SHIMADZU
Excellence in Science

Application Handbook

Materials Testing

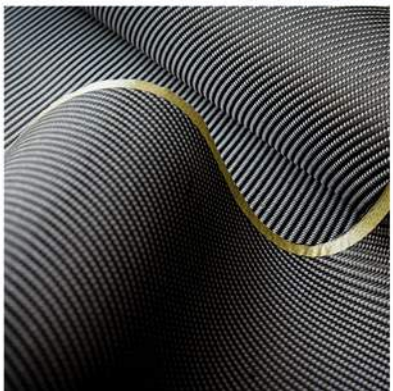

Introduction

Consumer and environmental protection, healthcare, quality control and product safety are key issues being pursued rigorously. In order to meet the requirements of international markets, standards and norms such as ISO, testing and inspection machines are applied in a vast number of industries. They help to support human health and individual well-being while preventing accidents and damage, enhancing comfort levels and enjoyment and providing peace of mind. Furthermore, testing machines offer data which serves to guide R&D towards improved materials and products.

This Materials Testing Application Handbook covers 112 applications of 8 industries, such as automotive, aerospace, biomaterials and medical, composites, food, metal, railroad, rubber and plastics industries. It is hands-on and solution-oriented. The applications described cover most-modern technologies, e.g. universal, fatigue and hardness testing and also high-speed video camera application.

Since 1917, Shimadzu has been manufacturing testing machines designed to meet the diverse needs of customers worldwide. To date, Shimadzu has sold tens of thousands of testing machines based on our primary product lines, including the Autograph series precision universal testers, UH series universal testing machines and Servopulser series fatigue testing machines. In addition, Shimadzu has marketed thousands of application-specific systems tailored to the unique needs of clients, and remains committed to providing customers with this same level of service in the future.

In addition to testing machines and equipment, Shimadzu as a worldwide leading manufacturer of analytical instrumentation systems provides high-level, sophisticated solutions in liquid and gas chromatography, mass spectrometry, TOC analysis, spectroscopy, consumables and software.

Our brand statement "Excellence in Science", reflects our desire and intention to respond to customer requirements by offering superior, world-class technologies. With a worldwide network of subsidiaries in 76 countries and circa 10.000 employees Shimadzu guarantees personal support for each customer.

Please see also our Application Handbooks on
- Liquid Chromatography
- Food & Beverages
- TOC
- Clinical
- GC/GC-MS.

www.shimadzu.eu/materials-testing-inspection

Contents

1. Automotive Industry

2. Aerospace Industry

3. Biomaterials and Medical Industry

4. Composite Industry

5. Food Industry

6. Metal Industry

7. Railroad Industry

8. Plastics and Rubber Industry

9. Others

SHIMADZU
Excellence in Science

1. Automotive Industry

1. Automotive Industry

EMOTION, SAFETY, COMFORT AND FUN

Cars are much more than just a means of transportation: although automobiles are technical products, they carry emotion, provide safety, offer comfort and generate fun. Cars are also part of cultures, and they play a role in business, private and family lives. Depending on the behavior of each single driver, cars can also be a means to endangering other road users.

The many tiers of the automotive industries provide a great deal of applications for material testing and inspection machines to make cars safer, more comfortable, efficient and environmentally responsible. The testing machines are used for engines, motors and power sources; bodies and interiors; lithium-ion rechargeable batteries and fuel cells; suspension and other power transmission systems; electronic instrumentation components and environmental conservation.

Cars may be the most complex technical mass market products which are comprehensively tested on a worldwide scale. International testing standards apply to single components as well as to cars as a whole. Please see the applications on the following pages for an overview of the wide range of testing. Materials tested are metals, non-metals and composites tested with destructive (Destructive Physical Analysis DPA) or non-destructive testing (NDT) methods in order to evaluate the properties of a material, component or system.

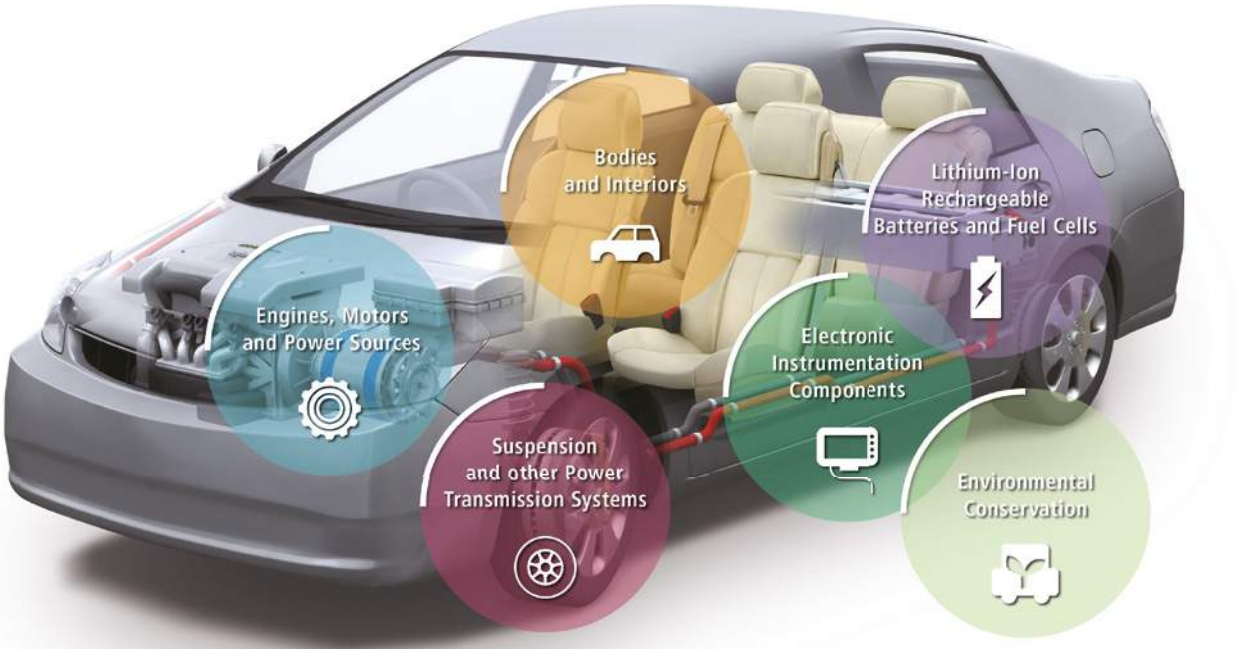

1. Automotive Industry

C225-E033	Three-axis endurance evaluations of automobile steering mechanisms
No.i245	Evaluation of temperature-dependent strength properties of lithium-ion battery separator by piercing and tensile testing
SCA_300_002	MCT compression test for structural materials of lithium-ion batteries
SCA_300_011	Evaluation of adhesive strength and hardness of protective surface layer of glass substrates
SCA_300_012	Evaluation of hardness of painted surface with Shimadzu dynamic ultra micro hardness tester model DUH
SCA_300_019	Hardness evaluation of thin film with Shimadzu dynamic ultra micro hardness tester
SCA_300_040	Evaluation of hardness of painted surface
SCA_300_049	Seat belt test tensile test according to manufacturer's specification
eV022	High-speed imaging of fuel injection in automotive engines
No.ei254	Compression after impact testing of composite
No.ei255	Compression testing of composite materials
No.36	Evaluating the fatigue strength of GFRP materials
No.30	Evaluating the strength of carbon fiber reinforced plastics (CFRP)
No.39	Evaluation of open-hole CFRP
No.i247	DIC analysis material testing by strain distribution visualization
No.8	Flexural testing of CFRP boards
No.16	Tensile testing of carbon fiber
No.31	Materials testing using digital image correlation
No.37	Observing the failure of open-hole CFRP samples in tensile tests
No.38	Observing the fracture of unidirectional CFRP in static tensile testing
No.ei256A	Open-hole compression testing of composite material
No.ei250	Shear test of composite material (V-notched beam)
No.ei251	Shear test of composite material (V-notched rail shear)
SCA_300_037	Compression-rupture test of carbon fibers with different tensile characteristics Shimadzu micro compression testing machine MCT
SCA_300_059	Observation of fracture in CFRP tensile test E001HPV
C225-E032	Ultrasonic fatigue testing system with an average stress loading mechanism
No.i244	Tensile test for metallic materials using strain rate control and stress rate control
SCA_300_035	A hardness measurement of surface treatment layer on a steel sample using Shimadzu dynamic ultra micro hardness tester, model DUH
SCA_300_045	Jigs for measuring Bauschinger effect
No.2	Flexural test of plastic ISO178
No.3	Tensile tests of plastic materials at low ISO527 1
No.4	Tensile test of rubber dumb bell specimens ISO37
No.5	Tear test of crescent shaped ISO34 1
No.6	Tear tests of angle shaped rubber specimens ISO34 1
No.7	Tensile tests of films ISO527 3
No.9	Measurements of modulus of elasticity and poisson's ratio for films ISO527

SHIMADZU
Excellence in Science

Three-Axis Endurance Evaluations of Automobile Steering Mechanisms

With Control via Actual Data, Endurance Evaluations Approximating Real Motion Can Easily Be Performed

Automobile steering units are important components that must be highly durable. There are also significant differences in driver arm strengths, so many cars are equipped with a power steering mechanism, which complicates the structure. In contrast, with luxury cars and sports cars, specifications are required that can achieve an operable feeling that heightens the sense of enhanced value. In regards to these new and diversified requirements, quantitation, not only evaluations by people, is increasingly needed. By combining three actuators with the 4830 controller, which is capable of high-accuracy control, this system can easily perform endurance tests under close to real conditions.

System Appearance

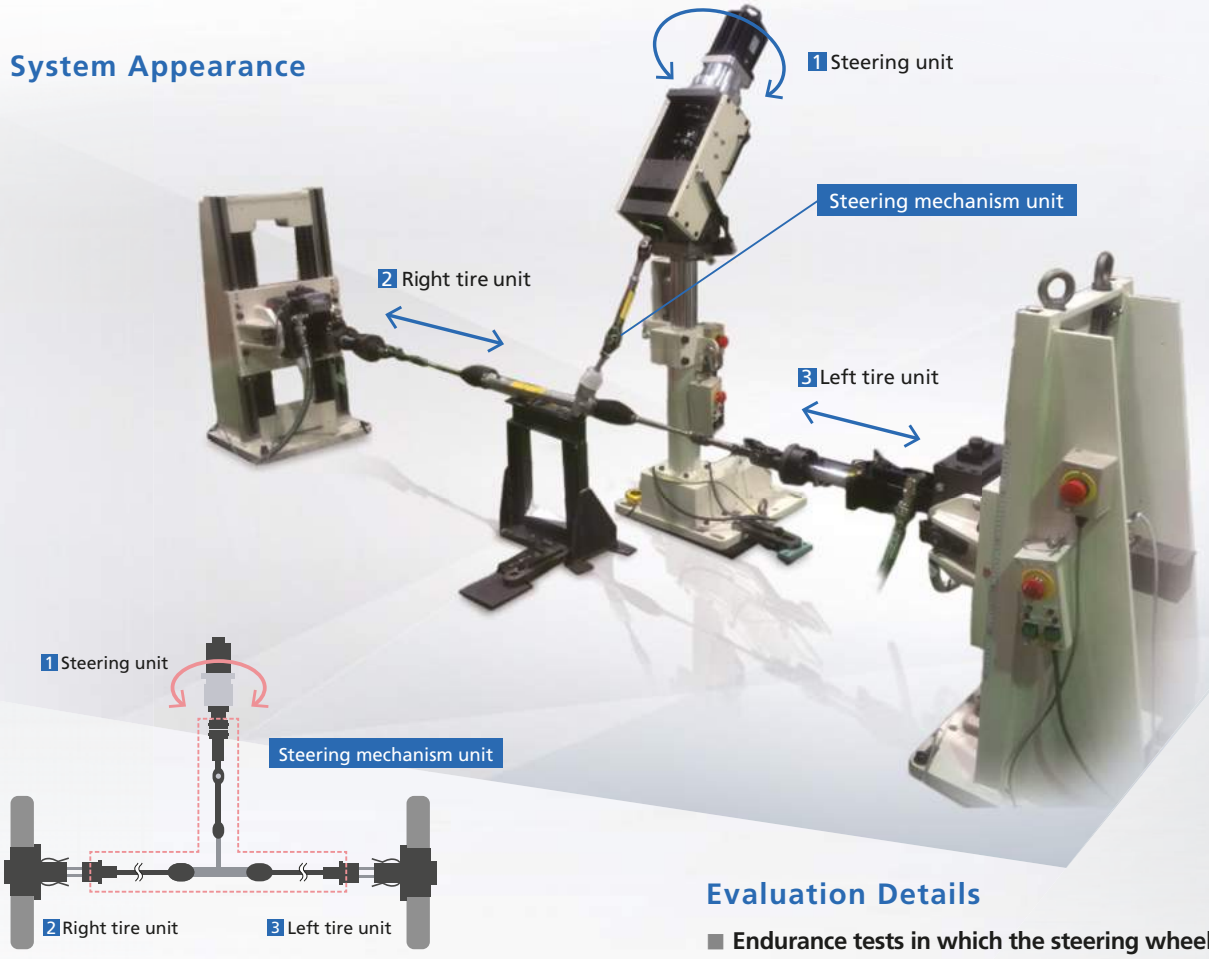

Endurance tests of the steering mechanism unit are performed by adding a rotational force via the steering wheel 1, and producing a reaction force originating from the tires in 2 and 3.

The reaction force from 2 and 3 corresponding to the rotational angle in 1 is obtained for use from an actual car.

Evaluation Details

- **Endurance tests in which the steering wheel is moved left and right more than one million times**
- **Endurance tests in which excessive force is applied to turn the steering wheel to the left or the right**
- **Quantitation of the sense of enhanced value (Rotational torque and angle of 1 and test force at 2 and 3 at each rotation point)**

Main Specifications

Left/Right Tire Units

1) Rated capacity: ±10 kN stroke ±100 mm
   (static maximum load capacity ±13 kN)
2) With trunnion pin
3) Maximum speed: 500 mm/sec
   (20 L/min hydraulic source, when unloaded)

Lifting Stand
(For the left/right tire units)

1) Height: 300 mm to 800 mm
   (electric lift, manual bolt fastening)
2) Angle: top/bottom ±10°
   (can change fastened or mobile) and horizontal ±10°

Steering Unit

1) Rated capacity: ±200 Nm, Angle: ±1080 deg
2) Maximum speed: 360 deg/sec
3) Excitation frequency: 0.01 Hz to 2 Hz (±5 deg or more)

4830 Controller

Lifting Stand
(For the steering unit)

1) Height: 800 mm to 1200 mm (electric lift, manual bolt fastening)
2) Angle: top/bottom 0° to 60° (can change fastened or mobile)

Data Processing Example (PC Screen)

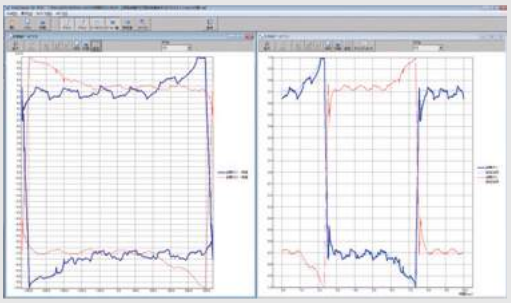

The left window shows the data chart results when the steering unit is turned to the left and right from the center position, and then returns to the center.

The window on the left shows a chart of angle versus test force.

The window on the right shows a chart of time versus test force.

The blue line is the test force for the right tire unit.

The red line is the test force for the left tire unit.

SHIMADZU

Shimadzu Corporation

www.shimadzu.com/an/

For Research Use Only. Not for use in diagnostic procedure.
This publication may contain references to products that are not available in your country. Please contact us to check the availability of these products in your country.
Company names, product/service names and logos used in this publication are trademarks and trade names of Shimadzu Corporation or its affiliates, whether or not they are used with trademark symbol "TM" or "®". Third-party trademarks and trade names may be used in this publication to refer to either the entities or their products/services. Shimadzu disclaims any proprietary interest in trademarks and trade names other than its own.

The contents of this publication are provided to you "as is" without warranty of any kind, and are subject to change without notice. Shimadzu does not assume any responsibility or liability for any damage, whether direct or indirect, relating to the use of this publication.

© Shimadzu Corporation, 2016

First Edition: August 2016

SHIMADZU

Application News

No.i245

Material Testing System

Evaluation of Temperature-Dependent Strength Properties of Lithium-Ion Battery Separator by Piercing and Tensile Testing

Introduction

Lithium-ion secondary cells, also called rechargeable batteries, (referred to here as "lithium-ion batteries") are widely used as energy sources for information terminals and consumer electronics, etc. because of their high energy density and cell voltage. Recently, their growing rate of dissemination into areas of general household applications, including hybrid and electric vehicles, is quite evident, and it appears obvious that the demand will further increase in the future.

Because lithium-ion batteries can sometimes become unstable due to short-circuit, over charging and discharging, impact, etc., a variety of protection mechanisms are incorporated at the battery component level to ensure safety.

Of these component parts, the lithium-ion battery separator prevents contact between the positive and negative electrodes, while at the same time playing a role as a spacer which permits the passage of lithium ions. However, it also performs the function of preventing a rise in battery temperature due to excessive current in the event of a short circuit.

Because the lithium-ion battery separator is set in place so that it comes into contact with the rough surfaces of the positive and negative terminals, high mechanical strength is required. This mechanical strength must be maintained even if there is some rise in temperature, which is common to some degree, for example, during battery charging. Therefore, we conducted piercing and tensile testing measurements of the separator to evaluate changes in strength with respect to changes in temperature. This document introduces actual examples of these tests.

Supplement) Regarding the lithium-ion battery separator, previous evaluation examples were also introduced in Application News T146 "Measurement of Separator in Lithium-Ion Battery" and i229 "Multi-Faceted Approach for Evaluating Lithium-Ion Battery Separators."

Piercing Test

The samples consisted of separators removed from two lithium-ion batteries (cylindrical) used in small electrical devices, and we measured the changes in piercing characteristics due to changes in environmental temperature. Fig. 1 shows an overview of the test conditions, and Table 1 presents details of the test conditions.

Fig. 1 Overview of Piercing Test

Table 1 Test Conditions (Piercing Test)

1) Instrument	Shimadzu AG-X Precision Universal Tester
2) Load cell capacity	1 kN
3) Jigs	Boil-in-bag piercing jig
4) Thermostatic chamber	TCR-1W
5) Load rate	50 mm/min
6) Temperature	25 °C, 60 °C, 90 °C
7) Software	TRAPEZIUMX (Single)

Fig. 2 shows the force – displacement curve, and Table 2 shows the maximum force and maximum displacement with respect to temperature.
Comparing the test results at 25 °C and 60 °C, it is evident that there is not much difference in the maximum force, but the maximum displacement is greater at 60 °C. Comparing characteristic values at 60 °C and 90 °C, the decrease in maximum force is obvious at 90 °C, but the maximum displacement value is about the same. From the above, it can be assumed that at 60 °C, there is no decrease in strength of the lithium-ion battery separator, despite the apparent increase in its elongation property.

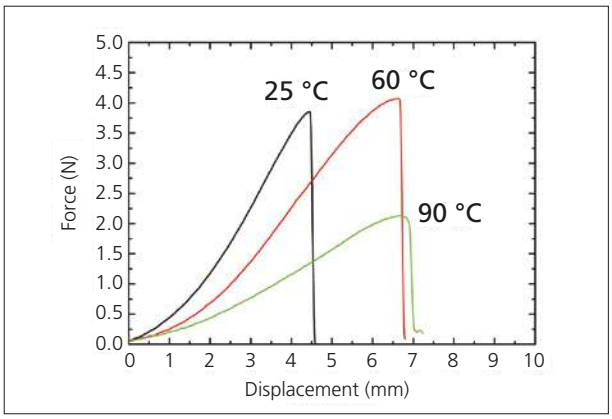

Fig. 2 Test Result (Piercing Test)

Table 2 Summary of Results (Piercing Test)

Temperature (°C)	Maximum Force (N)	Maximum Displacement (mm)
25	3.85	4.45
60	4.07	6.63
90	2.13	6.68

Tensile Test

The separators used for the tensile testing were removed from commercially available lithium-ion batteries (square-shaped), so 2 types of samples (below, referred to as samples (1) and (2)) which contained PE (polyethylene) as the principle constituent were used. When conducting the tensile tests, each separator sample (as shown in Fig. 3(a)) was fashioned into dumbbell-shaped specimens oriented in the lengthwise and widthwise directions of each separator, as shown in Fig. 3(b). The total length of all specimen was 35 mm, with the parallel section measuring 10 (L) × 2 (W) mm.

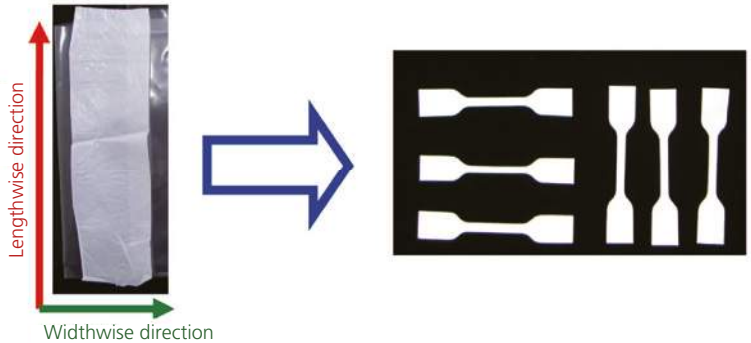

(a) Separator Sample (b) Dumbbell-Shaped Specimens (image)

Fig. 3 Test Samples

Table 3 shows the tensile test conditions that were used.

Table 3 Test Conditions (Tensile Test)

1) Instrument	Shimadzu AG-X Precision Universal Tester
2) Load cell capacity	100 N
3) Jig	50 N capacity pneumatic flat grips (flat surface teeth, pneumatic pressure 0.4 MPa)
4) Thermostatic chamber	TCR-1W
5) Load rate	50 mm/min
6) Temperature	25 °C, 60 °C, 90 °C
7) Software	TRAPEZIUMX (Single)

Fig. 4 and Fig. 5 show the stress – strain curves for the widthwise and lengthwise directions, respectively of sample (1). Fig. 6 and Fig. 7 show the stress – strain curves for the widthwise and lengthwise directions, respectively of sample (2). Table 4 shows the test values of the mechanical properties obtained at each temperature.

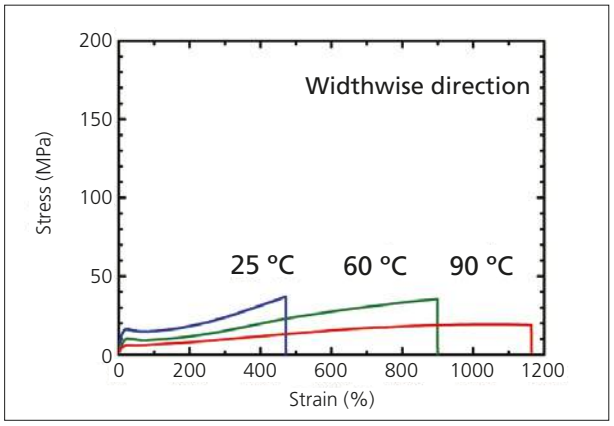

Fig. 4 Test Results (Sample (1), widthwise direction)

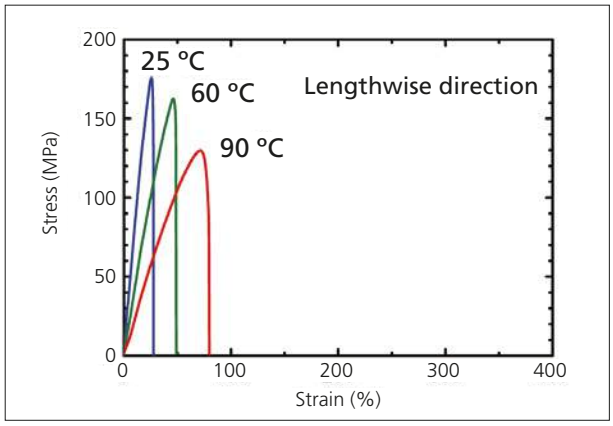

Fig. 5 Test Results (Sample (1), lengthwise direction)

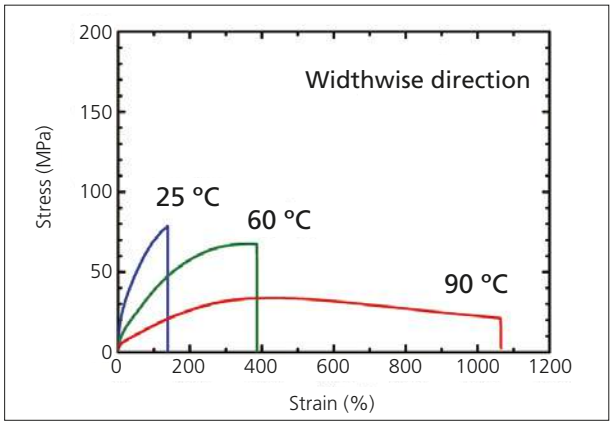

Fig. 6 Test Results (Sample (2), widthwise direction)

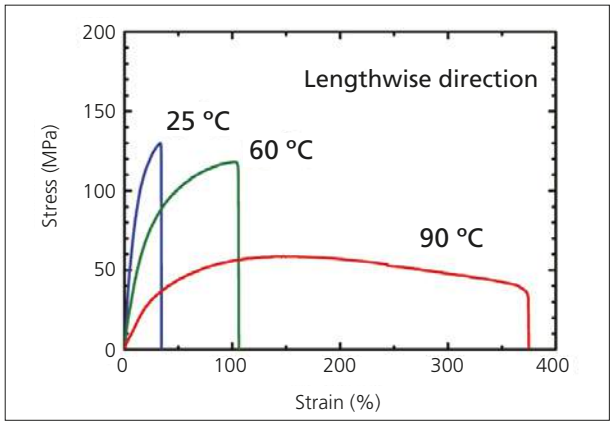

Fig. 7 Test Results (Sample (2), lengthwise direction)

Table 4 Summary of Results of Tensile Test

Sample	25 °C		60 °C		90 °C	
	Tensile Strength (MPa)	Strain at Break (%)	Tensile Strength (MPa)	Strain at Break (%)	Tensile Strength (MPa)	Strain at Break (%)
(1) Widthwise direction	36.9	471.4	35.4	898.8	19.3	1044.0
(1) Lengthwise direction	175.6	26.8	162.5	57.0	129.9	76.7
(2) Widthwise direction	78.2	138.5	68.8	347.6	33.8	427.9
(2) Lengthwise direction	129.5	34.1	118.3	105.3	58.7	367.2

In each of the samples, a lower tensile strength and greater elongation was seen in the widthwise direction than in the lengthwise direction. When comparing the numbers in Table 4, the lengthwise tensile strength for sample (1) is about 5 times greater than the widthwise tensile strength of sample (1). Also, the strain at break, for sample (1) in the lengthwise direction is lower by about a factor of 15 than that of sample (1) in the widthwise direction. From the above results, it is supposed that this separator (sample (1)) was manufactured using uniaxial drawing in the lengthwise direction. The widthwise tensile strength for sample (2) is about twice that of sample (1), and the strain at break is much lower. The tendency similar to that of sample (2) in the widthwise direction is seen with respect to sample (2) in the lengthwise direction. Therefore, due to the tendency of greater tensile strength and lower strain at break with sample (2) in the lengthwise direction, it is presumed that sample (2) was manufactured with a low biaxial drawing ratio, and that the drawing ratio in the lengthwise direction was greater than that in the widthwise direction.

The data obtained regarding the mechanical properties with respect to the sample temperature are also interesting. When comparing the sample strain at break and tensile strength at 25 °C and 60 °C, even though the strain at break value increased by a factor of 2 due to the test temperature increase to 60 °C, there was just a slight decrease in tensile strength. Similarly, when comparing the physical property measurement values at 60 °C and 90 °C, the strain at break showed the same tendency to greatly increase as when the values were compared at 25 °C and 60 °C. However, in this case, the tensile strength value shows a significant decrease. From the above, it is evident that the lithium-ion battery separators used in this test maintain excellent mechanical strength at 60 °C, notwithstanding its elevated elongation characteristics.

High-mechanical strength specifications are required for separators in order to withstand changing temperature in the cell. Here, as is clear from the results of piercing and tensile testing of lithium-ion battery separators under atmospheric temperature control, the mechanical properties of lithium-ion battery separators can be reliably evaluated using the Shimadzu Precision Universal Tester AG-X with its abundant array of accessories.

First Edition: January, 2012

SHIMADZU Corporation
www.shimadzu.com/an/

For Research Use Only. Not for use in diagnostic procedures.
The contents of this publication are provided to you “as is” without warranty of any kind, and are subject to change without notice.
Shimadzu does not assume any responsibility or liability for any damage, whether direct or indirect, relating to the use of this publication.

© Shimadzu Corporation, 2012

SHIMADZU
Excellence in Science

Application News

Material Testing System
MCT

Compression Test for Structural Materials of Lithium-Ion Batteries by MCT

No. SCA_300_002

■Introduction

Since lithium-ion batteries are light and small, they are used in a wide variety of products, from mobile electronic devices such as cellular phones and notebook PCs to electric cars and hybrid cars. Their inner structural materials are subjected to external force during production processes and to pressure during use. Therefore, evaluation of strength of each structural material is important to maintain consistent quality. A strength measurement was performed on thin or minute materials among various structural materials of lithium-ion batteries. Separators are usually evaluated by a tensile test or penetration test. A compression test is also important to evaluate them because they are compressed in some processes. Active materials of approximately 10 µm in size located near the electrode need to have a certain compression strength so they will not be destroyed during the coating process. Below are the results of compression tests performed on these materials using the MCT-211 Series Micro Compression Testing Machine.

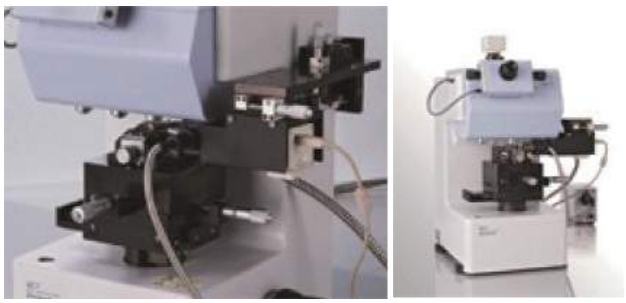

Fig. 1 External View of the MCT-211 Series (with the Side Observation Kit Mounted)

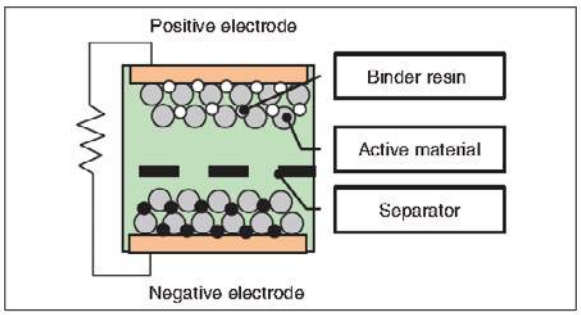

Fig. 2 Structure of Lithium-Ion Battery

■Compression Test on Separator of Lithium-Ion Battery

Table 1 shows the three types of specimens used for the measurement. Table 2 shows accessories used in the test and test conditions. Fig. 3 shows the conceptual diagram of the measurement. Table 3 shows the results of the compression tests on the three types of specimens. The specimens were evaluated by a compression rate where the same test force was applied. The results clearly show the difference among the three types. Fig. 4 is a graph indicating the test force - displacement relationship of each specimen. The inflexion point of specimen 2 is at around 10 mN (pressure of approximately 5 MPa), indicating that applying too much compression pressure causes plastic deformation to the separator.

Table 1 Specimens

1) Specimen Name	Separator		
2) Specimen Number	1	2	3
3) Thickness	20 µm	20 µm	10 µm

Table 2 Test Conditions

1) Upper Indenter	Flat indenter (with a diamond tip), 50 µm dia.
2) Test Mode	Load-unload test
3) Test Force (mN)	50
4) Loading Rate (mN/sec)	2.2
5) Holding Time (sec)	0
6) Test Method	A thin layer of liquid glue was applied to a glass plate, the separator was bonded to it, and a compression test was performed using the upper indenter. (See Fig. 2.)

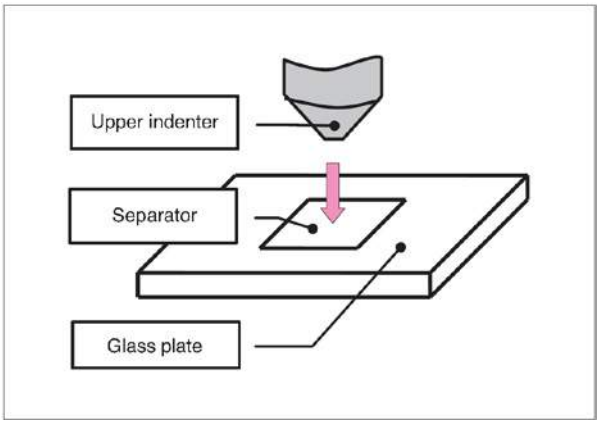

Fig. 3 Conceptual Diagram of Measurement

Table 3 Test Results

Specimen Name	Specimen Number	Maximum Force (mN)	Compression Variation (µm)	Compression Rate (%)
Separator	1	49.9	3.651	18.3
	2	49.9	3.371	16.9
	3	50.0	1.038	10.4

Note: The compression rate was calculated by the following calculation formula.
Compression rate (%) = (compression volume)/(thickness) × 100 (%)

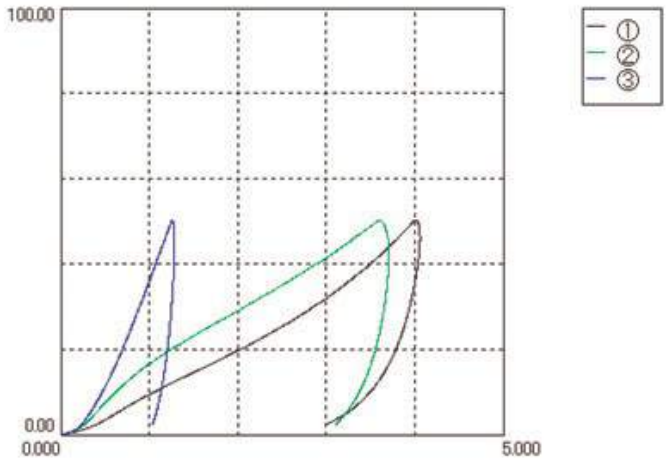

Fig. 4 Results of Compression Test

■Compression Test on Active Materials

A compression test was performed on two types of active material particles for positive electrode of lithium-ion battery. Table 4 shows test conditions and Fig. 5 shows an image of the test (compressed part). Measurement was performed ten times for each specimen. Then, average values were selected as a representative value for each specimen. (See Table 5 and Fig. 6.) The results clearly indicate the difference in the strength between the two active materials and lithium cobalt oxide (LiCoO2) was confirmed to have the higher strength. As shown above, the MCT-211 Series Micro Compression Testing Machine enables accurate and efficient evaluation of compression characteristics of thin or minute materials used inside lithium-ion battery.

Table 4 Test Conditions

1) Upper Indenter	Flat indenter (with a diamond tip), 50 μm dia.
2) Test Mode	Compression test
3) Test Force (mN)	50
4) Loading Rate (mN/sec)	2.2
5) Holding Time (sec)	0
6) Test Method	A very small amount of each specimen was spread on the lower compression plate and a compression test was performed on each single particle. (See Fig. 5.)

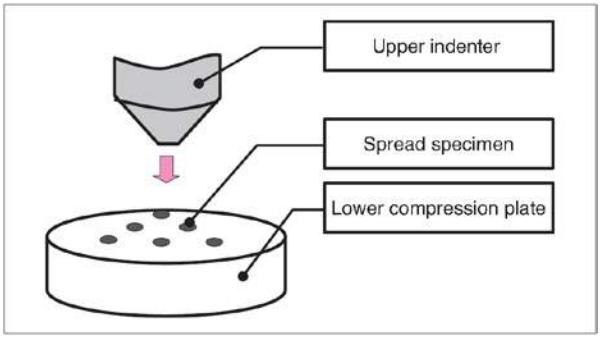

Fig. 5 Conceptual Diagram of the Compressed Part

Table 5 Test Results

Specimen Name	Fracture Force (mN)	Particle Diameter (µm)	Strength (MPa)
$LiMn_2O_4$	1.67	13.0	7.79
$LiCoO_2$	16.23	13.3	72.75

Note: Fracture strength was calculated by the following calculation formula (Based on JIS R1639-5∗1).

Cs = 2.48 P/πd2

Cs: Strength (MPa), P: Fracture force (N), d: Particle diameter (mm)

∗1: Test methods of properties of fi ne ceramic granules Part 5: Compressive strength of a single granule

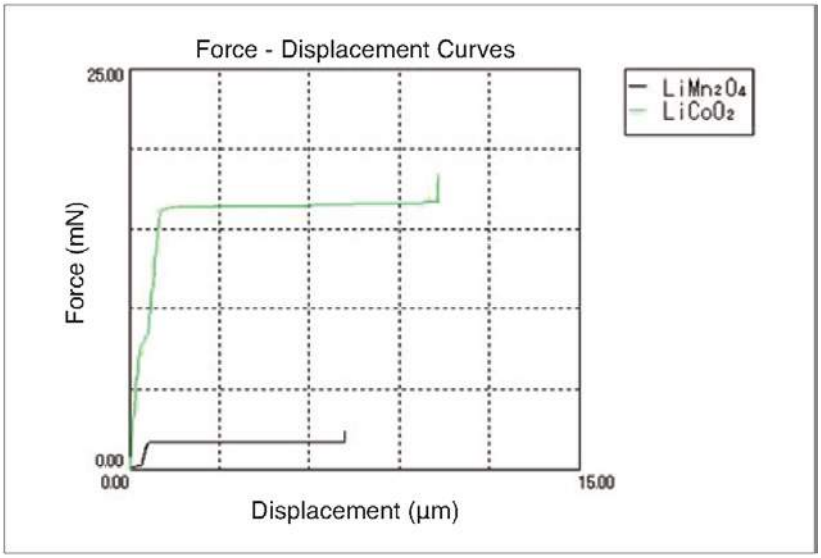

Fig. 6 Force - Displacement Curves

For Research Use Only. Not for use in diagnostic procedures.
The content of this publication shall not be reproduced, altered or sold for any commercial purpose without the written approval of Shimadzu. The information contained herein is provided to you "as is" without warranty of any kind including without limitation warranties as to its accuracy or completeness. Shimadzu does not assume any responsibility or liability for any damage, whether direct or indirect, relating to be the use of this publication. This publication is based upon the information available to Shimadzu on or before the date of publication, and subject to change without notice.

SHIMADZU
Excellence in Science

Application News

No. SCA_300_011

Material Testing System DUH

Evaluation of Adhesive Strength and Hardness of Protective Surface Layer of Glass Substrates

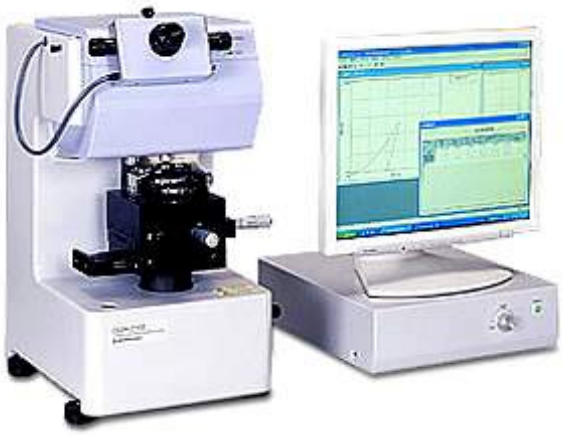

Rapid progress of thin film developing technology has accelerated expansion of film applications.
Thin film developing technologies based on vacuum evaporation, sputtering, or ion plating are featured not only in the improvement in quality of thin films, but also in adding new characteristics to a material, and are applied in various fields such as semiconductors, optical materials, and machine parts.
Adhesive strength and hardness are important factors for the evaluation of the mechanical strength of thin film that is produced by the aforementioned techniques.
Thin film that satisfies specifications of quality and properties may peel from its substrate board unless its adhesive strength is adequate. There may also be a problem of unimpeded wear and tear, if its hardness does not conform to specifications.
The following is an introduction to an evaluation of adhesive strength and hardness of a thin film on a glass substrate with Shimadzu Scanning Scratch Tester Model SST and Shimadzu Dynamic Ultra Micro Hardness Tester Model DUH.

■ Test conditions

SST-101:
(1) Stylus (needle): Diamond 100 µm
(2) Swing amplitude: 60 µm
(3) Scratch speed: 20 µm/s
(4) Max load: 20 gf
(5) Down speed of cartridge: 1 µm/s

DUH-211:
(1) Testing mode: Indenter pressing test
(2) Load: 2 gf
(3) Loading rate constant: 1 (0.029 gf/s)
(4) Indenter: 115° triangular pyramid

■ Test piece

1) Name: Surface protective thin film of glass substrate
2) Type: 1 through 3
3) Thickness of films: approx. 1µm or all

Test piece	Peeling load (gf)			
	1	2	3	4
No. 1	1.3	1.4	1.3	1.33
No. 2	2.5	2.4	2.5	2.47
No. 3	7.4	7.4	7.1	7.30

Table 1: Test results of SST

■ Test results

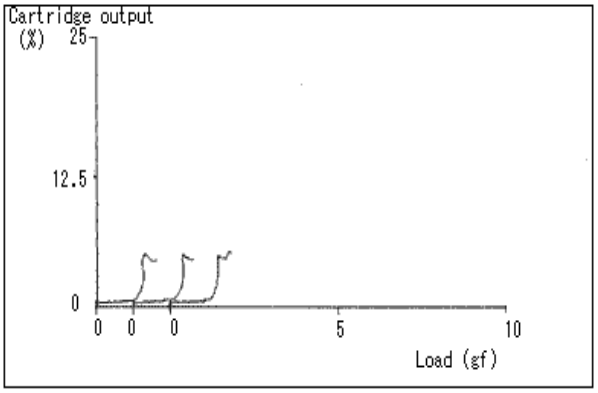

Figure 1: Load – cartridge output curves of test piece No.1 (with SST)

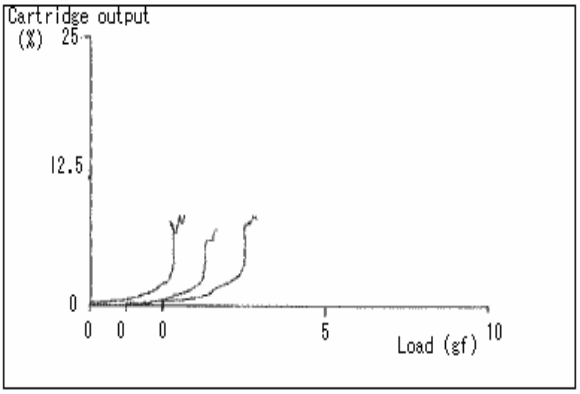

Figure 2: Load – cartridge output curves of test piece No.2 (with SST)

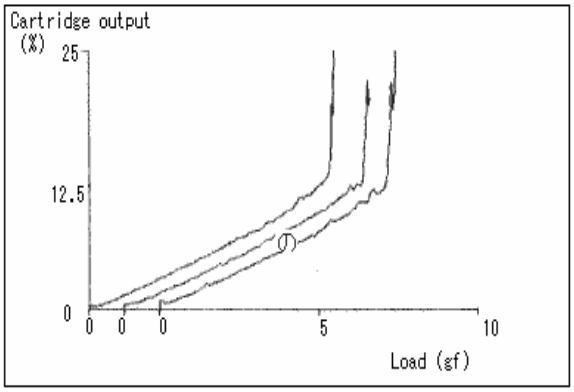

Figure 3: Load – cartridge output curves of test piece No.3 (with SST)

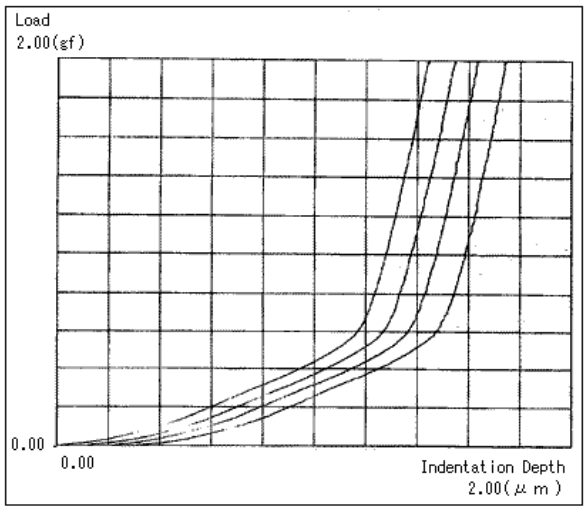

Figure 4: Load – indentation depth curves of test piece No.1 (with DUH)

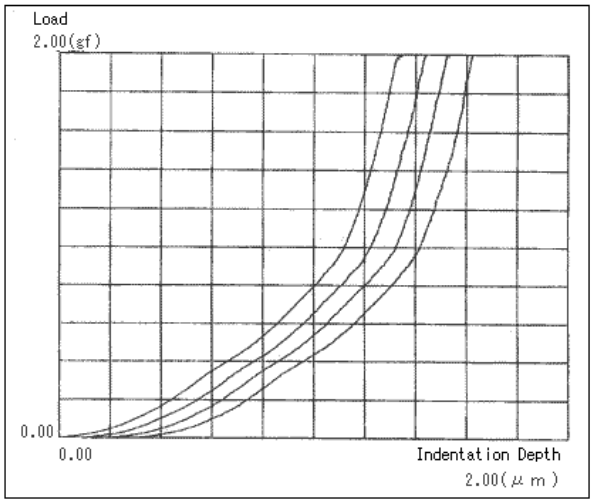

Figure 5: Load – indentation depth curves of test piece No.2 (with DUH)

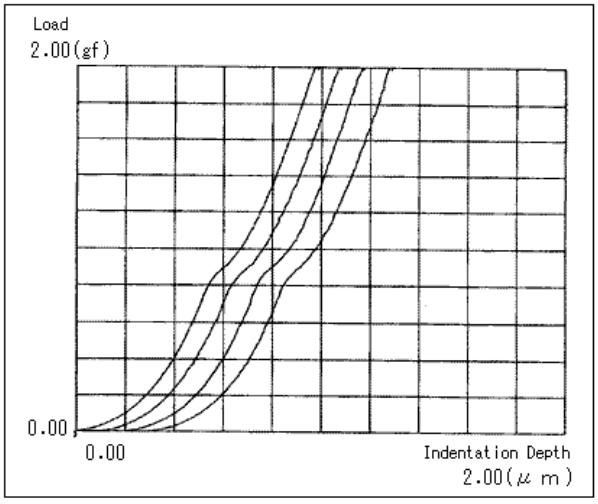

Figure 6: Load – indentation depth curves of test piece No.3 (with DUH)

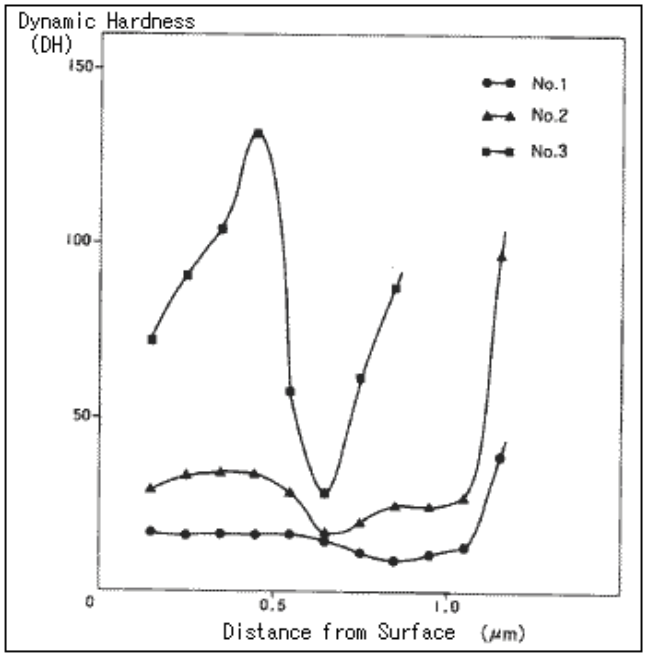

Figure 7: Hardness Distribution in Depth Direction

Hardness distribution was calculated by the following equation (Data analysis 2: Output data of load and indentation depth) as internal hardness distribution is not known from load-indentation depth curves.

$$DH_{m-n} = \frac{37{,}838 \cdot P_n \cdot \left(1 - \sqrt{\frac{P_m}{P_n}}\right)^2}{(D_n - D_m)^2}$$

Where $DH_{m\text{-}n}$: Hardness at indentation depth from D_m to D_n.
P_m, P_n: Load (gf)
D_m, D_n: Indentation depth (μm)

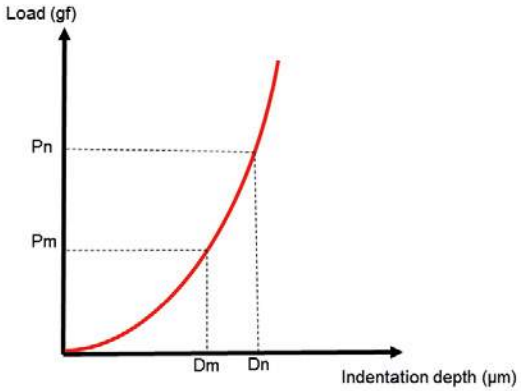

The result of peeling strength tests of surface protective films Nos.1-3 on glass substrates tested with Model SST-101 are shown in Table 1, from which it is known that adhesive strength estimated by the peeling load is greatest in the test piece No. 3 followed by No. 2 and No. 1, respectively. The hardness measurement's result is shown in Figs.4-6 in the form of load versus indentation depth curves. Hardness variation in depth direction is plotted in Fig.7 as well. According to this graph, it is known that the thin film hardness in the ultra-surface of specimen No. 3 is greatest among the three, and also that hardness of all the specimens gets lower at a depth below 0.5 μm, probably because cracks (ruptures) were produced during indentation. According to the hardness distribution curves from the surface down to 0.5 μm, hardness of test piece No. 3 (high adhesive strength) increases gradually, while the hardness of No. 1 (less adhesive strength) stays virtually unchanged.

For Research Use Only. Not for use in diagnostic procedures.
The content of this publication shall not be reproduced, altered or sold for any commercial purpose without the written approval of Shimadzu. The information contained herein is provided to you "as is" without warranty of any kind including without limitation warranties as to its accuracy or completeness. Shimadzu does not assume any responsibility or liability for any damage, whether direct or indirect, relating to be the use of this publication. This publication is based upon the information available to Shimadzu on or before the date of publication, and subject to change without notice.

SHIMADZU
Excellence in Science

Application News

No. SCA_300_012

Material Testing System DUH

Evaluation of Hardness of Painted Surface with Shimadzu Dynamic Ultra Micro Hardness Tester Model DUH

Painted surfaces are evaluated for properties such as weathering resistance, light resistance, adhesive strength, impact resistance and hardness by instrumental measurement, and for color, gloss, unevenness, rumples etc. by visual inspection. Of these, the hardness test of painted surfaces is most important in evaluating the quality of paint film. Wet paint is dried in order to transform wet paint into rigid paint film. Paint can be dried either by the natural drying method, in which the paint dries completely at room temperature, or by the forced drying method, in which paint is dried under high temperatures of approx. 100 to 250 degrees Celsius. The surface hardness of paint films differs depending on the kind of paint and the drying method. Information for evaluating hardness near the surface of paint film can be obtained by the ultra micro area measuring technique of the Shimadzu Dynamic Ultra Micro Hardness Tester Model DUH. The following presents the results of hardness tests performed on paint films of paints for general use dried either by the natural or by the forced drying method.

■ Measurement of surface hardness of paint films

Testing machine

TEST MODE	2
CAL. MODE	1 (115° Triangular Pyramid Indenter)
AUTO or MANUAL	AUTO
F.S. DEPTH	2 & 5 μm
MAX LOAD	9,81mN & 49,03 mN
LOADING SPEED	1 (0,1,4632 [mN/sec]) 5 (13,3240 [mN/sec])
TOUCH SPEED	50 (0,48 [mN/sec]) 50 (0,048 [mN/sec])
AFTER TIME	5 sec.
PRE TIME	5 sec.
LOT	5

Table 1 Test Conditions

(1) Paint film of meramin resin dried by forced drying

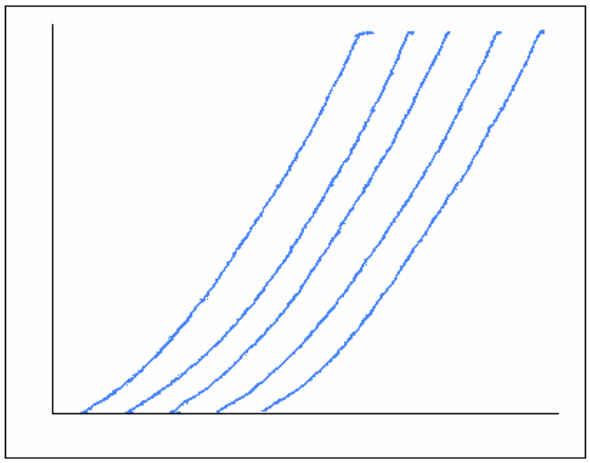

Fig.1 Indentation depth Load Curves of Painted Films of Meramin Resin

(2) Paint film of urethane resin dried by natural drying

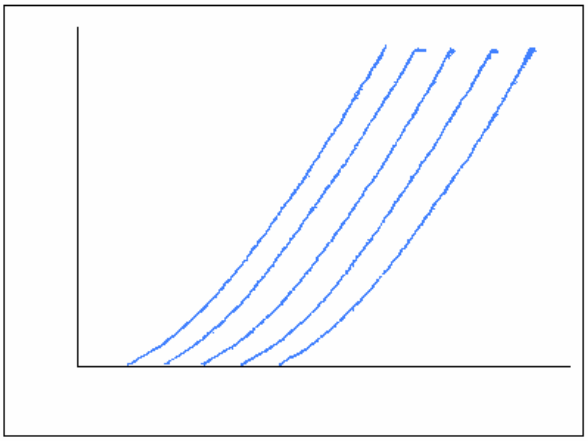

Fig.2 Indentation Depth Load Curves of Painted Films of Urethane Resin

(3) Paint film of acrylic resin dried by natural drying

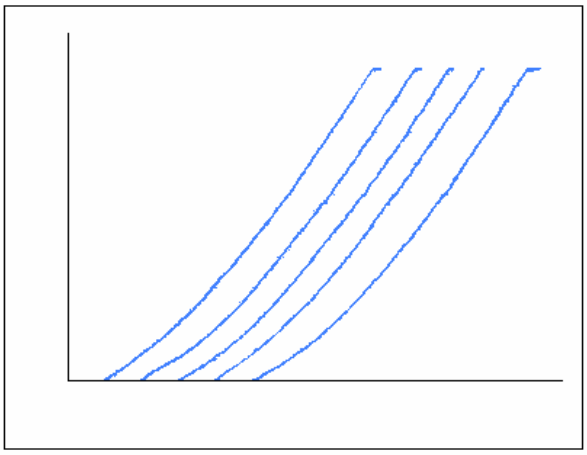

Fig.3 Indentation Depth Load Curves of Paint Films of Acrylic Resin

■ **Result of Measurements**

Sample Name	LOAD (mN)	DH (mean)
Meramin resin paint film thickness 38 µm - forced drying	9,81 mN	14,60
Overall thickness of paint film 177 µm	49,03 mN	12,00
Urethane resin paint film thickness 48 µm - forced drying	9,81 mN	13,00
Overall thickness of paint film 84 µm	49,03 mN	5,20
Acrylic resin paint film thickness 52 µm - forced drying	9,81 mN	10,50
Overall thickness of paint film 110 µm	49,03 mN	4,90

Table 2 Result of Measurements

Dynamic hardness is obtained based on the load value and indentation depth during the loading process. Since dynamic hardness is calculated from the indentation depth during the loading process, it includes both plastic deformation and elastic deformation.

DH: dynamic hardness
F: test load mN
h: dynamic indentation depth[2]
$DH115 = 3.8584 \times F / h^2$
DHT115: Dynamic hardness obtained with the triangular pyramid indenter with 115°tip angle

When LOAD is small, DEPTH is small, allowing the hardness of paint film at the outermost surface to be measured. When LOAD is large, DEPTH is also large, allowing the hardness at the deeper portion of paint film to be measured.
In tests on samples dried by natural drying and forced drying, a different trend was observed for the respective samples between the results of 9,81 mN and 49,03 mN LOADs. In other words, the difference between the data for 9,81 mN and 49,03 mN was large in case of natural drying, while significantly smaller in the case of forced drying. This indicates that forced drying creates hardness more evenly distributed throughout the depth of the paint film than natural drying.

* Please be advised that data obtained before the implementation of the current Weights and Measures Law may be presented in terms of gravimetric unit.

For Research Use Only. Not for use in diagnostic procedures.
The content of this publication shall not be reproduced, altered or sold for any commercial purpose without the written approval of Shimadzu. The information contained herein is provided to you "as is" without warranty of any kind including without limitation warranties as to its accuracy or completeness. Shimadzu does not assume any responsibility or liability for any damage, whether direct or indirect, relating to be the use of this publication. This publication is based upon the information available to Shimadzu on or before the date of publication, and subject to change without notice.

SHIMADZU
Excellence in Science

Application News

Material Testing System DUH

No. SCA_300_019

Hardness Evaluation of Thin Film with Shimadzu Dynamic Ultra Micro Hardness Tester (II)

■ Introduction

Thin film production technology has made a rapid progress and a great quantity of thin films are put to practical use in various applications. The evaluation of the hardness of thin films produced by CVD and PVD and surface coating layers plays an important role in production technology. In spite of such background, this method has not yet been definitively standardized, though some technical reports on hardness evaluation based on micro hardness method have been issued.

The Shimadzu Dynamic Micro Hardness Tester Model DUH, designed as a hardness evaluating machine, is also useful in the thin film market where a low electromagnetic load applying system is needed for information of material strength of a micro area on the basis of micro load measuring and controlling technique.

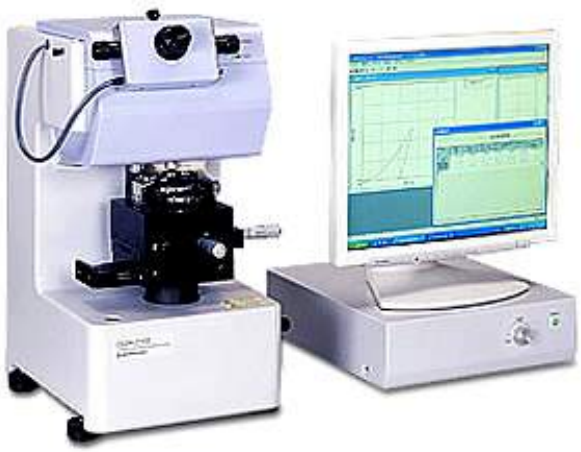

Fig. 1 External View of the DUH-211 series

In addition, a new method was developed for calculating dynamic hardness from the difference between two indentation depths at any two different loads, enabling calculation of hardness distribution in the depth direction. The following presents the results of two recent measurements.

■ Relation of load and indentation depth of a-Si thin film produced by CVD

DH hardness is calculated using the following equation, where D_1 and D_2 are depths at any two points on the chart and P_1 and P_2 are loads corresponding to D_1 and D_2 respectively.

$$DH = \alpha = \frac{P_2}{(D_2 - D_1)^2} \cdot \left(1 - \sqrt{\frac{P_1}{P_2}}\right)^2$$

The distances between D_1 and D_2 can be set freely. If D points are set at regular intervals, hardness distribution in depth direction is calculated.

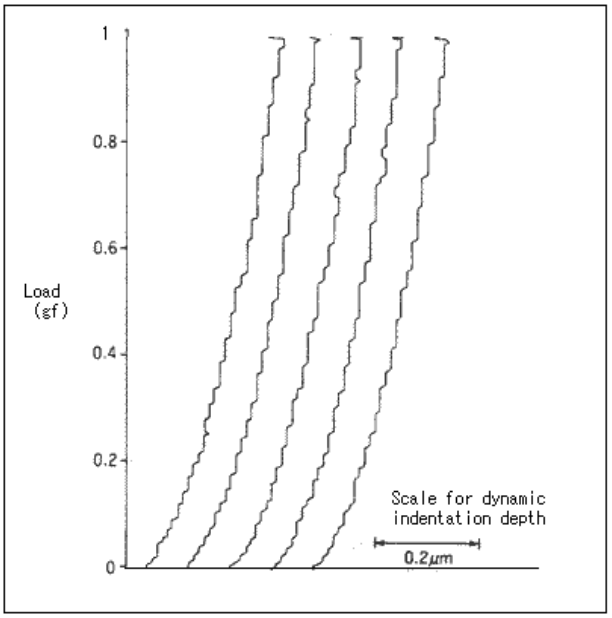

Fig. 2 Relation of Load versus Dynamic indentation depth of a-Si thin film

■ Evaluation of hardness distribution in depth direction for several kinds of thin films made by CVD

Hardness variation in the depth direction is shown for each thin film. These curves are useful to determine how hardness varies according to thin film processing conditions.

* Please be advised that data obtained before the implementation of the current Weights and Measures Law may be presented in terms of gravimetric unit

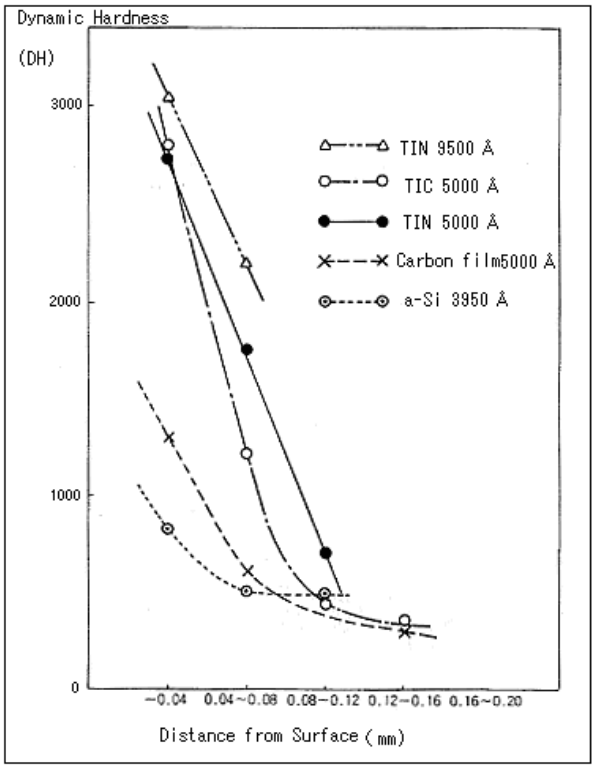

Fig. 3 Evaluation of Hardness distribution in depth direction for several kinds of thin films produced by CVD

For Research Use Only. Not for use in diagnostic procedures.
The content of this publication shall not be reproduced, altered or sold for any commercial purpose without the written approval of Shimadzu. The information contained herein is provided to you "as is" without warranty of any kind including without limitation warranties as to its accuracy or completeness. Shimadzu does not assume any responsibility or liability for any damage, whether direct or indirect, relating to be the use of this publication. This publication is based upon the information available to Shimadzu on or before the date of publication, and subject to change without notice.

SHIMADZU
Excellence in Science

Application News

Material Testing System DUH

No. SCA_300_040

Evaluation of Hardness of Painted Surface

Painted surfaces are evaluated for properties such as weathering resistance, light resistance, adhesive strength, impact resistance and hardness by instrumental measurement, and for color, gloss, unevenness, rumples etc. by visual inspection. Of these, the hardness test of painted surfaces is most important in evaluating the quality of paint film. Wet paint is dried in order to transform wet paint into rigid paint film. Paint can be dried either by the natural drying method, in which the paint dries completely at room temperature, or by the forced drying method, in which paint is dried under high temperatures of approx. 100 to 250 degrees Celsius. The surface hardness of paint films differs depending on the kind of paint and the drying method. Information for evaluating hardness near the surface of paint film can be obtained by the ultra-micro area measuring technique of the Shimadzu Dynamic Ultra Micro Hardness Tester Model DUH. The following presents the results of hardness tests performed on paint films of paints for general use dried either by the natural or by the forced drying method.

■ Measurement of surface hardness of paint films

TEST MODE	2
CAL. MODE	1 (115° Triangular Pyramid Indenter)
AUTO or MANUAL	AUTO
F.S. DEPTH	2 & 5 μm
MAX LOAD	9,81 mN & 49,03 mN
LOADING SPEED	1 (0,1,4632 [mN/sec]) 5 (13,3240 [mN/sec])
TOUCH SPEED	50 (0,48 [mN/sec]) 50 (0,048 [mN/sec])
AFTER TIME	5 sec.
PRE TIME	5 sec.
LOT	5

Table 1 Test Conditions

■ Paint film of Meramin Resin dried by forced drying

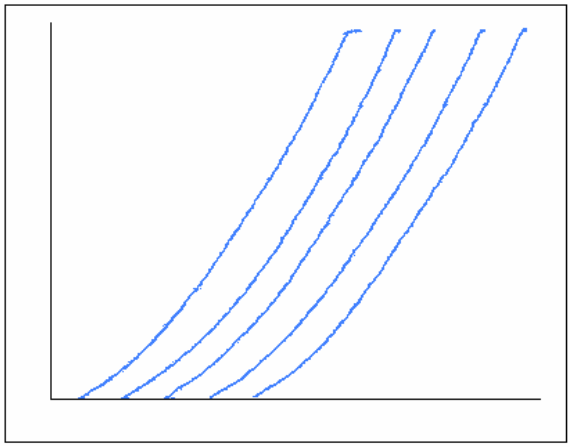

Fig. 1 Indentation depth Load Curves of Painted Films of Meramin Resin

■ Paint film of Urethane Resin dried by natural drying

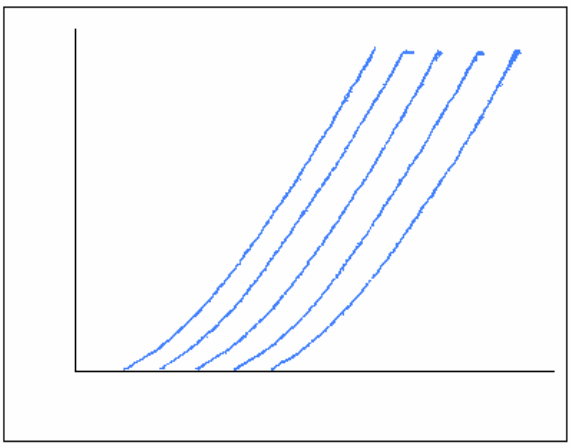

Fig. 2 Indentation Depht Load Curves of Painted Films of Urethane Resin

■ Paint film of acrylic resin dried by natural drying

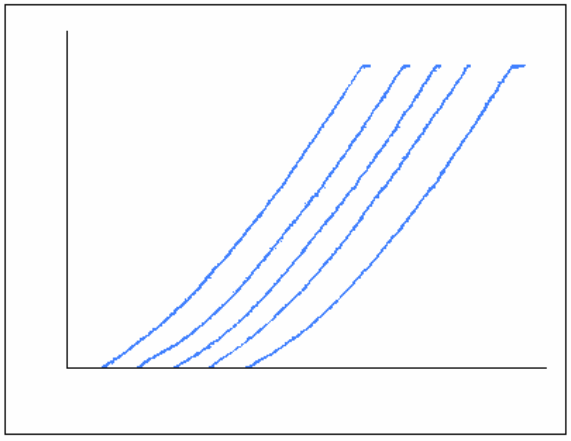

Fig. 3 Indentation Depth Load Curves of Paint Films of Acrylic Resin

Sample Name	LOAD (mN)	DH (mean)
Meramin resin paint film thickness 38 µm - forced drying	9,81 mN	14,60
Overall thickness of paint film 177 µm	49,03 mN	12,00
Urethane resin paint film thickness 48 µm - forced drying	9,81 mN	13,00
Overall thickness of paint film 84 µm	49,03 mN	5,20
Acrylic resin paint film thickness 52 µm - forced drying	9,81 mN	10,50
Overall thickness of paint film 110 µm	49,03 mN	4,90

Table 2 Result of Measurements

Dynamic hardness is obtained based on the load value and indentation depth during the loading process. Since dynamic hardness is calculated from the indentation depth during the loading process, it includes both plastic deformation and elastic deformation.

DH: dynamic hardness

F: test load mN

h: dynamic indentation depth2

DH115 = 3.8584×F／h2

DHT115: Dynamic hardness obtained with the triangular pyramid indenter with 115°tip angle

When LOAD is small, DEPTH is small, allowing the hardness of paint film at the outermost surface to be measured. When LOAD is large, DEPTH is also large, allowing the hardness at the deeper portion of paint film to be measured. In tests on samples dried by natural drying and forced drying, a different trend was observed for the respective samples between the results of 9,81 mN and 49,03 mN LOADs. In other words, the difference between the data for 9,81 mN and 49,03 mN was large in case of natural drying, while significantly smaller in the case of forced drying. This indicates that forced drying creates hardness more evenly distributed throughout the depth of the paint film than natural drying.

* Please be advised that data obtained before the implementation of the current Weights and Measures Law may be presented in terms of gravimetric unit.

For Research Use Only. Not for use in diagnostic procedures.
The content of this publication shall not be reproduced, altered or sold for any commercial purpose without the written approval of Shimadzu. The information contained herein is provided to you "as is" without warranty of any kind including without limitation warranties as to its accuracy or completeness. Shimadzu does not assume any responsibility or liability for any damage, whether direct or indirect, relating to be the use of this publication. This publication is based upon the information available to Shimadzu on or before the date of publication, and subject to change without notice.

SHIMADZU
Excellence in Science

Application News

Material Testing System AG-X plus

No. SCA_300_049

Seat Belt test Tensile test according to manufacturer's specification

■ Purpose and Definition:

The three point seat belt design, created by VOLVO in 1959, has saved approximately 1 000 000 lives worldwide since then. Tensile tests are a fundamental test within material science and is performed on more or less all materials. For seat belt manufacturers it´s of great importance to perform continuous quality control on the products they produce to ensure that the final product is according to specification and will withstand the forces, which occurs during an accident and again saving a life...

■ Equipment used:

Testing machine:	AG-100kNX with protective doors for camera.
Load cell:	100kN,1/1000 Class 0,5
Jig:	100kN belt grips.
Extensometer:	TRViewX single camera for protective doors, FOV 500 mm
Software:	Trapezium-X Single / Tensile.
Environment:	Room temp 21°+/-2°C, humidity ca. 50 +/-5% RHT
Test execution:	5 samples was prepared.

Sample length has to be long enough to be rolled on the grips and ensure a secure gripping.
In this case the total sample length was approximately 1200 mm.
There must still be enough grip separation to set the gauge length...

A method is prepared according to customer request. Test type is single and tensile. Test speed is set to 20 mm/min Gauge length is 200 mm and the TRViewX was selected as extensometer because of the sample dimensions and the violent break properties.
Some data points that are requested in this test are: Elongation at 980 daN, 1000 daN, 1110 daN and 1130 daN. Break elongation in %. Maximum force in daN. With the help of TrapeziumX all requested parameters are set quickly with a few clicks exactly according to the specification.

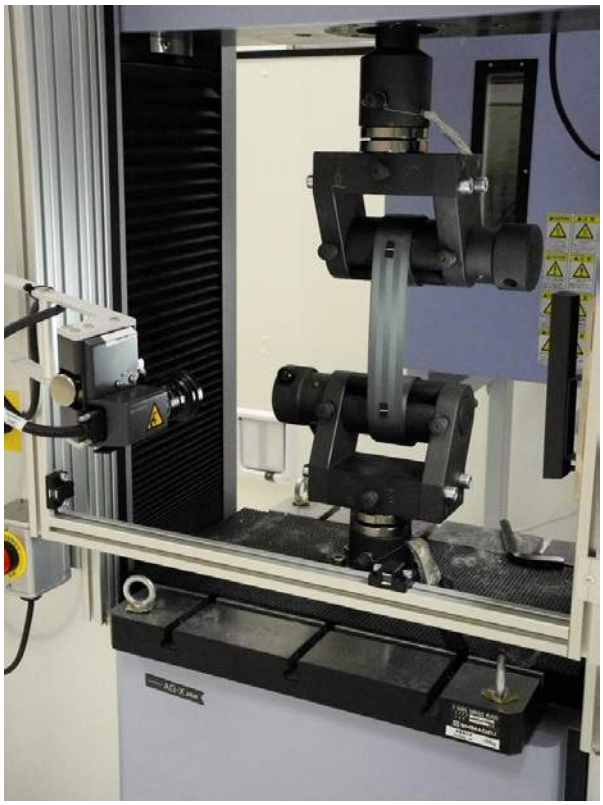

■ Test Results:

Tensile properties are always important in most materials and is the most common test made in universal testing machines. Generally, a customer is looking for elastic, maximum and break properties.

The fact that seat belts are tested we all understand very well and like in the measurements, purpose is to find out material strength and tensile properties at different loads.

Examples of applicable standards:
ASTM D6775 Test Method for Breaking Strength and Elongation of Textile Webbing, Tape and Braided Material

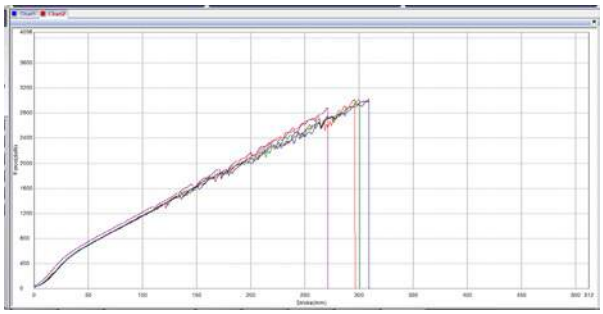

Results(Batch)

Name		Max_Force	980 Ext1(Strain)	1000 Ext1(Strain)	1110 Ext1(Strain)	1130 Ext1(Strain)	Break_Ext.1(Strain)
Parameter		Calc. at Entire Area	Force 980 daN	Force 1000 daN	Force 1110 daN	Force 1130 daN	Sensitivity: 10
Pass/Fail							
Unit		daN	%	%	%	%	%
Print		☑	☑	☑	☑	☑	☑
Belt 1	☑	3011,03	9,61522	9,84917	11,1243	11,2847	21,4502
Belt 3	☑	3027,53	9,75866	10,0505	11,2209	11,3641	22,4308
Belt 5	☑	2883,12	9,73363	9,97919	11,2152	11,4356	21,3222
Belt 7	☑	3004,81	9,69155	9,93767	11,1725	11,3387	22,0457
Belt 9	☑	2967,14	9,77825	10,0117	11,2215	11,4175	22,4387
Average		2982,73	9,71546	9,96565	11,1909	11,3681	21,9375
Standard Deviation		57,5262	0,06473	0,07722	0,04243	0,06089	0,52970
Maximum		3027,53	9,77825	10,0505	11,2215	11,4356	22,4387
Minimum		2883,12	9,61522	9,84917	11,1243	11,2847	21,3222
Range		144,410	0,16303	0,20133	0,09720	0,15090	1,11650
Median		3004,81	9,73363	9,97919	11,2152	11,3641	22,0457
Variation		0,01929	0,00666	0,00775	0,00379	0,00536	0,02415

SHIMADZU

Shimadzu Europa GmbH
www.shimadzu.eu

For Research Use Only. Not for use in diagnostic procedures.
The content of this publication shall not be reproduced, altered or sold for any commercial purpose without the written approval of Shimadzu. The information contained herein is provided to you "as is" without warranty of any kind including without limitation warranties as to its accuracy or completeness. Shimadzu does not assume any responsibility or liability for any damage, whether direct or indirect, relating to be the use of this publication. This publication is based upon the information available to Shimadzu on or before the date of publication, and subject to change without notice.

SHIMADZU
Excellence in Science

Application News

No.V22

High-Speed Video Camera

High-Speed Imaging of Fuel Injection in Automotive Engines

Introduction

An important observational method. As an example, gasoline being injected from the injector and adhering to the cylinder walls is considered to be a cause of fine particles with a diameter of 2.5 micrometers or smaller (PM2.5), harmful particles contained in exhaust gas. In addition, ensuring that the gasoline is refined and homogenized during injection is important in regards to improving fuel efficiency.
This article introduces images of fuel injection by an injector, and the collision of the injected spray against a wall surface, obtained using the HPV-X2 high-speed video camera.

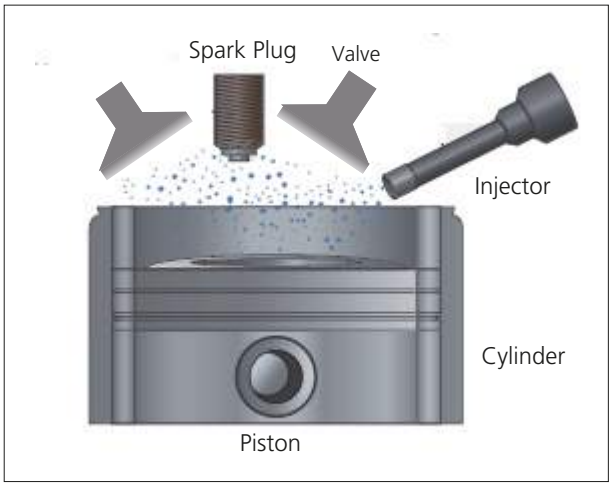

Fig. 1 Structure of an Automotive Engine

Measurement System

The HPV-X2 high-speed video camera was used in this experiment. Table 1 shows the instruments used. Instead of using a real engine, the experiment was performed with an injector placed on top and a flat plate below.

Table 1 Experimental equipment

High-Speed Video Camera	: HPV-X2
Microscope	: Long Range type
Light Source	: Strobe Light

Table 2 Imaging Conditions

Frame Rate: 10M frame/sec (Injection) 2M frame/sec (Collision)

Results

Fig. 2 shows the test configuration. Figs. 3 to 6 show images obtained. Images were recorded in proximity to the nozzle outlet, as well as 1 mm, 2 mm, and 4 mm below the nozzle. It is evident that the fuel collected in proximity to the nozzle disperses as it travels downwards.
The fuel injected from the nozzle ultimately collides with the cylinder wall. Fig. 7 shows how the fuel collides with the cylinder wall. Image (2) in Fig. 7 clearly shows the collision of a droplet approximately 40 µm in diameter with the wall. Among the droplets produced after the collision, a droplet as small as 10 µm in diameter could be confirmed as indicated by the arrow in image (9).

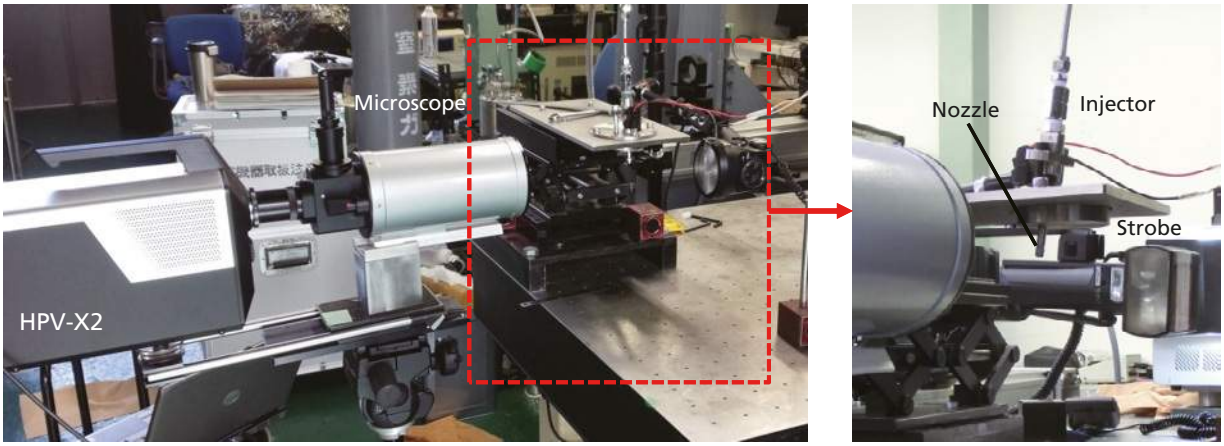

Overall Setup (left); Around the Nozzle (right)

Fig. 2 Test Configuration

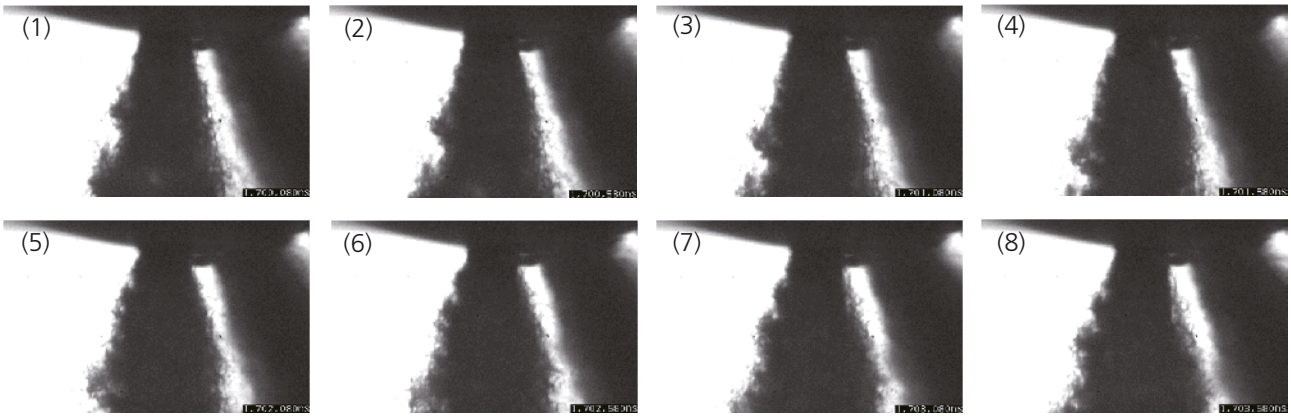

Fig. 3 Proximity to the Nozzle Outlet (500 nsec between images)

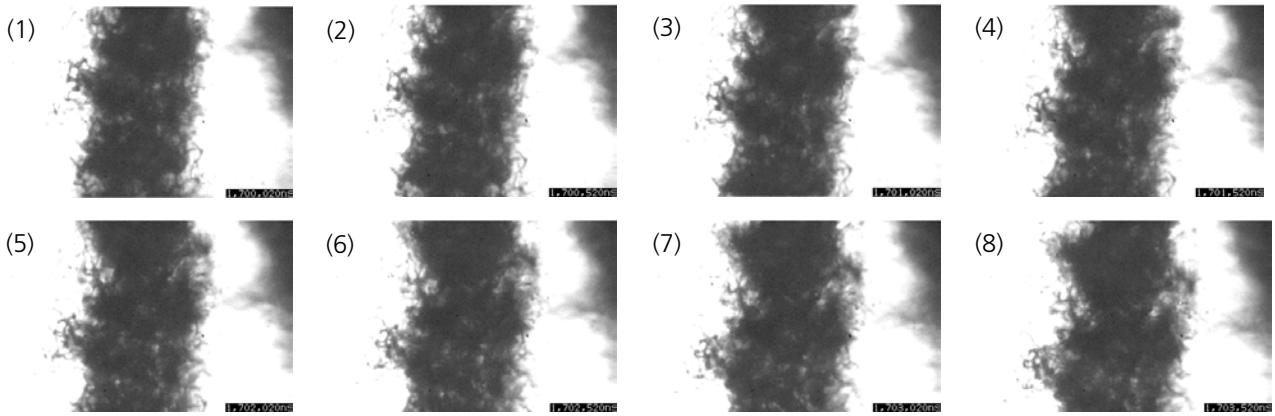

Fig. 4 1 mm Below the Nozzle (500 nsec between images)

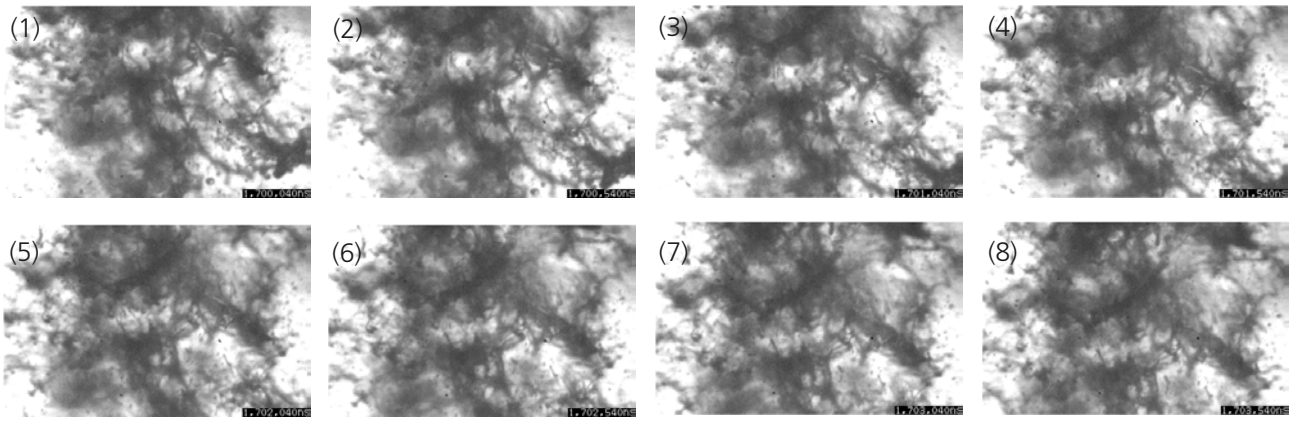

Fig. 5 2 mm Below the Nozzle (500 nsec between images)

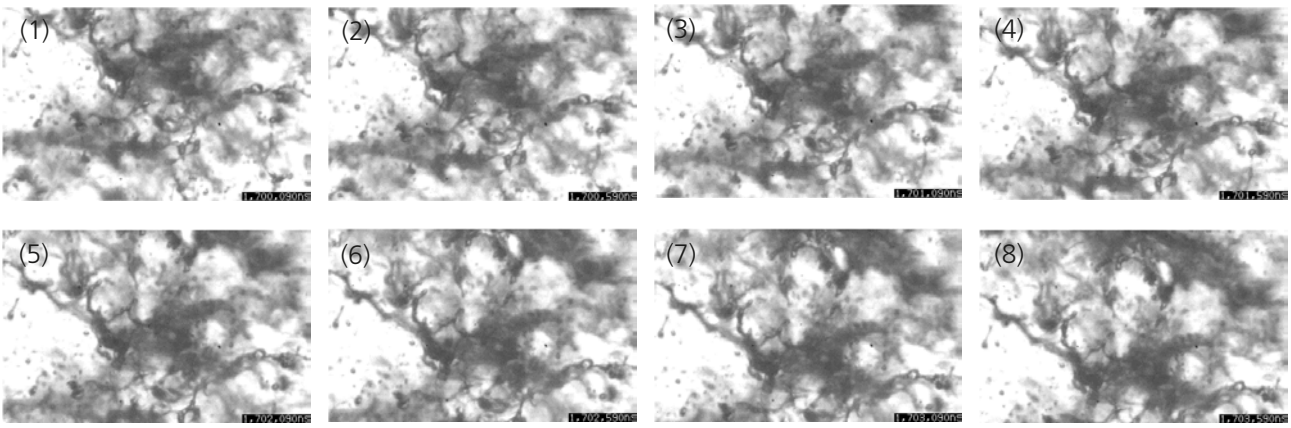

Fig. 6 4 mm Below the Nozzle (500 nsec between images)

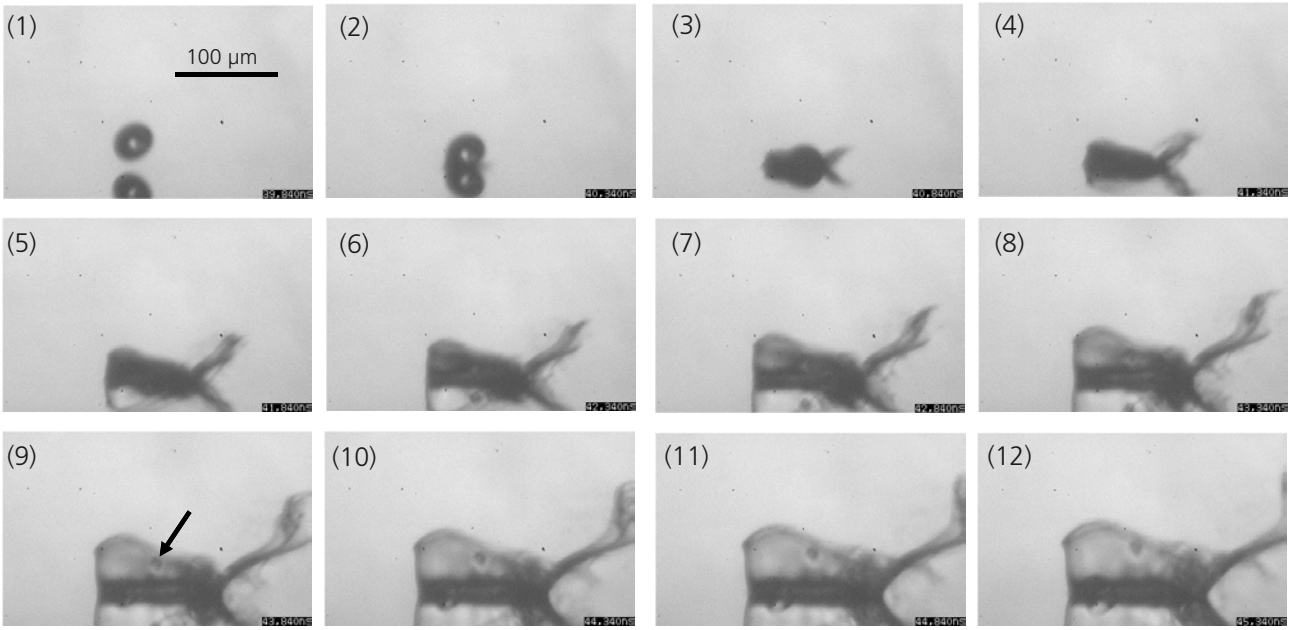

Data provided by: Professor Kawahara, Okayama University

Fig. 7 Collision with the Wall (500 nsec between images)

Conclusion

Images of fuel injection by an injector, and the collision of the injection spray against a wall surface were taken using the HPV-X2 high-speed video camera. The speed of injection from the injector is very fast, and may reach 140 m/sec depending on the injection pressure. As a result, a recording speed of at least 10 Mfps is required to observe such a high speed phenomenon with a microscope. With the conventional model (HPV-X), clear images were not obtained due to insufficient sensitivity.

The HPV-X2 has at least six times the sensitivity of the HPV-X however, so the fine structure of the injection spray and the quality of the liquid are captured even through a microscope. The collision of the injection spray with the wall is also clearly recorded, and the size of the scattered particles can be measured using image processing software. The use of the HPV-X2 in this way can thus serve a role in the development of automobile engine injectors.

First Edition: Jul. 2015

Shimadzu Corporation
www.shimadzu.com/an/

For Research Use Only. Not for use in diagnostic procedures.
The content of this publication shall not be reproduced, altered or sold for any commercial purpose without the written approval of Shimadzu.
The information contained herein is provided to you "as is" without warranty of any kind including without limitation warranties as to its accuracy or completeness. Shimadzu does not assume any responsibility or liability for any damage, whether direct or indirect, relating to the use of this publication. This publication is based upon the information available to Shimadzu on or before the date of publication, and subject to change without notice.

© Shimadzu Corporation, 2015

SHIMADZU
Excellence in Science

Application News

No.i254

Material Testing System

Compression After Impact Testing of Composite Material

Introduction

Carbon fiber reinforced plastic (CFRP) has a higher specific strength and rigidity than metals, and is used in aeronautics and astronautics to improve fuel consumption by reducing weight. However, CFRP only exhibits these superior properties in the direction of its fibers, and is not as strong perpendicular to its fibers or between its laminate layers. When force is applied to a CFRP laminate board, there is a possibility that delamination and matrix cracking will occur parallel to its fibers. Furthermore, CFRP is not particularly ductile, and is known to be susceptible to impacts. When a CFRP laminate board receives an impact load, it can result in internal matrix cracking and delamination that is not apparent on the material surface. There are many situations in which CFRP materials may sustain an impact load, such as if a tool being dropped onto a CFRP aircraft wing, or small stones hitting the a CFRP wing during landing. Consequently, tests are required for these scenarios. One of these tests is compression after impact (CAI) testing. CAI testing involves subjecting a specimen to a prescribed impact load, checking the state of damage to the specimen by a nondestructive method, and then performing compression testing of that specimen. This article describes CAI testing performed according to the ASTM D7137 (JIS K 7089) standard test method.

Measurements Taken Before Compression After Impact Testing

(1) Impact Test

The impact test involved dropping a 5 kg steel ball striker formed with a 16 mm diameter hemispherical point in the middle of the specimen. The specimen is fixed in place with four toggle clamps. The standard test method states that avoiding a second impact is preferred, so impact testing was performed with a mechanism that prevented second impacts. The impact energy recommended in the standard test method is 6.67 J per 1 mm of specimen thickness. For the purpose of comparison, the test was performed at four impact energies of 6.7, 5.0, 3.3, and 1.7 J per 1 mm thickness. Information on the specimen used is shown in Table 1. The test setup is shown in Fig. 1, and test conditions are shown in Table 2.

Table 1 Specimen Information

Dimensions [mm]	: 100 × 150 × 4.56
Lamination Method	: [45/0/−45/90] $_{ns}$
Material	: T800, 2252S-21

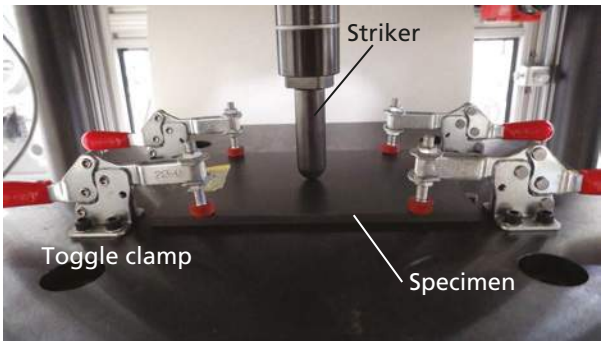

Fig. 1 Impact Test Setup

Table 2 Impact Test Conditions

Impact Energy	: 30.5, 22.9, 15.2, 7.6 [J]
No. of Tests	: n = 4

(2) Non-Destructive Inspection

After the impact test, the delamination area and maximum delamination length that resulted inside the laminate board were measured by nondestructive analysis. An ultrasonic flaw detection device is normally used for the non-destructive inspection step of CAI testing. The standard test method states that if ultrasonic flaw detection shows damage is present across more than half the width of the specimen, edge effects cannot be ignored and lowering the impact energy should be considered. Fig. 2 shows the setup for ultrasonic flaw detection.

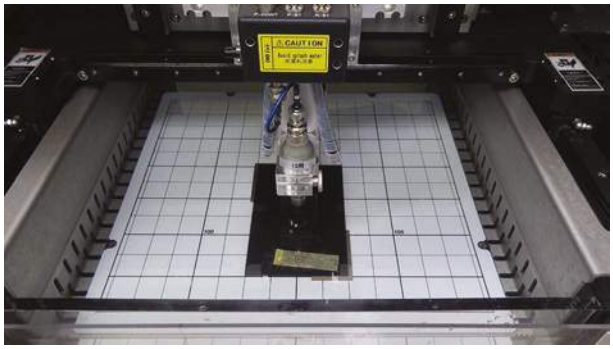

Fig. 2 Ultrasonic Flaw Detection

Fig. 3 shows the specimen after an impact test with an impact energy of 30.5 J. Fig. 3 shows an indentation in the middle of the specimen, but does not show the area of damage caused by delamination. Fig. 4 shows the results of ultrasonic flaw detection at each impact energy. The white areas in Fig. 4 are regions of delamination. Brighter areas show greater delamination. Comparison with Fig. 3 shows that delamination also occurs in areas other than the indentation in the center of the specimen, and the extent of internal damage cannot be determined based on external damage. The results also show that the damage area increases as the impact energy increases.

Fig. 3 Specimen After Impact Test (30.5 J Impact Energy)

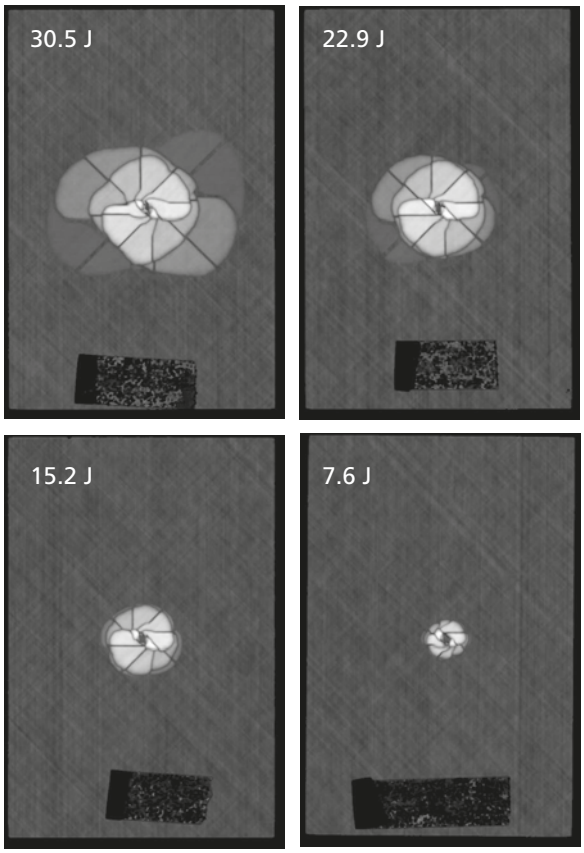

Fig. 4 Results of Ultrasonic Flaw Detection at Each Impact Energy

The damage area and maximum damage length are calculated from the images obtained by ultrasonic flaw detection. As an example, images used to calculate the damage area and maximum damage length after an impact energy of 30.5 J are shown in Fig. 5. Fig. 6 shows the relationship between damage area and impact energy, and Fig. 7 shows the relationship between maximum damage length and impact energy.

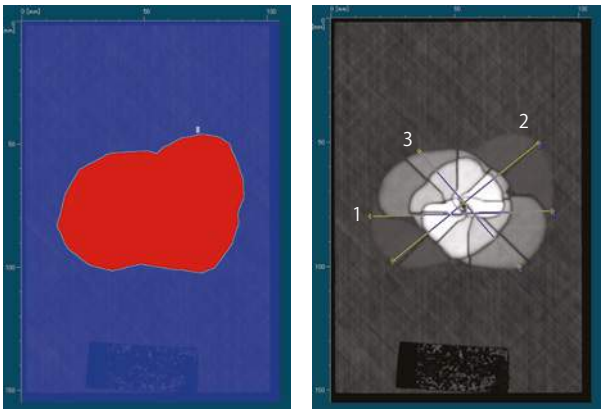

Region No.	Percentage Area (%)	Absolute Area (mm^2)
1	99.9988	3326.2400

No.	Length (mm)
1	73.03
2	75.50
3	61.37

Fig. 5 Images of Damaged Area and Maximum Damage Length

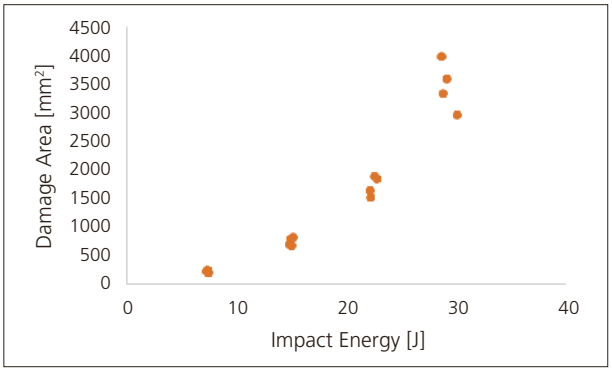

Fig. 6 Relationship between Damage Area and Impact Energy

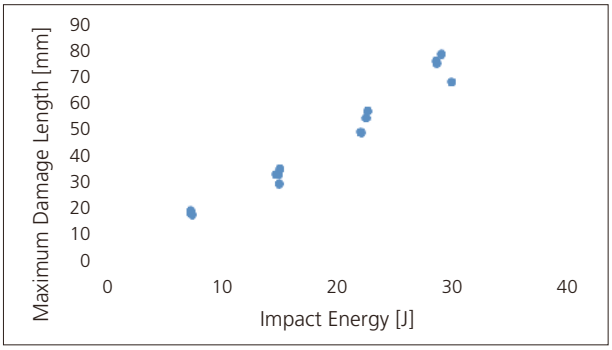

Fig. 7 Relationship between Maximum Damage Length and Impact Energy

Measurement System for Compression After Impact Testing

Two strain gauges must be attached to the front and back of the specimen. A specimen with strain gauges attached is shown in Fig. 8. The specimen shown in Fig. 8 is compressed at up to 10 % its expected compressive strength following impact in a longitudinal direction, and the CAI testing is performed after confirming the difference between front and rear strain gauges is within 10 %. Test conditions are shown in Table 3. The test setup is shown in Fig. 9, and test equipment used is shown in Table 4.

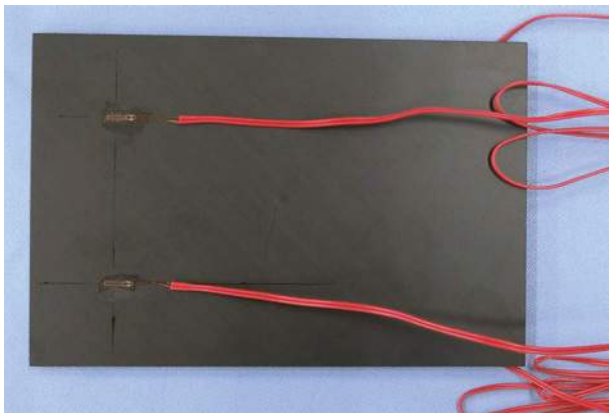

Fig. 8 Specimen

Table 3 Test Conditions

Test Speed	: 1.25 mm/min
No. of Tests	: n = 4

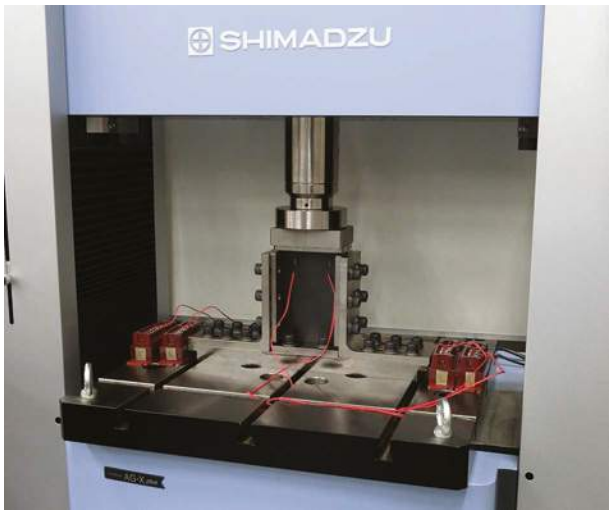

Fig. 9 Test Setup

Table 4 Experimental Equipment

Testing Machine	: AG-Xplus
Load Cell	: 250 kN
Test Jig	: Compression after impact test jig

Test Results

Examples of stress-strain curves at each impact energy are shown in Fig. 10. The compression-after-impact strength and mean compressive elastic modulus after impact are shown for each impact energy in Table 5. The standard test method states the compressive elastic modulus after impact should be calculated in the range of 0.1 % to 0.3 % strain. However, the breaking strain of one or more specimens was ≤ 0.3 % after the 30.5 J impact energy, and so for these specimens the elastic modulus was calculated from a linear region. Fig. 10 and Table 5 show the smaller the impact energy the larger the compression-after-impact strength. They also show the compressive elastic modulus after impact is almost constant regardless of impact energy.

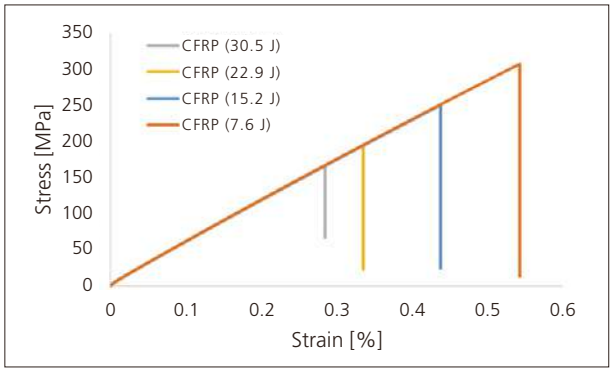

Fig. 10 Stress-Strain Curve

Table 5 Test Results (Mean)

Impact Energy [J]	Compression-After-Impact Strength [MPa]	Compressive Elastic Modulus After Impact [GPa]
30.5	162.9	57.2
22.9	203.3	56.4
15.2	246.4	56.0
7.6	308.6	56.3

The relationship between damage area and compression-after-impact strength is shown in Fig. 11, and the relationship between maximum damage length and compressive elastic modulus after impact is shown in Fig. 12. Fig. 11 and Fig. 12 show the smaller the damage area or maximum damage length, the larger the compression-after-impact strength. As a reference, the compressive strength of a specimen tested without applying any impact energy was 388 MPa.

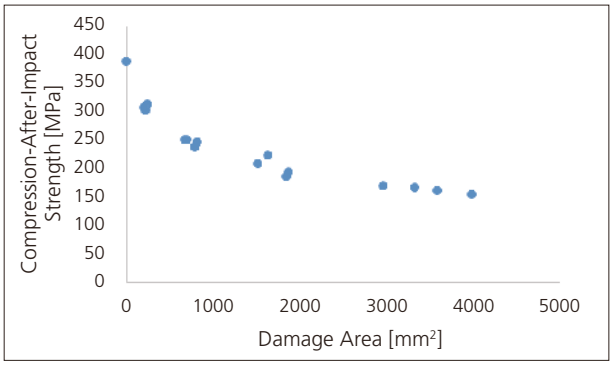

Fig. 11 Relationship between Damage Area and Compression-After-Impact Strength

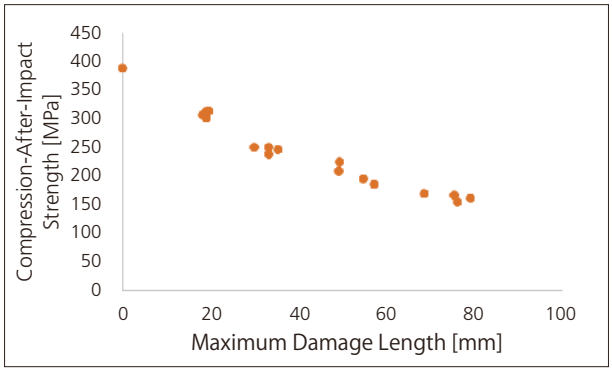

Fig. 12 Relationship between Maximum Damage Length and Compression-After-Impact Strength

Conclusion

CAI testing was performed on specimens at four different impact energies. As shown by the results, the larger the impact energy the smaller the compression-after-impact strength. Also, even a small amount of impact energy (in this experiment, an impact energy of 7.6 J amounted to 5 kg dropped from 0.15 m) reduced the compression-after-impact strength compared to the undamaged compressive strength, showing the importance of testing scenarios for impact loading. Shimadzu's testing system was used successfully to perform CAI testing according to ASTM D7137 (JIS K 7089), and can be used for evaluation of CFRP materials.

First Edition: Aug. 2016

Shimadzu Corporation
www.shimadzu.com/an/

For Research Use Only. Not for use in diagnostic procedure.
This publication may contain references to products that are not available in your country. Please contact us to check the availability of these products in your country.

The content of this publication shall not be reproduced, altered or sold for any commercial purpose without the written approval of Shimadzu. Company names, product/service names and logos used in this publication are trademarks and trade names of Shimadzu Corporation or its affiliates, whether or not they are used with trademark symbol "TM" or "®". Third-party trademarks and trade names may be used in this publication to refer to either the entities or their products/services. Shimadzu disclaims any proprietary interest in trademarks and trade names other than its own.

The information contained herein is provided to you "as is" without warranty of any kind including without limitation warranties as to its accuracy or completeness. Shimadzu does not assume any responsibility or liability for any damage, whether direct or indirect, relating to the use of this publication. This publication is based upon the information available to Shimadzu on or before the date of publication, and subject to change without notice.

© Shimadzu Corporation, 2016

SHIMADZU
Excellence in Science

Application News

No.i255

Material Testing System

Compression Test of Composite Material

Introduction

Even among composite materials, carbon fiber reinforced plastic (CFRP) has a particularly high specific strength, and is used in aeroplanes and some transport aircraft to improve fuel consumption by reducing weight. Compressive strength is an extremely important parameter in the design of composite materials that is always tested. However, due to the difficulty of testing compressive strength there is a variety of test methods. A major compression test method is the combined loading compression (CLC) method found in ASTM D6641. The CLC method can be performed with a simple jig structure, untabbed strip specimens, and can be used to simultaneously evaluate strength and measure elastic modulus. We performed compression testing of CFRP according to ASTM D6641.

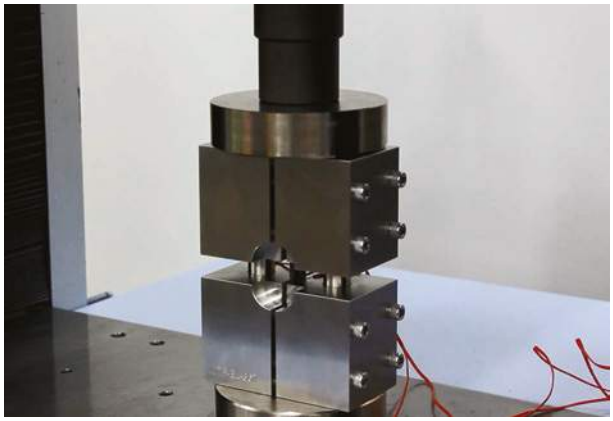

Fig. 1 Test Fixture

Measurement System

A CFRP specimen of T800S/3900 was used. Other information on the specimen is shown in Table 1. The test equipment used is shown in Table 2. Based on the CLC method in ASTM D6641, the specimen was attached to the jig shown in Fig. 1 and compressed using compression plate. Fig. 2 shows a photograph of the specimen. As shown in Fig. 2, a strain gauge was attached on the front and rear in the middle of the specimen. Outputs from the front and rear strain gauges confirmed that the specimen was aligned straight in the jig during specimen attachment. The specimen was attached using a torque wrench to fasten it in place uniformly. The test was performed with the test speed set to 1.3 mm/min.

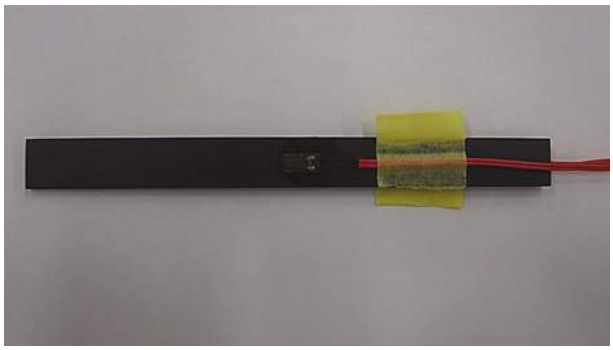

Fig. 2 Specimen

Table 1 Specimen Information

Length	: 140 mm
Width	: 13 mm
Thickness	: 3 mm
Lamination Method	: $[90/0]_{4S}$

Table 2 Experimental Equipment

Testing Machine	: AG-Xplus
Load Cell	: 50 kN
Test Jig	: CLC test fixture

Test Results

Measurements were performed twice, and stress-strain curves are shown in Fig. 3. The strain used is the mean strain taken from the front and rear sides of the specimen. The relationship between the first strain measurement and time is shown in Fig. 4 to show the outputs obtained from the strain gauges. Fig. 4 shows the outputs from both strain gauges were almost the same up to around 40 seconds, which is evidence that the test was successful. A small amount of deviation between the strain gauges arises after around 0.5 % strain, which is caused by a small amount of specimen flexure. Table 3 shows the test results. The mean compressive strength was 640.7 MPa, and the mean elastic modulus was 72.9 GPa. Elastic modulus was calculated using the mean of the strain gauge outputs.

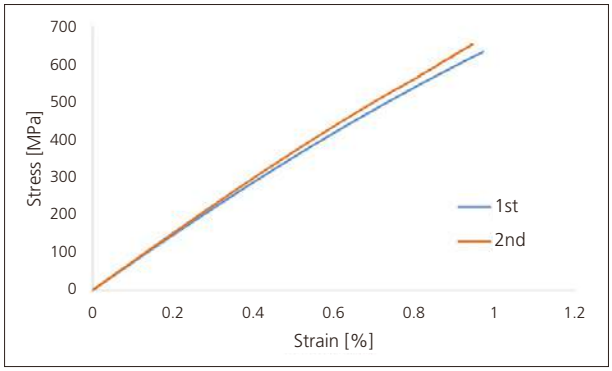

Fig. 3 Stress-Strain Curves (n = 2)

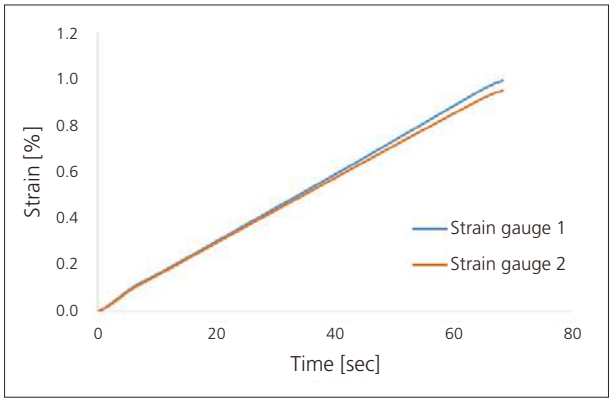

Fig. 4 Displacement-Time Curves (1st)

Table 3 Test Results

	Compressive Strength [MPa]	Elastic Modulus [GPa]
1st	629.9	71.4
2nd	651.4	74.3
Mean	640.7	72.9

Conclusion

Using this test system, compression testing of a CFRP was successfully performed according to ASTM D6641. Because this standard test method allows the testing of untabbed strip specimens, compressive strength and elastic modulus can be determined relatively easily for CFRPs.

First Edition: Aug. 2016

Shimadzu Corporation
www.shimadzu.com/an/

For Research Use Only. Not for use in diagnostic procedure.
This publication may contain references to products that are not available in your country. Please contact us to check the availability of these products in your country.

The content of this publication shall not be reproduced, altered or sold for any commercial purpose without the written approval of Shimadzu. Company names, product/service names and logos used in this publication are trademarks and trade names of Shimadzu Corporation or its affiliates, whether or not they are used with trademark symbol "TM" or "®". Third-party trademarks and trade names may be used in this publication to refer to either the entities or their products/services. Shimadzu disclaims any proprietary interest in trademarks and trade names other than its own.

The information contained herein is provided to you "as is" without warranty of any kind including without limitation warranties as to its accuracy or completeness. Shimadzu does not assume any responsibility or liability for any damage, whether direct or indirect, relating to the use of this publication. This publication is based upon the information available to Shimadzu on or before the date of publication, and subject to change without notice.

© Shimadzu Corporation, 2016

SHIMADZU
Excellence in Science

Application Data Sheet

No. 36

Servo Dynamic Systems

Material Testing & Inspection

Evaluating the Fatigue Strength of GFRP Materials

■ Introduction

As an ultra-high-strength composite material with superior heat resistance and electrical insulation properties, the use of glass fiber reinforced plastics (GFRP) has been increasing rapidly in automobiles, office equipment, consumer electronics, and other fields. Due to the use of GFRP materials in the automotive industry in particular, the impact resistance and fatigue strength of the material is increasingly being scrutinized and there is increasing demand for the development of GFRP materials that offer higher functionality or performance.

Shimadzu Servopulser series servo-hydraulic fatigue and endurance testing machines are able to accurately measure the fatigue strength of resins, composites, metals, and components, making them ideal for evaluating the fatigue strength of GFRP materials.

This issue of Shimadzu Application News describes an example of testing the fatigue strength of a GFRP composite material containing 20 % glass fiber in a polyamide resin. It also shows the change in the interior status of test samples as the fatigue test progresses, observed using a Shimadzu X-ray fluoroscopy system.

■ Testing Instruments and Samples

A Shimadzu EHF-LV20kN Servopulser series servo-hydraulic fatigue testing machine (a typical example is shown in Fig. 1) was used in conjunction with a Shimadzu SMX-225CT inspeXio X-ray fluoroscopy system used to observe the sample with X-ray fluoroscopy.

Sample details are as follows:

(1) Polymer: Polyamide
(2) Reinforcing material: 20 % glass fiber
(3) Sample shape:Hard plastic flat plate with 20 mm neck width
(4) Sample dimensions: 80(L) x 30(W) x 3(T) mm

■ Test Conditions

Before fatigue testing, static testing was performed using the following conditions to determine fatigue loading conditions. Static testing results are shown below.

(1) Tensile speed: 1 mm/min
(2) Chuck clamping distance: 40 mm
(3) Atmosphere: Room temperature of 25 °C
(4) Tensile strength (measurement results): 96 MPa

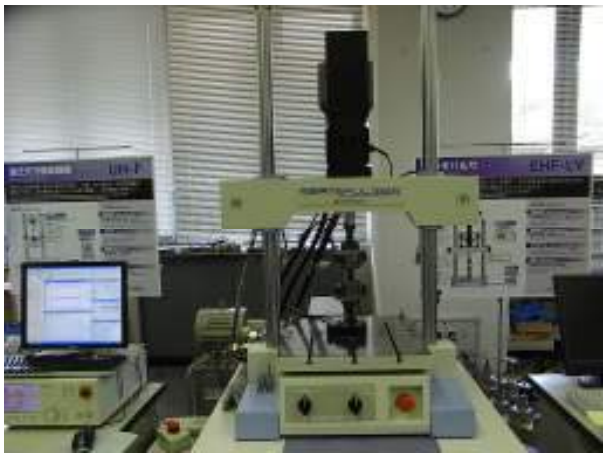

Fig.1 Shimadzu EHF-LV20kNX Servopulser Series Testing Machine

The following fatigue testing conditions (loading and data measurement/acquisition conditions) were determined based on the above static testing.

(1) Testing frequency: 10 Hz
(2) Maximum cyclic stress: Six levels, indicated below.
Level 1: 77 MPa (80 % of tensile strength)
Level 2: 67 MPa (70 % of tensile strength)
Level 3: 58 MPa (60 % of tensile strength)
Level 4: 48 MPa (50 % of tensile strength)
Level 5: 43 MPa (45 % of tensile strength)
Level 6: 38 MPa (40 % of tensile strength)
(3) Stress ratio:0 (given a minimum stress of 0 MPa)
(4) Atmosphere: Room temperature of 25 °C
(5) Testing machine: LV-20N Servopulser
(6) Test force measurement: 20,000 N load cell
(7) Chuck clamping distance: 40 mm
(8) Data acquisition: 2 kHz

(The testing machine is capable of measuring at frequencies up to 40 kHz.)

Six cyclic stress levels were decided based on the tensile strength (96 MPa) determined by static tensile testing, with a cyclic load stress ratio (minimum stress divided by maximum stress) of zero. (For example, level 1 applies a maximum stress of 77 MPa, a minimum stress of 0 MPa, and stress amplitude of 38.5 MPa.)

Though the testing machine is capable of cyclic loading at cycle rates up to 100 Hz, in this case a 10 Hz sine wave was used in consideration of sample heat generation.

Fig. 2 shows a sample mounted in the testing machine grips.

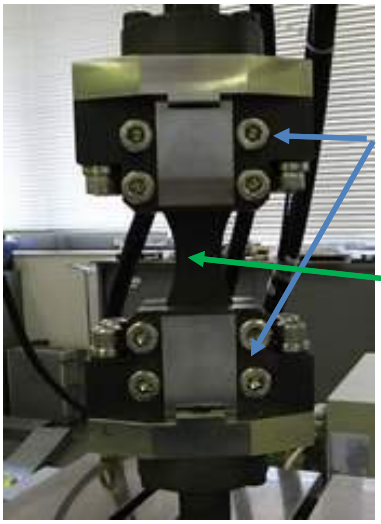

Fig. 2 Sample Mounted in Testing Machine

■ Test Results

Fig. 3 shows an example of peak stress (black) and displacement (blue) values (sine wave peak and valley values) measured from start of loading to sample fracture, given a stress level of 5.

The cyclic stress load applied to the sample causes it to gradually deform until a crack forms, after which the deformation increases rapidly and the sample fractures.

Fig. 4 is a stress versus cycle count plot for six stress levels (one sample for each level) that shows the relationship between the maximum stress load and the cycle count at sample fracture.

As shown in the results above, in addition to fatigue testing, the fatigue testing machine can also be used for a wide range of other strength testing, including static testing.

In addition, an industrial X-ray system was used to observe how the fiber orientation inside the GFRP material changes as the fatigue test progresses.

Fig. 5 shows the curious phenomenon of how the glass fibers inside the sample, which have no particular orientation before starting the fatigue test (left), begin to orient themselves a little in the longitudinal direction after a million load cycles (middle), and are all oriented in the longitudinal direction just before fracture (right).

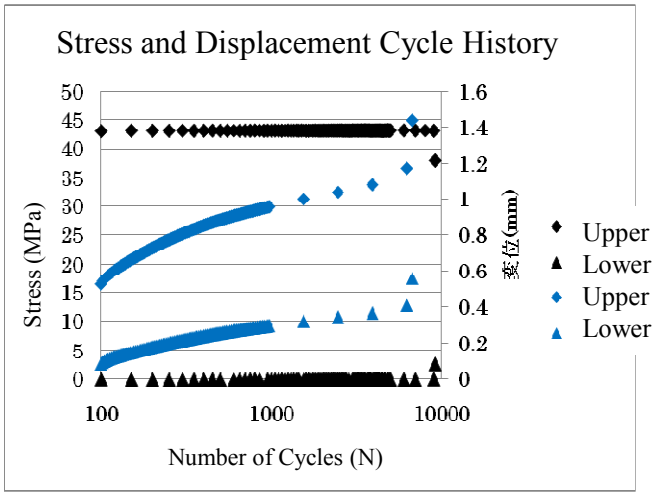

Fig. 3 Fatigue Test Results

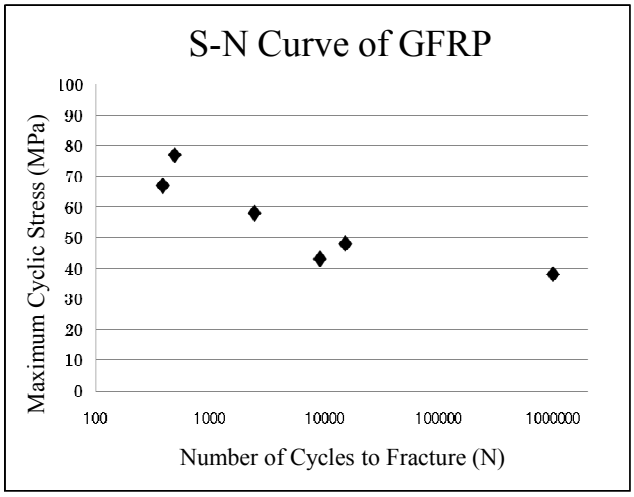

Fig. 4 Fatigue Test Results

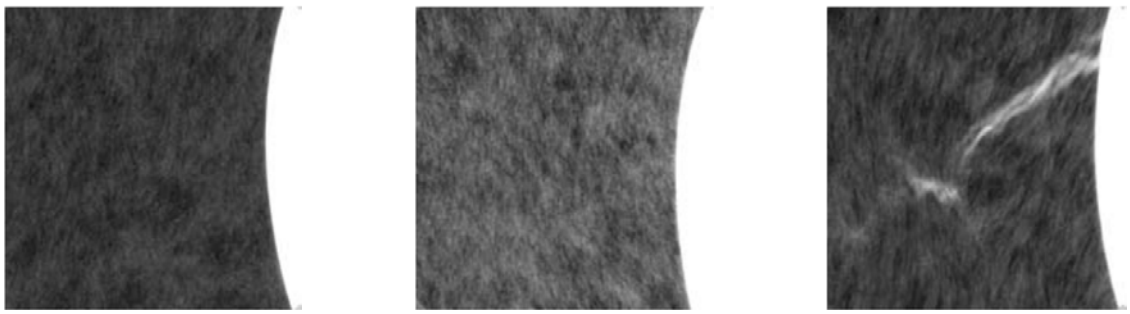

Start of Fatigue Test | After 1 Million Load Cycles | Just Before Fracture

Fig.5 Fiber Orientation Inside GFRP

Note: The analytical and measuring instruments described may not be sold in your country or region.

First Edition: July, 2015

SHIMADZU
Shimadzu Corporation
www.shimadzu.com/an/

For Research Use Only. Not for use in diagnostic procedures.
The content of this publication shall not be reproduced, altered or sold for any commercial purpose without the written approval of Shimadzu.
The information contained herein is provided to you "as is" without warranty of any kind including without limitation warranties as to its accuracy or completeness. Shimadzu does not assume any responsibility or liability for any damage, whether direct or indirect, relating to the use of this publication. This publication is based upon the information available to Shimadzu on or before the date of publication, and subject to change without notice.
© Shimadzu Corporation, 2015

SHIMADZU
Excellence in Science

Application Data Sheet

No. 30

Autograph Precision Universal Tester

Material Testing & Inspection

Evaluating the Strength of Carbon Fiber Reinforced Plastics (CFRP)

■Introduction

Various types of plastic materials have been developed that are light weight and also perform better than previous materials in terms of environmental resistance and in terms of strength. Consequently, there is a growing demand for such materials in aircraft, automotive, and many other fields.These plastic materials, such as carbon fiber reinforced plastic (CFRP), glass fiber reinforced plastic (GFRP), and aramid fiber reinforced plastic, are characterized by using fibers with advanced functionality (low weight, high strength, deformation resistance, corrosion resistance, and also heat resistance). Carbon fiber reinforced plastic (CFRP) is particularly representative of such materials and is increasingly used in sports equipment and other everyday products. Therefore, evaluating its strength, its fundamental feature, is very important.

This article presents results from testing carbon fiber reinforced plastic (CFRP) using a Shimadzu Autograph precision universal testing machine. (Test specimens and loading conditions conformed to JIS K7073-1988 Testing Method for Tensile Properties of Carbon Fiber Reinforced Plastics.)

■Measurement and Jigs

Specimens were Type-IV specified by JIS K7073-1988 (rectangular strips with no tabs). Tensile tests were conducted with an extensometer attached to measure longitudinal strain and a width sensor attached to measure lateral strain, as shown in Fig.1.

Fig. 1 Test Configuration

■Test Results

Test results indicate a tensile strength of 8.31×10^2 MPa, an elastic modulus of 5.76×10^5 MPa (determined from the slope between points at 100 MPa and 300 MPa), and a maximum tensile strain of 0.766 percent. Since these results were obtained using test specimens with fibers oriented perpendicular (lateral) to the direction of tensile load, the same test was performed with fibers oriented parallel (longitudinal) to the direction of tension. This resulted in an elastic modulus of about 13.00×10^5 MPa, which indicates a significant difference depending on the fiber orientation.

Fig.3 shows the relationship between stress and displacement in the direction perpendicular to tension, for the same test as before. A calculation of Poisson's ratio between 100 MPa and 300 MPa, as before, resulted in a value of 6.0×10^{-2}.

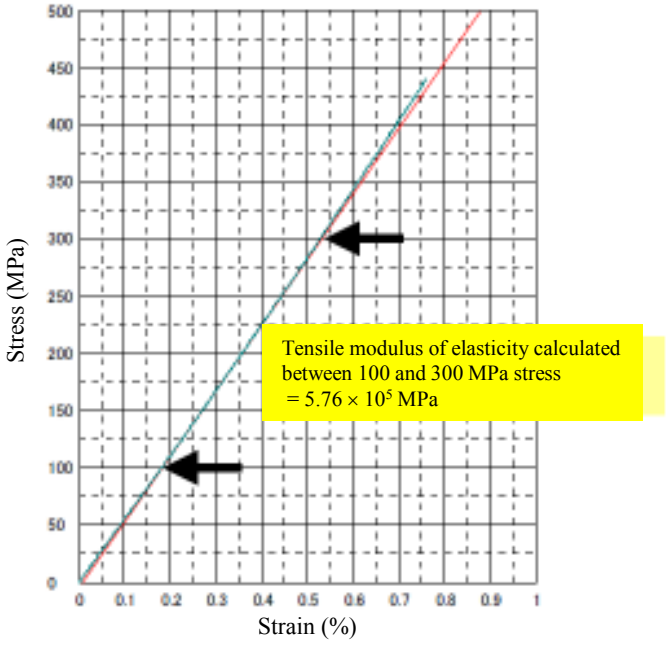

Fig.2 shows the results of testing to failure at a rate of 1 mm/min (stress vs. longitudinal strain curve).

Whereas the Poisson's ratio is about 0.3 for soft iron and about 0.46 to 0.49 for elastic rubber, the ratio for carbon fiber reinforced plastic (CFRP) is about one order of magnitude smaller, which means the deformation level of CFRP is extremely low.

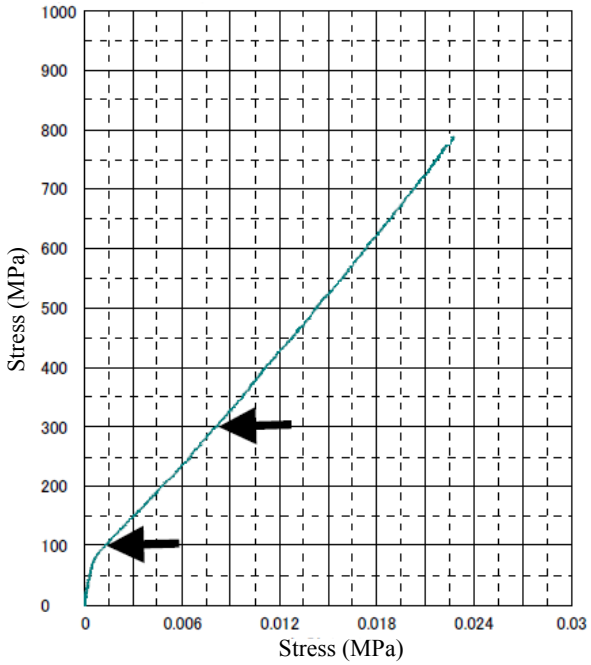

Fig. 3 Graph of Stress vs. Lateral Displacement

Poisson's ratio in left figure: 6.0×10^{-2}
(for range between 2 points, at 100 MPa and 300 MPa)

Method Used to Determine Poisson's Ratio
$\upsilon t = |\Delta\varepsilon 2/\Delta\varepsilon 1|$
υt: Poisson's ratio
$\Delta\varepsilon 1$: Strain increase in tensile direction
$\Delta\varepsilon 2$: Strain increase perpendicular to tension

■Test Conditions and Equipment Used

Tester:	AG-Xplus
Load Cell:	50 kN
Test Jig:	50 kN non-shift wedge type grips
Extensometer:	SG50-10 for measuring strain in tensile direction
	SGW-5 for measuring strain perpendicular to tensile direction
Software:	TRAPEZIUM X (Single)

AG-Xplus Floor-Type Precision Universal Tester

TRAPEZIUM X

■ A high-precision load cell is adopted. (The high-precision type is class 0.5; the standard-precision type is class 1.)
Accuracy is guaranteed over a wide range, from 1/1000 to 1/1 of the load cell capacity. This supports highly reliable test evaluations.

■ Crosshead speed range
Tests can be performed over a wide range from 0.0005 mm/min to 1,000 mm/min.

■ High-speed sampling
Ultrafast sampling, as fast as 0.2 msec, allows assessment of sudden changes in test force, such as when brittle materials fracture.

■ TRAPEZIUMX X operational software
Designed for intuitive operation, it offers a variety of convenient and user-friendly features.

■ Smart controller
Real-time test force and position data are readily confirmed, and the manual dial enables fine adjustments to jig positioning.

■ Optional Test Devices
A variety of tests can be performed by switching between an abundance of jigs in the lineup.

First Edition: July 2015

SHIMADZU
Shimadzu Corporation
www.shimadzu.com/an/

For Research Use Only. Not for use in diagnostic procedures.
The content of this publication shall not be reproduced, altered or sold for any commercial purpose without the written approval of Shimadzu.
The information contained herein is provided to you "as is" without warranty of any kind including without limitation warranties as to its accuracy or completeness. Shimadzu does not assume any responsibility or liability for any damage, whether direct or indirect, relating to the use of this publication. This publication is based upon the information available to Shimadzu on or before the date of publication, and subject to change without notice.
© Shimadzu Corporation, 2015

SHIMADZU
Excellence in Science

Application Data Sheet

No. 39

Autograph Precision Universal Testing Machine

Material Testing & Inspection

Evaluation of Open-Hole CFRP — Static Tensile Testing, Fracture Observation, and Internal Structure Observation —

■ Introduction

Recently, lightweight alternatives to conventional metal materials are being used as structural members where mechanical reliability is required. The main reason for this trend is that lighter products reduce transport weights, which reduces fuel consumption and carbon dioxide emissions during product transport. Fiber reinforced composite materials such as carbon fiber reinforced plastics (CFRP), which consist of a resin strengthened with carbon fibers, are extremely strong and light. Because of this, they are currently a material widely used in aircraft, and are expected to be used increasingly in various types of products, including automobiles, in order to make them lighter. For the development of fiber reinforced composite materials, not just a simple evaluation of their mechanical strength, but also the observation of failure events is important. In addition, from the perspective of quality management, the necessity for evaluation of internal structure of these materials, such as the oriented state of fibers and the presence of cracks, has increased.

In this article, we describe how we use a precision universal testing machine (Autograph AG-250kNXplus) and high-speed video camera (HyperVision HPV-X) (Fig. 1) to evaluate the static fracture behavior of a CFRP based on a test force attenuation graph and images of material failure. We also describe our subsequent examination of the state of the specimens internally using an X-ray CT system (inspeXio SMX-100CT) to investigate the state of fracture inside the specimen. Information on specimens is shown in Table 1. Specimens have a hole machined into their center that is 6 mm in diameter. Fracture is known to propagate easily through composite materials from the initial damage point, and when a crack or hole is present their strength is reduced markedly. Therefore, evaluation of the strength of open-hole specimens is extremely important from the perspective of the safe application of CFRP materials in aircraft, etc.

Table 1: Test Specimen Information

Laminate Structure	Dimensions L (mm) × W (mm) × T (mm), hole diameter (mm)
$[+45/0/-45/+90]_{2s}$	150 × 36 × 2.9, Φ6

Note: The CFRP laminate board used in the actual test was created by laying up prepreg material with fibers oriented in a single direction. The $[+45/0/-45/+90]_{2s}$ shown as the laminate structure in Table 1 refers to the laying up of 16 layers of material with fibers oriented at +45°, 0°, -45°, and +90° in two layer sets.

■ Static Tensile Testing (Ultra High Speed Sampling)

In this test, the change in load that occurs during specimen fracture was used as the signal for the HPV-X high-speed video camera to capture images. Specifically, the AG-Xplus precision universal testing machine was configured to create a signal when the test force on the specimen reaches half the maximum test force (referred to as Maximum test force in Fig. 3), with this signal being sent to the high-speed video camera. Static tensile testing and fracture observation were performed according to the conditions shown in Table 2. A test force-displacement plot for the open-hole quasi-isotropic CFRP(OH-CFRP) is shown in Fig. 2(a). A test force-time plot during the occurrence of material fracture is also shown in Fig. 2(b).

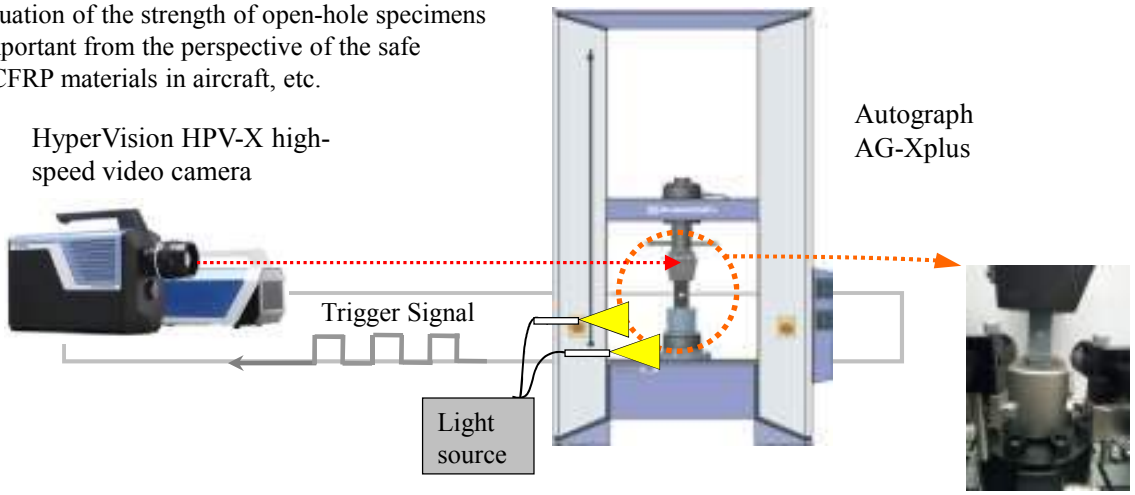

Fig.1: Testing Apparatus

Table 2: Test Conditions

Testing Machine	AG-Xplus
Load Cell Capacity	250 kN
Jig	Upper: 250 kN non-shift wedge type grips (with trapezoidal file teeth on grip faces for composite materials) Lower: 250 kN high-speed trigger-capable grips
Grip Space	100 mm
Loading Speed	1 mm/min
Test Temperature	Room temperature
Software	TRAPEZIUM X (Single)
Fracture Observation	HPV-X high-speed video camera (recording speed 600 kfps)
DIC Analysis	StrainMaster (LaVision GmbH.)

Note: fps stands for frames per second. This refers to the number of frames that can be captured in 1 second.

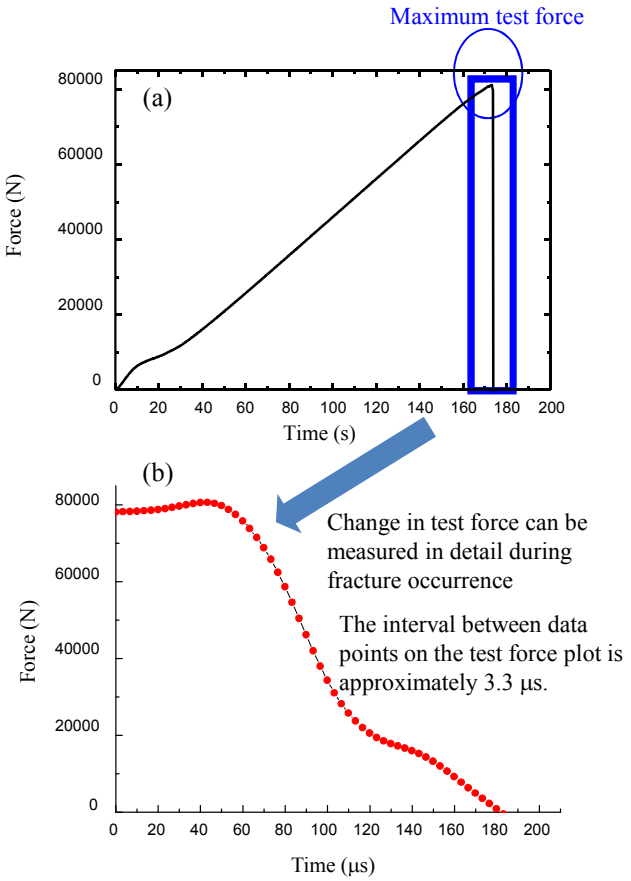

Fig. 2 (a) Test Force-Displacement Curve, and (b) Test Force-Time Curve (in Region of Maximum Test Force)

Fig. 2(a) can be interpreted to show the specimen fractured at the moment it reached the maximum test force, at which point the load on the specimen was suddenly released. This testing system can be used to perform high-speed sampling to measure in detail the change in test force in the region of maximum test force. The time interval between data points on the test force plot in Fig. 2(b) is 3.3 µs.

■ Fracture Observation (High Speed Imaging)

Images (1) through (8) in Fig. 3 capture the behavior of the specimen during fracture around the circular hole. Image (1) shows the moment cracks occur in a surface +45° layer. In this image, the tensile load being applied is deforming the circular hole, where hole diameter in the direction of the load is approximately 1.4 times that perpendicular to the load. In image (2), the cracks that occurred around the circular hole are propagating along the surface +45° layer. In images (3) through (6), a substantial change can be observed in the external appearance of the specimen near the end of the crack propagating to the bottom right from the circular hole. This suggests not only the surface layer, but internal layers are also fracturing. Based on the images of the same area and the state of the internal layers that can be slightly observed from the edges of the circular hole in images (7) and (8), the internal fracture has quickly propagated in the 18 µs period between images (3) and (8).

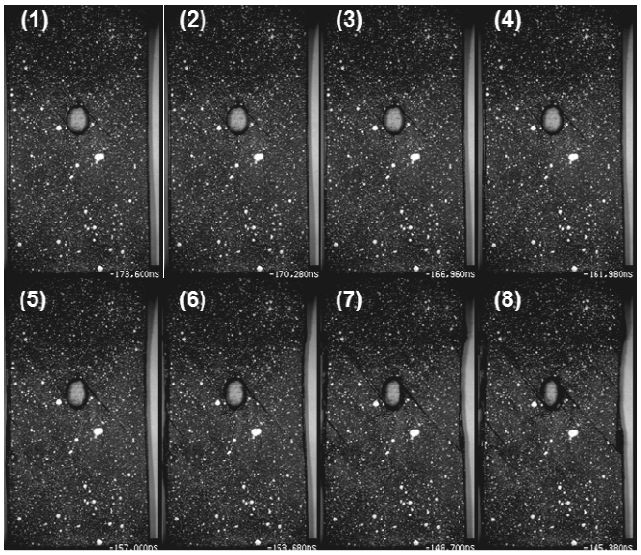

Fig. 3: Observations of OH-CFRP Fracture

First Edition: July 2015

Shimadzu Corporation
www.shimadzu.com/an/

For Research Use Only. Not for use in diagnostic procedures.
The content of this publication shall not be reproduced, altered or sold for any commercial purpose without the written approval of Shimadzu.
The information contained herein is provided to you "as is" without warranty of any kind including without limitation warranties as to its accuracy or completeness. Shimadzu does not assume any responsibility or liability for any damage, whether direct or indirect, relating to the use of this publication. This publication is based upon the information available to Shimadzu on or before the date of publication, and subject to change without notice.
© Shimadzu Corporation, 2015

Images (1) through (8) of Fig. 4 show the results of performing Digital image correlation (DIC) analysis on the fracture observation images of Fig. 3. Black signifies areas of the surface layer of the specimen under little strain, and red signifies areas under substantial strain. Looking at images (1) through (4), we can see that strain around the circular hole is focused diagonally toward the top-left (-45°) and toward the bottom-left (+45°) from the circular hole. Images (5) through (8) show the focusing of strain diagonally toward the bottom-right (-45°) and toward the top-right (+45°) from the circular hole in areas where it was not obvious in images (1) through (4). This shows an event is occurring in the surface layer of the specimen that is similar to the process of fracture often seen during tensile testing of ductile metal materials, which is crack propagation in the direction of maximum shearing stress.

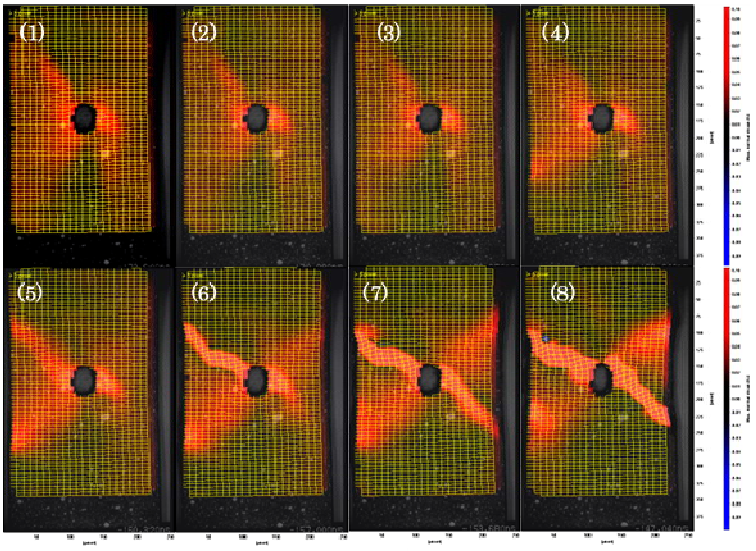

Fig. 4: Observation of OH-CFRP Fracture (DIC Analysis)

■ Internal Structure Observation (CT)

Next, internal observations were performed around the circular hole using a micro focus X-ray CT system to check the state of internal damage to the specimen. The SMX-100CT micro focus X-ray CT system (Fig. 5) is capable of capturing CT images at high magnification. The system rotates a specimen between an X-ray generator and an X-ray detector, uses a computer to calculate fluoroscopic images obtained from all 360° of rotation, then reconstructs a tomographic view of the specimen (Fig. 6). This system was used to perform a CT scan of the fracture area of the OH-CFRP after the static tensile testing and fracture observation performed as described in the previous section, so that the cracks that occurred inside can be observed.

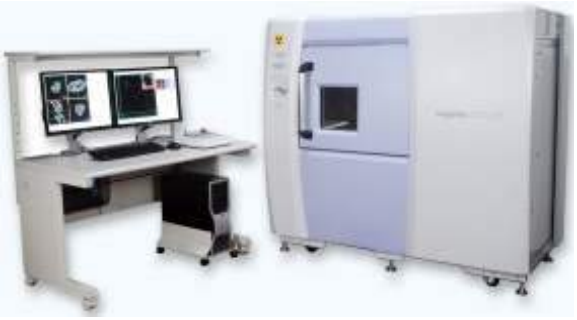

Fig. 5: Shimadzu inspeXio SMX-100CT Micro Focus X-Ray CT System

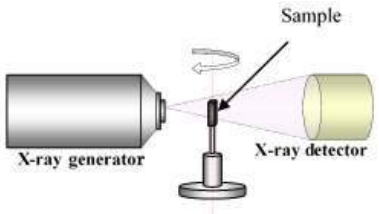

Fig. 6: Illustrated Example of X-Ray CT System Operation

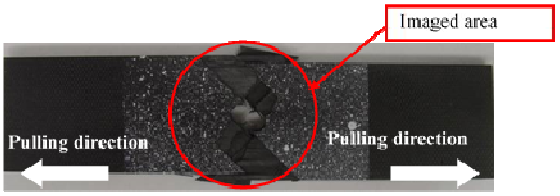

Fig. 7: Specimen After Static Tensile Testing (Specimen Used for CT Scan)

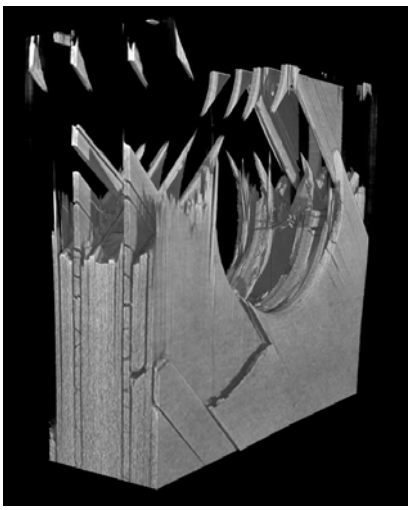

Fig. 8: Fracture Area 3D Image No. 1

First Edition: July 2015

SHIMADZU
Shimadzu Corporation
www.shimadzu.com/an/

For Research Use Only. Not for use in diagnostic procedures.
The content of this publication shall not be reproduced, altered or sold for any commercial purpose without the written approval of Shimadzu.
The information contained herein is provided to you "as is" without warranty of any kind including without limitation warranties as to its accuracy or completeness. Shimadzu does not assume any responsibility or liability for any damage, whether direct or indirect, relating to the use of this publication. This publication is based upon the information available to Shimadzu on or before the date of publication, and subject to change without notice.
© Shimadzu Corporation, 2015

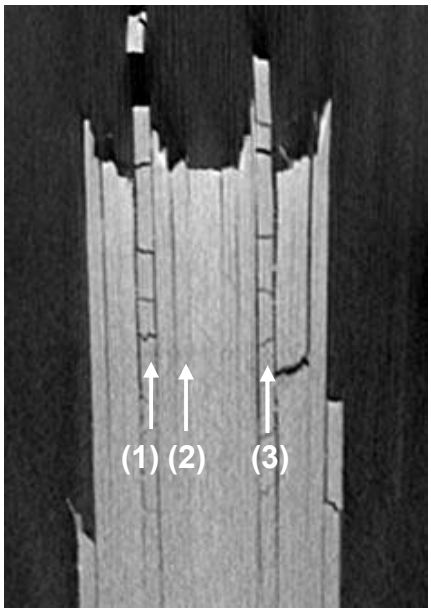

Fig. 9: CT Cross-Sectional Images of the Fracture Area

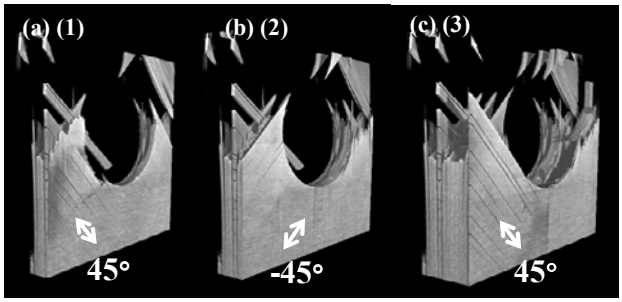

Fig. 10: Fracture Area 3D Image No. 2

Cross-sectional images of the specimen are shown as a 3D image in the 16 layers shown in Fig. 9, we can see that most cracks in the matrix occur in the +45° layer inside the specimen, indicated by the number (1) and (3). (shown in Fig. 10 (a) and Fig. 10 (b), respectively). In this layer, the carbon fibers are all aligned together in a +45° orientation, and the multiple matrix cracks occurring in this layer are probably due to the shearing force caused in this layer by tensile loading, together with deformation of adjacent layers in the direction of the loading. For comparison, a 3D image of the -45° layer inside the specimen (Fig. 9 (2)) is shown in Fig. 10 (b). As is clear from the image, the matrix cracks that occurred in the +45° layer have not occurred in the -45° layer. This difference in fracture state has probably arisen due to different shearing forces and load directions occurring in each layer. Such detailed observation of fracture surfaces associated with multiple matrix cracks was difficult by conventional methods, since to observe fracture surfaces the specimen was processed such as by cutting and embedding in resin, which changed the characteristics of the specimen. However, by using the high-resolution X-ray CT system as described in this article, there is little X-ray absorption difference between air and specimen, and it is possible to observe the state of complex internal damage, even for OH-CFRP in which microscopic damage is normally difficult to observe by X-ray.

■ Acknowledgment

We would like to extend our sincere gratitude to the Japan Aerospace Exploration Agency (JAXA) for their cooperation in the execution of this experiment.

Note: The analytical and measuring instruments described may not be sold in your country or region.

First Edition: July 2015

Shimadzu Corporation
www.shimadzu.com/an/

For Research Use Only. Not for use in diagnostic procedures.
The content of this publication shall not be reproduced, altered or sold for any commercial purpose without the written approval of Shimadzu.
The information contained herein is provided to you "as is" without warranty of any kind including without limitation warranties as to its accuracy or completeness. Shimadzu does not assume any responsibility or liability for any damage, whether direct or indirect, relating to the use of this publication. This publication is based upon the information available to Shimadzu on or before the date of publication, and subject to change without notice.
© Shimadzu Corporation, 2015

SHIMADZU
Excellence in Science

Application News

No.i247

Material Testing System

Material Testing by Strain Distribution Visualization – DIC Analysis –

Introduction

Strain distribution in samples is an increasingly important component of material testing.
As background to this trend, CAE (Computer Aided Engineering) is an analytical technology that is becoming widely used in the fields of science and industry due to the cost savings achieved through the reduced use of costly prototyping which is now being replaced by computerized product design simulation. A typical requirement is to conduct mechanical testing analysis of the region of a product in which strain is likely to occur, and to elucidate the correlation between the simulated analysis results and the strain distribution obtained in actual mechanical testing.
DIC (Digital Image Correlation) analysis is a technique used to compare the random patterns on the surface of a test sample before and after deformation to determine the degree of deformation of the sample. The advantages of this technique include the ability to measure displacement and strain distribution from a digital image without having to bring a sensor into contact with a test sample, and without requiring a complicated optical system. For these reasons, application development for DIC analysis is expanding into a wide range of fields in which measurement using existing technologies*1 has been difficult.

Here we introduce examples of DIC analysis of CFRP (Carbon Fiber Reinforced Plastic) and ABS resin high-speed tensile impact testing.

*1: Up to now, material strain distribution measurement has been conducted using various methods, including the direct attachment of large numbers of strain gauges to the test material. However, this method is not applicable for micro-sized samples to which strain gauges either cannot be attached, or attachment is difficult and complicated. These disadvantages also include the difficulty in measuring certain types of substances, such as films, that are easily affected by contact-type sensors.

Test Conditions

Fig. 1 shows the testing apparatus and software used in the high-speed tensile testing of CFRP. The test conditions are shown in Table 1, and information regarding the test specimens is shown in Table 2. For this experiment, special-shaped grips for composite materials were mounted to the HITS-T10 high-speed tensile testing machine, and the test specimen was affixed to the grips.
A high-speed HPV-2A video camera was mounted in front of the testing gap between the grips to collect video data of the specimen breaking, and the signal to start camera filming was a displacement signal from the high-speed tensile testing machine. The acquired video data was loaded into the StrainMaster (LaVision GmbH) DIC analysis software, and the strain distribution that occurred in the sample was analyzed.

HPV-2A High Speed Video Camera

Test Grips and Test Specimen

HITS-T10 High Speed Tensile Testing Machine

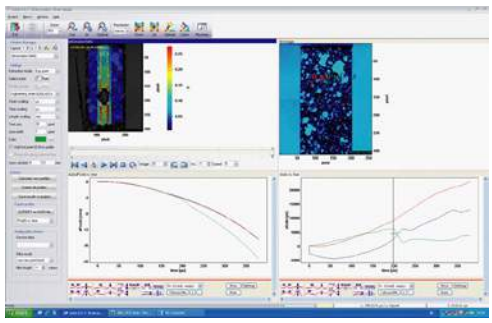
StrainMaster (LaVision GmbH)

Fig. 1 Testing Apparatus

Table 1 Test Conditions

Instrumentation	HITS-T10 high-speed tensile testing machine
	HPV-2A high-speed video camera
Test Force Measurement	10 kN load cell
Test Speed	10 m/s
Grips	Special grips for composite materials
Sampling	250 kHz
Imaging Speed	500 kfps
Light Source	Strobe
DIC Analysis	StrainMaster (LaVision GmbH) With cooperation of MARUBUN CORPORATION

Table 2 Samples

Samples (dimensions)	CFRP-OH*2 Laminate method $[0/90]_{2s}$*3 (Hole diameter ϕ1 mm, W8 × t0.4 reed-shaped)
	ABS resin (ASTM L-shaped test specimen Total length 60 mm, Parallel part 3.2 (W) × 3.2 (T) mm)
Marking	CFRP-OH*2 : White random pattern ABS resin : Black random pattern

*2: OH: Abbreviation for Open Hole. Refers to a hole that is opened in a CFRP plate.

*3: The CFRP laminate used in this experiment is prepared by laminating prepreg fibers oriented in one direction. The $[0/90]_{2s}$ specified for "Laminate method" in the table represents two sets of prepreg layers stacked in the 0 ° direction and 90 ° direction.

In this test, the HITS-T10 high speed tensile testing machine and HPV-2A high speed video camera were synchronized to take video at the instant the sample fractured. The sample was prepared prior to the test by spraying paint onto its surface in a random pattern, and the strain distribution on the surface of the test specimen was visualized by DIC analysis based on the amount of shift of the random pattern.

Test Results

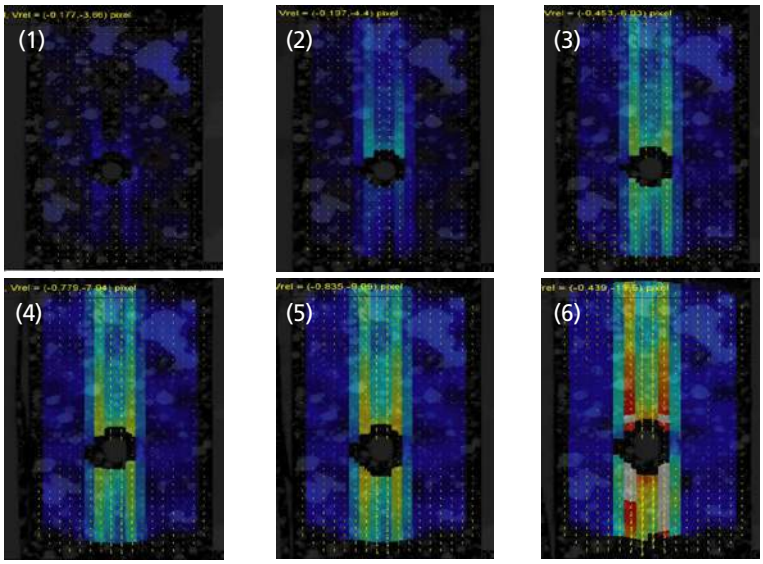

Fig. 2 Results of DIC Analysis of CFRP-OH Specimen

Fig. 2 and Fig. 3 show the DIC analysis results obtained in tensile testing of CFRP-OH and ABS resin test specimens, respectively. The images were extracted in the order of a typical time course analysis (image order corresponding to the numbers shown in images), from the start of the tensile test to the point that the specimen breaks. The appearance of coloring in the images corresponds to the strain distribution in the specimen. The amount of strain that occurs in the specimen corresponds to the degree of color warmth, with areas of darker color (such as blue-black) indicating low strain, and areas of brighter color (such as red-orange) indicating a greater degree of strain. It is clear that in Fig. 2, as the load is applied to the test specimen, the strain increases in the vicinity of the open hole. Because the test specimen is a $[0/90]_{2s}$ laminate material, it is believed that the fibers are aligned in the tensile direction in the test specimen surface layer which was subjected to random marking.

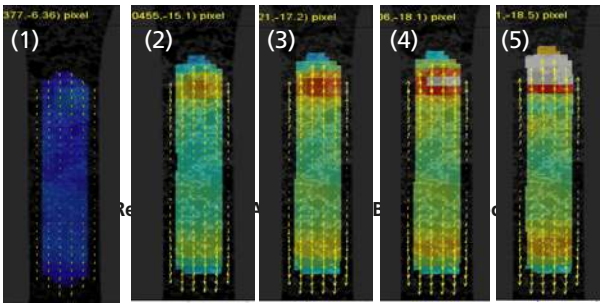

In Fig. 3, localized strain occurs from the edge of the parallel region of the test specimen, and as time progresses, localized strain is noticeable at the upper and lower edge of the parallel region.
Thus, by combining a high-speed tensile testing machine with a high-speed video camera, in addition to DIC analysis software, it has become possible to visualize the distribution of strain generated in a test specimen.

First Edition: Dce, 2012

Shimadzu Corporation
www.shimadzu.com/an/

For Research Use Only. Not for use in diagnostic procedures.
The content of this publication shall not be reproduced, altered or sold for any commercial purpose without the written approval of Shimadzu.
The information contained herein is provided to you "as is" without warranty of any kind including without limitation warranties as to its accuracy or completeness. Shimadzu does not assume any responsibility or liability for any damage, whether direct or indirect, relating to the use of this publication. This publication is based upon the information available to Shimadzu on or before the date of publication, and subject to change without notice.
© Shimadzu Corporation, 2012

SHIMADZU
Excellence in Science

Application Data Sheet

No. 8

Autograph Precision Universal Tester

Material Testing & Inspection

Flexural Testing of CFRP Boards

Standard No. JIS K 7074: 1988

Introduction

Carbon fiber reinforced plastic (CFRP) is a composite material with excellent relative strength. This plastic was quickly adopted in the aviation and space sectors, and has contributed significantly to reducing fuselage weight. Initially, this plastic was only used for partial replacement of metal materials. In the latest aircraft, however, composite materials, primarily CFRP, represent 50 % of the fuselage weight. Improved productivity and reduced costs are expected due to subsequent technical developments, and it can be expected that this plastic will also become popular as a main material in automobile frames. In this Data Sheet, a CFRP cloth was subjected to a flexural testing using a precision universal tester in order to evaluate the strength of the material.

F. Yano

Measurements and Jigs

In flexural testing specified in JIS K7074, a loading edge radius of 5 mm, and a support radius of 2 mm are specified. The specimen standard dimensions are specified as follows:

Length = 100 mm ± 1 mm
Width = 15 mm ± 0.2 mm
Thickness = 2 mm ± 0.4 mm

For tests performed using a specimen with the standard dimensions, the span between supports (L) will be 80 mm ± 0.2 mm. When TRAPEZIUM software is used, the flexural stress can be automatically calculated and plotted in a graph from the test force and the specimen dimensions. The flexural strength and other characteristic values can also be obtained from a few simple operations.

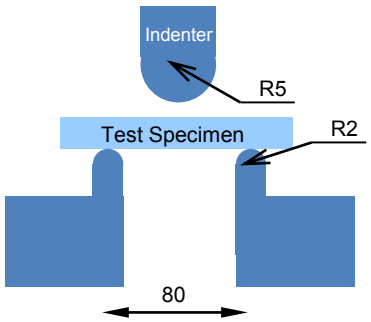

Fig. 1: Flexural Testing Schematic

Measurement Results

Fig. 2: Flexural Testing Status

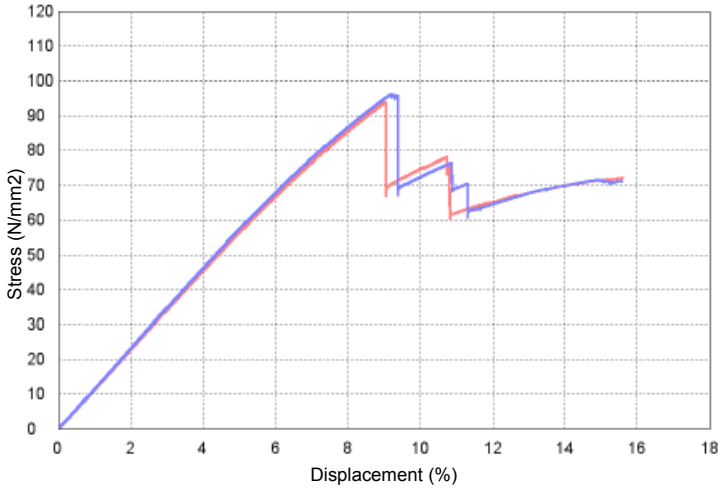

Fig. 3: Stress – Displacement Curve

Table 1: Test Conditions

Item	Set Value
Cell Capacity	5 kN
Load Speed	5 mm/min

Table 2: Test Results (Average)

Load at Fracture (N)	Bending Strength (%)
485	95

CFRP Flexural Testing System

Tester:	AG-Xplus
Load Cell:	5 kN
Test Jig:	Three-point bending test jig for plastics
Software:	TRAPEZIUM X (Single)

AG-Xplus Table-Top Precision Universal Tester

Features

- A high-precision load cell is adopted. (The high-precision type is class 0.5; the standard-precision type is class 1.)
  Accuracy is guaranteed over a wide range, from 1/1000 to 1/1 of the load cell capacity. This supports highly reliable test evaluations.
- Crosshead speed range
  Tests can be performed over a wide range from 0.0005 mm/min to 1,500 mm/min.
- High-speed sampling
  Ultrafast sampling, as fast as 0.2 msec. Sudden changes in test force, such as when brittle materials fracture, can be assessed.
- TRAPEZIUMX operational software
  Designed for intuitive operation, this software offers excellent convenience and user friendliness.
- Smart controller
  Real-time test force and position data is readily confirmed, and the manual dial can be used for fine adjustments to jig positioning.
- Optional Test Devices
  A variety of tests can be conducted by switching between an abundance of jigs in the lineup.

First Edition: February 2013

Shimadzu Corporation
www.shimadzu.com/an/

For Research Use Only. Not for use in diagnostic procedures.
The content of this publication shall not be reproduced, altered or sold for any commercial purpose without the written approval of Shimadzu.
The information contained herein is provided to you "as is" without warranty of any kind including without limitation warranties as to its accuracy or completeness. Shimadzu does not assume any responsibility or liability for any damage, whether direct or indirect, relating to the use of this publication. This publication is based upon the information available to Shimadzu on or before the date of publication, and subject to change without notice.
© Shimadzu Corporation, 2013

SHIMADZU
Excellence in Science

Application Data Sheet

No. 16

Autograph Precision Universal Tester

Material Testing & Inspection

Tensile Testing of Carbon Fiber

Standard No. ISO11566: 1996 (JIS R 7606: 2000)

Introduction

Carbon fiber is an important industrial material, being essential in carbon fiber reinforced plastics (CFRP), having a specific gravity one-fourth that of normal steels, and a specific strength of 7 times. In this Application Data Sheet, examples of tensile testing of single carbon fibers based on the ISO standard are introduced.

T. Murakami

Measurements and Jigs

In this test, the test sample is fixed to a test specimen mounting board made from a paper, metal, or resin sheet as shown in Fig. 1, installed in the grips, and the tensile test is performed. The standard describes in detail the shape of the mounting board, the type of adhesive used to fix the carbon fiber to the mounting board, and the procedure for installing the carbon fiber (for details refer to the standard). The tests were carried out using clip type grips whose grip force could be adjusted in accordance with the strength of the sample.

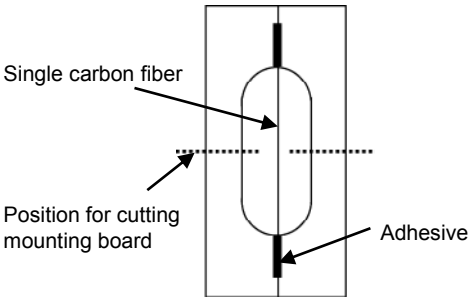

Fig. 1 Test Sample and Mounting Board (frame)

Measurement Results

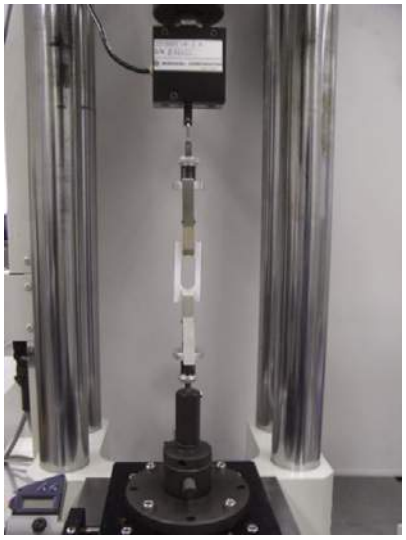

Fig. 2 Test Status

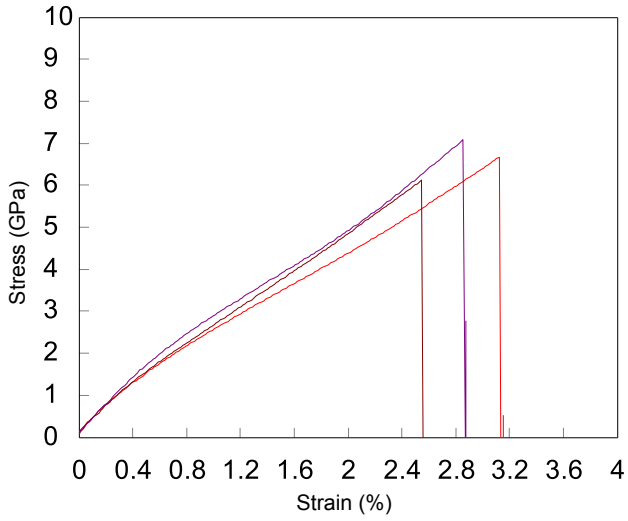

Fig. 3 Test Results

Table 1 Test Conditions

Item	Set Value
Test speed	1 mm/min
Distance between grips	25 mm

Table 2 Test Results (average)

Sample	Diameter	Tensile Strength	Elongation at Break
Carbon fiber	6 μm	7.1 GPa	2.84 %

Carbon Fiber Tensile Test System

Tester:	MST-I Type HR
Load Cell:	1 N
Test Jig:	1 N clip type grips (rubber-coated teeth), X-Y stage
Software:	TRAPEZIUM X (Single)

Shimadzu Autograph MST-1 Micro Strength Evaluation Testing Machine

Features

■ High Accuracy Displacement Measurement
A high accuracy (±0.2 μm) linear sensor has been adopted for measurement of displacement in the load direction. In addition, the backlash-free structure makes it possible to carry out testing with good accuracy. Displacement in the load direction of the test sample can be set accurately to a displacement display resolution of 0.02 μm and a control resolution of 0.005 μm.

■ Measurement of Micro Test Forces
A wide range of load cells from 0.5 N to 2 kN assures a precision of ±1 % for measurements of testing forces of 2 mN at minimum.

■ Positioning Very Small Test Samples
Using an X-Y stage (optional), very small test samples can be easily positioned. The position of the test samples can be observed using a stereo microscope.

■ High Rigidity Frame
A high rigidity frame (45 kN/mm minimum) has been adopted to enable measurement of minute displacements.

■ Optional Test Devices
A variety of tests can be accommodated by switching between an abundance of jigs in the lineup.

First Edition: February 2013

SHIMADZU

Shimadzu Corporation

www.shimadzu.com/an/

For Research Use Only. Not for use in diagnostic procedures.
The content of this publication shall not be reproduced, altered or sold for any commercial purpose without the written approval of Shimadzu. The information contained herein is provided to you "as is" without warranty of any kind including without limitation warranties as to its accuracy or completeness. Shimadzu does not assume any responsibility or liability for any damage, whether direct or indirect, relating to the use of this publication. This publication is based upon the information available to Shimadzu on or before the date of publication, and subject to change without notice.

© Shimadzu Corporation, 2013

SHIMADZU
Excellence in Science

Application Data Sheet

No. 31

Autograph Precision Universal Tester

Material Testing & Inspection

Materials Testing Using Digital Image Correlation

—3-Point Bending Test for Polypropylene and Open-Hole Tensile Test for Carbon Fiber Reinforced Thermo-Plastic—

■Introduction

In recent years, computer aided engineering (CAE), which has allowed significantly reducing the number of prototypes and costs required for product development by simulating product designs on a computer, has been widely used in scientific and industrial fields. This has resulted in an increased need to analyze the distribution of strain in test samples, where the areas prone to strain concentrations in such samples are evaluated by mechanical testing to determine the correlation between results from simulation and strain distribution obtained by mechanical testing.

Digital image correlation (DIC) analysis compares the random patterns on the surface of a test sample before and after deformation to determine the degree of deformation. A important feature of the method is that displacements can be measured and strain distributions analyzed from digital images, which means no sensors need to contact the test sample and no complicated optical systems are required. Consequently, DIC analysis is being used for a wide range of applications where strain is difficult to measure using conventional technology, such as analyzing the strain distribution in large structural members, materials at high temperatures, or micro-materials observed via a microscope.

This paper describes examples of using DIC analysis for 3-point bending tests of plastics and for open-hole tensile testing of thermoplastic carbon fiber reinforced plastics (CFRP) (fabric). The test data presented in this paper was obtained using a system comprising a Shimadzu AG-Xplus precision universal tester, a customized TRViewX non-contact video extensometer, and LaVision DaVis8 DIC analysis software. This system allows simultaneously acquiring JIS 0.5 class extensometer measurement results and video images for DIC analysis, as well as correlating DIC analysis results with test force data.

■Evaluation of Dependence on Distance Between Supports in 3-Point Bending Tests of Plastics

3-point bending tests are widely used throughout the world as a relatively easy way to evaluate the bending properties of materials. A photograph of the testing system is shown in Fig. 1. In 3-point bending tests, a punch applies a load to specimens supported at two points.

3-point bending test regulations for plastics (such as JIS K 7171 and ISO 178) specify that the L, the distance between supports, must be about 16 times greater than h, the specimen thickness (L/h ≈ 16), where this ratio, L/h, is an important factor for measuring the bending strength or bending elasticity correctly.[1), 2)] The following discusses L/h in more detail. Bending a specimen applies compressive stresses to the material above the center plane and tensile stresses below the center plane. The contribution of this compressive and tensile deformation to bending stresses is defined to be equal. Maximum bending stress occurs near the punch that applies the bending loads, where given a flat plate-shaped specimen, stress is defined as $\sigma_f = 3FL/2bh^2$. When a specimen bends, shear stresses also occur at the same time, where the shear stress is defined as $\tau = 3F/4bh$. Based on the above two equations, the relationship between specimen thickness and distance between supports is described by $L/h = \sigma_f/2\tau$. Given a uniformly formed specimen with a sufficiently large distance between the supports, relative to the specimen thickness, the definition of L/h indicates that the contribution of shear stresses in the specimen is small.[3) to 5)] To limit the effects of shear stresses during 3-point bending tests, the optimal L/h value must be specified for the specimen being tested.

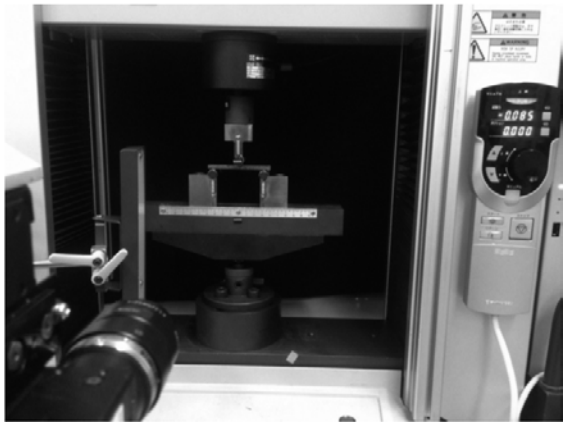

Fig. 1 3-Point Bending Testing System Using Non-Contact Video Extensometer

In the following example, a common plastic material, polypropylene, was tested by 3-point bending using three different distances between supports, and then DIC analysis was used to investigate how much the maximum shear stress distribution depends on the distance between supports. Test conditions are shown in Table 1.

Tests were performed at three L values (distance between supports), 64 mm for an L/h ratio of 16 specified in JIS K 7171, 48 mm for an L/h ratio of 12, where shear stress is predicted to have a large effect, and 32 mm for an L/h ratio of 8. Stress-strain curves obtained using different test conditions are shown in Fig. 2. Fig. 3 shows the maximum shear strain distribution near the elastic limit and near the maximum load point. Warmer colors indicate higher strain levels in the maximum shear strain distribution. This shows that at an L/h ratio of 16, strain is low even near the maximum load point and spreads out uniformly. However, L/h ratios of 8 and 12, where shear stress contribution is predicted to be large, generated large localized shear stresses near the maximum load point on the specimen surface under tension directly under the punch. Whereas localized shear stresses occurred from about the elastic limit for L/h ratio of 8, none were observed for the L/h ratio of 12.

This clearly shows that different deformation modes resulted from bending tests using different distances between supports and shows that DIC analysis provides an effective means of verifying the different modes. It also shows that L/h ratio of 16 recommended in the testing regulations is an appropriate value for 3-point bending tests.

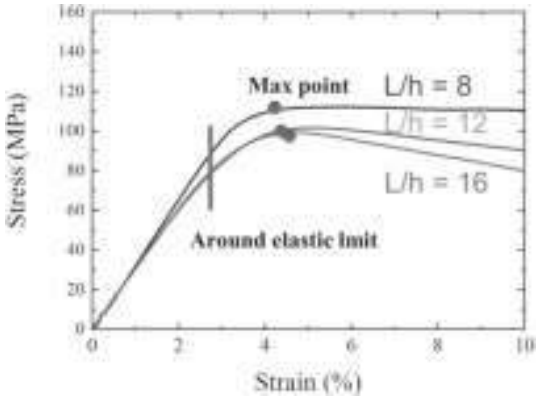

Fig. 2 Stress-Strain Curve

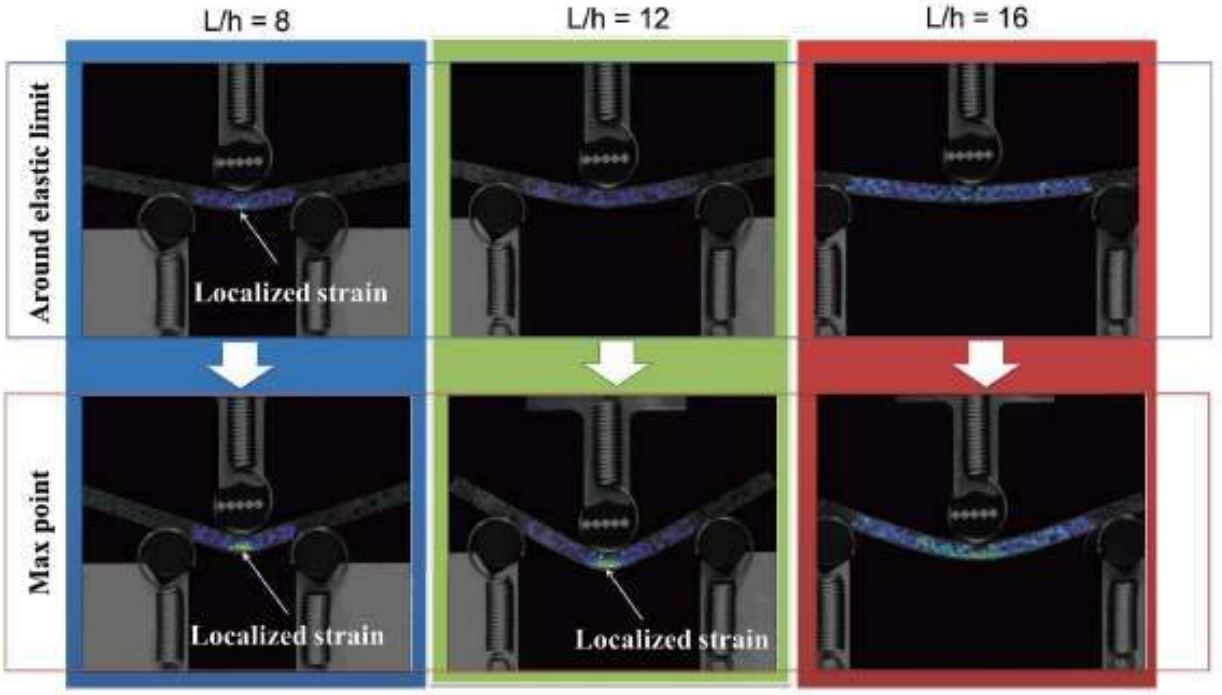

Fig. 3 Distribution of Maximum Shear Strain Around Elastic Limit and Maximum Load

Table 1 Test Conditions for 3-Point Bending Test of Plastic Material

1) Testing equipment	AG-Xplus precision universal tester
2) Load cell capacity	1 kN
3) Jig	Three-point bending test jig for plastic
4) Distance between supports	Three configurations: 32, 48, and 64 mm
5) Test speed	0.001 /s
6) Deflection measuring device	TRViewX120S non-contact video extensometer (customized)
7) Testing software	TRAPEZIUM X (Single)
8) DIC analysis software	DaVis8 (LaVision GMBH)
9) Specimen size	4 mm thick × 10 mm wide × 80 mm long

First Edition: July 2015

SHIMADZU
Shimadzu Corporation
www.shimadzu.com/an/

For Research Use Only. Not for use in diagnostic procedures.
The content of this publication shall not be reproduced, altered or sold for any commercial purpose without the written approval of Shimadzu.
The information contained herein is provided to you "as is" without warranty of any kind including without limitation warranties as to its accuracy or completeness. Shimadzu does not assume any responsibility or liability for any damage, whether direct or indirect, relating to the use of this publication. This publication is based upon the information available to Shimadzu on or before the date of publication, and subject to change without notice.
© Shimadzu Corporation, 2015

■Open-Hole Tensile Testing of Thermoplastic CFRP (Fabric)

Due to higher specific strength than steel materials, superior workability and formability than CFRP/epoxy, and short cycle times of only a few minutes possible for molding, thermoplastic CFRP materials are anticipated for use in production automobiles.[6)]

In general, CFRP materials start failing at the point where they are damaged. CFRP/epoxy used as structural materials in aircraft are mainly used for large components that are fastened with screws or rivets. Therefore, it is important to evaluate their open-hole tensile strength. The open-hole tensile test specified in ASTM D 5766, JIS K 7094, and other regulations is one of the essential evaluation criteria for understanding the properties of CFRP materials.[7), 8)]

In this case, we made a round hole in a thermoplastic CFRP specimen, applied a tensile load, and evaluated the resulting distribution of the maximum shear strain. Fig. 4 shows the testing system used for this test. Table 2 indicates testing conditions and information about the specimen. We chose to cut out type-I shaped specimens, as specified in JIS K 7094 (2012), from PA6 polymer-based thermoplastic CFRP material (with CF-3K flat woven $[0]_{10}$ fabric from Ichimura Sangyo), so that the fibers were oriented longitudinally.

The stress-strain curve obtained from testing is shown in Fig. 5 and the distribution of maximum shear strain that occurred on the observed specimen surface is shown in Fig. 6. Images (1) to (4) in Fig. 6 correspond to the numbers indicated on the stress-strain curve in Fig. 5.

Fig. 4 Open-Hole Tensile Testing System Using Non-Contact Video Extensometer

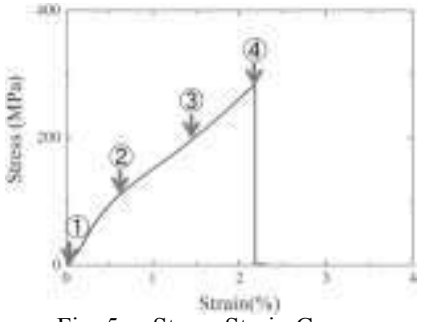

Fig. 5 Stress-Strain Curve

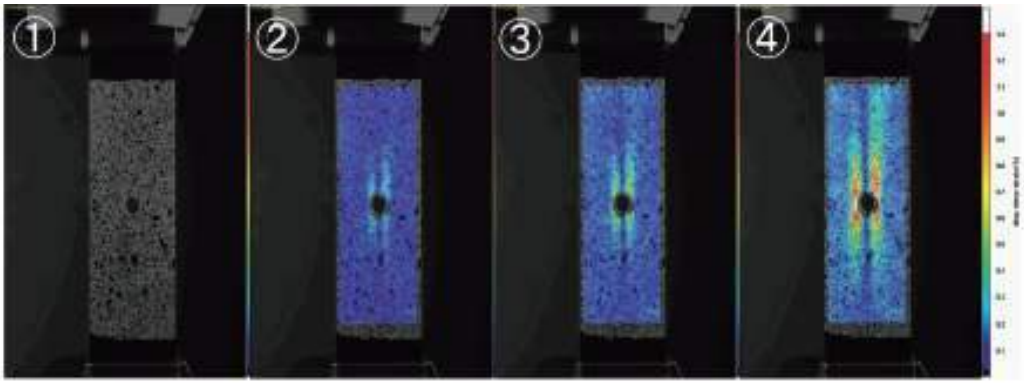

Fig. 6 Distribution of Maximum Shear Strain

Table 2 Test Conditions for Open-Hole Tensile Test of Carbon Fiber Reinforced Thermo-Plastic (Fabric)

1) Testing equipment	AG-Xplus precision universal tester
2) Load cell capacity	50 kN
3) Jig	50 kN non-shift wedge type grips (with trapezoidal file teeth on grip faces for flat specimens)
4) Distance between grips	100 mm
5) Test speed	0.5 mm/min
6) Deflection measuring device	TRViewX120S non-contact video extensometer (customized)
7) Testing software	TRAPEZIUM X (Single)
8) DIC analysis software	DaVis8 (LaVision GMBH)
9) Specimen size	2 mm thick × 36 mm wide × 150 mm long, with 6 mm diameter hole

First Edition: July 2015

SHIMADZU
Shimadzu Corporation
www.shimadzu.com/an/

For Research Use Only. Not for use in diagnostic procedures.
The content of this publication shall not be reproduced, altered or sold for any commercial purpose without the written approval of Shimadzu.
The information contained herein is provided to you "as is" without warranty of any kind including without limitation warranties as to its accuracy or completeness. Shimadzu does not assume any responsibility or liability for any damage, whether direct or indirect, relating to the use of this publication. This publication is based upon the information available to Shimadzu on or before the date of publication, and subject to change without notice.
© Shimadzu Corporation, 2015

The results showed that when the tensile load increased, the maximum shear strain distribution started near the tangent points on the left and right sides of the hole, and spread along the longitudinal direction of the specimen. Due to the orientation of the carbon fibers, the specimen has the greatest strength for bearing tensile loads in its longitudinal direction. The areas of strain concentration are the areas that contain continuous fibers, but they are presumably highly affected by the process of creating the hole. Fig. 7 is a photograph of the specimen after fracture. It shows that the specimen fractured in the direction perpendicular to the main tensile axis. The failure mode is typical of CFRP(fabric) specimens with an open hole, where cracking presumably progressed rapidly after the longitudinal carbon fibers near the hole fractured, resulting in specimen breaking.

Generally, open-hole tensile tests that involve creating a hole in specimens result in significantly lower stresses at the maximum load point, than for specimens without a hole, with some reports indicating a 1/3 to 1/2 drop in strength.[9), 10)] In addition to open-hole tensile testing, this research also involved tensile testing specimens without a hole for reference purposes. A resulting stress-strain curve and photograph of the specimen after fracture are shown in Figs. 8 and 9. The specimen fractured near the parallel area, at a value of about 700 MPa. In contrast, Fig. 5 indicates that the open-hole specimen failed at about 300 MPa, a result similar to CFRP/epoxy specimens.

Fig. 7 Picture of Fractured Specimen

■Conclusion

This paper describes using DIC analysis to evaluate the properties of polypropylene and thermoplastic CFRP (fabric), as examples of chemically engineered materials. However, there are many other types of chemically engineered materials available for which DIC analysis could be used for determining material properties, not only for bending or tensile tests, but also for various others tests, such as compression and shear tests. With high-speed video cameras developed in recent years that allow obtaining high-resolution video images with extremely high time resolution levels, technology has advanced to the point that DIC analysis can now be utilized to visualize strain distributions or obtain stress-strain curves for applications such as high-speed impact testing. Consequently, using DIC analysis for material testing in product design work provides an effective way of ensuring a higher level of safety and peace of mind by understanding the properties of the materials from various aspects.

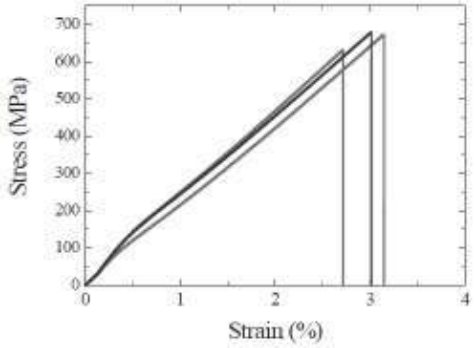

Fig. 8 Stress-Strain Curve

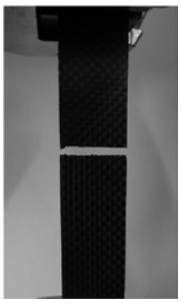

Fig. 9 Picture of Fractured Specimen

■References:

1) JIS K 7171: 2008 Plastics—Determination of flexural properties
2) ISO 178: 2001 Plastics—Determination of flexural properties
3) Masahiro Funabashi: Technology for Evaluating the Performance of Advanced Materials, Sangyo Gijutsu Service Center, pp. 286-287 (2014)
4) Leif A. Carlsson and R. Byron Pipes: Experimental Characterization of Advanced Composite Materials, Kokon Syoin, p. 75 (1990)
5) Ikuo Narisawa: Mechanical Properties of Plastics, Sigma Shuppan, pp. 105-108 (1994)
6) Takeshi Murakami and Tsuyoshi Matsuo: Summary of Presentations at the 39th Conference on Composite Materials, pp. 155-156 (2014)
7) ASTM D5766/D5766M -11 Standard Test Method for Open-Hole Tensile Strength of Polymer Matrix Composite Laminates
8) JIS K 7094: 2012 Test method for open-hole tensile strength of carbon fibre reinforced plastic
9) JAXA-ACDB Advanced Composites Database System http://www.jaxa-acdb.com/ (as of December 17, 2014)
10) Wisnom, M. R., Hallett, S. R., and Soutis, C.: Scaling effects in notched composites, Journal of composite materials, 44, 195-210 (2010)

First Edition: July 2015

SHIMADZU
Shimadzu Corporation
www.shimadzu.com/an/

For Research Use Only. Not for use in diagnostic procedures.
The content of this publication shall not be reproduced, altered or sold for any commercial purpose without the written approval of Shimadzu.
The information contained herein is provided to you "as is" without warranty of any kind including without limitation warranties as to its accuracy or completeness. Shimadzu does not assume any responsibility or liability for any damage, whether direct or indirect, relating to the use of this publication. This publication is based upon the information available to Shimadzu on or before the date of publication, and subject to change without notice.
© Shimadzu Corporation, 2015

SHIMADZU
Excellence in Science

Application Data Sheet

No. 37

High-speed Video Camera HPV-X2

Observing the Failure of Open-Hole CFRP Specimens in Tensile Testing

Synchronized Imaging Using Two High-Speed Video Cameras

■ Introduction

Offering superior specific strength, even compared to other composite materials, carbon fiber reinforced plastic (CFRP) is used in aircraft and some transport vehicles for the purpose of saving fuel through weight reduction. Composite materials have excellent mechanical properties. However, a general feature of composite materials is that their strength decreases markedly when they are notched. CFRP is no exception, so tests of notched specimens are important. In this case, testing is performed using specimens notched with a circular hole at the center. In this experiment, tensile tests were performed using CFRP (laminate method $[45/0/-45/90]_{2s}$) with a total length of 150 mm, a width of 36 mm, and a thickness of 2.5 mm, prepared with a 6 mm circular hole at the center. The failure process of CFRP was observed during the tensile test. In particular, it is important to confirm the failure process of weak regions, such as the periphery of circular holes, for CFRP development and to confirm the validity of CAE analysis. However, since the failure of CFRP is a brittle phenomenon, where failure occurs instantaneously, it cannot be confirmed with the naked eye. For this reason, high-speed video cameras are used to observe the failure. In this experiment, synchronized images were obtained at the front and the side of the specimens using two HPV-X2 high-speed video cameras.

■ Measurement system

In this experiment, the AG-X precision universal testing machine and two HPV-X2 high-speed video cameras were used. Table 1 shows the instruments used. To observe the specimen failure in a tensile test, a trigger signal synchronized to the failure must be transmitted to the high-speed video cameras. The failure starts on the periphery of the circular hole. Accordingly, aluminum foil was affixed to the periphery of the circular hole using adhesive, as shown in Fig. 1, so that conduction would be lost when the sample fails. The failure was observed using this timing to trigger the cameras.

Table 1 Testing Equipment

High-speed Camera	HPV-X2 ×2
Lens	105 mm Macro lens ×2
Illumination	Metal halide lump ×2
Testing Machine	AG-X plus
Load cell	100 kN
Grips	100 kN Non-shift wedge-type grips
Grip teeth	Trapezoidal file teeth for composite mater
Software	TRAPEZIUM X(Single)

Fig.1 Aluminum foil Trigger

■ Measurement Results

Table 2 shows the measurement conditions, and Fig. 2 shows the test configuration. As shown in Fig. 2, the failure of the specimen was recorded from the front by camera (1) and from the side by camera (2). Fig. 3 shows the test results from the AG-Xplus. Failure begins where the test force suddenly drops in Fig. 3. Fig. 4 shows the specimen failure observed from the front, and Fig. 5 from the side. Image (2) in Fig. 4 shows that the failure starts on the left side of the circular hole. In image (3), a crack also appears on the right side of the circular hole. Subsequently, cracks progressed in an orientation of 45 degrees, the orientation of the fibers in the outer layer. Further, as the test progressed, multiple cracks were confirmed, as in images (7) and (8). In the observation from the side, no failure was confirmed at the time the failure started, and was only initially confirmed in image (5). This is likely because the cracks started at the periphery of the circular hole reached the side of the specimen in image (5). Subsequently, failure was confirmed in multiple layers, except for the 0-degree layer, in image (6). Further, in image (7), failure was confirmed in the 0-degree layer, after which the failure progressed toward the outersurface. The final condition of the specimen is shown in Figs. 6 and 7.

Table 2 Measurement Conditions

Test speed	5 mm/min
Frame rate	1M frames/sec
	2M frames/sec

Fig.2 Test Configuration

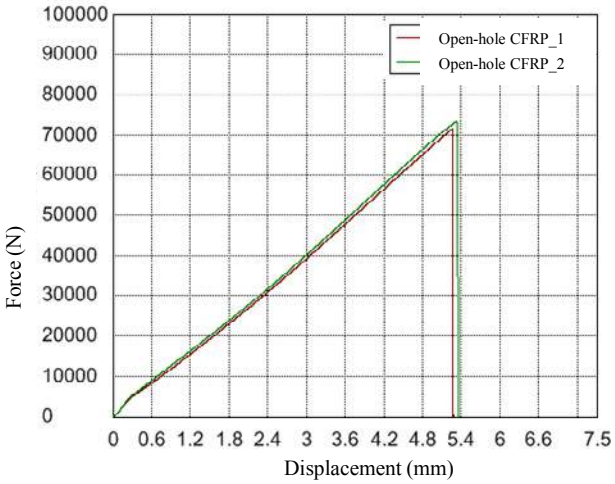

Fig.3 Test Results

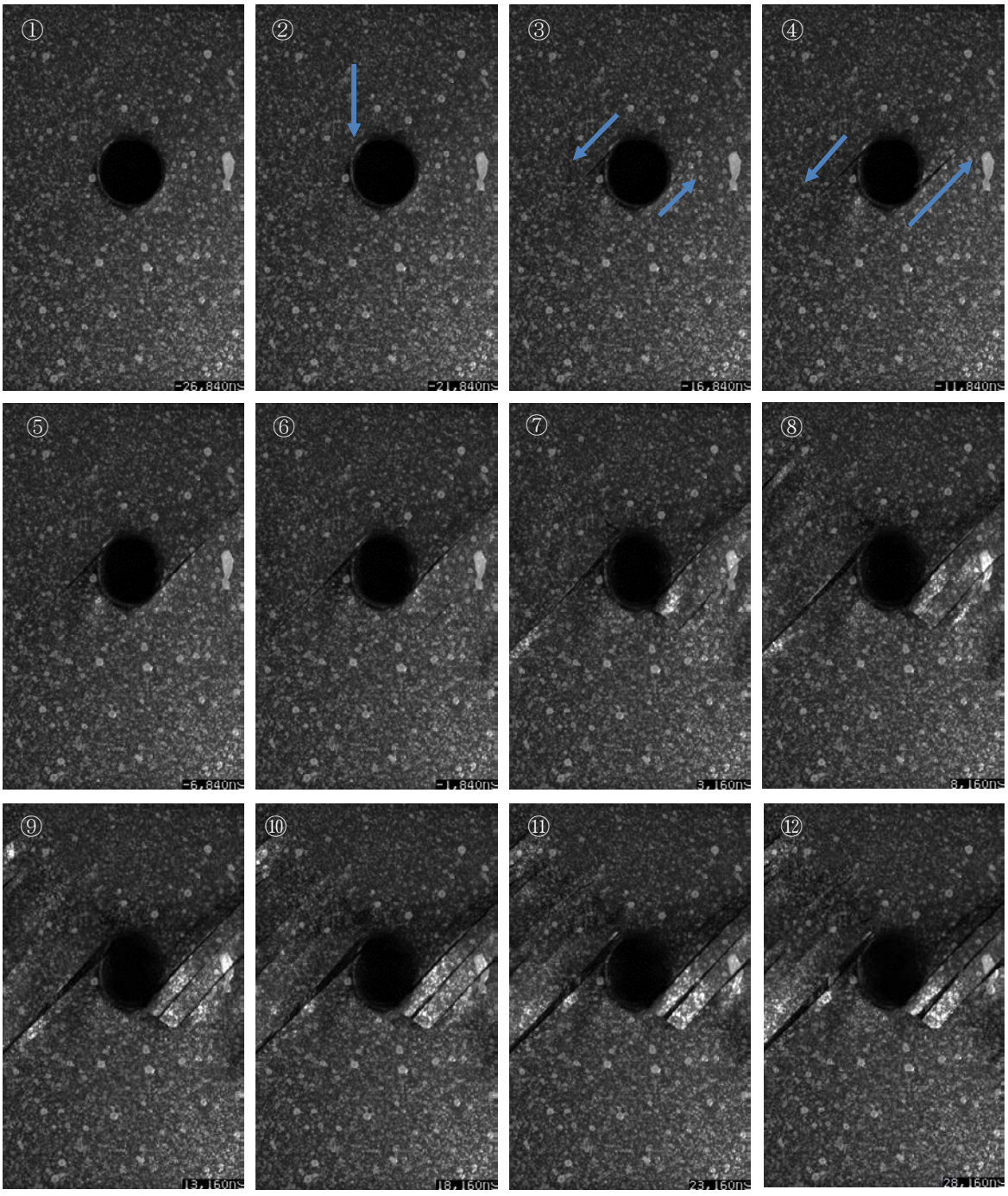

Fig.4 Images from Camera (1) (5 μs between images)

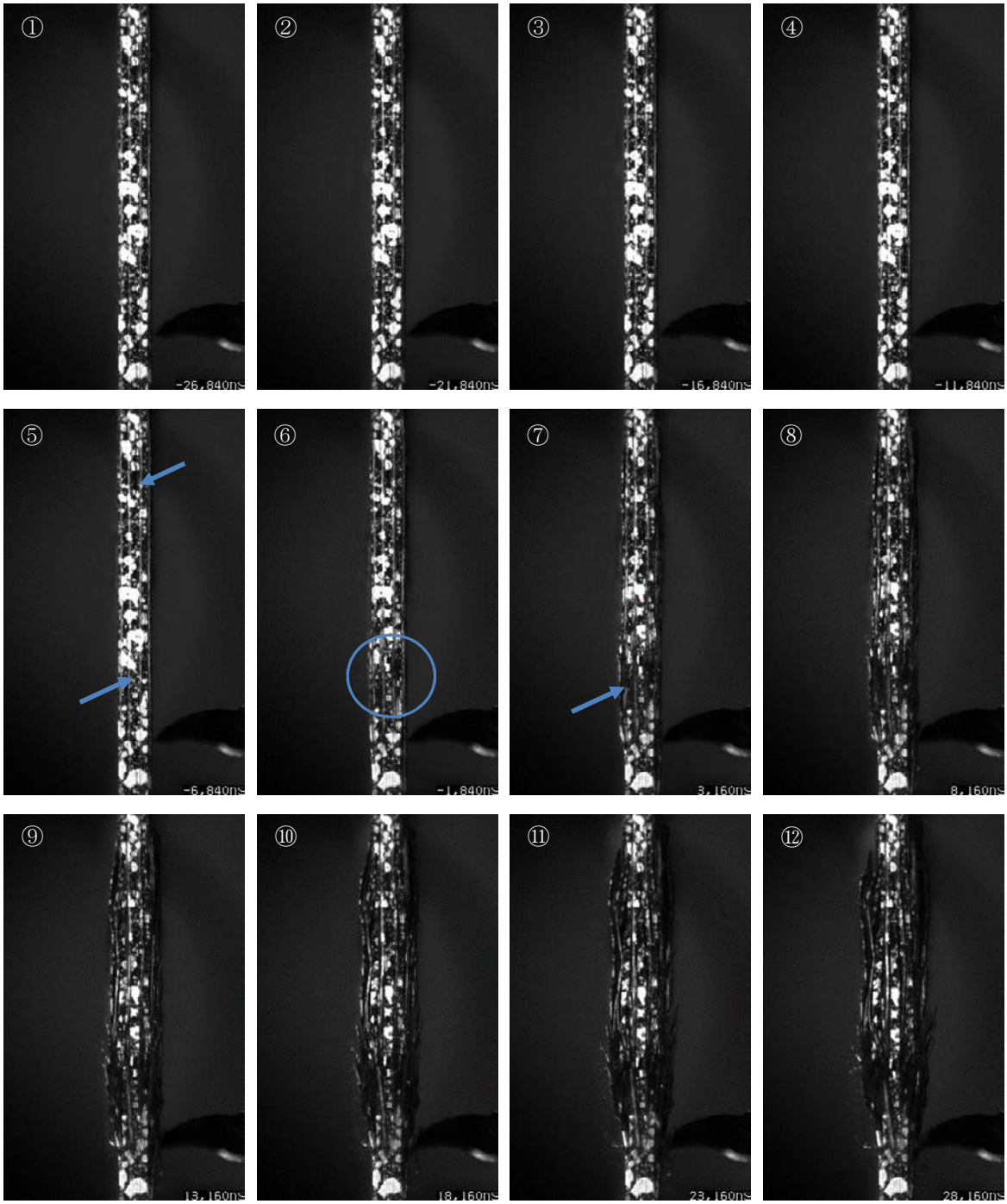

Fig.5 Images from Camera (2) (5 μs between images)

Fig.6 Specimen After Failure (front)

Fig.7 Specimen After Failure (side)

■ Conclusion

The conventional HPV-X does not have a synchronization function, and so is incapable of recording from two directions. Also, the sensitivity of the HPV-X is insufficient, so it cannot record at imaging speeds of 500 kfps or faster. The HPV-X2 is equipped with a synchronization function, and features improved sensitivity, so this instrument is capable of synchronized recordings at 2 Mfps, as in this case. As a result, failures can be observed in tensile tests of materials like CFRP that fail at high speeds.

Generally, failure observations are often recorded from the front of the specimen. However, adding recording from the side enables confirming the failure process that cannot be observed just from the front. In particular, with CFRP materials with different fiber orientations for each lamination layer, where failure progresses in different manner for each layer, as shown in this article, the failure process can be observed in more detail by recording from two directions.

First Edition: July, 2015

Shimadzu Corporation
www.shimadzu.com/an/

For Research Use Only. Not for use in diagnostic procedures.
The content of this publication shall not be reproduced, altered or sold for any commercial purpose without the written approval of Shimadzu.
The information contained herein is provided to you "as is" without warranty of any kind including without limitation warranties as to its accuracy or completeness. Shimadzu does not assume any responsibility or liability for any damage, whether direct or indirect, relating to the use of this publication. This publication is based upon the information available to Shimadzu on or before the date of publication, and subject to change without notice.
© Shimadzu Corporation, 2015

SHIMADZU
Excellence in Science

Application Data Sheet

No. 38

HPV-X2 High-Speed Video Camera

High-Speed Video Camera

Observing the Fracture of Unidirectional CFRP in Static Tensile Testing

■ Introduction

Carbon fiber reinforced plastic (CFRP) is a composite material with a particularly high specific strength. It is used in aircraft and in some transport equipment to reduce fuel costs by reducing weight. While it has some excellent mechanical characteristics as a composite material, when in-plane damage occurs it displays brittle failure behavior, with fracture propagating instantly from the point of damage. Consequently, CFRP development involves not only material testing, but also observation of material failure to check for fracture locations at weak points. Furthermore, material failure is observed to evaluate the validity of computer aided engineering (CAE) recently. As mentioned above, a CFRP fracture event occurs extremely quickly and cannot be observed by the naked eye, so a high-speed video camera is used. Shimadzu has published an Application News on this topic in the past (No. V017 Observing the Failure of CFRP Materials in High-Speed Tensile Tests). High-speed tensile testing involves an instantaneous testing time. To accommodate this, a strobe capable of emitting very intense light instantaneously is used to achieve an image capture speed of over 1 million frames/second. Meanwhile, static testing involves longer testing times with a metal halide lamp used as a light source for continuous lighting (a relatively weak light source compared to a strobe), which cannot produce enough light to capture images at more than 500 thousand frames/second.
The newly developed HPV-X2 camera is 6 times more sensitive than the previous HPV-X camera, which allows it to capture over 1 million frames/second using even a metal halide lamp as a light source. In this article, we demonstrate the observation of unidirectional CFRP failure in static testing.

■ Measurement

The AG-X precision universal testing machine and HPV-X2 high-speed video camera were used in experiments. The equipment used is shown in Table 1. Observing material failure during tensile testing requires a signal to trigger the high-speed video camera in time with material failure. Since cracks propagate in the direction of the unidirectional fibers when failure occurs in unidirectional CFRP, we attached aluminum foil perpendicular to the direction of the fibers with adhesive. A specimen with the aluminum foil attached is shown in Fig. 1. A break in conduction through the aluminum foil caused by a break in the specimen triggers observation of the failure event.

■ Results

A view of the test is shown in Fig. 2 and Fig. 3. As shown in Fig. 3, aluminum foil is also attached to the jigs around the specimen in order to focus light onto the specimen. Test conditions are shown in Table 2.

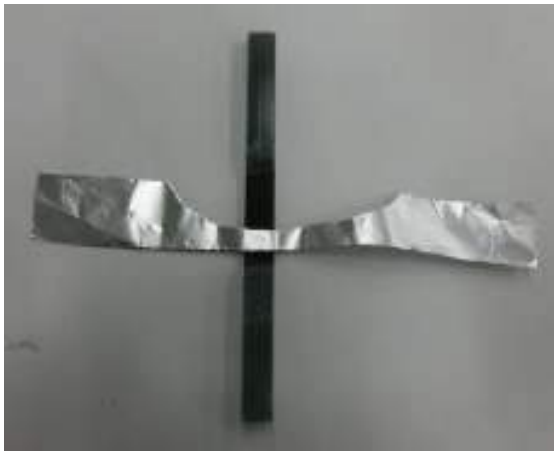

Fig. 1 Test Specimen

Table 1 Testing System

High-Speed Video Camera	HPV-X2
Lens	105 mm, F1.8
Lighting	Two metal halide lamps
Testing Machine	AG-Xplus
Load Cell	50 kN
Grip	50 kN non-shift wedge-type grips
Grip Face	Trapezoidal file teeth for composite materials
Software	TRAPEZIUM X (Single)

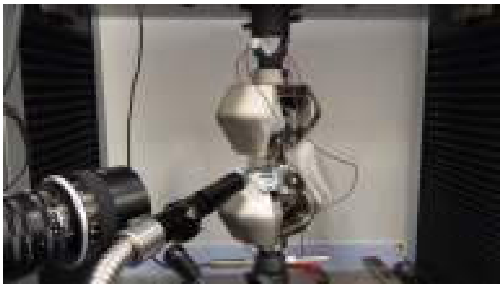

Fig. 2 View of the Test

Table 2 Test Conditions

Test speed	5 mm/min
Recording Speed	5 million frames/sec
Specimen Size	Width: 6 mm, thickness: 0.4 mm
Lamination Method	$[0]_2$

The failure of unidirectional CFRP is shown in Fig. 4. Longitudinal cracks can be seen on the left side of the specimen in image (2) of Fig. 4. In image (3), these cracks have propagated as far as the upper tab. Longitudinal cracks can also be seen on the right side of the specimen in image (3). Image (6) is a later view of the specimen as it is breaking apart. Using the HPV-X2 allows for the observation of CFRP failure during the static tensile test, which is useful for future CFRP development.

Fig. 3 View of the Test (Magnified View)

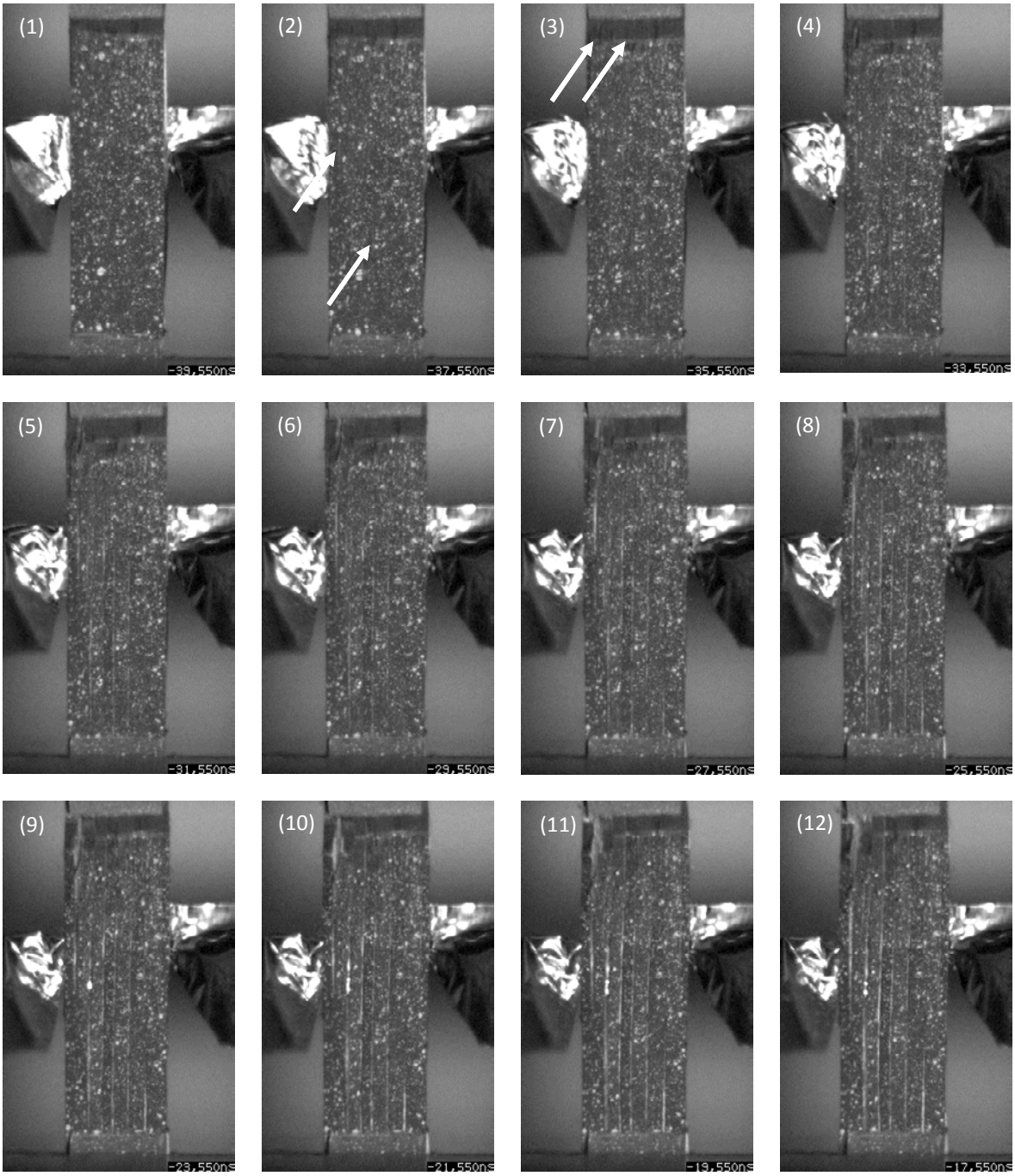

Fig. 4 Captured Images (Interval between captured images is 2 μs.)

First Edition: July, 2015

Shimadzu Corporation
www.shimadzu.com/an/

For Research Use Only. Not for use in diagnostic procedures.
The content of this publication shall not be reproduced, altered or sold for any commercial purpose without the written approval of Shimadzu.
The information contained herein is provided to you "as is" without warranty of any kind including without limitation warranties as to its accuracy or completeness. Shimadzu does not assume any responsibility or liability for any damage, whether direct or indirect, relating to the use of this publication. This publication is based upon the information available to Shimadzu on or before the date of publication, and subject to change without notice.
© Shimadzu Corporation, 2015

SHIMADZU
Excellence in Science

Application News

No.i256A

Material Testing System

Open-Hole Compression Test of Composite Material

Introduction

Carbon fiber reinforced plastic (CFRP) has gained attention due to their strength and low weight, and have quickly been adopted for use in aeronautics and astronautics. CFRP has excellent strength characteristics in terms of specific strength and high rigidity, but lose much of their strength when a cutout is made. Consequently, composite materials used in aeroplanes must be evaluated by tests that use specimens with a hole cut out of their center. We performed open-hole compression testing of a CFRP according to ASTM D6484.

Measurement System

The CFRP specimen used was T800S/3900. As shown in Fig. 1, a hole was created in the middle of the specimen. ASTM D6484 describes test methods in both SI and Imperial units, where the dimensions of the jigs and specimens differ in each. We performed testing with Imperial units. Specimen information is shown in Table 1.

ASTM D6484 includes two loading methods, which are described as Method A and Method B. In Method A, the specimen and test fixture are clamped in a gripping device, and the specimen is compressed by shear force applied by the fixture and gripping device. In Method B, compression plate is present at the ends of the specimen and fixture, and are used to compress the specimen. Method B was used, as shown in Fig. 2. Table 2 shows a list of the equipment used and Table 3 shows the test conditions used.

Table 1 Specimen Information

Length	: 305 mm
Width	: 38.1 mm
Thickness	: 3.1 mm
Lamination Method	: $[45/0/-45/92]_{2S}$

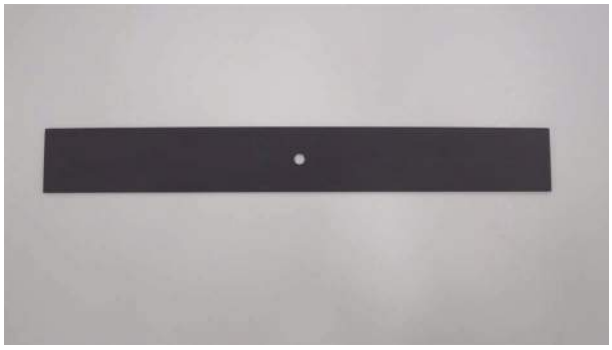

Fig. 1 Specimen

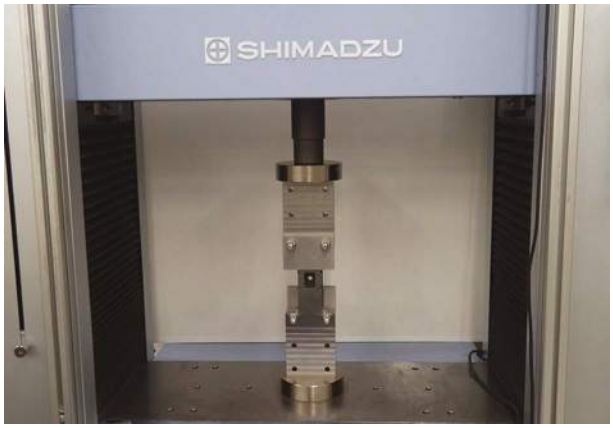

Fig. 2 Test Setup

Table 2 Experimental Equipment

Testing Machine	: AG-Xplus
Load Cell	: 50 kN
Test Fixture	: Open-Hole Compression Test Fixture

Table 3 Test Conditions

Test Speed : 2 mm/min

Results

Measurements were performed twice. Test results are shown in Table 4 and stress-displacement curves are shown in Fig. 3. As shown in Table 4, the mean open-hole compressive strength was 275.6 MPa.

Table 4 Test Results

Specimen Name	Open-Hole Compressive Strength
1st	278.2 MPa
2nd	273.0 MPa
Mean	275.6 MPa

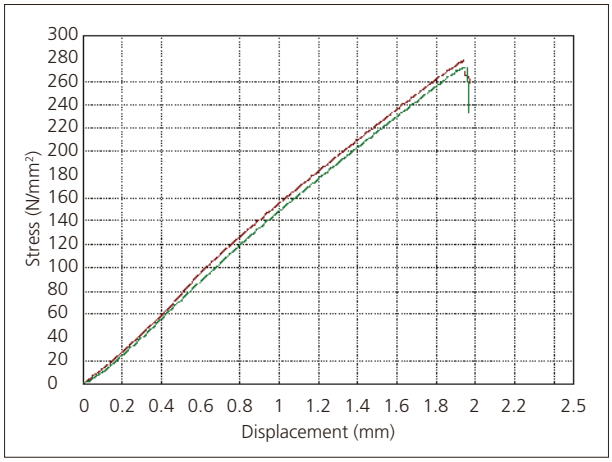

Fig. 3 Stress-Displacement Curves

Results (DIC Analysis)

Using the TRViewX non-contact extensometer allows for images and video of the specimen to be collected synchronized with test result collection. Also, applying a random pattern of paint to the observed specimen surface allows the images or video to be used to determine the strain distribution on the observed specimen surface during the test by DIC analysis[1]. Open-hole compression testing and DIC analysis were performed using the specimen described in Table 5. Fig. 4 shows a photograph of the open-hole compression test system with a non-contact extensometer. Fig. 5 shows strain distributions around the open hole in the specimen that were obtained by DIC analysis. Fig. 5 shows that strain accumulates at the vertical sides of the open hole (regions (1) and (3)), strain appears along the axis of compression from those points, and the final break occurs at the vertical sides of the hole. Meanwhile, almost no strain appears in the central part of the hole (region (2)) throughout the test. This strain distribution probably occurred due to a 0˚ fiber orientation on the surface of the specimen.

Table 5 Specimen Information (DIC)

Length	: 305 mm
Width	: 38 mm
Thickness	: 1.6 mm
Lamination Method	: $[0/90]_{2S}$

1) DIC analysis is an analysis method that measures strain and shows the strain distribution in a specimen based on movement of a random pattern of paint applied to the observed specimen surface before and during testing.

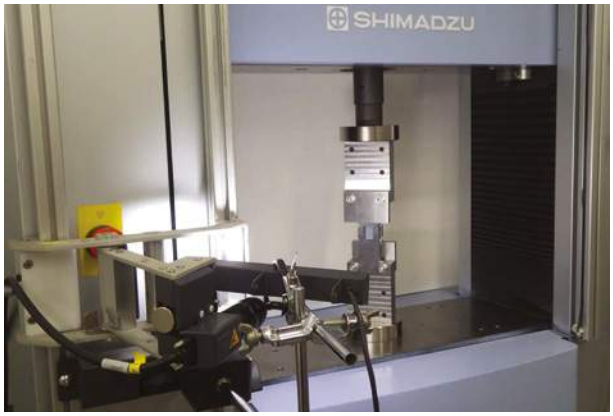

Fig. 4 Experimental Setup (DIC)

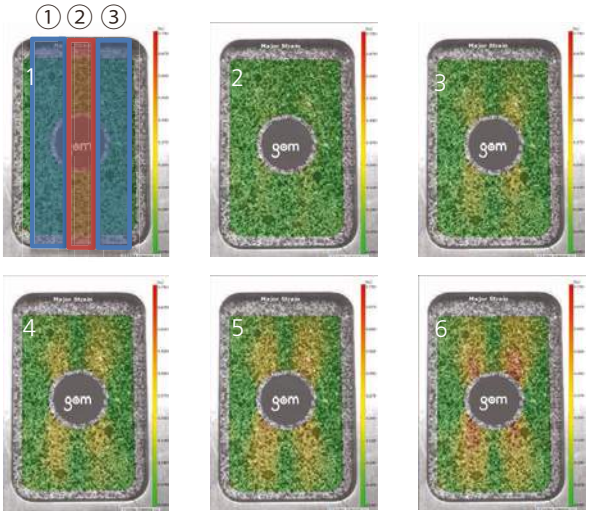

Fig. 5 DIC Analysis Results

Conclusion

Using this test system, open-hole compression testing of a CFRP was successfully performed according to ASTM D6484. Using a non-contact extensometer, we were also able to capture video (images) synchronized with the test force and crosshead displacement data obtained from the testing machine. Performing DIC analysis based on this video allowed an evaluation of the strain distribution on the observed specimen surface. This testing system will be extremely useful for the development of CFRPs and products that use CFRPs.

First Edition: Aug. 2016
Second Edition: Dec. 2016

SHIMADZU

Shimadzu Corporation
www.shimadzu.com/an/

For Research Use Only. Not for use in diagnostic procedure.
This publication may contain references to products that are not available in your country. Please contact us to check the availability of these products in your country.

The content of this publication shall not be reproduced, altered or sold for any commercial purpose without the written approval of Shimadzu. Company names, product/service names and logos used in this publication are trademarks and trade names of Shimadzu Corporation or its affiliates, whether or not they are used with trademark symbol "TM" or "®". Third-party trademarks and trade names may be used in this publication to refer to either the entities or their products/services. Shimadzu disclaims any proprietary interest in trademarks and trade names other than its own.

The information contained herein is provided to you "as is" without warranty of any kind including without limitation warranties as to its accuracy or completeness. Shimadzu does not assume any responsibility or liability for any damage, whether direct or indirect, relating to the use of this publication. This publication is based upon the information available to Shimadzu on or before the date of publication, and subject to change without notice.

© Shimadzu Corporation, 2016

SHIMADZU
Excellence in Science

Application News

No.i250

Material Testing System

Shear Test of Composite Material (V-Notched Beam)

Introduction

Carbon fiber reinforced plastic (CFRP) do not oxidize or rust and have a higher specific strength and stiffness than existing materials. Applications of CFRP are being investigated, with a focus on applications as industrial products that require strength and durability. Compared to existing homogeneous materials, composite materials like CFRP are anisotropic, and display complex failure behaviors as a result of tension, compression, bending, in-plane shear, out-of-plane shear, or a combination of these stresses arising from loading in the principal-axis direction. In recent years, use of CAE analysis in industry has become widespread since it can reduce numbers of prototypes and reduce the cost of new product development. Because values for each of the stress properties stated above are needed to increase precision when predicting product characteristics during product design, there is a strong demand for test methods able to evaluate pure failure behaviors in CFRP.

This article describes an example of V-notched beam method (Iosipescu method, ASTM D5379) that is widely used as an in-plane shear test method for composite material specimens. The test method can apply load as a pure in-plane shear stress on the evaluation area (see Fig. 1) by using a specimen cut with V-notches and supported at four asymmetrical points. Setting up the specimen and jig for this test method is relatively easy, and the test method can be used with a variety of CFRP laminate materials, including unidirectional materials, orthogonally laminated materials, and discontinuous fiber materials.

Measurement System

The equipment configuration is shown in Table 1. Information on the specimen prescribed by ASTM D5379 is shown in Fig. 1. The specimen is a $[0/90]_{10s}$ orthogonally laminated material made from Toray T800S prepreg that was molded in an autoclave. A two-axis strain gauge was attached at the mid-point between the upper and lower V-notches machined into the specimen (evaluation area), and oriented to measure strain in –45° and +45° directions. Shear strain can be calculated by inserting the strain values obtained from these two strain gauges into equation (1). Shear strain is a property needed to evaluate the shear modulus. In this test, strain gauges were attached on both the front and rear of the specimen. Calculating the mean of outputs obtained from strain gauges on both sides allows for more accurate measurement of the shear strain in the specimen, and confirms whether shear strain is being applied symmetrically on the front and rear of the specimen.

$$\gamma = |\varepsilon_{+45}| + |\varepsilon_{-45}|. \qquad \text{Equation (1)}$$

γ : Shear strain
ε_{+45} : Strain at +45°
ε_{-45} : Strain at –45°

Table 1 Test Conditions

Testing Machine	: AG-50kNX plus
Load Cell	: 50 kN
Test Jig	: ASTM D 5379 jig
Software	: TRAPEZIUM X (Single)
Test Speed	: 2 mm/min

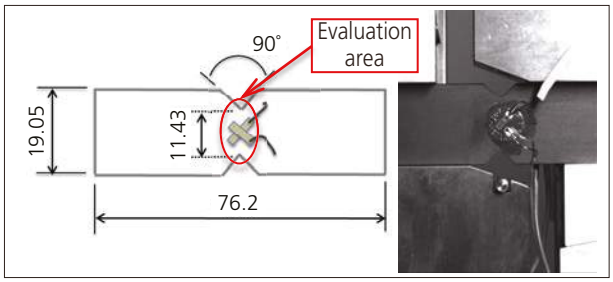

Fig. 1 Shape of Specimen

Fig. 2 Testing Apparatus

Fig. 3 Imaging Apparatus

The testing and imaging apparatus are shown in Fig. 2 and 3. Images captured using a TRViewX (Shimadzu Digital Video Extensometer) were gathered simultaneous to values obtained from the strain gauge outputs and specimen stress obtained by the testing apparatus. This made it easy to compare and evaluate images of the CFRP failure process against each specimen property values, something that was difficult to perform only with previous testing systems. Strain distribution can also be evaluated using digital image correlation (DIC, ARAMIS, GOMmbH) analysis of the images captured by TRViewX. To perform DIC analysis, paint must be sprayed on the specimen surface to create a random pattern on the front surface of the specimen.

Analytical Results

Each specimen property value obtained from this test is shown in Table 2. A photograph of the specimen after testing is shown in Fig. 4, a shear stress-normal strain curve is shown in Fig. 5 (strain values obtained from strain gauges), a shear stress-shear strain curve is shown in Fig. 6 (shear strain calculated from Equation (1)), and a shear stress-stroke curve is shown in Fig. 7. Table 2 shows that the results obtained for each shear property were highly reproducible. Fig. 5 and Fig. 6 show that the same strain values were obtained from the front and rear strain gauges, and highly symmetrical shear strain was applied to the specimen.

Table 2 Test Results

Specimen	Shear Modulus [GPa]	Shear Strength [MPa]
Test 1	4.62	136.0
Test 2	4.63	133.0
Test 3	4.50	131.0
Mean	4.58	133.0

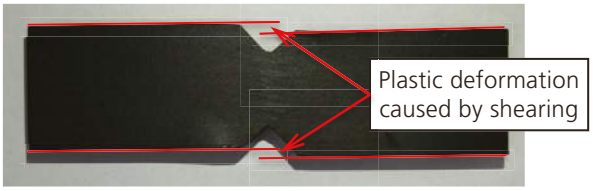

Fig. 4 Specimen After Testing

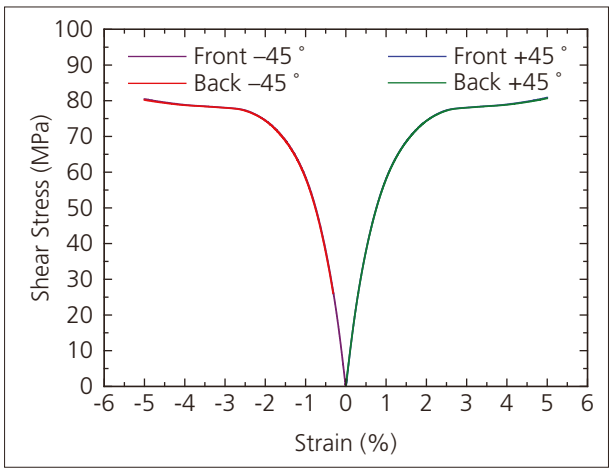

Fig. 5 Shear Stress-Normal Strain Curve

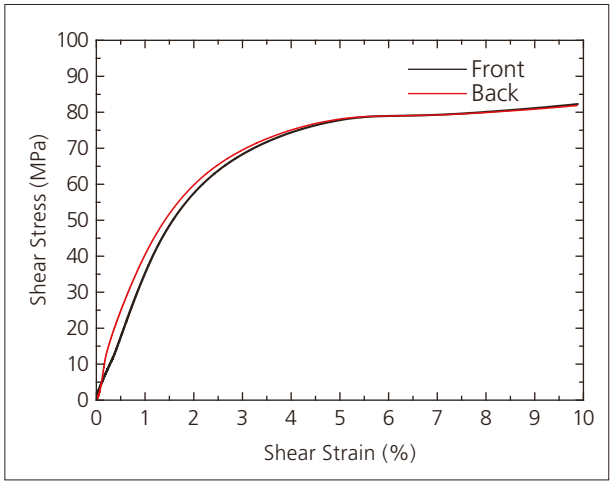

Fig. 6 Shear Stress-Shear Strain Curve

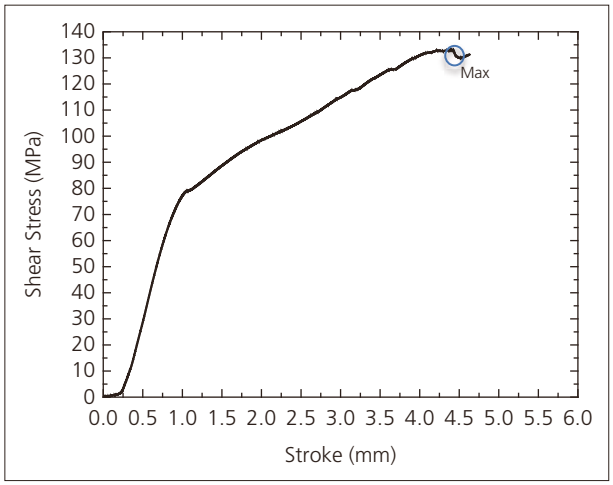

Fig. 7 Shear Stress-Stroke Curve

Failure of the specimen is shown in Fig. 8. Images of the shear strain distribution obtained by DIC analysis are shown in Fig. 9. The amount of strain occurring in the specimen is shown in terms of color, with low strain areas in cooler colors (black and blue) and high strain areas in warmer colors (orange and red). The images show that as the test progresses strain accumulates and is localized between the V-notches.

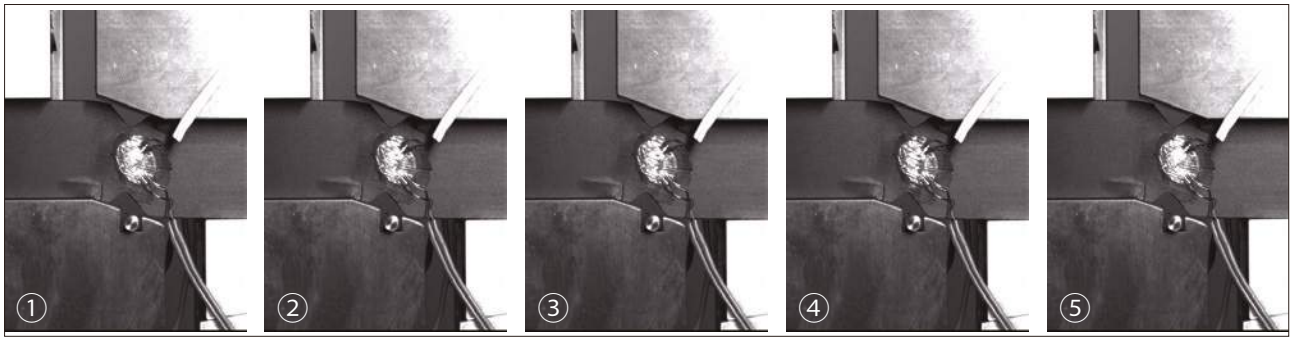

Fig. 8 Specimen e Failure Process (images show the point at which the specimen fails)

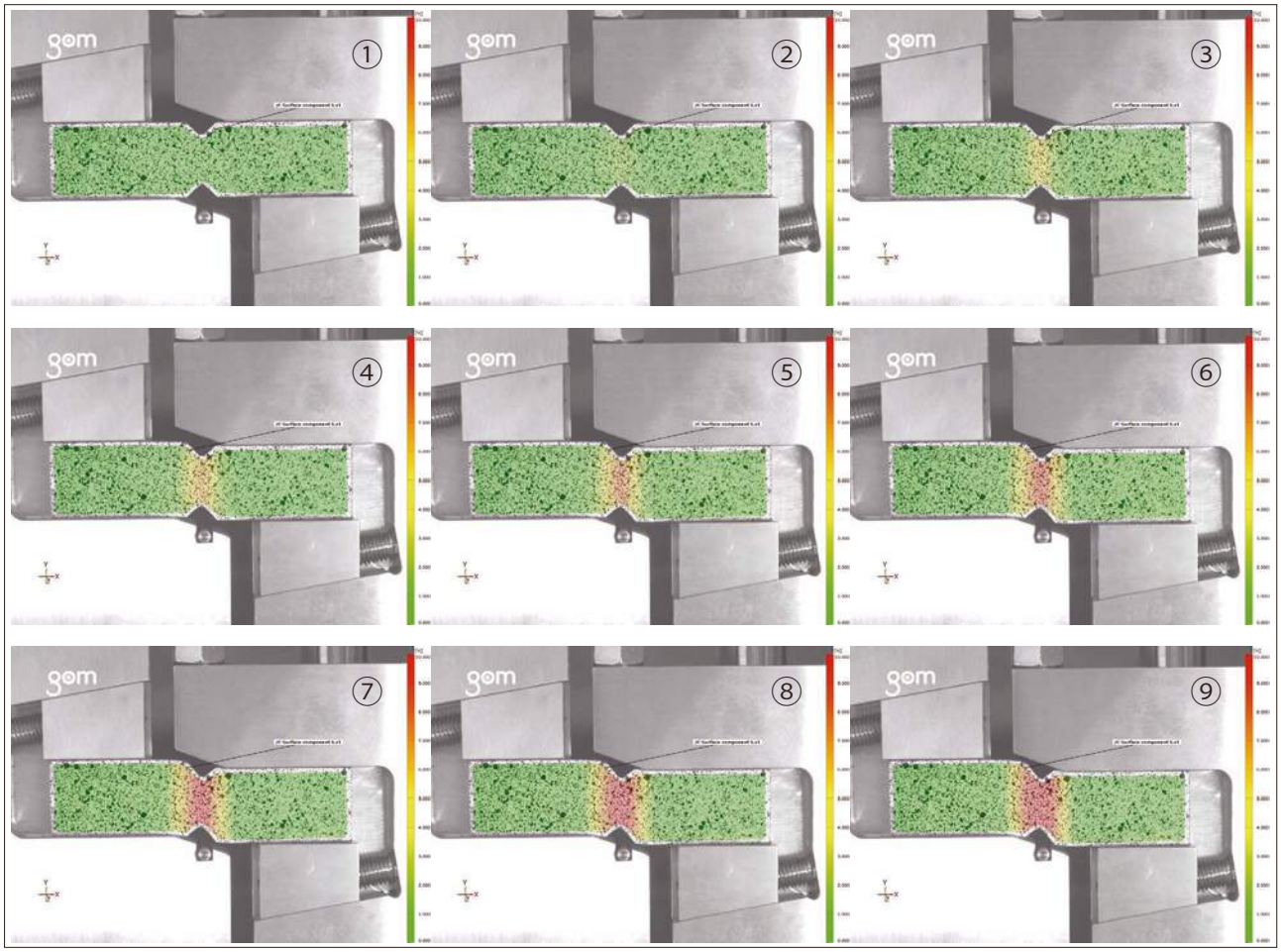

Fig. 9 Shear Strain Distribution (DIC analysis images)

Conclusion

We used this test system to successfully implement the V-notched beam method (ASTM D5379). In addition to evaluating the basic properties of shear modulus and shear strength, integrating a Digital Video Extensometer into the test system enabled us to capture reference data that can be used to elucidate the mechanism of failure of CFRP, allowing strain analysis to be performed in terms of specimen failure mode and DIC analysis.

First Edition: Aug. 2016

Shimadzu Corporation
www.shimadzu.com/an/

For Research Use Only. Not for use in diagnostic procedure.
This publication may contain references to products that are not available in your country. Please contact us to check the availability of these products in your country.

The content of this publication shall not be reproduced, altered or sold for any commercial purpose without the written approval of Shimadzu. Company names, product/service names and logos used in this publication are trademarks and trade names of Shimadzu Corporation or its affiliates, whether or not they are used with trademark symbol "TM" or "®". Third-party trademarks and trade names may be used in this publication to refer to either the entities or their products/services. Shimadzu disclaims any proprietary interest in trademarks and trade names other than its own.

The information contained herein is provided to you "as is" without warranty of any kind including without limitation warranties as to its accuracy or completeness. Shimadzu does not assume any responsibility or liability for any damage, whether direct or indirect, relating to the use of this publication. This publication is based upon the information available to Shimadzu on or before the date of publication, and subject to change without notice.

© Shimadzu Corporation, 2016

SHIMADZU
Excellence in Science

Application News

No.i251

Material Testing System

Shear Test of Composite Material (V-Notched Rail Shear)

Introduction

Carbon fiber reinforced plastic (CFRP) do not oxidize or rust and have a higher specific strength and stiffness than existing materials. Applications of CFRP are being investigated, with a focus on applications as industrial products that require strength and durability. Compared to existing homogeneous materials, composite materials like CFRP are anisotropic, and display complex failure behaviors as a result of tension, compression, bending, in-plane shear, out-of-plane shear, or a combination of these stresses arising from loading in the principal-axis direction. In recent years, use of CAE analysis in industry has become widespread since it can reduce numbers of prototypes and reduce the cost of new product development. Because values for each of the stress properties stated above are needed to increase precision when predicting product characteristics during product design, there is a strong demand for test methods able to evaluate pure failure behaviors in CFRP.

There are various tests methods for evaluating composite materials. Of these methods, two commonly used in-plane shear test methods to test in the direction of fibers in fiber reinforced composite materials and to test textile laminated materials are the Iosipescu method (ASTM D5379) that applies an asymmetrical four-point bending load to a specimen cut with notches, and method (ISO 14129) that applies a ±45° tensile load on laminated materials. We used the V-notched rail shear method (ASTM D7078) that can be used to test in-plane shear. Because this method uses a large gauge area on the specimen, it can accommodate specimens without holes and CRFP laminate materials that have discontinuous fibers.

Measurement System

The equipment configuration is shown in Table 1. Information on the specimen prescribed by ASTM D7078 is shown in Fig. 1. The specimen is a $[0/90]_{10s}$ orthogonally laminated material made from Toray T800S prepreg that was molded in an autoclave. The specimen has a 31-mm evaluation area (see Fig. 1), and two-axis strain gauges attached at the mid-point between the V-notches (center of evaluation area) that are able to measure strain in –45° and +45° directions. Shear strain can be calculated by inserting the strain values obtained from these two strain gauges into equation (1). Shear strain is a property needed to evaluate the shear modulus.

$$\gamma = |\varepsilon_{+45}| + |\varepsilon_{-45}|. \qquad \text{Equation (1)}$$

γ : Shear strain
ε_{+45} : Strain at +45°
ε_{-45} : Strain at –45°

In this test, strain gauges were attached on both the front and rear of the specimen. Calculating the mean of outputs obtained from strain gauges on both sides allows for more accurate measurement of the shear strain in the specimen, and confirms whether shear strain is being applied symmetrically on the front and rear of the specimen.

Table 1 Test Conditions

Testing Machine	: AG-50kNX plus
Load Cell	: 50 kN
Test Jig	: ASTM D7078 jig
Software	: TRAPEZIUM X (Single)
Test Speed	: 2 mm/min

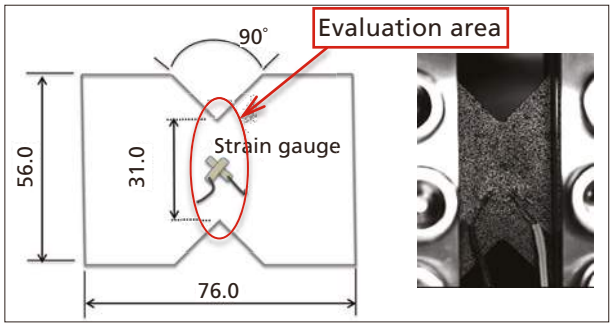

Fig. 1 Shape of Specimen

Fig. 2 Testing Apparatus

Fig. 3 Imaging Apparatus

The testing and imaging apparatus are shown in Fig. 2 and Fig. 3. Images captured using a TRViewX (Shimadzu Digital Video Extensometer) were gathered simultaneous to values obtained from the strain gauge outputs and specimen stress obtained by the testing apparatus. This made it easy to compare and evaluate images of the CFRP failure process against each specimen property values, something that was difficult to perform only with previous testing systems. Strain distribution can also be evaluated using digital image correlation (DIC, ARAMIS, GOMmbH) analysis of the images captured by TRViewX. To perform DIC analysis, paint must be sprayed on the specimen surface to create a random pattern on the front surface of the specimen.

Analytical Results

Each specimen property value obtained from this test is shown in Table 2. A photograph of the specimen after testing is shown in Fig. 4, a shear stress-normal strain curve is shown in Fig. 5 (strain values obtained from strain gauges), a shear stress-shear strain curve is shown in Fig. 6 (shear strain calculated from Equation (1)), and a shear stress-stroke curve is shown in Fig. 7. Table 2 shows that the results obtained for each shear property were highly reproducible. Fig. 5 and Fig. 6 show that the same strain values were obtained from the front and rear strain gauges, and highly symmetrical shear strain was applied to the specimen.

Table 2 Test Results

Specimen	Shear Modulus [GPa]	Shear Strength [MPa]
Test 1	4.63	121.72
Test 2	4.55	120.00
Test 3	4.58	120.05
Mean	4.59	120.60

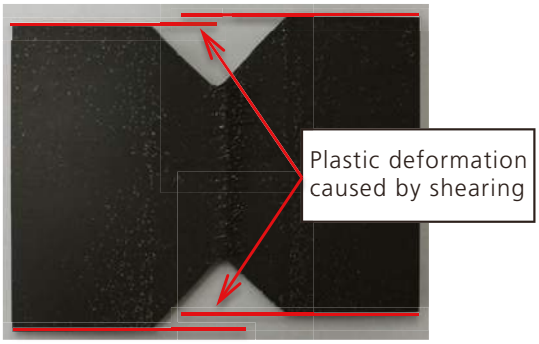

Fig. 4 Specimen After Testing

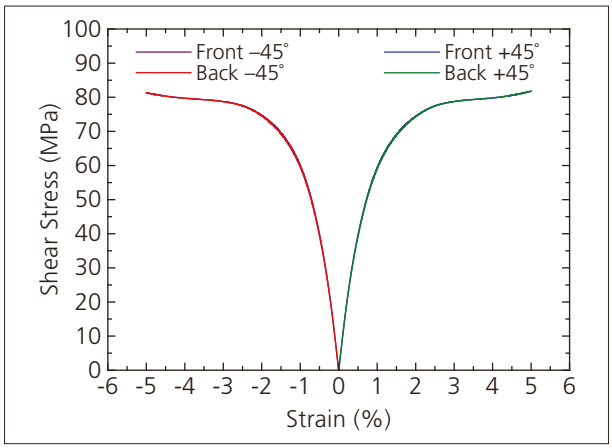

Fig. 5 Shear Stress-Normal Strain Curve

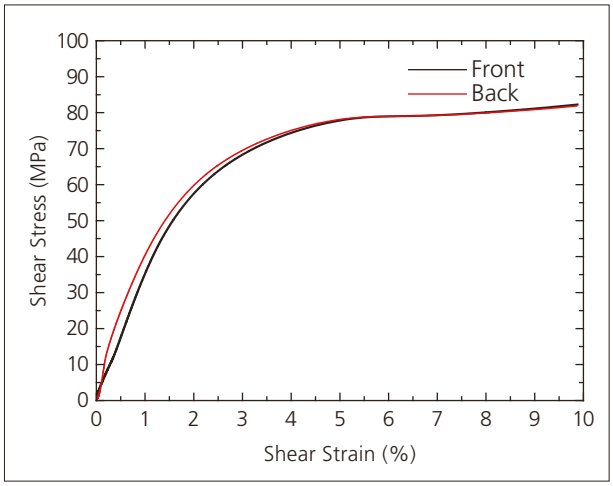

Fig. 6 Shear Stress-Shear Strain Curve

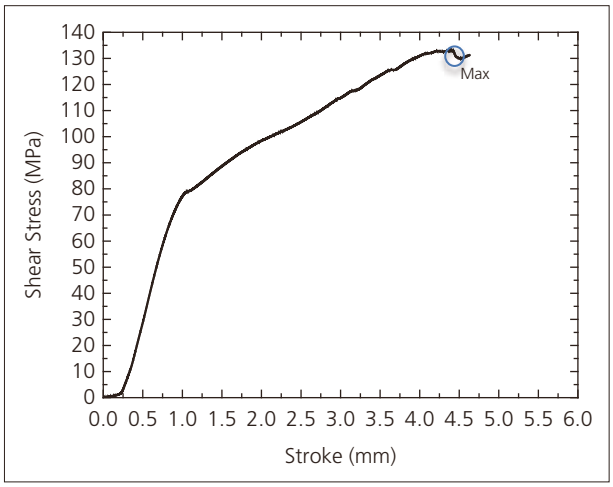

Fig. 7 Shear Stress-Stroke Curve

Failure of the specimen is shown in Fig. 8. A crack that appears close to the upper notch quickly propagates down toward the bottom notch during a simultaneous decrease in test force. Images of the shear strain distribution obtained by DIC analysis are shown in Fig. 9. The amount of strain occurring in the specimen is shown in terms of color, with low strain areas in cooler colors (black and blue) and high strain areas in warmer colors (orange and red). The images show that as the test progresses strain accumulates and is localized between the V-notches.

Fig. 8 Specimen Failure Process (images show the point at which the specimen fails)

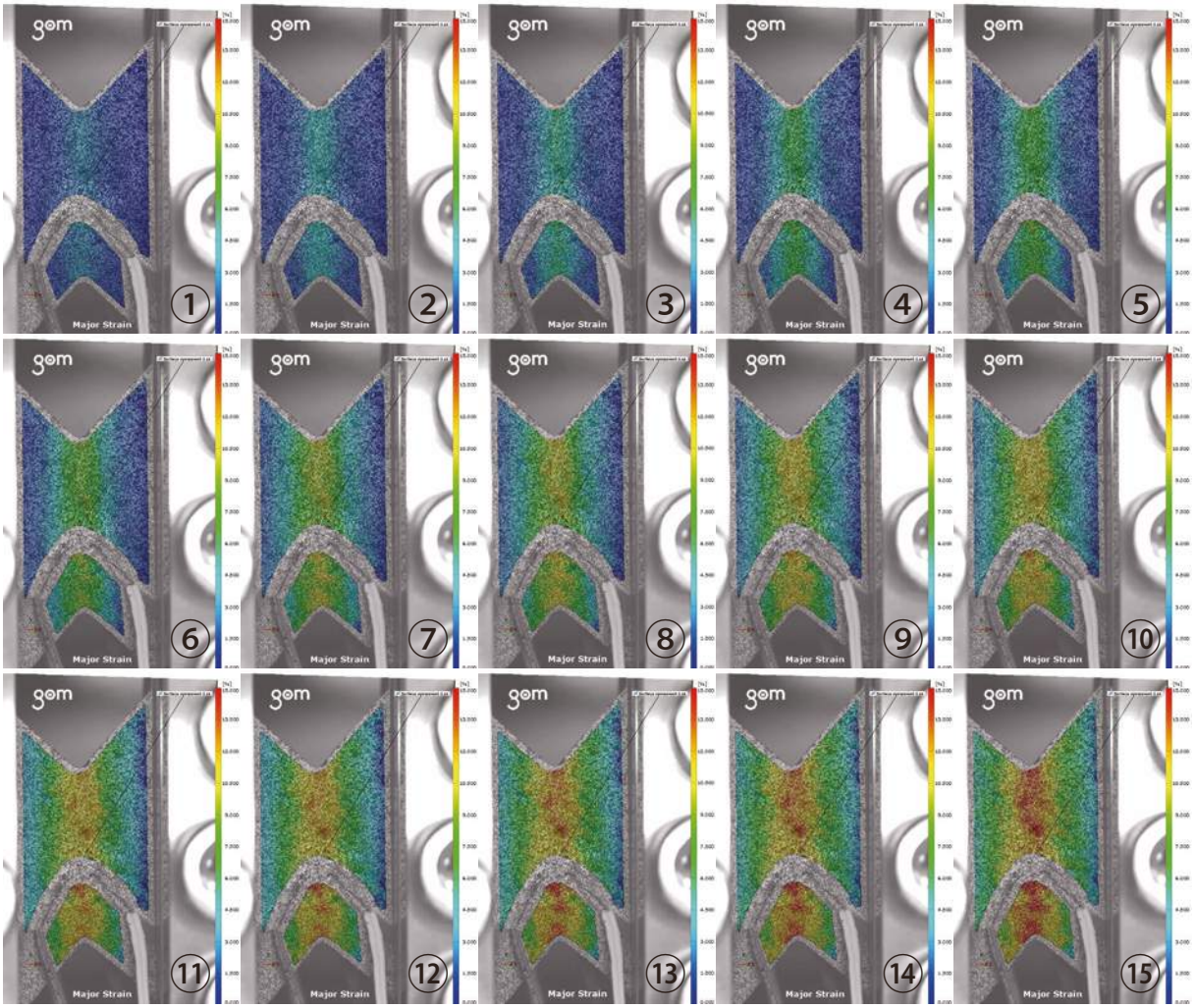

Fig. 9 Shear Strain Distribution (DIC analysis images)

Conclusion

We used this test system to successfully implement the V-notched rail shear method (ASTM D7078). In addition to evaluating the basic properties of shear modulus and shear strength, integrating a Digital Video Extensometer into the test system enabled us to capture reference data that can be used to elucidate the mechanism of failure of CFRP, allowing strain analysis to be performed in terms of specimen failure mode and DIC analysis.

First Edition: Aug. 2016

Shimadzu Corporation
www.shimadzu.com/an/

For Research Use Only. Not for use in diagnostic procedure.
This publication may contain references to products that are not available in your country. Please contact us to check the availability of these products in your country.

The content of this publication shall not be reproduced, altered or sold for any commercial purpose without the written approval of Shimadzu. Company names, product/service names and logos used in this publication are trademarks and trade names of Shimadzu Corporation or its affiliates, whether or not they are used with trademark symbol "TM" or "®". Third-party trademarks and trade names may be used in this publication to refer to either the entities or their products/services. Shimadzu disclaims any proprietary interest in trademarks and trade names other than its own.

The information contained herein is provided to you "as is" without warranty of any kind including without limitation warranties as to its accuracy or completeness. Shimadzu does not assume any responsibility or liability for any damage, whether direct or indirect, relating to the use of this publication. This publication is based upon the information available to Shimadzu on or before the date of publication, and subject to change without notice.

© Shimadzu Corporation, 2016

SHIMADZU
Excellence in Science

Application News

Material Testing System MCT

Compression-Rupture Test of Carbon Fibers with Different Tensile Characteristics Shimadzu Micro Compression Testing

No. SCA_300_037

■ Introduction

As the result of recent progress of research and development, carbon fiber materials have been put to practical use in a wide range of implements, including space aircraft parts, sporting goods like golf club shafts and tennis rackets, structure materials that must transmit X-rays, and acoustic materials.

A group of high-quality carbon fibers is further classified, according to its tensile strength, into several groups. One of these is a high-strength fiber group that features in excellent tensile strength; another is a high-elasticity fiber group characterized by high flexibility, but with a tensile strength of no more than around 2,000 MPa.

As described above, data on mechanical properties are indispensable information for classifying fibers.

The following is an example of tests for evaluation of physical behaviors under a compressive force applied to carbon fibers (single fibers) having different tensile strength levels with Shimadzu Micro Compression Testing Machine MCT.

■ Testing Conditions

(1) Testing mode: compression test
(2) Testing load: 200 gf
(3) Loading rate constant: 1 (4,230 gf/sec.)
(4) Calculation of strength: Compression strength is calculated by the following equation. *1

$$ST = 2 \cdot P \cdot \pi \cdot d \cdot L$$

where:
ST: tensile strength (kg/mm^2)
P: compression strength (kgf)
d: diameter of fiber (mm)
L: length of fiber (mm)

Note *1: from JIS A1113-1976 Method of tests for splitting tensile strength of concrete

■ Test Piece

(1) Name: Carbon fibers (PAN type carbon fibers)

(2) Types: 1 (high-ductility type)

2 (high-strength type)

3 (ultra-high elasticity type)

(3) Shape: See Fig. 1

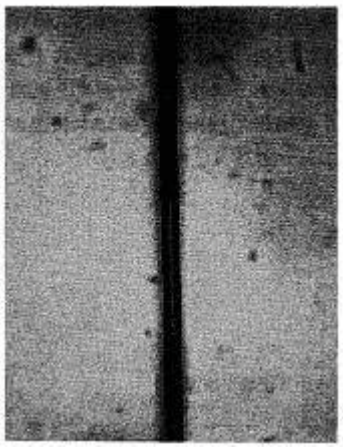

Fig. 1 A Microscopic photograph of Test Piece before Test

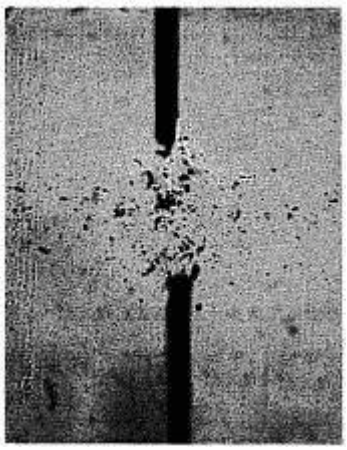

Fig. 2 A Microscopic photograph of Test Piece after Test

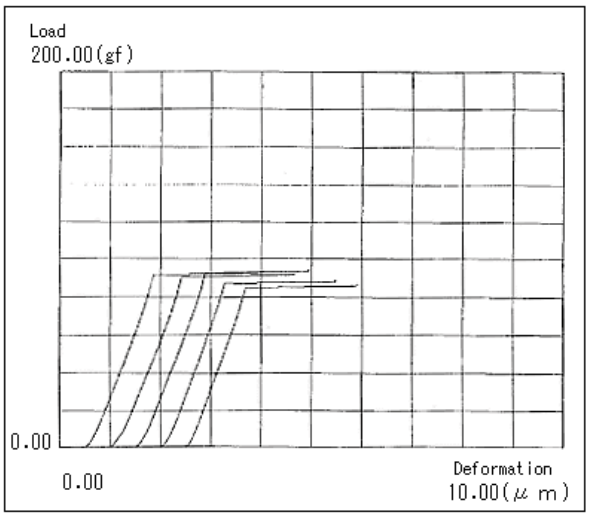

Fig. 3 Load- Deformation Curves of High Ductility Samples

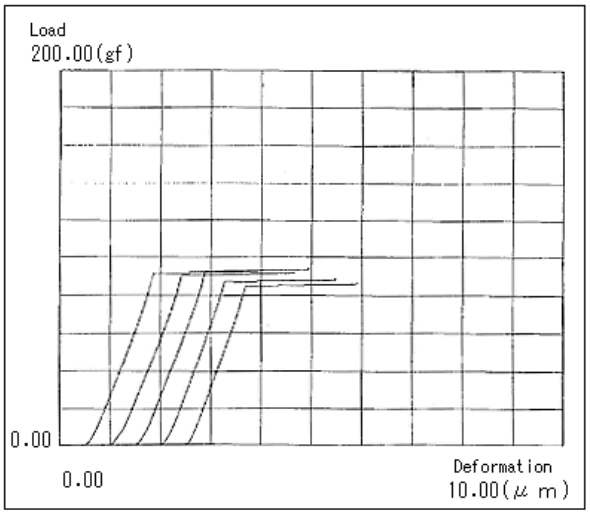

Fig.2 Load-Deformation Curves of High Ductility Samples

Fig. 4 Load- Deformation Curves of High Ductility Samples

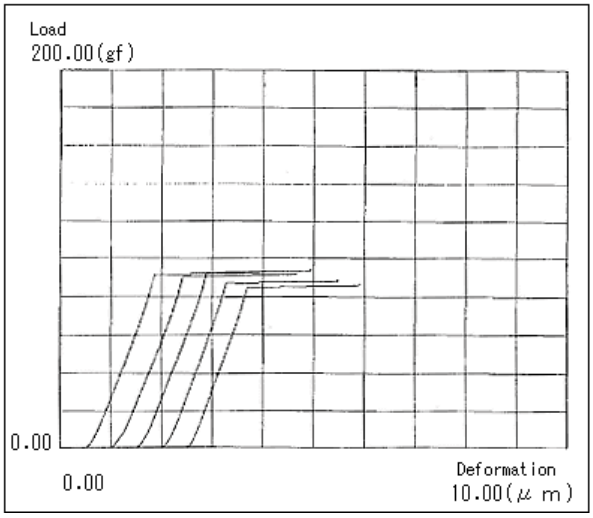

Fig. 5 Load- Deformation Curves of High Ductility Samples

Type of test piece	Compression-rupture strength(kgf/mm^2)	Standard deviation (kgf/mm^2)
High-ductility type	149.90	3.23
High-strength type	151.09	6.34
Ultra-high elasticity type	68.87	4.37

Table 1 Results of Compression-Rupture Test of Carbon Fibers

Note: The length of the indenter diameter (50 mm) was used for the length of fiber because the test piece was extraordinarily long.

■ Test Results

Table 1 shows a summary of test data, and Figs. 2-4 show the compression-rupture strength and the overlapping view of load-deformation curves for each test piece.

The difference of behavior between test pieces are observable in the load-deformation curves of Figs. 2-4.

The test pieces of the high-ductility type and the high-strength type have similar compression-rupture strength, while the ultra-high elasticity type has a remarkably low compression-rupture strength. (Refer to Table 1)

Admitting some deviation among the test data as a result of the surface conditions of the test pieces, the test results ensure that this testing machine is useful and effective for evaluation of mechanical properties of single fibers, provided that data are processed statistically.

* Please be advised that data obtained before the implementation of the current Weights and Measures Law may be presented in terms of gravimetric unit.

For Research Use Only. Not for use in diagnostic procedures.
The content of this publication shall not be reproduced, altered or sold for any commercial purpose without the written approval of Shimadzu. The information contained herein is provided to you "as is" without warranty of any kind including without limitation warranties as to its accuracy or completeness. Shimadzu does not assume any responsibility or liability for any damage, whether direct or indirect, relating to be the use of this publication. This publication is based upon the information available to Shimadzu on or before the date of publication, and subject to change without notice.

SHIMADZU
Excellence in Science

Application News

Material Testing System AG-X

No. SCA_300_059

Observation of fracture in CFRP tensile test

CFRP (carbon fiber reinforced plastic) has attracted attention as a high-performance composite material with high strength and rigidity, yet low in weight, and is being applied in various fields, such as for aircraft, railroad vehicles, automobiles and civil engineering. This example describes evaluating the characteristics of a flat plate specimen of CFRP material when a tensile load is applied (tensile test) and observing the fracture status. Tensile testing consisted of static testing of material strength and measuring the modulus of elasticity using a precision universal testing machine. In addition, high-rate tensile impact test was also performed. In the latter case, a high-speed video camera was used to record specimen fracture, which allowed capturing image data of the instant the CFRP material fractured.

■ Test specimen

The tensile test specimen tested in this example is shown in figure 1. Included 50 mm long CFRP tabs attached to both ends of the CFRP strip with thermosetting resin adhesive. Reinforcing the grip area with tabs ensures a stable tensile test with good reproducibility.

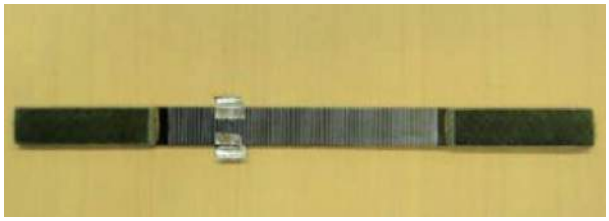

Figure 1: CFRP test specimen

Specimen details are as follows:

1) Material: unidirectional CFRP
2) Shape: strip (with tabs on both ends)
3) Specimen dimensions: for static tensile testing 200(L) x 12.5(W) x 1(T) mm. For recording image of impact fracture 70(L) x 6.25(W) x 0.3(T) mm

■ Static tensile test

A strain gauge type extensometer was attached to the specimen and a tensile test was performed using a precision testing machine. The extensometer was removed when strain exceeded the elasticity measurement range. It is also possible to measure strain by affixing a strain gauge instead of an extensometer. Tensile test parameters are indicated below.

(1) Tensile rate: 10 mm/min
(2) Grip distance: 100 mm
(3) Test force detection: 50 KN load cell
(4) Extensometer gauge length: 50 mm
(5) Elasticity calculation range: 5/10,000 to 25/10,000 strain

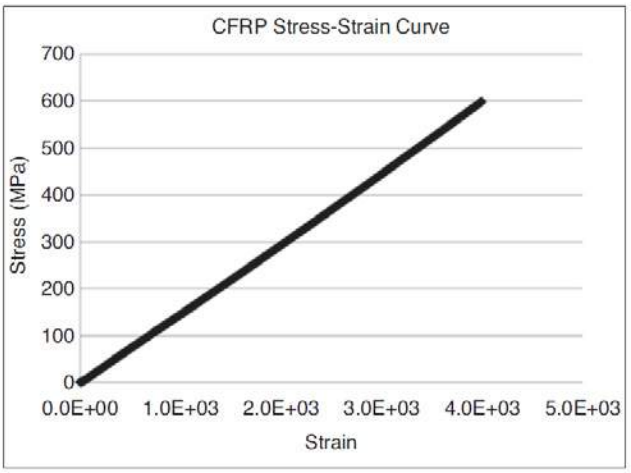

Figure 2: Static test results

The elasticity of CFRP specimen can be determined by calculating the slope of the given strain region (elasticity calculation range) in the stress-strain curve (figure 2) obtained from test results. Tensile strangth can be determined from the maximum stress in the stress-displacement curve (figure 3) before the specimen breaks.

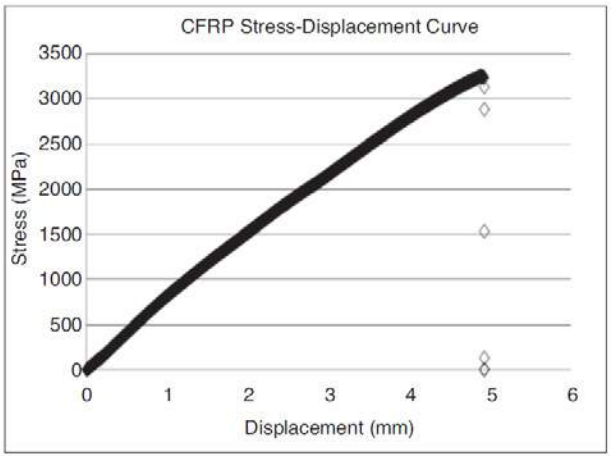

Figure 3: Static test results

The following values were obtained from the measurement data.

(1) Tensile strength: 346 GPa
(2) Elasticity: 148 GPa

The post-test status of the specimen is shown in figure 4. Compared to the starting status in figure 1, it clearly shows how the fibers within the resin have failed.

Figure 4: Specimen status after static test

■ Static tensile test

To verify functionality, development of composite materials involves not only static Static strength testing, but also involves the objective of ensuring active safety. Consequently, it is important to determine the shock strength and understand the process of fracture propagation. Therefore, the fracture process during tensile chock testing of a CFRP specimen was observed by combining a high-speed video camera with high-rate tensile shock test machine. Observation conditions are indicated below.

Specimen tensile rate:	6 m/s
Grip distance:	30 mm
Camera lens:	105 mm macro, with 2 x teleconverter
Camera lighting:	strobe
Camera trigger:	signal synchronized with tensile displacement is sent from testing machine to camera.

The setup used to record video of the test is shown in figure 5, with a high-speed video camera mounted about 450 mm in front of the specimen. Recording was activated by an external start trigger signal sent from the testing machine to the camera, which was synchronized to the tensile displacement. A strobe light synchronized to the video timing was used as lighting.

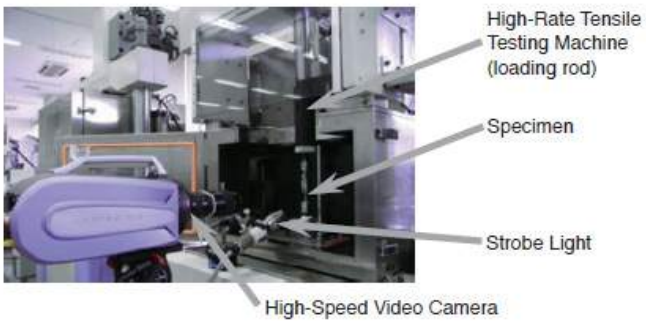

Figure 5: Setup of high-rate shock test

Using this test configuration, a load was applied to the CFRP specimen according to the parameters indicated above and a high-speed camera captured the instant of fracture, at 250.000 frames per second. This image data shown in figure 6.

This shows 8 consecutive frames, from (1) TO (8), with an interval of 4 microseconds between each frame. This camera features highly detailed image resolution of 312 horizontal by 260 vertical pixels that is constant, regardless of the frame rate.

This example shows, combining a high-speed video camera and material testing machine makes it possible to evaluate material properties and observe fracture behavior at the same time. This enables supporting a wide range of material development applications, from developing individual functionally enhanced resins to developing composite materials.

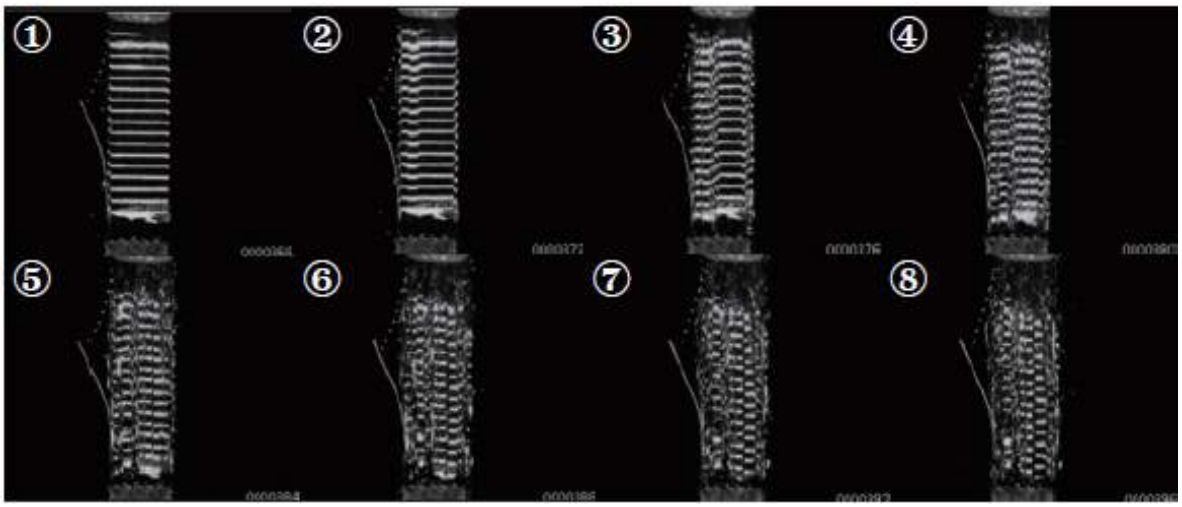

Figure 6: Images of specimen during fracture

For Research Use Only. Not for use in diagnostic procedures.
The content of this publication shall not be reproduced, altered or sold for any commercial purpose without the written approval of Shimadzu. The information contained herein is provided to you "as is" without warranty of any kind including without limitation warranties as to its accuracy or completeness. Shimadzu does not assume any responsibility or liability for any damage, whether direct or indirect, relating to be the use of this publication. This publication is based upon the information available to Shimadzu on or before the date of publication, and subject to change without notice.

SHIMADZU
Excellence in Science

Ultrasonic Fatigue Testing System with an Average Stress Loading Mechanism

For Gigacycle Fatigue Tests with Average Stress Loaded

Actual components are rarely used under conditions in which the average stress is zero. Despite this, the USF-2000A, a standard ultrasonic fatigue testing system, can only perform testing under zero average stress conditions.
Using an ultrasonic fatigue testing system equipped with an average stress loading mechanism, gigacycle fatigue tests can be performed with average tensile stress loaded.

System Appearance

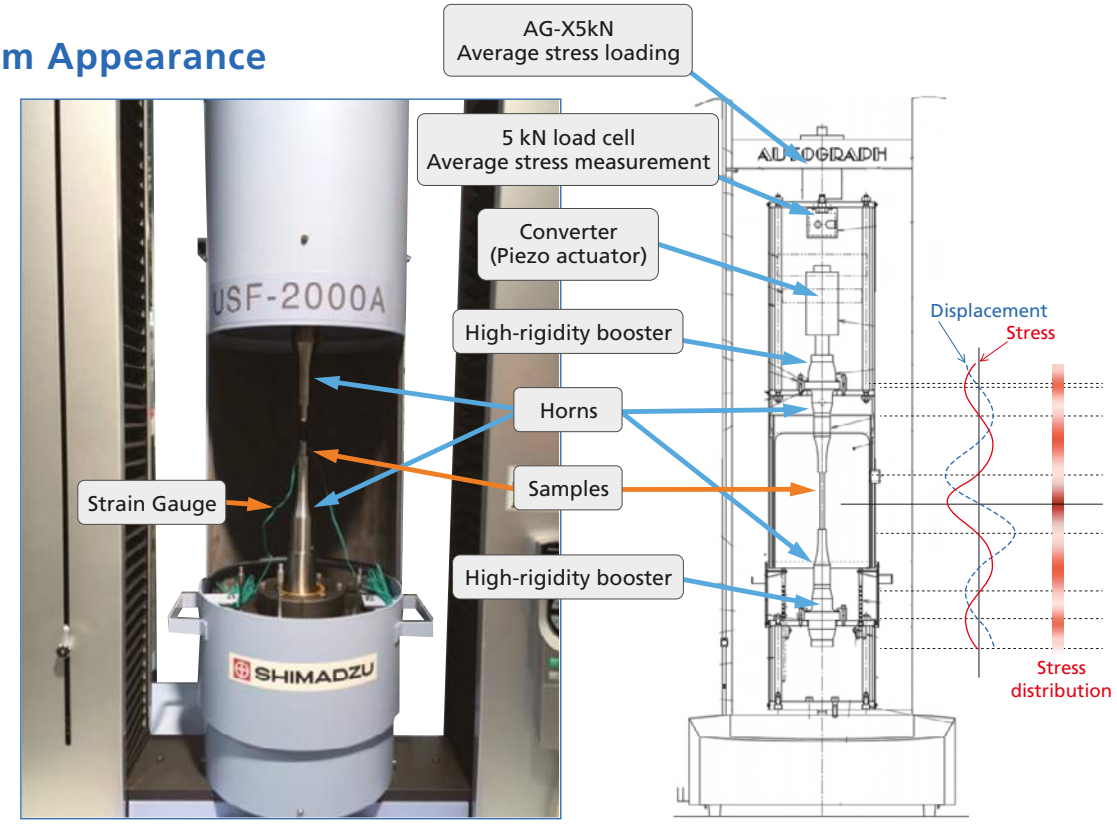

Ultrasonic Fatigue Testing System Effective for Gigacycle Fatigue Tests

With fatigue tests of high-strength steels, it is evident that internal fracture (fish-eye fracture), which is caused by inclusions and other micro defects, occurs at 107 cycles or more, a value considered the conventional fatigue limit.
An ultrasonic fatigue testing system is extremely effective when performing this sort of gigacycle fatigue test. (With a 100 Hz fatigue testing system, this would take 3 years, but if a 20 kHz ultrasonic fatigue testing system is used, testing can be completed in one week.)

Main Specifications

1) Test Frequency: 20 kHz ± 500 Hz

- The recommended test range is 20 kHz ± 30 Hz.
- The test frequency is determined by the resonance frequency of the sample.

2) Horn End Face Amplitude

Min. approx. ±10 µm
Max. approx. ±50 µm

- The minimum and maximum amplitudes are the end face amplitude values at amplitude outputs of 20 % and 100 % respectively. Accordingly, the minimum and maximum amplitude values will change somewhat depending on the shape of the sample.

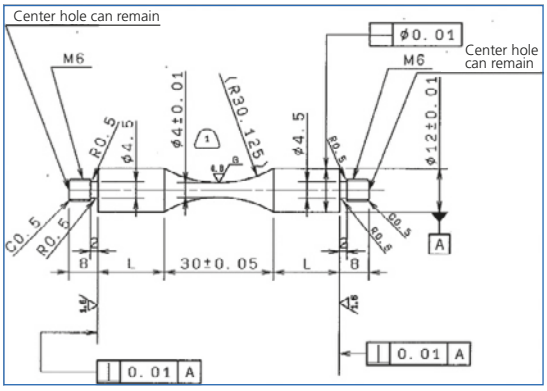

Standard Circular Tapered Sample

3) Test Stress

Standard circular tapered sample
Stress Min. 237 MPa
Max. 1186 MPa

- The test stress range can be changed by changing the sample shape.
- The minimum and maximum values are calculated with the end face amplitude values of 10 µm and 50 µm respectively.
- These are the values when the stress is within the elasticity range.

4) Average Stress

Max. 1.5 kN (tensile only)

- Average stress loads exceeding 1.5 kN are possible, but will have an impact on the service life of the horn.

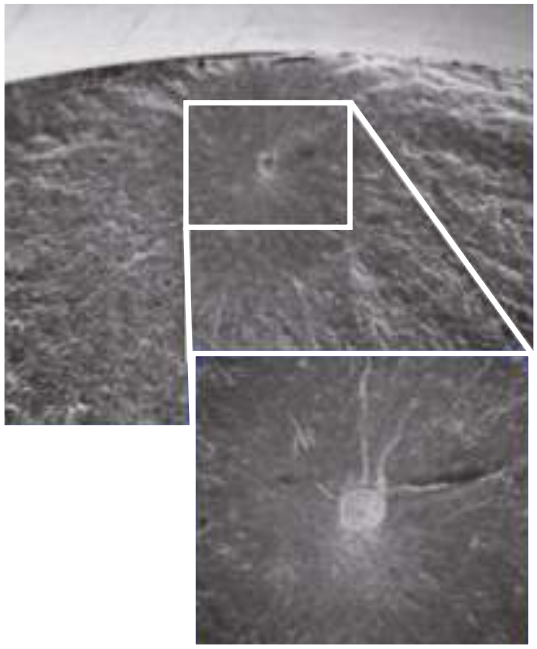
Surface of the Fatigued Fracture Originating from the Inclusion

■ Components

1	Ultrasonic resonance system Power supply, converter, booster (1 pair), horn (1 pair)
2	Personal computer (OS Windows 7) ADA/PIO interface board
3	Software Ultrasonic test control measurement software
4	Cooling system Air dryer, air piping • A separate 140 L/min air source is required.
5	Strain meter unit (option)
6	AG-X plus Autograph 5 kN + 250 extension
7	Average stress loading mechanism

Shimadzu Corporation
www.shimadzu.com/an/

For Research Use Only. Not for use in diagnostic procedure.
This publication may contain references to products that are not available in your country. Please contact us to check the availability of these products in your country.
Company names, product/service names and logos used in this publication are trademarks and trade names of Shimadzu Corporation or its affiliates, whether or not they are used with trademark symbol "TM" or "®". Third-party trademarks and trade names may be used in this publication to refer to either the entities or their products/services. Shimadzu disclaims any proprietary interest in trademarks and trade names other than its own.

The contents of this publication are provided to you "as is" without warranty of any kind, and are subject to change without notice. Shimadzu does not assume any responsibility or liability for any damage, whether direct or indirect, relating to the use of this publication.

© Shimadzu Corporation, 2016

First Edition: August 2016

SHIMADZU

Application News

No.i244

Material Testing System

Tensile Test for Metallic Materials Using Strain Rate Control and Stress Rate Control

Introduction

International standards for tensile testing of metallic materials have been revised as specified in ISO 6892 and JIS Z2241, such that strain rate control, where strain is measured with an extensometer, has recently been added as a test item to the current stress rate control method, in which a load is applied to a material until its yield point is reached. As a result, it can be assumed that there will be situations where both stress rate control and strain rate control tensile testing of metallic materials will be required.
Here, we introduce examples of strain rate control and stress rate control tensile testing of metallic samples, including cold-rolled steel, austenitic stainless steel, aluminium alloy and brass, according to ISO 6892, using the Shimadzu Autograph AG-50kNX Precision Universal Tester, and the SSG50-10H strain gauge type one-touch extensometer (Fig. 1, Fig. 2).

Fig. 1 Overview of Universal Testing System

Fig. 2 Specimen and Jigs for Tensile Testing

Specimens and Test Conditions

Information on the sample specimens are shown in Table 1, and the test conditions are shown in Table 2.

Table 1 Test Specimens

Sample Name	A	B	C	D
Material	Cold-rolled steel	Stainless steel (austenitic)	Aluminium alloy	Brass
Sample size	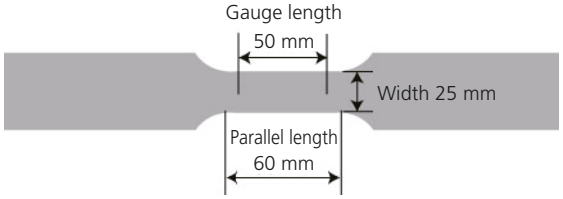 Width 25 mm, thickness 1 mm, gauge length 50 mm, parallel length 60 mm (JIS Z 2241 No. 5 test specimen)			

Table 2 Test Conditions

1) Load cell capacity	50 kN
2) Jig	50 kN Non-shift wedge type grips (file teeth for flat specimen)
3) Test speed	See Table 3
4) Test temperature	Ambient temperature
5) Software	TRAPEZIUMX (single)

Fig. 3 shows an image diagram of the test speed, and Table 3 and Table 4 show the applicable test speeds for the strain control and stress control tests, respectively.

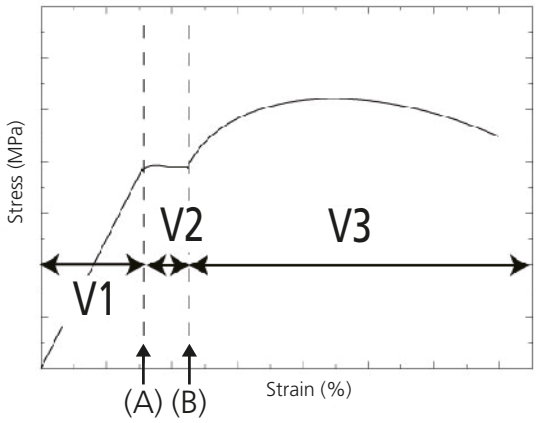

(A): Upper yield point (or its corresponding point)
(B): Upper limit of strain measurement (point after proof strength point)

Fig. 3 Image of Test Strain Rate

Table 3 Test Strain Rate (based on strain rate control)

V1: Strain rate	0.00025/s (1.5 %/min)
V2: Strain rate	0.00025/s (1.5 %/min)
V3: Predicted strain rate	0.0067/s (40 %/min)

Table 4 Test Stress Rate (based on stress rate control)

V1: Stress rate	10 MPa/s
V2: Strain rate	0.00083/s (5 %/min)
V3: Predicted strain rate	0.0067/s (40 %/min)

Test Results

Fig. 4 shows a diagram of the stress – stroke displacement for each sample using strain-rate control, and Table 5 shows their characteristic values. In Fig. 4, the point at which the stress becomes discontinuous, as indicated by the jump in the stress-stroke displacement curve, corresponds to the point at which the strain rate is switched.

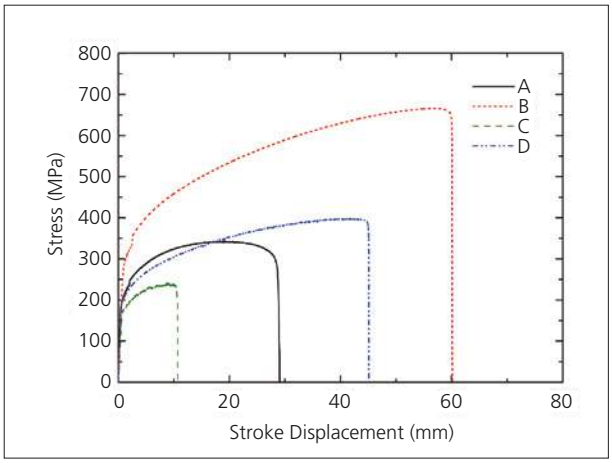

Fig. 4 Test Results for Each Metallic Material (stress-stroke curve based on strain rate control)

Table 5 Test results (Average n = 3)

Sample Name	Elastic Modulus (GPa)	0.2 % Proof Strength (MPa)	Tensile Strength (MPa)	Elongation at Break (%)
A (cold-rolled steel)	194	185.5	341.5	43.3
B (stainless steel)	200	278.5	660.8	55.0
C (aluminum)	71	170.1	236.3	13.0
D (brass)	109	193.1	398.1	49.1

Note 1) Strain rate refers to the amount of increase in strain, obtained using an extensometer to measure the gauge length of a test specimen, per unit time.
Note 2) Predicted strain rate was obtained using the displacement of the testing machine crosshead at each point in time and the test specimen's parallel length. Thus, it is defined as the increase in strain of the specimen's parallel length per unit time.

Fig. 5 (a) – (d) shows the strain rate and predicted strain rate obtained from tensile testing of the respective metallic materials using strain rate control. The red solid lines show the strain rate, the blue solid lines the predicted strain rate, and the black broken lines show the stress. In addition, the green dotted lines represent the permissible value ±20 % relative tolerance in the strain rate control (as specified in ISO 6892). As for the actual load rate, it is clear that the values are well within the permissible strain rate control range, indicating excellent strain rate control. Regarding samples A and B, displacement is measured up to 2 % of the gauge length using an extensometer. In the case of samples C and D, the strain measured using an extensometer was only up to 0.8 %, because of the appearance of serration when strain corresponding to about 1 % was applied.

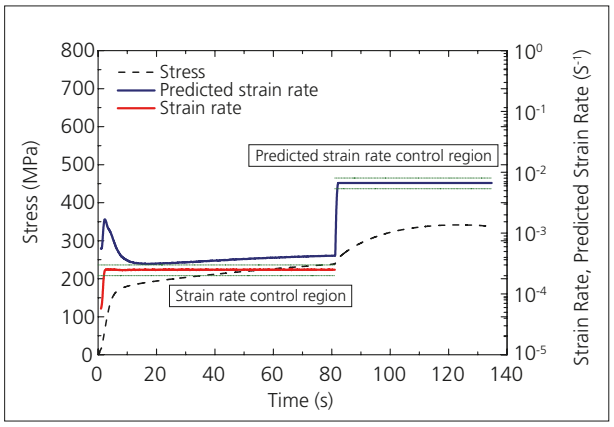

Fig. 5 (a) Test Results (Sample A)

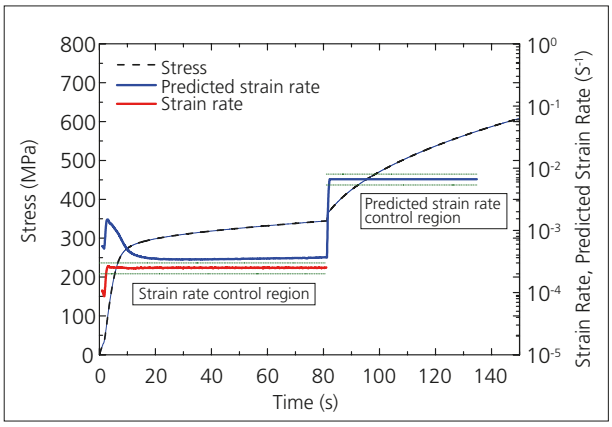

Fig. 5 (b) Test Results (Sample B)

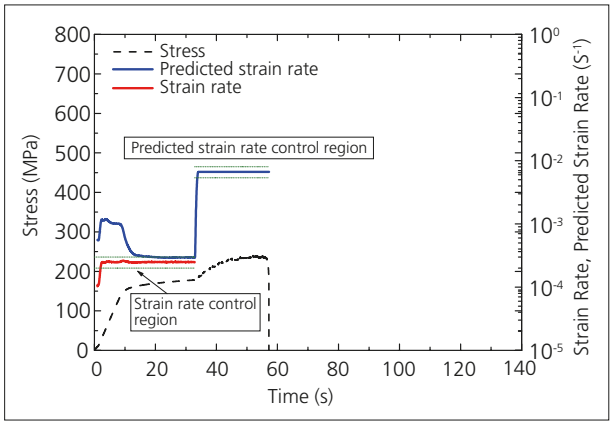

Fig. 5 (c) Test Results (Sample C)

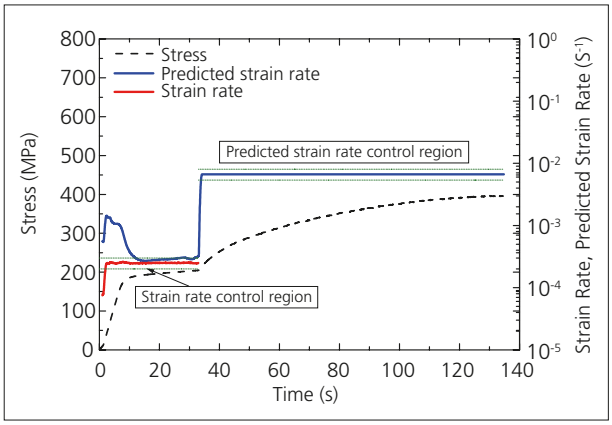

Fig. 5 (d) Test Results (Sample D)

Fig. 6 shows the stress-stroke displacement curve diagram obtained from tensile testing of each of the metallic materials using stress rate control, and the characteristic values are shown in Table 6.

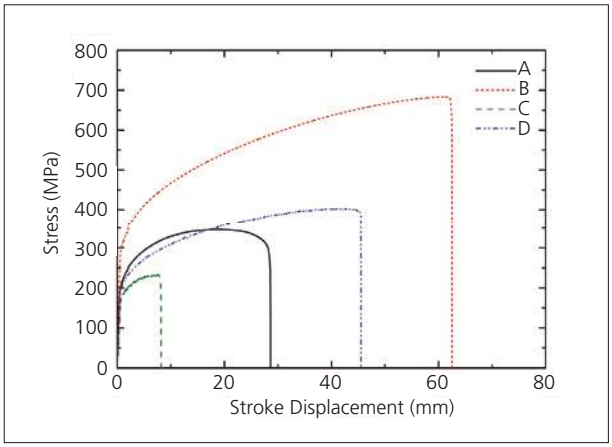

Fig. 6 Test Results (stress-stroke curve based on stress rate control)

Table 6 Test Results (Average n = 3)

Sample Name	Elastic Modulus (GPa)	0.2 % Proof Strength (MPa)	Tensile Strength (MPa)	Elongation at Break (%)
A (cold-rolled steel)	194	193.3	349.3	42.0
B (stainless steel)	205	290.7	687.0	54.8
C (aluminum)	69	177.0	233.5	12.6
D (brass)	112	196.7	405.5	48.8

Fig. 7 (a) – (d) shows the strain rate and predicted strain rate obtained from tensile testing of the respective metallic materials using stress rate control. The pink solid lines show the stress rate, the blue solid lines the predicted strain rate, and the black broken lines show the stress.

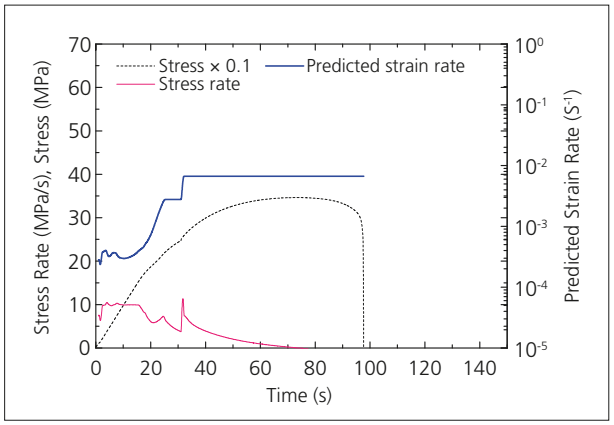

Fig. 7 (a) Test Results (Sample A)

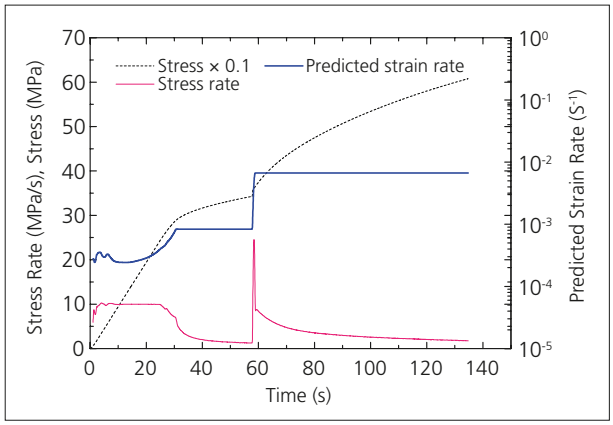

Fig. 7 (b) Test Results (Sample B)

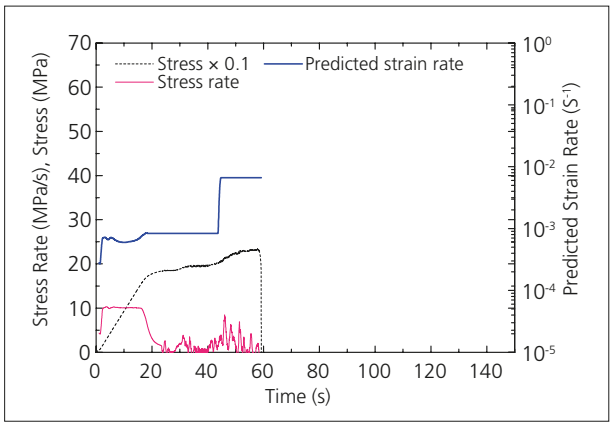

Fig. 7 (c) Test Results (Sample C)

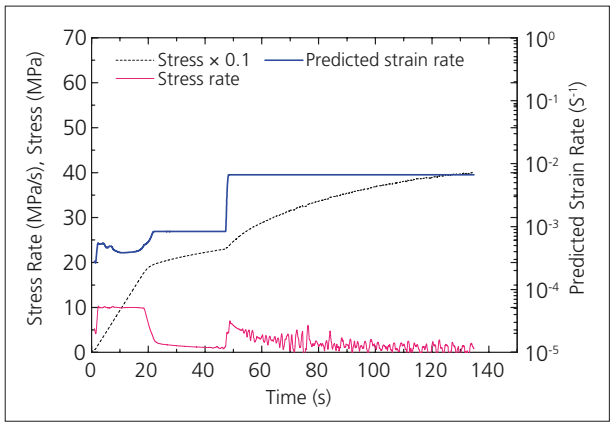

Fig. 7 (d) Test Results (Sample D)

It is clear that at the set rates, suitably stable data could be acquired for both stress rate and predicted strain rate.

The above results demonstrate that in the tensile testing of the various types of metallic materials using the Shimadzu Autograph AG-50kNX Precision Universal Tester, the strain rate control values were well within the range of the permissible values (± 20 %) specified in ISO 6892. Similarly, stable testing using stress rate control was also achieved. When using typical universal testing machines, testing control methods other than the crosshead rate control, e.g. strain rate control and stress rate control, normally require burdensome adjustment of the control gain depending on the material being tested. However, with this instrument, strain rate control and stress rate control in tensile testing of any metallic material are easily conducted because the gain is adjusted automatically (auto-tuning feature).

First Edition: January, 2012

SHIMADZU

SHIMADZU Corporation
www.shimadzu.com/an/

For Research Use Only. Not for use in diagnostic procedures.
The contents of this publication are provided to you "as is" without warranty of any kind, and are subject to change without notice.
Shimadzu does not assume any responsibility or liability for any damage, whether direct or indirect, relating to the use of this publication.

© Shimadzu Corporation, 2012

SHIMADZU
Excellence in Science

Application News

Material Testing System DUH

No. SCA_300_035

A hardness measurement of surface treatment layer on a steel sample using Shimadzu Dynamic Ultra Micro Hardness Tester, Model DUH

Recent years have seen intensive requests for engineering materials with higher function ability and longer life, and as a result, surface treatment for such materials has become popular. Under this circumstance, hardness testers with micro load are enjoying an increasing demand. In this regards, a test report is herein introduced on the hardness distribution measured from the sample surface toward depth direction with an interval of 2 µm, using Shimadzu Dynamic Ultra Micro Hardness Tester Model DUH.

■ Test Parameters

1) Sample: plating layer on a metal plate (See Fig. 1)

2) Indenter: tip angle 136°, square pyramid indenter (Vickers indenter)

3) Measuring mode: load-load-hold test (mode 1)

4) Test load: 2.0 gf

5) Loading speed: 0.029 gf/sec.

6) Load hold-time: 10 sec.

■ Test Method

1) Vickers Hardness
Testing procedures, the distance between the indentation center and the sample edge shall be 2.5 time the diagonal length or more (the diagonal length is 2.6 µm or less). The test load was determined in accordance with this specification, and the tests were performed near the mid depth of the plating layer.

2) Hardness distribution measurements were performed at the location and with the depth intervals of 2 µm starting from the sample surface as shown in Fig. 2

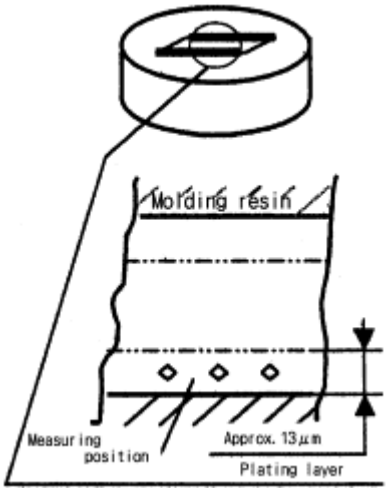

Fig. 1

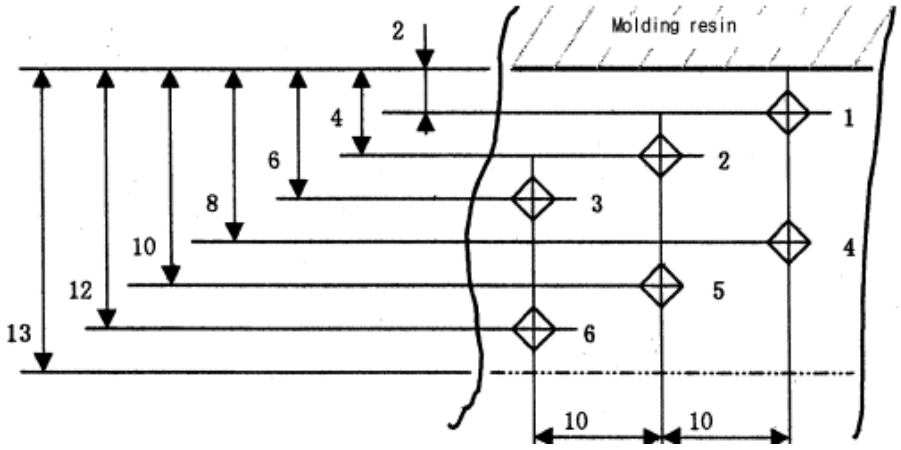

Fig. 2

■ Test Results

The average of five measurements is shown in Table 1, and the load-indentation depth curve is in Fig. 3

Test Load (gf)	Depth (μm)	Dynamic Hardness DHV
2,001	0,206	1065

Table 1 Hardness Test Result

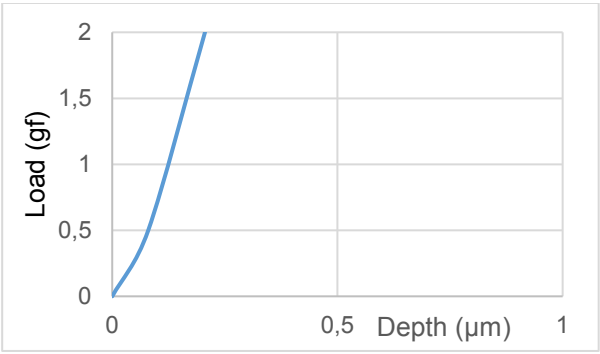

Fig. 3 Load-Indentation depth curve

Dynamic Hardness was determined by the following formula:

$$DHV = \frac{37{,}838 \cdot P}{h^2}$$

Where:

DHV: Dynamic hardness by Vickers Indenter

P: Test Load (gf)

H: Indentation depth (μm)

■ Test Results

Result of five tests with a depth interval of 2 μm is listed in Table 2.

Test Load (gf)	DHV					
	1	2	3	4	5	6
2,0	847	1001	1070	1103	966	925

Table 2 Hardness Distribution

..

■ **Dynamic hardness was determined by the same formula as item 1) above.**

The Relation of depth and hardness is shown in Fig. 4.

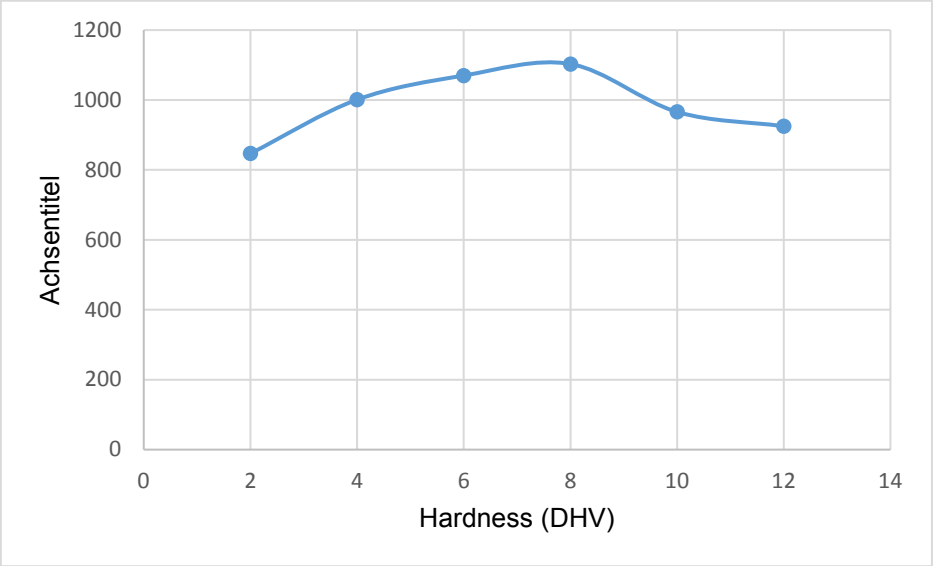

Fig. 4

Fig. 4 indicates a tendency that hardness increases as depth increases, reaches the max. at mid depth of the plating layer, and decreases thereafter.

For Research Use Only. Not for use in diagnostic procedures.
The content of this publication shall not be reproduced, altered or sold for any commercial purpose without the written approval of Shimadzu. The information contained herein is provided to you "as is" without warranty of any kind including without limitation warranties as to its accuracy or completeness. Shimadzu does not assume any responsibility or liability for any damage, whether direct or indirect, relating to be the use of this publication. This publication is based upon the information available to Shimadzu on or before the date of publication, and subject to change without notice.

SHIMADZU
Excellence in Science

Application News

Material Testing System AG-X

No. SCA_300_045

Jigs for Measuring Bauschinger Effect

Use Autograph to simply perform in-plane reverse loading tests on sheet metal.

■ In-Plane Reverse Loading Test

It is a testing method, where a sheet metal is subjected to tensile ➡ compression ➡ tensile reverse loading and continuously measuring the stress-strain curve. It can be used to make highly accurate measurements of the Bauschinger effect or the strain dependence of the elastic modulus required for forming simulation. In-plane reverse loading is possible by gripping the specimen with a die (comb grips) movable in the testing axis direction to prevent a specimen from buckling.

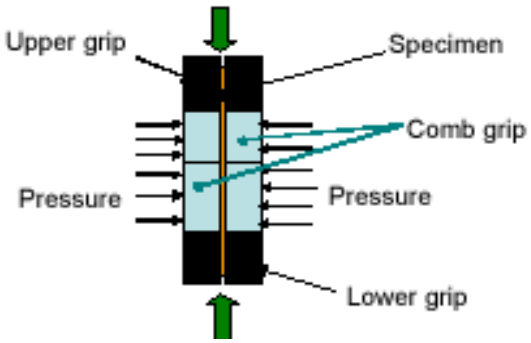

■ Features

Space-saving:

Perform tests by attaching the jigs to Autograph. No specialized equipment required.

Good operability:

The jigs can be used sideways, making specimen setting easy. All operations from attachment of the jigs to testing can be performed by one person.

Simple displacement measurement:

Extension of the specimen can be measured using the strain gauge type extensometer. No need to attach a strain gauge to the specimen, making it possible to perform tests more efficiently.

Simple operation:

Any straightening pressure can be set easily using the hydraulic jack and hydraulic hand pump.

■ External View of Jigs

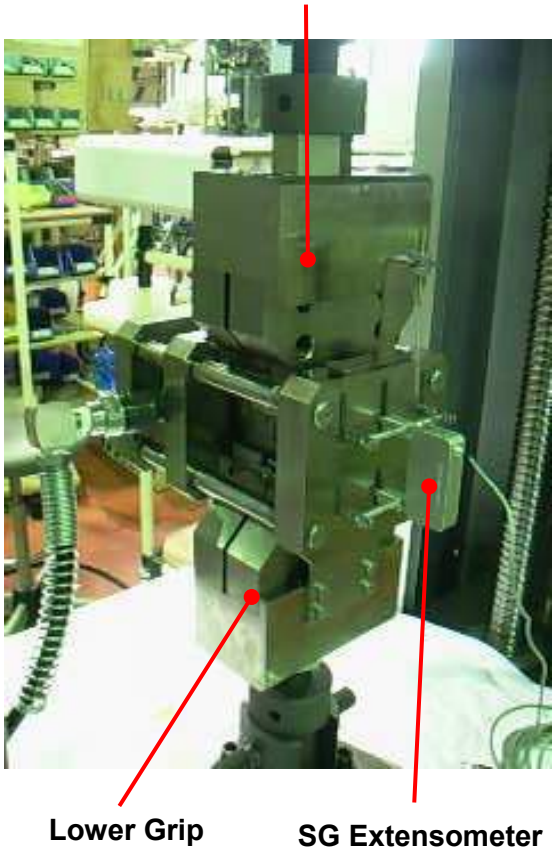

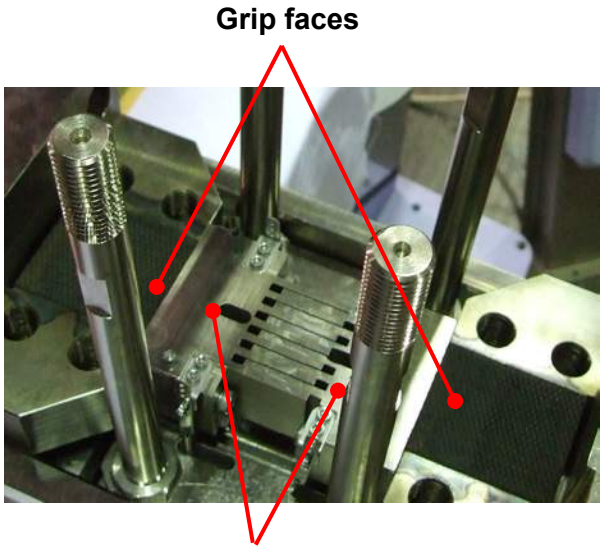

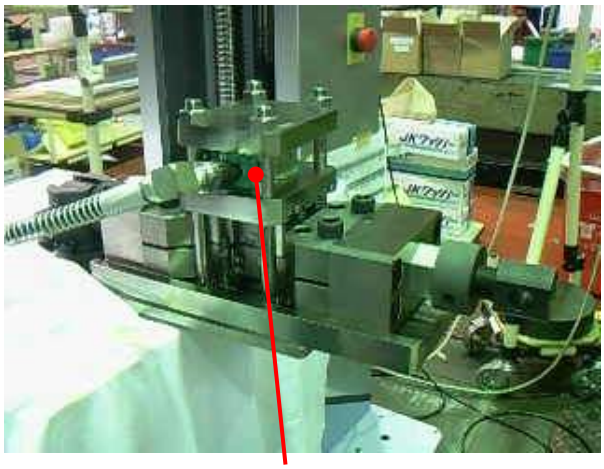

■ Example of Test Results True Stress-True Strain Curve

Specimen: DP780 high strength steel, sheet thickness 1.4 mm

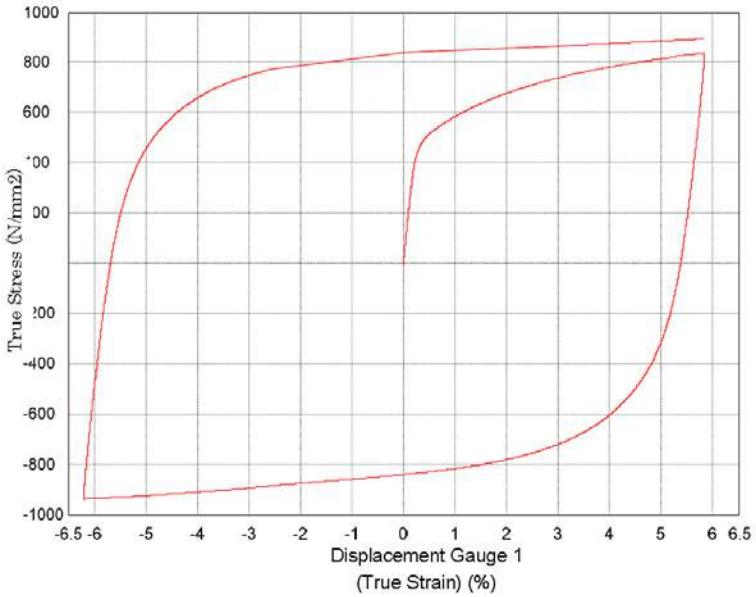

Specifications		
Applicable Testing Machine		AG-100kN
Loading Capacity		Tensile: 100 kN / Compression: 100 kN
Buckling Prevention Unit	Hydraulic Unit	Hydraulic hand pump
	Straightening Pressure	Max. 40 kN
Extensometer	Type	Strain gauge type
	Gauge Length	50 mm
	Measurement Range	+50 %/-10 %
	Measurement Precision	JIS B 7741 Class 1
Applicable Specimen	JIS 5	L200 mm x W40 mm
		Parallel section L60 mm x W40 mm
		1–3 mm thick
	JIS 5 Special Size (Wide specimen)	L200 mm x W45 mm
		Parallel section L60 mm x W35 mm
		1–3 mm thick
Operational Temp. Range		Room temperature

The test data is used with kind permission from G-TEKT Corporation

For Research Use Only. Not for use in diagnostic procedures.
The content of this publication shall not be reproduced, altered or sold for any commercial purpose without the written approval of Shimadzu. The information contained herein is provided to you "as is" without warranty of any kind including without limitation warranties as to its accuracy or completeness. Shimadzu does not assume any responsibility or liability for any damage, whether direct or indirect, relating to be the use of this publication. This publication is based upon the information available to Shimadzu on or before the date of publication, and subject to change without notice.

SHIMADZU
Excellence in Science

Application Data Sheet

No. 2

Autograph Precision Universal Tester

Material Testing & Inspection

Flexural Testing of Plastics

Standard No. ISO178: 2010 (JIS K 7171: 1994)

Introduction

In recent years, a large variety of synthetic resin (plastic) materials has become available for use in a diversity of products. They are used in applications that take advantage of their respective characteristics. For example, polyethylene (PE) is cheap and easy to mold, and thus used for containers, packaging film, and other everyday applications. In contrast, polycarbonate (PC) is transparent, has a high mechanical strength, and is heat-resistant; consequently, it is used for CDs and DVDs in the electrical and electronics fields, as well as in transportation equipment, optics, and medical fields.

In this Data Sheet, flexural testings are performed on four materials, including polyvinyl chloride (PVC) and polypropylene (PP).

T. Murakami

Measurements and Jigs

In plastic flexural testings, the width of the two supports and central loading edge must be larger than the width of the specimen, and parallelism within ± 0.2 mm is required. The loading edge radius is 5 mm ±0.1 mm, and the supports radius is specified as 2 mm ± 0.2 mm for specimens with a thickness of 3 mm or less, and 5 mm ± 0.2 mm for specimens with a thickness exceeding 3 mm. The span must be adjusted to a value of 16 (± 1) times the specimen thickness. In this test, since a 4 mm-thick specimen is used, the span is set to 64 mm (specimen thickness of 4 mm × 16 = 64 mm).

Measurement Results

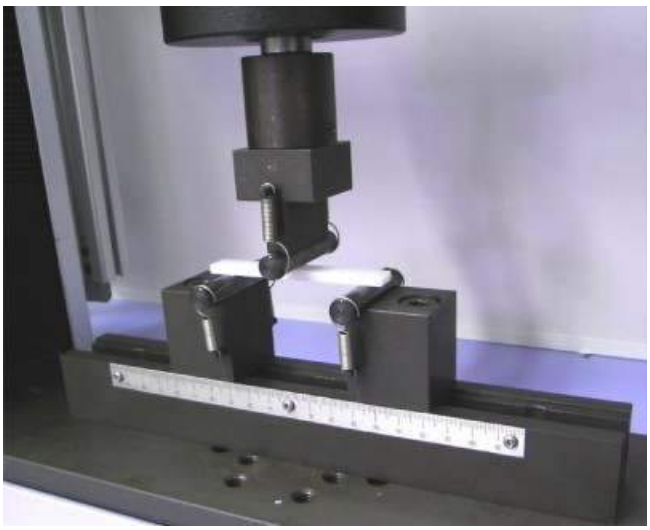

Fig. 1: Test Status

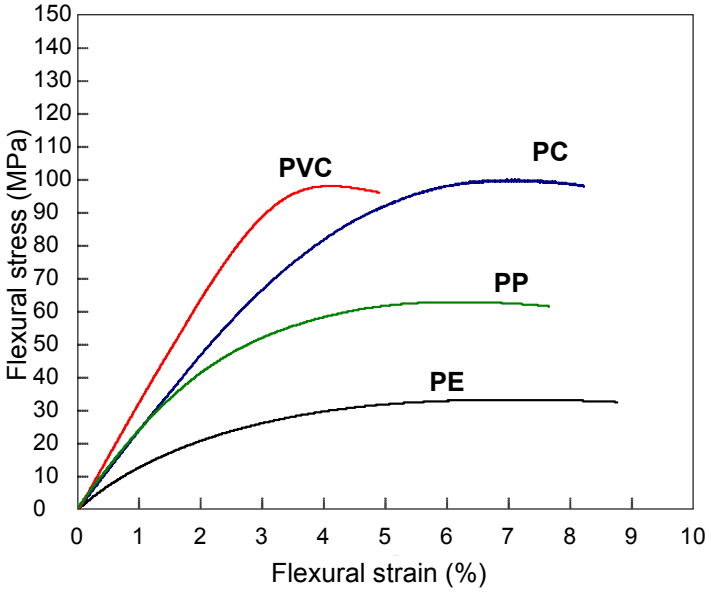

Fig. 2: Relationship Between Flexural Stress and Flexural Strain

Table 1: Test Conditions

Item	Set Value
Test Speed	2 mm/min
Span	64 mm

Table 2: Test Results

Sample	Flexural Modulus (MPa)	Flexural Strength (MPa)
PE (polyethylene)	1527	33.0
PC (polycarbonate)	2378	99.7
PVC (polyvinyl chloride)	3257	97.8
PP (polypropylene)	2559	62.6

Plastic Flexural Testing System

Tester:	AGS-X
Load Cell:	1 kN
Test Jig:	Three-point bending test jig for plastics (loading edge radius.: 5 mm, supports radius.: 3 mm)
Software:	TRAPEZIUM LITE X

AGS-X Table-Top Precision Universal Tester

Features

- A high-precision load cell is adopted. (The high-precision type is class 0.5; the standard-precision type is class 1.) Accuracy is guaranteed over a wide range, from 1/500 to 1/1 of the load cell capacity. This supports highly reliable test evaluations.
- Crosshead speed range
  Tests can be performed over a wide range from 0.001 mm/min to 1,000 mm/min.
- High-speed sampling
  High-speed sampling, as fast as 1 msec.
- TRAPEZIUMX LITE X operational software
  This is simple, highly effective software.
- Jog controller (optional)
  This allows hand-held control of the crosshead position. Fine position adjustment is possible using the jog dial.
- Optional Test Devices
  A variety of tests can be conducted by switching between an abundance of jigs in the lineup.

First Edition: February 2013

Shimadzu Corporation
www.shimadzu.com/an/

For Research Use Only. Not for use in diagnostic procedures.
The content of this publication shall not be reproduced, altered or sold for any commercial purpose without the written approval of Shimadzu.
The information contained herein is provided to you "as is" without warranty of any kind including without limitation warranties as to its accuracy or completeness. Shimadzu does not assume any responsibility or liability for any damage, whether direct or indirect, relating to the use of this publication. This publication is based upon the information available to Shimadzu on or before the date of publication, and subject to change without notice.
© Shimadzu Corporation, 2013

SHIMADZU
Excellence in Science

Application Data Sheet

No. 3

Autograph Precision Universal Tester

Material Testing & Inspection

Tensile Tests of Plastic Materials at Low Temperatures (-40 °C)

Standard No. ISO527-1: 2012 (JIS K 7161: 1994)

Introduction

Tensile tests are widely used to evaluate plastic materials, and the results are used as indices for new materials development and for implementing quality control. Items evaluated as tensile characteristics of plastic materials include the tensile modulus, strength, and break strain. In this Data Sheet, the tensile modulus of polypropylene (PP) and polyvinyl chloride (PVC) specimens (dumbbell shaped and cut types) was calculated based on displacement data acquired using an extensometer at a low temperature of -40 °C. In addition, the strength and break strain for the respective plastic materials were also evaluated.

T. Murakami

Measurements and Jigs

In finding a sample's tensile modulus, it is necessary to use an extensometer capable of measuring tiny deformations of the sample with high accuracy. Measurements of crosshead travel distances include errors not only from sample deformation, but also from load cell and test jig deformation. When the deformation region is very small, the ratio of the error becomes significant, so this data is not suitable for tensile modulus calculations. In such cases, an extensometer that can measure changes in the gauge length with an accuracy of at least ±1 % must be used. When measuring the modulus of elasticity with a 50 mm gauge length, this corresponds to an accuracy of ±1μm. In this test, a one-touch contact type extensometer, capable of operating even in a -40 °C environment, was used.

Measurement Results

Fig. 1: Test Status

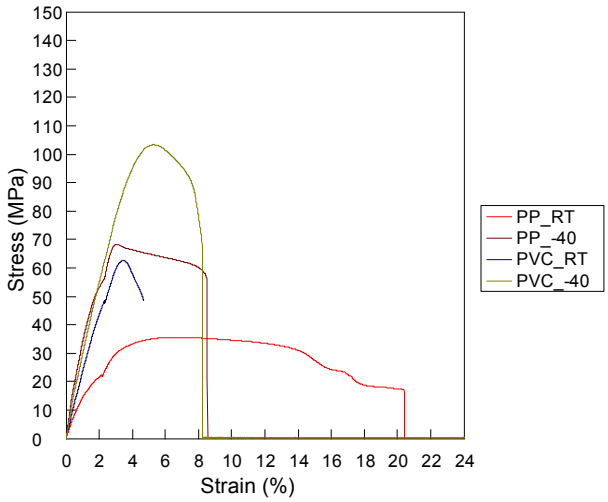

Fig. 2: Relationship Between Stress and Strain

In the results, samples with an "RT" suffix were measured in a room temperature environment, and those with a "-40" suffix were measured at -40 °C. In all cases, measurement was performed at a test speed of 1 mm/min up to 2 %, and then at a test speed of 50 mm/min. In the room temperature measurements, the extensometer measurement range was exceeded, so the extensometer was removed at the 2 % position.

Table 1: Test Results

Sample	Tensile Modulus (MPa)	Strength (MPa)	Break Strain (%)
PP_RT	1955	36	20.2
PP_-40	5333	68	7.8
PVC_RT	3150	63	4.3
PVC_-40	3942	103	7.1

Plastic Material Thermostatic Tensile Test System

Tester:	AGS-X
Load Cell:	5 kN
Test Jig:	5 kN pneumatic flat grips (Single-side file teeth grip faces)
Extensometer:	Strain gauge type one-touch extensometer EPC-50-10
External Amplifier:	ESA-CU200
Thermostatic Chamber:	TCR2W
Software:	TRAPEZIUM LITE X

AGS-X Table-Top Precision Universal Tester

Features

- A high-precision load cell is adopted. (The high-precision type is class 0.5; the standard-precision type is class 1.) Accuracy is guaranteed over a wide range, from 1/500 to 1/1 of the load cell capacity. This supports highly reliable test evaluations.
- Crosshead speed range
  Tests can be performed over a wide range from 0.001 mm/min to 1,000 mm/min.
- High-speed sampling
  High-speed sampling, as fast as 1 msec.
- TRAPEZIUMX LITE X operational software
  This is simple, highly effective software.
- Jog controller (optional)
  This allows hand-held control of the crosshead position. Fine position adjustment is possible using the jog dial.
- Optional Test Devices
  A variety of tests can be conducted by switching between an abundance of jigs in the lineup.

First Edition: February 2013

Shimadzu Corporation
www.shimadzu.com/an/

For Research Use Only. Not for use in diagnostic procedures.
The content of this publication shall not be reproduced, altered or sold for any commercial purpose without the written approval of Shimadzu.
The information contained herein is provided to you "as is" without warranty of any kind including without limitation warranties as to its accuracy or completeness. Shimadzu does not assume any responsibility or liability for any damage, whether direct or indirect, relating to the use of this publication. This publication is based upon the information available to Shimadzu on or before the date of publication, and subject to change without notice.
© Shimadzu Corporation, 2013

SHIMADZU
Excellence in Science

Application Data Sheet

No. 4

Autograph Precision Universal Tester

Material Testing & Inspection

Tensile Tests of Rubber Dumb-bell Specimens

Standard No. ISO37: 2005 (JIS K6251: 2010)

Introduction

Rubber materials have characteristic mechanical properties including elasticity and flexibility, and are widely used for industrial parts, construction materials, and housewares. In particular, a diverse range of synthetic rubber materials with differing properties suited to match their application have been developed. Measuring these mechanical properties is extremely important to ensure quality control and for new materials development. This Data Sheet introduces an example of the evaluation of three synthetic rubber (main components: chloroprene [1]; urethane [2]) specimens (dumb-bell test pieces). Static tensile tests were performed, and the specimens were evaluated with respect to tensile strength, stress at given elongation, and elongation at break, which are aspects of their basic mechanical properties.

T. Murakami

Measurements and Jigs

In tensile tests of rubber dumb-bell specimens, the grips must tighten automatically. When tensile loads are applied to rubber materials, they elongate and their thickness decreases. For this reason, if there is no automatic tightening mechanism, the specimen will inadvertently break free of the grip before the maximum load is applied, making favorable measurements impossible. Accordingly, in rubber tensile tests, it is necessary to use pneumatic parallel grippers, pantograph grips, eccentric roller type grips, Henry Scott type grips, or other grips equipped with this feature.

Measurement Results

Fig. 1: Test Status

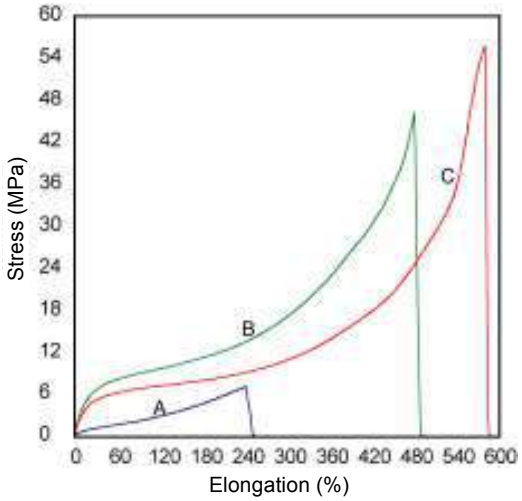

Fig. 2: Relationship Between Stress and Elongation

Table 1: Test Conditions

Item	Set Value
Test Speed	500 mm/min
Initial Distance between Grips	60 mm
Gauge Length	20 mm

Table 2: Test Results

Sample	Main Component	Tensile Strength (MPa)	Stress at 100 % Elongation (MPa)	Stress at 200 % Elongation (MPa)	Elongation at Break (%)
A	Chloroprene	7.1	2.4	5.4	242.3
B	Urethane	47.1	9.3	11.9	478.1
C	Urethane	55.5	7.0	8.4	572.6

The tensile test results for the three samples are shown in Table 2. A graph showing the stress-elongation relationship for the samples is shown in Fig. 2. Clear differences in mechanical properties such as tensile strength and elongation at break are apparent between the samples.

Rubber (Dumb-bells test pieces) Tensile Test System

Tester:	AGS-X
Load Cell:	1 kN
Test Jig:	1 kN pneumatic flat grips (Single-side file teeth grip faces)
Extensometer:	SES-1000 type extensometer for soft specimens
Software:	TRAPEZIUM LITE X

AGS-X Table-Top Precision Universal Tester

Features

- A high-precision load cell is adopted. (The high-precision type is class 0.5; the standard-precision type is class 1.) Accuracy is guaranteed over a wide range, from 1/500 to 1/1 of the load cell capacity. This supports highly reliable test evaluations.
- Crosshead speed range
  Tests can be performed over a wide range from 0.001 mm/min to 1,000 mm/min.
- High-speed sampling
  High-speed sampling, as fast as 1 msec.
- TRAPEZIUMX LITE X operational software
  This is simple, highly effective software.
- Jog controller (optional)
  This allows hand-held control of the crosshead position. Fine position adjustment is possible using the jog dial.
- Optional Test Devices
  A variety of tests can be conducted by switching between an abundance of jigs in the lineup.

First Edition: February 2013

Shimadzu Corporation
www.shimadzu.com/an/

For Research Use Only. Not for use in diagnostic procedures.
The content of this publication shall not be reproduced, altered or sold for any commercial purpose without the written approval of Shimadzu.
The information contained herein is provided to you "as is" without warranty of any kind including without limitation warranties as to its accuracy or completeness. Shimadzu does not assume any responsibility or liability for any damage, whether direct or indirect, relating to the use of this publication. This publication is based upon the information available to Shimadzu on or before the date of publication, and subject to change without notice.
© Shimadzu Corporation, 2013

SHIMADZU
Excellence in Science

Application Data Sheet

No. 5

Autograph Precision Universal Tester

Material Testing & Inspection

Tear Tests of Crescent-shaped Rubber Specimens

Standard No. ISO34-1: 2004 (JIS K6252: 2007)

Introduction

Rubber materials have characteristic mechanical properties including elasticity and flexibility, and are widely used for industrial parts, construction materials, and housewares. In particular, a diverse range of synthetic rubber materials with differing properties suited to match their application have been developed. Measuring these mechanical properties is extremely important to ensure quality control and for new materials development. This Data Sheet introduces an example of the evaluation of two synthetic rubber specimens (crescent-shaped specimens). Tear tests were performed, and the specimens were evaluated with respect to tear strength, one of their basic mechanical properties.

T. Murakami, J. Sakai

Measurements and Jigs

Tear tests of crescent-shaped rubber specimens require grips that tighten automatically as the tear force increases. When tensile loads are applied to rubber materials, they elongate and their thickness decreases. For this reason, if there is no automatic tightening mechanism, the specimen will inadvertently break free of the grips before the maximum tear force is applied, making favorable measurements impossible. Accordingly, in rubber tear tests, it is necessary to use pneumatic parallel grippers, pantograph grips, eccentric roller type grips, Henry Scott type grips, or other grips equipped with this feature.

Measurement Results

Fig. 1: Test Status

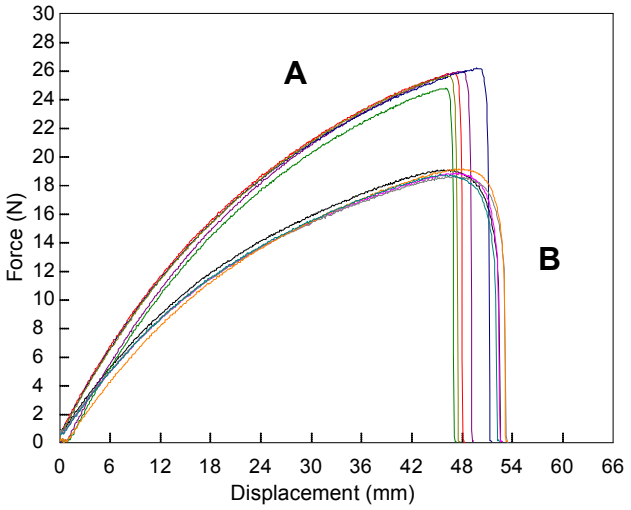

Fig. 2: Relationship Between Force and Displacement

Table 1: Test Conditions

Item	Set Value
Test Speed	500 mm/min
Initial Distance between Grips	60 mm

Table 2: Test Results (Average)

Sample	Main Component	Max. Force (N)	Tear Strength (kN/m)
A	CR rubber (black)	25.9	13.0
B	CR rubber (white)	18.9	9.5

The tear test results for the two samples are shown in Table 2. A graph showing the force-displacement relationship for each sample is shown in Fig. 2. Differences in tear strength between the samples are clearly apparent.

Rubber Tear Test System

Tester:	AGS-X
Load Cell:	1 kN
Test Jig:	1 kN pneumatic flat grips (Single-side file teeth grip faces)
Software:	TRAPEZIUM LITE X

AGS-X Table-Top Precision Universal Tester

Features

- A high-precision load cell is adopted. (The high-precision type is class 0.5; the standard-precision type is class 1.) Accuracy is guaranteed over a wide range, from 1/500 to 1/1 of the load cell capacity. This supports highly reliable test evaluations.
- Crosshead speed range
  Tests can be performed over a wide range from 0.001 mm/min to 1,000 mm/min.
- High-speed sampling
  High-speed sampling, as fast as 1 msec.
- TRAPEZIUMX LITE X operational software
  This is simple, highly effective software.
- Jog controller (optional)
  This allows hand-held control of the crosshead position. Fine position adjustment is possible using the jog dial.
- Optional Test Devices
  A variety of tests can be conducted by switching between an abundance of jigs in the lineup.

First Edition: February 2013

Shimadzu Corporation
www.shimadzu.com/an/

For Research Use Only. Not for use in diagnostic procedures.
The content of this publication shall not be reproduced, altered or sold for any commercial purpose without the written approval of Shimadzu.
The information contained herein is provided to you "as is" without warranty of any kind including without limitation warranties as to its accuracy or completeness. Shimadzu does not assume any responsibility or liability for any damage, whether direct or indirect, relating to the use of this publication. This publication is based upon the information available to Shimadzu on or before the date of publication, and subject to change without notice.
© Shimadzu Corporation, 2013

SHIMADZU
Excellence in Science

Application Data Sheet

No. 6

Autograph Precision Universal Tester

Material Testing & Inspection

Tear Tests of Angle-Shaped Rubber Specimens

Standard No. ISO34-1: 2004 (JIS K6252: 2007)

Introduction

Rubber materials have characteristic mechanical properties including elasticity and flexibility, and are widely used for industrial parts, construction materials, and housewares. In particular, a diverse range of synthetic rubber materials with differing properties suited to match their application have been developed. Measuring these mechanical properties is extremely important to ensure quality control and for new materials development. This Data Sheet introduces an example of the evaluation of two synthetic rubber specimens (angle-shaped specimens). Tear tests were performed, and the specimens were evaluated with respect to tear strength, one of their basic mechanical properties.

T. Murakami, J. Sakai

Measurements and Jigs

Tear tests of angle-shaped rubber specimens require grips that tighten automatically as the tear force increases. When tensile loads are applied to rubber materials, they elongate and their thickness decreases. For this reason, if there is no automatic tightening mechanism, the specimen will inadvertently break free of the grips before the maximum tear force is applied, making favorable measurements impossible. Accordingly, in rubber tear tests, it is necessary to use pneumatic parallel grippers, pantograph grips, eccentric roller type grips, Henry Scott type grips, or other grips equipped with this feature.

Measurement Results

Fig. 1: Test Status

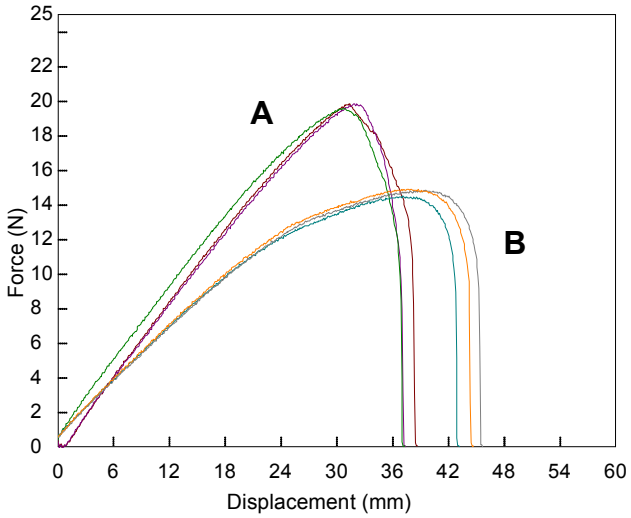

Fig. 2: Relationship Between Force and Displacement

Table 1: Test Conditions

Item	Set Value
Test Speed	500 mm/min
Initial Distance between Grips	60 mm

Table 2: Test Results (Average)

Sample	Main Component	Max. Force (N)	Tear Strength (kN/m)
A	CR rubber (black)	19.7	9.85
B	CR rubber (white)	14.7	7.35

The tear test results for the two samples are shown in Table 2. A graph showing the force-displacement relationship for each sample is shown in Fig. 2. Differences in tear strength between the samples are clearly apparent.

Rubber Tear Test System

Tester:	AGS-X
Load Cell:	1 kN
Test Jig:	1 kN pneumatic flat grips (Single-side file teeth grip faces)
Software:	TRAPEZIUM LITE X

AGS-X Table-Top Precision Universal Tester

Features

- A high-precision load cell is adopted. (The high-precision type is class 0.5; the standard-precision type is class 1.) Accuracy is guaranteed over a wide range, from 1/500 to 1/1 of the load cell capacity. This supports highly reliable test evaluations.
- Crosshead speed range
  Tests can be performed over a wide range from 0.001 mm/min to 1,000 mm/min.
- High-speed sampling
  High-speed sampling, as fast as 1 msec.
- TRAPEZIUMX LITE X operational software
  This is simple, highly effective software.
- Jog controller (optional)
  This allows hand-held control of the crosshead position. Fine position adjustment is possible using the jog dial.
- Optional Test Devices
  A variety of tests can be conducted by switching between an abundance of jigs in the lineup.

First Edition: February 2013

Shimadzu Corporation
www.shimadzu.com/an/

For Research Use Only. Not for use in diagnostic procedures.
The content of this publication shall not be reproduced, altered or sold for any commercial purpose without the written approval of Shimadzu.
The information contained herein is provided to you "as is" without warranty of any kind including without limitation warranties as to its accuracy or completeness. Shimadzu does not assume any responsibility or liability for any damage, whether direct or indirect, relating to the use of this publication. This publication is based upon the information available to Shimadzu on or before the date of publication, and subject to change without notice.
© Shimadzu Corporation, 2013

SHIMADZU
Excellence in Science

Application Data Sheet

No. 7

Autograph Precision Universal Tester

Material Testing & Inspection

Tensile Tests of Films

Standard No. ISO527-3: 2012 (JIS K 7127: 1999)

Introduction

Tensile tests are widely used to evaluate plastic materials, and the results are used as indices for new materials development and for implementing quality control. Items widely evaluated as tensile characteristics of plastic materials include the tensile modulus, strength, and break strain. In this Data Sheet, break strain was measured based on displacement data acquired using an extensometer. The strength was also evaluated.

T. Murakami

Measurements and Jigs

Non-contact type extensometers capable of displacement measurements without affecting the sample properties are effective for accurately measuring the break strain of a film. In measuring such physical properties, the sample must be gripped evenly, suppressing the occurrence of wrinkles, so it is important to choose the grips carefully. As in this test, the use of a non-contact type extensometer/width sensor and foil grips is recommended for film tensile tests.

Measurement Results

Fig. 1: Test Status

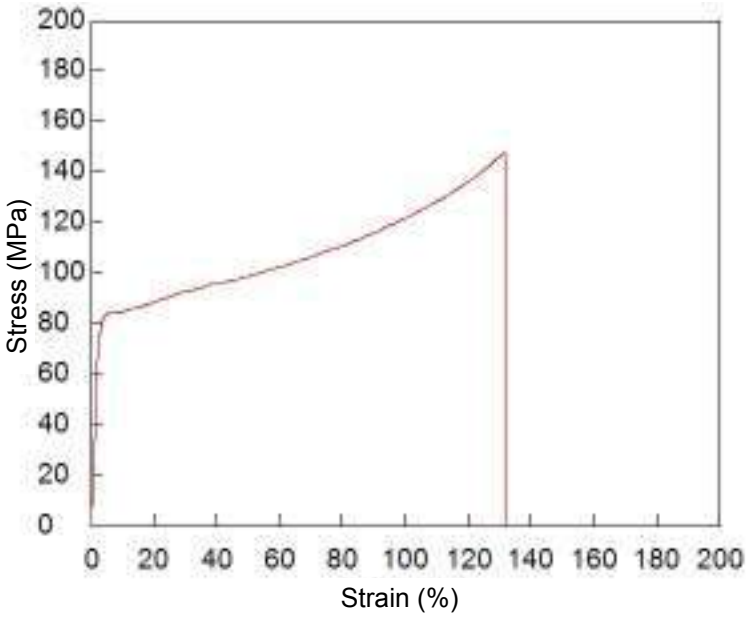

Fig. 2: Relationship Between Stress and Strain

Table 1: Test Conditions

Item	Set Value
Test Speed	50 mm/min
Initial Distance between Grips	100 mm

Table 2: Test Results

Sample	Thickness (μm)	Strength (MPa)	Break Strain (%)
PET Film	150	148	132

Film Tensile Test System

Tester:	AGS-X
Load Cell:	1 kN
Test Jig:	1 kN grips for foils
Extensometer:	TRViewX 240S non-contact extensometer/width sensor
Software:	TRAPEZIUM X

AGS-X Table-Top Precision Universal Tester

Features

- A high-precision load cell is adopted. (The high-precision type is class 0.5; the standard-precision type is class 1.) Accuracy is guaranteed over a wide range, from 1/500 to 1/1 of the load cell capacity. This supports highly reliable test evaluations.
- Crosshead speed range
  Tests can be performed over a wide range from 0.001 mm/min to 1,000 mm/min.
- High-speed sampling
  High-speed sampling, as fast as 1 msec.
- TRAPEZIUMX operational software
  Designed for intuitive operation, this software offers excellent convenience and user friendliness.
- Jog controller (optional)
  This allows hand-held control of the crosshead position. Fine position adjustment is possible using the jog dial.
- Optional Test Devices
  A variety of tests can be conducted by switching between an abundance of jigs in the lineup.

First Edition: February 2013

SHIMADZU

Shimadzu Corporation

www.shimadzu.com/an/

For Research Use Only. Not for use in diagnostic procedures.
The content of this publication shall not be reproduced, altered or sold for any commercial purpose without the written approval of Shimadzu.
The information contained herein is provided to you "as is" without warranty of any kind including without limitation warranties as to its accuracy or completeness. Shimadzu does not assume any responsibility or liability for any damage, whether direct or indirect, relating to the use of this publication. This publication is based upon the information available to Shimadzu on or before the date of publication, and subject to change without notice.

© Shimadzu Corporation, 2013

SHIMADZU
Excellence in Science

Application Data Sheet

No. 9

Autograph Precision Universal Tester

Material Testing & Inspection

Measurements of Modulus of Elasticity and Poisson's Ratio for Films

Standard Nos. ISO527-3: 2012 (JIS K 7127: 1999)
ISO527-1: 2012 (JIS K 7161: 1994)

Introduction

Tensile tests are widely used to evaluate plastic materials, and the results are used as indices for new materials development and for implementing quality control. Items evaluated as tensile characteristics of plastic materials include the tensile modulus, Poisson's ratio, strength, and break strain. With films, there are no standards specified with respect to test methods for the tensile elastic modulus and Poisson's ratio, yet there are demands for measurements of these values. In this Data Sheet, measurements of the tensile modulus and Poisson's ratio were performed for a PET film based on elongation and width data acquired using a non-contact type extensometer/width sensor.

T. Murakami

Measurements and Jigs

Non-contact type extensometers/width sensors capable of fine displacement measurements without affecting the sample properties are required to accurately obtain the tensile modulus and Poisson's ratio for a film. In measuring such physical properties, the sample must be gripped evenly, suppressing the occurrence of wrinkles, so it is important to choose the grips carefully. The use of a non-contact type extensometer/width sensor and foil grips is recommended for film tensile tests.

Measurement Results

Fig. 1: Test Status

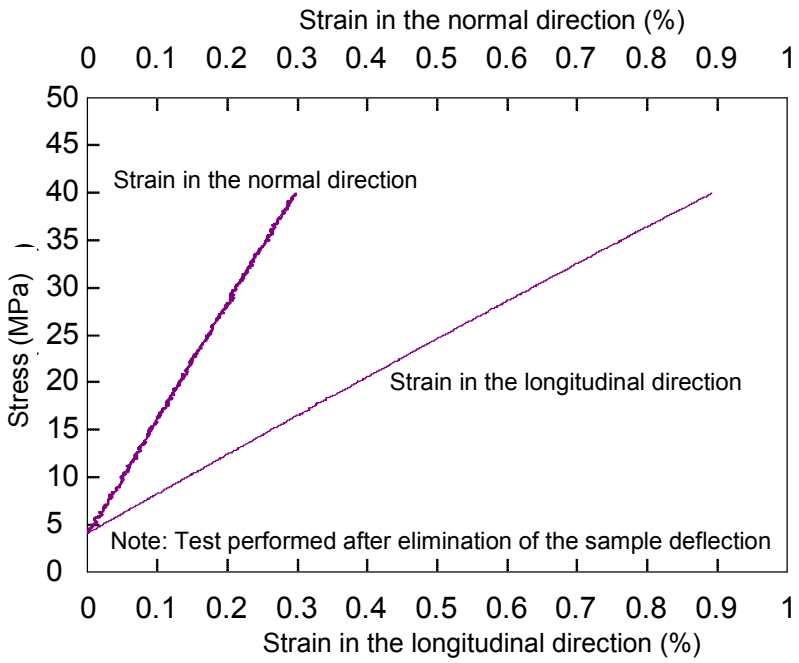

Fig. 2: Relationship Between Stress and Strain

Table 1: Test Conditions

Item	Set Value
Test Speed	1 mm/min
Initial distance Between Grip	100 mm
Gauge Length	40 mm

Table 2: Test Results

Sample	Thickness (μm)	Tensile Modulus (MPa)	Poisson's Ratio
PET Film	25	4139	0.37

Young's Modulus Measurement System for Film

Tester:	AG-Xplus
Load Cell:	1 kN
Test Jig:	1 kN grips for foils
Extensometer:	TRViewX 55S non-contact extensometer/width sensor
Software:	TRAPEZIUM X (Single)

AG-Xplus Table-Top Precision Universal Tester

Features

- A high-precision load cell is adopted. (The high-precision type is class 0.5; the standard-precision type is class 1.) Accuracy is guaranteed over a wide range, from 1/1000 to 1/1 of the load cell capacity. This supports highly reliable test evaluations.
- Crosshead speed range
  Tests can be performed over a wide range from 0.0005 mm/min to 1,500 mm/min.
- High-speed sampling
  Ultrafast sampling, as fast as 0.2 msec. Sudden changes in test force, such as when brittle materials fracture, can be assessed.
- TRAPEZIUMX X operational software
  Designed for intuitive operation, this software offers excellent convenience and user friendliness.
- Smart controller
  Real-time test force and position data is readily confirmed, and the manual dial can be used for fine adjustments to jig positioning.
- Optional Test Devices
  A variety of tests can be conducted by switching between an abundance of jigs in the lineup.

First Edition: February 2013

Shimadzu Corporation
www.shimadzu.com/an/

For Research Use Only. Not for use in diagnostic procedures.
The content of this publication shall not be reproduced, altered or sold for any commercial purpose without the written approval of Shimadzu.
The information contained herein is provided to you "as is" without warranty of any kind including without limitation warranties as to its accuracy or completeness. Shimadzu does not assume any responsibility or liability for any damage, whether direct or indirect, relating to the use of this publication. This publication is based upon the information available to Shimadzu on or before the date of publication, and subject to change without notice.
© Shimadzu Corporation, 2013

SHIMADZU
Excellence in Science

2. Aerospace Industry

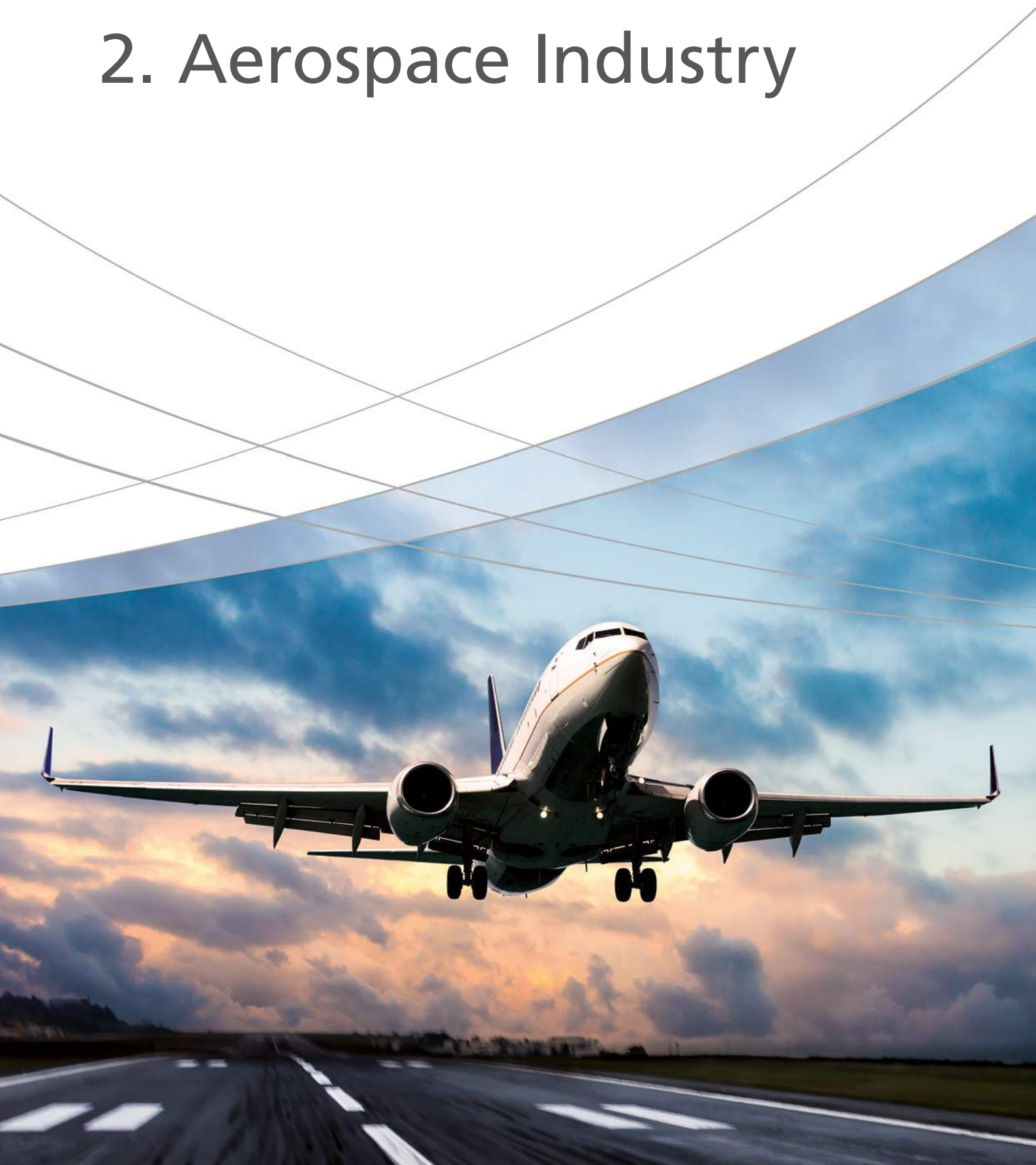

2. Aerospace Industry

EVEN LIGHTER INNOVATIVE MATERIALS

Materials used in aircraft can be broadly categorized into metal, non-metal and composite materials. All are light but strong, offering excellent machinability and heat resistance, and have been developed to provide the properties required for aircraft.

Metals are the major materials used in aircraft structures, of which the majority are aluminum alloys. Titanium alloys and stainless steel are also used for parts around the afterburner and for components subjected to the jet exhaust.

Since plastics are light, easy to color-mold, transparent to electromagnetic waves and also good electrical and thermal insulators, they are widely used for window glass, interior material and so on.

Apart from applications in reinforcement of glass-fiber-reinforced resins, glass materials are inserted between the aircraft outer surface and interior lining as sound and thermal insulators.

Since synthetic rubber materials offer better resistance to weather, heat, oil and chemicals than natural rubber, they are widely used in gaskets, packing, hoses, duct couplings and waterproof sheets. Natural rubber is commonly used in aircraft tires due to superior rubber elasticity, tear strength and abrasive resistance.

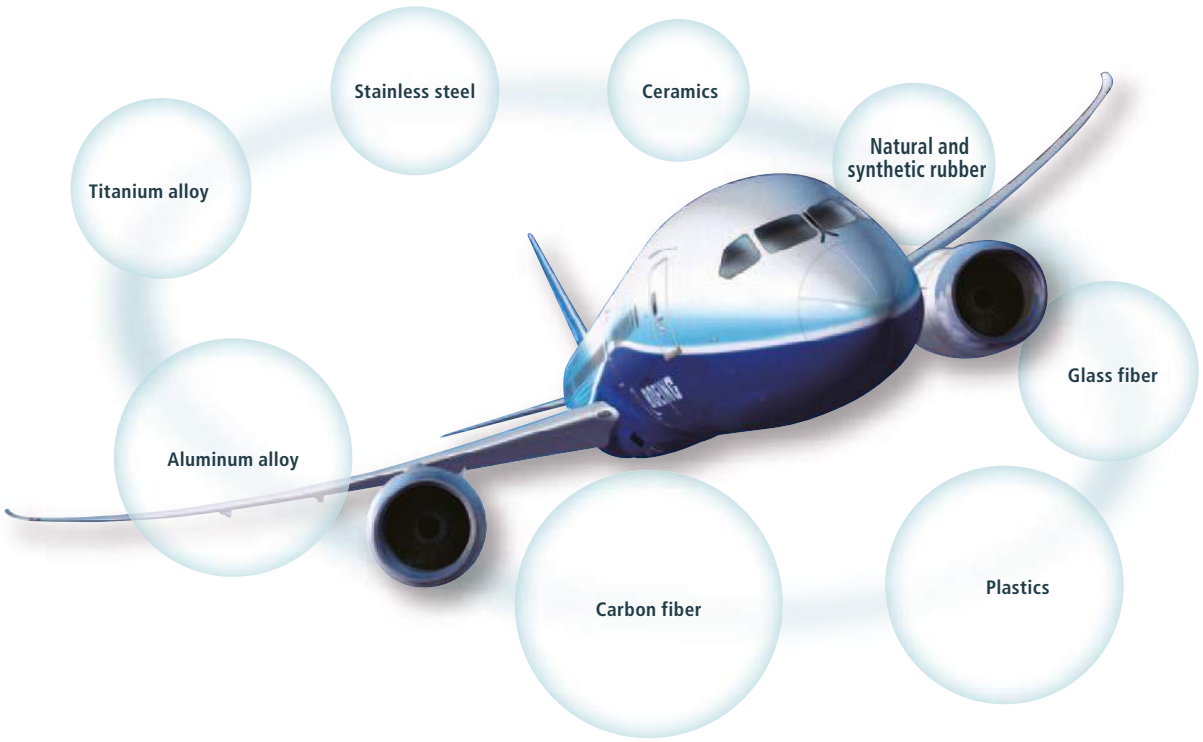

2. Aerospace Industry

C225-E032	Ultrasonic fatigue testing system with an average stress loading mechanism
SCA_300_001	Very high cycle fatigue (VHCF) assessment of laser additive manufactured (LAM) AlSi12 alloy
No.ei254	Compression after impact testing of composite
No.ei255	Compression testing of composite materials
No.36	Evaluating the fatigue strength of GFRP materials
No.30	Evaluating the strength of carbon fiber reinforced plastics (CFRP)
No.39	Evaluation of open-hole CFRP
No.i247	DIC analysis material testing by strain distribution visualization
No.8	Flexural testing of CFRP boards
No.16	Tensile testing of carbon fiber
No.31	Materials testing using digital image correlation
No.37	Observing the failure of open-hole CFRP samples in tensile tests
No.38	Observing the fracture of unidirectional CFRP in static tensile testing
No.ei256A	Open-hole compression testing of composite material
No.ei250	Shear test of composite material (V-notched beam)
No.ei251	Shear test of composite material (V-notched rail shear)
SCA_300_037	Compression-rupture test of carbon fibers with different tensile characteristics Shimadzu micro compression testing machine MCT
SCA_300_059	Observation of fracture in CFRP tensile test E001HPV
C225-E032	Ultrasonic fatigue testing system with an average stress loading mechanism
No.i244	Tensile test for metallic materials using strain rate control and stress rate control
SCA_300_035	A hardness measurement of surface treatment layer on a steel sample using Shimadzu dynamic ultra micro hardness tester, model DUH
No.2	Flexural test of plastic ISO178
No.3	Tensile tests of plastic materials at low ISO527 1
No.4	Tensile test of rubber dumb bell specimens ISO37
No.5	Tear test of crescent shaped ISO34 1
No.6	Tear tests of angle shaped rubber specimens ISO34 1
No.7	Tensile tests of films ISO527 3
No.9	Measurements of modulus of elasticity and poisson's ratio for films ISO527

SHIMADZU
Excellence in Science

Ultrasonic Fatigue Testing System with an Average Stress Loading Mechanism

For Gigacycle Fatigue Tests with Average Stress Loaded

Actual components are rarely used under conditions in which the average stress is zero. Despite this, the USF-2000A, a standard ultrasonic fatigue testing system, can only perform testing under zero average stress conditions.
Using an ultrasonic fatigue testing system equipped with an average stress loading mechanism, gigacycle fatigue tests can be performed with average tensile stress loaded.

System Appearance

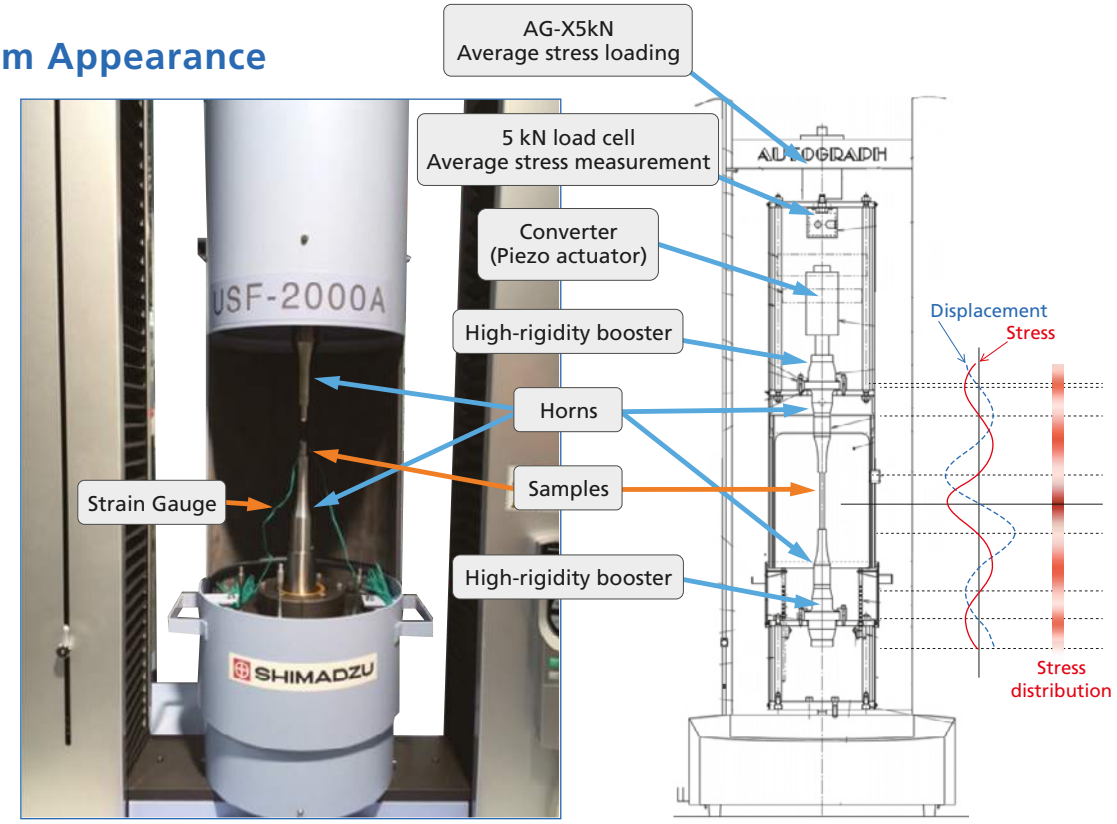

Ultrasonic Fatigue Testing System Effective for Gigacycle Fatigue Tests

With fatigue tests of high-strength steels, it is evident that internal fracture (fish-eye fracture), which is caused by inclusions and other micro defects, occurs at 107 cycles or more, a value considered the conventional fatigue limit.
An ultrasonic fatigue testing system is extremely effective when performing this sort of gigacycle fatigue test. (With a 100 Hz fatigue testing system, this would take 3 years, but if a 20 kHz ultrasonic fatigue testing system is used, testing can be completed in one week.)

Main Specifications

1) Test Frequency: 20 kHz ± 500 Hz

- The recommended test range is 20 kHz ± 30 Hz.
- The test frequency is determined by the resonance frequency of the sample.

2) Horn End Face Amplitude

Min. approx. ±10 µm
Max. approx. ±50 µm

- The minimum and maximum amplitudes are the end face amplitude values at amplitude outputs of 20 % and 100 % respectively. Accordingly, the minimum and maximum amplitude values will change somewhat depending on the shape of the sample.

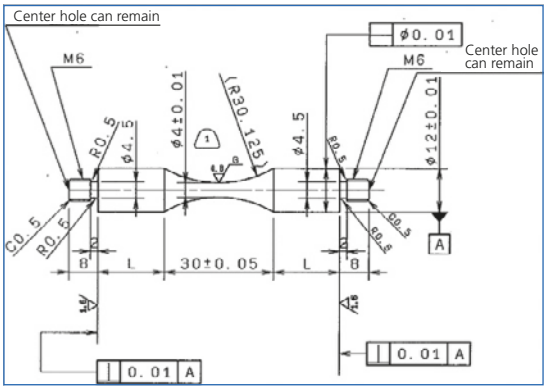

Standard Circular Tapered Sample

3) Test Stress

Standard circular tapered sample
Stress Min. 237 MPa
Max. 1186 MPa

- The test stress range can be changed by changing the sample shape.
- The minimum and maximum values are calculated with the end face amplitude values of 10 µm and 50 µm respectively.
- These are the values when the stress is within the elasticity range.

4) Average Stress

Max. 1.5 kN (tensile only)

- Average stress loads exceeding 1.5 kN are possible, but will have an impact on the service life of the horn.

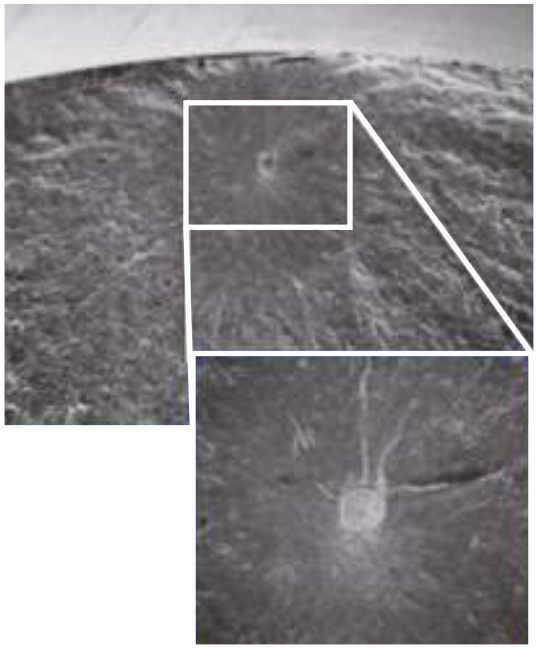
Surface of the Fatigued Fracture Originating from the Inclusion

■ Components

1	Ultrasonic resonance system Power supply, converter, booster (1 pair), horn (1 pair)
2	Personal computer (OS Windows 7) ADA/PIO interface board
3	Software Ultrasonic test control measurement software
4	Cooling system Air dryer, air piping • A separate 140 L/min air source is required.
5	Strain meter unit (option)
6	AG-X plus Autograph 5 kN + 250 extension
7	Average stress loading mechanism

Shimadzu Corporation
www.shimadzu.com/an/

For Research Use Only. Not for use in diagnostic procedure.
This publication may contain references to products that are not available in your country. Please contact us to check the availability of these products in your country.
Company names, product/service names and logos used in this publication are trademarks and trade names of Shimadzu Corporation or its affiliates, whether or not they are used with trademark symbol "TM" or "®". Third-party trademarks and trade names may be used in this publication to refer to either the entities or their products/services. Shimadzu disclaims any proprietary interest in trademarks and trade names other than its own.

The contents of this publication are provided to you "as is" without warranty of any kind, and are subject to change without notice. Shimadzu does not assume any responsibility or liability for any damage, whether direct or indirect, relating to the use of this publication.

© Shimadzu Corporation, 2016

First Edition: August 2016

SHIMADZU

Application News

No. SCA_300_001

Shimadzu Ultrasonic Fatigue Testing System

Very High Cycle Fatigue (VHCF) Assessment of Laser Additive Manufactured (LAM) AlSi12 Alloy

■ Introduction

Selective laser melting (SLM) is a laser additive manufacturing process where parts are additively manufactured using powder material with the aid of laser energy. Three-dimensional CAD model is provided as an input to the SLM machine, which scans the geometry after slicing the geometry into 2D layers. The laser energy selectively melts the powder particles at the desired location of the component to be manufactured. The unique manufacturing capability of SLM process makes it suitable for aerospace, automotive and biomedical applications. Several alloys like aluminum, titanium, steel and nickel-based alloys have been processed by SLM technique [1,2]. Although the fatigue strength diminishes for SLM processed materials in the “as-built” condition due to the process-inherent surface roughness, fatigue performance after post-processing is suitable for many applications in the aviation and medical industry [1].

Contrary to the previous assumption that the materials do not fail under fatigue if the applied stress is below the so-called fatigue limit; with the availability of the novel very high cycle fatigue (VHCF) testing techniques, it has been found that materials do fail under fatigue loading even when the stresses are below the conventional fatigue limit, suggesting the non-existence of such a limit [3,4]. Some alloys of both lattice types (bcc and fcc) show a change in crack initiation site from surface to subsurface in a region from HCF to VHCF [5].

■ Experimental methodology

The test samples of AlSi12 alloy were manufactured using a commercially available SLM system in an inert environment using argon gas. The details of the processing setup and parameters can be viewed in [1]. Quasi-static tensile tests were carried out according to ISO 6892-1:2009. Continuous load increase tests were carried out starting at low stress amplitude of 30 MPa. Stress amplitude was increased slowly at a rate of 10 MPa / 10^4 cycles. Load increase tests and constant amplitude testes were carried out at a frequency of 20 Hz. The results of process optimization, quasi-static properties, high cycle fatigue properties and the measurement methodology for characterization of process-induced defects are published in [2,6]. Two types of configurations are investigated in this study. For the batch I, no pre-heating of the base plate was applied; whereas samples of batch II were manufactured with a base plate heating (BPH) at 200 °C.

Very high cycle fatigue (VHCF) tests were carried out on an ultrasonic fatigue testing system at a frequency of 20 kHz. Fig. 1 shows the overview of the USF-2000 testing system by Shimadzu (http://www.shimadzu.de/usf-2000) and Fig. 2 explains the detailed principle of the test setup. Piezoelectric crystal is used in the actuator, which resonates at a fixed frequency of 20 kHz. In the ultrasonic fatigue testing system, vibrations are designed so that the longitudinal waves transmitted through the solid body resonate.

Fig. 1: Overview of the ultrasonic fatigue testing system USF-2000 by Shimadzu

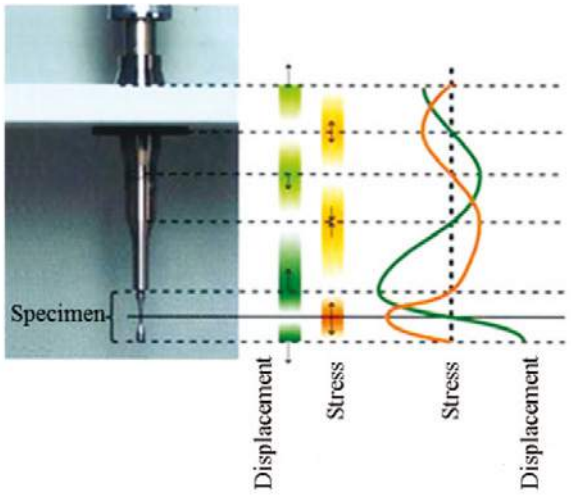

Fig. 2: Functional principle of specimen loading at ultrasonic fatigue testing system USF-2000

The specimen with geometry shown in Fig. 3 is clamped only at one threaded end on USF and is free at the bottom end. The specimen is designed in a way that maximum stress is experienced at the middle of the specimen and the maximum displacement occurs at the free end of the specimen. To eliminate the temperature effect due to high test frequency, the specimens were cooled with compressed air during tests and the tests were performed at a pulse-pause ratio of 50:50 i.e. the system was set to resonance for 200 ms and then stopped for the next 200 ms to cool down.

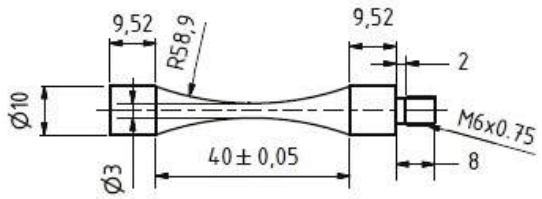

Fig. 3: Specimen geometry for ultrasonic fatigue tests

Experiments for determination of the fatigue strength at 10^9 cycles were performed according to stair-case method. If a specimen at ultrasonic frequency failed at less than 10^9 cycles, the stress amplitude is decreased by 5 MPa for the next experiment. If the specimen did not fail at 10^9 cycles, the stress amplitude was increased by 5 MPa in the subsequent test. Failure of the specimen is based on the change is resonance frequency. When the micro-crack leads to final fracture, the natural frequency of the system reduces than the operating frequency of the system and the test is terminated.

■ Results

Fig. 4 shows exemplary surface micrographs for the two investigated batches. The remnant porosity is viewed as only the gas porosity. A difference in the pore fraction of the samples without and with base plate heating is observed. In the samples with base plate heating, large size gas pores are absent which are very critical for fatigue performance. The reduction of large pores is attributed to the de-gassing in the manufacturing chamber due to pre-heating.

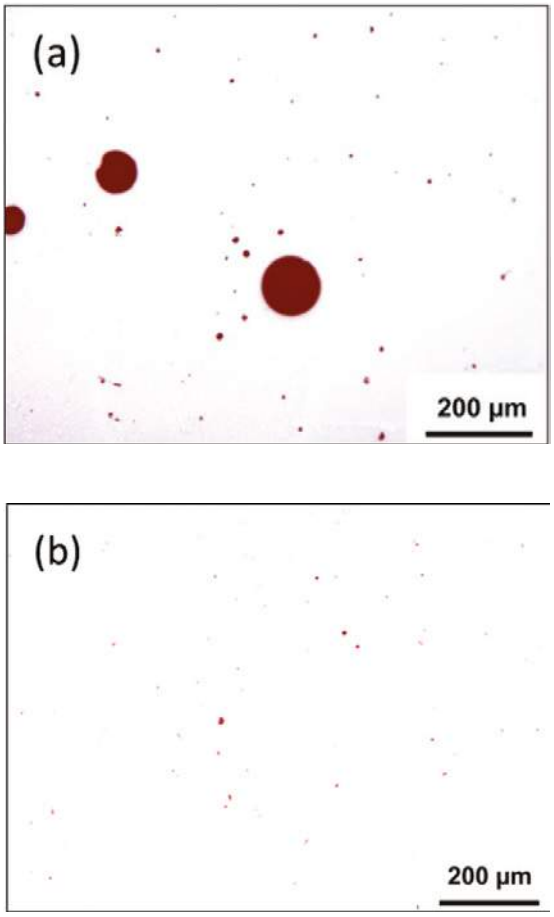

Fig. 4: Exemplary surface micrograph for sample without base plate heating (a); and with base plate heating (b)

Fig. 5 represents S-N curves for batches I and II in the region from high cycle fatigue (HCF) to very high cycle fatigue (VHCF). Experiments showed that the fatigue fracture occurs beyond high cycle fatigue region in both batches. The results of the experiments indicate that fatigue strength in very high cycle regime of samples manufactured with base plate heating is about 45% higher than fatigue strength of sample without base plate heating. Fatigue strength at one giga cycle for batches I and II is 60.5 ± 4.7 MPa and 88.7 ± 3.3 MPa, respectively. This increase in strength is attributed to elimination of the micro pores.

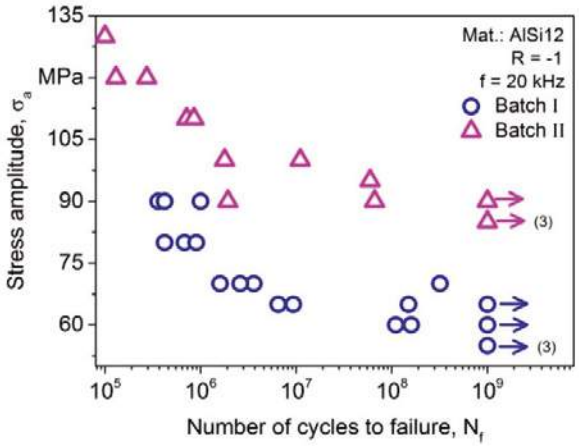

Fig. 5: S-N characterization for ultrasonic fatigue testing results

■ Outlook

New developments in testing machines enabled to go beyond the previously known limits of knowledge. This opens the door towards more intensive testing in the most realistic conditions. The new capabilities in testing machines shall provide researchers with powerful tools to further investigate the effect of processing parameters on the resulting functional performance in a wide range.

■ References

[1] Siddique, S.; Wycisk, E.; Frieling, G.; Emmelmann, C.; Walther, F.: Microstructural and mechanical properties of selective laser melted Al 4047. Applied Mechanics and Materials 752-753 (2015) 485–490.

[2] Siddique, S.; Imran, M.; Wycisk, E.; Emmelmann, C.; Walther, F.: Influence of process-induced microstructure and imperfections on mechanical properties of AlSi12 processed by selective laser melting. Journal of Materials Processing Technology 221 (2015) 205–213.

[3] Pyttel, B.; Schwerdt, D.; Berger, C.: Very high cycle fatigue – Is there a fatigue limit? International Journal of Fatigue 33 (2011) 49–58.

[4] Benedetti, M.; Fontanari, V., Bandini, M.: Very high cycle fatigue resistance of shot-peened high strength aluminium alloys. Experimental and Applied Mechanics 4 (2013) 203–211.

[5] Morrissey, R.J.; Nicholas, T.: Fatigue strength of Ti-6Al-4V at very long lives. International Journal of Fatigue 27 (2005) 1608–1612.

[6] Siddique, S.; Imran, M.; Rauer, M.; Kaloudis, M.; Wycisk, E.; Emmelmann, C.; Walther, F.: Computed tomography for characterization of fatigue performance of selective laser melted parts. Materials & Design 83 (2015) 661-669.

■ Contact Address

TU Dortmund University
Materials Test Engineering (WPT)
M.Sc. Shafaqat Siddique
Baroper Str. 303
D-44227 Dortmund

Tel.: +49 (0)231 755-8165
Fax: +49 (0)231 755-8029
E-Mail: shafaqat.siddique@tu-dortmund.de
Web: www.wpt-info.de

TU Dortmund University
Materials Test Engineering (WPT)
Prof. Dr.-Ing. Frank Walther
Baroper Str. 303
D-44227 Dortmund

Tel.: +49 (0)231 755-8028
Fax: +49 (0)231 755-8029
E-Mail: frank.walther@tu-dortmund.de
Web: www.wpt-info.de

For Research Use Only. Not for use in diagnostic procedures.
The content of this publication shall not be reproduced, altered or sold for any commercial purpose without the written approval of Shimadzu. The information contained herein is provided to you "as is" without warranty of any kind including without limitation warranties as to its accuracy or completeness. Shimadzu does not assume any responsibility or liability for any damage, whether direct or indirect, relating to be the use of this publication. This publication is based upon the information available to Shimadzu on or before the date of publication, and subject to change without notice.

SHIMADZU
Excellence in Science

Application News

No.i254

Material Testing System

Compression After Impact Testing of Composite Material

Introduction

Carbon fiber reinforced plastic (CFRP) has a higher specific strength and rigidity than metals, and is used in aeronautics and astronautics to improve fuel consumption by reducing weight. However, CFRP only exhibits these superior properties in the direction of its fibers, and is not as strong perpendicular to its fibers or between its laminate layers. When force is applied to a CFRP laminate board, there is a possibility that delamination and matrix cracking will occur parallel to its fibers. Furthermore, CFRP is not particularly ductile, and is known to be susceptible to impacts. When a CFRP laminate board receives an impact load, it can result in internal matrix cracking and delamination that is not apparent on the material surface. There are many situations in which CFRP materials may sustain an impact load, such as if a tool being dropped onto a CFRP aircraft wing, or small stones hitting the a CFRP wing during landing. Consequently, tests are required for these scenarios. One of these tests is compression after impact (CAI) testing. CAI testing involves subjecting a specimen to a prescribed impact load, checking the state of damage to the specimen by a nondestructive method, and then performing compression testing of that specimen. This article describes CAI testing performed according to the ASTM D7137 (JIS K 7089) standard test method.

Measurements Taken Before Compression After Impact Testing

(1) Impact Test

The impact test involved dropping a 5 kg steel ball striker formed with a 16 mm diameter hemispherical point in the middle of the specimen. The specimen is fixed in place with four toggle clamps. The standard test method states that avoiding a second impact is preferred, so impact testing was performed with a mechanism that prevented second impacts. The impact energy recommended in the standard test method is 6.67 J per 1 mm of specimen thickness. For the purpose of comparison, the test was performed at four impact energies of 6.7, 5.0, 3.3, and 1.7 J per 1 mm thickness. Information on the specimen used is shown in Table 1. The test setup is shown in Fig. 1, and test conditions are shown in Table 2.

Table 1 Specimen Information

Dimensions [mm]	: 100 × 150 × 4.56
Lamination Method	: [45/0/−45/90] $_{ns}$
Material	: T800, 2252S-21

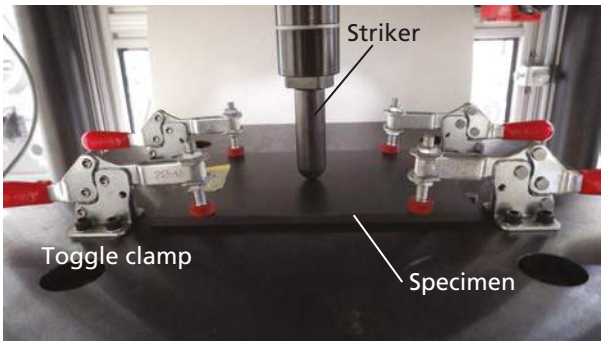

Fig. 1 Impact Test Setup

Table 2 Impact Test Conditions

Impact Energy	: 30.5, 22.9, 15.2, 7.6 [J]
No. of Tests	: n = 4

(2) Non-Destructive Inspection

After the impact test, the delamination area and maximum delamination length that resulted inside the laminate board were measured by nondestructive analysis. An ultrasonic flaw detection device is normally used for the non-destructive inspection step of CAI testing. The standard test method states that if ultrasonic flaw detection shows damage is present across more than half the width of the specimen, edge effects cannot be ignored and lowering the impact energy should be considered. Fig. 2 shows the setup for ultrasonic flaw detection.

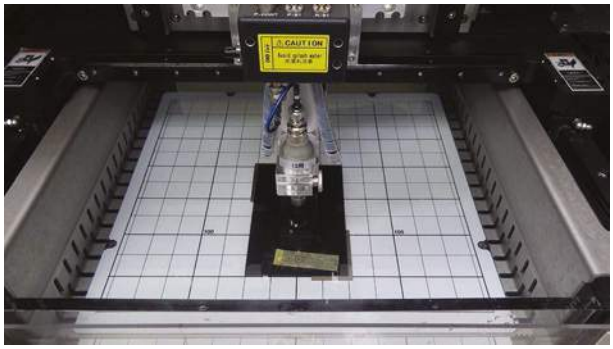

Fig. 2 Ultrasonic Flaw Detection

Fig. 3 shows the specimen after an impact test with an impact energy of 30.5 J. Fig. 3 shows an indentation in the middle of the specimen, but does not show the area of damage caused by delamination. Fig. 4 shows the results of ultrasonic flaw detection at each impact energy. The white areas in Fig. 4 are regions of delamination. Brighter areas show greater delamination. Comparison with Fig. 3 shows that delamination also occurs in areas other than the indentation in the center of the specimen, and the extent of internal damage cannot be determined based on external damage. The results also show that the damage area increases as the impact energy increases.

Fig. 3 Specimen After Impact Test (30.5 J Impact Energy)

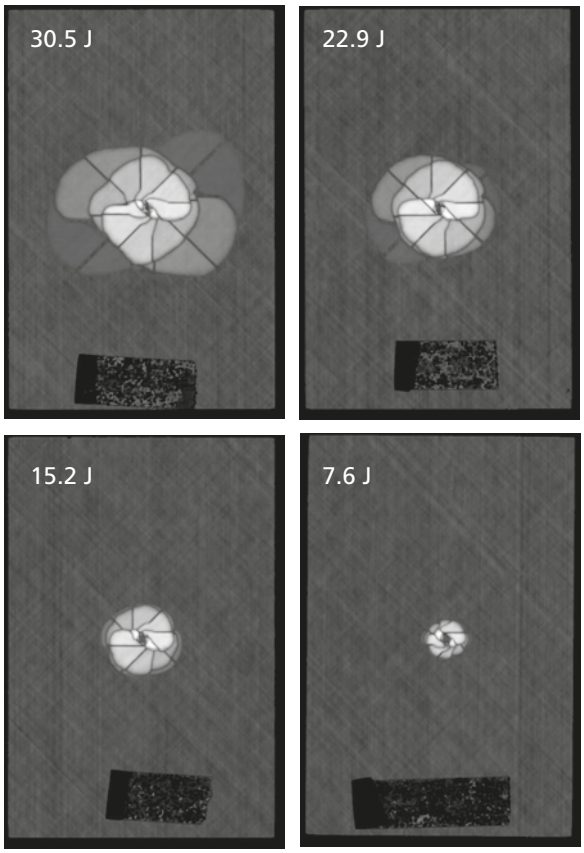

Fig. 4 Results of Ultrasonic Flaw Detection at Each Impact Energy

The damage area and maximum damage length are calculated from the images obtained by ultrasonic flaw detection. As an example, images used to calculate the damage area and maximum damage length after an impact energy of 30.5 J are shown in Fig. 5. Fig. 6 shows the relationship between damage area and impact energy, and Fig. 7 shows the relationship between maximum damage length and impact energy.

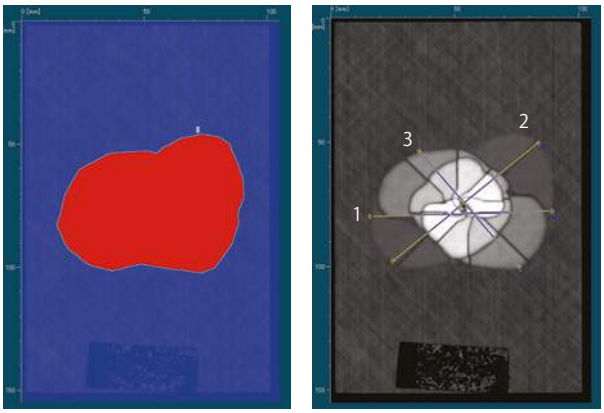

Region No.	Percentage Area (%)	Absolute Area (mm^2)
1	99.9988	3326.2400

No.	Length (mm)
1	73.03
2	75.50
3	61.37

Fig. 5 Images of Damaged Area and Maximum Damage Length

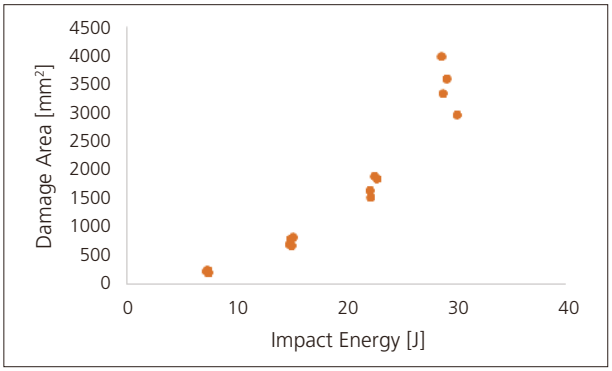

Fig. 6 Relationship between Damage Area and Impact Energy

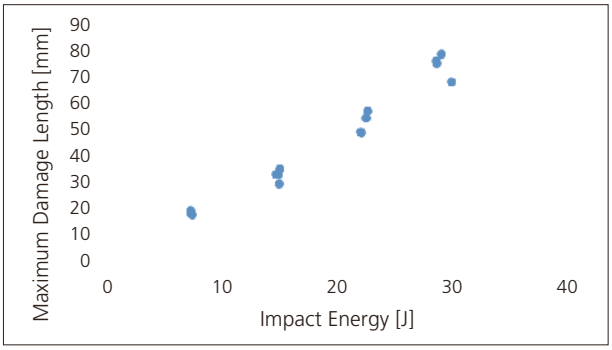

Fig. 7 Relationship between Maximum Damage Length and Impact Energy

Measurement System for Compression After Impact Testing

Two strain gauges must be attached to the front and back of the specimen. A specimen with strain gauges attached is shown in Fig. 8. The specimen shown in Fig. 8 is compressed at up to 10 % its expected compressive strength following impact in a longitudinal direction, and the CAI testing is performed after confirming the difference between front and rear strain gauges is within 10 %. Test conditions are shown in Table 3. The test setup is shown in Fig. 9, and test equipment used is shown in Table 4.

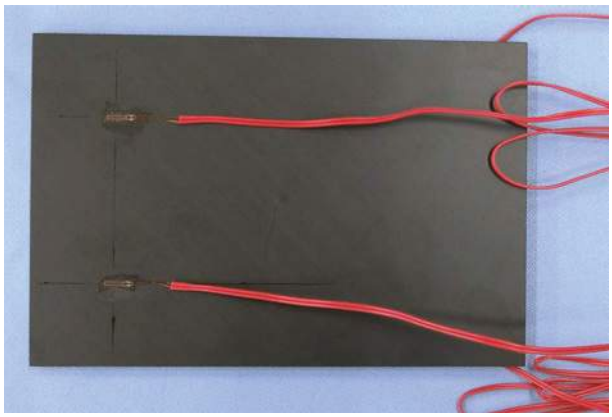

Fig. 8 Specimen

Table 3 Test Conditions

Test Speed	: 1.25 mm/min
No. of Tests	: n = 4

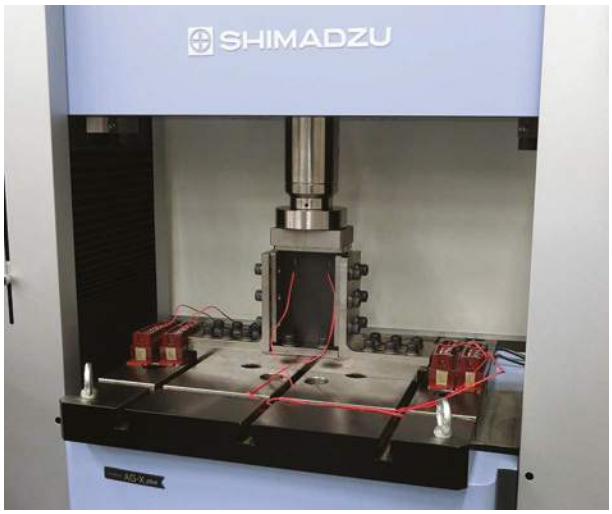

Fig. 9 Test Setup

Table 4 Experimental Equipment

Testing Machine	: AG-Xplus
Load Cell	: 250 kN
Test Jig	: Compression after impact test jig

Test Results

Examples of stress-strain curves at each impact energy are shown in Fig. 10. The compression-after-impact strength and mean compressive elastic modulus after impact are shown for each impact energy in Table 5. The standard test method states the compressive elastic modulus after impact should be calculated in the range of 0.1 % to 0.3 % strain. However, the breaking strain of one or more specimens was ≤ 0.3 % after the 30.5 J impact energy, and so for these specimens the elastic modulus was calculated from a linear region. Fig. 10 and Table 5 show the smaller the impact energy the larger the compression-after-impact strength. They also show the compressive elastic modulus after impact is almost constant regardless of impact energy.

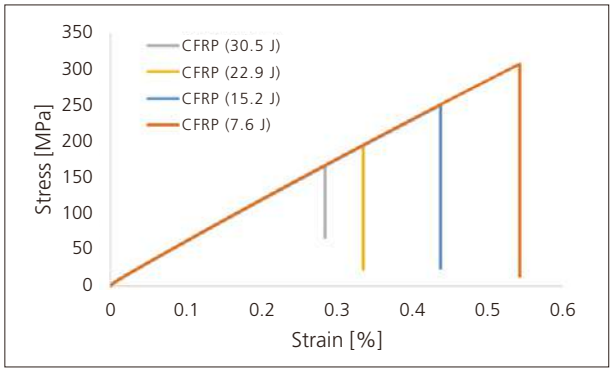

Fig. 10 Stress-Strain Curve

Table 5 Test Results (Mean)

Impact Energy [J]	Compression-After-Impact Strength [MPa]	Compressive Elastic Modulus After Impact [GPa]
30.5	162.9	57.2
22.9	203.3	56.4
15.2	246.4	56.0
7.6	308.6	56.3

The relationship between damage area and compression-after-impact strength is shown in Fig. 11, and the relationship between maximum damage length and compressive elastic modulus after impact is shown in Fig. 12. Fig. 11 and Fig. 12 show the smaller the damage area or maximum damage length, the larger the compression-after-impact strength. As a reference, the compressive strength of a specimen tested without applying any impact energy was 388 MPa.

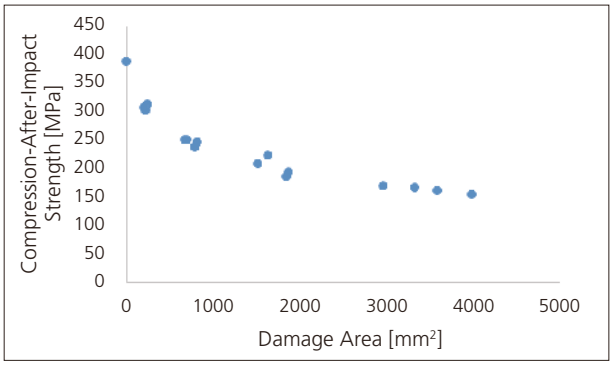

Fig. 11 Relationship between Damage Area and Compression-After-Impact Strength

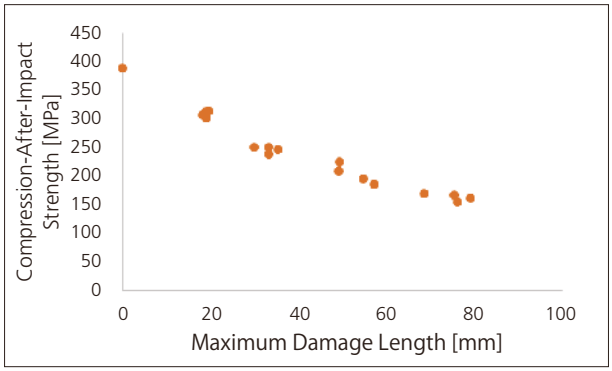

Fig. 12 Relationship between Maximum Damage Length and Compression-After-Impact Strength

Conclusion

CAI testing was performed on specimens at four different impact energies. As shown by the results, the larger the impact energy the smaller the compression-after-impact strength. Also, even a small amount of impact energy (in this experiment, an impact energy of 7.6 J amounted to 5 kg dropped from 0.15 m) reduced the compression-after-impact strength compared to the undamaged compressive strength, showing the importance of testing scenarios for impact loading. Shimadzu's testing system was used successfully to perform CAI testing according to ASTM D7137 (JIS K 7089), and can be used for evaluation of CFRP materials.

First Edition: Aug. 2016

Shimadzu Corporation
www.shimadzu.com/an/

For Research Use Only. Not for use in diagnostic procedure.
This publication may contain references to products that are not available in your country. Please contact us to check the availability of these products in your country.

The content of this publication shall not be reproduced, altered or sold for any commercial purpose without the written approval of Shimadzu. Company names, product/service names and logos used in this publication are trademarks and trade names of Shimadzu Corporation or its affiliates, whether or not they are used with trademark symbol "TM" or "®". Third-party trademarks and trade names may be used in this publication to refer to either the entities or their products/services. Shimadzu disclaims any proprietary interest in trademarks and trade names other than its own.

The information contained herein is provided to you "as is" without warranty of any kind including without limitation warranties as to its accuracy or completeness. Shimadzu does not assume any responsibility or liability for any damage, whether direct or indirect, relating to the use of this publication. This publication is based upon the information available to Shimadzu on or before the date of publication, and subject to change without notice.

© Shimadzu Corporation, 2016

SHIMADZU
Excellence in Science

Application News

No.i255

Material Testing System

Compression Test of Composite Material

Introduction

Even among composite materials, carbon fiber reinforced plastic (CFRP) has a particularly high specific strength, and is used in aeroplanes and some transport aircraft to improve fuel consumption by reducing weight. Compressive strength is an extremely important parameter in the design of composite materials that is always tested. However, due to the difficulty of testing compressive strength there is a variety of test methods. A major compression test method is the combined loading compression (CLC) method found in ASTM D6641. The CLC method can be performed with a simple jig structure, untabbed strip specimens, and can be used to simultaneously evaluate strength and measure elastic modulus. We performed compression testing of CFRP according to ASTM D6641.

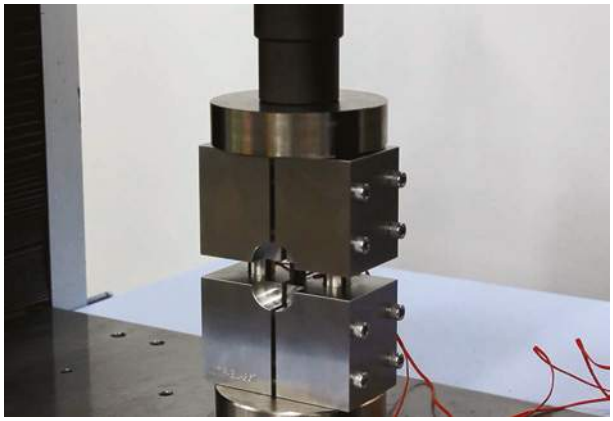

Fig. 1 Test Fixture

Measurement System

A CFRP specimen of T800S/3900 was used. Other information on the specimen is shown in Table 1. The test equipment used is shown in Table 2. Based on the CLC method in ASTM D6641, the specimen was attached to the jig shown in Fig. 1 and compressed using compression plate. Fig. 2 shows a photograph of the specimen. As shown in Fig. 2, a strain gauge was attached on the front and rear in the middle of the specimen. Outputs from the front and rear strain gauges confirmed that the specimen was aligned straight in the jig during specimen attachment. The specimen was attached using a torque wrench to fasten it in place uniformly. The test was performed with the test speed set to 1.3 mm/min.

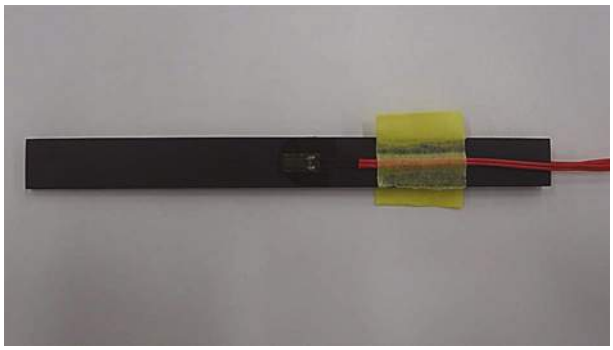

Fig. 2 Specimen

Table 1 Specimen Information

Length	: 140 mm
Width	: 13 mm
Thickness	: 3 mm
Lamination Method	: $[90/0]_{4S}$

Table 2 Experimental Equipment

Testing Machine	: AG-Xplus
Load Cell	: 50 kN
Test Jig	: CLC test fixture

Test Results

Measurements were performed twice, and stress-strain curves are shown in Fig. 3. The strain used is the mean strain taken from the front and rear sides of the specimen. The relationship between the first strain measurement and time is shown in Fig. 4 to show the outputs obtained from the strain gauges. Fig. 4 shows the outputs from both strain gauges were almost the same up to around 40 seconds, which is evidence that the test was successful. A small amount of deviation between the strain gauges arises after around 0.5 % strain, which is caused by a small amount of specimen flexure. Table 3 shows the test results. The mean compressive strength was 640.7 MPa, and the mean elastic modulus was 72.9 GPa. Elastic modulus was calculated using the mean of the strain gauge outputs.

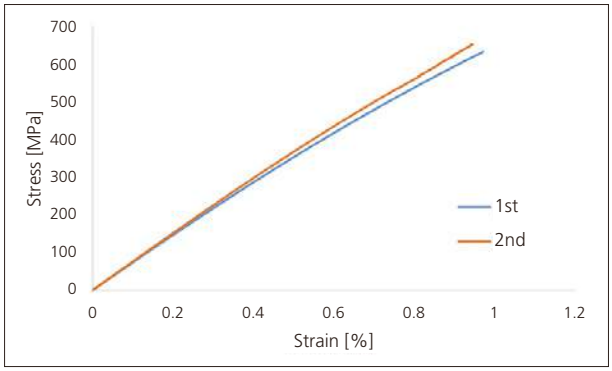

Fig. 3 Stress-Strain Curves (n = 2)

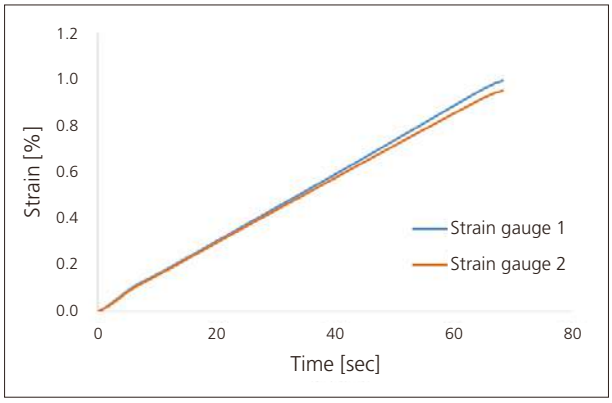

Fig. 4 Displacement-Time Curves (1st)

Table 3 Test Results

	Compressive Strength [MPa]	Elastic Modulus [GPa]
1st	629.9	71.4
2nd	651.4	74.3
Mean	640.7	72.9

Conclusion

Using this test system, compression testing of a CFRP was successfully performed according to ASTM D6641. Because this standard test method allows the testing of untabbed strip specimens, compressive strength and elastic modulus can be determined relatively easily for CFRPs.

First Edition: Aug. 2016

Shimadzu Corporation
www.shimadzu.com/an/

For Research Use Only. Not for use in diagnostic procedure.
This publication may contain references to products that are not available in your country. Please contact us to check the availability of these products in your country.

The content of this publication shall not be reproduced, altered or sold for any commercial purpose without the written approval of Shimadzu. Company names, product/service names and logos used in this publication are trademarks and trade names of Shimadzu Corporation or its affiliates, whether or not they are used with trademark symbol "TM" or "®". Third-party trademarks and trade names may be used in this publication to refer to either the entities or their products/services. Shimadzu disclaims any proprietary interest in trademarks and trade names other than its own.

The information contained herein is provided to you "as is" without warranty of any kind including without limitation warranties as to its accuracy or completeness. Shimadzu does not assume any responsibility or liability for any damage, whether direct or indirect, relating to the use of this publication. This publication is based upon the information available to Shimadzu on or before the date of publication, and subject to change without notice.

© Shimadzu Corporation, 2016

SHIMADZU
Excellence in Science

Application Data Sheet

No. 36

Servo Dynamic Systems

Material Testing & Inspection

Evaluating the Fatigue Strength of GFRP Materials

■ Introduction

As an ultra-high-strength composite material with superior heat resistance and electrical insulation properties, the use of glass fiber reinforced plastics (GFRP) has been increasing rapidly in automobiles, office equipment, consumer electronics, and other fields. Due to the use of GFRP materials in the automotive industry in particular, the impact resistance and fatigue strength of the material is increasingly being scrutinized and there is increasing demand for the development of GFRP materials that offer higher functionality or performance.

Shimadzu Servopulser series servo-hydraulic fatigue and endurance testing machines are able to accurately measure the fatigue strength of resins, composites, metals, and components, making them ideal for evaluating the fatigue strength of GFRP materials.

This issue of Shimadzu Application News describes an example of testing the fatigue strength of a GFRP composite material containing 20 % glass fiber in a polyamide resin. It also shows the change in the interior status of test samples as the fatigue test progresses, observed using a Shimadzu X-ray fluoroscopy system.

■ Testing Instruments and Samples

A Shimadzu EHF-LV20kN Servopulser series servo-hydraulic fatigue testing machine (a typical example is shown in Fig. 1) was used in conjunction with a Shimadzu SMX-225CT inspeXio X-ray fluoroscopy system used to observe the sample with X-ray fluoroscopy.

Sample details are as follows:

(1) Polymer: Polyamide
(2) Reinforcing material: 20 % glass fiber
(3) Sample shape:Hard plastic flat plate with 20 mm neck width
(4) Sample dimensions: 80(L) x 30(W) x 3(T) mm

■ Test Conditions

Before fatigue testing, static testing was performed using the following conditions to determine fatigue loading conditions. Static testing results are shown below.

(1) Tensile speed: 1 mm/min
(2) Chuck clamping distance: 40 mm
(3) Atmosphere: Room temperature of 25 °C
(4) Tensile strength (measurement results): 96 MPa

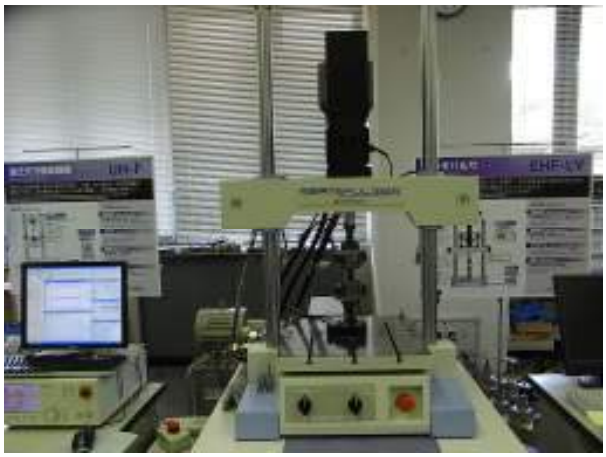

Fig.1 Shimadzu EHF-LV20kNX Servopulser Series Testing Machine

The following fatigue testing conditions (loading and data measurement/acquisition conditions) were determined based on the above static testing.

(1) Testing frequency: 10 Hz
(2) Maximum cyclic stress: Six levels, indicated below.
Level 1: 77 MPa (80 % of tensile strength)
Level 2: 67 MPa (70 % of tensile strength)
Level 3: 58 MPa (60 % of tensile strength)
Level 4: 48 MPa (50 % of tensile strength)
Level 5: 43 MPa (45 % of tensile strength)
Level 6: 38 MPa (40 % of tensile strength)
(3) Stress ratio:0 (given a minimum stress of 0 MPa)
(4) Atmosphere: Room temperature of 25 °C
(5) Testing machine: LV-20N Servopulser
(6) Test force measurement: 20,000 N load cell
(7) Chuck clamping distance: 40 mm
(8) Data acquisition: 2 kHz

(The testing machine is capable of measuring at frequencies up to 40 kHz.)

Six cyclic stress levels were decided based on the tensile strength (96 MPa) determined by static tensile testing, with a cyclic load stress ratio (minimum stress divided by maximum stress) of zero. (For example, level 1 applies a maximum stress of 77 MPa, a minimum stress of 0 MPa, and stress amplitude of 38.5 MPa.)

Though the testing machine is capable of cyclic loading at cycle rates up to 100 Hz, in this case a 10 Hz sine wave was used in consideration of sample heat generation.

Fig. 2 shows a sample mounted in the testing machine grips.

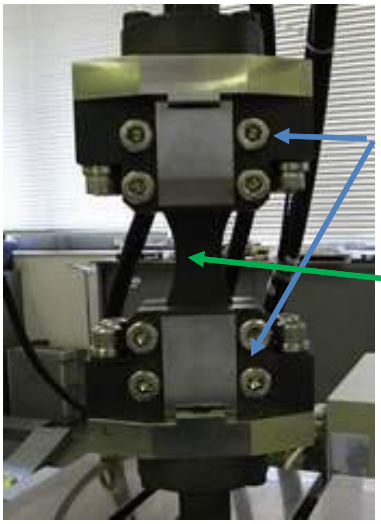

Fig. 2 Sample Mounted in Testing Machine

■ Test Results

Fig. 3 shows an example of peak stress (black) and displacement (blue) values (sine wave peak and valley values) measured from start of loading to sample fracture, given a stress level of 5.

The cyclic stress load applied to the sample causes it to gradually deform until a crack forms, after which the deformation increases rapidly and the sample fractures.

Fig. 4 is a stress versus cycle count plot for six stress levels (one sample for each level) that shows the relationship between the maximum stress load and the cycle count at sample fracture.

As shown in the results above, in addition to fatigue testing, the fatigue testing machine can also be used for a wide range of other strength testing, including static testing.

In addition, an industrial X-ray system was used to observe how the fiber orientation inside the GFRP material changes as the fatigue test progresses.

Fig. 5 shows the curious phenomenon of how the glass fibers inside the sample, which have no particular orientation before starting the fatigue test (left), begin to orient themselves a little in the longitudinal direction after a million load cycles (middle), and are all oriented in the longitudinal direction just before fracture (right).

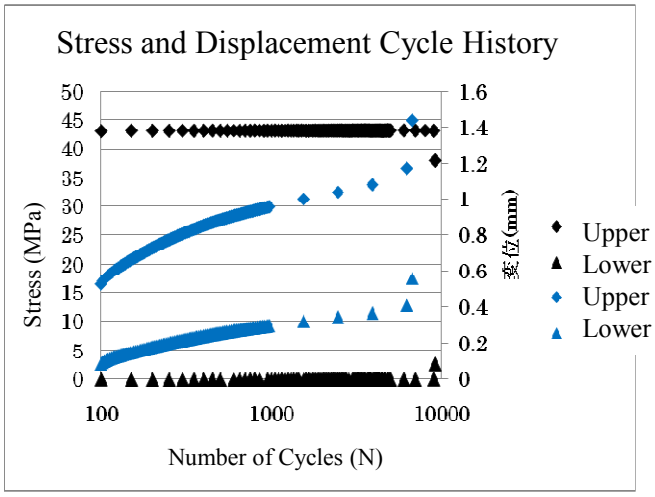

Fig. 3 Fatigue Test Results

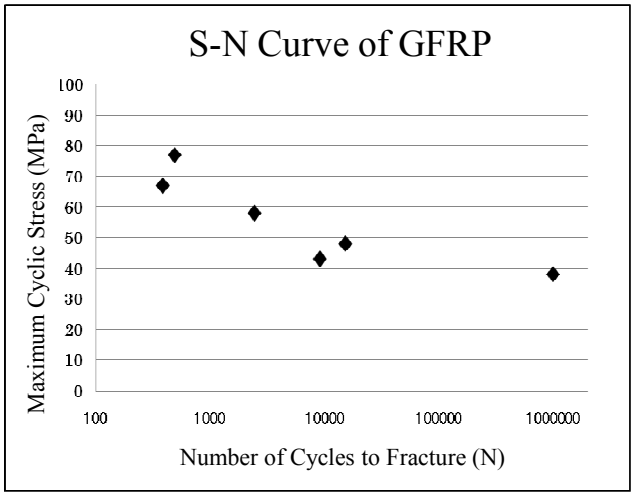

Fig. 4 Fatigue Test Results

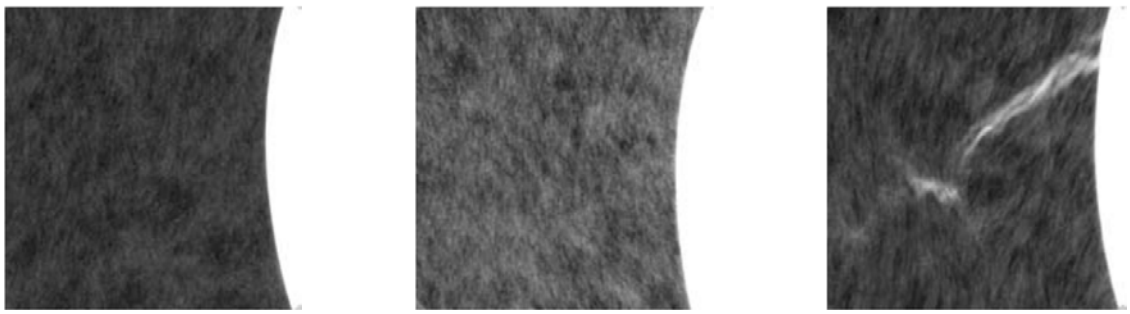

Start of Fatigue Test | After 1 Million Load Cycles | Just Before Fracture

Fig.5 Fiber Orientation Inside GFRP

Note: The analytical and measuring instruments described may not be sold in your country or region.

First Edition: July, 2015

SHIMADZU
Shimadzu Corporation
www.shimadzu.com/an/

For Research Use Only. Not for use in diagnostic procedures.
The content of this publication shall not be reproduced, altered or sold for any commercial purpose without the written approval of Shimadzu.
The information contained herein is provided to you "as is" without warranty of any kind including without limitation warranties as to its accuracy or completeness. Shimadzu does not assume any responsibility or liability for any damage, whether direct or indirect, relating to the use of this publication. This publication is based upon the information available to Shimadzu on or before the date of publication, and subject to change without notice.
© Shimadzu Corporation, 2015

SHIMADZU
Excellence in Science

Application Data Sheet

No. 30

Autograph Precision Universal Tester

Material Testing & Inspection

Evaluating the Strength of Carbon Fiber Reinforced Plastics (CFRP)

■Introduction

Various types of plastic materials have been developed that are light weight and also perform better than previous materials in terms of environmental resistance and in terms of strength. Consequently, there is a growing demand for such materials in aircraft, automotive, and many other fields.These plastic materials, such as carbon fiber reinforced plastic (CFRP), glass fiber reinforced plastic (GFRP), and aramid fiber reinforced plastic, are characterized by using fibers with advanced functionality (low weight, high strength, deformation resistance, corrosion resistance, and also heat resistance). Carbon fiber reinforced plastic (CFRP) is particularly representative of such materials and is increasingly used in sports equipment and other everyday products. Therefore, evaluating its strength, its fundamental feature, is very important.

This article presents results from testing carbon fiber reinforced plastic (CFRP) using a Shimadzu Autograph precision universal testing machine. (Test specimens and loading conditions conformed to JIS K7073-1988 Testing Method for Tensile Properties of Carbon Fiber Reinforced Plastics.)

■Measurement and Jigs

Specimens were Type-IV specified by JIS K7073-1988 (rectangular strips with no tabs). Tensile tests were conducted with an extensometer attached to measure longitudinal strain and a width sensor attached to measure lateral strain, as shown in Fig.1.

Fig. 1 Test Configuration

■Test Results

Test results indicate a tensile strength of 8.31×10^2 MPa, an elastic modulus of 5.76×10^5 MPa (determined from the slope between points at 100 MPa and 300 MPa), and a maximum tensile strain of 0.766 percent. Since these results were obtained using test specimens with fibers oriented perpendicular (lateral) to the direction of tensile load, the same test was performed with fibers oriented parallel (longitudinal) to the direction of tension. This resulted in an elastic modulus of about 13.00×10^5 MPa, which indicates a significant difference depending on the fiber orientation.

Fig.3 shows the relationship between stress and displacement in the direction perpendicular to tension, for the same test as before. A calculation of Poisson's ratio between 100 MPa and 300 MPa, as before, resulted in a value of 6.0×10^{-2}.

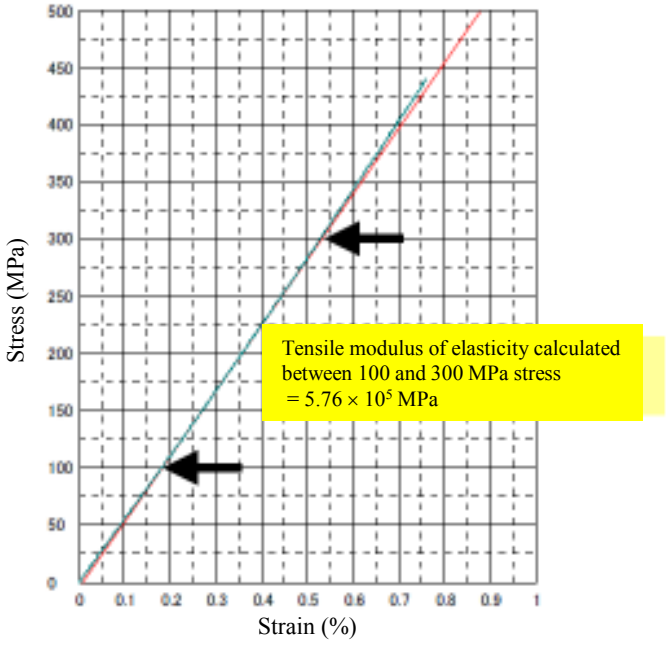

Fig.2 shows the results of testing to failure at a rate of 1 mm/min (stress vs. longitudinal strain curve).

Whereas the Poisson's ratio is about 0.3 for soft iron and about 0.46 to 0.49 for elastic rubber, the ratio for carbon fiber reinforced plastic (CFRP) is about one order of magnitude smaller, which means the deformation level of CFRP is extremely low.

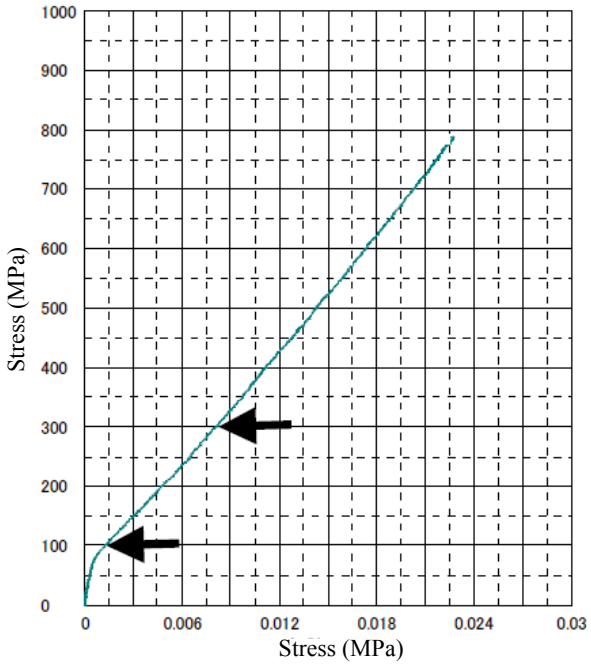

Fig. 3 Graph of Stress vs. Lateral Displacement

Poisson's ratio in left figure: 6.0×10^{-2}
(for range between 2 points, at 100 MPa and 300 MPa)

Method Used to Determine Poisson's Ratio
$\upsilon t = |\Delta\varepsilon 2/\Delta\varepsilon 1|$
υt: Poisson's ratio
$\Delta\varepsilon 1$: Strain increase in tensile direction
$\Delta\varepsilon 2$: Strain increase perpendicular to tension

■Test Conditions and Equipment Used

Tester:	AG-Xplus
Load Cell:	50 kN
Test Jig:	50 kN non-shift wedge type grips
Extensometer:	SG50-10 for measuring strain in tensile direction
	SGW-5 for measuring strain perpendicular to tensile direction
Software:	TRAPEZIUM X (Single)

AG-Xplus Floor-Type Precision Universal Tester

TRAPEZIUM X

■ A high-precision load cell is adopted. (The high-precision type is class 0.5; the standard-precision type is class 1.)
Accuracy is guaranteed over a wide range, from 1/1000 to 1/1 of the load cell capacity. This supports highly reliable test evaluations.

■ Crosshead speed range
Tests can be performed over a wide range from 0.0005 mm/min to 1,000 mm/min.

■ High-speed sampling
Ultrafast sampling, as fast as 0.2 msec, allows assessment of sudden changes in test force, such as when brittle materials fracture.

■ TRAPEZIUMX X operational software
Designed for intuitive operation, it offers a variety of convenient and user-friendly features.

■ Smart controller
Real-time test force and position data are readily confirmed, and the manual dial enables fine adjustments to jig positioning.

■ Optional Test Devices
A variety of tests can be performed by switching between an abundance of jigs in the lineup.

First Edition: July 2015

SHIMADZU
Shimadzu Corporation
www.shimadzu.com/an/

For Research Use Only. Not for use in diagnostic procedures.
The content of this publication shall not be reproduced, altered or sold for any commercial purpose without the written approval of Shimadzu.
The information contained herein is provided to you "as is" without warranty of any kind including without limitation warranties as to its accuracy or completeness. Shimadzu does not assume any responsibility or liability for any damage, whether direct or indirect, relating to the use of this publication. This publication is based upon the information available to Shimadzu on or before the date of publication, and subject to change without notice.
© Shimadzu Corporation, 2015

SHIMADZU
Excellence in Science

Application Data Sheet

No. 39

Autograph Precision Universal Testing Machine

Material Testing & Inspection

Evaluation of Open-Hole CFRP — Static Tensile Testing, Fracture Observation, and Internal Structure Observation —

■ Introduction

Recently, lightweight alternatives to conventional metal materials are being used as structural members where mechanical reliability is required. The main reason for this trend is that lighter products reduce transport weights, which reduces fuel consumption and carbon dioxide emissions during product transport. Fiber reinforced composite materials such as carbon fiber reinforced plastics (CFRP), which consist of a resin strengthened with carbon fibers, are extremely strong and light. Because of this, they are currently a material widely used in aircraft, and are expected to be used increasingly in various types of products, including automobiles, in order to make them lighter. For the development of fiber reinforced composite materials, not just a simple evaluation of their mechanical strength, but also the observation of failure events is important. In addition, from the perspective of quality management, the necessity for evaluation of internal structure of these materials, such as the oriented state of fibers and the presence of cracks, has increased.

In this article, we describe how we use a precision universal testing machine (Autograph AG-250kNXplus) and high-speed video camera (HyperVision HPV-X) (Fig. 1) to evaluate the static fracture behavior of a CFRP based on a test force attenuation graph and images of material failure. We also describe our subsequent examination of the state of the specimens internally using an X-ray CT system (inspeXio SMX-100CT) to investigate the state of fracture inside the specimen. Information on specimens is shown in Table 1. Specimens have a hole machined into their center that is 6 mm in diameter. Fracture is known to propagate easily through composite materials from the initial damage point, and when a crack or hole is present their strength is reduced markedly. Therefore, evaluation of the strength of open-hole specimens is extremely important from the perspective of the safe application of CFRP materials in aircraft, etc.

Table 1: Test Specimen Information

Laminate Structure	Dimensions L (mm) × W (mm) × T (mm), hole diameter (mm)
$[+45/0/-45/+90]_{2s}$	150 × 36 × 2.9, Φ6

Note: The CFRP laminate board used in the actual test was created by laying up prepreg material with fibers oriented in a single direction. The $[+45/0/-45/+90]_{2s}$ shown as the laminate structure in Table 1 refers to the laying up of 16 layers of material with fibers oriented at +45°, 0°, -45°, and +90° in two layer sets.

■ Static Tensile Testing (Ultra High Speed Sampling)

In this test, the change in load that occurs during specimen fracture was used as the signal for the HPV-X high-speed video camera to capture images. Specifically, the AG-Xplus precision universal testing machine was configured to create a signal when the test force on the specimen reaches half the maximum test force (referred to as Maximum test force in Fig. 3), with this signal being sent to the high-speed video camera. Static tensile testing and fracture observation were performed according to the conditions shown in Table 2. A test force-displacement plot for the open-hole quasi-isotropic CFRP(OH-CFRP) is shown in Fig. 2(a). A test force-time plot during the occurrence of material fracture is also shown in Fig. 2(b).

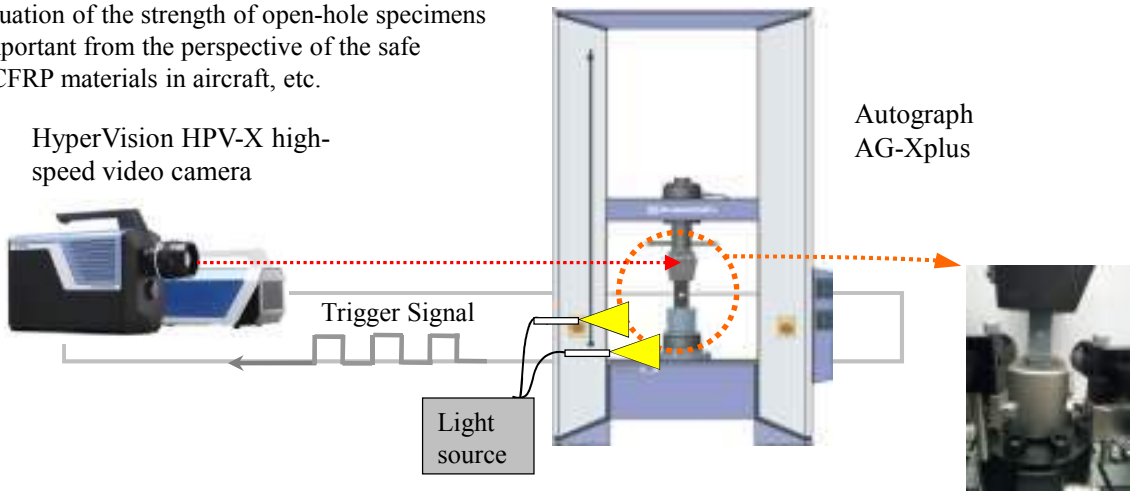

Fig.1: Testing Apparatus

Table 2: Test Conditions

Testing Machine	AG-Xplus
Load Cell Capacity	250 kN
Jig	Upper: 250 kN non-shift wedge type grips (with trapezoidal file teeth on grip faces for composite materials) Lower: 250 kN high-speed trigger-capable grips
Grip Space	100 mm
Loading Speed	1 mm/min
Test Temperature	Room temperature
Software	TRAPEZIUM X (Single)
Fracture Observation	HPV-X high-speed video camera (recording speed 600 kfps)
DIC Analysis	StrainMaster (LaVision GmbH.)

Note: fps stands for frames per second. This refers to the number of frames that can be captured in 1 second.

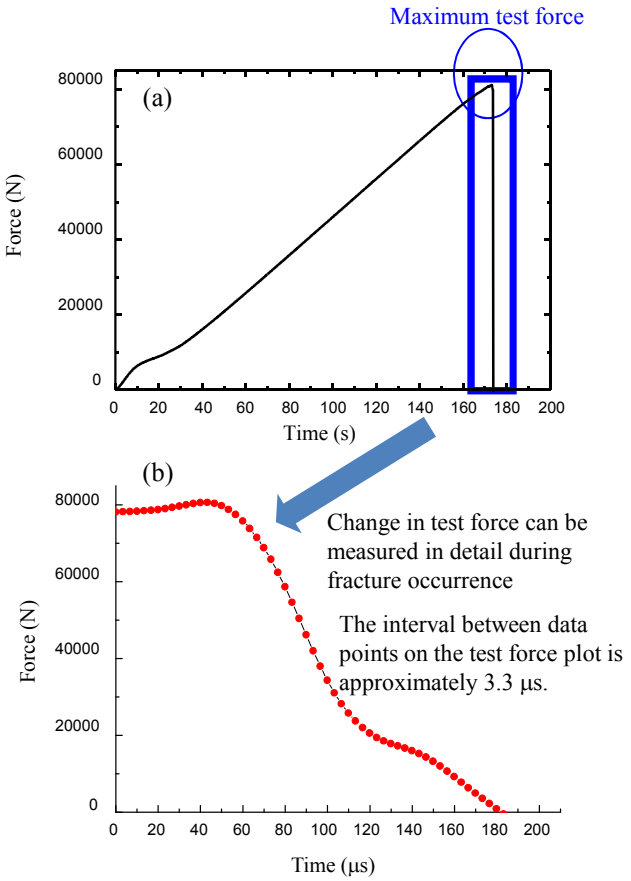

Fig. 2 (a) Test Force-Displacement Curve, and (b) Test Force-Time Curve (in Region of Maximum Test Force)

Fig. 2(a) can be interpreted to show the specimen fractured at the moment it reached the maximum test force, at which point the load on the specimen was suddenly released. This testing system can be used to perform high-speed sampling to measure in detail the change in test force in the region of maximum test force. The time interval between data points on the test force plot in Fig. 2(b) is 3.3 µs.

■ Fracture Observation (High Speed Imaging)

Images (1) through (8) in Fig. 3 capture the behavior of the specimen during fracture around the circular hole. Image (1) shows the moment cracks occur in a surface +45° layer. In this image, the tensile load being applied is deforming the circular hole, where hole diameter in the direction of the load is approximately 1.4 times that perpendicular to the load. In image (2), the cracks that occurred around the circular hole are propagating along the surface +45° layer. In images (3) through (6), a substantial change can be observed in the external appearance of the specimen near the end of the crack propagating to the bottom right from the circular hole. This suggests not only the surface layer, but internal layers are also fracturing. Based on the images of the same area and the state of the internal layers that can be slightly observed from the edges of the circular hole in images (7) and (8), the internal fracture has quickly propagated in the 18 µs period between images (3) and (8).

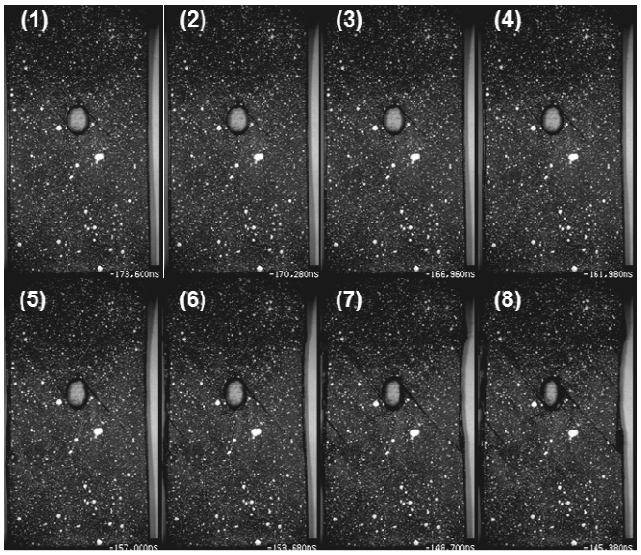

Fig. 3: Observations of OH-CFRP Fracture

First Edition: July 2015

Shimadzu Corporation
www.shimadzu.com/an/

For Research Use Only. Not for use in diagnostic procedures.
The content of this publication shall not be reproduced, altered or sold for any commercial purpose without the written approval of Shimadzu.
The information contained herein is provided to you "as is" without warranty of any kind including without limitation warranties as to its accuracy or completeness. Shimadzu does not assume any responsibility or liability for any damage, whether direct or indirect, relating to the use of this publication. This publication is based upon the information available to Shimadzu on or before the date of publication, and subject to change without notice.
© Shimadzu Corporation, 2015

Images (1) through (8) of Fig. 4 show the results of performing Digital image correlation (DIC) analysis on the fracture observation images of Fig. 3. Black signifies areas of the surface layer of the specimen under little strain, and red signifies areas under substantial strain. Looking at images (1) through (4), we can see that strain around the circular hole is focused diagonally toward the top-left (-45°) and toward the bottom-left (+45°) from the circular hole. Images (5) through (8) show the focusing of strain diagonally toward the bottom-right (-45°) and toward the top-right (+45°) from the circular hole in areas where it was not obvious in images (1) through (4). This shows an event is occurring in the surface layer of the specimen that is similar to the process of fracture often seen during tensile testing of ductile metal materials, which is crack propagation in the direction of maximum shearing stress.

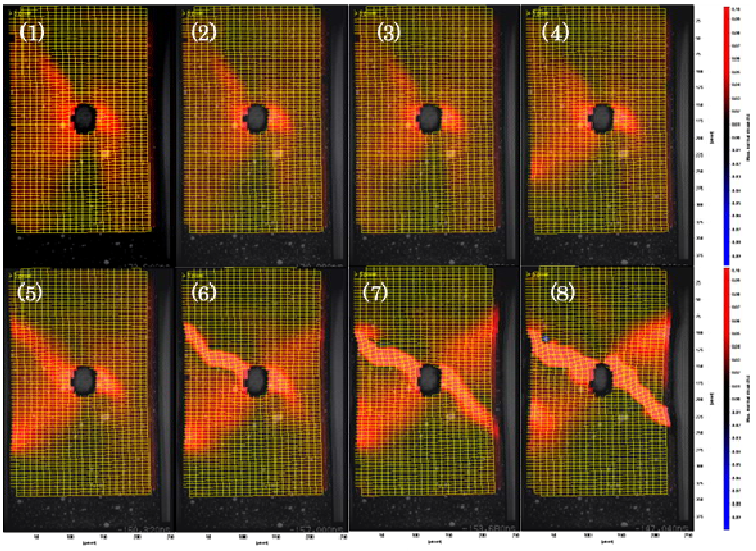

Fig. 4: Observation of OH-CFRP Fracture (DIC Analysis)

■ Internal Structure Observation (CT)

Next, internal observations were performed around the circular hole using a micro focus X-ray CT system to check the state of internal damage to the specimen. The SMX-100CT micro focus X-ray CT system (Fig. 5) is capable of capturing CT images at high magnification. The system rotates a specimen between an X-ray generator and an X-ray detector, uses a computer to calculate fluoroscopic images obtained from all 360° of rotation, then reconstructs a tomographic view of the specimen (Fig. 6). This system was used to perform a CT scan of the fracture area of the OH-CFRP after the static tensile testing and fracture observation performed as described in the previous section, so that the cracks that occurred inside can be observed.

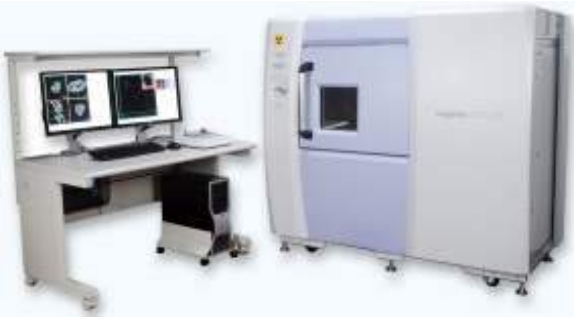

Fig. 5: Shimadzu inspeXio SMX-100CT Micro Focus X-Ray CT System

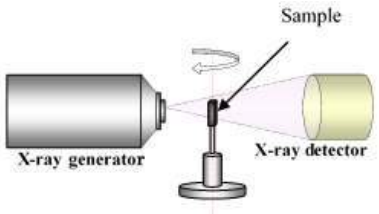

Fig. 6: Illustrated Example of X-Ray CT System Operation

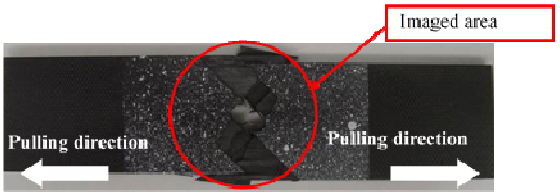

Fig. 7: Specimen After Static Tensile Testing (Specimen Used for CT Scan)

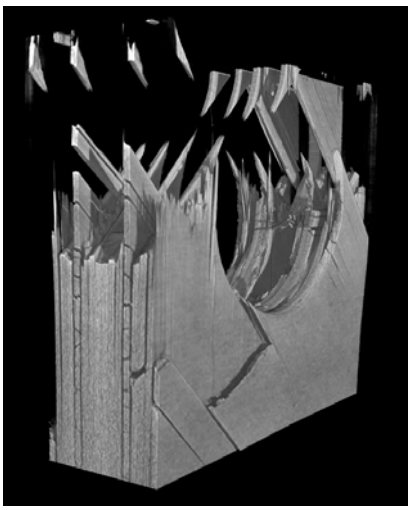

Fig. 8: Fracture Area 3D Image No. 1

First Edition: July 2015

SHIMADZU
Shimadzu Corporation
www.shimadzu.com/an/

For Research Use Only. Not for use in diagnostic procedures.
The content of this publication shall not be reproduced, altered or sold for any commercial purpose without the written approval of Shimadzu.
The information contained herein is provided to you "as is" without warranty of any kind including without limitation warranties as to its accuracy or completeness. Shimadzu does not assume any responsibility or liability for any damage, whether direct or indirect, relating to the use of this publication. This publication is based upon the information available to Shimadzu on or before the date of publication, and subject to change without notice.
© Shimadzu Corporation, 2015

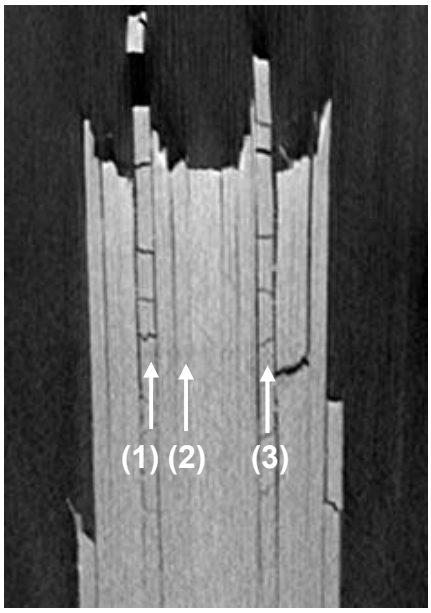

Fig. 9: CT Cross-Sectional Images of the Fracture Area

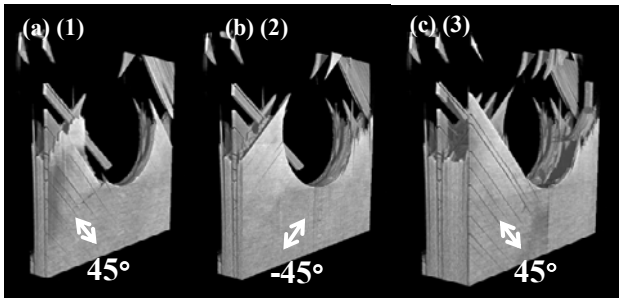

Fig. 10: Fracture Area 3D Image No. 2

Cross-sectional images of the specimen are shown as a 3D image in the 16 layers shown in Fig. 9, we can see that most cracks in the matrix occur in the +45° layer inside the specimen, indicated by the number (1) and (3). (shown in Fig. 10 (a) and Fig. 10 (b), respectively). In this layer, the carbon fibers are all aligned together in a +45° orientation, and the multiple matrix cracks occurring in this layer are probably due to the shearing force caused in this layer by tensile loading, together with deformation of adjacent layers in the direction of the loading. For comparison, a 3D image of the -45° layer inside the specimen (Fig. 9 (2)) is shown in Fig. 10 (b). As is clear from the image, the matrix cracks that occurred in the +45° layer have not occurred in the -45° layer. This difference in fracture state has probably arisen due to different shearing forces and load directions occurring in each layer. Such detailed observation of fracture surfaces associated with multiple matrix cracks was difficult by conventional methods, since to observe fracture surfaces the specimen was processed such as by cutting and embedding in resin, which changed the characteristics of the specimen. However, by using the high-resolution X-ray CT system as described in this article, there is little X-ray absorption difference between air and specimen, and it is possible to observe the state of complex internal damage, even for OH-CFRP in which microscopic damage is normally difficult to observe by X-ray.

■ Acknowledgment

We would like to extend our sincere gratitude to the Japan Aerospace Exploration Agency (JAXA) for their cooperation in the execution of this experiment.

Note: The analytical and measuring instruments described may not be sold in your country or region.

First Edition: July 2015

Shimadzu Corporation
www.shimadzu.com/an/

For Research Use Only. Not for use in diagnostic procedures.
The content of this publication shall not be reproduced, altered or sold for any commercial purpose without the written approval of Shimadzu.
The information contained herein is provided to you "as is" without warranty of any kind including without limitation warranties as to its accuracy or completeness. Shimadzu does not assume any responsibility or liability for any damage, whether direct or indirect, relating to the use of this publication. This publication is based upon the information available to Shimadzu on or before the date of publication, and subject to change without notice.
© Shimadzu Corporation, 2015

SHIMADZU
Excellence in Science

Application News

No.i247

Material Testing System

Material Testing by Strain Distribution Visualization – DIC Analysis –

Introduction

Strain distribution in samples is an increasingly important component of material testing.
As background to this trend, CAE (Computer Aided Engineering) is an analytical technology that is becoming widely used in the fields of science and industry due to the cost savings achieved through the reduced use of costly prototyping which is now being replaced by computerized product design simulation. A typical requirement is to conduct mechanical testing analysis of the region of a product in which strain is likely to occur, and to elucidate the correlation between the simulated analysis results and the strain distribution obtained in actual mechanical testing.
DIC (Digital Image Correlation) analysis is a technique used to compare the random patterns on the surface of a test sample before and after deformation to determine the degree of deformation of the sample. The advantages of this technique include the ability to measure displacement and strain distribution from a digital image without having to bring a sensor into contact with a test sample, and without requiring a complicated optical system. For these reasons, application development for DIC analysis is expanding into a wide range of fields in which measurement using existing technologies*1 has been difficult.

Here we introduce examples of DIC analysis of CFRP (Carbon Fiber Reinforced Plastic) and ABS resin high-speed tensile impact testing.

*1: Up to now, material strain distribution measurement has been conducted using various methods, including the direct attachment of large numbers of strain gauges to the test material. However, this method is not applicable for micro-sized samples to which strain gauges either cannot be attached, or attachment is difficult and complicated. These disadvantages also include the difficulty in measuring certain types of substances, such as films, that are easily affected by contact-type sensors.

Test Conditions

Fig. 1 shows the testing apparatus and software used in the high-speed tensile testing of CFRP. The test conditions are shown in Table 1, and information regarding the test specimens is shown in Table 2. For this experiment, special-shaped grips for composite materials were mounted to the HITS-T10 high-speed tensile testing machine, and the test specimen was affixed to the grips.
A high-speed HPV-2A video camera was mounted in front of the testing gap between the grips to collect video data of the specimen breaking, and the signal to start camera filming was a displacement signal from the high-speed tensile testing machine. The acquired video data was loaded into the StrainMaster (LaVision GmbH) DIC analysis software, and the strain distribution that occurred in the sample was analyzed.

HPV-2A High Speed Video Camera

Test Grips and Test Specimen

HITS-T10 High Speed Tensile Testing Machine

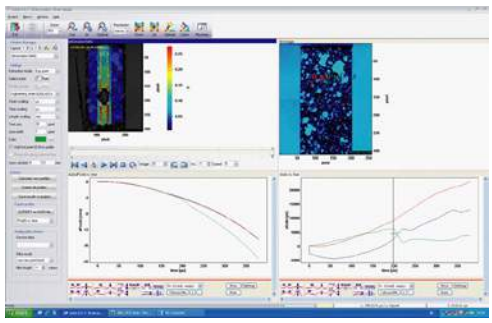
StrainMaster (LaVision GmbH)

Fig. 1 Testing Apparatus

Table 1 Test Conditions

Instrumentation	HITS-T10 high-speed tensile testing machine
	HPV-2A high-speed video camera
Test Force Measurement	10 kN load cell
Test Speed	10 m/s
Grips	Special grips for composite materials
Sampling	250 kHz
Imaging Speed	500 kfps
Light Source	Strobe
DIC Analysis	StrainMaster (LaVision GmbH) With cooperation of MARUBUN CORPORATION

Table 2 Samples

Samples (dimensions)	CFRP-OH*2 Laminate method $[0/90]_{2s}$*3 (Hole diameter ϕ1 mm, W8 × t0.4 reed-shaped)
	ABS resin (ASTM L-shaped test specimen Total length 60 mm, Parallel part 3.2 (W) × 3.2 (T) mm)
Marking	CFRP-OH*2 : White random pattern ABS resin : Black random pattern

*2: OH: Abbreviation for Open Hole. Refers to a hole that is opened in a CFRP plate.

*3: The CFRP laminate used in this experiment is prepared by laminating prepreg fibers oriented in one direction. The $[0/90]_{2s}$ specified for "Laminate method" in the table represents two sets of prepreg layers stacked in the 0 ° direction and 90 ° direction.

In this test, the HITS-T10 high speed tensile testing machine and HPV-2A high speed video camera were synchronized to take video at the instant the sample fractured. The sample was prepared prior to the test by spraying paint onto its surface in a random pattern, and the strain distribution on the surface of the test specimen was visualized by DIC analysis based on the amount of shift of the random pattern.

Test Results

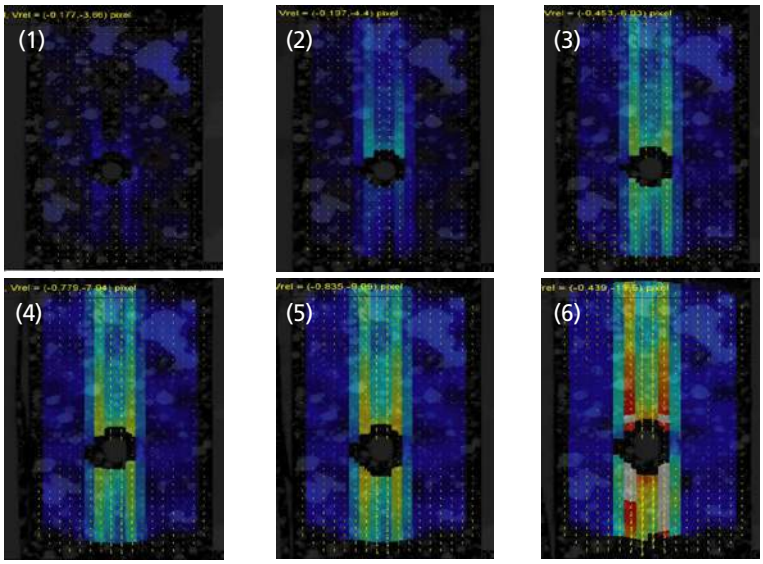

Fig. 2 Results of DIC Analysis of CFRP-OH Specimen

Fig. 2 and Fig. 3 show the DIC analysis results obtained in tensile testing of CFRP-OH and ABS resin test specimens, respectively. The images were extracted in the order of a typical time course analysis (image order corresponding to the numbers shown in images), from the start of the tensile test to the point that the specimen breaks. The appearance of coloring in the images corresponds to the strain distribution in the specimen. The amount of strain that occurs in the specimen corresponds to the degree of color warmth, with areas of darker color (such as blue-black) indicating low strain, and areas of brighter color (such as red-orange) indicating a greater degree of strain. It is clear that in Fig. 2, as the load is applied to the test specimen, the strain increases in the vicinity of the open hole. Because the test specimen is a $[0/90]_{2s}$ laminate material, it is believed that the fibers are aligned in the tensile direction in the test specimen surface layer which was subjected to random marking.

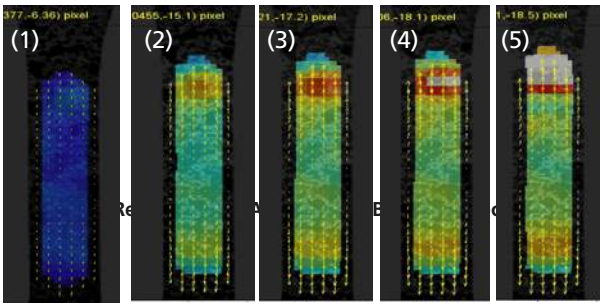

In Fig. 3, localized strain occurs from the edge of the parallel region of the test specimen, and as time progresses, localized strain is noticeable at the upper and lower edge of the parallel region.
Thus, by combining a high-speed tensile testing machine with a high-speed video camera, in addition to DIC analysis software, it has become possible to visualize the distribution of strain generated in a test specimen.

First Edition: Dce, 2012

Shimadzu Corporation
www.shimadzu.com/an/

For Research Use Only. Not for use in diagnostic procedures.
The content of this publication shall not be reproduced, altered or sold for any commercial purpose without the written approval of Shimadzu.
The information contained herein is provided to you "as is" without warranty of any kind including without limitation warranties as to its accuracy or completeness. Shimadzu does not assume any responsibility or liability for any damage, whether direct or indirect, relating to the use of this publication. This publication is based upon the information available to Shimadzu on or before the date of publication, and subject to change without notice.
© Shimadzu Corporation, 2012

SHIMADZU
Excellence in Science

Application Data Sheet

No. 8

Autograph Precision Universal Tester

Material Testing & Inspection

Flexural Testing of CFRP Boards

Standard No. JIS K 7074: 1988

Introduction

Carbon fiber reinforced plastic (CFRP) is a composite material with excellent relative strength. This plastic was quickly adopted in the aviation and space sectors, and has contributed significantly to reducing fuselage weight. Initially, this plastic was only used for partial replacement of metal materials. In the latest aircraft, however, composite materials, primarily CFRP, represent 50 % of the fuselage weight. Improved productivity and reduced costs are expected due to subsequent technical developments, and it can be expected that this plastic will also become popular as a main material in automobile frames. In this Data Sheet, a CFRP cloth was subjected to a flexural testing using a precision universal tester in order to evaluate the strength of the material.

F. Yano

Measurements and Jigs

In flexural testing specified in JIS K7074, a loading edge radius of 5 mm, and a support radius of 2 mm are specified. The specimen standard dimensions are specified as follows:

Length = 100 mm ± 1 mm
Width = 15 mm ± 0.2 mm
Thickness = 2 mm ± 0.4 mm

For tests performed using a specimen with the standard dimensions, the span between supports (L) will be 80 mm ± 0.2 mm. When TRAPEZIUM software is used, the flexural stress can be automatically calculated and plotted in a graph from the test force and the specimen dimensions. The flexural strength and other characteristic values can also be obtained from a few simple operations.

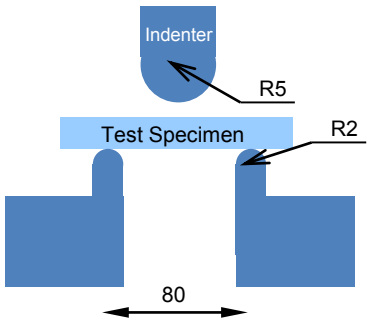

Fig. 1: Flexural Testing Schematic

Measurement Results

Fig. 2: Flexural Testing Status

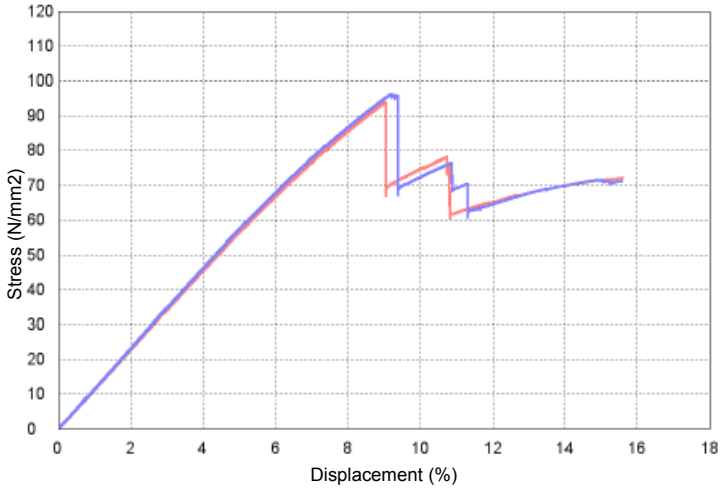

Fig. 3: Stress – Displacement Curve

Table 1: Test Conditions

Item	Set Value
Cell Capacity	5 kN
Load Speed	5 mm/min

Table 2: Test Results (Average)

Load at Fracture (N)	Bending Strength (%)
485	95

CFRP Flexural Testing System

Tester:	AG-Xplus
Load Cell:	5 kN
Test Jig:	Three-point bending test jig for plastics
Software:	TRAPEZIUM X (Single)

AG-Xplus Table-Top Precision Universal Tester

Features

- A high-precision load cell is adopted. (The high-precision type is class 0.5; the standard-precision type is class 1.)
  Accuracy is guaranteed over a wide range, from 1/1000 to 1/1 of the load cell capacity. This supports highly reliable test evaluations.
- Crosshead speed range
  Tests can be performed over a wide range from 0.0005 mm/min to 1,500 mm/min.
- High-speed sampling
  Ultrafast sampling, as fast as 0.2 msec. Sudden changes in test force, such as when brittle materials fracture, can be assessed.
- TRAPEZIUMX operational software
  Designed for intuitive operation, this software offers excellent convenience and user friendliness.
- Smart controller
  Real-time test force and position data is readily confirmed, and the manual dial can be used for fine adjustments to jig positioning.
- Optional Test Devices
  A variety of tests can be conducted by switching between an abundance of jigs in the lineup.

First Edition: February 2013

Shimadzu Corporation
www.shimadzu.com/an/

For Research Use Only. Not for use in diagnostic procedures.
The content of this publication shall not be reproduced, altered or sold for any commercial purpose without the written approval of Shimadzu.
The information contained herein is provided to you "as is" without warranty of any kind including without limitation warranties as to its accuracy or completeness. Shimadzu does not assume any responsibility or liability for any damage, whether direct or indirect, relating to the use of this publication. This publication is based upon the information available to Shimadzu on or before the date of publication, and subject to change without notice.
© Shimadzu Corporation, 2013

SHIMADZU
Excellence in Science

Application Data Sheet

No. 16

Autograph Precision Universal Tester

Material Testing & Inspection

Tensile Testing of Carbon Fiber

Standard No. ISO11566: 1996 (JIS R 7606: 2000)

Introduction

Carbon fiber is an important industrial material, being essential in carbon fiber reinforced plastics (CFRP), having a specific gravity one-fourth that of normal steels, and a specific strength of 7 times. In this Application Data Sheet, examples of tensile testing of single carbon fibers based on the ISO standard are introduced.

T. Murakami

Measurements and Jigs

In this test, the test sample is fixed to a test specimen mounting board made from a paper, metal, or resin sheet as shown in Fig. 1, installed in the grips, and the tensile test is performed. The standard describes in detail the shape of the mounting board, the type of adhesive used to fix the carbon fiber to the mounting board, and the procedure for installing the carbon fiber (for details refer to the standard). The tests were carried out using clip type grips whose grip force could be adjusted in accordance with the strength of the sample.

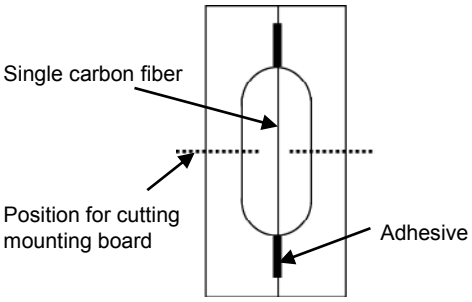

Fig. 1 Test Sample and Mounting Board (frame)

Measurement Results

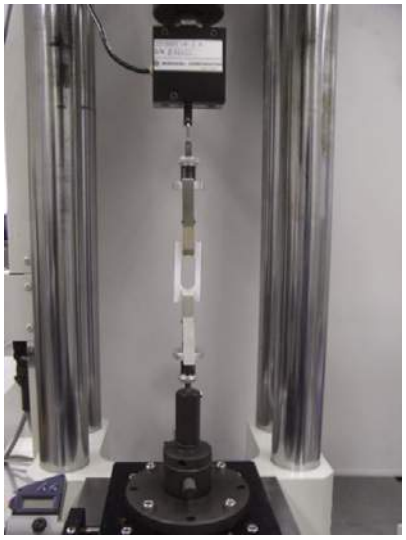

Fig. 2 Test Status

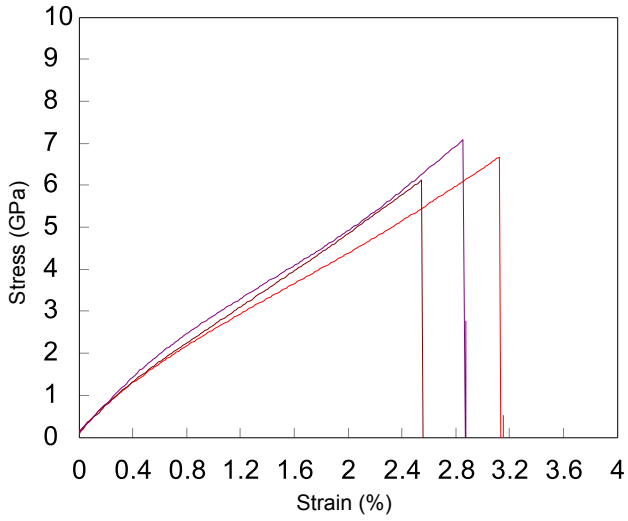

Fig. 3 Test Results

Table 1 Test Conditions

Item	Set Value
Test speed	1 mm/min
Distance between grips	25 mm

Table 2 Test Results (average)

Sample	Diameter	Tensile Strength	Elongation at Break
Carbon fiber	6 μm	7.1 GPa	2.84 %

Carbon Fiber Tensile Test System

Tester:	MST-I Type HR
Load Cell:	1 N
Test Jig:	1 N clip type grips (rubber-coated teeth), X-Y stage
Software:	TRAPEZIUM X (Single)

Shimadzu Autograph MST-1 Micro Strength Evaluation Testing Machine

Features

■ High Accuracy Displacement Measurement
A high accuracy (±0.2 μm) linear sensor has been adopted for measurement of displacement in the load direction. In addition, the backlash-free structure makes it possible to carry out testing with good accuracy. Displacement in the load direction of the test sample can be set accurately to a displacement display resolution of 0.02 μm and a control resolution of 0.005 μm.

■ Measurement of Micro Test Forces
A wide range of load cells from 0.5 N to 2 kN assures a precision of ±1 % for measurements of testing forces of 2 mN at minimum.

■ Positioning Very Small Test Samples
Using an X-Y stage (optional), very small test samples can be easily positioned. The position of the test samples can be observed using a stereo microscope.

■ High Rigidity Frame
A high rigidity frame (45 kN/mm minimum) has been adopted to enable measurement of minute displacements.

■ Optional Test Devices
A variety of tests can be accommodated by switching between an abundance of jigs in the lineup.

First Edition: February 2013

SHIMADZU

Shimadzu Corporation

www.shimadzu.com/an/

For Research Use Only. Not for use in diagnostic procedures.
The content of this publication shall not be reproduced, altered or sold for any commercial purpose without the written approval of Shimadzu. The information contained herein is provided to you "as is" without warranty of any kind including without limitation warranties as to its accuracy or completeness. Shimadzu does not assume any responsibility or liability for any damage, whether direct or indirect, relating to the use of this publication. This publication is based upon the information available to Shimadzu on or before the date of publication, and subject to change without notice.

© Shimadzu Corporation, 2013

SHIMADZU
Excellence in Science

Application Data Sheet

No. 31

Autograph Precision Universal Tester

Material Testing & Inspection

Materials Testing Using Digital Image Correlation

—3-Point Bending Test for Polypropylene and Open-Hole Tensile Test for Carbon Fiber Reinforced Thermo-Plastic—

■Introduction

In recent years, computer aided engineering (CAE), which has allowed significantly reducing the number of prototypes and costs required for product development by simulating product designs on a computer, has been widely used in scientific and industrial fields. This has resulted in an increased need to analyze the distribution of strain in test samples, where the areas prone to strain concentrations in such samples are evaluated by mechanical testing to determine the correlation between results from simulation and strain distribution obtained by mechanical testing.

Digital image correlation (DIC) analysis compares the random patterns on the surface of a test sample before and after deformation to determine the degree of deformation. A important feature of the method is that displacements can be measured and strain distributions analyzed from digital images, which means no sensors need to contact the test sample and no complicated optical systems are required. Consequently, DIC analysis is being used for a wide range of applications where strain is difficult to measure using conventional technology, such as analyzing the strain distribution in large structural members, materials at high temperatures, or micro-materials observed via a microscope.

This paper describes examples of using DIC analysis for 3-point bending tests of plastics and for open-hole tensile testing of thermoplastic carbon fiber reinforced plastics (CFRP) (fabric). The test data presented in this paper was obtained using a system comprising a Shimadzu AG-Xplus precision universal tester, a customized TRViewX non-contact video extensometer, and LaVision DaVis8 DIC analysis software. This system allows simultaneously acquiring JIS 0.5 class extensometer measurement results and video images for DIC analysis, as well as correlating DIC analysis results with test force data.

■Evaluation of Dependence on Distance Between Supports in 3-Point Bending Tests of Plastics

3-point bending tests are widely used throughout the world as a relatively easy way to evaluate the bending properties of materials. A photograph of the testing system is shown in Fig. 1. In 3-point bending tests, a punch applies a load to specimens supported at two points.

3-point bending test regulations for plastics (such as JIS K 7171 and ISO 178) specify that the L, the distance between supports, must be about 16 times greater than h, the specimen thickness (L/h ≈ 16), where this ratio, L/h, is an important factor for measuring the bending strength or bending elasticity correctly.[1), 2)] The following discusses L/h in more detail. Bending a specimen applies compressive stresses to the material above the center plane and tensile stresses below the center plane. The contribution of this compressive and tensile deformation to bending stresses is defined to be equal. Maximum bending stress occurs near the punch that applies the bending loads, where given a flat plate-shaped specimen, stress is defined as $\sigma_f = 3FL/2bh^2$. When a specimen bends, shear stresses also occur at the same time, where the shear stress is defined as $\tau = 3F/4bh$. Based on the above two equations, the relationship between specimen thickness and distance between supports is described by $L/h = \sigma_f/2\tau$. Given a uniformly formed specimen with a sufficiently large distance between the supports, relative to the specimen thickness, the definition of L/h indicates that the contribution of shear stresses in the specimen is small.[3) to 5)] To limit the effects of shear stresses during 3-point bending tests, the optimal L/h value must be specified for the specimen being tested.

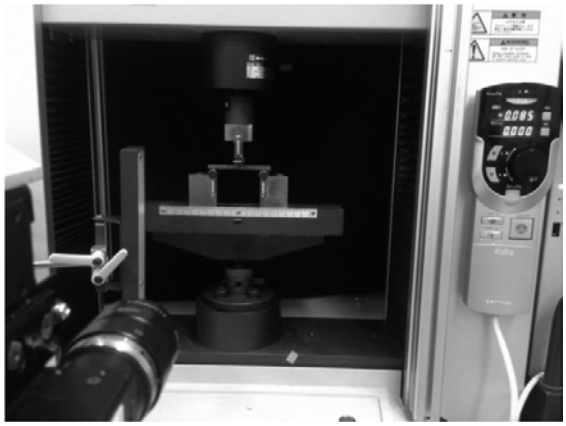

Fig. 1 3-Point Bending Testing System Using Non-Contact Video Extensometer

In the following example, a common plastic material, polypropylene, was tested by 3-point bending using three different distances between supports, and then DIC analysis was used to investigate how much the maximum shear stress distribution depends on the distance between supports. Test conditions are shown in Table 1.

Tests were performed at three L values (distance between supports), 64 mm for an L/h ratio of 16 specified in JIS K 7171, 48 mm for an L/h ratio of 12, where shear stress is predicted to have a large effect, and 32 mm for an L/h ratio of 8. Stress-strain curves obtained using different test conditions are shown in Fig. 2. Fig. 3 shows the maximum shear strain distribution near the elastic limit and near the maximum load point. Warmer colors indicate higher strain levels in the maximum shear strain distribution. This shows that at an L/h ratio of 16, strain is low even near the maximum load point and spreads out uniformly. However, L/h ratios of 8 and 12, where shear stress contribution is predicted to be large, generated large localized shear stresses near the maximum load point on the specimen surface under tension directly under the punch. Whereas localized shear stresses occurred from about the elastic limit for L/h ratio of 8, none were observed for the L/h ratio of 12.

This clearly shows that different deformation modes resulted from bending tests using different distances between supports and shows that DIC analysis provides an effective means of verifying the different modes. It also shows that L/h ratio of 16 recommended in the testing regulations is an appropriate value for 3-point bending tests.

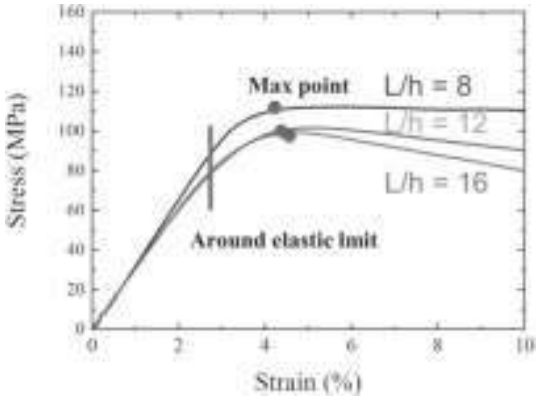

Fig. 2 Stress-Strain Curve

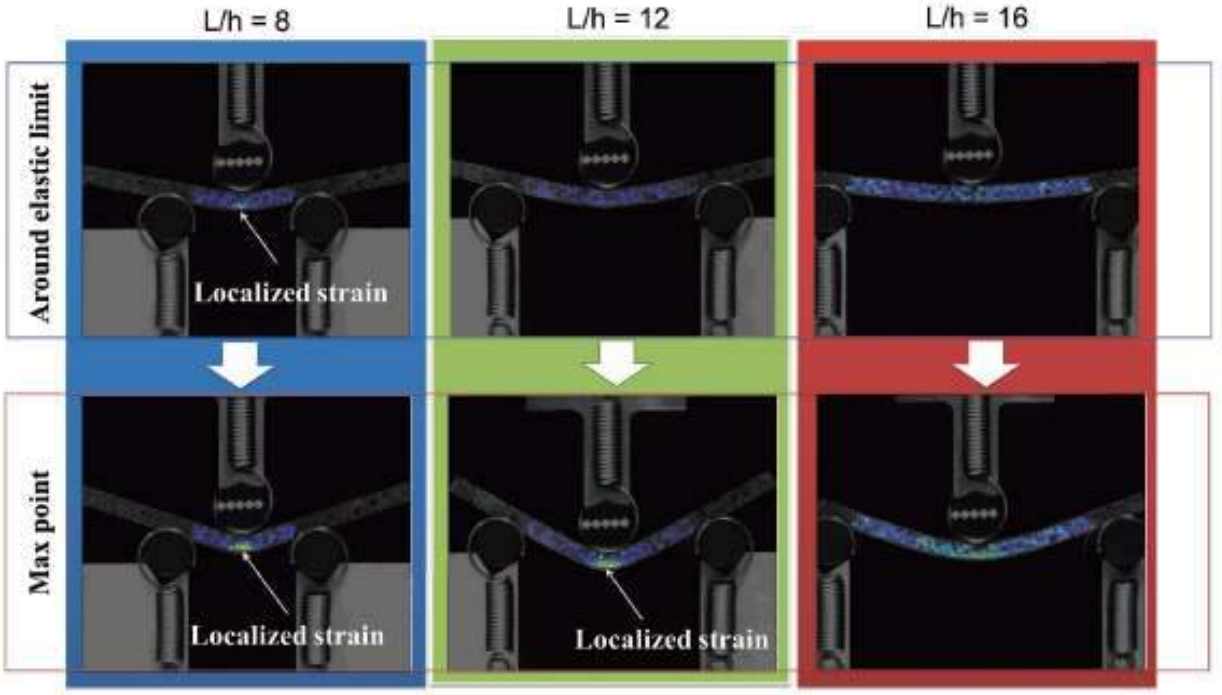

Fig. 3 Distribution of Maximum Shear Strain Around Elastic Limit and Maximum Load

Table 1 Test Conditions for 3-Point Bending Test of Plastic Material

1) Testing equipment	AG-Xplus precision universal tester
2) Load cell capacity	1 kN
3) Jig	Three-point bending test jig for plastic
4) Distance between supports	Three configurations: 32, 48, and 64 mm
5) Test speed	0.001 /s
6) Deflection measuring device	TRViewX120S non-contact video extensometer (customized)
7) Testing software	TRAPEZIUM X (Single)
8) DIC analysis software	DaVis8 (LaVision GMBH)
9) Specimen size	4 mm thick × 10 mm wide × 80 mm long

First Edition: July 2015

SHIMADZU
Shimadzu Corporation
www.shimadzu.com/an/

For Research Use Only. Not for use in diagnostic procedures.
The content of this publication shall not be reproduced, altered or sold for any commercial purpose without the written approval of Shimadzu.
The information contained herein is provided to you "as is" without warranty of any kind including without limitation warranties as to its accuracy or completeness. Shimadzu does not assume any responsibility or liability for any damage, whether direct or indirect, relating to the use of this publication. This publication is based upon the information available to Shimadzu on or before the date of publication, and subject to change without notice.
© Shimadzu Corporation, 2015

■Open-Hole Tensile Testing of Thermoplastic CFRP (Fabric)

Due to higher specific strength than steel materials, superior workability and formability than CFRP/epoxy, and short cycle times of only a few minutes possible for molding, thermoplastic CFRP materials are anticipated for use in production automobiles.[6)]

In general, CFRP materials start failing at the point where they are damaged. CFRP/epoxy used as structural materials in aircraft are mainly used for large components that are fastened with screws or rivets. Therefore, it is important to evaluate their open-hole tensile strength. The open-hole tensile test specified in ASTM D 5766, JIS K 7094, and other regulations is one of the essential evaluation criteria for understanding the properties of CFRP materials.[7), 8)]

In this case, we made a round hole in a thermoplastic CFRP specimen, applied a tensile load, and evaluated the resulting distribution of the maximum shear strain. Fig. 4 shows the testing system used for this test. Table 2 indicates testing conditions and information about the specimen. We chose to cut out type-I shaped specimens, as specified in JIS K 7094 (2012), from PA6 polymer-based thermoplastic CFRP material (with CF-3K flat woven $[0]_{10}$ fabric from Ichimura Sangyo), so that the fibers were oriented longitudinally.

The stress-strain curve obtained from testing is shown in Fig. 5 and the distribution of maximum shear strain that occurred on the observed specimen surface is shown in Fig. 6. Images (1) to (4) in Fig. 6 correspond to the numbers indicated on the stress-strain curve in Fig. 5.

Fig. 4 Open-Hole Tensile Testing System Using Non-Contact Video Extensometer

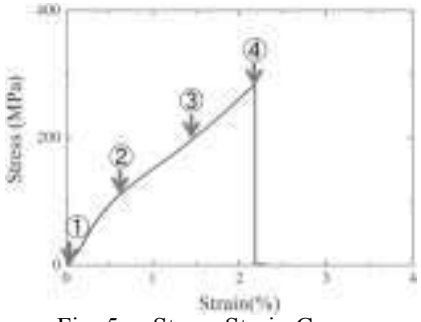

Fig. 5 Stress-Strain Curve

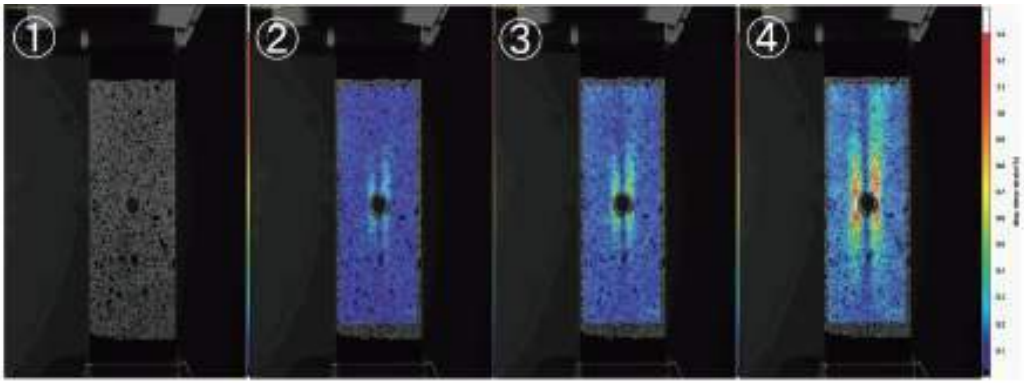

Fig. 6 Distribution of Maximum Shear Strain

Table 2 Test Conditions for Open-Hole Tensile Test of Carbon Fiber Reinforced Thermo-Plastic (Fabric)

1) Testing equipment	AG-Xplus precision universal tester
2) Load cell capacity	50 kN
3) Jig	50 kN non-shift wedge type grips (with trapezoidal file teeth on grip faces for flat specimens)
4) Distance between grips	100 mm
5) Test speed	0.5 mm/min
6) Deflection measuring device	TRViewX120S non-contact video extensometer (customized)
7) Testing software	TRAPEZIUM X (Single)
8) DIC analysis software	DaVis8 (LaVision GMBH)
9) Specimen size	2 mm thick × 36 mm wide × 150 mm long, with 6 mm diameter hole

First Edition: July 2015

SHIMADZU
Shimadzu Corporation
www.shimadzu.com/an/

For Research Use Only. Not for use in diagnostic procedures.
The content of this publication shall not be reproduced, altered or sold for any commercial purpose without the written approval of Shimadzu.
The information contained herein is provided to you "as is" without warranty of any kind including without limitation warranties as to its accuracy or completeness. Shimadzu does not assume any responsibility or liability for any damage, whether direct or indirect, relating to the use of this publication. This publication is based upon the information available to Shimadzu on or before the date of publication, and subject to change without notice.
© Shimadzu Corporation, 2015

The results showed that when the tensile load increased, the maximum shear strain distribution started near the tangent points on the left and right sides of the hole, and spread along the longitudinal direction of the specimen. Due to the orientation of the carbon fibers, the specimen has the greatest strength for bearing tensile loads in its longitudinal direction. The areas of strain concentration are the areas that contain continuous fibers, but they are presumably highly affected by the process of creating the hole. Fig. 7 is a photograph of the specimen after fracture. It shows that the specimen fractured in the direction perpendicular to the main tensile axis. The failure mode is typical of CFRP(fabric) specimens with an open hole, where cracking presumably progressed rapidly after the longitudinal carbon fibers near the hole fractured, resulting in specimen breaking.

Generally, open-hole tensile tests that involve creating a hole in specimens result in significantly lower stresses at the maximum load point, than for specimens without a hole, with some reports indicating a 1/3 to 1/2 drop in strength.[9), 10)] In addition to open-hole tensile testing, this research also involved tensile testing specimens without a hole for reference purposes. A resulting stress-strain curve and photograph of the specimen after fracture are shown in Figs. 8 and 9. The specimen fractured near the parallel area, at a value of about 700 MPa. In contrast, Fig. 5 indicates that the open-hole specimen failed at about 300 MPa, a result similar to CFRP/epoxy specimens.

Fig. 7 Picture of Fractured Specimen

■Conclusion

This paper describes using DIC analysis to evaluate the properties of polypropylene and thermoplastic CFRP (fabric), as examples of chemically engineered materials. However, there are many other types of chemically engineered materials available for which DIC analysis could be used for determining material properties, not only for bending or tensile tests, but also for various others tests, such as compression and shear tests. With high-speed video cameras developed in recent years that allow obtaining high-resolution video images with extremely high time resolution levels, technology has advanced to the point that DIC analysis can now be utilized to visualize strain distributions or obtain stress-strain curves for applications such as high-speed impact testing. Consequently, using DIC analysis for material testing in product design work provides an effective way of ensuring a higher level of safety and peace of mind by understanding the properties of the materials from various aspects.

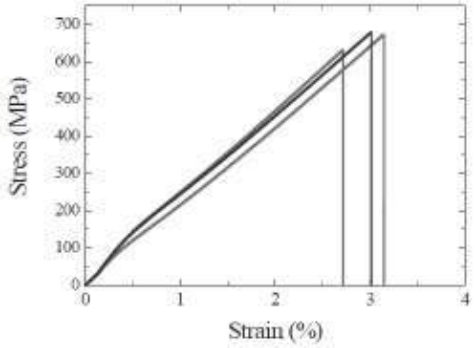

Fig. 8 Stress-Strain Curve

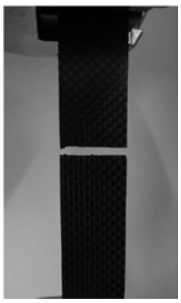

Fig. 9 Picture of Fractured Specimen

■References:

1) JIS K 7171: 2008 Plastics—Determination of flexural properties
2) ISO 178: 2001 Plastics—Determination of flexural properties
3) Masahiro Funabashi: Technology for Evaluating the Performance of Advanced Materials, Sangyo Gijutsu Service Center, pp. 286-287 (2014)
4) Leif A. Carlsson and R. Byron Pipes: Experimental Characterization of Advanced Composite Materials, Kokon Syoin, p. 75 (1990)
5) Ikuo Narisawa: Mechanical Properties of Plastics, Sigma Shuppan, pp. 105-108 (1994)
6) Takeshi Murakami and Tsuyoshi Matsuo: Summary of Presentations at the 39th Conference on Composite Materials, pp. 155-156 (2014)
7) ASTM D5766/D5766M -11 Standard Test Method for Open-Hole Tensile Strength of Polymer Matrix Composite Laminates
8) JIS K 7094: 2012 Test method for open-hole tensile strength of carbon fibre reinforced plastic
9) JAXA-ACDB Advanced Composites Database System http://www.jaxa-acdb.com/ (as of December 17, 2014)
10) Wisnom, M. R., Hallett, S. R., and Soutis, C.: Scaling effects in notched composites, Journal of composite materials, 44, 195-210 (2010)

First Edition: July 2015

SHIMADZU
Shimadzu Corporation
www.shimadzu.com/an/

For Research Use Only. Not for use in diagnostic procedures.
The content of this publication shall not be reproduced, altered or sold for any commercial purpose without the written approval of Shimadzu.
The information contained herein is provided to you "as is" without warranty of any kind including without limitation warranties as to its accuracy or completeness. Shimadzu does not assume any responsibility or liability for any damage, whether direct or indirect, relating to the use of this publication. This publication is based upon the information available to Shimadzu on or before the date of publication, and subject to change without notice.
© Shimadzu Corporation, 2015

SHIMADZU
Excellence in Science

Application Data Sheet

No. 37

High-speed Video Camera HPV-X2

Observing the Failure of Open-Hole CFRP Specimens in Tensile Testing

Synchronized Imaging Using Two High-Speed Video Cameras

■ Introduction

Offering superior specific strength, even compared to other composite materials, carbon fiber reinforced plastic (CFRP) is used in aircraft and some transport vehicles for the purpose of saving fuel through weight reduction. Composite materials have excellent mechanical properties. However, a general feature of composite materials is that their strength decreases markedly when they are notched. CFRP is no exception, so tests of notched specimens are important. In this case, testing is performed using specimens notched with a circular hole at the center. In this experiment, tensile tests were performed using CFRP (laminate method $[45/0/-45/90]_{2s}$) with a total length of 150 mm, a width of 36 mm, and a thickness of 2.5 mm, prepared with a 6 mm circular hole at the center. The failure process of CFRP was observed during the tensile test. In particular, it is important to confirm the failure process of weak regions, such as the periphery of circular holes, for CFRP development and to confirm the validity of CAE analysis. However, since the failure of CFRP is a brittle phenomenon, where failure occurs instantaneously, it cannot be confirmed with the naked eye. For this reason, high-speed video cameras are used to observe the failure. In this experiment, synchronized images were obtained at the front and the side of the specimens using two HPV-X2 high-speed video cameras.

■ Measurement system

In this experiment, the AG-X precision universal testing machine and two HPV-X2 high-speed video cameras were used. Table 1 shows the instruments used. To observe the specimen failure in a tensile test, a trigger signal synchronized to the failure must be transmitted to the high-speed video cameras. The failure starts on the periphery of the circular hole. Accordingly, aluminum foil was affixed to the periphery of the circular hole using adhesive, as shown in Fig. 1, so that conduction would be lost when the sample fails. The failure was observed using this timing to trigger the cameras.

Table 1 Testing Equipment

High-speed Camera	HPV-X2 ×2
Lens	105 mm Macro lens ×2
Illumination	Metal halide lump ×2
Testing Machine	AG-X plus
Load cell	100 kN
Grips	100 kN Non-shift wedge-type grips
Grip teeth	Trapezoidal file teeth for composite mater
Software	TRAPEZIUM X(Single)

Fig.1 Aluminum foil Trigger

■ Measurement Results

Table 2 shows the measurement conditions, and Fig. 2 shows the test configuration. As shown in Fig. 2, the failure of the specimen was recorded from the front by camera (1) and from the side by camera (2). Fig. 3 shows the test results from the AG-Xplus. Failure begins where the test force suddenly drops in Fig. 3. Fig. 4 shows the specimen failure observed from the front, and Fig. 5 from the side. Image (2) in Fig. 4 shows that the failure starts on the left side of the circular hole. In image (3), a crack also appears on the right side of the circular hole. Subsequently, cracks progressed in an orientation of 45 degrees, the orientation of the fibers in the outer layer. Further, as the test progressed, multiple cracks were confirmed, as in images (7) and (8). In the observation from the side, no failure was confirmed at the time the failure started, and was only initially confirmed in image (5). This is likely because the cracks started at the periphery of the circular hole reached the side of the specimen in image (5). Subsequently, failure was confirmed in multiple layers, except for the 0-degree layer, in image (6). Further, in image (7), failure was confirmed in the 0-degree layer, after which the failure progressed toward the outersurface. The final condition of the specimen is shown in Figs. 6 and 7.

Table 2 Measurement Conditions

Test speed	5 mm/min
Frame rate	1M frames/sec
	2M frames/sec

Fig.2 Test Configuration

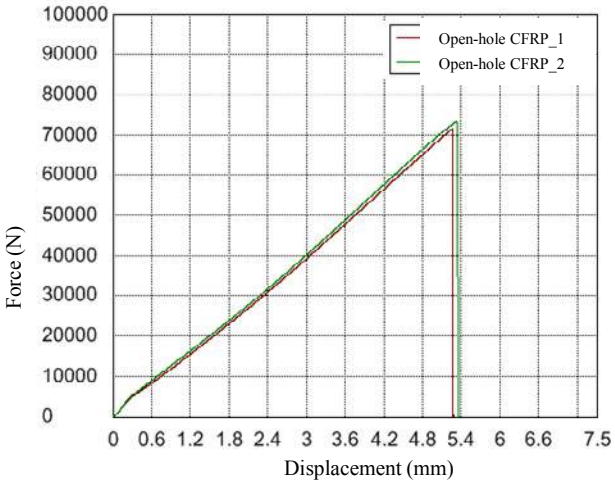

Fig.3 Test Results

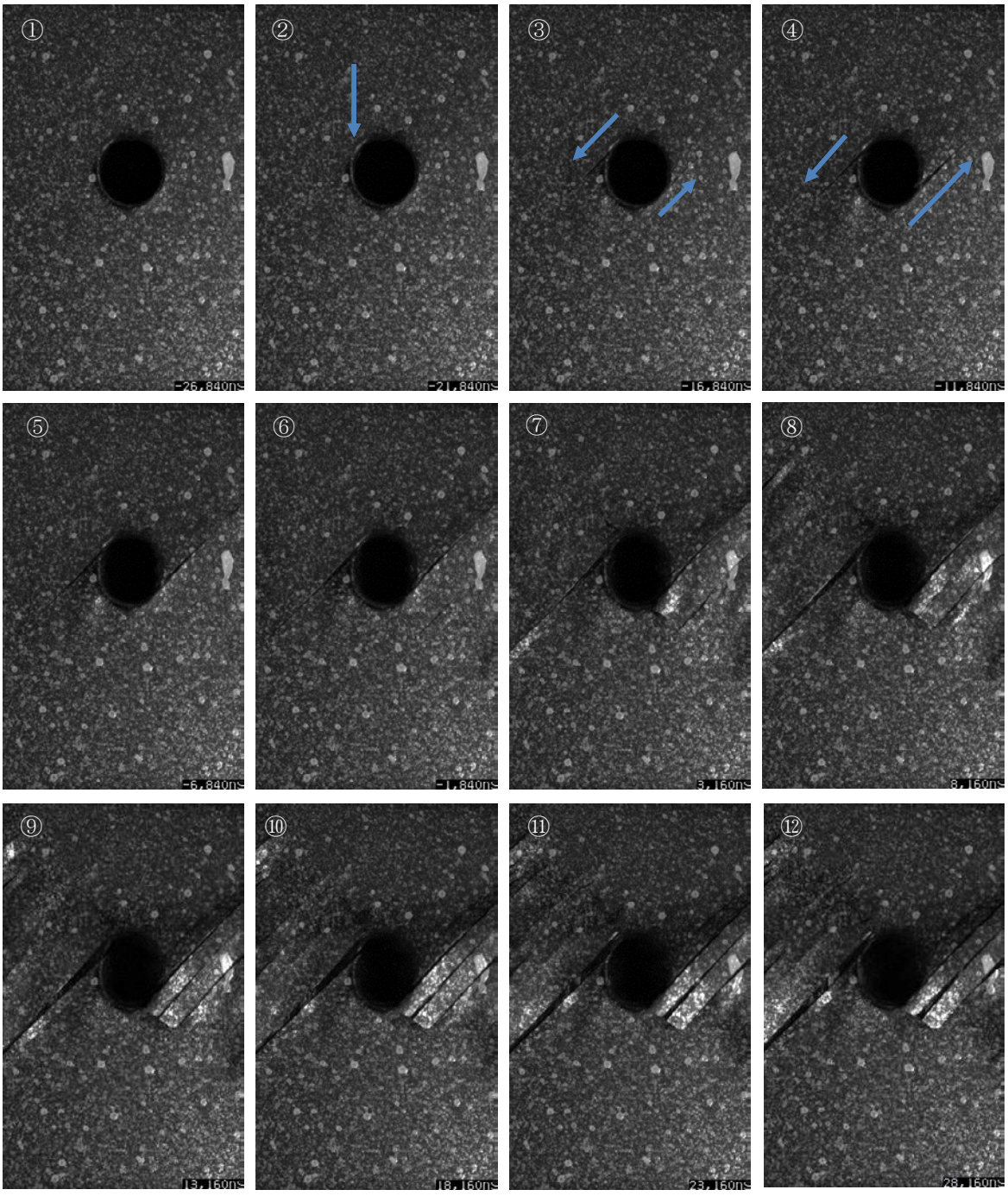

Fig.4 Images from Camera (1) (5 μs between images)

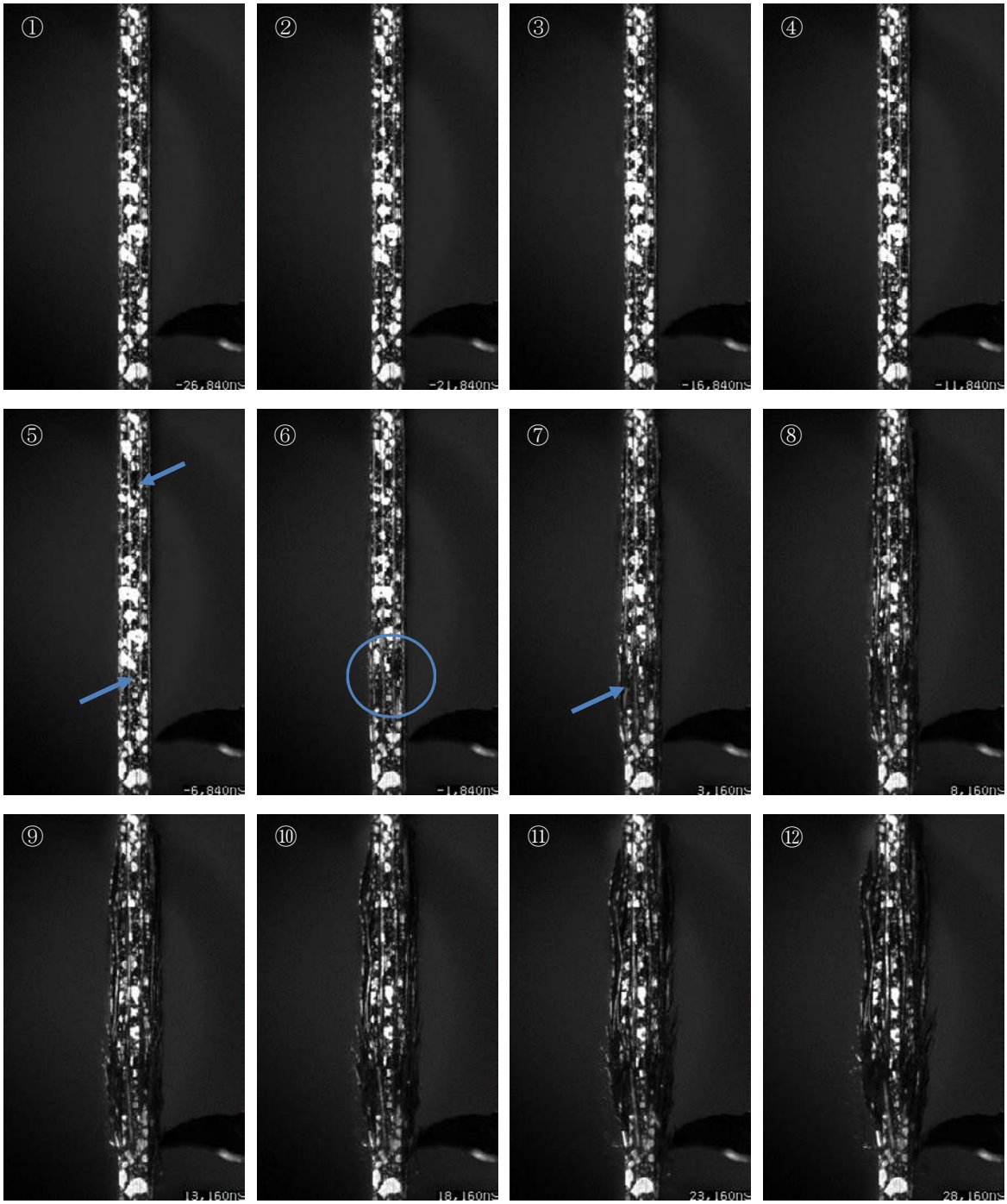

Fig.5 Images from Camera (2) (5 μs between images)

Fig.6 Specimen After Failure (front)

Fig.7 Specimen After Failure (side)

■ Conclusion

The conventional HPV-X does not have a synchronization function, and so is incapable of recording from two directions. Also, the sensitivity of the HPV-X is insufficient, so it cannot record at imaging speeds of 500 kfps or faster. The HPV-X2 is equipped with a synchronization function, and features improved sensitivity, so this instrument is capable of synchronized recordings at 2 Mfps, as in this case. As a result, failures can be observed in tensile tests of materials like CFRP that fail at high speeds.

Generally, failure observations are often recorded from the front of the specimen. However, adding recording from the side enables confirming the failure process that cannot be observed just from the front. In particular, with CFRP materials with different fiber orientations for each lamination layer, where failure progresses in different manner for each layer, as shown in this article, the failure process can be observed in more detail by recording from two directions.

First Edition: July, 2015

Shimadzu Corporation
www.shimadzu.com/an/

For Research Use Only. Not for use in diagnostic procedures.
The content of this publication shall not be reproduced, altered or sold for any commercial purpose without the written approval of Shimadzu.
The information contained herein is provided to you "as is" without warranty of any kind including without limitation warranties as to its accuracy or completeness. Shimadzu does not assume any responsibility or liability for any damage, whether direct or indirect, relating to the use of this publication. This publication is based upon the information available to Shimadzu on or before the date of publication, and subject to change without notice.
© Shimadzu Corporation, 2015

SHIMADZU
Excellence in Science

Application Data Sheet

No. 38

HPV-X2 High-Speed Video Camera

High-Speed Video Camera

Observing the Fracture of Unidirectional CFRP in Static Tensile Testing

■ Introduction

Carbon fiber reinforced plastic (CFRP) is a composite material with a particularly high specific strength. It is used in aircraft and in some transport equipment to reduce fuel costs by reducing weight. While it has some excellent mechanical characteristics as a composite material, when in-plane damage occurs it displays brittle failure behavior, with fracture propagating instantly from the point of damage. Consequently, CFRP development involves not only material testing, but also observation of material failure to check for fracture locations at weak points. Furthermore, material failure is observed to evaluate the validity of computer aided engineering (CAE) recently. As mentioned above, a CFRP fracture event occurs extremely quickly and cannot be observed by the naked eye, so a high-speed video camera is used. Shimadzu has published an Application News on this topic in the past (No. V017 Observing the Failure of CFRP Materials in High-Speed Tensile Tests). High-speed tensile testing involves an instantaneous testing time. To accommodate this, a strobe capable of emitting very intense light instantaneously is used to achieve an image capture speed of over 1 million frames/second. Meanwhile, static testing involves longer testing times with a metal halide lamp used as a light source for continuous lighting (a relatively weak light source compared to a strobe), which cannot produce enough light to capture images at more than 500 thousand frames/second.
The newly developed HPV-X2 camera is 6 times more sensitive than the previous HPV-X camera, which allows it to capture over 1 million frames/second using even a metal halide lamp as a light source. In this article, we demonstrate the observation of unidirectional CFRP failure in static testing.

■ Measurement

The AG-X precision universal testing machine and HPV-X2 high-speed video camera were used in experiments. The equipment used is shown in Table 1. Observing material failure during tensile testing requires a signal to trigger the high-speed video camera in time with material failure. Since cracks propagate in the direction of the unidirectional fibers when failure occurs in unidirectional CFRP, we attached aluminum foil perpendicular to the direction of the fibers with adhesive. A specimen with the aluminum foil attached is shown in Fig. 1. A break in conduction through the aluminum foil caused by a break in the specimen triggers observation of the failure event.

■ Results

A view of the test is shown in Fig. 2 and Fig. 3. As shown in Fig. 3, aluminum foil is also attached to the jigs around the specimen in order to focus light onto the specimen. Test conditions are shown in Table 2.

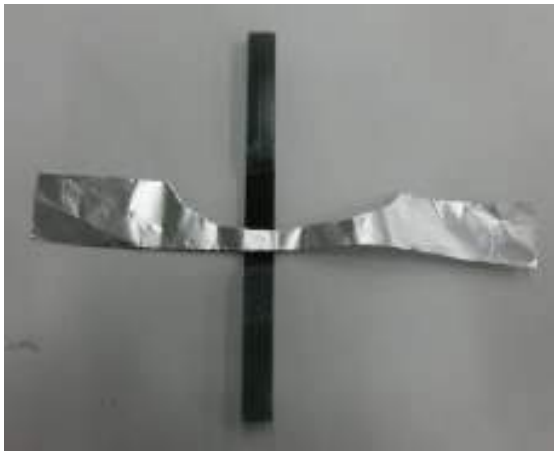

Fig. 1 Test Specimen

Table 1 Testing System

High-Speed Video Camera	HPV-X2
Lens	105 mm, F1.8
Lighting	Two metal halide lamps
Testing Machine	AG-Xplus
Load Cell	50 kN
Grip	50 kN non-shift wedge-type grips
Grip Face	Trapezoidal file teeth for composite materials
Software	TRAPEZIUM X (Single)

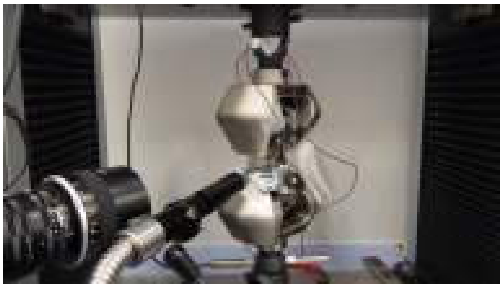

Fig. 2 View of the Test

Table 2 Test Conditions

Test speed	5 mm/min
Recording Speed	5 million frames/sec
Specimen Size	Width: 6 mm, thickness: 0.4 mm
Lamination Method	$[0]_2$

The failure of unidirectional CFRP is shown in Fig. 4. Longitudinal cracks can be seen on the left side of the specimen in image (2) of Fig. 4. In image (3), these cracks have propagated as far as the upper tab. Longitudinal cracks can also be seen on the right side of the specimen in image (3). Image (6) is a later view of the specimen as it is breaking apart. Using the HPV-X2 allows for the observation of CFRP failure during the static tensile test, which is useful for future CFRP development.

Fig. 3 View of the Test (Magnified View)

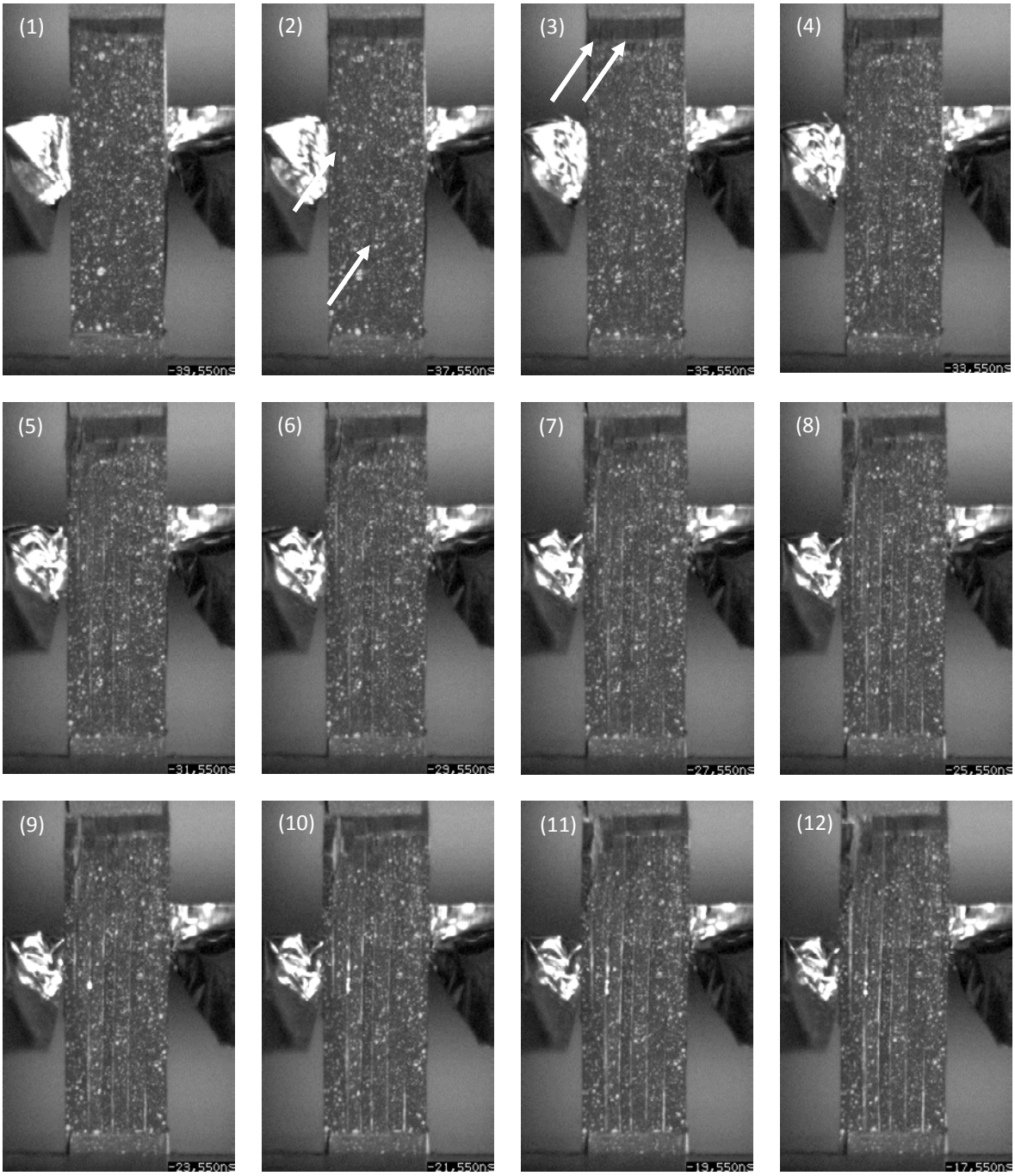

Fig. 4 Captured Images (Interval between captured images is 2 μs.)

First Edition: July, 2015

Shimadzu Corporation
www.shimadzu.com/an/

For Research Use Only. Not for use in diagnostic procedures.
The content of this publication shall not be reproduced, altered or sold for any commercial purpose without the written approval of Shimadzu.
The information contained herein is provided to you "as is" without warranty of any kind including without limitation warranties as to its accuracy or completeness. Shimadzu does not assume any responsibility or liability for any damage, whether direct or indirect, relating to the use of this publication. This publication is based upon the information available to Shimadzu on or before the date of publication, and subject to change without notice.
© Shimadzu Corporation, 2015

SHIMADZU
Excellence in Science

Application News

No.i256A

Material Testing System

Open-Hole Compression Test of Composite Material

Introduction

Carbon fiber reinforced plastic (CFRP) has gained attention due to their strength and low weight, and have quickly been adopted for use in aeronautics and astronautics. CFRP has excellent strength characteristics in terms of specific strength and high rigidity, but lose much of their strength when a cutout is made. Consequently, composite materials used in aeroplanes must be evaluated by tests that use specimens with a hole cut out of their center. We performed open-hole compression testing of a CFRP according to ASTM D6484.

Measurement System

The CFRP specimen used was T800S/3900. As shown in Fig. 1, a hole was created in the middle of the specimen. ASTM D6484 describes test methods in both SI and Imperial units, where the dimensions of the jigs and specimens differ in each. We performed testing with Imperial units. Specimen information is shown in Table 1.

ASTM D6484 includes two loading methods, which are described as Method A and Method B. In Method A, the specimen and test fixture are clamped in a gripping device, and the specimen is compressed by shear force applied by the fixture and gripping device. In Method B, compression plate is present at the ends of the specimen and fixture, and are used to compress the specimen. Method B was used, as shown in Fig. 2. Table 2 shows a list of the equipment used and Table 3 shows the test conditions used.

Table 1 Specimen Information

Length	: 305 mm
Width	: 38.1 mm
Thickness	: 3.1 mm
Lamination Method	: $[45/0/-45/92]_{2S}$

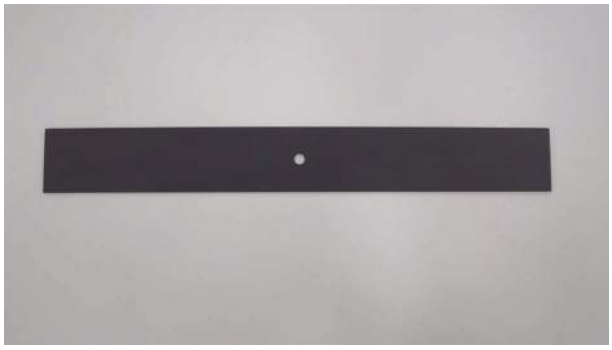

Fig. 1 Specimen

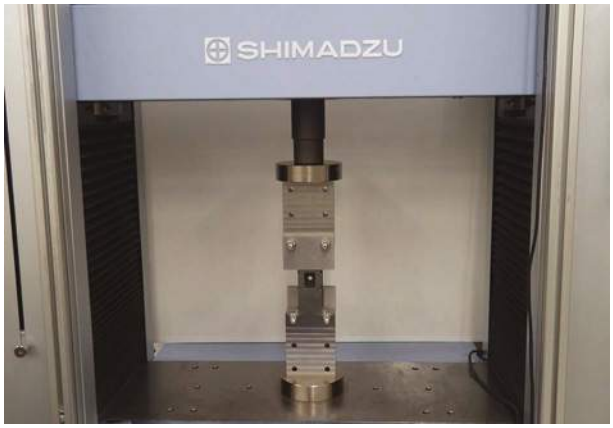

Fig. 2 Test Setup

Table 2 Experimental Equipment

Testing Machine	: AG-Xplus
Load Cell	: 50 kN
Test Fixture	: Open-Hole Compression Test Fixture

Table 3 Test Conditions

Test Speed : 2 mm/min

Results

Measurements were performed twice. Test results are shown in Table 4 and stress-displacement curves are shown in Fig. 3. As shown in Table 4, the mean open-hole compressive strength was 275.6 MPa.

Table 4 Test Results

Specimen Name	Open-Hole Compressive Strength
1st	278.2 MPa
2nd	273.0 MPa
Mean	275.6 MPa

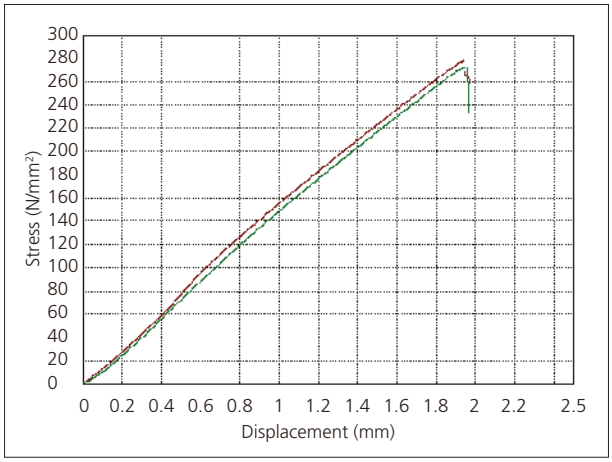

Fig. 3 Stress-Displacement Curves

Results (DIC Analysis)

Using the TRViewX non-contact extensometer allows for images and video of the specimen to be collected synchronized with test result collection. Also, applying a random pattern of paint to the observed specimen surface allows the images or video to be used to determine the strain distribution on the observed specimen surface during the test by DIC analysis[1]. Open-hole compression testing and DIC analysis were performed using the specimen described in Table 5. Fig. 4 shows a photograph of the open-hole compression test system with a non-contact extensometer. Fig. 5 shows strain distributions around the open hole in the specimen that were obtained by DIC analysis. Fig. 5 shows that strain accumulates at the vertical sides of the open hole (regions (1) and (3)), strain appears along the axis of compression from those points, and the final break occurs at the vertical sides of the hole. Meanwhile, almost no strain appears in the central part of the hole (region (2)) throughout the test. This strain distribution probably occurred due to a 0˚ fiber orientation on the surface of the specimen.

Table 5 Specimen Information (DIC)

Length	: 305 mm
Width	: 38 mm
Thickness	: 1.6 mm
Lamination Method	: $[0/90]_{2S}$

1) DIC analysis is an analysis method that measures strain and shows the strain distribution in a specimen based on movement of a random pattern of paint applied to the observed specimen surface before and during testing.

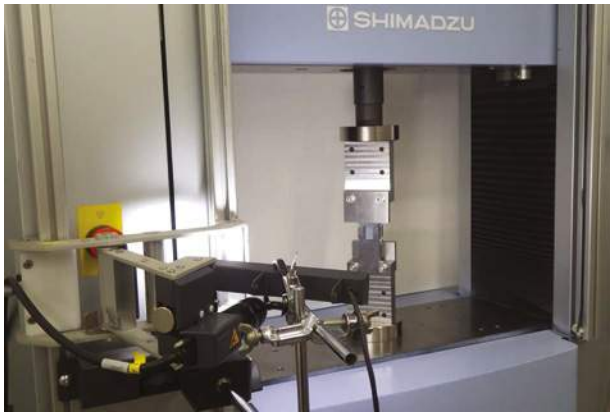

Fig. 4 Experimental Setup (DIC)

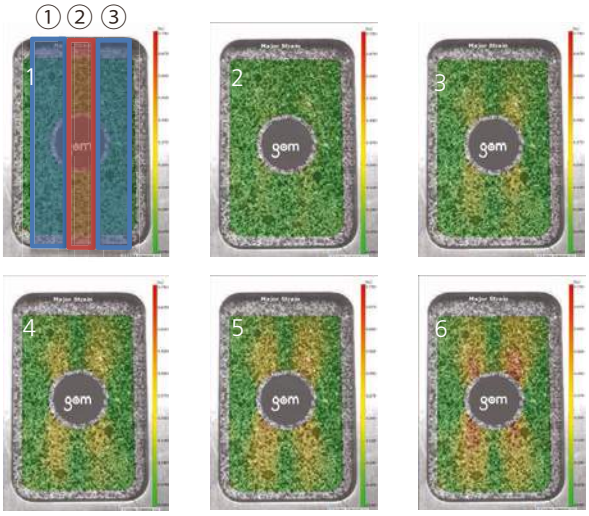

Fig. 5 DIC Analysis Results

Conclusion

Using this test system, open-hole compression testing of a CFRP was successfully performed according to ASTM D6484. Using a non-contact extensometer, we were also able to capture video (images) synchronized with the test force and crosshead displacement data obtained from the testing machine. Performing DIC analysis based on this video allowed an evaluation of the strain distribution on the observed specimen surface. This testing system will be extremely useful for the development of CFRPs and products that use CFRPs.

First Edition: Aug. 2016
Second Edition: Dec. 2016

SHIMADZU

Shimadzu Corporation
www.shimadzu.com/an/

For Research Use Only. Not for use in diagnostic procedure.
This publication may contain references to products that are not available in your country. Please contact us to check the availability of these products in your country.

The content of this publication shall not be reproduced, altered or sold for any commercial purpose without the written approval of Shimadzu. Company names, product/service names and logos used in this publication are trademarks and trade names of Shimadzu Corporation or its affiliates, whether or not they are used with trademark symbol "TM" or "®". Third-party trademarks and trade names may be used in this publication to refer to either the entities or their products/services. Shimadzu disclaims any proprietary interest in trademarks and trade names other than its own.

The information contained herein is provided to you "as is" without warranty of any kind including without limitation warranties as to its accuracy or completeness. Shimadzu does not assume any responsibility or liability for any damage, whether direct or indirect, relating to the use of this publication. This publication is based upon the information available to Shimadzu on or before the date of publication, and subject to change without notice.

© Shimadzu Corporation, 2016

SHIMADZU
Excellence in Science

Application News

No.i250

Material Testing System

Shear Test of Composite Material (V-Notched Beam)

Introduction

Carbon fiber reinforced plastic (CFRP) do not oxidize or rust and have a higher specific strength and stiffness than existing materials. Applications of CFRP are being investigated, with a focus on applications as industrial products that require strength and durability. Compared to existing homogeneous materials, composite materials like CFRP are anisotropic, and display complex failure behaviors as a result of tension, compression, bending, in-plane shear, out-of-plane shear, or a combination of these stresses arising from loading in the principal-axis direction. In recent years, use of CAE analysis in industry has become widespread since it can reduce numbers of prototypes and reduce the cost of new product development. Because values for each of the stress properties stated above are needed to increase precision when predicting product characteristics during product design, there is a strong demand for test methods able to evaluate pure failure behaviors in CFRP.

This article describes an example of V-notched beam method (Iosipescu method, ASTM D5379) that is widely used as an in-plane shear test method for composite material specimens. The test method can apply load as a pure in-plane shear stress on the evaluation area (see Fig. 1) by using a specimen cut with V-notches and supported at four asymmetrical points. Setting up the specimen and jig for this test method is relatively easy, and the test method can be used with a variety of CFRP laminate materials, including unidirectional materials, orthogonally laminated materials, and discontinuous fiber materials.

Measurement System

The equipment configuration is shown in Table 1. Information on the specimen prescribed by ASTM D5379 is shown in Fig. 1. The specimen is a $[0/90]_{10s}$ orthogonally laminated material made from Toray T800S prepreg that was molded in an autoclave. A two-axis strain gauge was attached at the mid-point between the upper and lower V-notches machined into the specimen (evaluation area), and oriented to measure strain in –45° and +45° directions. Shear strain can be calculated by inserting the strain values obtained from these two strain gauges into equation (1). Shear strain is a property needed to evaluate the shear modulus. In this test, strain gauges were attached on both the front and rear of the specimen. Calculating the mean of outputs obtained from strain gauges on both sides allows for more accurate measurement of the shear strain in the specimen, and confirms whether shear strain is being applied symmetrically on the front and rear of the specimen.

$$\gamma = |\varepsilon_{+45}| + |\varepsilon_{-45}|. \qquad \text{Equation (1)}$$

γ : Shear strain
ε_{+45} : Strain at +45°
ε_{-45} : Strain at –45°

Table 1 Test Conditions

Testing Machine	: AG-50kNX plus
Load Cell	: 50 kN
Test Jig	: ASTM D 5379 jig
Software	: TRAPEZIUM X (Single)
Test Speed	: 2 mm/min

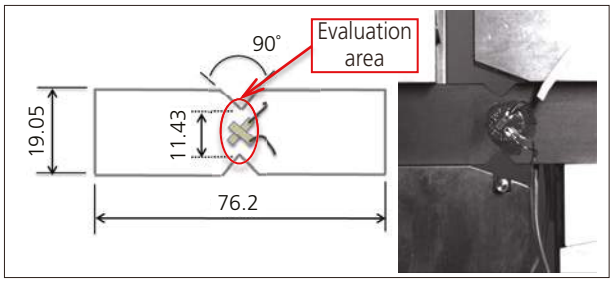

Fig. 1 Shape of Specimen

Fig. 2 Testing Apparatus

Fig. 3 Imaging Apparatus

The testing and imaging apparatus are shown in Fig. 2 and 3. Images captured using a TRViewX (Shimadzu Digital Video Extensometer) were gathered simultaneous to values obtained from the strain gauge outputs and specimen stress obtained by the testing apparatus. This made it easy to compare and evaluate images of the CFRP failure process against each specimen property values, something that was difficult to perform only with previous testing systems. Strain distribution can also be evaluated using digital image correlation (DIC, ARAMIS, GOMmbH) analysis of the images captured by TRViewX. To perform DIC analysis, paint must be sprayed on the specimen surface to create a random pattern on the front surface of the specimen.

Analytical Results

Each specimen property value obtained from this test is shown in Table 2. A photograph of the specimen after testing is shown in Fig. 4, a shear stress-normal strain curve is shown in Fig. 5 (strain values obtained from strain gauges), a shear stress-shear strain curve is shown in Fig. 6 (shear strain calculated from Equation (1)), and a shear stress-stroke curve is shown in Fig. 7. Table 2 shows that the results obtained for each shear property were highly reproducible. Fig. 5 and Fig. 6 show that the same strain values were obtained from the front and rear strain gauges, and highly symmetrical shear strain was applied to the specimen.

Table 2 Test Results

Specimen	Shear Modulus [GPa]	Shear Strength [MPa]
Test 1	4.62	136.0
Test 2	4.63	133.0
Test 3	4.50	131.0
Mean	4.58	133.0

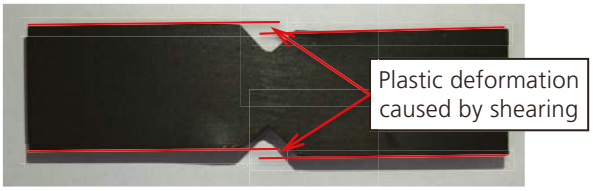

Fig. 4 Specimen After Testing

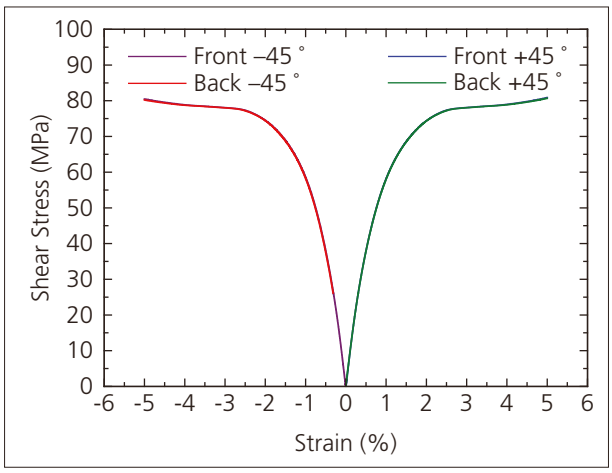

Fig. 5 Shear Stress-Normal Strain Curve

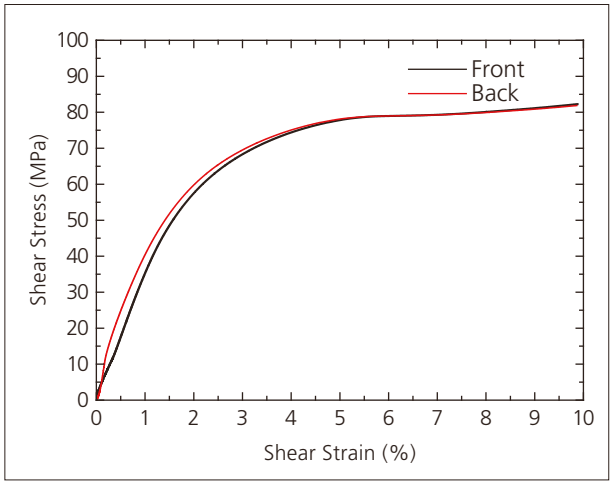

Fig. 6 Shear Stress-Shear Strain Curve

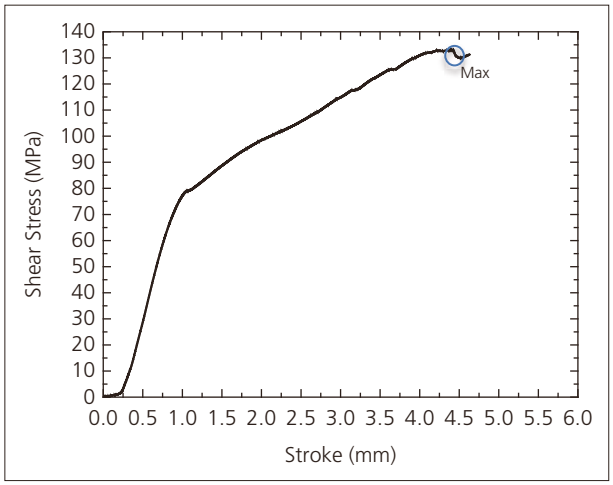

Fig. 7 Shear Stress-Stroke Curve

Failure of the specimen is shown in Fig. 8. Images of the shear strain distribution obtained by DIC analysis are shown in Fig. 9. The amount of strain occurring in the specimen is shown in terms of color, with low strain areas in cooler colors (black and blue) and high strain areas in warmer colors (orange and red). The images show that as the test progresses strain accumulates and is localized between the V-notches.

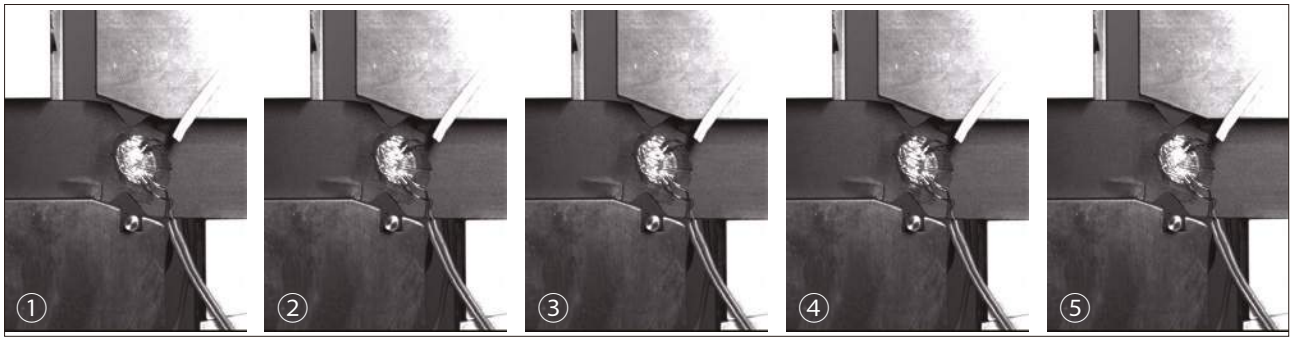

Fig. 8 Specimen e Failure Process (images show the point at which the specimen fails)

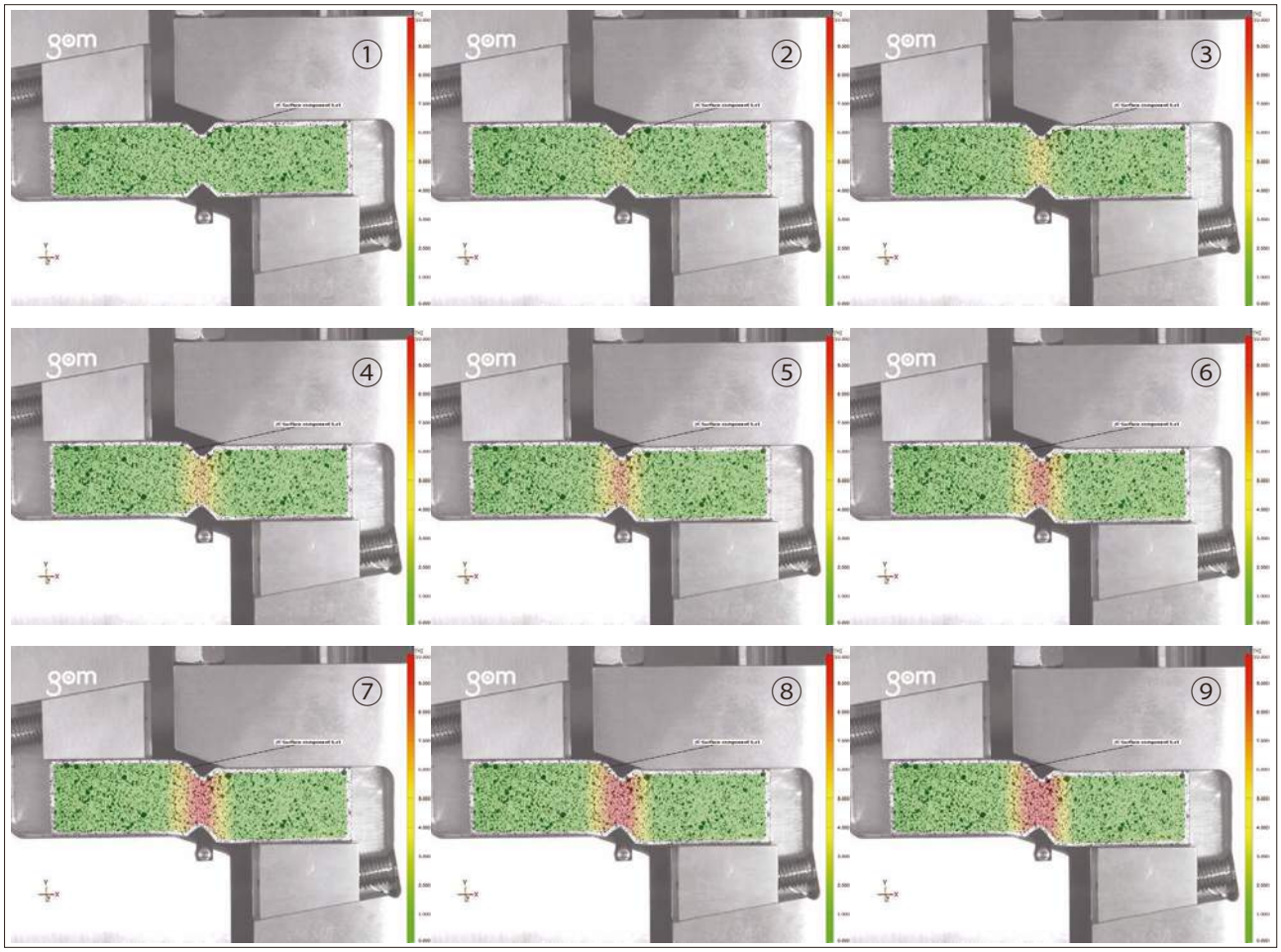

Fig. 9 Shear Strain Distribution (DIC analysis images)

Conclusion

We used this test system to successfully implement the V-notched beam method (ASTM D5379). In addition to evaluating the basic properties of shear modulus and shear strength, integrating a Digital Video Extensometer into the test system enabled us to capture reference data that can be used to elucidate the mechanism of failure of CFRP, allowing strain analysis to be performed in terms of specimen failure mode and DIC analysis.

First Edition: Aug. 2016

Shimadzu Corporation
www.shimadzu.com/an/

For Research Use Only. Not for use in diagnostic procedure.
This publication may contain references to products that are not available in your country. Please contact us to check the availability of these products in your country.

The content of this publication shall not be reproduced, altered or sold for any commercial purpose without the written approval of Shimadzu. Company names, product/service names and logos used in this publication are trademarks and trade names of Shimadzu Corporation or its affiliates, whether or not they are used with trademark symbol "TM" or "®". Third-party trademarks and trade names may be used in this publication to refer to either the entities or their products/services. Shimadzu disclaims any proprietary interest in trademarks and trade names other than its own.

The information contained herein is provided to you "as is" without warranty of any kind including without limitation warranties as to its accuracy or completeness. Shimadzu does not assume any responsibility or liability for any damage, whether direct or indirect, relating to the use of this publication. This publication is based upon the information available to Shimadzu on or before the date of publication, and subject to change without notice.

© Shimadzu Corporation, 2016

SHIMADZU
Excellence in Science

Application News

No.i251

Material Testing System

Shear Test of Composite Material (V-Notched Rail Shear)

Introduction

Carbon fiber reinforced plastic (CFRP) do not oxidize or rust and have a higher specific strength and stiffness than existing materials. Applications of CFRP are being investigated, with a focus on applications as industrial products that require strength and durability. Compared to existing homogeneous materials, composite materials like CFRP are anisotropic, and display complex failure behaviors as a result of tension, compression, bending, in-plane shear, out-of-plane shear, or a combination of these stresses arising from loading in the principal-axis direction. In recent years, use of CAE analysis in industry has become widespread since it can reduce numbers of prototypes and reduce the cost of new product development. Because values for each of the stress properties stated above are needed to increase precision when predicting product characteristics during product design, there is a strong demand for test methods able to evaluate pure failure behaviors in CFRP.

There are various tests methods for evaluating composite materials. Of these methods, two commonly used in-plane shear test methods to test in the direction of fibers in fiber reinforced composite materials and to test textile laminated materials are the Iosipescu method (ASTM D5379) that applies an asymmetrical four-point bending load to a specimen cut with notches, and method (ISO 14129) that applies a ±45° tensile load on laminated materials. We used the V-notched rail shear method (ASTM D7078) that can be used to test in-plane shear. Because this method uses a large gauge area on the specimen, it can accommodate specimens without holes and CRFP laminate materials that have discontinuous fibers.

Measurement System

The equipment configuration is shown in Table 1. Information on the specimen prescribed by ASTM D7078 is shown in Fig. 1. The specimen is a $[0/90]_{10s}$ orthogonally laminated material made from Toray T800S prepreg that was molded in an autoclave. The specimen has a 31-mm evaluation area (see Fig. 1), and two-axis strain gauges attached at the mid-point between the V-notches (center of evaluation area) that are able to measure strain in –45° and +45° directions. Shear strain can be calculated by inserting the strain values obtained from these two strain gauges into equation (1). Shear strain is a property needed to evaluate the shear modulus.

$$\gamma = |\varepsilon_{+45}| + |\varepsilon_{-45}|. \qquad \text{Equation (1)}$$

γ : Shear strain
ε_{+45} : Strain at +45°
ε_{-45} : Strain at –45°

In this test, strain gauges were attached on both the front and rear of the specimen. Calculating the mean of outputs obtained from strain gauges on both sides allows for more accurate measurement of the shear strain in the specimen, and confirms whether shear strain is being applied symmetrically on the front and rear of the specimen.

Table 1 Test Conditions

Testing Machine	: AG-50kNX plus
Load Cell	: 50 kN
Test Jig	: ASTM D7078 jig
Software	: TRAPEZIUM X (Single)
Test Speed	: 2 mm/min

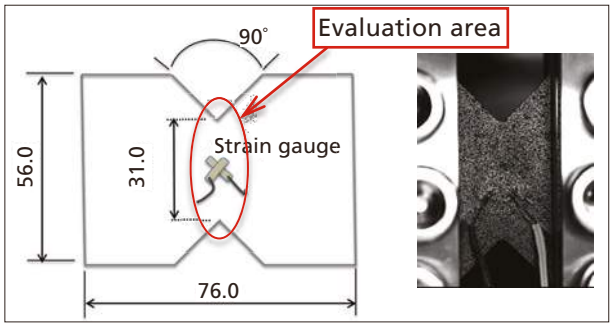

Fig. 1 Shape of Specimen

Fig. 2 Testing Apparatus

Fig. 3 Imaging Apparatus

The testing and imaging apparatus are shown in Fig. 2 and Fig. 3. Images captured using a TRViewX (Shimadzu Digital Video Extensometer) were gathered simultaneous to values obtained from the strain gauge outputs and specimen stress obtained by the testing apparatus. This made it easy to compare and evaluate images of the CFRP failure process against each specimen property values, something that was difficult to perform only with previous testing systems. Strain distribution can also be evaluated using digital image correlation (DIC, ARAMIS, GOMmbH) analysis of the images captured by TRViewX. To perform DIC analysis, paint must be sprayed on the specimen surface to create a random pattern on the front surface of the specimen.

Analytical Results

Each specimen property value obtained from this test is shown in Table 2. A photograph of the specimen after testing is shown in Fig. 4, a shear stress-normal strain curve is shown in Fig. 5 (strain values obtained from strain gauges), a shear stress-shear strain curve is shown in Fig. 6 (shear strain calculated from Equation (1)), and a shear stress-stroke curve is shown in Fig. 7. Table 2 shows that the results obtained for each shear property were highly reproducible. Fig. 5 and Fig. 6 show that the same strain values were obtained from the front and rear strain gauges, and highly symmetrical shear strain was applied to the specimen.

Table 2 Test Results

Specimen	Shear Modulus [GPa]	Shear Strength [MPa]
Test 1	4.63	121.72
Test 2	4.55	120.00
Test 3	4.58	120.05
Mean	4.59	120.60

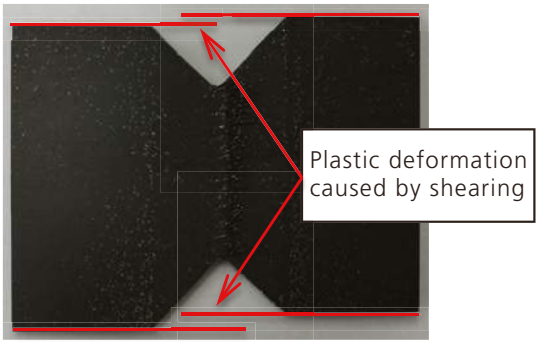

Fig. 4 Specimen After Testing

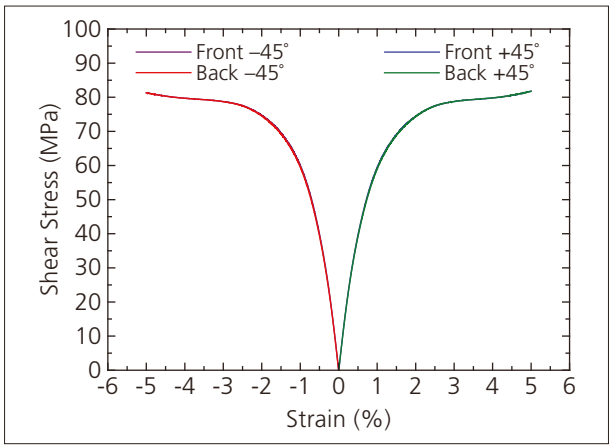

Fig. 5 Shear Stress-Normal Strain Curve

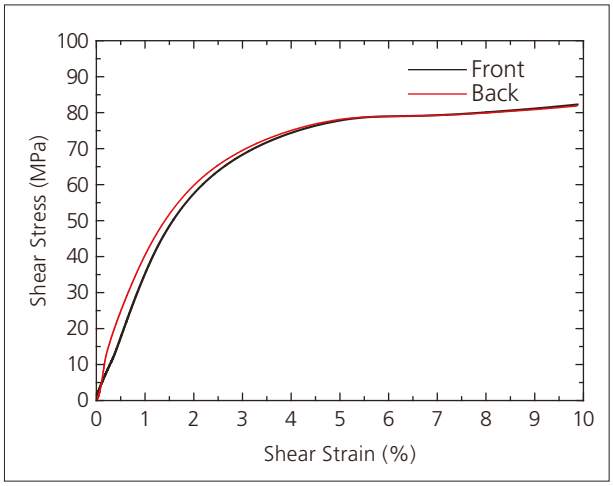

Fig. 6 Shear Stress-Shear Strain Curve

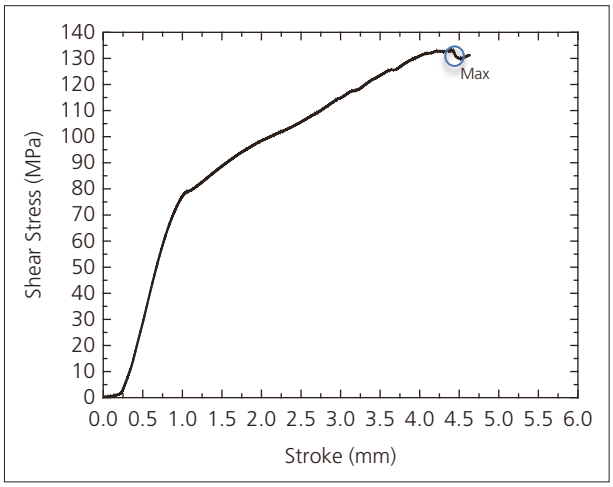

Fig. 7 Shear Stress-Stroke Curve

Failure of the specimen is shown in Fig. 8. A crack that appears close to the upper notch quickly propagates down toward the bottom notch during a simultaneous decrease in test force. Images of the shear strain distribution obtained by DIC analysis are shown in Fig. 9. The amount of strain occurring in the specimen is shown in terms of color, with low strain areas in cooler colors (black and blue) and high strain areas in warmer colors (orange and red). The images show that as the test progresses strain accumulates and is localized between the V-notches.

Fig. 8 Specimen Failure Process (images show the point at which the specimen fails)

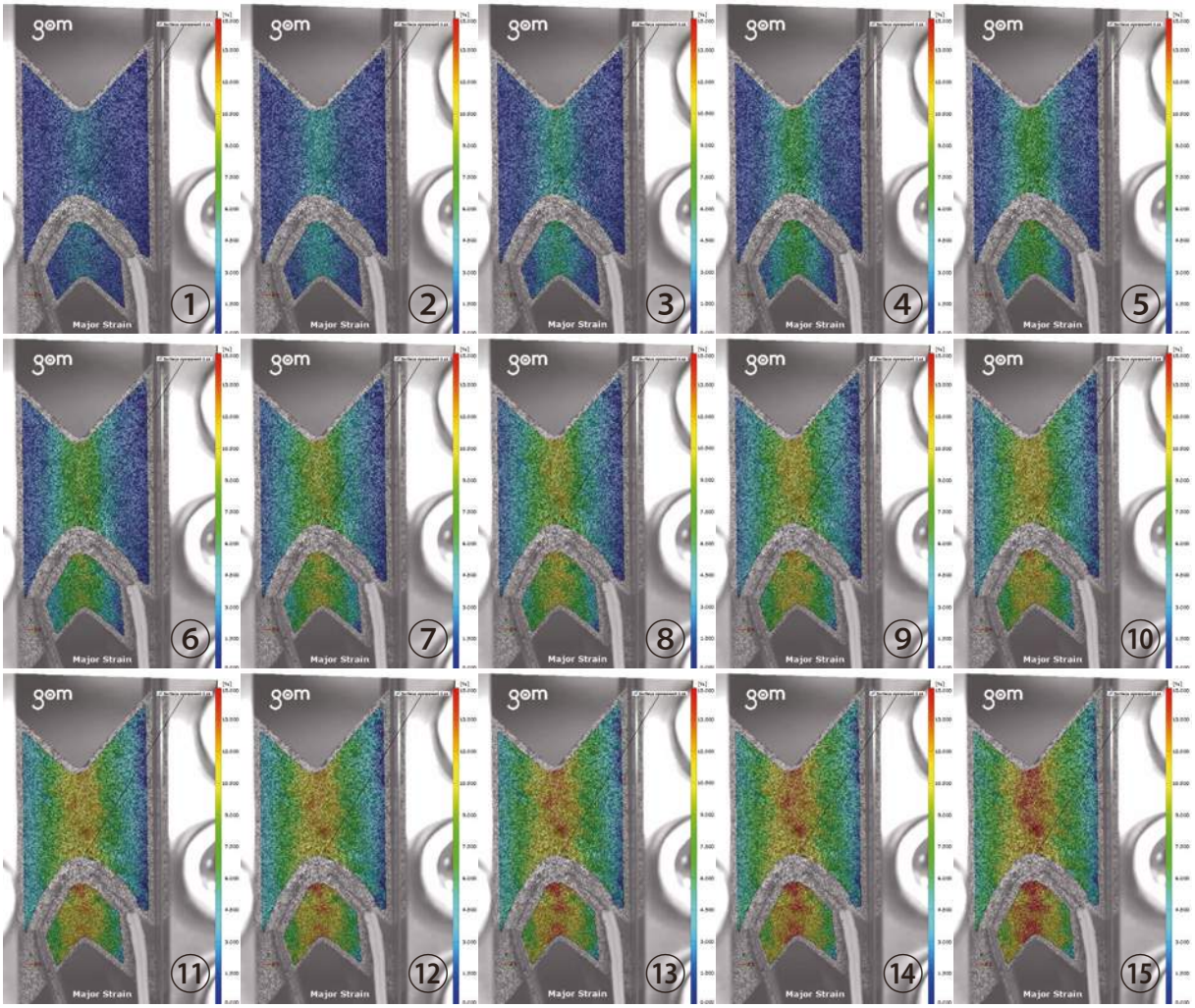

Fig. 9 Shear Strain Distribution (DIC analysis images)

Conclusion

We used this test system to successfully implement the V-notched rail shear method (ASTM D7078). In addition to evaluating the basic properties of shear modulus and shear strength, integrating a Digital Video Extensometer into the test system enabled us to capture reference data that can be used to elucidate the mechanism of failure of CFRP, allowing strain analysis to be performed in terms of specimen failure mode and DIC analysis.

First Edition: Aug. 2016

Shimadzu Corporation
www.shimadzu.com/an/

For Research Use Only. Not for use in diagnostic procedure.
This publication may contain references to products that are not available in your country. Please contact us to check the availability of these products in your country.

The content of this publication shall not be reproduced, altered or sold for any commercial purpose without the written approval of Shimadzu. Company names, product/service names and logos used in this publication are trademarks and trade names of Shimadzu Corporation or its affiliates, whether or not they are used with trademark symbol "TM" or "®". Third-party trademarks and trade names may be used in this publication to refer to either the entities or their products/services. Shimadzu disclaims any proprietary interest in trademarks and trade names other than its own.

The information contained herein is provided to you "as is" without warranty of any kind including without limitation warranties as to its accuracy or completeness. Shimadzu does not assume any responsibility or liability for any damage, whether direct or indirect, relating to the use of this publication. This publication is based upon the information available to Shimadzu on or before the date of publication, and subject to change without notice.

© Shimadzu Corporation, 2016

SHIMADZU
Excellence in Science

Application News

Material Testing System MCT

Compression-Rupture Test of Carbon Fibers with Different Tensile Characteristics Shimadzu Micro Compression Testing

No. SCA_300_037

■ Introduction

As the result of recent progress of research and development, carbon fiber materials have been put to practical use in a wide range of implements, including space aircraft parts, sporting goods like golf club shafts and tennis rackets, structure materials that must transmit X-rays, and acoustic materials.

A group of high-quality carbon fibers is further classified, according to its tensile strength, into several groups. One of these is a high-strength fiber group that features in excellent tensile strength; another is a high-elasticity fiber group characterized by high flexibility, but with a tensile strength of no more than around 2,000 MPa.

As described above, data on mechanical properties are indispensable information for classifying fibers.

The following is an example of tests for evaluation of physical behaviors under a compressive force applied to carbon fibers (single fibers) having different tensile strength levels with Shimadzu Micro Compression Testing Machine MCT.

■ Testing Conditions

(1) Testing mode: compression test
(2) Testing load: 200 gf
(3) Loading rate constant: 1 (4,230 gf/sec.)
(4) Calculation of strength: Compression strength is calculated by the following equation. *1

$$ST = 2 \cdot P \cdot \pi \cdot d \cdot L$$

where:
ST: tensile strength (kg/mm^2)
P: compression strength (kgf)
d: diameter of fiber (mm)
L: length of fiber (mm)

Note *1: from JIS A1113-1976 Method of tests for splitting tensile strength of concrete

■ Test Piece

(1) Name: Carbon fibers (PAN type carbon fibers)

(2) Types: 1 (high-ductility type)

2 (high-strength type)

3 (ultra-high elasticity type)

(3) Shape: See Fig. 1

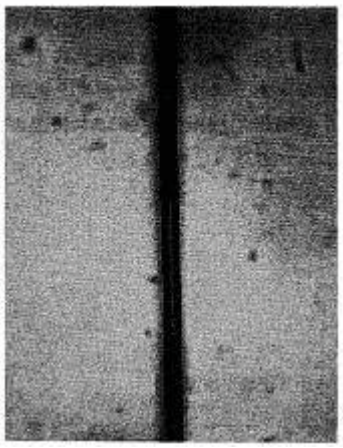

Fig. 1 A Microscopic photograph of Test Piece before Test

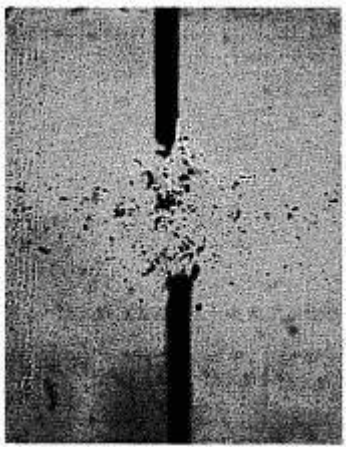

Fig. 2 A Microscopic photograph of Test Piece after Test

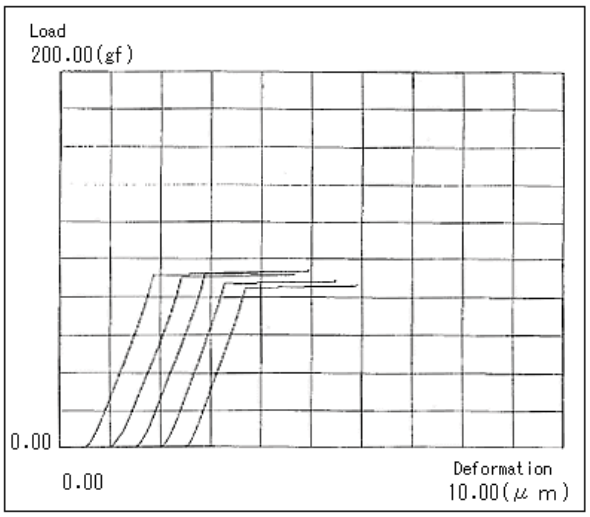

Fig. 3 Load- Deformation Curves of High Ductility Samples

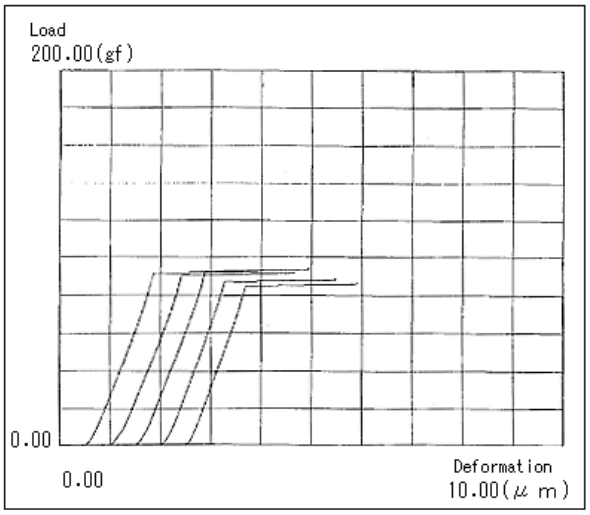

Fig.2 Load-Deformation Curves of High Ductility Samples

Fig. 4 Load- Deformation Curves of High Ductility Samples

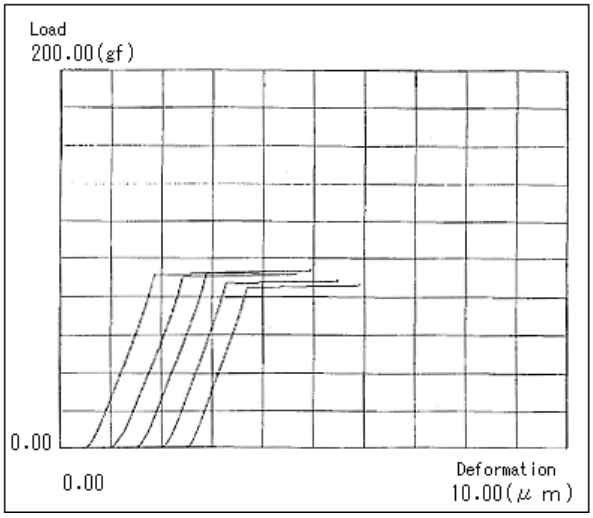

Fig. 5 Load- Deformation Curves of High Ductility Samples

Type of test piece	Compression-rupture strength(kgf/mm^2)	Standard deviation (kgf/mm^2)
High-ductility type	149.90	3.23
High-strength type	151.09	6.34
Ultra-high elasticity type	68.87	4.37

Table 1 Results of Compression-Rupture Test of Carbon Fibers

Note: The length of the indenter diameter (50 mm) was used for the length of fiber because the test piece was extraordinarily long.

■ Test Results

Table 1 shows a summary of test data, and Figs. 2-4 show the compression-rupture strength and the overlapping view of load-deformation curves for each test piece.

The difference of behavior between test pieces are observable in the load-deformation curves of Figs. 2-4.

The test pieces of the high-ductility type and the high-strength type have similar compression-rupture strength, while the ultra-high elasticity type has a remarkably low compression-rupture strength. (Refer to Table 1)

Admitting some deviation among the test data as a result of the surface conditions of the test pieces, the test results ensure that this testing machine is useful and effective for evaluation of mechanical properties of single fibers, provided that data are processed statistically.

* Please be advised that data obtained before the implementation of the current Weights and Measures Law may be presented in terms of gravimetric unit.

For Research Use Only. Not for use in diagnostic procedures.
The content of this publication shall not be reproduced, altered or sold for any commercial purpose without the written approval of Shimadzu. The information contained herein is provided to you "as is" without warranty of any kind including without limitation warranties as to its accuracy or completeness. Shimadzu does not assume any responsibility or liability for any damage, whether direct or indirect, relating to be the use of this publication. This publication is based upon the information available to Shimadzu on or before the date of publication, and subject to change without notice.

SHIMADZU
Excellence in Science

Application News

Material Testing System AG-X

No. SCA_300_059

Observation of fracture in CFRP tensile test

CFRP (carbon fiber reinforced plastic) has attracted attention as a high-performance composite material with high strength and rigidity, yet low in weight, and is being applied in various fields, such as for aircraft, railroad vehicles, automobiles and civil engineering. This example describes evaluating the characteristics of a flat plate specimen of CFRP material when a tensile load is applied (tensile test) and observing the fracture status. Tensile testing consisted of static testing of material strength and measuring the modulus of elasticity using a precision universal testing machine. In addition, high-rate tensile impact test was also performed. In the latter case, a high-speed video camera was used to record specimen fracture, which allowed capturing image data of the instant the CFRP material fractured.

■ Test specimen

The tensile test specimen tested in this example is shown in figure 1. Included 50 mm long CFRP tabs attached to both ends of the CFRP strip with thermosetting resin adhesive. Reinforcing the grip area with tabs ensures a stable tensile test with good reproducibility.

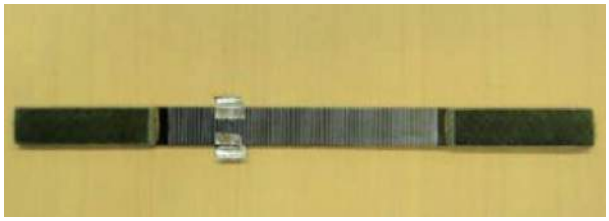

Figure 1: CFRP test specimen

Specimen details are as follows:

1) Material: unidirectional CFRP
2) Shape: strip (with tabs on both ends)
3) Specimen dimensions: for static tensile testing 200(L) x 12.5(W) x 1(T) mm. For recording image of impact fracture 70(L) x 6.25(W) x 0.3(T) mm

■ Static tensile test

A strain gauge type extensometer was attached to the specimen and a tensile test was performed using a precision testing machine. The extensometer was removed when strain exceeded the elasticity measurement range. It is also possible to measure strain by affixing a strain gauge instead of an extensometer. Tensile test parameters are indicated below.

(1) Tensile rate: 10 mm/min
(2) Grip distance: 100 mm
(3) Test force detection: 50 KN load cell
(4) Extensometer gauge length: 50 mm
(5) Elasticity calculation range: 5/10,000 to 25/10,000 strain

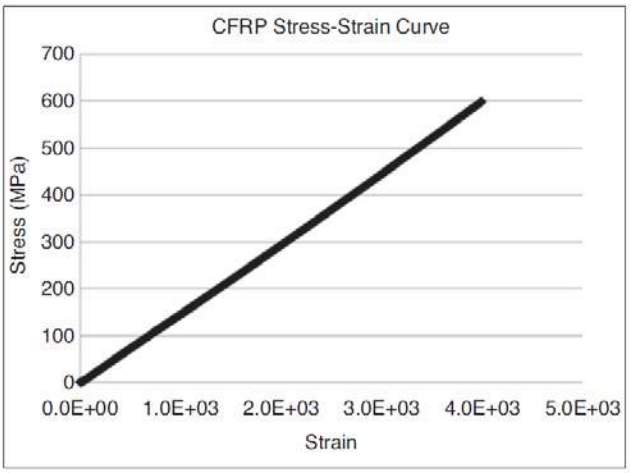

Figure 2: Static test results

The elasticity of CFRP specimen can be determined by calculating the slope of the given strain region (elasticity calculation range) in the stress-strain curve (figure 2) obtained from test results. Tensile strangth can be determined from the maximum stress in the stress-displacement curve (figure 3) before the specimen breaks.

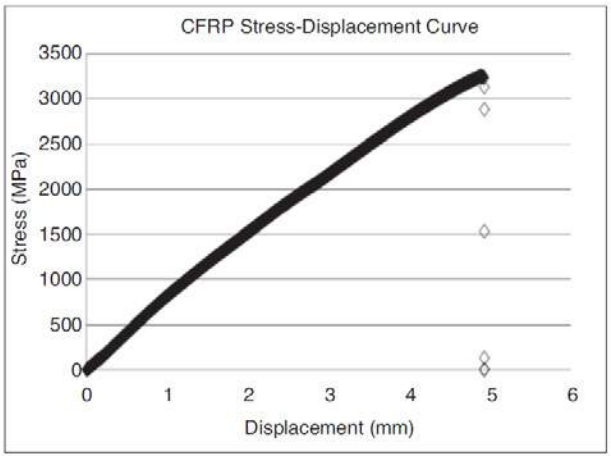

Figure 3: Static test results

The following values were obtained from the measurement data.

(1) Tensile strength: 346 GPa
(2) Elasticity: 148 GPa

The post-test status of the specimen is shown in figure 4. Compared to the starting status in figure 1, it clearly shows how the fibers within the resin have failed.

Figure 4: Specimen status after static test

■ Static tensile test

To verify functionality, development of composite materials involves not only static Static strength testing, but also involves the objective of ensuring active safety. Consequently, it is important to determine the shock strength and understand the process of fracture propagation. Therefore, the fracture process during tensile chock testing of a CFRP specimen was observed by combining a high-speed video camera with high-rate tensile shock test machine. Observation conditions are indicated below.

Specimen tensile rate:	6 m/s
Grip distance:	30 mm
Camera lens:	105 mm macro, with 2 x teleconverter
Camera lighting:	strobe
Camera trigger:	signal synchronized with tensile displacement is sent from testing machine to camera.

The setup used to record video of the test is shown in figure 5, with a high-speed video camera mounted about 450 mm in front of the specimen. Recording was activated by an external start trigger signal sent from the testing machine to the camera, which was synchronized to the tensile displacement. A strobe light synchronized to the video timing was used as lighting.

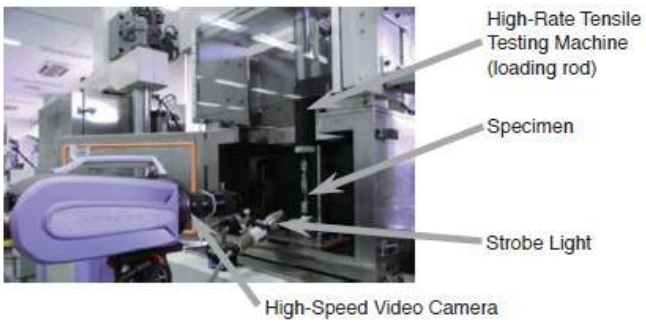

Figure 5: Setup of high-rate shock test

Using this test configuration, a load was applied to the CFRP specimen according to the parameters indicated above and a high-speed camera captured the instant of fracture, at 250.000 frames per second. This image data shown in figure 6.

This shows 8 consecutive frames, from (1) TO (8), with an interval of 4 microseconds between each frame. This camera features highly detailed image resolution of 312 horizontal by 260 vertical pixels that is constant, regardless of the frame rate.

This example shows, combining a high-speed video camera and material testing machine makes it possible to evaluate material properties and observe fracture behavior at the same time. This enables supporting a wide range of material development applications, from developing individual functionally enhanced resins to developing composite materials.

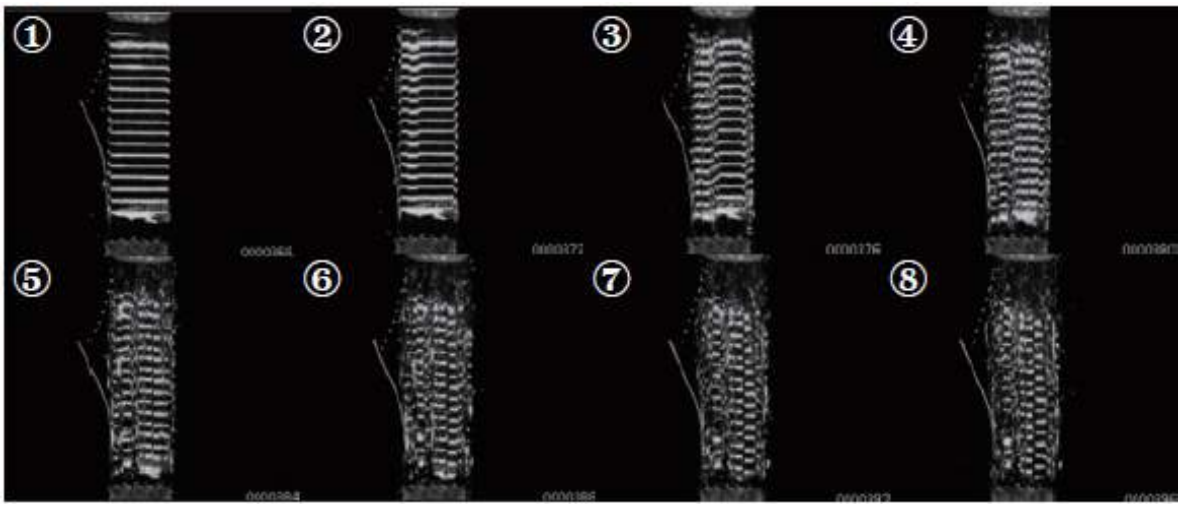

Figure 6: Images of specimen during fracture

For Research Use Only. Not for use in diagnostic procedures.
The content of this publication shall not be reproduced, altered or sold for any commercial purpose without the written approval of Shimadzu. The information contained herein is provided to you "as is" without warranty of any kind including without limitation warranties as to its accuracy or completeness. Shimadzu does not assume any responsibility or liability for any damage, whether direct or indirect, relating to be the use of this publication. This publication is based upon the information available to Shimadzu on or before the date of publication, and subject to change without notice.

SHIMADZU
Excellence in Science

Ultrasonic Fatigue Testing System with an Average Stress Loading Mechanism

For Gigacycle Fatigue Tests with Average Stress Loaded

Actual components are rarely used under conditions in which the average stress is zero. Despite this, the USF-2000A, a standard ultrasonic fatigue testing system, can only perform testing under zero average stress conditions.
Using an ultrasonic fatigue testing system equipped with an average stress loading mechanism, gigacycle fatigue tests can be performed with average tensile stress loaded.

System Appearance

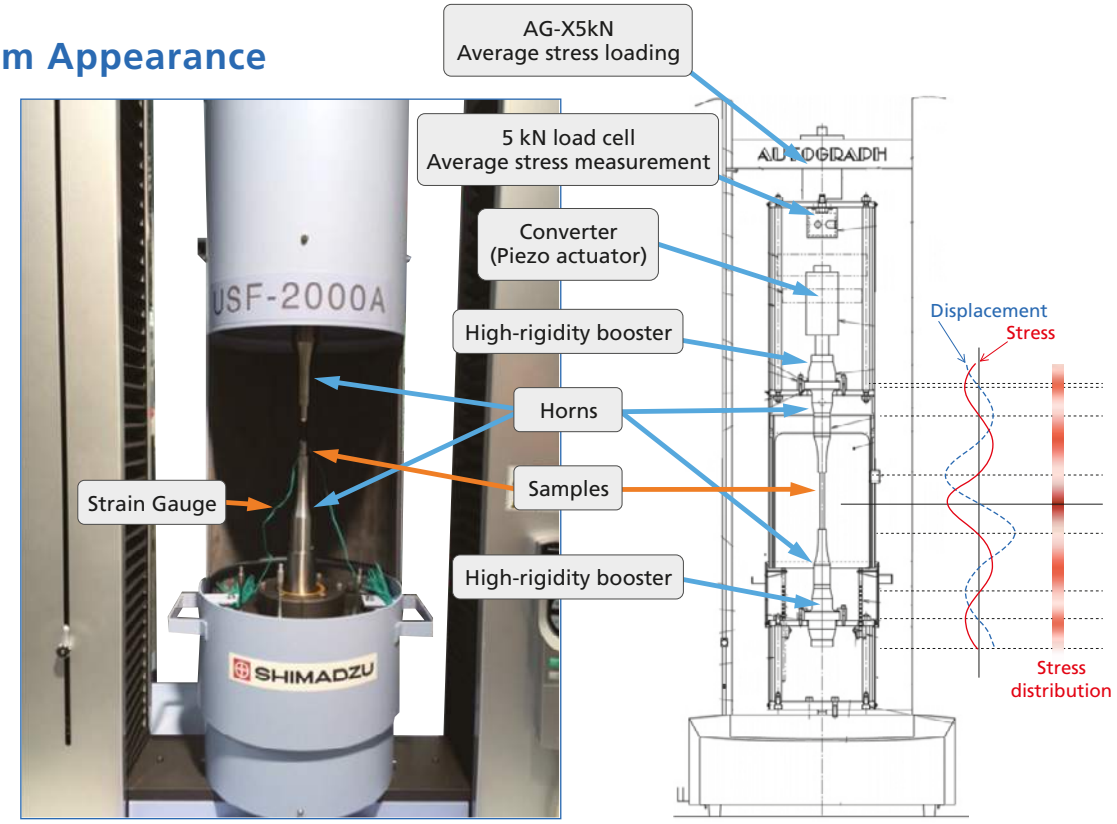

Ultrasonic Fatigue Testing System Effective for Gigacycle Fatigue Tests

With fatigue tests of high-strength steels, it is evident that internal fracture (fish-eye fracture), which is caused by inclusions and other micro defects, occurs at 107 cycles or more, a value considered the conventional fatigue limit.
An ultrasonic fatigue testing system is extremely effective when performing this sort of gigacycle fatigue test. (With a 100 Hz fatigue testing system, this would take 3 years, but if a 20 kHz ultrasonic fatigue testing system is used, testing can be completed in one week.)

Main Specifications

1) Test Frequency: 20 kHz ± 500 Hz

- The recommended test range is 20 kHz ± 30 Hz.
- The test frequency is determined by the resonance frequency of the sample.

2) Horn End Face Amplitude

Min. approx. ±10 µm
Max. approx. ±50 µm

- The minimum and maximum amplitudes are the end face amplitude values at amplitude outputs of 20 % and 100 % respectively. Accordingly, the minimum and maximum amplitude values will change somewhat depending on the shape of the sample.

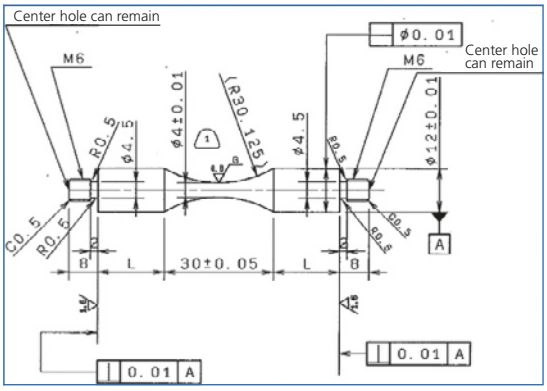

Standard Circular Tapered Sample

3) Test Stress

Standard circular tapered sample
Stress Min. 237 MPa
Max. 1186 MPa

- The test stress range can be changed by changing the sample shape.
- The minimum and maximum values are calculated with the end face amplitude values of 10 µm and 50 µm respectively.
- These are the values when the stress is within the elasticity range.

4) Average Stress

Max. 1.5 kN (tensile only)

- Average stress loads exceeding 1.5 kN are possible, but will have an impact on the service life of the horn.

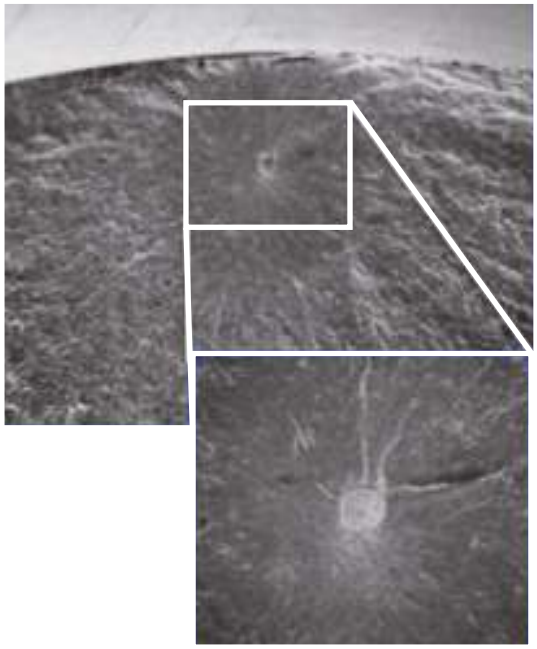
Surface of the Fatigued Fracture Originating from the Inclusion

■ Components

1	Ultrasonic resonance system Power supply, converter, booster (1 pair), horn (1 pair)
2	Personal computer (OS Windows 7) ADA/PIO interface board
3	Software Ultrasonic test control measurement software
4	Cooling system Air dryer, air piping • A separate 140 L/min air source is required.
5	Strain meter unit (option)
6	AG-X plus Autograph 5 kN + 250 extension
7	Average stress loading mechanism

Shimadzu Corporation
www.shimadzu.com/an/

For Research Use Only. Not for use in diagnostic procedure.
This publication may contain references to products that are not available in your country. Please contact us to check the availability of these products in your country.
Company names, product/service names and logos used in this publication are trademarks and trade names of Shimadzu Corporation or its affiliates, whether or not they are used with trademark symbol "TM" or "®". Third-party trademarks and trade names may be used in this publication to refer to either the entities or their products/services. Shimadzu disclaims any proprietary interest in trademarks and trade names other than its own.

The contents of this publication are provided to you "as is" without warranty of any kind, and are subject to change without notice. Shimadzu does not assume any responsibility or liability for any damage, whether direct or indirect, relating to the use of this publication.

© Shimadzu Corporation, 2016

First Edition: August 2016

SHIMADZU

Application News

No.i244

Material Testing System

Tensile Test for Metallic Materials Using Strain Rate Control and Stress Rate Control

Introduction

International standards for tensile testing of metallic materials have been revised as specified in ISO 6892 and JIS Z2241, such that strain rate control, where strain is measured with an extensometer, has recently been added as a test item to the current stress rate control method, in which a load is applied to a material until its yield point is reached. As a result, it can be assumed that there will be situations where both stress rate control and strain rate control tensile testing of metallic materials will be required.
Here, we introduce examples of strain rate control and stress rate control tensile testing of metallic samples, including cold-rolled steel, austenitic stainless steel, aluminium alloy and brass, according to ISO 6892, using the Shimadzu Autograph AG-50kNX Precision Universal Tester, and the SSG50-10H strain gauge type one-touch extensometer (Fig. 1, Fig. 2).

Fig. 1 Overview of Universal Testing System

Fig. 2 Specimen and Jigs for Tensile Testing

Specimens and Test Conditions

Information on the sample specimens are shown in Table 1, and the test conditions are shown in Table 2.

Table 1 Test Specimens

Sample Name	A	B	C	D
Material	Cold-rolled steel	Stainless steel (austenitic)	Aluminium alloy	Brass
Sample size	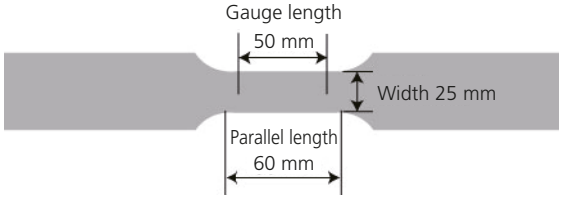 Width 25 mm, thickness 1 mm, gauge length 50 mm, parallel length 60 mm (JIS Z 2241 No. 5 test specimen)			

Table 2 Test Conditions

1) Load cell capacity	50 kN
2) Jig	50 kN Non-shift wedge type grips (file teeth for flat specimen)
3) Test speed	See Table 3
4) Test temperature	Ambient temperature
5) Software	TRAPEZIUMX (single)

Fig. 3 shows an image diagram of the test speed, and Table 3 and Table 4 show the applicable test speeds for the strain control and stress control tests, respectively.

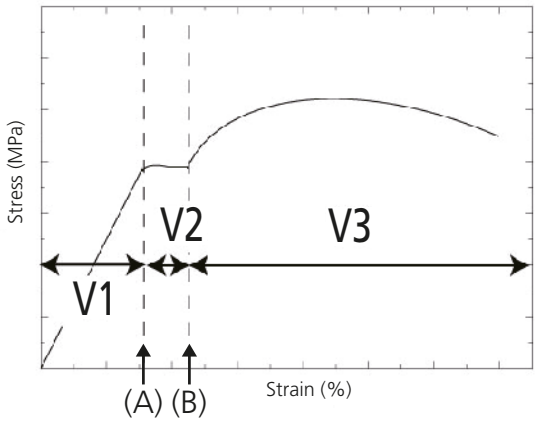

(A): Upper yield point (or its corresponding point)
(B): Upper limit of strain measurement (point after proof strength point)

Fig. 3 Image of Test Strain Rate

Table 3 Test Strain Rate (based on strain rate control)

V1: Strain rate	0.00025/s (1.5 %/min)
V2: Strain rate	0.00025/s (1.5 %/min)
V3: Predicted strain rate	0.0067/s (40 %/min)

Table 4 Test Stress Rate (based on stress rate control)

V1: Stress rate	10 MPa/s
V2: Strain rate	0.00083/s (5 %/min)
V3: Predicted strain rate	0.0067/s (40 %/min)

Test Results

Fig. 4 shows a diagram of the stress – stroke displacement for each sample using strain-rate control, and Table 5 shows their characteristic values. In Fig. 4, the point at which the stress becomes discontinuous, as indicated by the jump in the stress-stroke displacement curve, corresponds to the point at which the strain rate is switched.

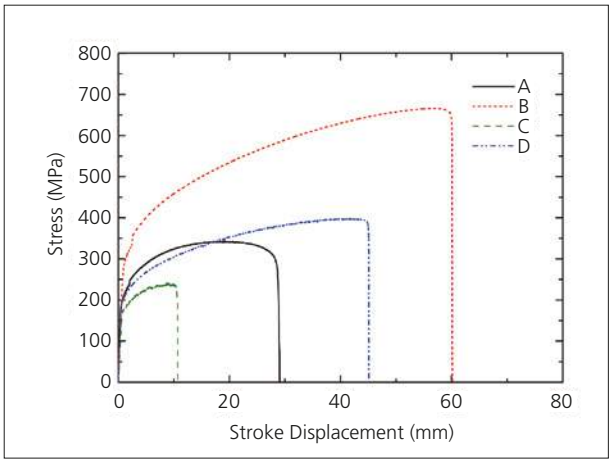

Fig. 4 Test Results for Each Metallic Material (stress-stroke curve based on strain rate control)

Table 5 Test results (Average n = 3)

Sample Name	Elastic Modulus (GPa)	0.2 % Proof Strength (MPa)	Tensile Strength (MPa)	Elongation at Break (%)
A (cold-rolled steel)	194	185.5	341.5	43.3
B (stainless steel)	200	278.5	660.8	55.0
C (aluminum)	71	170.1	236.3	13.0
D (brass)	109	193.1	398.1	49.1

Note 1) Strain rate refers to the amount of increase in strain, obtained using an extensometer to measure the gauge length of a test specimen, per unit time.
Note 2) Predicted strain rate was obtained using the displacement of the testing machine crosshead at each point in time and the test specimen's parallel length. Thus, it is defined as the increase in strain of the specimen's parallel length per unit time.

Fig. 5 (a) – (d) shows the strain rate and predicted strain rate obtained from tensile testing of the respective metallic materials using strain rate control. The red solid lines show the strain rate, the blue solid lines the predicted strain rate, and the black broken lines show the stress. In addition, the green dotted lines represent the permissible value ±20 % relative tolerance in the strain rate control (as specified in ISO 6892). As for the actual load rate, it is clear that the values are well within the permissible strain rate control range, indicating excellent strain rate control. Regarding samples A and B, displacement is measured up to 2 % of the gauge length using an extensometer. In the case of samples C and D, the strain measured using an extensometer was only up to 0.8 %, because of the appearance of serration when strain corresponding to about 1 % was applied.

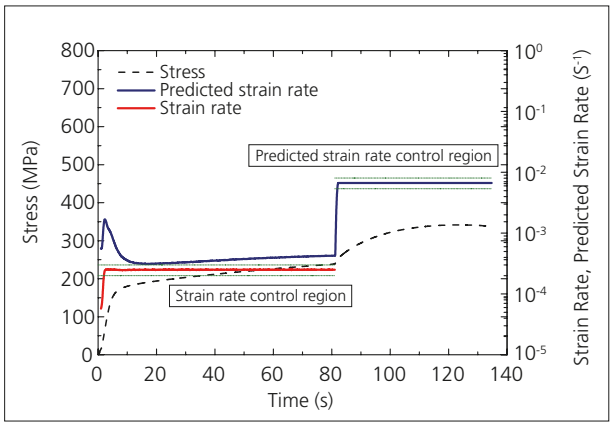

Fig. 5 (a) Test Results (Sample A)

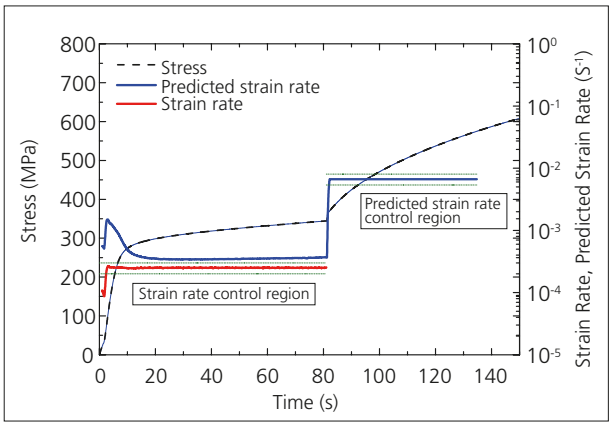

Fig. 5 (b) Test Results (Sample B)

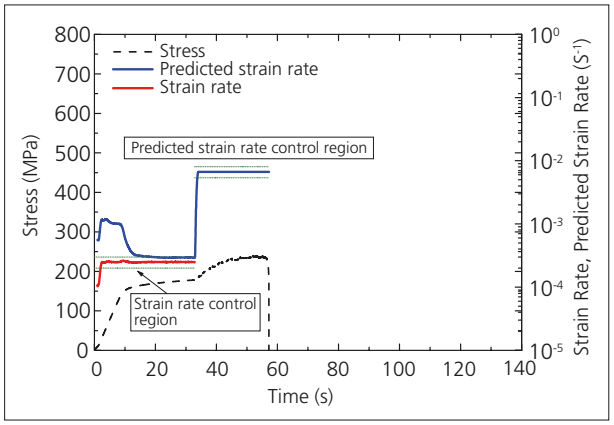

Fig. 5 (c) Test Results (Sample C)

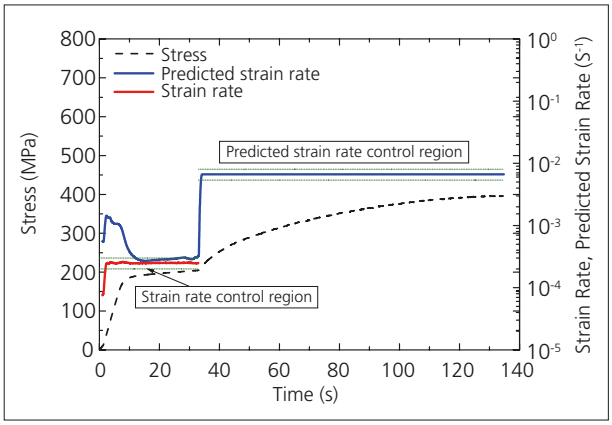

Fig. 5 (d) Test Results (Sample D)

Fig. 6 shows the stress-stroke displacement curve diagram obtained from tensile testing of each of the metallic materials using stress rate control, and the characteristic values are shown in Table 6.

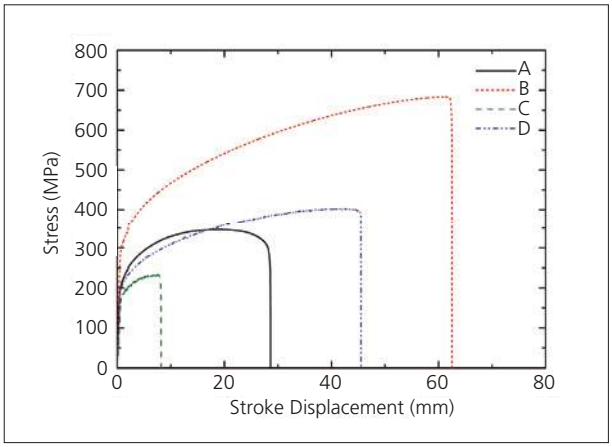

Fig. 6 Test Results (stress-stroke curve based on stress rate control)

Table 6 Test Results (Average n = 3)

Sample Name	Elastic Modulus (GPa)	0.2 % Proof Strength (MPa)	Tensile Strength (MPa)	Elongation at Break (%)
A (cold-rolled steel)	194	193.3	349.3	42.0
B (stainless steel)	205	290.7	687.0	54.8
C (aluminum)	69	177.0	233.5	12.6
D (brass)	112	196.7	405.5	48.8

Fig. 7 (a) – (d) shows the strain rate and predicted strain rate obtained from tensile testing of the respective metallic materials using stress rate control. The pink solid lines show the stress rate, the blue solid lines the predicted strain rate, and the black broken lines show the stress.

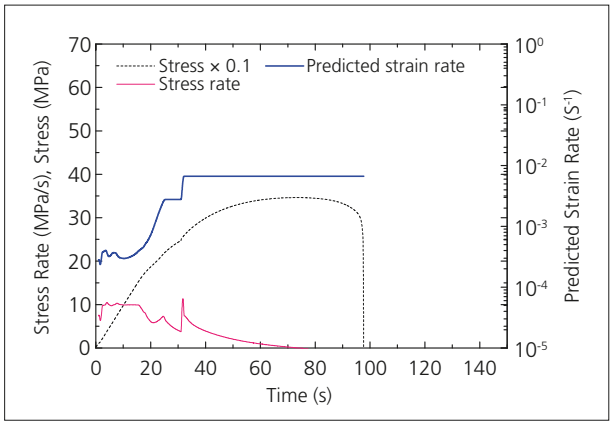

Fig. 7 (a) Test Results (Sample A)

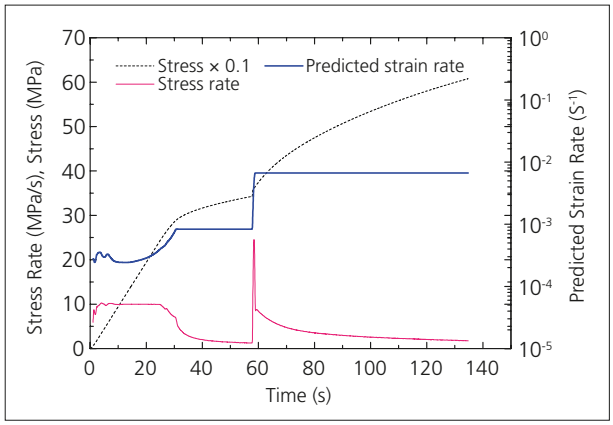

Fig. 7 (b) Test Results (Sample B)

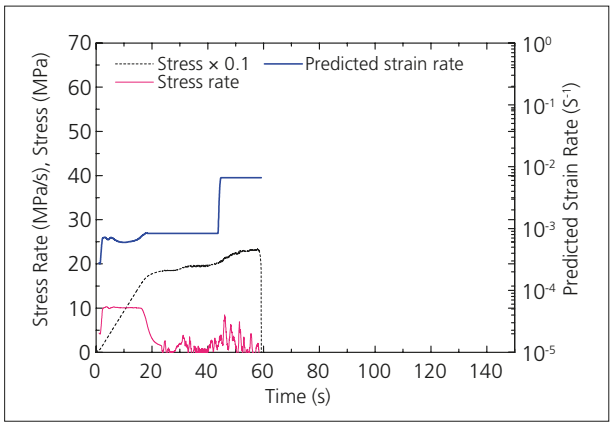

Fig. 7 (c) Test Results (Sample C)

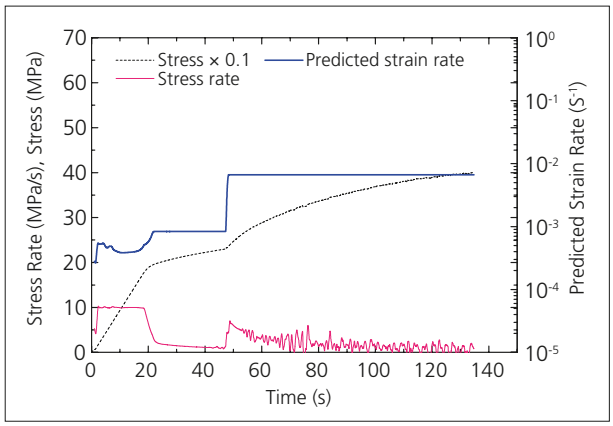

Fig. 7 (d) Test Results (Sample D)

It is clear that at the set rates, suitably stable data could be acquired for both stress rate and predicted strain rate.

The above results demonstrate that in the tensile testing of the various types of metallic materials using the Shimadzu Autograph AG-50kNX Precision Universal Tester, the strain rate control values were well within the range of the permissible values (± 20 %) specified in ISO 6892. Similarly, stable testing using stress rate control was also achieved. When using typical universal testing machines, testing control methods other than the crosshead rate control, e.g. strain rate control and stress rate control, normally require burdensome adjustment of the control gain depending on the material being tested. However, with this instrument, strain rate control and stress rate control in tensile testing of any metallic material are easily conducted because the gain is adjusted automatically (auto-tuning feature).

First Edition: January, 2012

SHIMADZU

SHIMADZU Corporation
www.shimadzu.com/an/

For Research Use Only. Not for use in diagnostic procedures.
The contents of this publication are provided to you "as is" without warranty of any kind, and are subject to change without notice.
Shimadzu does not assume any responsibility or liability for any damage, whether direct or indirect, relating to the use of this publication.

© Shimadzu Corporation, 2012

SHIMADZU
Excellence in Science

Application News

Material Testing System DUH

No. SCA_300_035

A hardness measurement of surface treatment layer on a steel sample using Shimadzu Dynamic Ultra Micro Hardness Tester, Model DUH

Recent years have seen intensive requests for engineering materials with higher function ability and longer life, and as a result, surface treatment for such materials has become popular. Under this circumstance, hardness testers with micro load are enjoying an increasing demand. In this regards, a test report is herein introduced on the hardness distribution measured from the sample surface toward depth direction with an interval of 2 µm, using Shimadzu Dynamic Ultra Micro Hardness Tester Model DUH.

■ Test Parameters

1) Sample: plating layer on a metal plate (See Fig. 1)

2) Indenter: tip angle 136°, square pyramid indenter (Vickers indenter)

3) Measuring mode: load-load-hold test (mode 1)

4) Test load: 2.0 gf

5) Loading speed: 0.029 gf/sec.

6) Load hold-time: 10 sec.

■ Test Method

1) Vickers Hardness
Testing procedures, the distance between the indentation center and the sample edge shall be 2.5 time the diagonal length or more (the diagonal length is 2.6 µm or less). The test load was determined in accordance with this specification, and the tests were performed near the mid depth of the plating layer.

2) Hardness distribution measurements were performed at the location and with the depth intervals of 2 µm starting from the sample surface as shown in Fig. 2

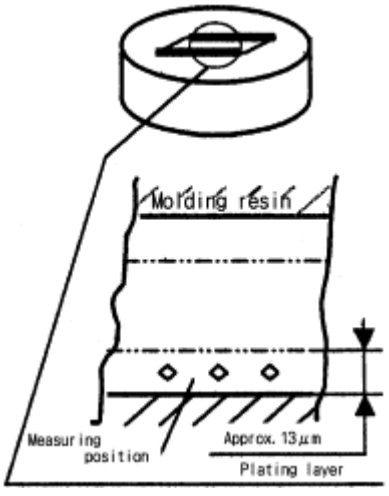

Fig. 1

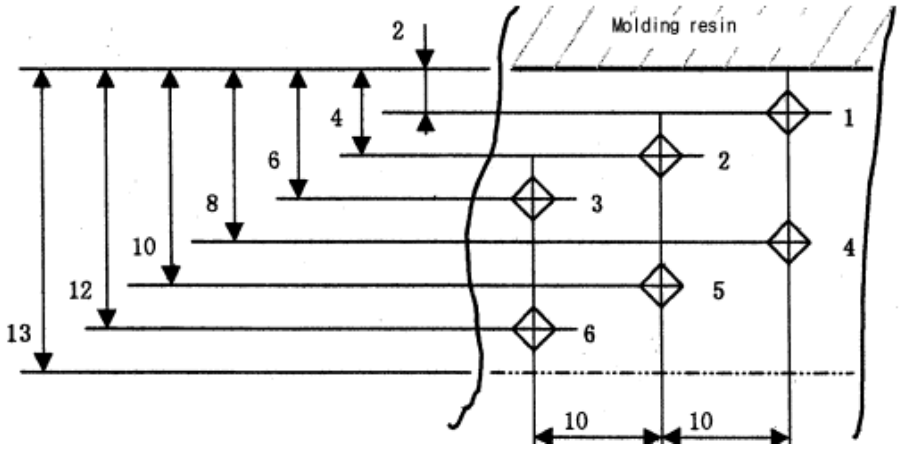

Fig. 2

■ Test Results

The average of five measurements is shown in Table 1, and the load-indentation depth curve is in Fig. 3

Test Load (gf)	Depth (μm)	Dynamic Hardness DHV
2,001	0,206	1065

Table 1 Hardness Test Result

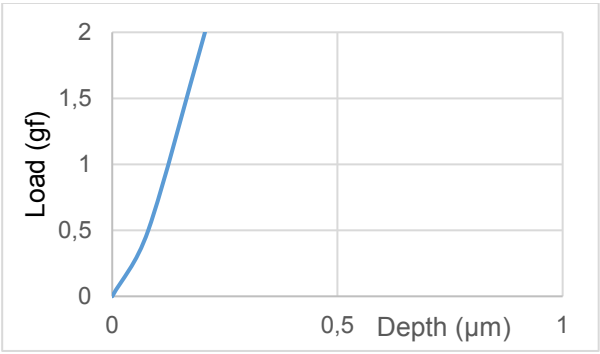

Fig. 3 Load-Indentation depth curve

Dynamic Hardness was determined by the following formula:

$$DHV = \frac{37{,}838 \cdot P}{h^2}$$

Where:

DHV: Dynamic hardness by Vickers Indenter

P: Test Load (gf)

H: Indentation depth (μm)

■ Test Results

Result of five tests with a depth interval of 2 μm is listed in Table 2.

Test Load (gf)	DHV					
	1	2	3	4	5	6
2,0	847	1001	1070	1103	966	925

Table 2 Hardness Distribution

..

■ **Dynamic hardness was determined by the same formula as item 1) above.**

The Relation of depth and hardness is shown in Fig. 4.

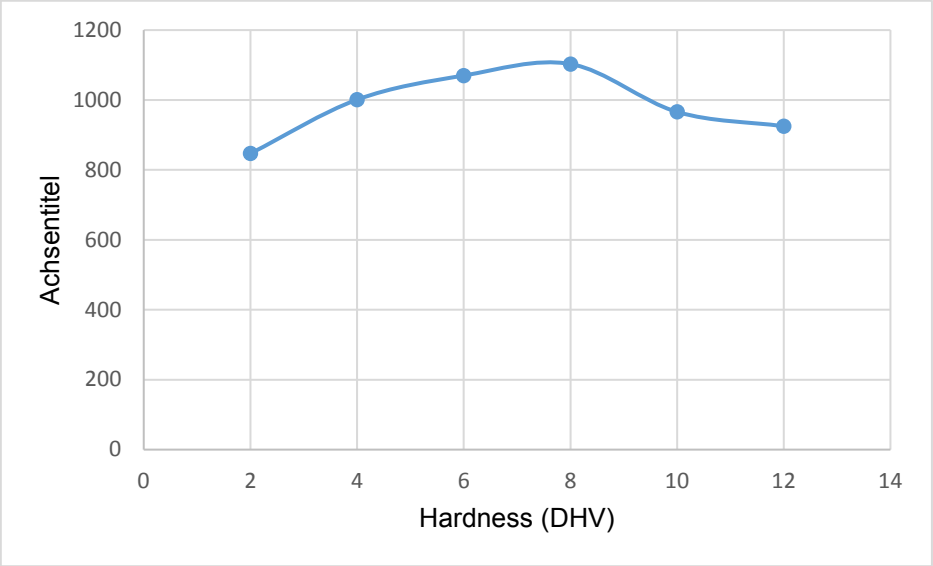

Fig. 4

Fig. 4 indicates a tendency that hardness increases as depth increases, reaches the max. at mid depth of the plating layer, and decreases thereafter.

For Research Use Only. Not for use in diagnostic procedures.
The content of this publication shall not be reproduced, altered or sold for any commercial purpose without the written approval of Shimadzu. The information contained herein is provided to you "as is" without warranty of any kind including without limitation warranties as to its accuracy or completeness. Shimadzu does not assume any responsibility or liability for any damage, whether direct or indirect, relating to be the use of this publication. This publication is based upon the information available to Shimadzu on or before the date of publication, and subject to change without notice.

SHIMADZU
Excellence in Science

Application Data Sheet

No. 2

Autograph Precision Universal Tester

Material Testing & Inspection

Flexural Testing of Plastics

Standard No. ISO178: 2010 (JIS K 7171: 1994)

Introduction

In recent years, a large variety of synthetic resin (plastic) materials has become available for use in a diversity of products. They are used in applications that take advantage of their respective characteristics. For example, polyethylene (PE) is cheap and easy to mold, and thus used for containers, packaging film, and other everyday applications. In contrast, polycarbonate (PC) is transparent, has a high mechanical strength, and is heat-resistant; consequently, it is used for CDs and DVDs in the electrical and electronics fields, as well as in transportation equipment, optics, and medical fields.

In this Data Sheet, flexural testings are performed on four materials, including polyvinyl chloride (PVC) and polypropylene (PP).

T. Murakami

Measurements and Jigs

In plastic flexural testings, the width of the two supports and central loading edge must be larger than the width of the specimen, and parallelism within ± 0.2 mm is required. The loading edge radius is 5 mm ±0.1 mm, and the supports radius is specified as 2 mm ± 0.2 mm for specimens with a thickness of 3 mm or less, and 5 mm ± 0.2 mm for specimens with a thickness exceeding 3 mm. The span must be adjusted to a value of 16 (± 1) times the specimen thickness. In this test, since a 4 mm-thick specimen is used, the span is set to 64 mm (specimen thickness of 4 mm × 16 = 64 mm).

Measurement Results

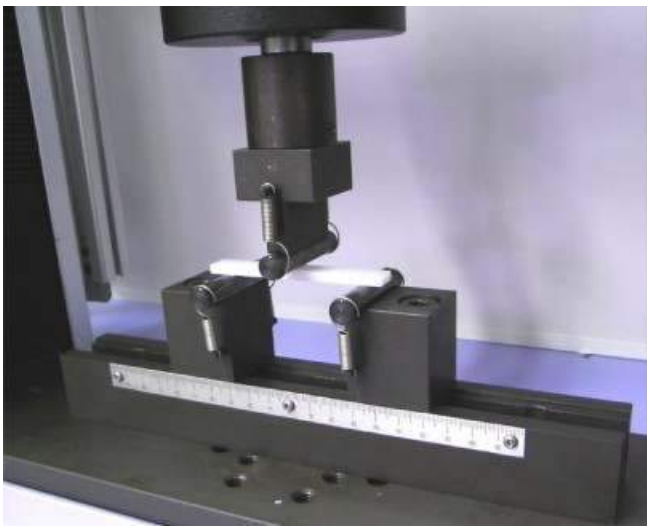

Fig. 1: Test Status

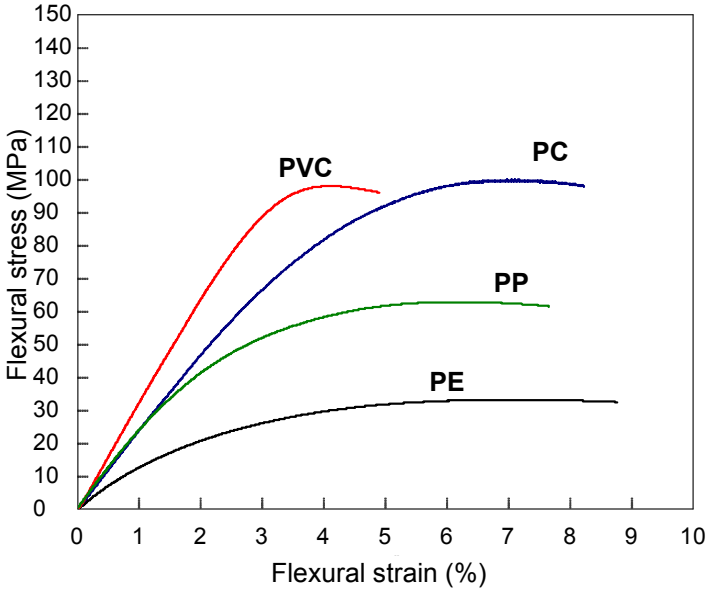

Fig. 2: Relationship Between Flexural Stress and Flexural Strain

Table 1: Test Conditions

Item	Set Value
Test Speed	2 mm/min
Span	64 mm

Table 2: Test Results

Sample	Flexural Modulus (MPa)	Flexural Strength (MPa)
PE (polyethylene)	1527	33.0
PC (polycarbonate)	2378	99.7
PVC (polyvinyl chloride)	3257	97.8
PP (polypropylene)	2559	62.6

Plastic Flexural Testing System

Tester:	AGS-X
Load Cell:	1 kN
Test Jig:	Three-point bending test jig for plastics (loading edge radius.: 5 mm, supports radius.: 3 mm)
Software:	TRAPEZIUM LITE X

AGS-X Table-Top Precision Universal Tester

Features

- A high-precision load cell is adopted. (The high-precision type is class 0.5; the standard-precision type is class 1.) Accuracy is guaranteed over a wide range, from 1/500 to 1/1 of the load cell capacity. This supports highly reliable test evaluations.
- Crosshead speed range
  Tests can be performed over a wide range from 0.001 mm/min to 1,000 mm/min.
- High-speed sampling
  High-speed sampling, as fast as 1 msec.
- TRAPEZIUMX LITE X operational software
  This is simple, highly effective software.
- Jog controller (optional)
  This allows hand-held control of the crosshead position. Fine position adjustment is possible using the jog dial.
- Optional Test Devices
  A variety of tests can be conducted by switching between an abundance of jigs in the lineup.

First Edition: February 2013

Shimadzu Corporation
www.shimadzu.com/an/

For Research Use Only. Not for use in diagnostic procedures.
The content of this publication shall not be reproduced, altered or sold for any commercial purpose without the written approval of Shimadzu.
The information contained herein is provided to you "as is" without warranty of any kind including without limitation warranties as to its accuracy or completeness. Shimadzu does not assume any responsibility or liability for any damage, whether direct or indirect, relating to the use of this publication. This publication is based upon the information available to Shimadzu on or before the date of publication, and subject to change without notice.
© Shimadzu Corporation, 2013

SHIMADZU
Excellence in Science

Application Data Sheet

No. 3

Autograph Precision Universal Tester

Material Testing & Inspection

Tensile Tests of Plastic Materials at Low Temperatures (-40 °C)

Standard No. ISO527-1: 2012 (JIS K 7161: 1994)

Introduction

Tensile tests are widely used to evaluate plastic materials, and the results are used as indices for new materials development and for implementing quality control. Items evaluated as tensile characteristics of plastic materials include the tensile modulus, strength, and break strain. In this Data Sheet, the tensile modulus of polypropylene (PP) and polyvinyl chloride (PVC) specimens (dumbbell shaped and cut types) was calculated based on displacement data acquired using an extensometer at a low temperature of -40 °C. In addition, the strength and break strain for the respective plastic materials were also evaluated.

T. Murakami

Measurements and Jigs

In finding a sample's tensile modulus, it is necessary to use an extensometer capable of measuring tiny deformations of the sample with high accuracy. Measurements of crosshead travel distances include errors not only from sample deformation, but also from load cell and test jig deformation. When the deformation region is very small, the ratio of the error becomes significant, so this data is not suitable for tensile modulus calculations. In such cases, an extensometer that can measure changes in the gauge length with an accuracy of at least ±1 % must be used. When measuring the modulus of elasticity with a 50 mm gauge length, this corresponds to an accuracy of ±1μm. In this test, a one-touch contact type extensometer, capable of operating even in a -40 °C environment, was used.

Measurement Results

Fig. 1: Test Status

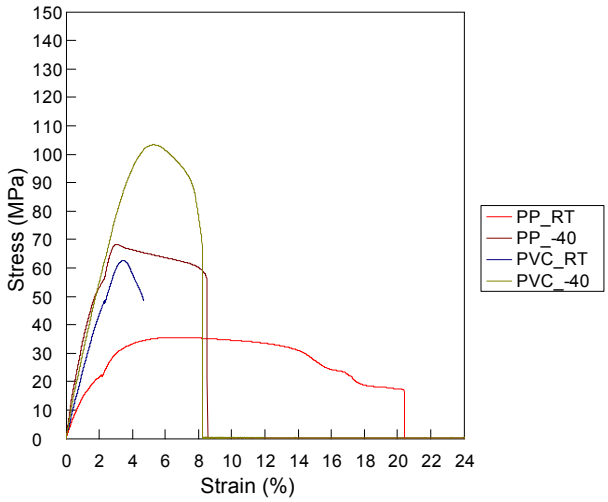

Fig. 2: Relationship Between Stress and Strain

In the results, samples with an "RT" suffix were measured in a room temperature environment, and those with a "-40" suffix were measured at -40 °C. In all cases, measurement was performed at a test speed of 1 mm/min up to 2 %, and then at a test speed of 50 mm/min. In the room temperature measurements, the extensometer measurement range was exceeded, so the extensometer was removed at the 2 % position.

Table 1: Test Results

Sample	Tensile Modulus (MPa)	Strength (MPa)	Break Strain (%)
PP_RT	1955	36	20.2
PP_-40	5333	68	7.8
PVC_RT	3150	63	4.3
PVC_-40	3942	103	7.1

Plastic Material Thermostatic Tensile Test System

Tester:	AGS-X
Load Cell:	5 kN
Test Jig:	5 kN pneumatic flat grips (Single-side file teeth grip faces)
Extensometer:	Strain gauge type one-touch extensometer EPC-50-10
External Amplifier:	ESA-CU200
Thermostatic Chamber:	TCR2W
Software:	TRAPEZIUM LITE X

AGS-X Table-Top Precision Universal Tester

Features

- A high-precision load cell is adopted. (The high-precision type is class 0.5; the standard-precision type is class 1.) Accuracy is guaranteed over a wide range, from 1/500 to 1/1 of the load cell capacity. This supports highly reliable test evaluations.
- Crosshead speed range
  Tests can be performed over a wide range from 0.001 mm/min to 1,000 mm/min.
- High-speed sampling
  High-speed sampling, as fast as 1 msec.
- TRAPEZIUMX LITE X operational software
  This is simple, highly effective software.
- Jog controller (optional)
  This allows hand-held control of the crosshead position. Fine position adjustment is possible using the jog dial.
- Optional Test Devices
  A variety of tests can be conducted by switching between an abundance of jigs in the lineup.

First Edition: February 2013

Shimadzu Corporation
www.shimadzu.com/an/

For Research Use Only. Not for use in diagnostic procedures.
The content of this publication shall not be reproduced, altered or sold for any commercial purpose without the written approval of Shimadzu.
The information contained herein is provided to you "as is" without warranty of any kind including without limitation warranties as to its accuracy or completeness. Shimadzu does not assume any responsibility or liability for any damage, whether direct or indirect, relating to the use of this publication. This publication is based upon the information available to Shimadzu on or before the date of publication, and subject to change without notice.
© Shimadzu Corporation, 2013

SHIMADZU
Excellence in Science

Application Data Sheet

No. 4

Autograph Precision Universal Tester

Material Testing & Inspection

Tensile Tests of Rubber Dumb-bell Specimens

Standard No. ISO37: 2005 (JIS K6251: 2010)

Introduction

Rubber materials have characteristic mechanical properties including elasticity and flexibility, and are widely used for industrial parts, construction materials, and housewares. In particular, a diverse range of synthetic rubber materials with differing properties suited to match their application have been developed. Measuring these mechanical properties is extremely important to ensure quality control and for new materials development. This Data Sheet introduces an example of the evaluation of three synthetic rubber (main components: chloroprene [1]; urethane [2]) specimens (dumb-bell test pieces). Static tensile tests were performed, and the specimens were evaluated with respect to tensile strength, stress at given elongation, and elongation at break, which are aspects of their basic mechanical properties.

T. Murakami

Measurements and Jigs

In tensile tests of rubber dumb-bell specimens, the grips must tighten automatically. When tensile loads are applied to rubber materials, they elongate and their thickness decreases. For this reason, if there is no automatic tightening mechanism, the specimen will inadvertently break free of the grip before the maximum load is applied, making favorable measurements impossible. Accordingly, in rubber tensile tests, it is necessary to use pneumatic parallel grippers, pantograph grips, eccentric roller type grips, Henry Scott type grips, or other grips equipped with this feature.

Measurement Results

Fig. 1: Test Status

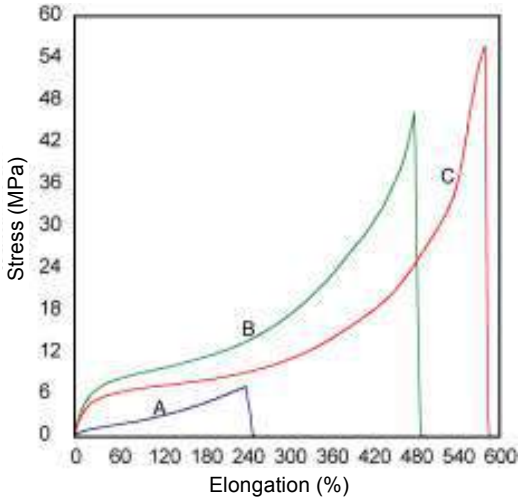

Fig. 2: Relationship Between Stress and Elongation

Table 1: Test Conditions

Item	Set Value
Test Speed	500 mm/min
Initial Distance between Grips	60 mm
Gauge Length	20 mm

Table 2: Test Results

Sample	Main Component	Tensile Strength (MPa)	Stress at 100 % Elongation (MPa)	Stress at 200 % Elongation (MPa)	Elongation at Break (%)
A	Chloroprene	7.1	2.4	5.4	242.3
B	Urethane	47.1	9.3	11.9	478.1
C	Urethane	55.5	7.0	8.4	572.6

The tensile test results for the three samples are shown in Table 2. A graph showing the stress-elongation relationship for the samples is shown in Fig. 2. Clear differences in mechanical properties such as tensile strength and elongation at break are apparent between the samples.

Rubber (Dumb-bells test pieces) Tensile Test System

Tester:	AGS-X
Load Cell:	1 kN
Test Jig:	1 kN pneumatic flat grips (Single-side file teeth grip faces)
Extensometer:	SES-1000 type extensometer for soft specimens
Software:	TRAPEZIUM LITE X

AGS-X Table-Top Precision Universal Tester

Features

- A high-precision load cell is adopted. (The high-precision type is class 0.5; the standard-precision type is class 1.) Accuracy is guaranteed over a wide range, from 1/500 to 1/1 of the load cell capacity. This supports highly reliable test evaluations.
- Crosshead speed range
  Tests can be performed over a wide range from 0.001 mm/min to 1,000 mm/min.
- High-speed sampling
  High-speed sampling, as fast as 1 msec.
- TRAPEZIUMX LITE X operational software
  This is simple, highly effective software.
- Jog controller (optional)
  This allows hand-held control of the crosshead position. Fine position adjustment is possible using the jog dial.
- Optional Test Devices
  A variety of tests can be conducted by switching between an abundance of jigs in the lineup.

First Edition: February 2013

Shimadzu Corporation
www.shimadzu.com/an/

For Research Use Only. Not for use in diagnostic procedures.
The content of this publication shall not be reproduced, altered or sold for any commercial purpose without the written approval of Shimadzu.
The information contained herein is provided to you "as is" without warranty of any kind including without limitation warranties as to its accuracy or completeness. Shimadzu does not assume any responsibility or liability for any damage, whether direct or indirect, relating to the use of this publication. This publication is based upon the information available to Shimadzu on or before the date of publication, and subject to change without notice.
© Shimadzu Corporation, 2013

SHIMADZU
Excellence in Science

Application Data Sheet

No. 5

Autograph Precision Universal Tester

Material Testing & Inspection

Tear Tests of Crescent-shaped Rubber Specimens

Standard No. ISO34-1: 2004 (JIS K6252: 2007)

Introduction

Rubber materials have characteristic mechanical properties including elasticity and flexibility, and are widely used for industrial parts, construction materials, and housewares. In particular, a diverse range of synthetic rubber materials with differing properties suited to match their application have been developed. Measuring these mechanical properties is extremely important to ensure quality control and for new materials development. This Data Sheet introduces an example of the evaluation of two synthetic rubber specimens (crescent-shaped specimens). Tear tests were performed, and the specimens were evaluated with respect to tear strength, one of their basic mechanical properties.

T. Murakami, J. Sakai

Measurements and Jigs

Tear tests of crescent-shaped rubber specimens require grips that tighten automatically as the tear force increases. When tensile loads are applied to rubber materials, they elongate and their thickness decreases. For this reason, if there is no automatic tightening mechanism, the specimen will inadvertently break free of the grips before the maximum tear force is applied, making favorable measurements impossible. Accordingly, in rubber tear tests, it is necessary to use pneumatic parallel grippers, pantograph grips, eccentric roller type grips, Henry Scott type grips, or other grips equipped with this feature.

Measurement Results

Fig. 1: Test Status

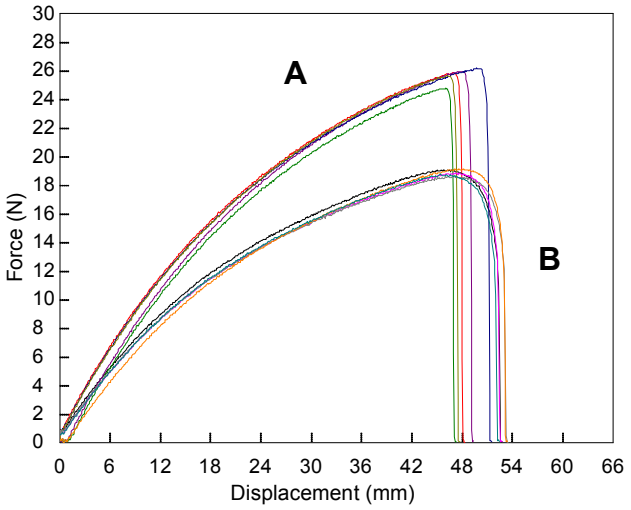

Fig. 2: Relationship Between Force and Displacement

Table 1: Test Conditions

Item	Set Value
Test Speed	500 mm/min
Initial Distance between Grips	60 mm

Table 2: Test Results (Average)

Sample	Main Component	Max. Force (N)	Tear Strength (kN/m)
A	CR rubber (black)	25.9	13.0
B	CR rubber (white)	18.9	9.5

The tear test results for the two samples are shown in Table 2. A graph showing the force-displacement relationship for each sample is shown in Fig. 2. Differences in tear strength between the samples are clearly apparent.

Rubber Tear Test System

Tester:	AGS-X
Load Cell:	1 kN
Test Jig:	1 kN pneumatic flat grips (Single-side file teeth grip faces)
Software:	TRAPEZIUM LITE X

AGS-X Table-Top Precision Universal Tester

Features

- A high-precision load cell is adopted. (The high-precision type is class 0.5; the standard-precision type is class 1.) Accuracy is guaranteed over a wide range, from 1/500 to 1/1 of the load cell capacity. This supports highly reliable test evaluations.
- Crosshead speed range
  Tests can be performed over a wide range from 0.001 mm/min to 1,000 mm/min.
- High-speed sampling
  High-speed sampling, as fast as 1 msec.
- TRAPEZIUMX LITE X operational software
  This is simple, highly effective software.
- Jog controller (optional)
  This allows hand-held control of the crosshead position. Fine position adjustment is possible using the jog dial.
- Optional Test Devices
  A variety of tests can be conducted by switching between an abundance of jigs in the lineup.

First Edition: February 2013

Shimadzu Corporation
www.shimadzu.com/an/

For Research Use Only. Not for use in diagnostic procedures.
The content of this publication shall not be reproduced, altered or sold for any commercial purpose without the written approval of Shimadzu.
The information contained herein is provided to you "as is" without warranty of any kind including without limitation warranties as to its accuracy or completeness. Shimadzu does not assume any responsibility or liability for any damage, whether direct or indirect, relating to the use of this publication. This publication is based upon the information available to Shimadzu on or before the date of publication, and subject to change without notice.
© Shimadzu Corporation, 2013

SHIMADZU
Excellence in Science

Application Data Sheet

No. 6

Autograph Precision Universal Tester

Material Testing & Inspection

Tear Tests of Angle-Shaped Rubber Specimens

Standard No. ISO34-1: 2004 (JIS K6252: 2007)

Introduction

Rubber materials have characteristic mechanical properties including elasticity and flexibility, and are widely used for industrial parts, construction materials, and housewares. In particular, a diverse range of synthetic rubber materials with differing properties suited to match their application have been developed. Measuring these mechanical properties is extremely important to ensure quality control and for new materials development. This Data Sheet introduces an example of the evaluation of two synthetic rubber specimens (angle-shaped specimens). Tear tests were performed, and the specimens were evaluated with respect to tear strength, one of their basic mechanical properties.

T. Murakami, J. Sakai

Measurements and Jigs

Tear tests of angle-shaped rubber specimens require grips that tighten automatically as the tear force increases. When tensile loads are applied to rubber materials, they elongate and their thickness decreases. For this reason, if there is no automatic tightening mechanism, the specimen will inadvertently break free of the grips before the maximum tear force is applied, making favorable measurements impossible. Accordingly, in rubber tear tests, it is necessary to use pneumatic parallel grippers, pantograph grips, eccentric roller type grips, Henry Scott type grips, or other grips equipped with this feature.

Measurement Results

Fig. 1: Test Status

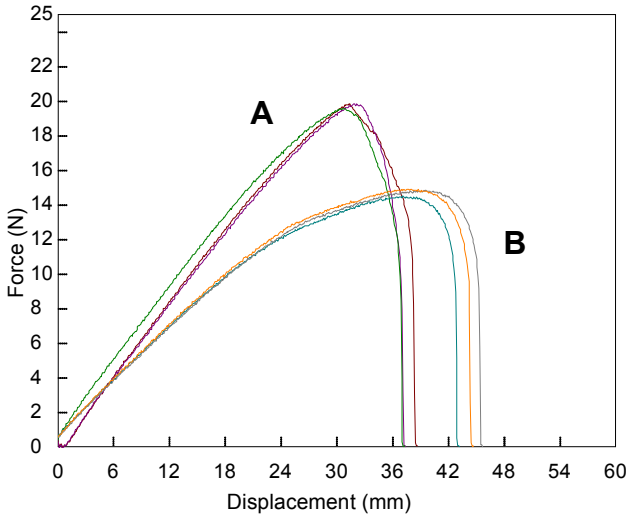

Fig. 2: Relationship Between Force and Displacement

Table 1: Test Conditions

Item	Set Value
Test Speed	500 mm/min
Initial Distance between Grips	60 mm

Table 2: Test Results (Average)

Sample	Main Component	Max. Force (N)	Tear Strength (kN/m)
A	CR rubber (black)	19.7	9.85
B	CR rubber (white)	14.7	7.35

The tear test results for the two samples are shown in Table 2. A graph showing the force-displacement relationship for each sample is shown in Fig. 2. Differences in tear strength between the samples are clearly apparent.

Rubber Tear Test System

Tester:	AGS-X
Load Cell:	1 kN
Test Jig:	1 kN pneumatic flat grips (Single-side file teeth grip faces)
Software:	TRAPEZIUM LITE X

AGS-X Table-Top Precision Universal Tester

Features

- A high-precision load cell is adopted. (The high-precision type is class 0.5; the standard-precision type is class 1.) Accuracy is guaranteed over a wide range, from 1/500 to 1/1 of the load cell capacity. This supports highly reliable test evaluations.
- Crosshead speed range
  Tests can be performed over a wide range from 0.001 mm/min to 1,000 mm/min.
- High-speed sampling
  High-speed sampling, as fast as 1 msec.
- TRAPEZIUMX LITE X operational software
  This is simple, highly effective software.
- Jog controller (optional)
  This allows hand-held control of the crosshead position. Fine position adjustment is possible using the jog dial.
- Optional Test Devices
  A variety of tests can be conducted by switching between an abundance of jigs in the lineup.

First Edition: February 2013

Shimadzu Corporation
www.shimadzu.com/an/

For Research Use Only. Not for use in diagnostic procedures.
The content of this publication shall not be reproduced, altered or sold for any commercial purpose without the written approval of Shimadzu.
The information contained herein is provided to you "as is" without warranty of any kind including without limitation warranties as to its accuracy or completeness. Shimadzu does not assume any responsibility or liability for any damage, whether direct or indirect, relating to the use of this publication. This publication is based upon the information available to Shimadzu on or before the date of publication, and subject to change without notice.
© Shimadzu Corporation, 2013

SHIMADZU
Excellence in Science

Application Data Sheet

No. 7

Autograph Precision Universal Tester

Material Testing & Inspection

Tensile Tests of Films

Standard No. ISO527-3: 2012 (JIS K 7127: 1999)

Introduction

Tensile tests are widely used to evaluate plastic materials, and the results are used as indices for new materials development and for implementing quality control. Items widely evaluated as tensile characteristics of plastic materials include the tensile modulus, strength, and break strain. In this Data Sheet, break strain was measured based on displacement data acquired using an extensometer. The strength was also evaluated.

T. Murakami

Measurements and Jigs

Non-contact type extensometers capable of displacement measurements without affecting the sample properties are effective for accurately measuring the break strain of a film. In measuring such physical properties, the sample must be gripped evenly, suppressing the occurrence of wrinkles, so it is important to choose the grips carefully. As in this test, the use of a non-contact type extensometer/width sensor and foil grips is recommended for film tensile tests.

Measurement Results

Fig. 1: Test Status

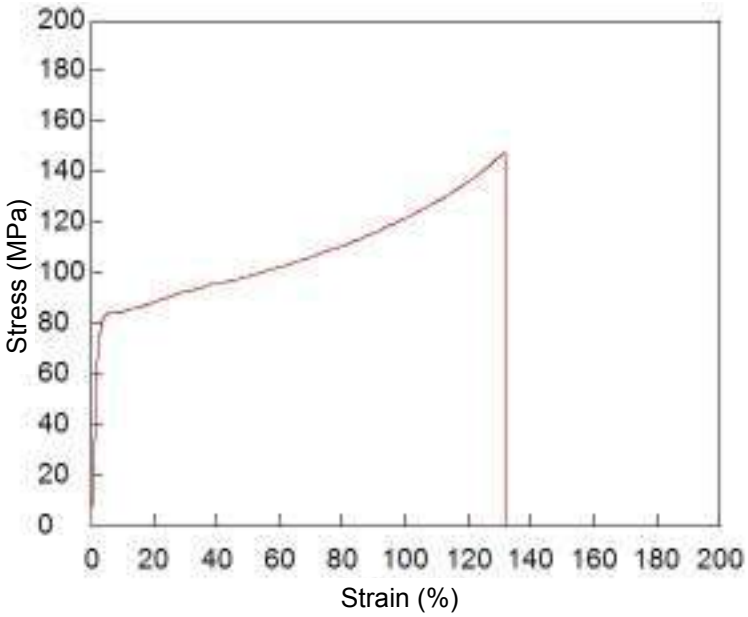

Fig. 2: Relationship Between Stress and Strain

Table 1: Test Conditions

Item	Set Value
Test Speed	50 mm/min
Initial Distance between Grips	100 mm

Table 2: Test Results

Sample	Thickness (μm)	Strength (MPa)	Break Strain (%)
PET Film	150	148	132

Film Tensile Test System

Tester:	AGS-X
Load Cell:	1 kN
Test Jig:	1 kN grips for foils
Extensometer:	TRViewX 240S non-contact extensometer/width sensor
Software:	TRAPEZIUM X

AGS-X Table-Top Precision Universal Tester

Features

- A high-precision load cell is adopted. (The high-precision type is class 0.5; the standard-precision type is class 1.) Accuracy is guaranteed over a wide range, from 1/500 to 1/1 of the load cell capacity. This supports highly reliable test evaluations.
- Crosshead speed range
  Tests can be performed over a wide range from 0.001 mm/min to 1,000 mm/min.
- High-speed sampling
  High-speed sampling, as fast as 1 msec.
- TRAPEZIUMX operational software
  Designed for intuitive operation, this software offers excellent convenience and user friendliness.
- Jog controller (optional)
  This allows hand-held control of the crosshead position. Fine position adjustment is possible using the jog dial.
- Optional Test Devices
  A variety of tests can be conducted by switching between an abundance of jigs in the lineup.

First Edition: February 2013

SHIMADZU

Shimadzu Corporation

www.shimadzu.com/an/

For Research Use Only. Not for use in diagnostic procedures.
The content of this publication shall not be reproduced, altered or sold for any commercial purpose without the written approval of Shimadzu.
The information contained herein is provided to you "as is" without warranty of any kind including without limitation warranties as to its accuracy or completeness. Shimadzu does not assume any responsibility or liability for any damage, whether direct or indirect, relating to the use of this publication. This publication is based upon the information available to Shimadzu on or before the date of publication, and subject to change without notice.

© Shimadzu Corporation, 2013

SHIMADZU
Excellence in Science

Application Data Sheet

No. 9

Autograph Precision Universal Tester

Material Testing & Inspection

Measurements of Modulus of Elasticity and Poisson's Ratio for Films

Standard Nos. ISO527-3: 2012 (JIS K 7127: 1999)
ISO527-1: 2012 (JIS K 7161: 1994)

Introduction

Tensile tests are widely used to evaluate plastic materials, and the results are used as indices for new materials development and for implementing quality control. Items evaluated as tensile characteristics of plastic materials include the tensile modulus, Poisson's ratio, strength, and break strain. With films, there are no standards specified with respect to test methods for the tensile elastic modulus and Poisson's ratio, yet there are demands for measurements of these values. In this Data Sheet, measurements of the tensile modulus and Poisson's ratio were performed for a PET film based on elongation and width data acquired using a non-contact type extensometer/width sensor.

T. Murakami

Measurements and Jigs

Non-contact type extensometers/width sensors capable of fine displacement measurements without affecting the sample properties are required to accurately obtain the tensile modulus and Poisson's ratio for a film. In measuring such physical properties, the sample must be gripped evenly, suppressing the occurrence of wrinkles, so it is important to choose the grips carefully. The use of a non-contact type extensometer/width sensor and foil grips is recommended for film tensile tests.

Measurement Results

Fig. 1: Test Status

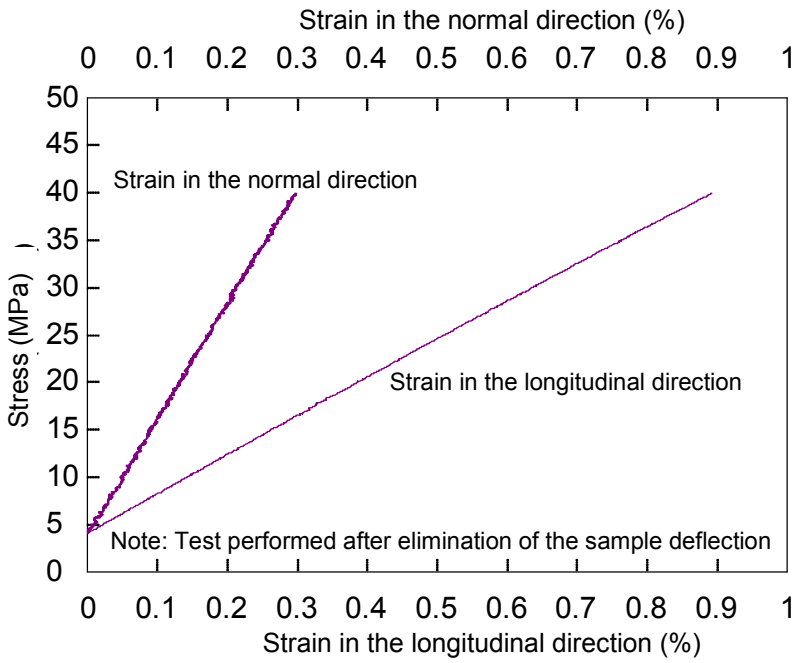

Fig. 2: Relationship Between Stress and Strain

Table 1: Test Conditions

Item	Set Value
Test Speed	1 mm/min
Initial distance Between Grip	100 mm
Gauge Length	40 mm

Table 2: Test Results

Sample	Thickness (μm)	Tensile Modulus (MPa)	Poisson's Ratio
PET Film	25	4139	0.37

Young's Modulus Measurement System for Film

Tester:	AG-Xplus
Load Cell:	1 kN
Test Jig:	1 kN grips for foils
Extensometer:	TRViewX 55S non-contact extensometer/width sensor
Software:	TRAPEZIUM X (Single)

AG-Xplus Table-Top Precision Universal Tester

Features

- A high-precision load cell is adopted. (The high-precision type is class 0.5; the standard-precision type is class 1.) Accuracy is guaranteed over a wide range, from 1/1000 to 1/1 of the load cell capacity. This supports highly reliable test evaluations.
- Crosshead speed range
  Tests can be performed over a wide range from 0.0005 mm/min to 1,500 mm/min.
- High-speed sampling
  Ultrafast sampling, as fast as 0.2 msec. Sudden changes in test force, such as when brittle materials fracture, can be assessed.
- TRAPEZIUMX X operational software
  Designed for intuitive operation, this software offers excellent convenience and user friendliness.
- Smart controller
  Real-time test force and position data is readily confirmed, and the manual dial can be used for fine adjustments to jig positioning.
- Optional Test Devices
  A variety of tests can be conducted by switching between an abundance of jigs in the lineup.

First Edition: February 2013

Shimadzu Corporation
www.shimadzu.com/an/

For Research Use Only. Not for use in diagnostic procedures.
The content of this publication shall not be reproduced, altered or sold for any commercial purpose without the written approval of Shimadzu.
The information contained herein is provided to you "as is" without warranty of any kind including without limitation warranties as to its accuracy or completeness. Shimadzu does not assume any responsibility or liability for any damage, whether direct or indirect, relating to the use of this publication. This publication is based upon the information available to Shimadzu on or before the date of publication, and subject to change without notice.
© Shimadzu Corporation, 2013

SHIMADZU
Excellence in Science

3. Biomaterials and Medical Industry

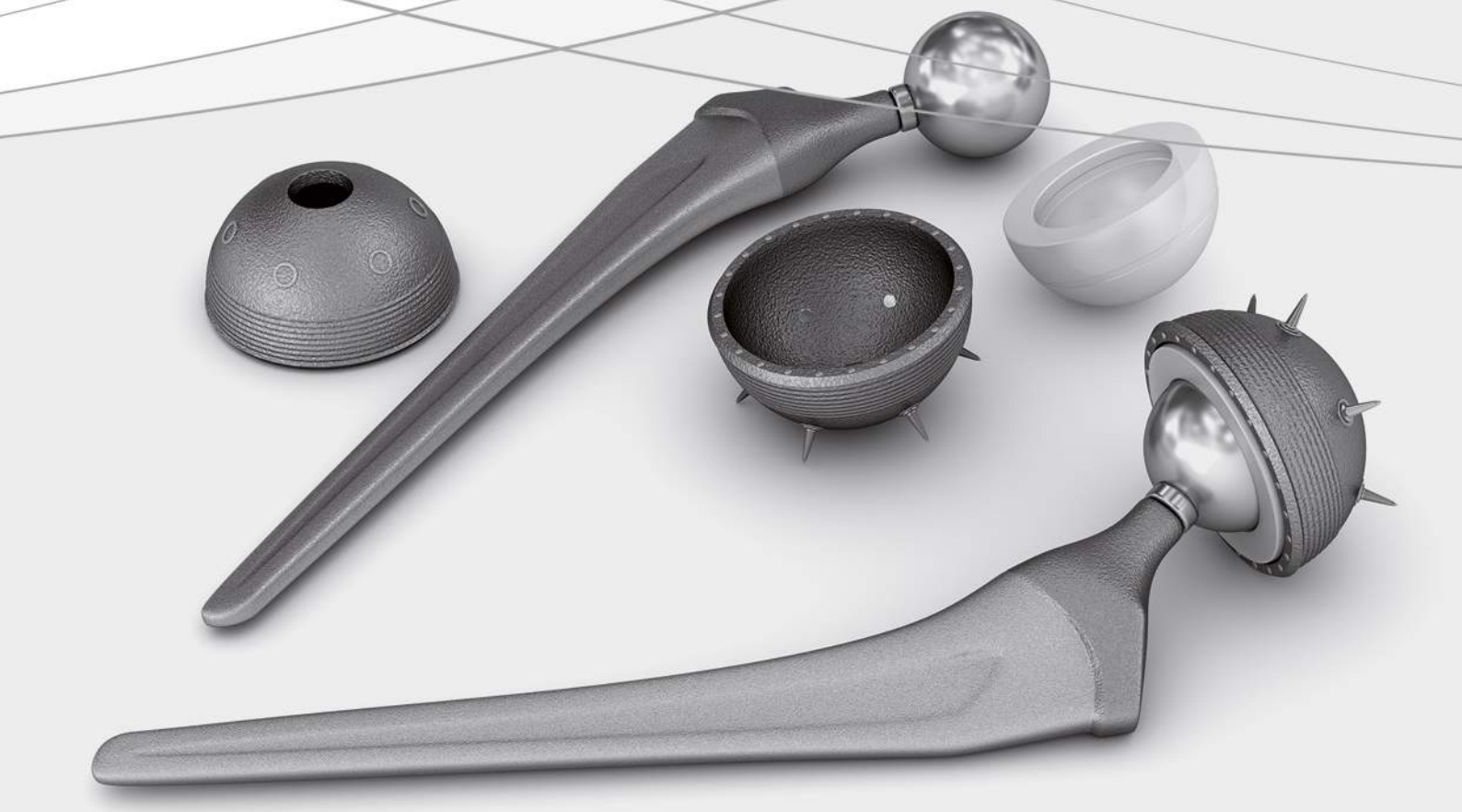

3. Biomaterials and Medical Industry

DEVELOPMENT OF ADVANCED MEDICAL TREATMENTS

World population was just two billion in 1927, but reached seven billion in 2011 and is expected to be ten billion by the end of the 21st century. At the same time, so-called advanced countries are becoming aging societies. This dramatic growth in population and life-expectancy is said to result from more sophisticated medicine, which in turn will require more advanced medical technology.

The medical equipment and biomaterials industries have experienced a vast number of innovations and developments over the past decade. In addition, great strides have been made in materials and technologies; therapeutic strategies and surgical techniques have progressed dramatically. For instance, a broken femur can now be replaced by an implant, and inserting small metal stents weighing just a few grams into the neurovascular system can prevent strokes due to plaque or arterial stenosis.

To guarantee the safety and efficacy of medical equipment and technologies in the wake of such medical breakthroughs, active efforts are being made to reinforce evaluation criteria and the regulations governing the standardization of measuring instruments and test methods. Medical equipment manufacturers and research organizations around the world are conducting research and development into medical equipment based on mechanical properties evaluation and finite element analysis.

Shimadzu applies its technical expertise cultivated through physical testing, quality control and full-scale testing in materials development to the fields of leading-edge medicine and biomaterials evaluation.

3. Biomaterials and Medical Industry

No.ei252	Orthodontic implant fatigue testing
SCA_300_058	Measurement of press-trough package force and tablet break force

SHIMADZU
Excellence in Science

Application News

No.i252

Material Testing System

Orthodontic Implant Fatigue Testing

Introduction

Dental implantation normally refers to a method of treatment that involves embedding a titanium implant in the jaw bone and fitting an artificial tooth onto this implant to return the function and aesthetic appearance of the original tooth. Orthodontic implantation uses implant technology to affix artificial material into bone. Embedding artificial material into bone has advantages of orthodontic therapies that use implants, such as being able to secure a stronger anchor, increasing the range of movement of the teeth, increasing the likelihood of using therapies that do not require tooth removal, and increasing the scope of non-surgical orthodontic therapy. However, fluoride solutions used in mouthwash can have a negative effect on the durability of titanium implants. Consequently, fatigue testing of orthodontic implants must be performed in solution so its effect can be determined and more durable orthodontic implants developed. We performed fatigue testing of an orthodontic implant in pure water at 37 ˚C, and report the results.

Measurement System

The Electromagnetic Force Fatigue and Endurance Test System MMT-101NV-10 was used for testing. Testing was performed in pure water at 37 ˚C using a thermostatic water immersion test unit. Testing was performed as shown in Fig. 1, and the test equipment used is shown in Table 1.

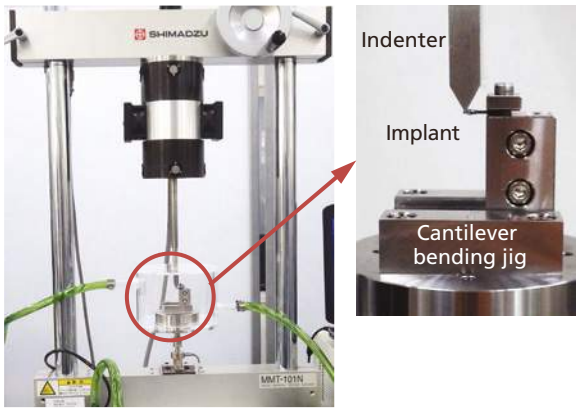

Fig. 1 Test Overview

Table 1 Experimental Equipment

Testing machine	: MMT-101NV-10
Load Cell	: 100 N
Jig	: Implant cantilever bending jig
Tank	: Thermostatic water immersion test unit

Results

(1) Static testing

First, static testing was performed to determine the loading level for fatigue testing. Test conditions are shown in Table 2, and the static test results are shown in Fig. 2. Based on static test results, the mean maximum strength was 35.4 N.

Table 2 Test Conditions

Testing Speed	: 5 mm/min
Test Environment	: Room temperature, in air
Number of Tests	: n = 5

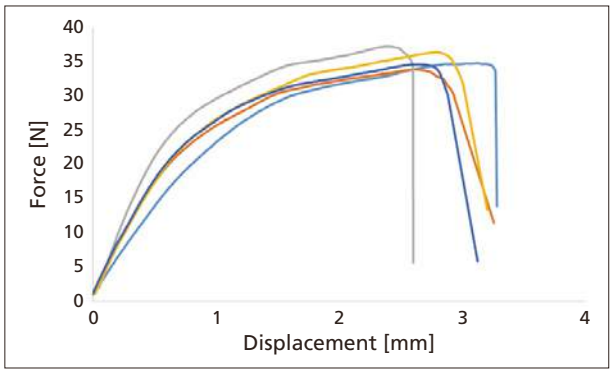

Fig. 2 Results of Static Testing

(2) Fatigue testing

The loading level for fatigue testing was determined based on the static test results. The test conditions used in fatigue testing are shown in Table 3.

Table 3 Test Conditions

Max. Force	: 30, 25, 20, 15, 12.5, 11, 10, 9, 8, 7
Stress Ratio	: 0.1
Frequency	: 10 Hz
Test Environment	: 37 ˚C, in pure water
Max. Number of Repetitions	: 5,000,000
Number of Tests	: n = 1

Test results are shown in Fig. 3. Fig. 3 shows that at a maximum force ≤ 11 N the number of cycles to failure was < 10,000, and there was no particular increase in the number of cycles to failure. At test forces ≤ 10 N, the maximum force fell and the number of cycles to failure increased substantially. At a maximum force of 7 N, failure did not occur at < 5,000,000 cycles.

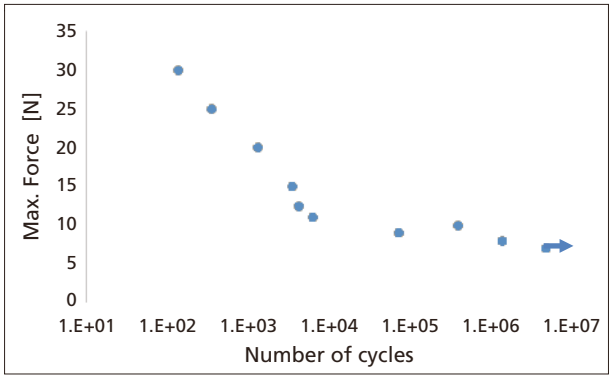

Fig. 3 S-N Curve

Conclusion

We performed cantilever bending fatigue testing of an orthodontic implant at 37 ˚C in pure water. The orthodontic implant we tested had a small number of cycles to failure at maximum forces ≥ 11 N (≥ 31 % of static strength), but this number of cycles to failure increased at forces ≤ 10 N (≤ 28 % of static strength). We plan to perform more fatigue testing in fluoride compound-containing mouthwash solution. This report shows that Shimadzu's test system can be used to perform cantilever bending fatigue testing of orthodontic implants in solution, and may be used for the development and evaluation of orthodontic implants.

First Edition: Jul. 2016

Shimadzu Corporation
www.shimadzu.com/an/

For Research Use Only. Not for use in diagnostic procedure.
This publication may contain references to products that are not available in your country. Please contact us to check the availability of these products in your country.

The content of this publication shall not be reproduced, altered or sold for any commercial purpose without the written approval of Shimadzu. Company names, product/service names and logos used in this publication are trademarks and trade names of Shimadzu Corporation or its affiliates, whether or not they are used with trademark symbol "TM" or "®". Third-party trademarks and trade names may be used in this publication to refer to either the entities or their products/services. Shimadzu disclaims any proprietary interest in trademarks and trade names other than its own.

The information contained herein is provided to you "as is" without warranty of any kind including without limitation warranties as to its accuracy or completeness. Shimadzu does not assume any responsibility or liability for any damage, whether direct or indirect, relating to the use of this publication. This publication is based upon the information available to Shimadzu on or before the date of publication, and subject to change without notice.

© Shimadzu Corporation, 2016

SHIMADZU
Excellence in Science

Application News

Material Testing System EZ-X

No. SCA_300_058

Measurement of Press-Trough Package Force and Tablet Break Force

Many tablets and capsules are packaged in thin metallic (aluminum etc.) and plastic materials. This type of package is referred to as a PTP (press trough package) or PTP sheet, and serves to protect the contained tablets and capsules and facilitate handling of the contents. Therefore, quality control is necessary to ensure that the package does not peel excessively, and that the tablet is not too difficult to dispense.

Figure 1: PTP packaged tablets

Figure 2: Testing machine (EZ-SX)

Here, using the Shimadzu EZ-X compact table-top universal testing machine and the TrapeziumX material testing software, we introduce an example of the adhesive strength of the PTP package, in addition to the force required to break a tablet in half.

■ Press-Dispense test for PTP packaged tablets

As shown in figure 4, the test was performed by pushing the tablet out of the PTP package using an upper 10 mm spherical press jig at a test speed of 50 mm/min, and a fix platform below. In this case the result obtained was a maximum test force mean value of 24.3 N. The judgment as to whether or not the tablet is easy to push out can be obtained from the maximum test force, which is applicable to product development and quality control.

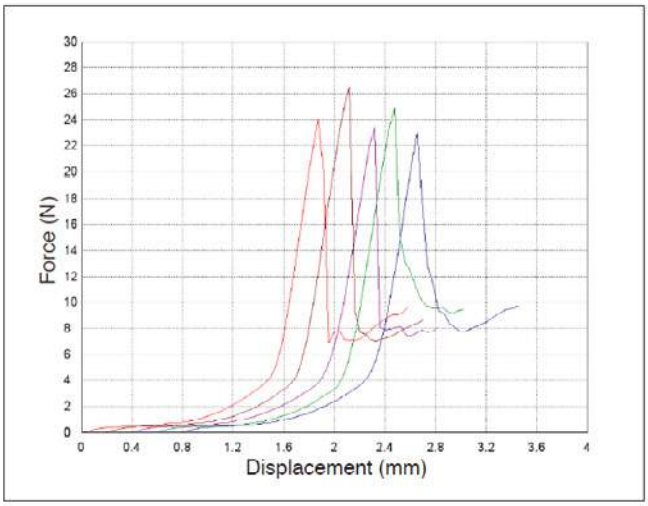

Figure 3: Results of press-dispense test

Figure 4: View of testing machine during measurement

■ Peel test for PTP packages

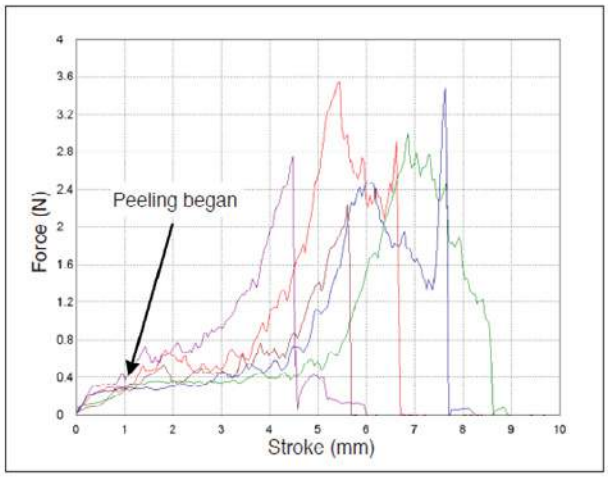

Figure 5: Results of peel test

Figure 6: Testing machine during measurement

As shown in figure 6, using a 100N pantograph type jigs above and fixing platform below, we performed the test by peeling the aluminum foil off from the underside of the PTP package at a test speed of 50 mm/min. peeling began at about 0.3 N, and at the package edge the force was about 3 N.

■ Break test of tablets

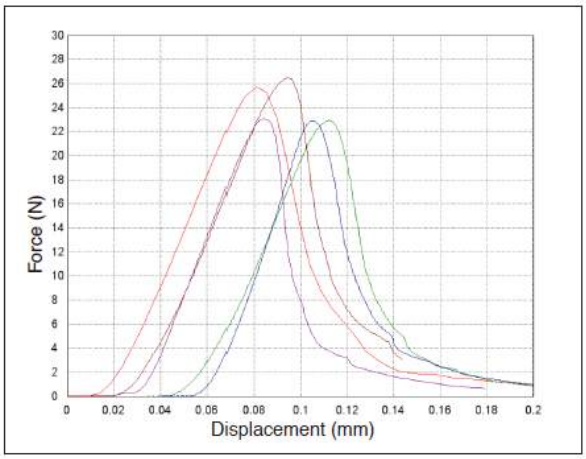

Figure 7: Results of break force test

Figure 8: Testing machine during measurement

■ Summary

Some tablets have a groove in the center, allowing each to be taken whole by adults or via a half dose by children. Accordingly, it must be able to be broken in half using some suitable degree of force. As a suitable method of simulating this breaking in half, that tablet was placed above the bend test jig supports (5 mm distance between supports), and measurement was conducted at a test speed of 0.5 mm/min until the tablet broke. As shown in the measurement result graph of figure 7, the force required to break the tablet in half (mean value of maximum test force) was about 24 N.

By using this kind of measurement, the depth of the tablet center groove can be optimized so that the tablet is easily and accuratelly broken in half.

Thus, by combining the Shimadzu EZ-X compact table-top universal testing machine with the abundant selection of test jigs, test force evaluation of drug products including the packaging material can be conducted easily.

For Research Use Only. Not for use in diagnostic procedures.
The content of this publication shall not be reproduced, altered or sold for any commercial purpose without the written approval of Shimadzu. The information contained herein is provided to you "as is" without warranty of any kind including without limitation warranties as to its accuracy or completeness. Shimadzu does not assume any responsibility or liability for any damage, whether direct or indirect, relating to be the use of this publication. This publication is based upon the information available to Shimadzu on or before the date of publication, and subject to change without notice.

SHIMADZU
Excellence in Science

4. Composite Industry

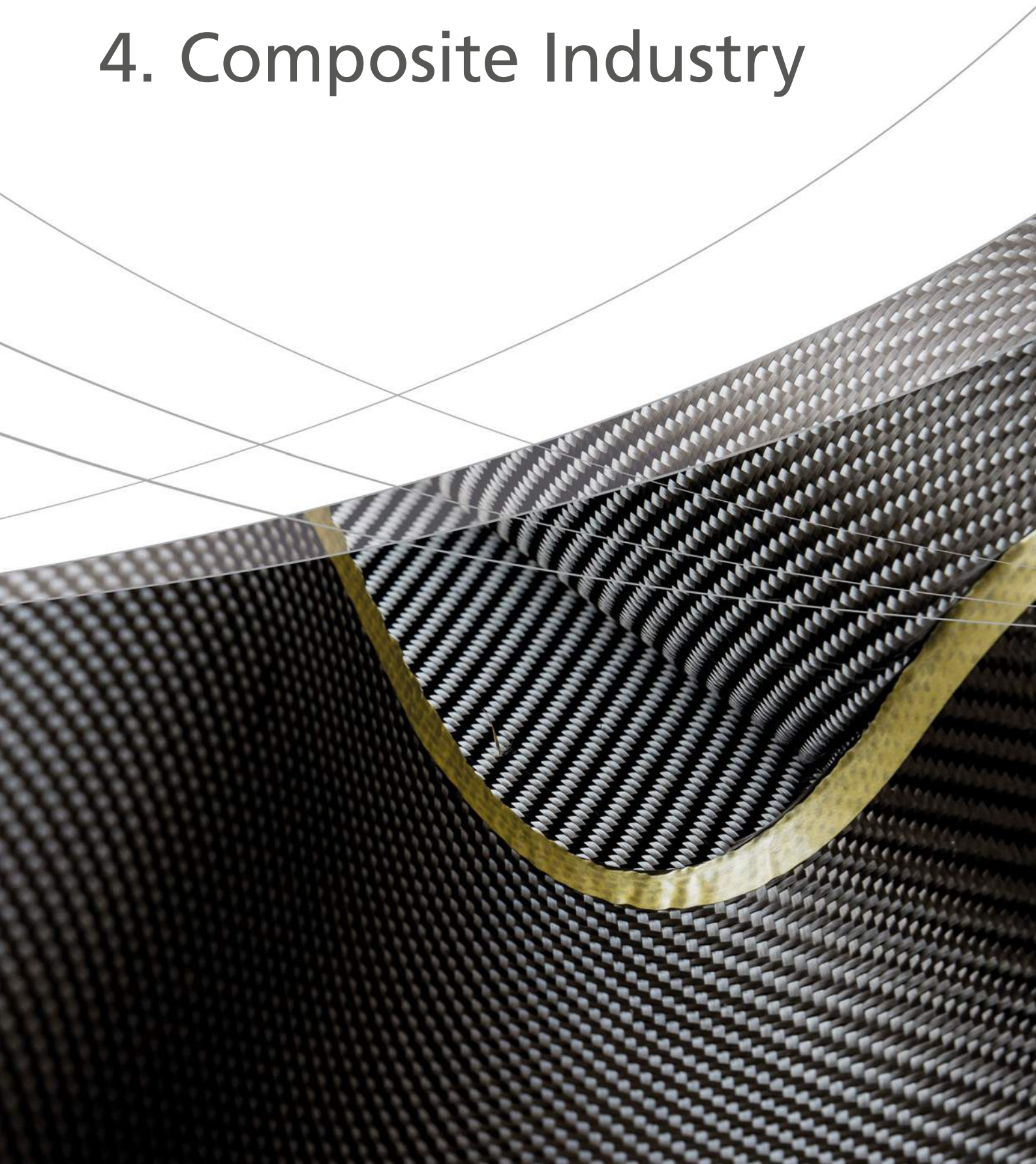

4. Composite Industry

GROWING USE OF COMPOSITE MATERIALS

Composites combine different materials to achieve greater specific strength than is available from a single material. The evaluation of fundamental mechanical properties is essential for new materials. Ongoing standardization of sample shapes and test methods is intended to improve the stability of material quality while enhancing reliability.

Fiber-reinforced plastics (FRP) are typical composite materials. Among these are glass-fiber-reinforced plastics (GFRP) which are widely used for aircraft wing fillets, fairings, control surfaces, radomes, wing tips and cabin floors. Carbon-fiber-reinforced plastics (CFRP) combine plastics with carbon fibers having high specific modulus of elasticity and specific strength; they are applied in important components such as aircraft wings and center wing boxes as well as horizontal and vertical stabilizers.

Aircraft are designed to meet the requirements indicated in the design standards. Inspection and testing of aircraft structure and strength are performed at the manufacturing stage, and flight testing is conducted to confirm the performance and flying quality of the completed aircraft. Testing includes static and fatigue testing at the materials development stage, endurance testing of all parts and components, and impact testing to evaluate the fast fracture characteristics of the materials.

In recent years, it has become more important to observe fracture behavior. High-speed video cameras are now commonly used to perform more sophisticated evaluations through synchronized observations of the tested material behavior and the S-S curve.

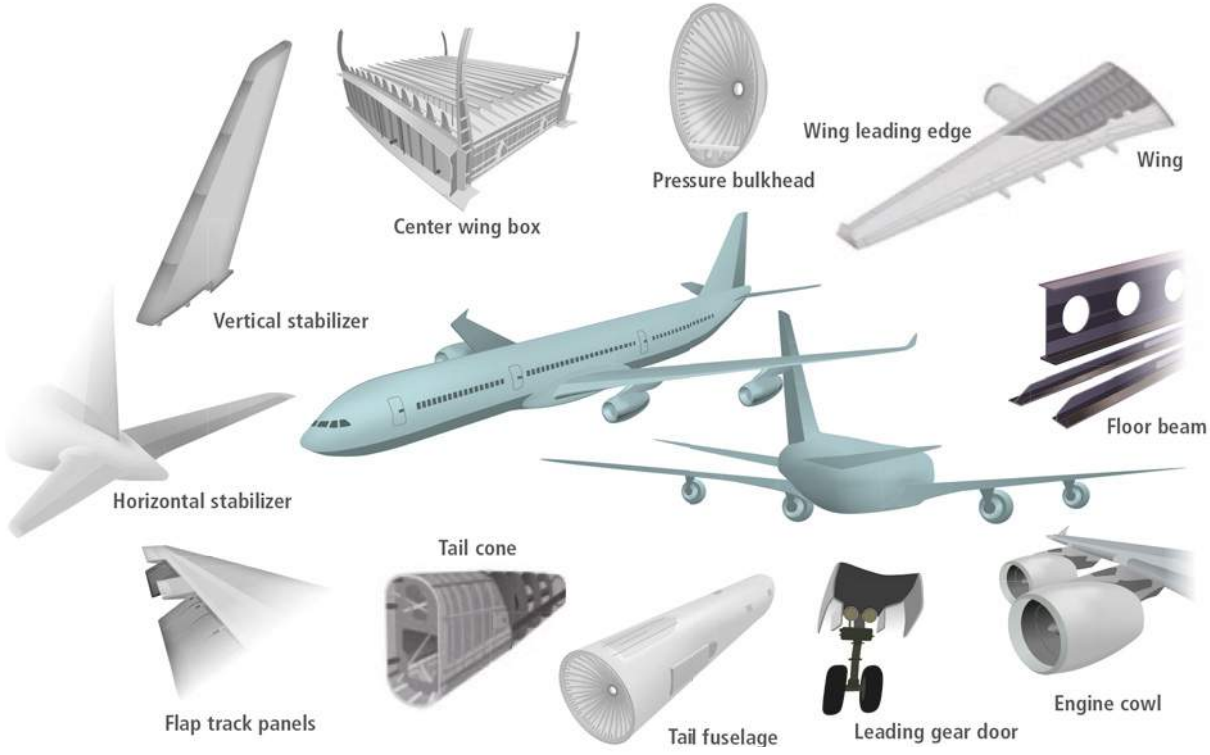

Some part in which CFRP is used

4. Composite Industry

No_ei254	Compression after impact testing of composite
No_ei255	Compression testing of composite materials
No.36	Evaluating the fatigue strength of GFRP materials
No.30	Evaluating the strength of carbon fiber reinforced plastics (CFRP)
No.39	Evaluation of open-hole CFRP
No.i247	DIC analysis material testing by strain distribution visualization
No.8	Flexural testing of CFRP boards
No.16	Tensile testing of carbon fiber
No.31	Materials testing using digital image correlation
No.37	Observing the failure of open-hole CFRP samples in tensile tests
No.38	Observing the fracture of unidirectional CFRP in static tensile testing
No.ei256A	Open-hole compression testing of composite material
No.ei250	Shear test of composite material (V-notched beam)
No.ei251	Shear test of composite material (V-notched rail shear)
SCA_300_037	Compression-rupture test of carbon fibers with different tensile characteristics Shimadzu micro compression testing machine MCT
SCA_300_055	Viscosity evaluation of thermoplastic resins (GFRP)
SCA_300_056	Viscosity evaluation of thermoplastic resins (GFRP)
SCA_300_059	Observation of fracture in CFRP tensile test E001HPV

SHIMADZU
Excellence in Science

Application News

No.i254

Material Testing System

Compression After Impact Testing of Composite Material

Introduction

Carbon fiber reinforced plastic (CFRP) has a higher specific strength and rigidity than metals, and is used in aeronautics and astronautics to improve fuel consumption by reducing weight. However, CFRP only exhibits these superior properties in the direction of its fibers, and is not as strong perpendicular to its fibers or between its laminate layers. When force is applied to a CFRP laminate board, there is a possibility that delamination and matrix cracking will occur parallel to its fibers. Furthermore, CFRP is not particularly ductile, and is known to be susceptible to impacts. When a CFRP laminate board receives an impact load, it can result in internal matrix cracking and delamination that is not apparent on the material surface. There are many situations in which CFRP materials may sustain an impact load, such as if a tool being dropped onto a CFRP aircraft wing, or small stones hitting the a CFRP wing during landing. Consequently, tests are required for these scenarios. One of these tests is compression after impact (CAI) testing. CAI testing involves subjecting a specimen to a prescribed impact load, checking the state of damage to the specimen by a nondestructive method, and then performing compression testing of that specimen. This article describes CAI testing performed according to the ASTM D7137 (JIS K 7089) standard test method.

Measurements Taken Before Compression After Impact Testing

(1) Impact Test

The impact test involved dropping a 5 kg steel ball striker formed with a 16 mm diameter hemispherical point in the middle of the specimen. The specimen is fixed in place with four toggle clamps. The standard test method states that avoiding a second impact is preferred, so impact testing was performed with a mechanism that prevented second impacts. The impact energy recommended in the standard test method is 6.67 J per 1 mm of specimen thickness. For the purpose of comparison, the test was performed at four impact energies of 6.7, 5.0, 3.3, and 1.7 J per 1 mm thickness. Information on the specimen used is shown in Table 1. The test setup is shown in Fig. 1, and test conditions are shown in Table 2.

Table 1 Specimen Information

Dimensions [mm]	: 100 × 150 × 4.56
Lamination Method	: [45/0/−45/90] $_{ns}$
Material	: T800, 2252S-21

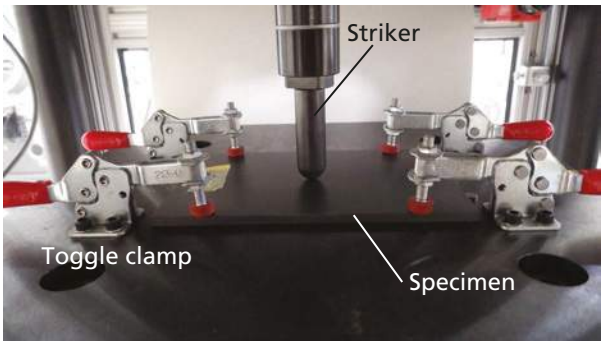

Fig. 1 Impact Test Setup

Table 2 Impact Test Conditions

Impact Energy	: 30.5, 22.9, 15.2, 7.6 [J]
No. of Tests	: n = 4

(2) Non-Destructive Inspection

After the impact test, the delamination area and maximum delamination length that resulted inside the laminate board were measured by nondestructive analysis. An ultrasonic flaw detection device is normally used for the non-destructive inspection step of CAI testing. The standard test method states that if ultrasonic flaw detection shows damage is present across more than half the width of the specimen, edge effects cannot be ignored and lowering the impact energy should be considered. Fig. 2 shows the setup for ultrasonic flaw detection.

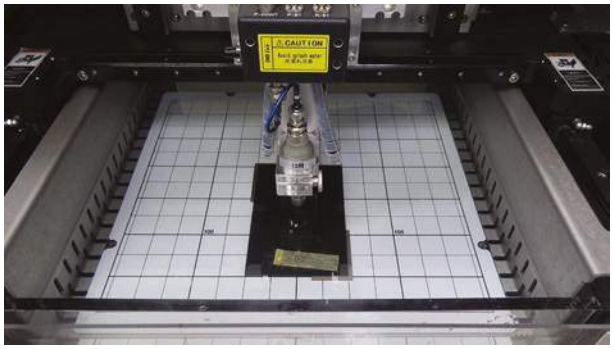

Fig. 2 Ultrasonic Flaw Detection

Fig. 3 shows the specimen after an impact test with an impact energy of 30.5 J. Fig. 3 shows an indentation in the middle of the specimen, but does not show the area of damage caused by delamination. Fig. 4 shows the results of ultrasonic flaw detection at each impact energy. The white areas in Fig. 4 are regions of delamination. Brighter areas show greater delamination. Comparison with Fig. 3 shows that delamination also occurs in areas other than the indentation in the center of the specimen, and the extent of internal damage cannot be determined based on external damage. The results also show that the damage area increases as the impact energy increases.

Fig. 3 Specimen After Impact Test (30.5 J Impact Energy)

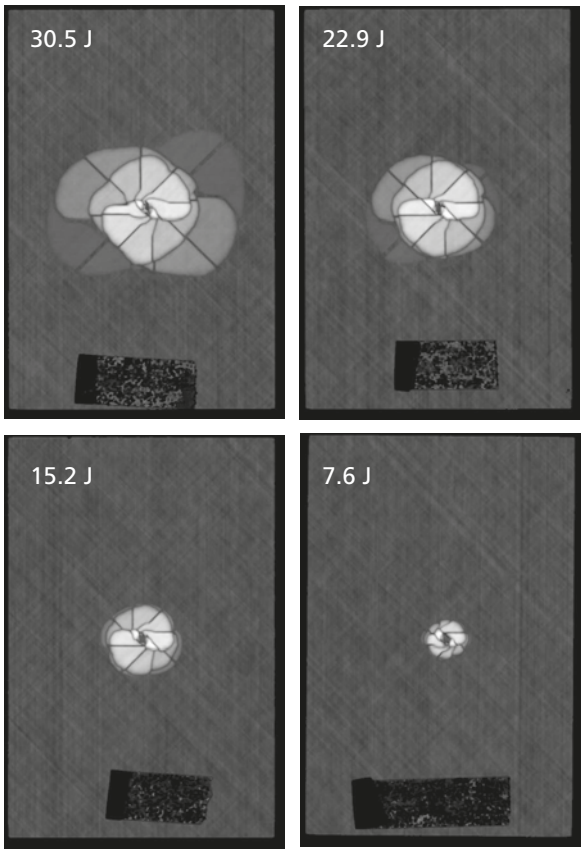

Fig. 4 Results of Ultrasonic Flaw Detection at Each Impact Energy

The damage area and maximum damage length are calculated from the images obtained by ultrasonic flaw detection. As an example, images used to calculate the damage area and maximum damage length after an impact energy of 30.5 J are shown in Fig. 5. Fig. 6 shows the relationship between damage area and impact energy, and Fig. 7 shows the relationship between maximum damage length and impact energy.

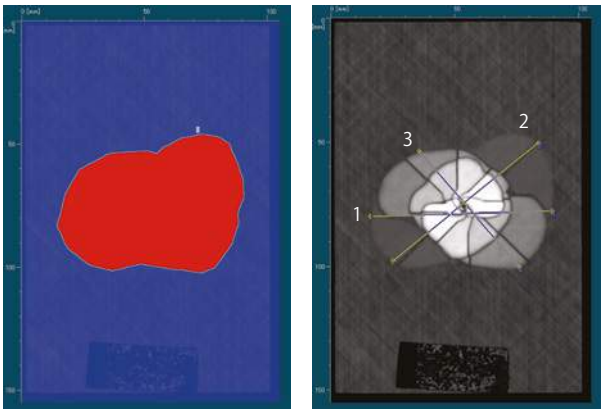

Region No.	Percentage Area (%)	Absolute Area (mm^2)
1	99.9988	3326.2400

No.	Length (mm)
1	73.03
2	75.50
3	61.37

Fig. 5 Images of Damaged Area and Maximum Damage Length

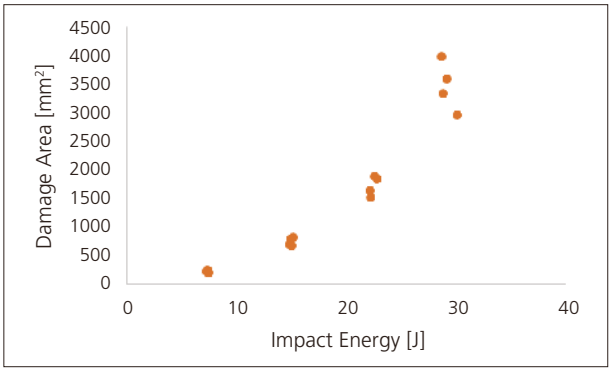

Fig. 6 Relationship between Damage Area and Impact Energy

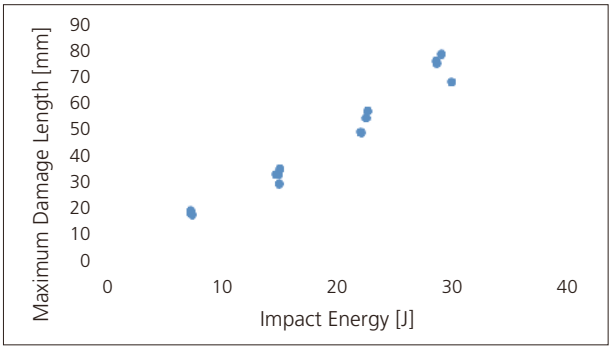

Fig. 7 Relationship between Maximum Damage Length and Impact Energy

Measurement System for Compression After Impact Testing

Two strain gauges must be attached to the front and back of the specimen. A specimen with strain gauges attached is shown in Fig. 8. The specimen shown in Fig. 8 is compressed at up to 10 % its expected compressive strength following impact in a longitudinal direction, and the CAI testing is performed after confirming the difference between front and rear strain gauges is within 10 %. Test conditions are shown in Table 3. The test setup is shown in Fig. 9, and test equipment used is shown in Table 4.

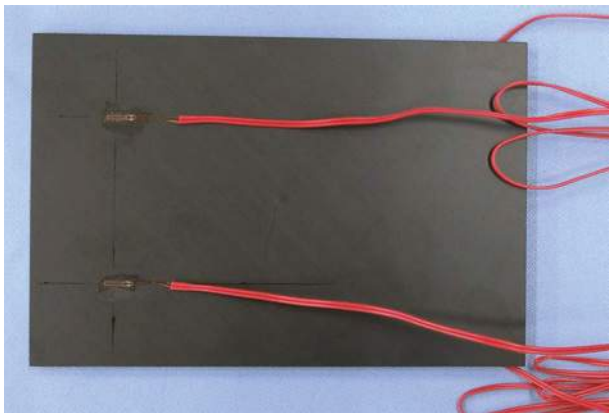

Fig. 8 Specimen

Table 3 Test Conditions

Test Speed	: 1.25 mm/min
No. of Tests	: n = 4

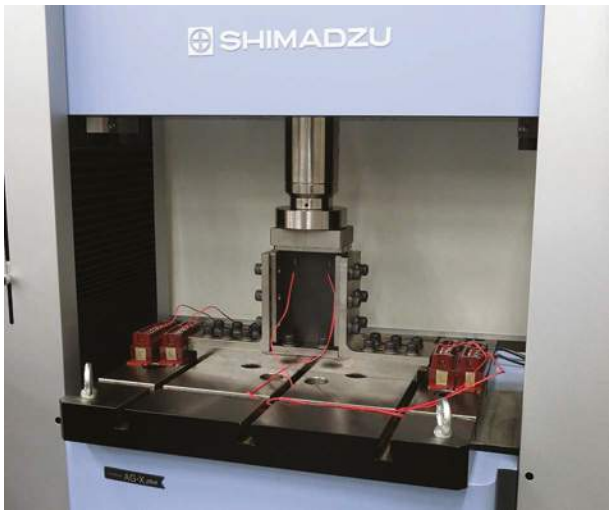

Fig. 9 Test Setup

Table 4 Experimental Equipment

Testing Machine	: AG-Xplus
Load Cell	: 250 kN
Test Jig	: Compression after impact test jig

Test Results

Examples of stress-strain curves at each impact energy are shown in Fig. 10. The compression-after-impact strength and mean compressive elastic modulus after impact are shown for each impact energy in Table 5. The standard test method states the compressive elastic modulus after impact should be calculated in the range of 0.1 % to 0.3 % strain. However, the breaking strain of one or more specimens was ≤ 0.3 % after the 30.5 J impact energy, and so for these specimens the elastic modulus was calculated from a linear region. Fig. 10 and Table 5 show the smaller the impact energy the larger the compression-after-impact strength. They also show the compressive elastic modulus after impact is almost constant regardless of impact energy.

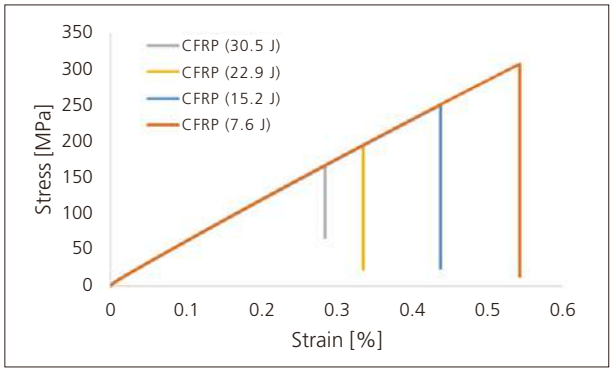

Fig. 10 Stress-Strain Curve

Table 5 Test Results (Mean)

Impact Energy [J]	Compression-After-Impact Strength [MPa]	Compressive Elastic Modulus After Impact [GPa]
30.5	162.9	57.2
22.9	203.3	56.4
15.2	246.4	56.0
7.6	308.6	56.3

The relationship between damage area and compression-after-impact strength is shown in Fig. 11, and the relationship between maximum damage length and compressive elastic modulus after impact is shown in Fig. 12. Fig. 11 and Fig. 12 show the smaller the damage area or maximum damage length, the larger the compression-after-impact strength. As a reference, the compressive strength of a specimen tested without applying any impact energy was 388 MPa.

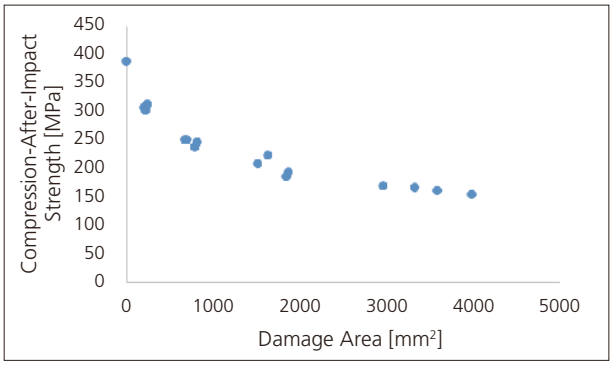

Fig. 11 Relationship between Damage Area and Compression-After-Impact Strength

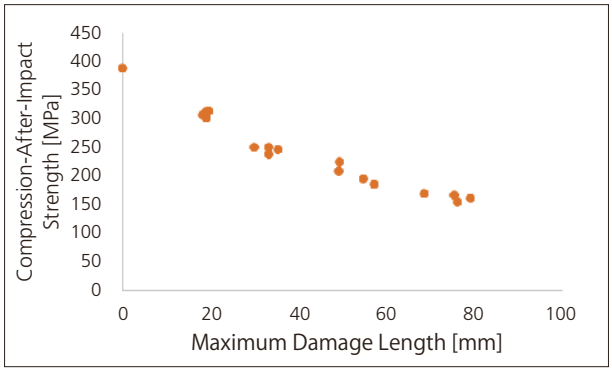

Fig. 12 Relationship between Maximum Damage Length and Compression-After-Impact Strength

Conclusion

CAI testing was performed on specimens at four different impact energies. As shown by the results, the larger the impact energy the smaller the compression-after-impact strength. Also, even a small amount of impact energy (in this experiment, an impact energy of 7.6 J amounted to 5 kg dropped from 0.15 m) reduced the compression-after-impact strength compared to the undamaged compressive strength, showing the importance of testing scenarios for impact loading. Shimadzu's testing system was used successfully to perform CAI testing according to ASTM D7137 (JIS K 7089), and can be used for evaluation of CFRP materials.

First Edition: Aug. 2016

Shimadzu Corporation
www.shimadzu.com/an/

For Research Use Only. Not for use in diagnostic procedure.
This publication may contain references to products that are not available in your country. Please contact us to check the availability of these products in your country.

The content of this publication shall not be reproduced, altered or sold for any commercial purpose without the written approval of Shimadzu. Company names, product/service names and logos used in this publication are trademarks and trade names of Shimadzu Corporation or its affiliates, whether or not they are used with trademark symbol "TM" or "®". Third-party trademarks and trade names may be used in this publication to refer to either the entities or their products/services. Shimadzu disclaims any proprietary interest in trademarks and trade names other than its own.

The information contained herein is provided to you "as is" without warranty of any kind including without limitation warranties as to its accuracy or completeness. Shimadzu does not assume any responsibility or liability for any damage, whether direct or indirect, relating to the use of this publication. This publication is based upon the information available to Shimadzu on or before the date of publication, and subject to change without notice.

© Shimadzu Corporation, 2016

SHIMADZU
Excellence in Science

Application News

No.i255

Material Testing System

Compression Test of Composite Material

Introduction

Even among composite materials, carbon fiber reinforced plastic (CFRP) has a particularly high specific strength, and is used in aeroplanes and some transport aircraft to improve fuel consumption by reducing weight. Compressive strength is an extremely important parameter in the design of composite materials that is always tested. However, due to the difficulty of testing compressive strength there is a variety of test methods. A major compression test method is the combined loading compression (CLC) method found in ASTM D6641. The CLC method can be performed with a simple jig structure, untabbed strip specimens, and can be used to simultaneously evaluate strength and measure elastic modulus. We performed compression testing of CFRP according to ASTM D6641.

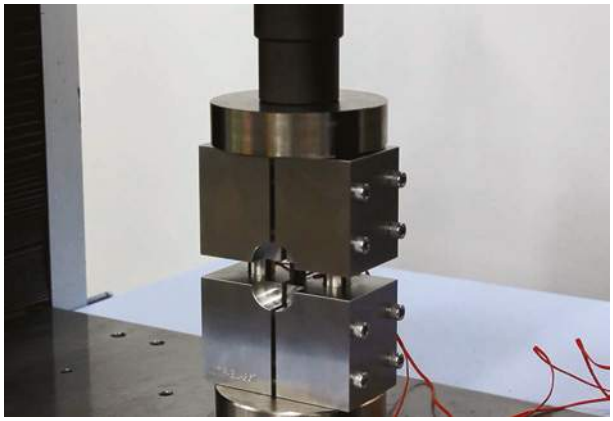

Fig. 1 Test Fixture

Measurement System

A CFRP specimen of T800S/3900 was used. Other information on the specimen is shown in Table 1. The test equipment used is shown in Table 2. Based on the CLC method in ASTM D6641, the specimen was attached to the jig shown in Fig. 1 and compressed using compression plate. Fig. 2 shows a photograph of the specimen. As shown in Fig. 2, a strain gauge was attached on the front and rear in the middle of the specimen. Outputs from the front and rear strain gauges confirmed that the specimen was aligned straight in the jig during specimen attachment. The specimen was attached using a torque wrench to fasten it in place uniformly. The test was performed with the test speed set to 1.3 mm/min.

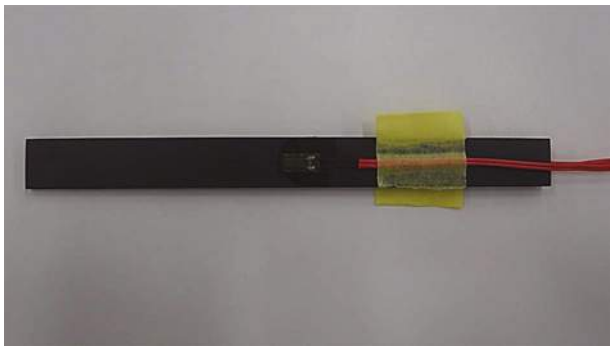

Fig. 2 Specimen

Table 1 Specimen Information

Length	: 140 mm
Width	: 13 mm
Thickness	: 3 mm
Lamination Method	: $[90/0]_{4S}$

Table 2 Experimental Equipment

Testing Machine	: AG-Xplus
Load Cell	: 50 kN
Test Jig	: CLC test fixture

Test Results

Measurements were performed twice, and stress-strain curves are shown in Fig. 3. The strain used is the mean strain taken from the front and rear sides of the specimen. The relationship between the first strain measurement and time is shown in Fig. 4 to show the outputs obtained from the strain gauges. Fig. 4 shows the outputs from both strain gauges were almost the same up to around 40 seconds, which is evidence that the test was successful. A small amount of deviation between the strain gauges arises after around 0.5 % strain, which is caused by a small amount of specimen flexure. Table 3 shows the test results. The mean compressive strength was 640.7 MPa, and the mean elastic modulus was 72.9 GPa. Elastic modulus was calculated using the mean of the strain gauge outputs.

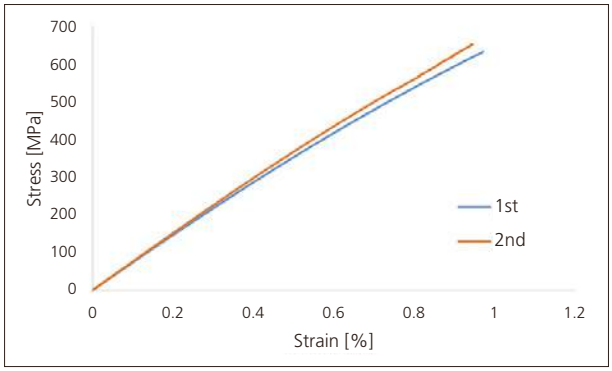

Fig. 3 Stress-Strain Curves (n = 2)

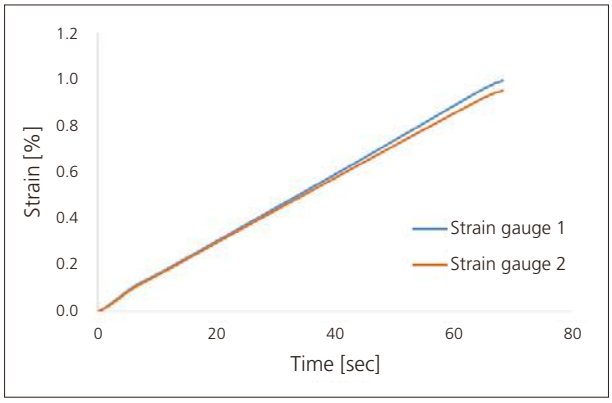

Fig. 4 Displacement-Time Curves (1st)

Table 3 Test Results

	Compressive Strength [MPa]	Elastic Modulus [GPa]
1st	629.9	71.4
2nd	651.4	74.3
Mean	640.7	72.9

Conclusion

Using this test system, compression testing of a CFRP was successfully performed according to ASTM D6641. Because this standard test method allows the testing of untabbed strip specimens, compressive strength and elastic modulus can be determined relatively easily for CFRPs.

First Edition: Aug. 2016

Shimadzu Corporation
www.shimadzu.com/an/

For Research Use Only. Not for use in diagnostic procedure.
This publication may contain references to products that are not available in your country. Please contact us to check the availability of these products in your country.

The content of this publication shall not be reproduced, altered or sold for any commercial purpose without the written approval of Shimadzu. Company names, product/service names and logos used in this publication are trademarks and trade names of Shimadzu Corporation or its affiliates, whether or not they are used with trademark symbol "TM" or "®". Third-party trademarks and trade names may be used in this publication to refer to either the entities or their products/services. Shimadzu disclaims any proprietary interest in trademarks and trade names other than its own.

The information contained herein is provided to you "as is" without warranty of any kind including without limitation warranties as to its accuracy or completeness. Shimadzu does not assume any responsibility or liability for any damage, whether direct or indirect, relating to the use of this publication. This publication is based upon the information available to Shimadzu on or before the date of publication, and subject to change without notice.

© Shimadzu Corporation, 2016

SHIMADZU
Excellence in Science

Application Data Sheet

No. 36

Servo Dynamic Systems

Material Testing & Inspection

Evaluating the Fatigue Strength of GFRP Materials

■ Introduction

As an ultra-high-strength composite material with superior heat resistance and electrical insulation properties, the use of glass fiber reinforced plastics (GFRP) has been increasing rapidly in automobiles, office equipment, consumer electronics, and other fields. Due to the use of GFRP materials in the automotive industry in particular, the impact resistance and fatigue strength of the material is increasingly being scrutinized and there is increasing demand for the development of GFRP materials that offer higher functionality or performance.

Shimadzu Servopulser series servo-hydraulic fatigue and endurance testing machines are able to accurately measure the fatigue strength of resins, composites, metals, and components, making them ideal for evaluating the fatigue strength of GFRP materials.

This issue of Shimadzu Application News describes an example of testing the fatigue strength of a GFRP composite material containing 20 % glass fiber in a polyamide resin. It also shows the change in the interior status of test samples as the fatigue test progresses, observed using a Shimadzu X-ray fluoroscopy system.

■ Testing Instruments and Samples

A Shimadzu EHF-LV20kN Servopulser series servo-hydraulic fatigue testing machine (a typical example is shown in Fig. 1) was used in conjunction with a Shimadzu SMX-225CT inspeXio X-ray fluoroscopy system used to observe the sample with X-ray fluoroscopy.

Sample details are as follows:

(1) Polymer: Polyamide
(2) Reinforcing material: 20 % glass fiber
(3) Sample shape:Hard plastic flat plate with 20 mm neck width
(4) Sample dimensions: 80(L) x 30(W) x 3(T) mm

■ Test Conditions

Before fatigue testing, static testing was performed using the following conditions to determine fatigue loading conditions. Static testing results are shown below.

(1) Tensile speed: 1 mm/min
(2) Chuck clamping distance: 40 mm
(3) Atmosphere: Room temperature of 25 °C
(4) Tensile strength (measurement results): 96 MPa

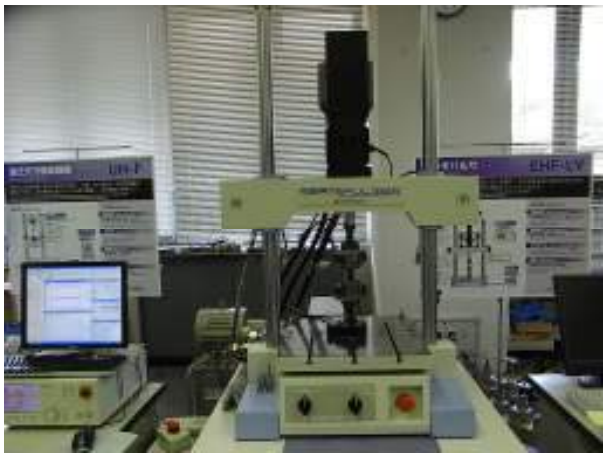

Fig.1 Shimadzu EHF-LV20kNX Servopulser Series Testing Machine

The following fatigue testing conditions (loading and data measurement/acquisition conditions) were determined based on the above static testing.

(1) Testing frequency: 10 Hz
(2) Maximum cyclic stress: Six levels, indicated below.
Level 1: 77 MPa (80 % of tensile strength)
Level 2: 67 MPa (70 % of tensile strength)
Level 3: 58 MPa (60 % of tensile strength)
Level 4: 48 MPa (50 % of tensile strength)
Level 5: 43 MPa (45 % of tensile strength)
Level 6: 38 MPa (40 % of tensile strength)
(3) Stress ratio:0 (given a minimum stress of 0 MPa)
(4) Atmosphere: Room temperature of 25 °C
(5) Testing machine: LV-20N Servopulser
(6) Test force measurement: 20,000 N load cell
(7) Chuck clamping distance: 40 mm
(8) Data acquisition: 2 kHz

(The testing machine is capable of measuring at frequencies up to 40 kHz.)

Six cyclic stress levels were decided based on the tensile strength (96 MPa) determined by static tensile testing, with a cyclic load stress ratio (minimum stress divided by maximum stress) of zero. (For example, level 1 applies a maximum stress of 77 MPa, a minimum stress of 0 MPa, and stress amplitude of 38.5 MPa.)

Though the testing machine is capable of cyclic loading at cycle rates up to 100 Hz, in this case a 10 Hz sine wave was used in consideration of sample heat generation.

Fig. 2 shows a sample mounted in the testing machine grips.

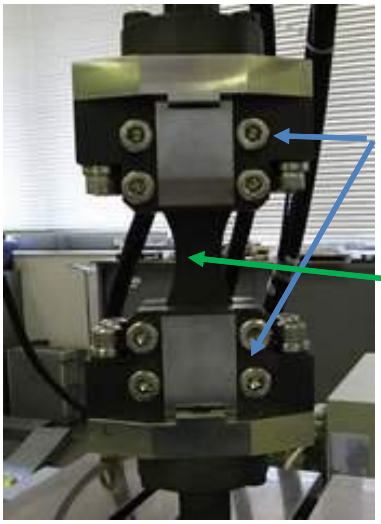

Fig. 2 Sample Mounted in Testing Machine

■ Test Results

Fig. 3 shows an example of peak stress (black) and displacement (blue) values (sine wave peak and valley values) measured from start of loading to sample fracture, given a stress level of 5.

The cyclic stress load applied to the sample causes it to gradually deform until a crack forms, after which the deformation increases rapidly and the sample fractures.

Fig. 4 is a stress versus cycle count plot for six stress levels (one sample for each level) that shows the relationship between the maximum stress load and the cycle count at sample fracture.

As shown in the results above, in addition to fatigue testing, the fatigue testing machine can also be used for a wide range of other strength testing, including static testing.

In addition, an industrial X-ray system was used to observe how the fiber orientation inside the GFRP material changes as the fatigue test progresses.

Fig. 5 shows the curious phenomenon of how the glass fibers inside the sample, which have no particular orientation before starting the fatigue test (left), begin to orient themselves a little in the longitudinal direction after a million load cycles (middle), and are all oriented in the longitudinal direction just before fracture (right).

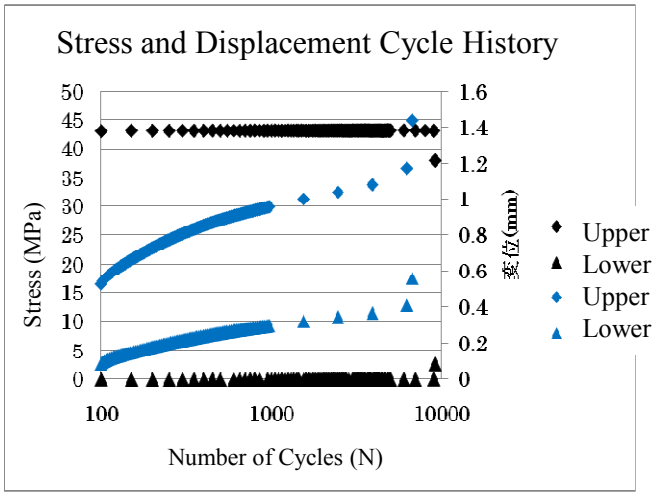

Fig. 3 Fatigue Test Results

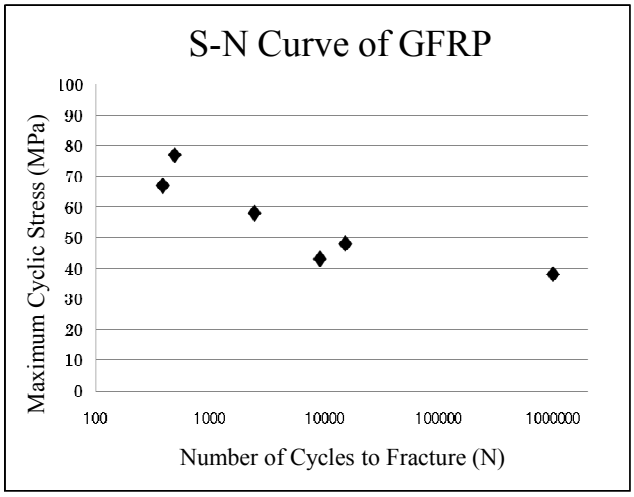

Fig. 4 Fatigue Test Results

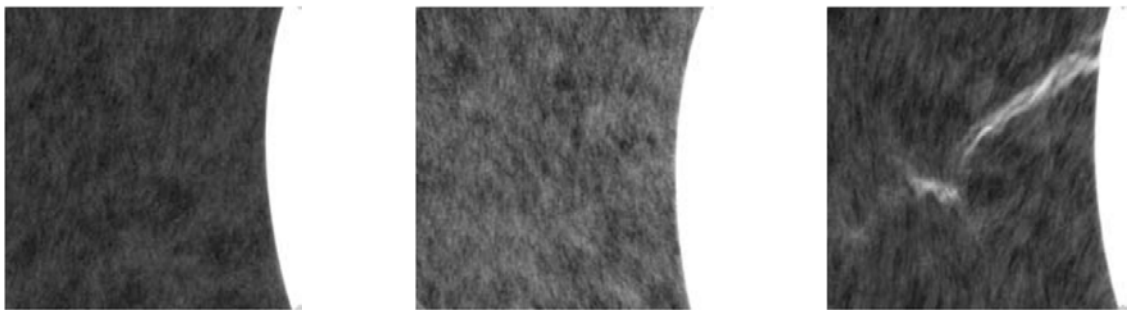

Start of Fatigue Test | After 1 Million Load Cycles | Just Before Fracture

Fig.5 Fiber Orientation Inside GFRP

Note: The analytical and measuring instruments described may not be sold in your country or region.

First Edition: July, 2015

SHIMADZU
Shimadzu Corporation
www.shimadzu.com/an/

For Research Use Only. Not for use in diagnostic procedures.
The content of this publication shall not be reproduced, altered or sold for any commercial purpose without the written approval of Shimadzu.
The information contained herein is provided to you "as is" without warranty of any kind including without limitation warranties as to its accuracy or completeness. Shimadzu does not assume any responsibility or liability for any damage, whether direct or indirect, relating to the use of this publication. This publication is based upon the information available to Shimadzu on or before the date of publication, and subject to change without notice.
© Shimadzu Corporation, 2015

SHIMADZU
Excellence in Science

Application Data Sheet

No. 30

Autograph Precision Universal Tester

Material Testing & Inspection

Evaluating the Strength of Carbon Fiber Reinforced Plastics (CFRP)

■Introduction

Various types of plastic materials have been developed that are light weight and also perform better than previous materials in terms of environmental resistance and in terms of strength. Consequently, there is a growing demand for such materials in aircraft, automotive, and many other fields.These plastic materials, such as carbon fiber reinforced plastic (CFRP), glass fiber reinforced plastic (GFRP), and aramid fiber reinforced plastic, are characterized by using fibers with advanced functionality (low weight, high strength, deformation resistance, corrosion resistance, and also heat resistance). Carbon fiber reinforced plastic (CFRP) is particularly representative of such materials and is increasingly used in sports equipment and other everyday products. Therefore, evaluating its strength, its fundamental feature, is very important.

This article presents results from testing carbon fiber reinforced plastic (CFRP) using a Shimadzu Autograph precision universal testing machine. (Test specimens and loading conditions conformed to JIS K7073-1988 Testing Method for Tensile Properties of Carbon Fiber Reinforced Plastics.)

■Measurement and Jigs

Specimens were Type-IV specified by JIS K7073-1988 (rectangular strips with no tabs). Tensile tests were conducted with an extensometer attached to measure longitudinal strain and a width sensor attached to measure lateral strain, as shown in Fig.1.

Fig. 1 Test Configuration

■Test Results

Test results indicate a tensile strength of 8.31×10^2 MPa, an elastic modulus of 5.76×10^5 MPa (determined from the slope between points at 100 MPa and 300 MPa), and a maximum tensile strain of 0.766 percent. Since these results were obtained using test specimens with fibers oriented perpendicular (lateral) to the direction of tensile load, the same test was performed with fibers oriented parallel (longitudinal) to the direction of tension. This resulted in an elastic modulus of about 13.00×10^5 MPa, which indicates a significant difference depending on the fiber orientation.

Fig.3 shows the relationship between stress and displacement in the direction perpendicular to tension, for the same test as before. A calculation of Poisson's ratio between 100 MPa and 300 MPa, as before, resulted in a value of 6.0×10^{-2}.

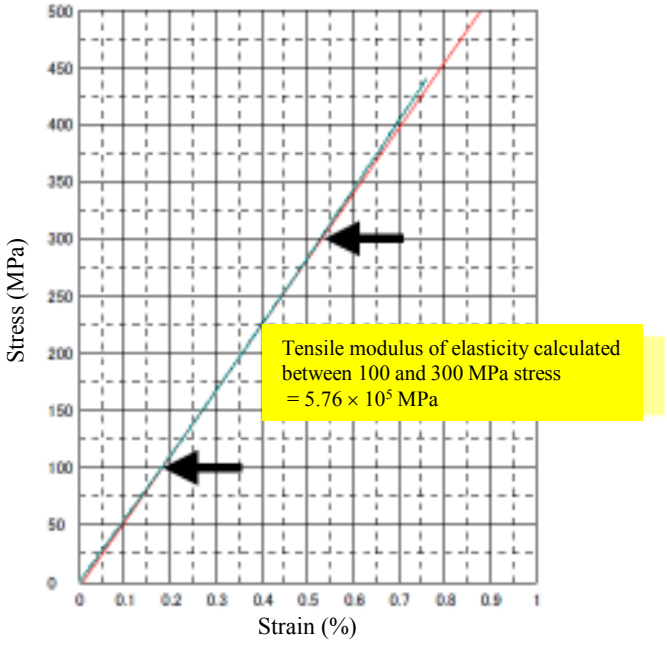

Fig.2 shows the results of testing to failure at a rate of 1 mm/min (stress vs. longitudinal strain curve).

Whereas the Poisson's ratio is about 0.3 for soft iron and about 0.46 to 0.49 for elastic rubber, the ratio for carbon fiber reinforced plastic (CFRP) is about one order of magnitude smaller, which means the deformation level of CFRP is extremely low.

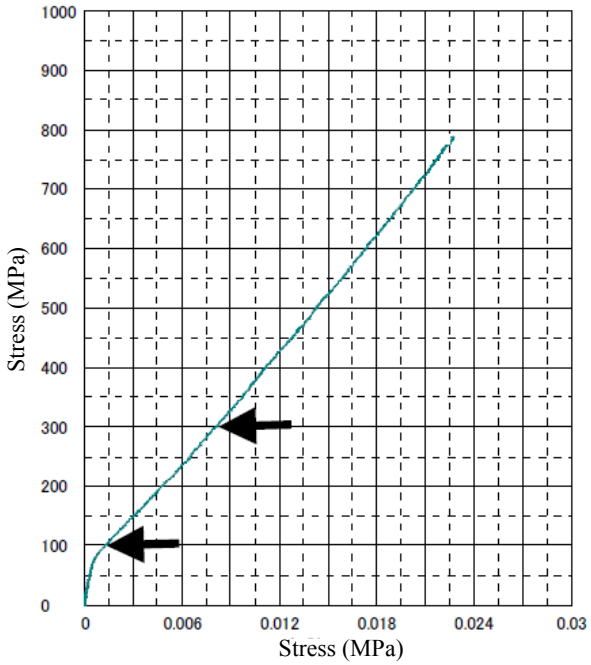

Fig. 3 Graph of Stress vs. Lateral Displacement

Poisson's ratio in left figure: 6.0×10^{-2}
(for range between 2 points, at 100 MPa and 300 MPa)

Method Used to Determine Poisson's Ratio
$\upsilon t = |\Delta\varepsilon 2/\Delta\varepsilon 1|$
υt: Poisson's ratio
$\Delta\varepsilon 1$: Strain increase in tensile direction
$\Delta\varepsilon 2$: Strain increase perpendicular to tension

■Test Conditions and Equipment Used

Tester:	AG-Xplus
Load Cell:	50 kN
Test Jig:	50 kN non-shift wedge type grips
Extensometer:	SG50-10 for measuring strain in tensile direction
	SGW-5 for measuring strain perpendicular to tensile direction
Software:	TRAPEZIUM X (Single)

AG-Xplus Floor-Type Precision Universal Tester

TRAPEZIUM X

■ A high-precision load cell is adopted. (The high-precision type is class 0.5; the standard-precision type is class 1.)
Accuracy is guaranteed over a wide range, from 1/1000 to 1/1 of the load cell capacity. This supports highly reliable test evaluations.

■ Crosshead speed range
Tests can be performed over a wide range from 0.0005 mm/min to 1,000 mm/min.

■ High-speed sampling
Ultrafast sampling, as fast as 0.2 msec, allows assessment of sudden changes in test force, such as when brittle materials fracture.

■ TRAPEZIUMX X operational software
Designed for intuitive operation, it offers a variety of convenient and user-friendly features.

■ Smart controller
Real-time test force and position data are readily confirmed, and the manual dial enables fine adjustments to jig positioning.

■ Optional Test Devices
A variety of tests can be performed by switching between an abundance of jigs in the lineup.

First Edition: July 2015

SHIMADZU
Shimadzu Corporation
www.shimadzu.com/an/

For Research Use Only. Not for use in diagnostic procedures.
The content of this publication shall not be reproduced, altered or sold for any commercial purpose without the written approval of Shimadzu.
The information contained herein is provided to you "as is" without warranty of any kind including without limitation warranties as to its accuracy or completeness. Shimadzu does not assume any responsibility or liability for any damage, whether direct or indirect, relating to the use of this publication. This publication is based upon the information available to Shimadzu on or before the date of publication, and subject to change without notice.
© Shimadzu Corporation, 2015

SHIMADZU
Excellence in Science

Application Data Sheet

No. 39

Autograph Precision Universal Testing Machine

Material Testing & Inspection

Evaluation of Open-Hole CFRP — Static Tensile Testing, Fracture Observation, and Internal Structure Observation —

■ Introduction

Recently, lightweight alternatives to conventional metal materials are being used as structural members where mechanical reliability is required. The main reason for this trend is that lighter products reduce transport weights, which reduces fuel consumption and carbon dioxide emissions during product transport. Fiber reinforced composite materials such as carbon fiber reinforced plastics (CFRP), which consist of a resin strengthened with carbon fibers, are extremely strong and light. Because of this, they are currently a material widely used in aircraft, and are expected to be used increasingly in various types of products, including automobiles, in order to make them lighter. For the development of fiber reinforced composite materials, not just a simple evaluation of their mechanical strength, but also the observation of failure events is important. In addition, from the perspective of quality management, the necessity for evaluation of internal structure of these materials, such as the oriented state of fibers and the presence of cracks, has increased.

In this article, we describe how we use a precision universal testing machine (Autograph AG-250kNXplus) and high-speed video camera (HyperVision HPV-X) (Fig. 1) to evaluate the static fracture behavior of a CFRP based on a test force attenuation graph and images of material failure. We also describe our subsequent examination of the state of the specimens internally using an X-ray CT system (inspeXio SMX-100CT) to investigate the state of fracture inside the specimen. Information on specimens is shown in Table 1. Specimens have a hole machined into their center that is 6 mm in diameter. Fracture is known to propagate easily through composite materials from the initial damage point, and when a crack or hole is present their strength is reduced markedly. Therefore, evaluation of the strength of open-hole specimens is extremely important from the perspective of the safe application of CFRP materials in aircraft, etc.

Table 1: Test Specimen Information

Laminate Structure	Dimensions L (mm) × W (mm) × T (mm), hole diameter (mm)
$[+45/0/-45/+90]_{2s}$	150 × 36 × 2.9, Φ6

Note: The CFRP laminate board used in the actual test was created by laying up prepreg material with fibers oriented in a single direction. The $[+45/0/-45/+90]_{2s}$ shown as the laminate structure in Table 1 refers to the laying up of 16 layers of material with fibers oriented at +45°, 0°, -45°, and +90° in two layer sets.

■ Static Tensile Testing (Ultra High Speed Sampling)

In this test, the change in load that occurs during specimen fracture was used as the signal for the HPV-X high-speed video camera to capture images. Specifically, the AG-Xplus precision universal testing machine was configured to create a signal when the test force on the specimen reaches half the maximum test force (referred to as Maximum test force in Fig. 3), with this signal being sent to the high-speed video camera. Static tensile testing and fracture observation were performed according to the conditions shown in Table 2. A test force-displacement plot for the open-hole quasi-isotropic CFRP(OH-CFRP) is shown in Fig. 2(a). A test force-time plot during the occurrence of material fracture is also shown in Fig. 2(b).

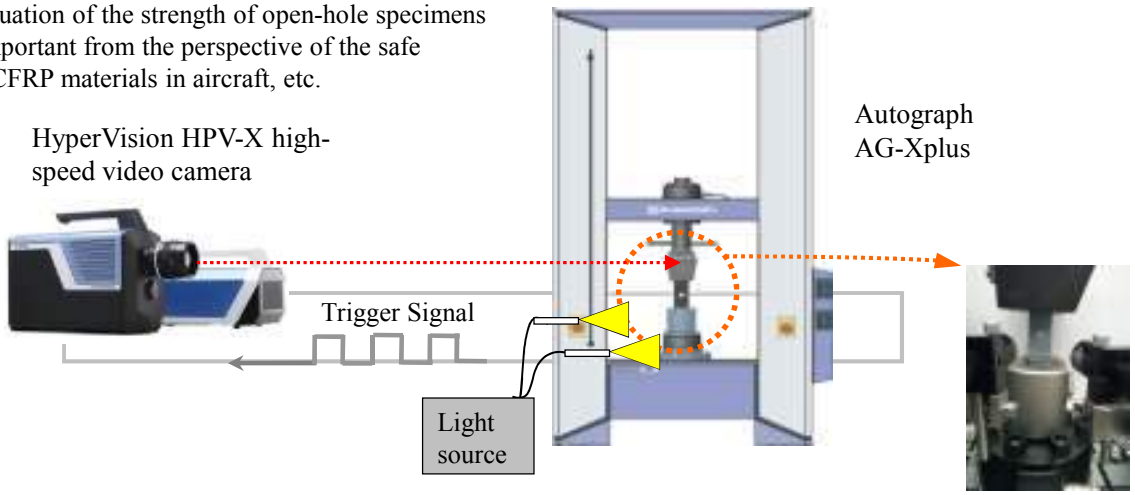

Fig.1: Testing Apparatus

Table 2: Test Conditions

Testing Machine	AG-Xplus
Load Cell Capacity	250 kN
Jig	Upper: 250 kN non-shift wedge type grips (with trapezoidal file teeth on grip faces for composite materials) Lower: 250 kN high-speed trigger-capable grips
Grip Space	100 mm
Loading Speed	1 mm/min
Test Temperature	Room temperature
Software	TRAPEZIUM X (Single)
Fracture Observation	HPV-X high-speed video camera (recording speed 600 kfps)
DIC Analysis	StrainMaster (LaVision GmbH.)

Note: fps stands for frames per second. This refers to the number of frames that can be captured in 1 second.

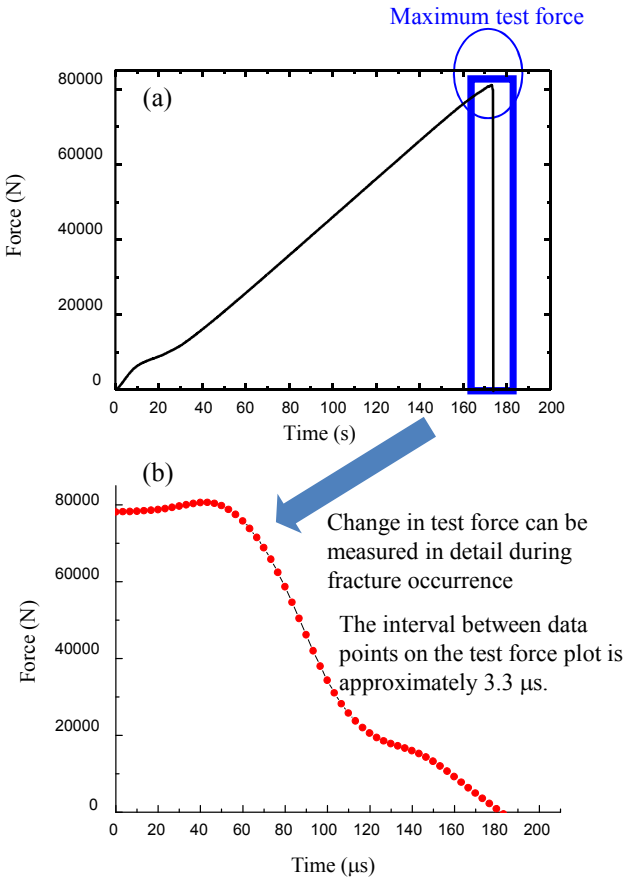

Fig. 2 (a) Test Force-Displacement Curve, and (b) Test Force-Time Curve (in Region of Maximum Test Force)

Fig. 2(a) can be interpreted to show the specimen fractured at the moment it reached the maximum test force, at which point the load on the specimen was suddenly released. This testing system can be used to perform high-speed sampling to measure in detail the change in test force in the region of maximum test force. The time interval between data points on the test force plot in Fig. 2(b) is 3.3 µs.

■ Fracture Observation (High Speed Imaging)

Images (1) through (8) in Fig. 3 capture the behavior of the specimen during fracture around the circular hole. Image (1) shows the moment cracks occur in a surface +45° layer. In this image, the tensile load being applied is deforming the circular hole, where hole diameter in the direction of the load is approximately 1.4 times that perpendicular to the load. In image (2), the cracks that occurred around the circular hole are propagating along the surface +45° layer. In images (3) through (6), a substantial change can be observed in the external appearance of the specimen near the end of the crack propagating to the bottom right from the circular hole. This suggests not only the surface layer, but internal layers are also fracturing. Based on the images of the same area and the state of the internal layers that can be slightly observed from the edges of the circular hole in images (7) and (8), the internal fracture has quickly propagated in the 18 µs period between images (3) and (8).

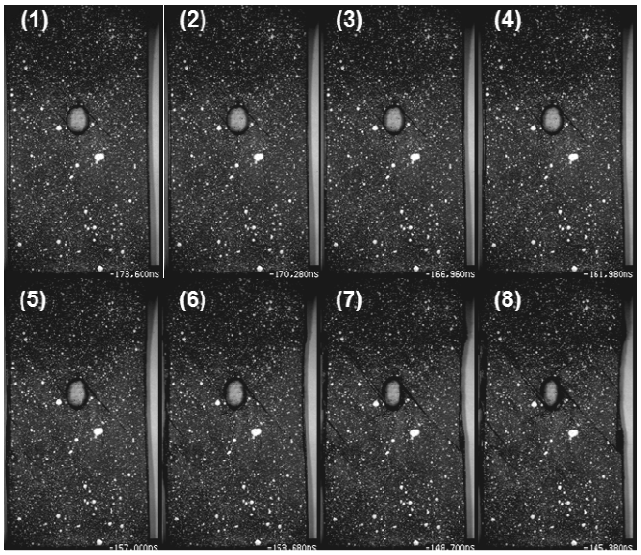

Fig. 3: Observations of OH-CFRP Fracture

First Edition: July 2015

Shimadzu Corporation
www.shimadzu.com/an/

For Research Use Only. Not for use in diagnostic procedures.
The content of this publication shall not be reproduced, altered or sold for any commercial purpose without the written approval of Shimadzu.
The information contained herein is provided to you "as is" without warranty of any kind including without limitation warranties as to its accuracy or completeness. Shimadzu does not assume any responsibility or liability for any damage, whether direct or indirect, relating to the use of this publication. This publication is based upon the information available to Shimadzu on or before the date of publication, and subject to change without notice.
© Shimadzu Corporation, 2015

Images (1) through (8) of Fig. 4 show the results of performing Digital image correlation (DIC) analysis on the fracture observation images of Fig. 3. Black signifies areas of the surface layer of the specimen under little strain, and red signifies areas under substantial strain. Looking at images (1) through (4), we can see that strain around the circular hole is focused diagonally toward the top-left (-45°) and toward the bottom-left (+45°) from the circular hole. Images (5) through (8) show the focusing of strain diagonally toward the bottom-right (-45°) and toward the top-right (+45°) from the circular hole in areas where it was not obvious in images (1) through (4). This shows an event is occurring in the surface layer of the specimen that is similar to the process of fracture often seen during tensile testing of ductile metal materials, which is crack propagation in the direction of maximum shearing stress.

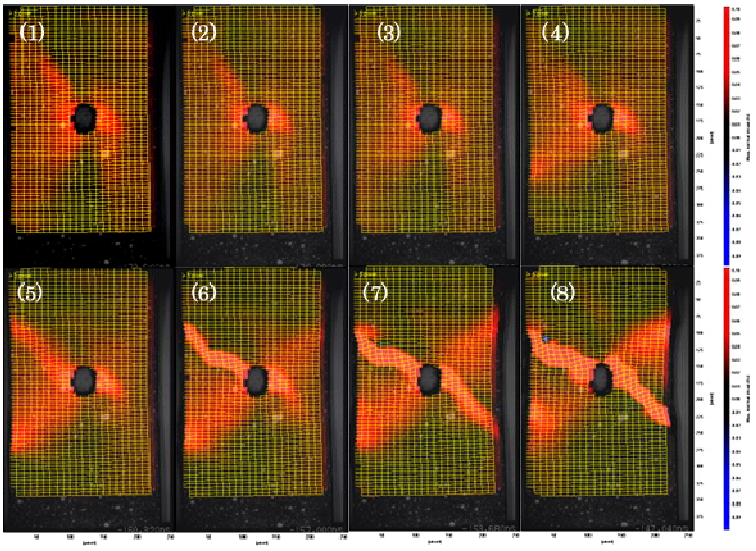

Fig. 4: Observation of OH-CFRP Fracture (DIC Analysis)

■ Internal Structure Observation (CT)

Next, internal observations were performed around the circular hole using a micro focus X-ray CT system to check the state of internal damage to the specimen. The SMX-100CT micro focus X-ray CT system (Fig. 5) is capable of capturing CT images at high magnification. The system rotates a specimen between an X-ray generator and an X-ray detector, uses a computer to calculate fluoroscopic images obtained from all 360° of rotation, then reconstructs a tomographic view of the specimen (Fig. 6). This system was used to perform a CT scan of the fracture area of the OH-CFRP after the static tensile testing and fracture observation performed as described in the previous section, so that the cracks that occurred inside can be observed.

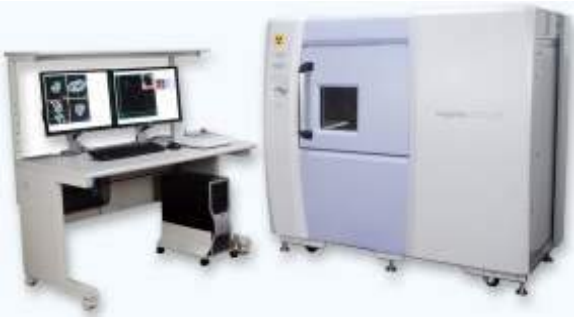

Fig. 5: Shimadzu inspeXio SMX-100CT Micro Focus X-Ray CT System

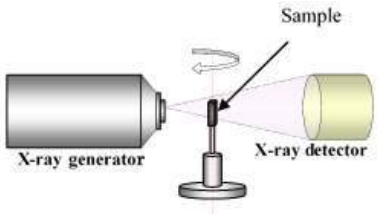

Fig. 6: Illustrated Example of X-Ray CT System Operation

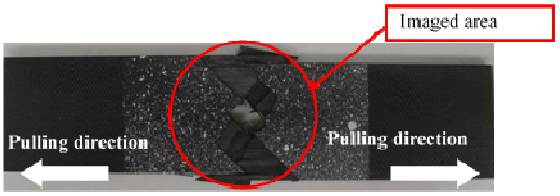

Fig. 7: Specimen After Static Tensile Testing (Specimen Used for CT Scan)

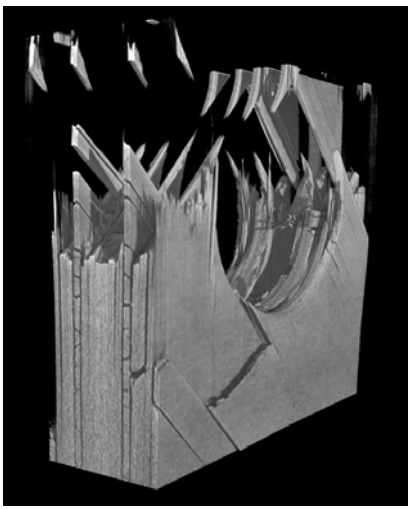

Fig. 8: Fracture Area 3D Image No. 1

First Edition: July 2015

SHIMADZU
Shimadzu Corporation
www.shimadzu.com/an/

For Research Use Only. Not for use in diagnostic procedures.
The content of this publication shall not be reproduced, altered or sold for any commercial purpose without the written approval of Shimadzu.
The information contained herein is provided to you "as is" without warranty of any kind including without limitation warranties as to its accuracy or completeness. Shimadzu does not assume any responsibility or liability for any damage, whether direct or indirect, relating to the use of this publication. This publication is based upon the information available to Shimadzu on or before the date of publication, and subject to change without notice.
© Shimadzu Corporation, 2015

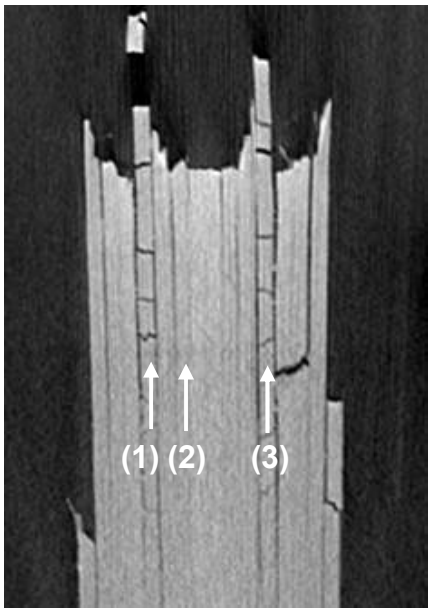

Fig. 9: CT Cross-Sectional Images of the Fracture Area

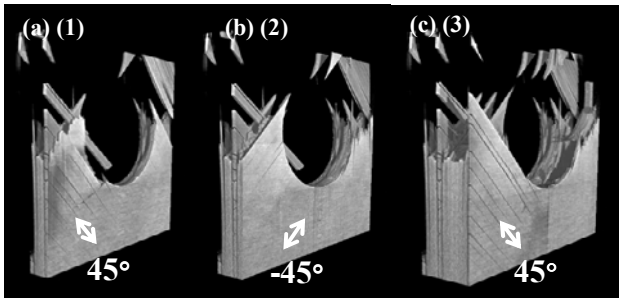

Fig. 10: Fracture Area 3D Image No. 2

Cross-sectional images of the specimen are shown as a 3D image in the 16 layers shown in Fig. 9, we can see that most cracks in the matrix occur in the +45° layer inside the specimen, indicated by the number (1) and (3). (shown in Fig. 10 (a) and Fig. 10 (b), respectively). In this layer, the carbon fibers are all aligned together in a +45° orientation, and the multiple matrix cracks occurring in this layer are probably due to the shearing force caused in this layer by tensile loading, together with deformation of adjacent layers in the direction of the loading. For comparison, a 3D image of the -45° layer inside the specimen (Fig. 9 (2)) is shown in Fig. 10 (b). As is clear from the image, the matrix cracks that occurred in the +45° layer have not occurred in the -45° layer. This difference in fracture state has probably arisen due to different shearing forces and load directions occurring in each layer. Such detailed observation of fracture surfaces associated with multiple matrix cracks was difficult by conventional methods, since to observe fracture surfaces the specimen was processed such as by cutting and embedding in resin, which changed the characteristics of the specimen. However, by using the high-resolution X-ray CT system as described in this article, there is little X-ray absorption difference between air and specimen, and it is possible to observe the state of complex internal damage, even for OH-CFRP in which microscopic damage is normally difficult to observe by X-ray.

■ Acknowledgment

We would like to extend our sincere gratitude to the Japan Aerospace Exploration Agency (JAXA) for their cooperation in the execution of this experiment.

Note: The analytical and measuring instruments described may not be sold in your country or region.

First Edition: July 2015

Shimadzu Corporation
www.shimadzu.com/an/

For Research Use Only. Not for use in diagnostic procedures.
The content of this publication shall not be reproduced, altered or sold for any commercial purpose without the written approval of Shimadzu.
The information contained herein is provided to you "as is" without warranty of any kind including without limitation warranties as to its accuracy or completeness. Shimadzu does not assume any responsibility or liability for any damage, whether direct or indirect, relating to the use of this publication. This publication is based upon the information available to Shimadzu on or before the date of publication, and subject to change without notice.
© Shimadzu Corporation, 2015

SHIMADZU
Excellence in Science

Application News

No.i247

Material Testing System

Material Testing by Strain Distribution Visualization – DIC Analysis –

Introduction

Strain distribution in samples is an increasingly important component of material testing.
As background to this trend, CAE (Computer Aided Engineering) is an analytical technology that is becoming widely used in the fields of science and industry due to the cost savings achieved through the reduced use of costly prototyping which is now being replaced by computerized product design simulation. A typical requirement is to conduct mechanical testing analysis of the region of a product in which strain is likely to occur, and to elucidate the correlation between the simulated analysis results and the strain distribution obtained in actual mechanical testing.
DIC (Digital Image Correlation) analysis is a technique used to compare the random patterns on the surface of a test sample before and after deformation to determine the degree of deformation of the sample. The advantages of this technique include the ability to measure displacement and strain distribution from a digital image without having to bring a sensor into contact with a test sample, and without requiring a complicated optical system. For these reasons, application development for DIC analysis is expanding into a wide range of fields in which measurement using existing technologies*1 has been difficult.

Here we introduce examples of DIC analysis of CFRP (Carbon Fiber Reinforced Plastic) and ABS resin high-speed tensile impact testing.

*1: Up to now, material strain distribution measurement has been conducted using various methods, including the direct attachment of large numbers of strain gauges to the test material. However, this method is not applicable for micro-sized samples to which strain gauges either cannot be attached, or attachment is difficult and complicated. These disadvantages also include the difficulty in measuring certain types of substances, such as films, that are easily affected by contact-type sensors.

Test Conditions

Fig. 1 shows the testing apparatus and software used in the high-speed tensile testing of CFRP. The test conditions are shown in Table 1, and information regarding the test specimens is shown in Table 2. For this experiment, special-shaped grips for composite materials were mounted to the HITS-T10 high-speed tensile testing machine, and the test specimen was affixed to the grips.
A high-speed HPV-2A video camera was mounted in front of the testing gap between the grips to collect video data of the specimen breaking, and the signal to start camera filming was a displacement signal from the high-speed tensile testing machine. The acquired video data was loaded into the StrainMaster (LaVision GmbH) DIC analysis software, and the strain distribution that occurred in the sample was analyzed.

HPV-2A High Speed Video Camera

Test Grips and Test Specimen

HITS-T10 High Speed Tensile Testing Machine

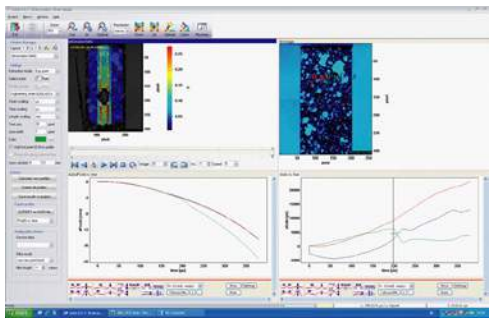
StrainMaster (LaVision GmbH)

Fig. 1 Testing Apparatus

Table 1 Test Conditions

Instrumentation	HITS-T10 high-speed tensile testing machine
	HPV-2A high-speed video camera
Test Force Measurement	10 kN load cell
Test Speed	10 m/s
Grips	Special grips for composite materials
Sampling	250 kHz
Imaging Speed	500 kfps
Light Source	Strobe
DIC Analysis	StrainMaster (LaVision GmbH) With cooperation of MARUBUN CORPORATION

Table 2 Samples

Samples (dimensions)	CFRP-OH*2 Laminate method $[0/90]_{2s}$*3 (Hole diameter ϕ1 mm, W8 × t0.4 reed-shaped)
	ABS resin (ASTM L-shaped test specimen Total length 60 mm, Parallel part 3.2 (W) × 3.2 (T) mm)
Marking	CFRP-OH*2 : White random pattern ABS resin : Black random pattern

*2: OH: Abbreviation for Open Hole. Refers to a hole that is opened in a CFRP plate.

*3: The CFRP laminate used in this experiment is prepared by laminating prepreg fibers oriented in one direction. The $[0/90]_{2s}$ specified for "Laminate method" in the table represents two sets of prepreg layers stacked in the 0 ° direction and 90 ° direction.

In this test, the HITS-T10 high speed tensile testing machine and HPV-2A high speed video camera were synchronized to take video at the instant the sample fractured. The sample was prepared prior to the test by spraying paint onto its surface in a random pattern, and the strain distribution on the surface of the test specimen was visualized by DIC analysis based on the amount of shift of the random pattern.

Test Results

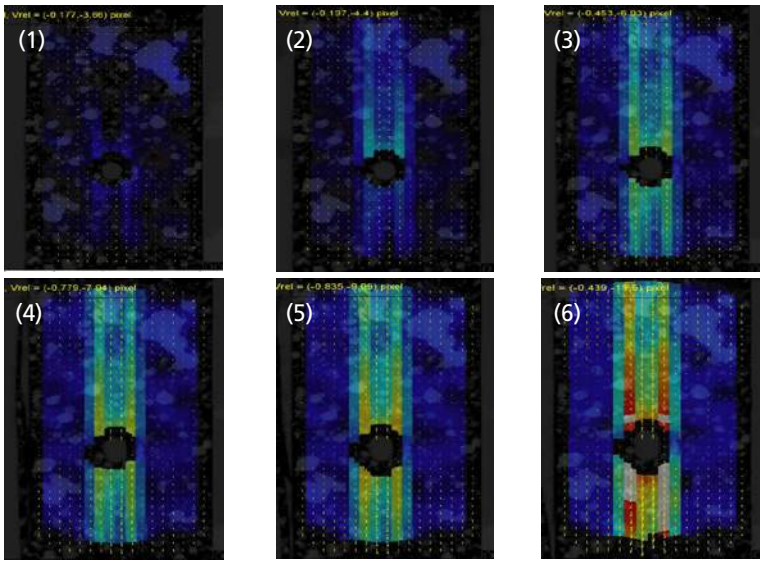

Fig. 2 Results of DIC Analysis of CFRP-OH Specimen

Fig. 2 and Fig. 3 show the DIC analysis results obtained in tensile testing of CFRP-OH and ABS resin test specimens, respectively. The images were extracted in the order of a typical time course analysis (image order corresponding to the numbers shown in images), from the start of the tensile test to the point that the specimen breaks. The appearance of coloring in the images corresponds to the strain distribution in the specimen. The amount of strain that occurs in the specimen corresponds to the degree of color warmth, with areas of darker color (such as blue-black) indicating low strain, and areas of brighter color (such as red-orange) indicating a greater degree of strain. It is clear that in Fig. 2, as the load is applied to the test specimen, the strain increases in the vicinity of the open hole. Because the test specimen is a $[0/90]_{2s}$ laminate material, it is believed that the fibers are aligned in the tensile direction in the test specimen surface layer which was subjected to random marking.

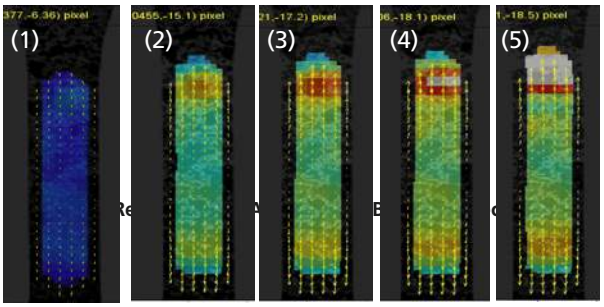

In Fig. 3, localized strain occurs from the edge of the parallel region of the test specimen, and as time progresses, localized strain is noticeable at the upper and lower edge of the parallel region.
Thus, by combining a high-speed tensile testing machine with a high-speed video camera, in addition to DIC analysis software, it has become possible to visualize the distribution of strain generated in a test specimen.

First Edition: Dce, 2012

Shimadzu Corporation
www.shimadzu.com/an/

For Research Use Only. Not for use in diagnostic procedures.
The content of this publication shall not be reproduced, altered or sold for any commercial purpose without the written approval of Shimadzu.
The information contained herein is provided to you "as is" without warranty of any kind including without limitation warranties as to its accuracy or completeness. Shimadzu does not assume any responsibility or liability for any damage, whether direct or indirect, relating to the use of this publication. This publication is based upon the information available to Shimadzu on or before the date of publication, and subject to change without notice.
© Shimadzu Corporation, 2012

SHIMADZU
Excellence in Science

Application Data Sheet

No. 8

Autograph Precision Universal Tester

Material Testing & Inspection

Flexural Testing of CFRP Boards

Standard No. JIS K 7074: 1988

Introduction

Carbon fiber reinforced plastic (CFRP) is a composite material with excellent relative strength. This plastic was quickly adopted in the aviation and space sectors, and has contributed significantly to reducing fuselage weight. Initially, this plastic was only used for partial replacement of metal materials. In the latest aircraft, however, composite materials, primarily CFRP, represent 50 % of the fuselage weight. Improved productivity and reduced costs are expected due to subsequent technical developments, and it can be expected that this plastic will also become popular as a main material in automobile frames. In this Data Sheet, a CFRP cloth was subjected to a flexural testing using a precision universal tester in order to evaluate the strength of the material.

F. Yano

Measurements and Jigs

In flexural testing specified in JIS K7074, a loading edge radius of 5 mm, and a support radius of 2 mm are specified. The specimen standard dimensions are specified as follows:

Length = 100 mm ± 1 mm
Width = 15 mm ± 0.2 mm
Thickness = 2 mm ± 0.4 mm

For tests performed using a specimen with the standard dimensions, the span between supports (L) will be 80 mm ± 0.2 mm. When TRAPEZIUM software is used, the flexural stress can be automatically calculated and plotted in a graph from the test force and the specimen dimensions. The flexural strength and other characteristic values can also be obtained from a few simple operations.

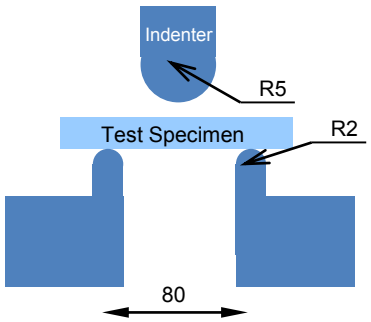

Fig. 1: Flexural Testing Schematic

Measurement Results

Fig. 2: Flexural Testing Status

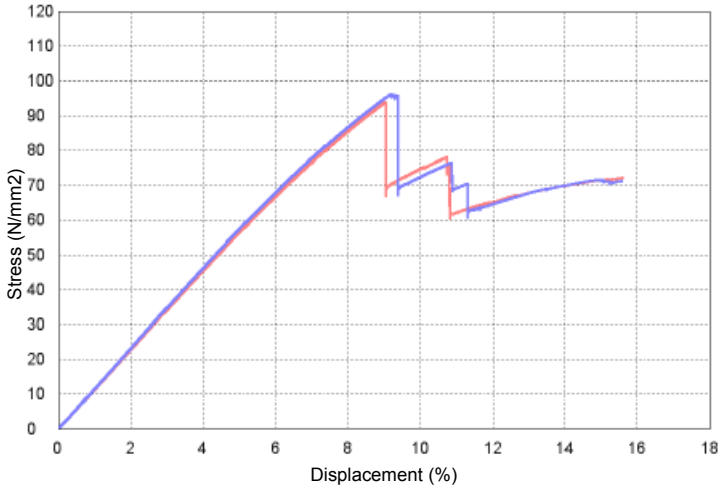

Fig. 3: Stress – Displacement Curve

Table 1: Test Conditions

Item	Set Value
Cell Capacity	5 kN
Load Speed	5 mm/min

Table 2: Test Results (Average)

Load at Fracture (N)	Bending Strength (%)
485	95

CFRP Flexural Testing System

Tester:	AG-Xplus
Load Cell:	5 kN
Test Jig:	Three-point bending test jig for plastics
Software:	TRAPEZIUM X (Single)

AG-Xplus Table-Top Precision Universal Tester

Features

- A high-precision load cell is adopted. (The high-precision type is class 0.5; the standard-precision type is class 1.)
  Accuracy is guaranteed over a wide range, from 1/1000 to 1/1 of the load cell capacity. This supports highly reliable test evaluations.
- Crosshead speed range
  Tests can be performed over a wide range from 0.0005 mm/min to 1,500 mm/min.
- High-speed sampling
  Ultrafast sampling, as fast as 0.2 msec. Sudden changes in test force, such as when brittle materials fracture, can be assessed.
- TRAPEZIUMX operational software
  Designed for intuitive operation, this software offers excellent convenience and user friendliness.
- Smart controller
  Real-time test force and position data is readily confirmed, and the manual dial can be used for fine adjustments to jig positioning.
- Optional Test Devices
  A variety of tests can be conducted by switching between an abundance of jigs in the lineup.

First Edition: February 2013

Shimadzu Corporation
www.shimadzu.com/an/

For Research Use Only. Not for use in diagnostic procedures.
The content of this publication shall not be reproduced, altered or sold for any commercial purpose without the written approval of Shimadzu.
The information contained herein is provided to you "as is" without warranty of any kind including without limitation warranties as to its accuracy or completeness. Shimadzu does not assume any responsibility or liability for any damage, whether direct or indirect, relating to the use of this publication. This publication is based upon the information available to Shimadzu on or before the date of publication, and subject to change without notice.
© Shimadzu Corporation, 2013

SHIMADZU
Excellence in Science

Application Data Sheet

No. 16

Autograph Precision Universal Tester

Material Testing & Inspection

Tensile Testing of Carbon Fiber

Standard No. ISO11566: 1996 (JIS R 7606: 2000)

Introduction

Carbon fiber is an important industrial material, being essential in carbon fiber reinforced plastics (CFRP), having a specific gravity one-fourth that of normal steels, and a specific strength of 7 times. In this Application Data Sheet, examples of tensile testing of single carbon fibers based on the ISO standard are introduced.

T. Murakami

Measurements and Jigs

In this test, the test sample is fixed to a test specimen mounting board made from a paper, metal, or resin sheet as shown in Fig. 1, installed in the grips, and the tensile test is performed. The standard describes in detail the shape of the mounting board, the type of adhesive used to fix the carbon fiber to the mounting board, and the procedure for installing the carbon fiber (for details refer to the standard). The tests were carried out using clip type grips whose grip force could be adjusted in accordance with the strength of the sample.

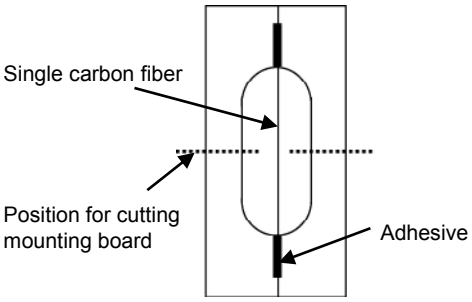

Fig. 1 Test Sample and Mounting Board (frame)

Measurement Results

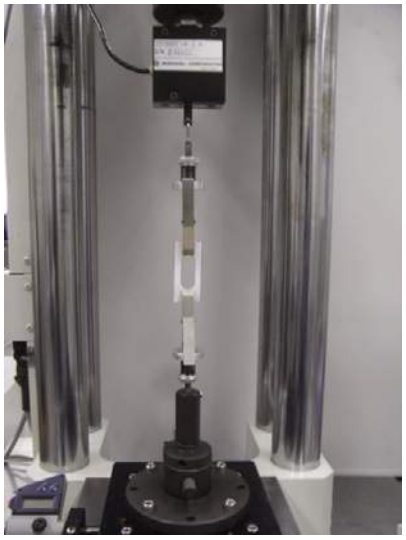

Fig. 2 Test Status

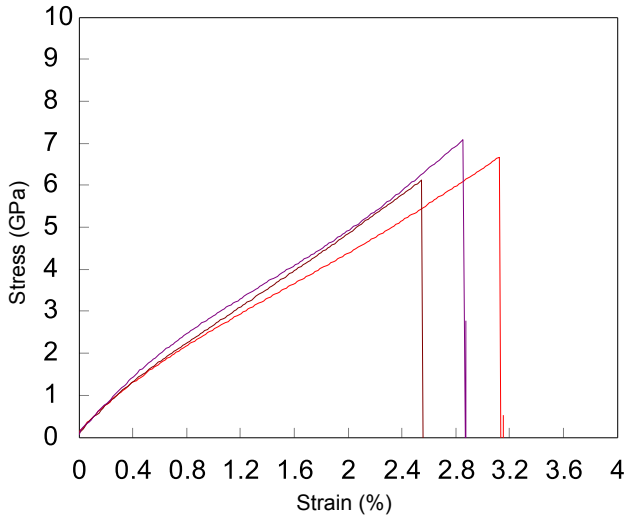

Fig. 3 Test Results

Table 1 Test Conditions

Item	Set Value
Test speed	1 mm/min
Distance between grips	25 mm

Table 2 Test Results (average)

Sample	Diameter	Tensile Strength	Elongation at Break
Carbon fiber	6 μm	7.1 GPa	2.84 %

Carbon Fiber Tensile Test System

Tester:	MST-I Type HR
Load Cell:	1 N
Test Jig:	1 N clip type grips (rubber-coated teeth), X-Y stage
Software:	TRAPEZIUM X (Single)

Shimadzu Autograph MST-1 Micro Strength Evaluation Testing Machine

Features

■ High Accuracy Displacement Measurement
A high accuracy (±0.2 μm) linear sensor has been adopted for measurement of displacement in the load direction. In addition, the backlash-free structure makes it possible to carry out testing with good accuracy. Displacement in the load direction of the test sample can be set accurately to a displacement display resolution of 0.02 μm and a control resolution of 0.005 μm.

■ Measurement of Micro Test Forces
A wide range of load cells from 0.5 N to 2 kN assures a precision of ±1 % for measurements of testing forces of 2 mN at minimum.

■ Positioning Very Small Test Samples
Using an X-Y stage (optional), very small test samples can be easily positioned. The position of the test samples can be observed using a stereo microscope.

■ High Rigidity Frame
A high rigidity frame (45 kN/mm minimum) has been adopted to enable measurement of minute displacements.

■ Optional Test Devices
A variety of tests can be accommodated by switching between an abundance of jigs in the lineup.

First Edition: February 2013

SHIMADZU

Shimadzu Corporation

www.shimadzu.com/an/

For Research Use Only. Not for use in diagnostic procedures.
The content of this publication shall not be reproduced, altered or sold for any commercial purpose without the written approval of Shimadzu. The information contained herein is provided to you "as is" without warranty of any kind including without limitation warranties as to its accuracy or completeness. Shimadzu does not assume any responsibility or liability for any damage, whether direct or indirect, relating to the use of this publication. This publication is based upon the information available to Shimadzu on or before the date of publication, and subject to change without notice.

© Shimadzu Corporation, 2013

SHIMADZU
Excellence in Science

Application Data Sheet

No. 31

Autograph Precision Universal Tester

Material Testing & Inspection

Materials Testing Using Digital Image Correlation

—3-Point Bending Test for Polypropylene and Open-Hole Tensile Test for Carbon Fiber Reinforced Thermo-Plastic—

■Introduction

In recent years, computer aided engineering (CAE), which has allowed significantly reducing the number of prototypes and costs required for product development by simulating product designs on a computer, has been widely used in scientific and industrial fields. This has resulted in an increased need to analyze the distribution of strain in test samples, where the areas prone to strain concentrations in such samples are evaluated by mechanical testing to determine the correlation between results from simulation and strain distribution obtained by mechanical testing.

Digital image correlation (DIC) analysis compares the random patterns on the surface of a test sample before and after deformation to determine the degree of deformation. A important feature of the method is that displacements can be measured and strain distributions analyzed from digital images, which means no sensors need to contact the test sample and no complicated optical systems are required. Consequently, DIC analysis is being used for a wide range of applications where strain is difficult to measure using conventional technology, such as analyzing the strain distribution in large structural members, materials at high temperatures, or micro-materials observed via a microscope.

This paper describes examples of using DIC analysis for 3-point bending tests of plastics and for open-hole tensile testing of thermoplastic carbon fiber reinforced plastics (CFRP) (fabric). The test data presented in this paper was obtained using a system comprising a Shimadzu AG-Xplus precision universal tester, a customized TRViewX non-contact video extensometer, and LaVision DaVis8 DIC analysis software. This system allows simultaneously acquiring JIS 0.5 class extensometer measurement results and video images for DIC analysis, as well as correlating DIC analysis results with test force data.

■Evaluation of Dependence on Distance Between Supports in 3-Point Bending Tests of Plastics

3-point bending tests are widely used throughout the world as a relatively easy way to evaluate the bending properties of materials. A photograph of the testing system is shown in Fig. 1. In 3-point bending tests, a punch applies a load to specimens supported at two points.

3-point bending test regulations for plastics (such as JIS K 7171 and ISO 178) specify that the L, the distance between supports, must be about 16 times greater than h, the specimen thickness (L/h ≈ 16), where this ratio, L/h, is an important factor for measuring the bending strength or bending elasticity correctly.[1), 2)] The following discusses L/h in more detail. Bending a specimen applies compressive stresses to the material above the center plane and tensile stresses below the center plane. The contribution of this compressive and tensile deformation to bending stresses is defined to be equal. Maximum bending stress occurs near the punch that applies the bending loads, where given a flat plate-shaped specimen, stress is defined as $\sigma_f = 3FL/2bh^2$. When a specimen bends, shear stresses also occur at the same time, where the shear stress is defined as $\tau = 3F/4bh$. Based on the above two equations, the relationship between specimen thickness and distance between supports is described by $L/h = \sigma_f/2\tau$. Given a uniformly formed specimen with a sufficiently large distance between the supports, relative to the specimen thickness, the definition of L/h indicates that the contribution of shear stresses in the specimen is small.[3) to 5)] To limit the effects of shear stresses during 3-point bending tests, the optimal L/h value must be specified for the specimen being tested.

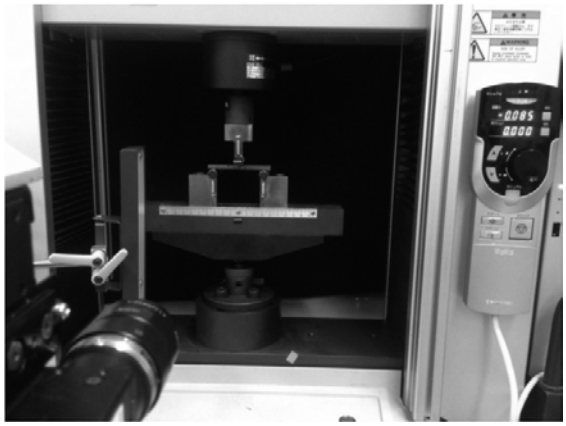

Fig. 1 3-Point Bending Testing System Using Non-Contact Video Extensometer

In the following example, a common plastic material, polypropylene, was tested by 3-point bending using three different distances between supports, and then DIC analysis was used to investigate how much the maximum shear stress distribution depends on the distance between supports. Test conditions are shown in Table 1.

Tests were performed at three L values (distance between supports), 64 mm for an L/h ratio of 16 specified in JIS K 7171, 48 mm for an L/h ratio of 12, where shear stress is predicted to have a large effect, and 32 mm for an L/h ratio of 8. Stress-strain curves obtained using different test conditions are shown in Fig. 2. Fig. 3 shows the maximum shear strain distribution near the elastic limit and near the maximum load point. Warmer colors indicate higher strain levels in the maximum shear strain distribution. This shows that at an L/h ratio of 16, strain is low even near the maximum load point and spreads out uniformly. However, L/h ratios of 8 and 12, where shear stress contribution is predicted to be large, generated large localized shear stresses near the maximum load point on the specimen surface under tension directly under the punch. Whereas localized shear stresses occurred from about the elastic limit for L/h ratio of 8, none were observed for the L/h ratio of 12.

This clearly shows that different deformation modes resulted from bending tests using different distances between supports and shows that DIC analysis provides an effective means of verifying the different modes. It also shows that L/h ratio of 16 recommended in the testing regulations is an appropriate value for 3-point bending tests.

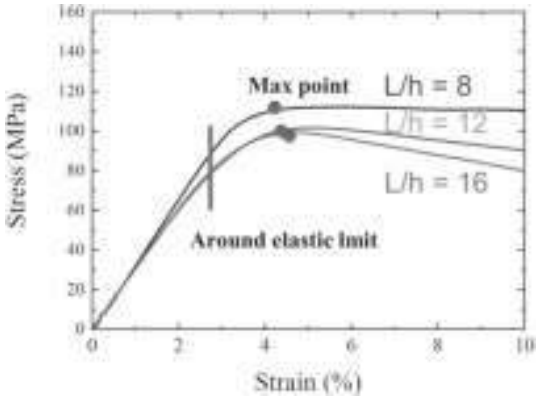

Fig. 2 Stress-Strain Curve

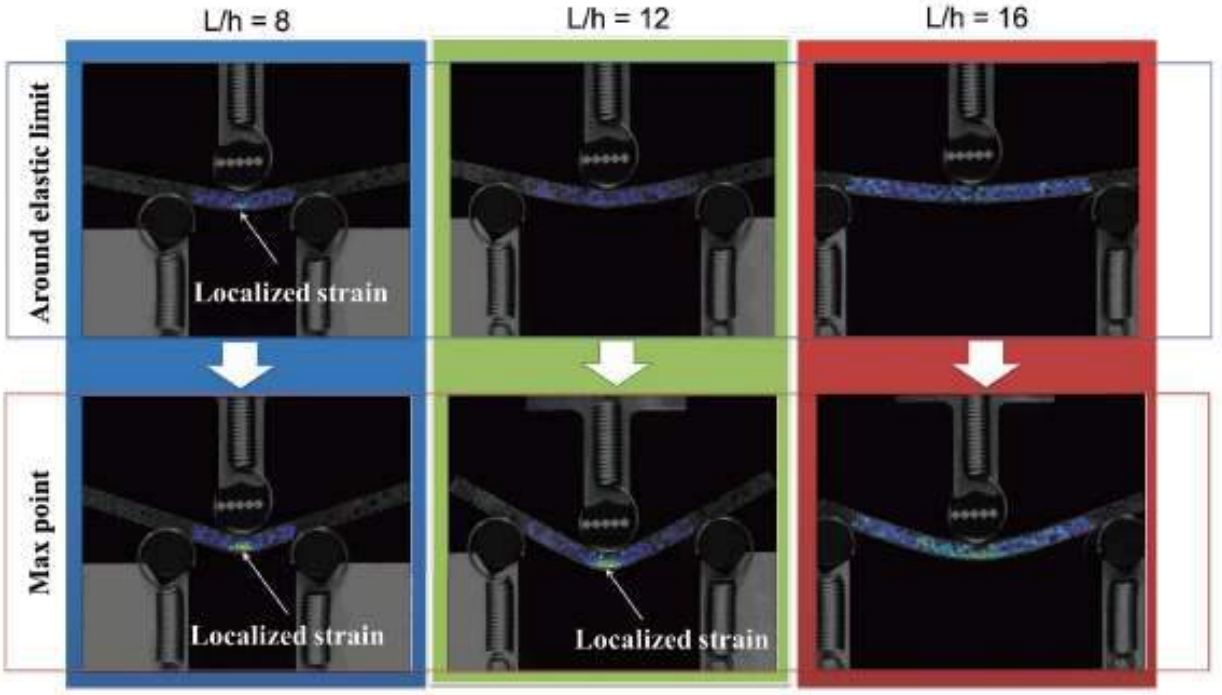

Fig. 3 Distribution of Maximum Shear Strain Around Elastic Limit and Maximum Load

Table 1 Test Conditions for 3-Point Bending Test of Plastic Material

1) Testing equipment	AG-Xplus precision universal tester
2) Load cell capacity	1 kN
3) Jig	Three-point bending test jig for plastic
4) Distance between supports	Three configurations: 32, 48, and 64 mm
5) Test speed	0.001 /s
6) Deflection measuring device	TRViewX120S non-contact video extensometer (customized)
7) Testing software	TRAPEZIUM X (Single)
8) DIC analysis software	DaVis8 (LaVision GMBH)
9) Specimen size	4 mm thick × 10 mm wide × 80 mm long

First Edition: July 2015

SHIMADZU
Shimadzu Corporation
www.shimadzu.com/an/

For Research Use Only. Not for use in diagnostic procedures.
The content of this publication shall not be reproduced, altered or sold for any commercial purpose without the written approval of Shimadzu.
The information contained herein is provided to you "as is" without warranty of any kind including without limitation warranties as to its accuracy or completeness. Shimadzu does not assume any responsibility or liability for any damage, whether direct or indirect, relating to the use of this publication. This publication is based upon the information available to Shimadzu on or before the date of publication, and subject to change without notice.
© Shimadzu Corporation, 2015

■Open-Hole Tensile Testing of Thermoplastic CFRP (Fabric)

Due to higher specific strength than steel materials, superior workability and formability than CFRP/epoxy, and short cycle times of only a few minutes possible for molding, thermoplastic CFRP materials are anticipated for use in production automobiles.[6)]

In general, CFRP materials start failing at the point where they are damaged. CFRP/epoxy used as structural materials in aircraft are mainly used for large components that are fastened with screws or rivets. Therefore, it is important to evaluate their open-hole tensile strength. The open-hole tensile test specified in ASTM D 5766, JIS K 7094, and other regulations is one of the essential evaluation criteria for understanding the properties of CFRP materials.[7), 8)]

In this case, we made a round hole in a thermoplastic CFRP specimen, applied a tensile load, and evaluated the resulting distribution of the maximum shear strain. Fig. 4 shows the testing system used for this test. Table 2 indicates testing conditions and information about the specimen. We chose to cut out type-I shaped specimens, as specified in JIS K 7094 (2012), from PA6 polymer-based thermoplastic CFRP material (with CF-3K flat woven $[0]_{10}$ fabric from Ichimura Sangyo), so that the fibers were oriented longitudinally.

The stress-strain curve obtained from testing is shown in Fig. 5 and the distribution of maximum shear strain that occurred on the observed specimen surface is shown in Fig. 6. Images (1) to (4) in Fig. 6 correspond to the numbers indicated on the stress-strain curve in Fig. 5.

Fig. 4 Open-Hole Tensile Testing System Using Non-Contact Video Extensometer

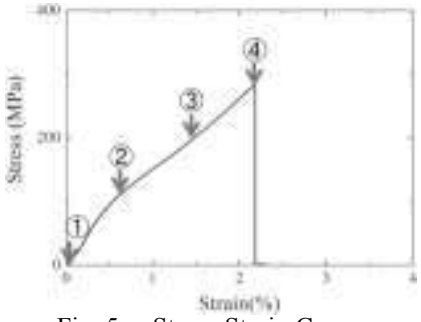

Fig. 5 Stress-Strain Curve

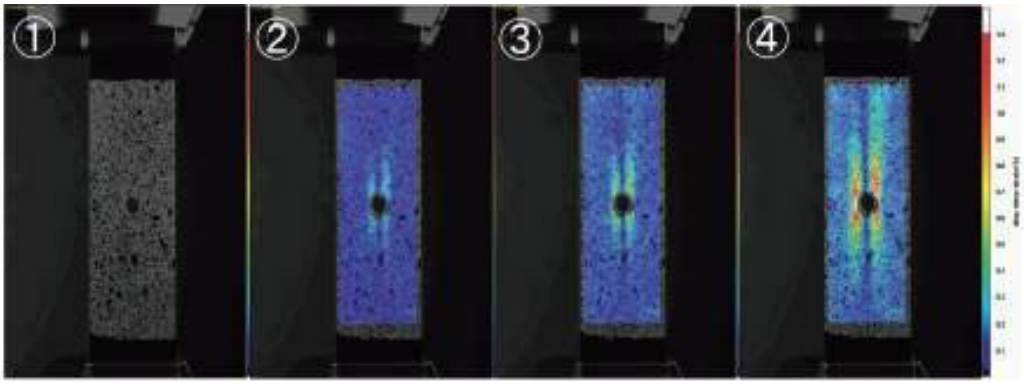

Fig. 6 Distribution of Maximum Shear Strain

Table 2 Test Conditions for Open-Hole Tensile Test of Carbon Fiber Reinforced Thermo-Plastic (Fabric)

1) Testing equipment	AG-Xplus precision universal tester
2) Load cell capacity	50 kN
3) Jig	50 kN non-shift wedge type grips (with trapezoidal file teeth on grip faces for flat specimens)
4) Distance between grips	100 mm
5) Test speed	0.5 mm/min
6) Deflection measuring device	TRViewX120S non-contact video extensometer (customized)
7) Testing software	TRAPEZIUM X (Single)
8) DIC analysis software	DaVis8 (LaVision GMBH)
9) Specimen size	2 mm thick × 36 mm wide × 150 mm long, with 6 mm diameter hole

First Edition: July 2015

SHIMADZU
Shimadzu Corporation
www.shimadzu.com/an/

For Research Use Only. Not for use in diagnostic procedures.
The content of this publication shall not be reproduced, altered or sold for any commercial purpose without the written approval of Shimadzu.
The information contained herein is provided to you "as is" without warranty of any kind including without limitation warranties as to its accuracy or completeness. Shimadzu does not assume any responsibility or liability for any damage, whether direct or indirect, relating to the use of this publication. This publication is based upon the information available to Shimadzu on or before the date of publication, and subject to change without notice.
© Shimadzu Corporation, 2015

The results showed that when the tensile load increased, the maximum shear strain distribution started near the tangent points on the left and right sides of the hole, and spread along the longitudinal direction of the specimen. Due to the orientation of the carbon fibers, the specimen has the greatest strength for bearing tensile loads in its longitudinal direction. The areas of strain concentration are the areas that contain continuous fibers, but they are presumably highly affected by the process of creating the hole. Fig. 7 is a photograph of the specimen after fracture. It shows that the specimen fractured in the direction perpendicular to the main tensile axis. The failure mode is typical of CFRP(fabric) specimens with an open hole, where cracking presumably progressed rapidly after the longitudinal carbon fibers near the hole fractured, resulting in specimen breaking.

Generally, open-hole tensile tests that involve creating a hole in specimens result in significantly lower stresses at the maximum load point, than for specimens without a hole, with some reports indicating a 1/3 to 1/2 drop in strength.[9), 10)] In addition to open-hole tensile testing, this research also involved tensile testing specimens without a hole for reference purposes. A resulting stress-strain curve and photograph of the specimen after fracture are shown in Figs. 8 and 9. The specimen fractured near the parallel area, at a value of about 700 MPa. In contrast, Fig. 5 indicates that the open-hole specimen failed at about 300 MPa, a result similar to CFRP/epoxy specimens.

Fig. 7 Picture of Fractured Specimen

■Conclusion

This paper describes using DIC analysis to evaluate the properties of polypropylene and thermoplastic CFRP (fabric), as examples of chemically engineered materials. However, there are many other types of chemically engineered materials available for which DIC analysis could be used for determining material properties, not only for bending or tensile tests, but also for various others tests, such as compression and shear tests. With high-speed video cameras developed in recent years that allow obtaining high-resolution video images with extremely high time resolution levels, technology has advanced to the point that DIC analysis can now be utilized to visualize strain distributions or obtain stress-strain curves for applications such as high-speed impact testing. Consequently, using DIC analysis for material testing in product design work provides an effective way of ensuring a higher level of safety and peace of mind by understanding the properties of the materials from various aspects.

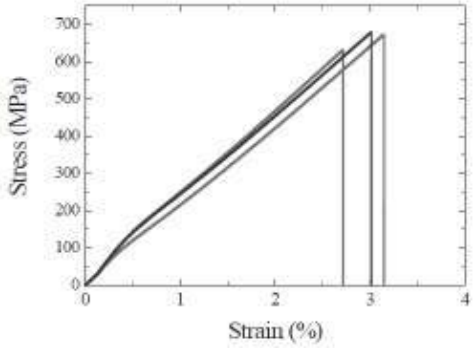

Fig. 8 Stress-Strain Curve

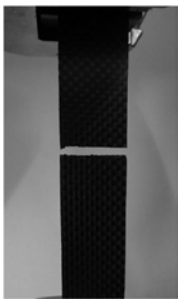

Fig. 9 Picture of Fractured Specimen

■References:

1) JIS K 7171: 2008 Plastics—Determination of flexural properties
2) ISO 178: 2001 Plastics—Determination of flexural properties
3) Masahiro Funabashi: Technology for Evaluating the Performance of Advanced Materials, Sangyo Gijutsu Service Center, pp. 286-287 (2014)
4) Leif A. Carlsson and R. Byron Pipes: Experimental Characterization of Advanced Composite Materials, Kokon Syoin, p. 75 (1990)
5) Ikuo Narisawa: Mechanical Properties of Plastics, Sigma Shuppan, pp. 105-108 (1994)
6) Takeshi Murakami and Tsuyoshi Matsuo: Summary of Presentations at the 39th Conference on Composite Materials, pp. 155-156 (2014)
7) ASTM D5766/D5766M -11 Standard Test Method for Open-Hole Tensile Strength of Polymer Matrix Composite Laminates
8) JIS K 7094: 2012 Test method for open-hole tensile strength of carbon fibre reinforced plastic
9) JAXA-ACDB Advanced Composites Database System http://www.jaxa-acdb.com/ (as of December 17, 2014)
10) Wisnom, M. R., Hallett, S. R., and Soutis, C.: Scaling effects in notched composites, Journal of composite materials, 44, 195-210 (2010)

First Edition: July 2015

SHIMADZU
Shimadzu Corporation
www.shimadzu.com/an/

For Research Use Only. Not for use in diagnostic procedures.
The content of this publication shall not be reproduced, altered or sold for any commercial purpose without the written approval of Shimadzu.
The information contained herein is provided to you "as is" without warranty of any kind including without limitation warranties as to its accuracy or completeness. Shimadzu does not assume any responsibility or liability for any damage, whether direct or indirect, relating to the use of this publication. This publication is based upon the information available to Shimadzu on or before the date of publication, and subject to change without notice.
© Shimadzu Corporation, 2015

SHIMADZU
Excellence in Science

Application Data Sheet

No. 37

High-speed Video Camera HPV-X2

Observing the Failure of Open-Hole CFRP Specimens in Tensile Testing

Synchronized Imaging Using Two High-Speed Video Cameras

■ Introduction

Offering superior specific strength, even compared to other composite materials, carbon fiber reinforced plastic (CFRP) is used in aircraft and some transport vehicles for the purpose of saving fuel through weight reduction. Composite materials have excellent mechanical properties. However, a general feature of composite materials is that their strength decreases markedly when they are notched. CFRP is no exception, so tests of notched specimens are important. In this case, testing is performed using specimens notched with a circular hole at the center. In this experiment, tensile tests were performed using CFRP (laminate method $[45/0/-45/90]_{2s}$) with a total length of 150 mm, a width of 36 mm, and a thickness of 2.5 mm, prepared with a 6 mm circular hole at the center. The failure process of CFRP was observed during the tensile test. In particular, it is important to confirm the failure process of weak regions, such as the periphery of circular holes, for CFRP development and to confirm the validity of CAE analysis. However, since the failure of CFRP is a brittle phenomenon, where failure occurs instantaneously, it cannot be confirmed with the naked eye. For this reason, high-speed video cameras are used to observe the failure. In this experiment, synchronized images were obtained at the front and the side of the specimens using two HPV-X2 high-speed video cameras.

■ Measurement system

In this experiment, the AG-X precision universal testing machine and two HPV-X2 high-speed video cameras were used. Table 1 shows the instruments used. To observe the specimen failure in a tensile test, a trigger signal synchronized to the failure must be transmitted to the high-speed video cameras. The failure starts on the periphery of the circular hole. Accordingly, aluminum foil was affixed to the periphery of the circular hole using adhesive, as shown in Fig. 1, so that conduction would be lost when the sample fails. The failure was observed using this timing to trigger the cameras.

Table 1 Testing Equipment

High-speed Camera	HPV-X2 ×2
Lens	105 mm Macro lens ×2
Illumination	Metal halide lump ×2
Testing Machine	AG-X plus
Load cell	100 kN
Grips	100 kN Non-shift wedge-type grips
Grip teeth	Trapezoidal file teeth for composite mater
Software	TRAPEZIUM X(Single)

Fig.1 Aluminum foil Trigger

■ Measurement Results

Table 2 shows the measurement conditions, and Fig. 2 shows the test configuration. As shown in Fig. 2, the failure of the specimen was recorded from the front by camera (1) and from the side by camera (2). Fig. 3 shows the test results from the AG-Xplus. Failure begins where the test force suddenly drops in Fig. 3. Fig. 4 shows the specimen failure observed from the front, and Fig. 5 from the side. Image (2) in Fig. 4 shows that the failure starts on the left side of the circular hole. In image (3), a crack also appears on the right side of the circular hole. Subsequently, cracks progressed in an orientation of 45 degrees, the orientation of the fibers in the outer layer. Further, as the test progressed, multiple cracks were confirmed, as in images (7) and (8). In the observation from the side, no failure was confirmed at the time the failure started, and was only initially confirmed in image (5). This is likely because the cracks started at the periphery of the circular hole reached the side of the specimen in image (5). Subsequently, failure was confirmed in multiple layers, except for the 0-degree layer, in image (6). Further, in image (7), failure was confirmed in the 0-degree layer, after which the failure progressed toward the outersurface. The final condition of the specimen is shown in Figs. 6 and 7.

Table 2 Measurement Conditions

Test speed	5 mm/min
Frame rate	1M frames/sec
	2M frames/sec

Fig.2 Test Configuration

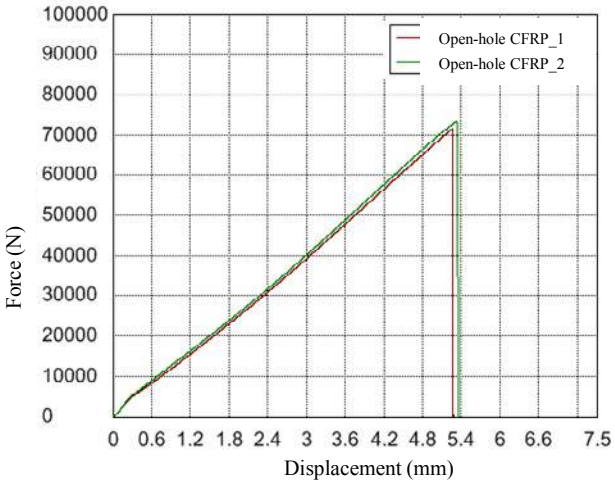

Fig.3 Test Results

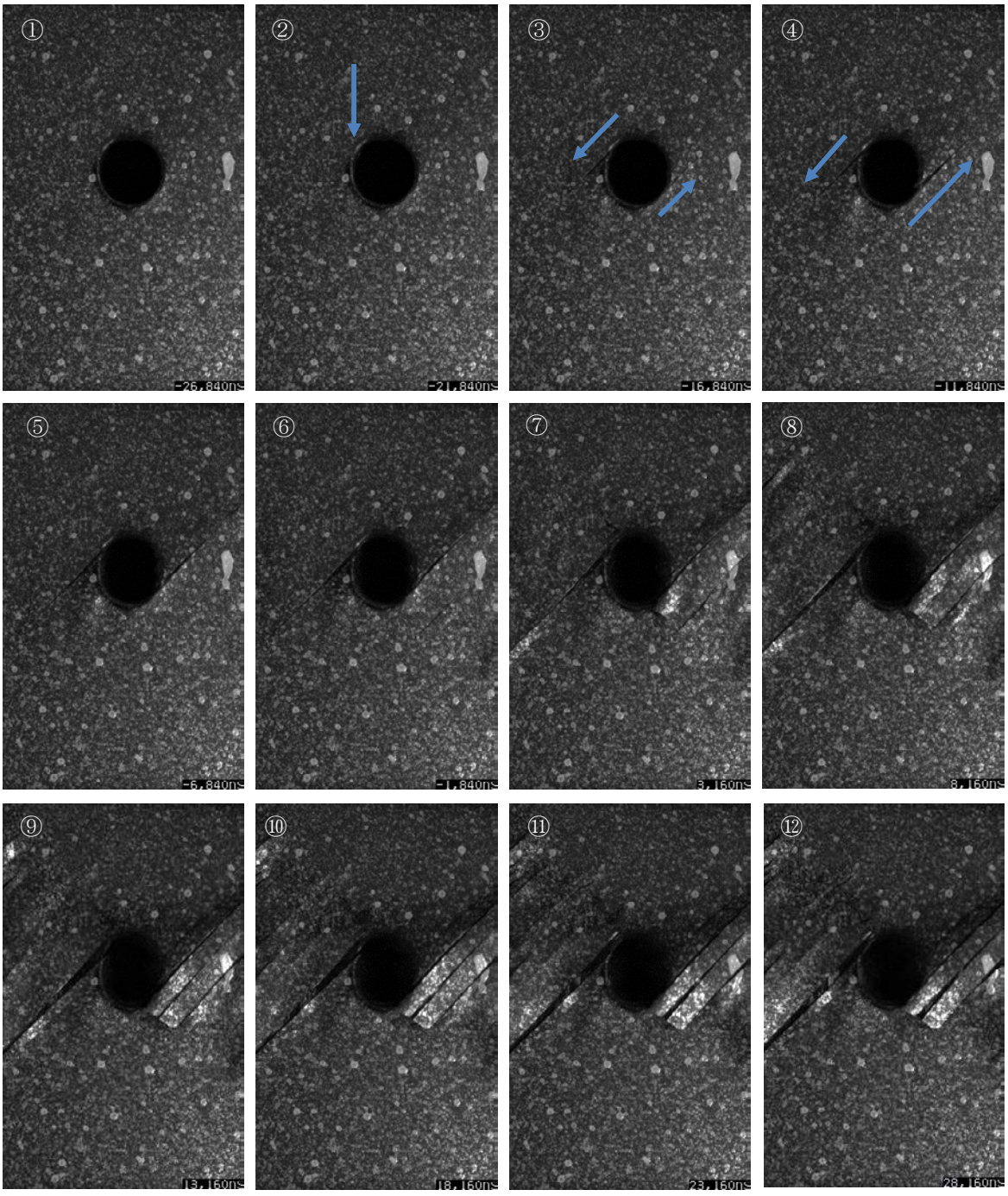

Fig.4 Images from Camera (1) (5 μs between images)

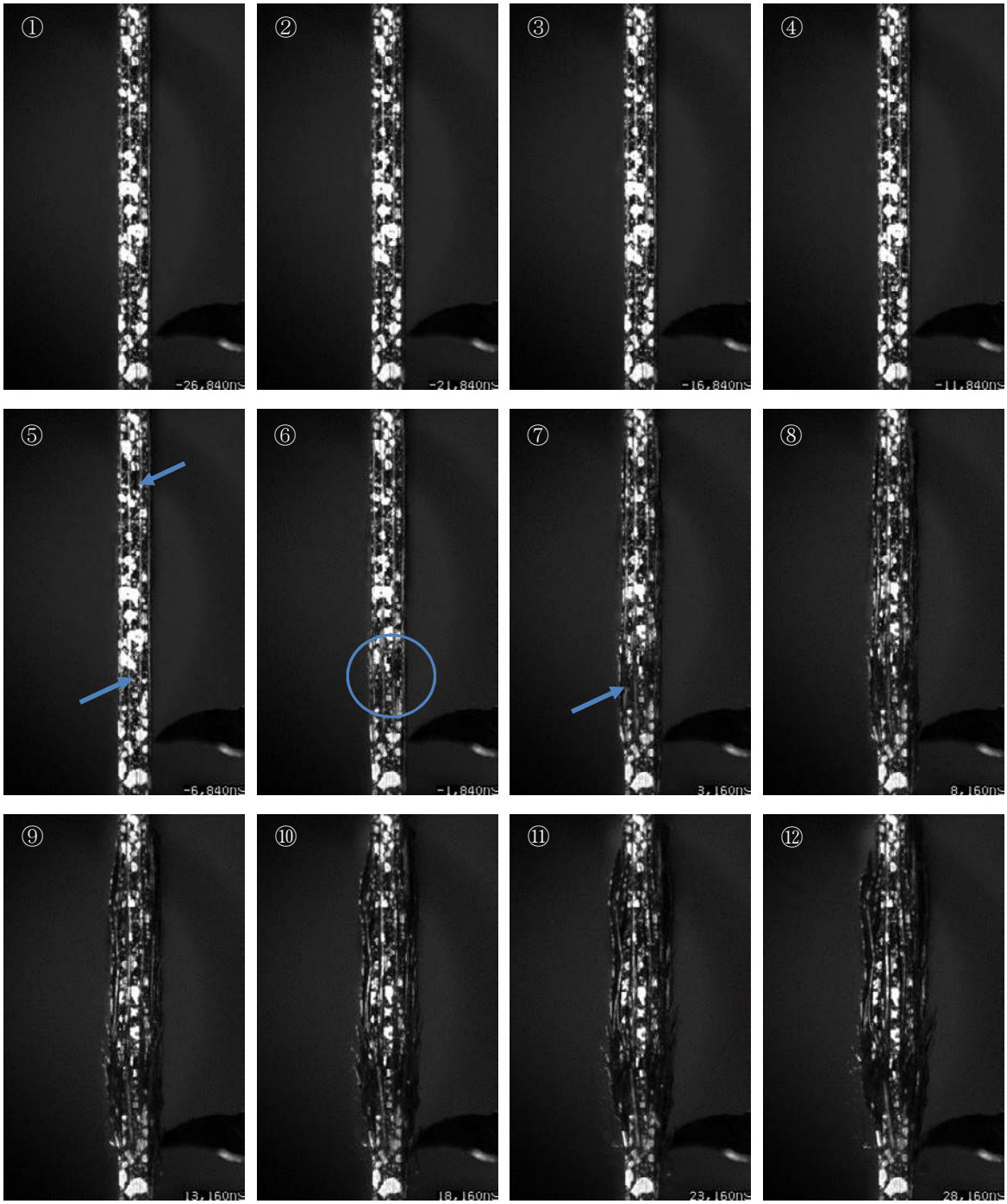

Fig.5 Images from Camera (2) (5 μs between images)

Fig.6 Specimen After Failure (front)

Fig.7 Specimen After Failure (side)

■ Conclusion

The conventional HPV-X does not have a synchronization function, and so is incapable of recording from two directions. Also, the sensitivity of the HPV-X is insufficient, so it cannot record at imaging speeds of 500 kfps or faster. The HPV-X2 is equipped with a synchronization function, and features improved sensitivity, so this instrument is capable of synchronized recordings at 2 Mfps, as in this case. As a result, failures can be observed in tensile tests of materials like CFRP that fail at high speeds.

Generally, failure observations are often recorded from the front of the specimen. However, adding recording from the side enables confirming the failure process that cannot be observed just from the front. In particular, with CFRP materials with different fiber orientations for each lamination layer, where failure progresses in different manner for each layer, as shown in this article, the failure process can be observed in more detail by recording from two directions.

First Edition: July, 2015

Shimadzu Corporation
www.shimadzu.com/an/

For Research Use Only. Not for use in diagnostic procedures.
The content of this publication shall not be reproduced, altered or sold for any commercial purpose without the written approval of Shimadzu.
The information contained herein is provided to you "as is" without warranty of any kind including without limitation warranties as to its accuracy or completeness. Shimadzu does not assume any responsibility or liability for any damage, whether direct or indirect, relating to the use of this publication. This publication is based upon the information available to Shimadzu on or before the date of publication, and subject to change without notice.
© Shimadzu Corporation, 2015

SHIMADZU
Excellence in Science

Application Data Sheet

No. 38

HPV-X2 High-Speed Video Camera

High-Speed Video Camera

Observing the Fracture of Unidirectional CFRP in Static Tensile Testing

■ Introduction

Carbon fiber reinforced plastic (CFRP) is a composite material with a particularly high specific strength. It is used in aircraft and in some transport equipment to reduce fuel costs by reducing weight. While it has some excellent mechanical characteristics as a composite material, when in-plane damage occurs it displays brittle failure behavior, with fracture propagating instantly from the point of damage. Consequently, CFRP development involves not only material testing, but also observation of material failure to check for fracture locations at weak points. Furthermore, material failure is observed to evaluate the validity of computer aided engineering (CAE) recently. As mentioned above, a CFRP fracture event occurs extremely quickly and cannot be observed by the naked eye, so a high-speed video camera is used. Shimadzu has published an Application News on this topic in the past (No. V017 Observing the Failure of CFRP Materials in High-Speed Tensile Tests). High-speed tensile testing involves an instantaneous testing time. To accommodate this, a strobe capable of emitting very intense light instantaneously is used to achieve an image capture speed of over 1 million frames/second. Meanwhile, static testing involves longer testing times with a metal halide lamp used as a light source for continuous lighting (a relatively weak light source compared to a strobe), which cannot produce enough light to capture images at more than 500 thousand frames/second.
The newly developed HPV-X2 camera is 6 times more sensitive than the previous HPV-X camera, which allows it to capture over 1 million frames/second using even a metal halide lamp as a light source. In this article, we demonstrate the observation of unidirectional CFRP failure in static testing.

■ Measurement

The AG-X precision universal testing machine and HPV-X2 high-speed video camera were used in experiments. The equipment used is shown in Table 1. Observing material failure during tensile testing requires a signal to trigger the high-speed video camera in time with material failure. Since cracks propagate in the direction of the unidirectional fibers when failure occurs in unidirectional CFRP, we attached aluminum foil perpendicular to the direction of the fibers with adhesive. A specimen with the aluminum foil attached is shown in Fig. 1. A break in conduction through the aluminum foil caused by a break in the specimen triggers observation of the failure event.

■ Results

A view of the test is shown in Fig. 2 and Fig. 3. As shown in Fig. 3, aluminum foil is also attached to the jigs around the specimen in order to focus light onto the specimen. Test conditions are shown in Table 2.

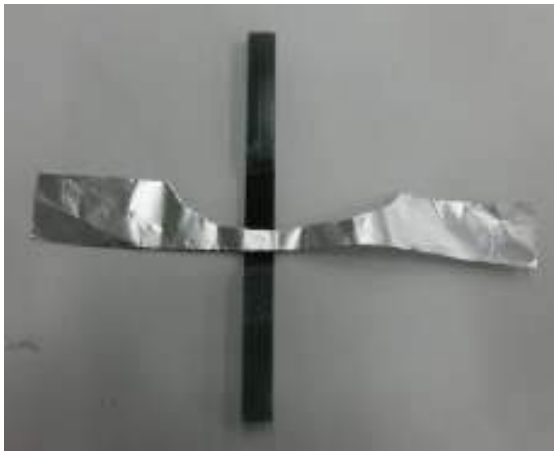

Fig. 1 Test Specimen

Table 1 Testing System

High-Speed Video Camera	HPV-X2
Lens	105 mm, F1.8
Lighting	Two metal halide lamps
Testing Machine	AG-Xplus
Load Cell	50 kN
Grip	50 kN non-shift wedge-type grips
Grip Face	Trapezoidal file teeth for composite materials
Software	TRAPEZIUM X (Single)

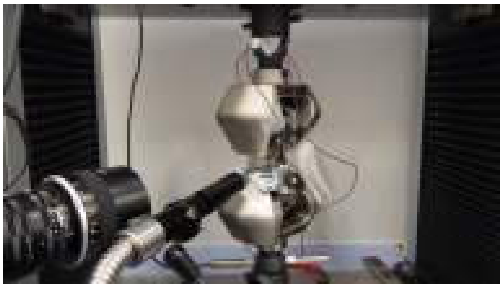

Fig. 2 View of the Test

Table 2 Test Conditions

Test speed	5 mm/min
Recording Speed	5 million frames/sec
Specimen Size	Width: 6 mm, thickness: 0.4 mm
Lamination Method	$[0]_2$

The failure of unidirectional CFRP is shown in Fig. 4. Longitudinal cracks can be seen on the left side of the specimen in image (2) of Fig. 4. In image (3), these cracks have propagated as far as the upper tab. Longitudinal cracks can also be seen on the right side of the specimen in image (3). Image (6) is a later view of the specimen as it is breaking apart. Using the HPV-X2 allows for the observation of CFRP failure during the static tensile test, which is useful for future CFRP development.

Fig. 3 View of the Test (Magnified View)

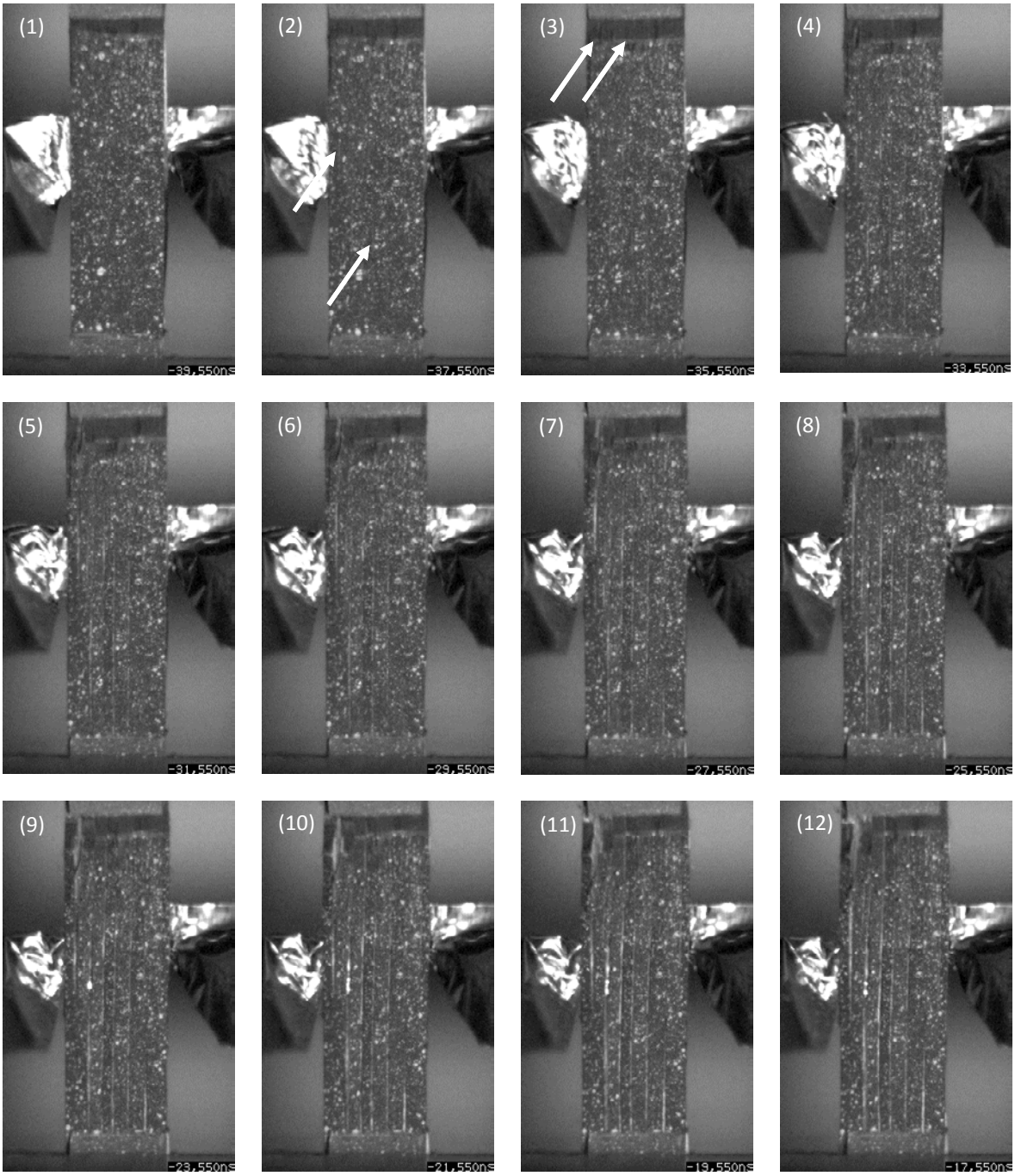

Fig. 4 Captured Images (Interval between captured images is 2 μs.)

First Edition: July, 2015

Shimadzu Corporation
www.shimadzu.com/an/

For Research Use Only. Not for use in diagnostic procedures.
The content of this publication shall not be reproduced, altered or sold for any commercial purpose without the written approval of Shimadzu.
The information contained herein is provided to you "as is" without warranty of any kind including without limitation warranties as to its accuracy or completeness. Shimadzu does not assume any responsibility or liability for any damage, whether direct or indirect, relating to the use of this publication. This publication is based upon the information available to Shimadzu on or before the date of publication, and subject to change without notice.
© Shimadzu Corporation, 2015

SHIMADZU
Excellence in Science

Application News

No.i256A

Material Testing System

Open-Hole Compression Test of Composite Material

Introduction

Carbon fiber reinforced plastic (CFRP) has gained attention due to their strength and low weight, and have quickly been adopted for use in aeronautics and astronautics. CFRP has excellent strength characteristics in terms of specific strength and high rigidity, but lose much of their strength when a cutout is made. Consequently, composite materials used in aeroplanes must be evaluated by tests that use specimens with a hole cut out of their center. We performed open-hole compression testing of a CFRP according to ASTM D6484.

Measurement System

The CFRP specimen used was T800S/3900. As shown in Fig. 1, a hole was created in the middle of the specimen. ASTM D6484 describes test methods in both SI and Imperial units, where the dimensions of the jigs and specimens differ in each. We performed testing with Imperial units. Specimen information is shown in Table 1.

ASTM D6484 includes two loading methods, which are described as Method A and Method B. In Method A, the specimen and test fixture are clamped in a gripping device, and the specimen is compressed by shear force applied by the fixture and gripping device. In Method B, compression plate is present at the ends of the specimen and fixture, and are used to compress the specimen. Method B was used, as shown in Fig. 2. Table 2 shows a list of the equipment used and Table 3 shows the test conditions used.

Table 1 Specimen Information

Length	: 305 mm
Width	: 38.1 mm
Thickness	: 3.1 mm
Lamination Method	: $[45/0/-45/92]_{2S}$

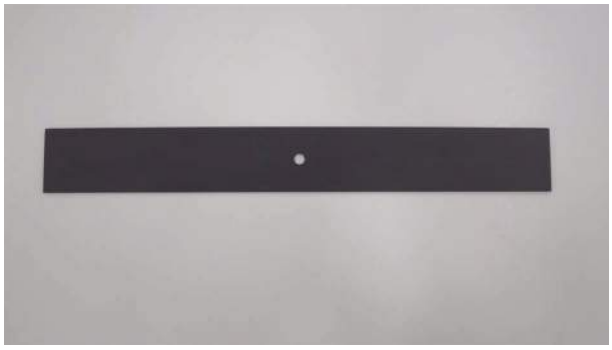

Fig. 1 Specimen

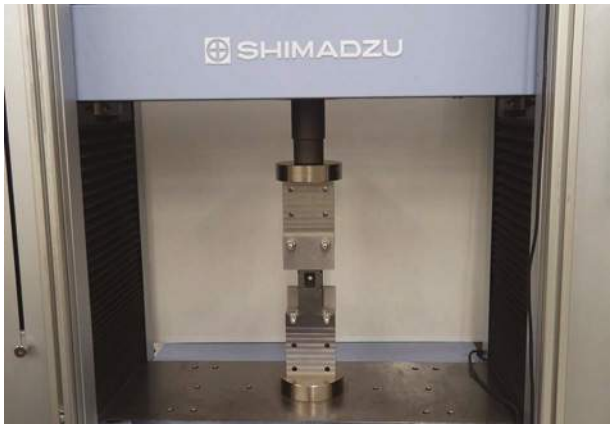

Fig. 2 Test Setup

Table 2 Experimental Equipment

Testing Machine	: AG-Xplus
Load Cell	: 50 kN
Test Fixture	: Open-Hole Compression Test Fixture

Table 3 Test Conditions

Test Speed : 2 mm/min

Results

Measurements were performed twice. Test results are shown in Table 4 and stress-displacement curves are shown in Fig. 3. As shown in Table 4, the mean open-hole compressive strength was 275.6 MPa.

Table 4 Test Results

Specimen Name	Open-Hole Compressive Strength
1st	278.2 MPa
2nd	273.0 MPa
Mean	275.6 MPa

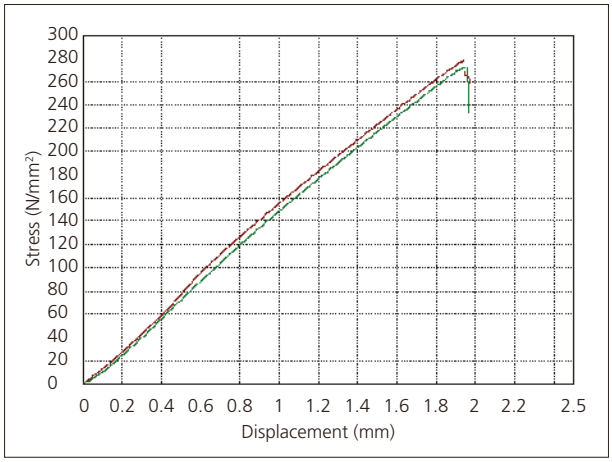

Fig. 3 Stress-Displacement Curves

Results (DIC Analysis)

Using the TRViewX non-contact extensometer allows for images and video of the specimen to be collected synchronized with test result collection. Also, applying a random pattern of paint to the observed specimen surface allows the images or video to be used to determine the strain distribution on the observed specimen surface during the test by DIC analysis[1]. Open-hole compression testing and DIC analysis were performed using the specimen described in Table 5. Fig. 4 shows a photograph of the open-hole compression test system with a non-contact extensometer. Fig. 5 shows strain distributions around the open hole in the specimen that were obtained by DIC analysis. Fig. 5 shows that strain accumulates at the vertical sides of the open hole (regions (1) and (3)), strain appears along the axis of compression from those points, and the final break occurs at the vertical sides of the hole. Meanwhile, almost no strain appears in the central part of the hole (region (2)) throughout the test. This strain distribution probably occurred due to a 0˚ fiber orientation on the surface of the specimen.

Table 5 Specimen Information (DIC)

Length	: 305 mm
Width	: 38 mm
Thickness	: 1.6 mm
Lamination Method	: $[0/90]_{2S}$

1) DIC analysis is an analysis method that measures strain and shows the strain distribution in a specimen based on movement of a random pattern of paint applied to the observed specimen surface before and during testing.

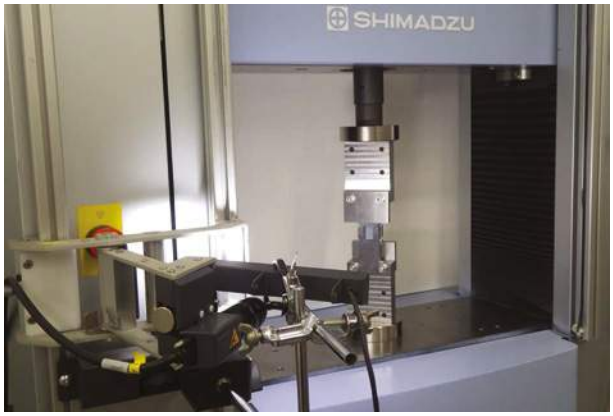

Fig. 4 Experimental Setup (DIC)

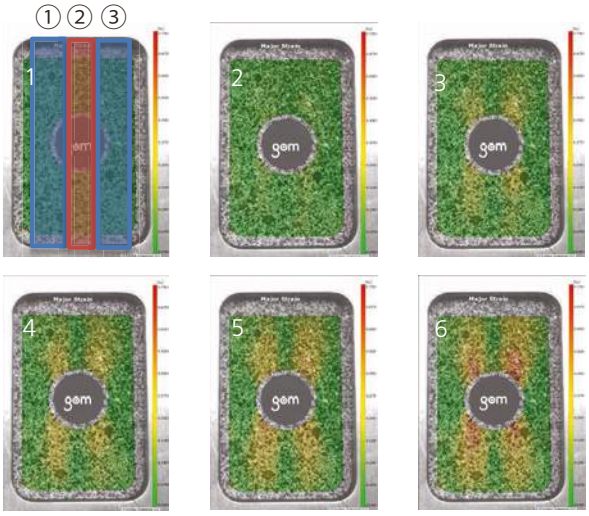

Fig. 5 DIC Analysis Results

Conclusion

Using this test system, open-hole compression testing of a CFRP was successfully performed according to ASTM D6484. Using a non-contact extensometer, we were also able to capture video (images) synchronized with the test force and crosshead displacement data obtained from the testing machine. Performing DIC analysis based on this video allowed an evaluation of the strain distribution on the observed specimen surface. This testing system will be extremely useful for the development of CFRPs and products that use CFRPs.

First Edition: Aug. 2016
Second Edition: Dec. 2016

SHIMADZU

Shimadzu Corporation
www.shimadzu.com/an/

For Research Use Only. Not for use in diagnostic procedure.
This publication may contain references to products that are not available in your country. Please contact us to check the availability of these products in your country.

The content of this publication shall not be reproduced, altered or sold for any commercial purpose without the written approval of Shimadzu. Company names, product/service names and logos used in this publication are trademarks and trade names of Shimadzu Corporation or its affiliates, whether or not they are used with trademark symbol "TM" or "®". Third-party trademarks and trade names may be used in this publication to refer to either the entities or their products/services. Shimadzu disclaims any proprietary interest in trademarks and trade names other than its own.

The information contained herein is provided to you "as is" without warranty of any kind including without limitation warranties as to its accuracy or completeness. Shimadzu does not assume any responsibility or liability for any damage, whether direct or indirect, relating to the use of this publication. This publication is based upon the information available to Shimadzu on or before the date of publication, and subject to change without notice.

© Shimadzu Corporation, 2016

SHIMADZU
Excellence in Science

Application News

No.i250

Material Testing System

Shear Test of Composite Material (V-Notched Beam)

Introduction

Carbon fiber reinforced plastic (CFRP) do not oxidize or rust and have a higher specific strength and stiffness than existing materials. Applications of CFRP are being investigated, with a focus on applications as industrial products that require strength and durability. Compared to existing homogeneous materials, composite materials like CFRP are anisotropic, and display complex failure behaviors as a result of tension, compression, bending, in-plane shear, out-of-plane shear, or a combination of these stresses arising from loading in the principal-axis direction. In recent years, use of CAE analysis in industry has become widespread since it can reduce numbers of prototypes and reduce the cost of new product development. Because values for each of the stress properties stated above are needed to increase precision when predicting product characteristics during product design, there is a strong demand for test methods able to evaluate pure failure behaviors in CFRP.

This article describes an example of V-notched beam method (Iosipescu method, ASTM D5379) that is widely used as an in-plane shear test method for composite material specimens. The test method can apply load as a pure in-plane shear stress on the evaluation area (see Fig. 1) by using a specimen cut with V-notches and supported at four asymmetrical points. Setting up the specimen and jig for this test method is relatively easy, and the test method can be used with a variety of CFRP laminate materials, including unidirectional materials, orthogonally laminated materials, and discontinuous fiber materials.

Measurement System

The equipment configuration is shown in Table 1. Information on the specimen prescribed by ASTM D5379 is shown in Fig. 1. The specimen is a $[0/90]_{10s}$ orthogonally laminated material made from Toray T800S prepreg that was molded in an autoclave. A two-axis strain gauge was attached at the mid-point between the upper and lower V-notches machined into the specimen (evaluation area), and oriented to measure strain in –45° and +45° directions. Shear strain can be calculated by inserting the strain values obtained from these two strain gauges into equation (1). Shear strain is a property needed to evaluate the shear modulus. In this test, strain gauges were attached on both the front and rear of the specimen. Calculating the mean of outputs obtained from strain gauges on both sides allows for more accurate measurement of the shear strain in the specimen, and confirms whether shear strain is being applied symmetrically on the front and rear of the specimen.

$$\gamma = |\varepsilon_{+45}| + |\varepsilon_{-45}|. \qquad \text{Equation (1)}$$

γ : Shear strain
ε_{+45} : Strain at +45°
ε_{-45} : Strain at –45°

Table 1 Test Conditions

Testing Machine	: AG-50kNX plus
Load Cell	: 50 kN
Test Jig	: ASTM D 5379 jig
Software	: TRAPEZIUM X (Single)
Test Speed	: 2 mm/min

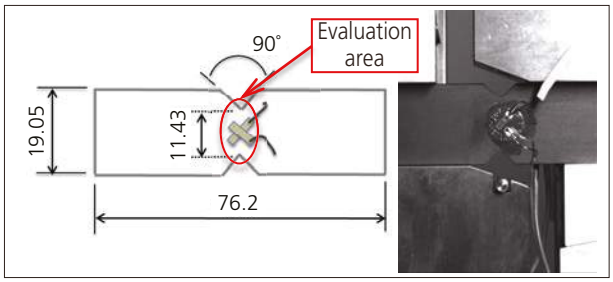

Fig. 1 Shape of Specimen

Fig. 2 Testing Apparatus

Fig. 3 Imaging Apparatus

The testing and imaging apparatus are shown in Fig. 2 and 3. Images captured using a TRViewX (Shimadzu Digital Video Extensometer) were gathered simultaneous to values obtained from the strain gauge outputs and specimen stress obtained by the testing apparatus. This made it easy to compare and evaluate images of the CFRP failure process against each specimen property values, something that was difficult to perform only with previous testing systems. Strain distribution can also be evaluated using digital image correlation (DIC, ARAMIS, GOMmbH) analysis of the images captured by TRViewX. To perform DIC analysis, paint must be sprayed on the specimen surface to create a random pattern on the front surface of the specimen.

Analytical Results

Each specimen property value obtained from this test is shown in Table 2. A photograph of the specimen after testing is shown in Fig. 4, a shear stress-normal strain curve is shown in Fig. 5 (strain values obtained from strain gauges), a shear stress-shear strain curve is shown in Fig. 6 (shear strain calculated from Equation (1)), and a shear stress-stroke curve is shown in Fig. 7. Table 2 shows that the results obtained for each shear property were highly reproducible. Fig. 5 and Fig. 6 show that the same strain values were obtained from the front and rear strain gauges, and highly symmetrical shear strain was applied to the specimen.

Table 2 Test Results

Specimen	Shear Modulus [GPa]	Shear Strength [MPa]
Test 1	4.62	136.0
Test 2	4.63	133.0
Test 3	4.50	131.0
Mean	4.58	133.0

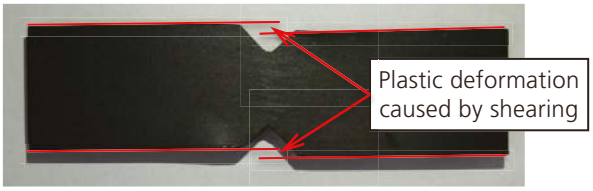

Fig. 4 Specimen After Testing

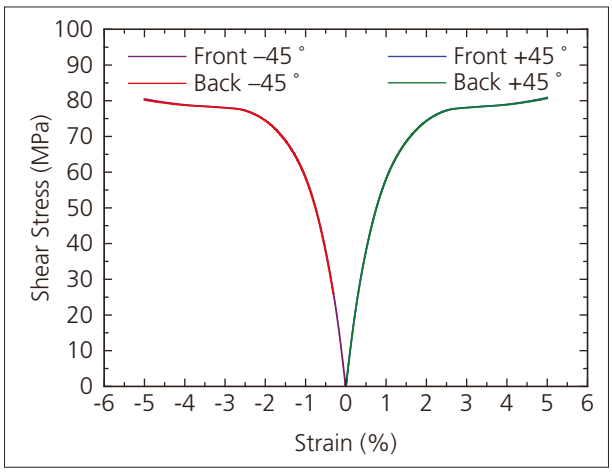

Fig. 5 Shear Stress-Normal Strain Curve

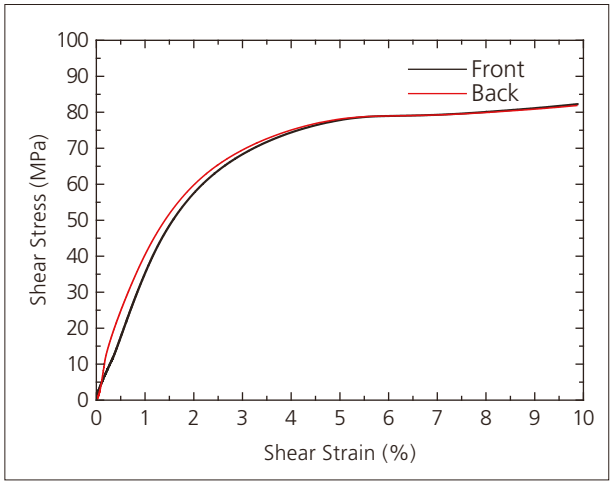

Fig. 6 Shear Stress-Shear Strain Curve

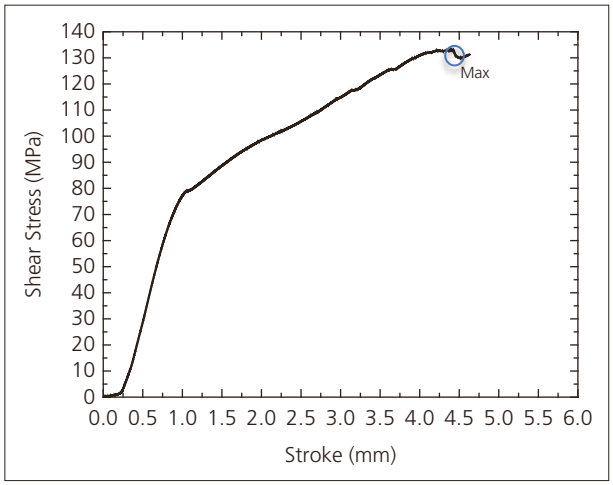

Fig. 7 Shear Stress-Stroke Curve

Failure of the specimen is shown in Fig. 8. Images of the shear strain distribution obtained by DIC analysis are shown in Fig. 9. The amount of strain occurring in the specimen is shown in terms of color, with low strain areas in cooler colors (black and blue) and high strain areas in warmer colors (orange and red). The images show that as the test progresses strain accumulates and is localized between the V-notches.

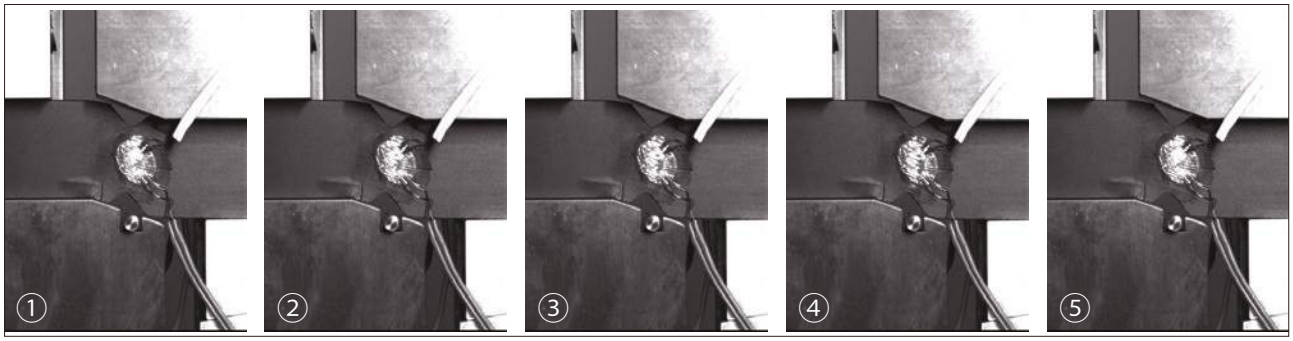

Fig. 8 Specimen e Failure Process (images show the point at which the specimen fails)

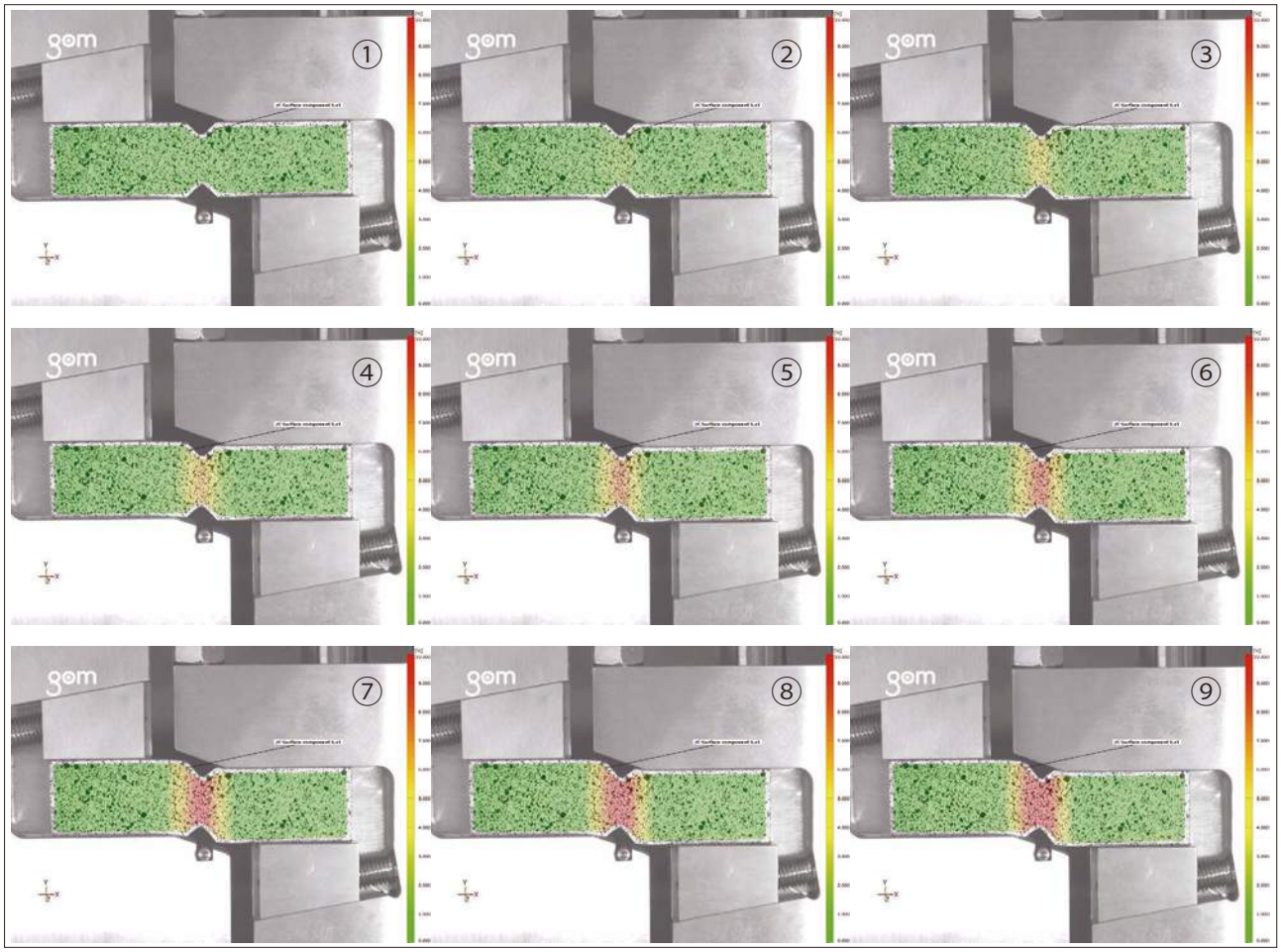

Fig. 9 Shear Strain Distribution (DIC analysis images)

Conclusion

We used this test system to successfully implement the V-notched beam method (ASTM D5379). In addition to evaluating the basic properties of shear modulus and shear strength, integrating a Digital Video Extensometer into the test system enabled us to capture reference data that can be used to elucidate the mechanism of failure of CFRP, allowing strain analysis to be performed in terms of specimen failure mode and DIC analysis.

First Edition: Aug. 2016

Shimadzu Corporation
www.shimadzu.com/an/

For Research Use Only. Not for use in diagnostic procedure.
This publication may contain references to products that are not available in your country. Please contact us to check the availability of these products in your country.

The content of this publication shall not be reproduced, altered or sold for any commercial purpose without the written approval of Shimadzu. Company names, product/service names and logos used in this publication are trademarks and trade names of Shimadzu Corporation or its affiliates, whether or not they are used with trademark symbol "TM" or "®". Third-party trademarks and trade names may be used in this publication to refer to either the entities or their products/services. Shimadzu disclaims any proprietary interest in trademarks and trade names other than its own.

The information contained herein is provided to you "as is" without warranty of any kind including without limitation warranties as to its accuracy or completeness. Shimadzu does not assume any responsibility or liability for any damage, whether direct or indirect, relating to the use of this publication. This publication is based upon the information available to Shimadzu on or before the date of publication, and subject to change without notice.

© Shimadzu Corporation, 2016

SHIMADZU
Excellence in Science

Application News

No.i251

Material Testing System

Shear Test of Composite Material (V-Notched Rail Shear)

Introduction

Carbon fiber reinforced plastic (CFRP) do not oxidize or rust and have a higher specific strength and stiffness than existing materials. Applications of CFRP are being investigated, with a focus on applications as industrial products that require strength and durability. Compared to existing homogeneous materials, composite materials like CFRP are anisotropic, and display complex failure behaviors as a result of tension, compression, bending, in-plane shear, out-of-plane shear, or a combination of these stresses arising from loading in the principal-axis direction. In recent years, use of CAE analysis in industry has become widespread since it can reduce numbers of prototypes and reduce the cost of new product development. Because values for each of the stress properties stated above are needed to increase precision when predicting product characteristics during product design, there is a strong demand for test methods able to evaluate pure failure behaviors in CFRP.

There are various tests methods for evaluating composite materials. Of these methods, two commonly used in-plane shear test methods to test in the direction of fibers in fiber reinforced composite materials and to test textile laminated materials are the Iosipescu method (ASTM D5379) that applies an asymmetrical four-point bending load to a specimen cut with notches, and method (ISO 14129) that applies a ±45° tensile load on laminated materials. We used the V-notched rail shear method (ASTM D7078) that can be used to test in-plane shear. Because this method uses a large gauge area on the specimen, it can accommodate specimens without holes and CRFP laminate materials that have discontinuous fibers.

Measurement System

The equipment configuration is shown in Table 1. Information on the specimen prescribed by ASTM D7078 is shown in Fig. 1. The specimen is a $[0/90]_{10s}$ orthogonally laminated material made from Toray T800S prepreg that was molded in an autoclave. The specimen has a 31-mm evaluation area (see Fig. 1), and two-axis strain gauges attached at the mid-point between the V-notches (center of evaluation area) that are able to measure strain in –45° and +45° directions. Shear strain can be calculated by inserting the strain values obtained from these two strain gauges into equation (1). Shear strain is a property needed to evaluate the shear modulus.

$$\gamma = |\varepsilon_{+45}| + |\varepsilon_{-45}|. \qquad \text{Equation (1)}$$

γ : Shear strain
ε_{+45} : Strain at +45°
ε_{-45} : Strain at –45°

In this test, strain gauges were attached on both the front and rear of the specimen. Calculating the mean of outputs obtained from strain gauges on both sides allows for more accurate measurement of the shear strain in the specimen, and confirms whether shear strain is being applied symmetrically on the front and rear of the specimen.

Table 1 Test Conditions

Testing Machine	: AG-50kNX plus
Load Cell	: 50 kN
Test Jig	: ASTM D7078 jig
Software	: TRAPEZIUM X (Single)
Test Speed	: 2 mm/min

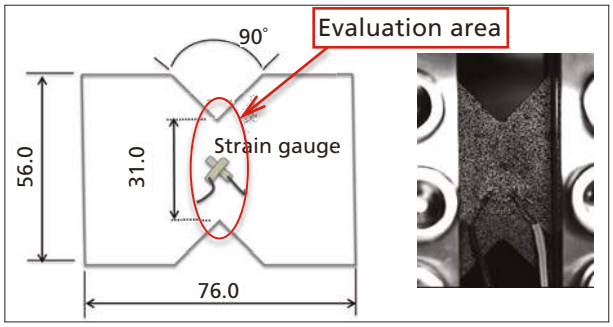

Fig. 1 Shape of Specimen

Fig. 2 Testing Apparatus

Fig. 3 Imaging Apparatus

The testing and imaging apparatus are shown in Fig. 2 and Fig. 3. Images captured using a TRViewX (Shimadzu Digital Video Extensometer) were gathered simultaneous to values obtained from the strain gauge outputs and specimen stress obtained by the testing apparatus. This made it easy to compare and evaluate images of the CFRP failure process against each specimen property values, something that was difficult to perform only with previous testing systems. Strain distribution can also be evaluated using digital image correlation (DIC, ARAMIS, GOMmbH) analysis of the images captured by TRViewX. To perform DIC analysis, paint must be sprayed on the specimen surface to create a random pattern on the front surface of the specimen.

Analytical Results

Each specimen property value obtained from this test is shown in Table 2. A photograph of the specimen after testing is shown in Fig. 4, a shear stress-normal strain curve is shown in Fig. 5 (strain values obtained from strain gauges), a shear stress-shear strain curve is shown in Fig. 6 (shear strain calculated from Equation (1)), and a shear stress-stroke curve is shown in Fig. 7. Table 2 shows that the results obtained for each shear property were highly reproducible. Fig. 5 and Fig. 6 show that the same strain values were obtained from the front and rear strain gauges, and highly symmetrical shear strain was applied to the specimen.

Table 2 Test Results

Specimen	Shear Modulus [GPa]	Shear Strength [MPa]
Test 1	4.63	121.72
Test 2	4.55	120.00
Test 3	4.58	120.05
Mean	4.59	120.60

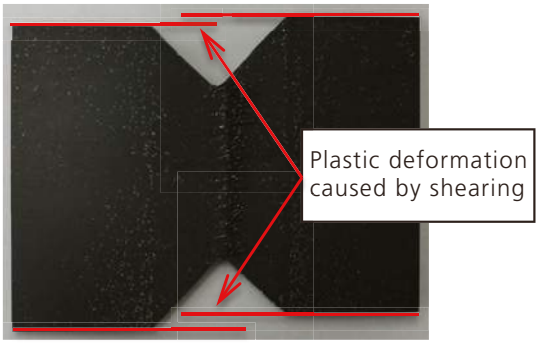

Fig. 4 Specimen After Testing

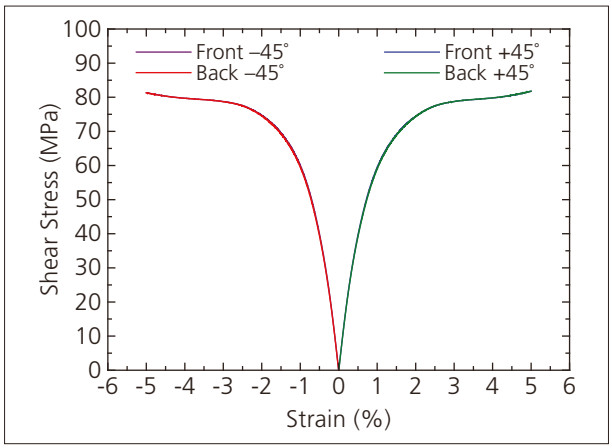

Fig. 5 Shear Stress-Normal Strain Curve

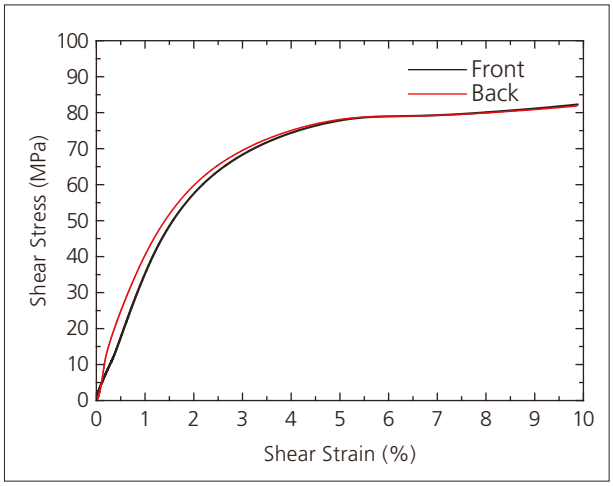

Fig. 6 Shear Stress-Shear Strain Curve

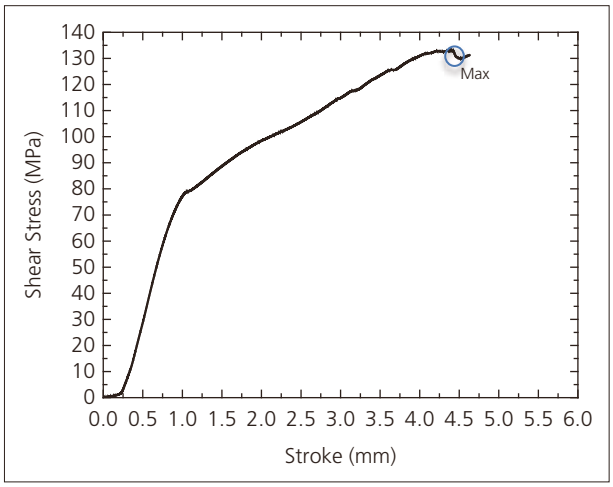

Fig. 7 Shear Stress-Stroke Curve

Failure of the specimen is shown in Fig. 8. A crack that appears close to the upper notch quickly propagates down toward the bottom notch during a simultaneous decrease in test force. Images of the shear strain distribution obtained by DIC analysis are shown in Fig. 9. The amount of strain occurring in the specimen is shown in terms of color, with low strain areas in cooler colors (black and blue) and high strain areas in warmer colors (orange and red). The images show that as the test progresses strain accumulates and is localized between the V-notches.

Fig. 8 Specimen Failure Process (images show the point at which the specimen fails)

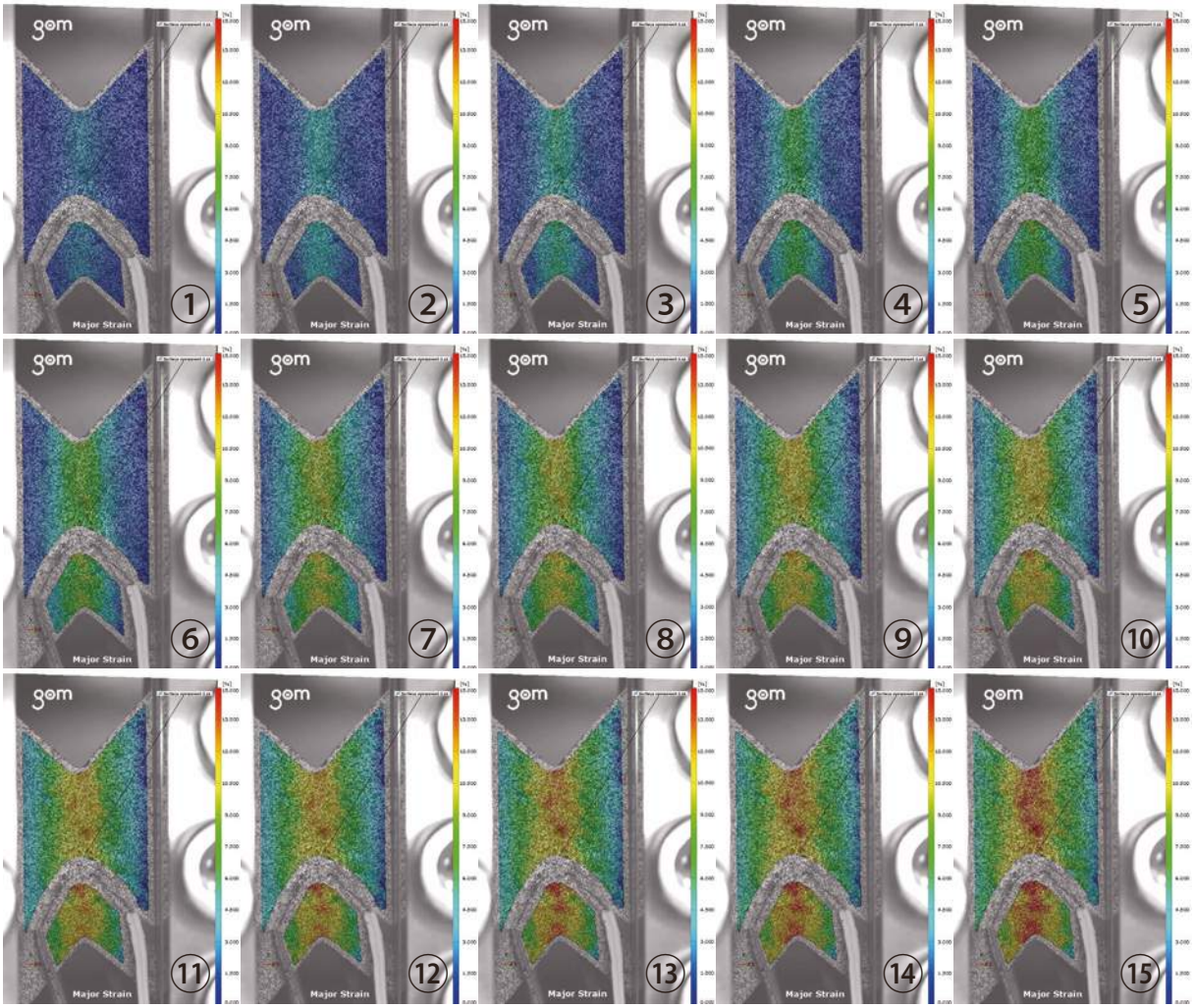

Fig. 9 Shear Strain Distribution (DIC analysis images)

Conclusion

We used this test system to successfully implement the V-notched rail shear method (ASTM D7078). In addition to evaluating the basic properties of shear modulus and shear strength, integrating a Digital Video Extensometer into the test system enabled us to capture reference data that can be used to elucidate the mechanism of failure of CFRP, allowing strain analysis to be performed in terms of specimen failure mode and DIC analysis.

First Edition: Aug. 2016

Shimadzu Corporation
www.shimadzu.com/an/

For Research Use Only. Not for use in diagnostic procedure.
This publication may contain references to products that are not available in your country. Please contact us to check the availability of these products in your country.

The content of this publication shall not be reproduced, altered or sold for any commercial purpose without the written approval of Shimadzu. Company names, product/service names and logos used in this publication are trademarks and trade names of Shimadzu Corporation or its affiliates, whether or not they are used with trademark symbol "TM" or "®". Third-party trademarks and trade names may be used in this publication to refer to either the entities or their products/services. Shimadzu disclaims any proprietary interest in trademarks and trade names other than its own.

The information contained herein is provided to you "as is" without warranty of any kind including without limitation warranties as to its accuracy or completeness. Shimadzu does not assume any responsibility or liability for any damage, whether direct or indirect, relating to the use of this publication. This publication is based upon the information available to Shimadzu on or before the date of publication, and subject to change without notice.

© Shimadzu Corporation, 2016

SHIMADZU
Excellence in Science

Application News

Material Testing System MCT

Compression-Rupture Test of Carbon Fibers with Different Tensile Characteristics Shimadzu Micro Compression Testing

No. SCA_300_037

■ Introduction

As the result of recent progress of research and development, carbon fiber materials have been put to practical use in a wide range of implements, including space aircraft parts, sporting goods like golf club shafts and tennis rackets, structure materials that must transmit X-rays, and acoustic materials.

A group of high-quality carbon fibers is further classified, according to its tensile strength, into several groups. One of these is a high-strength fiber group that features in excellent tensile strength; another is a high-elasticity fiber group characterized by high flexibility, but with a tensile strength of no more than around 2,000 MPa.

As described above, data on mechanical properties are indispensable information for classifying fibers.

The following is an example of tests for evaluation of physical behaviors under a compressive force applied to carbon fibers (single fibers) having different tensile strength levels with Shimadzu Micro Compression Testing Machine MCT.

■ Testing Conditions

(1) Testing mode: compression test
(2) Testing load: 200 gf
(3) Loading rate constant: 1 (4,230 gf/sec.)
(4) Calculation of strength: Compression strength is calculated by the following equation. *1

$$ST = 2 \cdot P \cdot \pi \cdot d \cdot L$$

where:
ST: tensile strength (kg/mm^2)
P: compression strength (kgf)
d: diameter of fiber (mm)
L: length of fiber (mm)

Note *1: from JIS A1113-1976 Method of tests for splitting tensile strength of concrete

■ Test Piece

(1) Name: Carbon fibers (PAN type carbon fibers)

(2) Types: 1 (high-ductility type)

2 (high-strength type)

3 (ultra-high elasticity type)

(3) Shape: See Fig. 1

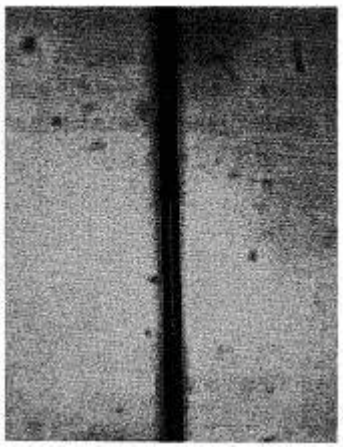

Fig. 1 A Microscopic photograph of Test Piece before Test

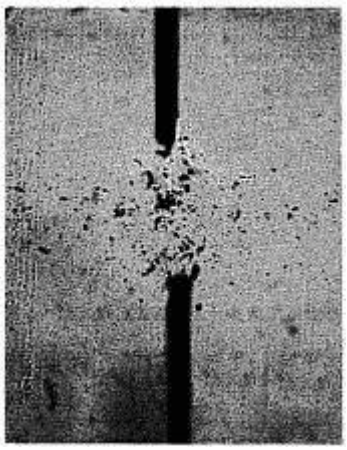

Fig. 2 A Microscopic photograph of Test Piece after Test

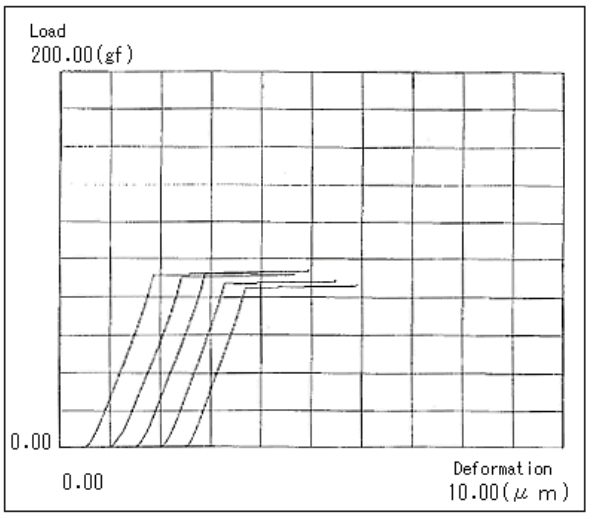

Fig. 3 Load- Deformation Curves of High Ductility Samples

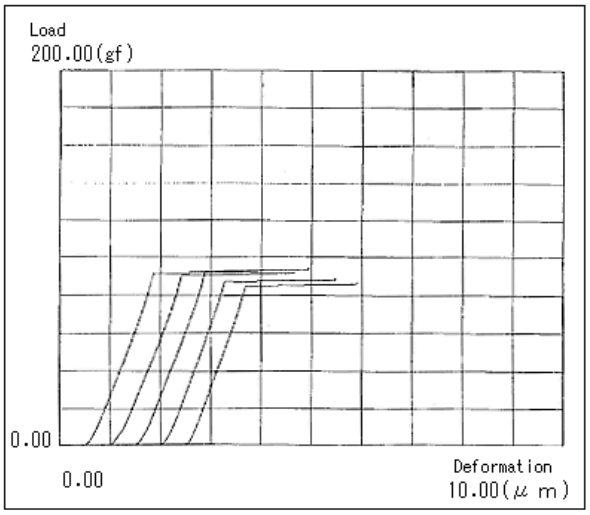

Fig.2 Load-Deformation Curves of High Ductility Samples

Fig. 4 Load- Deformation Curves of High Ductility Samples

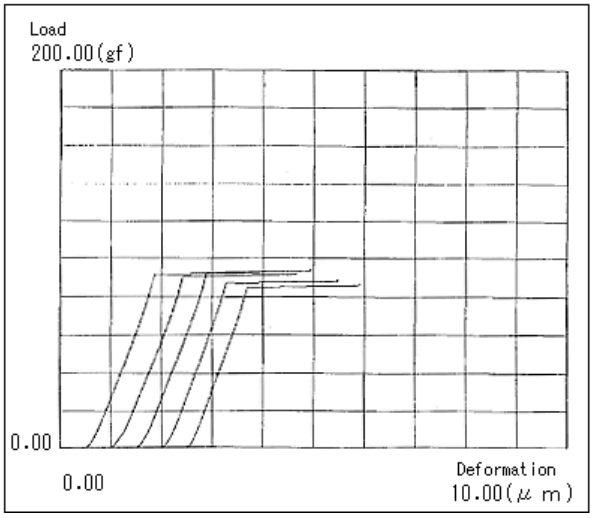

Fig. 5 Load- Deformation Curves of High Ductility Samples

Type of test piece	Compression-rupture strength(kgf/mm^2)	Standard deviation (kgf/mm^2)
High-ductility type	149.90	3.23
High-strength type	151.09	6.34
Ultra-high elasticity type	68.87	4.37

Table 1 Results of Compression-Rupture Test of Carbon Fibers

Note: The length of the indenter diameter (50 mm) was used for the length of fiber because the test piece was extraordinarily long.

■ Test Results

Table 1 shows a summary of test data, and Figs. 2-4 show the compression-rupture strength and the overlapping view of load-deformation curves for each test piece.

The difference of behavior between test pieces are observable in the load-deformation curves of Figs. 2-4.

The test pieces of the high-ductility type and the high-strength type have similar compression-rupture strength, while the ultra-high elasticity type has a remarkably low compression-rupture strength. (Refer to Table 1)

Admitting some deviation among the test data as a result of the surface conditions of the test pieces, the test results ensure that this testing machine is useful and effective for evaluation of mechanical properties of single fibers, provided that data are processed statistically.

* Please be advised that data obtained before the implementation of the current Weights and Measures Law may be presented in terms of gravimetric unit.

For Research Use Only. Not for use in diagnostic procedures.
The content of this publication shall not be reproduced, altered or sold for any commercial purpose without the written approval of Shimadzu. The information contained herein is provided to you "as is" without warranty of any kind including without limitation warranties as to its accuracy or completeness. Shimadzu does not assume any responsibility or liability for any damage, whether direct or indirect, relating to be the use of this publication. This publication is based upon the information available to Shimadzu on or before the date of publication, and subject to change without notice.

SHIMADZU
Excellence in Science

Application News

Material Testing System CFT

No. SCA_300_055

Viscosity Evaluation of Thermoplastic Resins (GFRP)

■ Introduction

Most mass produced molded plastic products are injection-molded. The appropriate temperature and pressure for injection molding differs depending on the type of resin and shape of the die, over-filling, under-filling, sink marks, voids, or other molding defects. Even if appropriate molding parameters are used, any changes in the status of the resin raw materials used could cause molding defects as well. Therefore, it control the quality of resin raw materials on a daily basis. Furthermore, it is important to perform the daily resin high pressure conditions that approximate molding conditions, which is not possible using the melt flowrate measurement method.

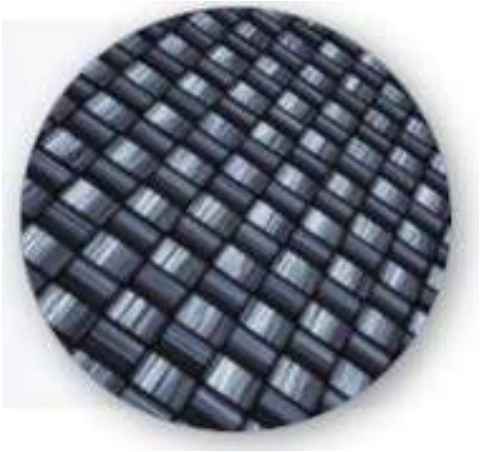

■ Viscosity Evaluation Using Constant Temperature Method

Polycarbonate (PC) samples of various molecular weights containing 33 % glass fiber (GF) were measured using constant temperature method. The flow curves clearly show that the higher the molecular weight, the higher the sample's viscosity.

Test Method	Constant temperature test
Die Diameter	1 mm
Die Length	10 mm
Test Temperature	280 ℃
Test Pressure	1.96 MPa
Preheating Time	300 sec
Sample Size	1.5 g

Test Conditions

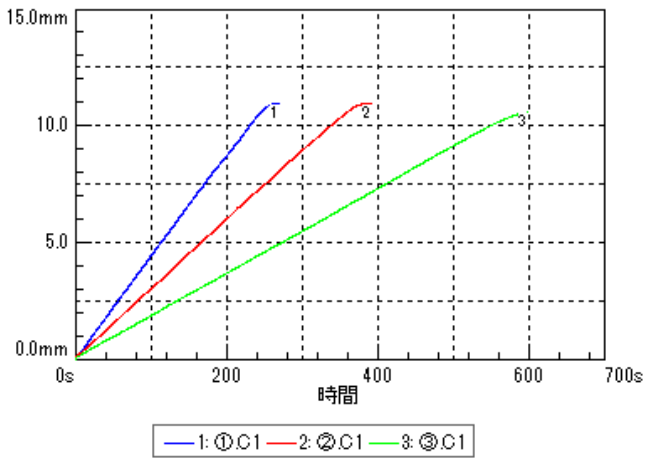

Test result

Sample No.	Component	Molecular Weight	GF Ratio (%)	Shear Rate (S^{-1})	Viscosity (Pa•s)
1	PC/SGF	17000	33	44,7	1,098
2	PC/SGF	22000	33	30,6	1,604
3	PC/SGF	26000	33	18,5	2,657

Test Results

■ Selection of Measurement Method According to Material

Constant Temperature Method

In the testing method based on the use of a constant temperature, two calculation points on the piston's descent are set beforehand. The calculation is conducted using either the limiting method or the automatic method. In the limiting method, the flowrate is determined from the stroke-time curve of the piston between the above two points. In the automatic method, the stroke-time curve is divided into 20 segments, and the flowrate is determined from the gradients of the curves of those segments except for the first and last segment, with the maximum value taken automatically as the flowrate.

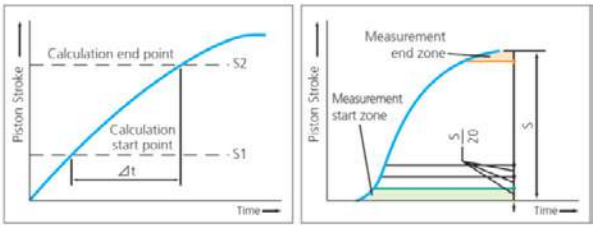

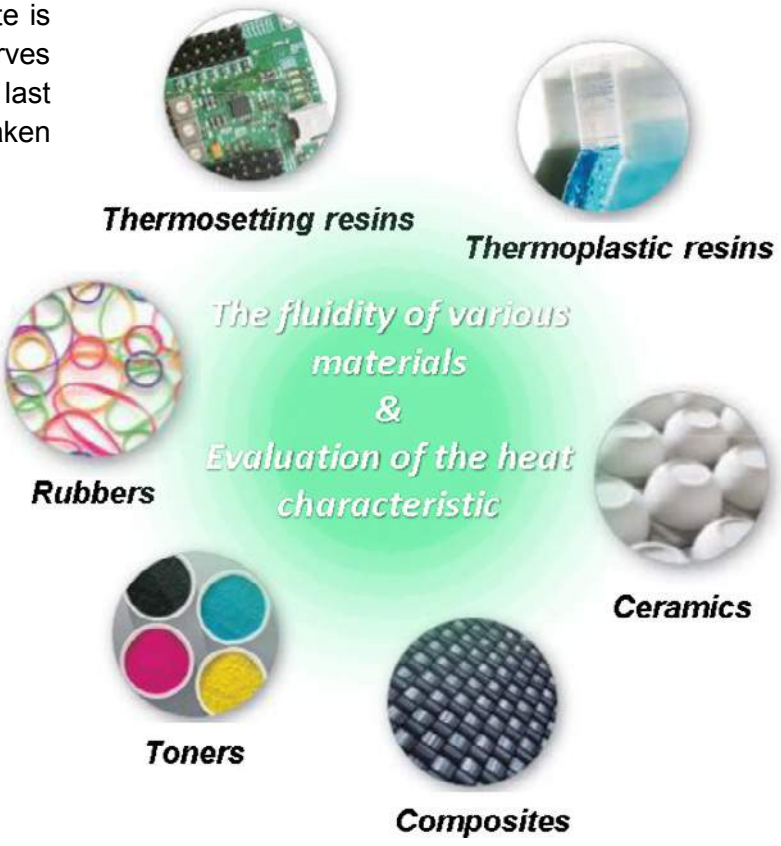

SHIMADZU

Shimadzu Europa GmbH
www.shimadzu.eu

For Research Use Only. Not for use in diagnostic procedures.
The content of this publication shall not be reproduced, altered or sold for any commercial purpose without the written approval of Shimadzu. The information contained herein is provided to you "as is" without warranty of any kind including without limitation warranties as to its accuracy or completeness. Shimadzu does not assume any responsibility or liability for any damage, whether direct or indirect, relating to be the use of this publication. This publication is based upon the information available to Shimadzu on or before the date of publication, and subject to change without notice.

SHIMADZU
Excellence in Science

Application News

Material Testing System CFT

No. SCA_300_056

Viscosity Evaluation of Thermoplastic Resins (GFRP)

Most mass produced molded plastic products are injection-molded. The appropriate temperature and pressure for injection molding differs depending on the type of resin and shape of the die, over-filling, under-filling, sink marks, voids, or other molding defects. Even if appropriate molding parameters are used, any changes in the status of the resin raw materials used could cause molding defects as well. Therefore, it control the quality of resin raw materials on a daily basis. Furthermore, it is important to perform the daily resin high pressure conditions that approximate molding conditions, which is not possible using the melt flowrate measurement method.

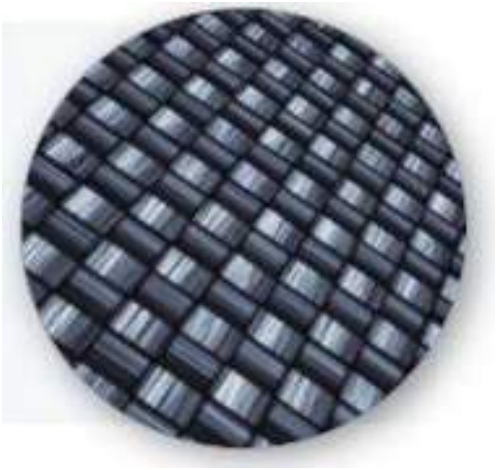

■ Changes in Viscosity Due to Moisture Absorption Time

The change in resin viscosity due to moisture absorption was measured using sample (1), with a molecular weight of 17,000. After drying for 13 hours in a vacuum environment at 100 °C, the sample was left in a room with a temperature of about 23 °C and about 50 % relative humidity for constant temperature testing. The graph shows that the fluidity increases and viscosity decreases as more moisture is absorbed. The results show that about 4 hours after leaving the sample there, viscosity drops sharply and then almost stops decreasing after about 24 hours. Due to the large changes in resin viscosity that result from moisture absorption, using resin materials that have not been controlled for moisture can result in injection molding failures.

Therefore, such injection molding problems can be avoided by using a CFT-EX series flowtester to measure the viscosity to ensure that it iswithin given standards before molding the parts.

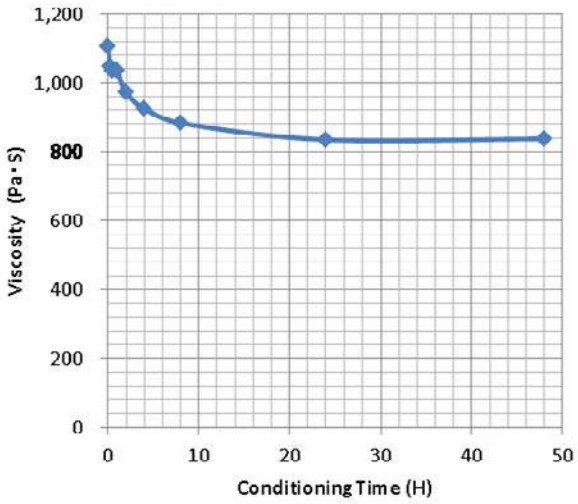

Test Results

Conditioning Time(H)	Share Rate (s^{-1})	Viscosity (Pa・s)
0	44,38	1,105
0,25	46,84	1,047
0,5	47,35	1,036
1	47,38	1,035
2	50,41	973
4	53,03	925
8	55,54	883
24	58,77	834
48	58,61	837

Test Results

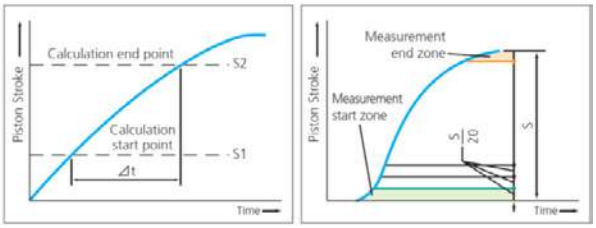

Limiting Method Automatic Method

■ Selection of Measurement Method According to Material

Constant Temperature Method

In the testing method based on the use of a constant temperature, two calculation points on the piston's descent are set beforehand. The calculation is conducted using either the limiting method or the automatic method. In the limiting method, the flowrate is determined from the stroke-time curve of the piston between the above two points. In the automatic method, the stroke-time curve is divided into 20 segments, and the flowrate is determined from the gradients of the curves of those segments except for the first and last segment, with the maximum value taken automatically as the flowrate.

■ CFT-EX Series

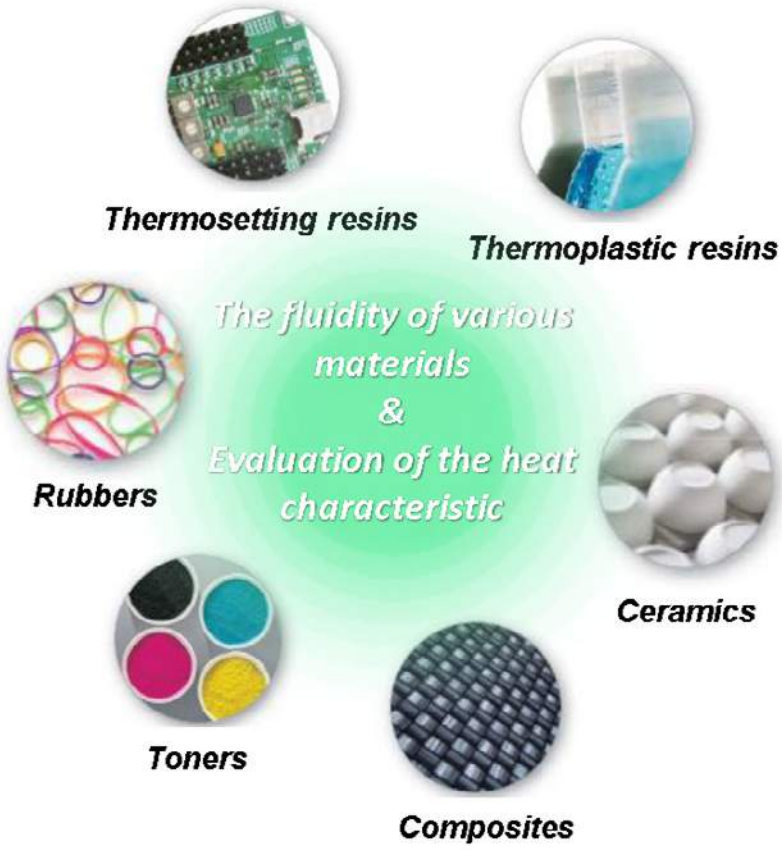

For Research Use Only. Not for use in diagnostic procedures.
The content of this publication shall not be reproduced, altered or sold for any commercial purpose without the written approval of Shimadzu. The information contained herein is provided to you "as is" without warranty of any kind including without limitation warranties as to its accuracy or completeness. Shimadzu does not assume any responsibility or liability for any damage, whether direct or indirect, relating to be the use of this publication. This publication is based upon the information available to Shimadzu on or before the date of publication, and subject to change without notice.

SHIMADZU
Excellence in Science

Application News

Material Testing System AG-X

No. SCA_300_059

Observation of fracture in CFRP tensile test

CFRP (carbon fiber reinforced plastic) has attracted attention as a high-performance composite material with high strength and rigidity, yet low in weight, and is being applied in various fields, such as for aircraft, railroad vehicles, automobiles and civil engineering. This example describes evaluating the characteristics of a flat plate specimen of CFRP material when a tensile load is applied (tensile test) and observing the fracture status. Tensile testing consisted of static testing of material strength and measuring the modulus of elasticity using a precision universal testing machine. In addition, high-rate tensile impact test was also performed. In the latter case, a high-speed video camera was used to record specimen fracture, which allowed capturing image data of the instant the CFRP material fractured.

■ Test specimen

The tensile test specimen tested in this example is shown in figure 1. Included 50 mm long CFRP tabs attached to both ends of the CFRP strip with thermosetting resin adhesive. Reinforcing the grip area with tabs ensures a stable tensile test with good reproducibility.

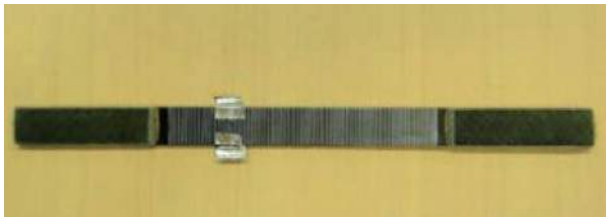

Figure 1: CFRP test specimen

Specimen details are as follows:

1) Material: unidirectional CFRP
2) Shape: strip (with tabs on both ends)
3) Specimen dimensions: for static tensile testing 200(L) x 12.5(W) x 1(T) mm. For recording image of impact fracture 70(L) x 6.25(W) x 0.3(T) mm

■ Static tensile test

A strain gauge type extensometer was attached to the specimen and a tensile test was performed using a precision testing machine. The extensometer was removed when strain exceeded the elasticity measurement range. It is also possible to measure strain by affixing a strain gauge instead of an extensometer. Tensile test parameters are indicated below.

(1) Tensile rate: 10 mm/min
(2) Grip distance: 100 mm
(3) Test force detection: 50 KN load cell
(4) Extensometer gauge length: 50 mm
(5) Elasticity calculation range: 5/10,000 to 25/10,000 strain

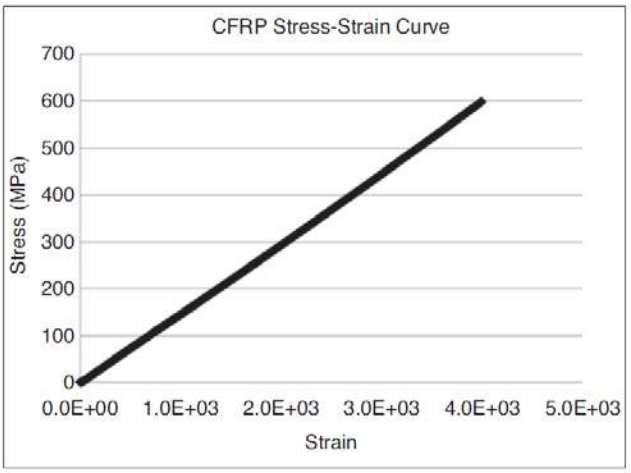

Figure 2: Static test results

The elasticity of CFRP specimen can be determined by calculating the slope of the given strain region (elasticity calculation range) in the stress-strain curve (figure 2) obtained from test results. Tensile strangth can be determined from the maximum stress in the stress-displacement curve (figure 3) before the specimen breaks.

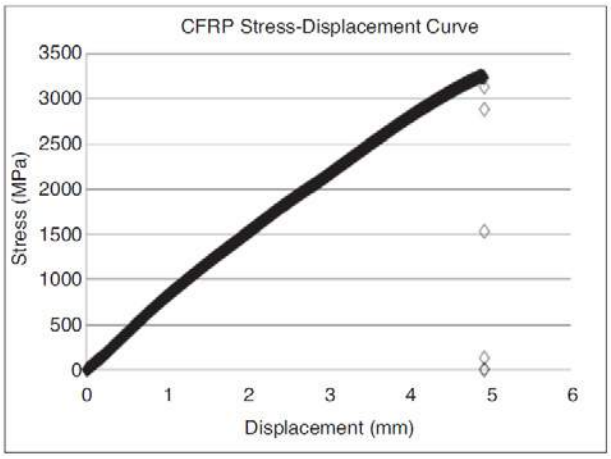

Figure 3: Static test results

The following values were obtained from the measurement data.

(1) Tensile strength: 346 GPa
(2) Elasticity: 148 GPa

The post-test status of the specimen is shown in figure 4. Compared to the starting status in figure 1, it clearly shows how the fibers within the resin have failed.

Figure 4: Specimen status after static test

■ Static tensile test

To verify functionality, development of composite materials involves not only static Static strength testing, but also involves the objective of ensuring active safety. Consequently, it is important to determine the shock strength and understand the process of fracture propagation. Therefore, the fracture process during tensile chock testing of a CFRP specimen was observed by combining a high-speed video camera with high-rate tensile shock test machine. Observation conditions are indicated below.

Specimen tensile rate:	6 m/s
Grip distance:	30 mm
Camera lens:	105 mm macro, with 2 x teleconverter
Camera lighting:	strobe
Camera trigger:	signal synchronized with tensile displacement is sent from testing machine to camera.

The setup used to record video of the test is shown in figure 5, with a high-speed video camera mounted about 450 mm in front of the specimen. Recording was activated by an external start trigger signal sent from the testing machine to the camera, which was synchronized to the tensile displacement. A strobe light synchronized to the video timing was used as lighting.

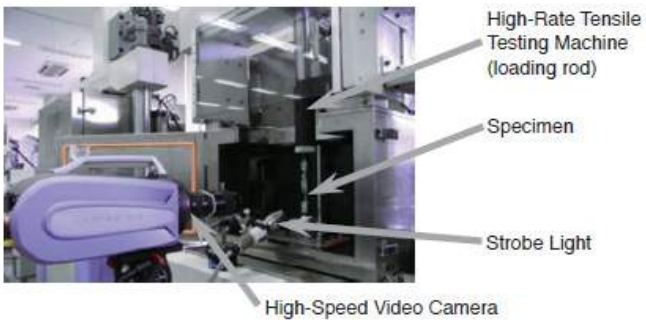

Figure 5: Setup of high-rate shock test

Using this test configuration, a load was applied to the CFRP specimen according to the parameters indicated above and a high-speed camera captured the instant of fracture, at 250.000 frames per second. This image data shown in figure 6.

This shows 8 consecutive frames, from (1) TO (8), with an interval of 4 microseconds between each frame. This camera features highly detailed image resolution of 312 horizontal by 260 vertical pixels that is constant, regardless of the frame rate.

This example shows, combining a high-speed video camera and material testing machine makes it possible to evaluate material properties and observe fracture behavior at the same time. This enables supporting a wide range of material development applications, from developing individual functionally enhanced resins to developing composite materials.

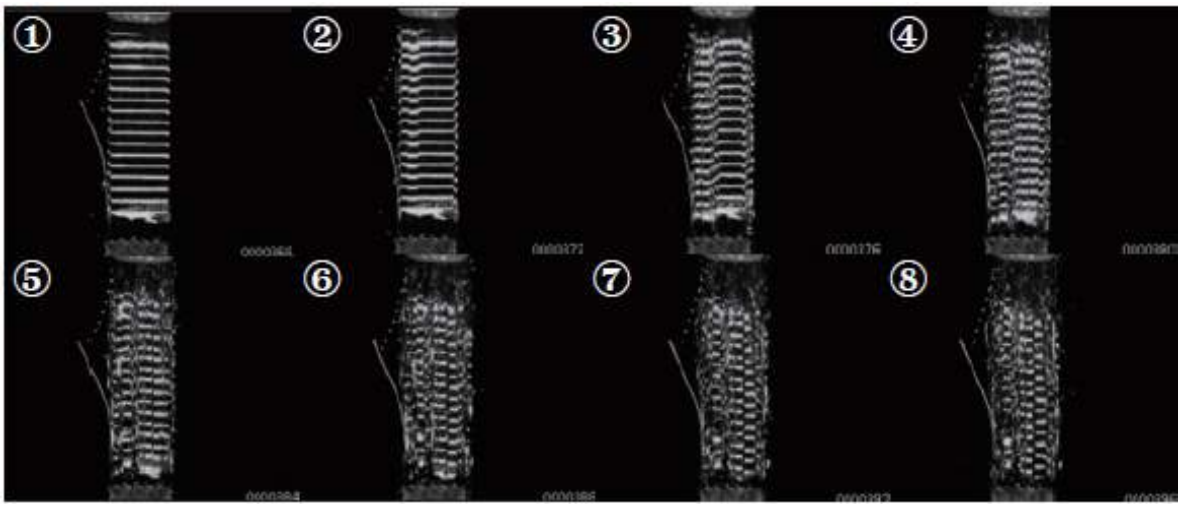

Figure 6: Images of specimen during fracture

For Research Use Only. Not for use in diagnostic procedures.
The content of this publication shall not be reproduced, altered or sold for any commercial purpose without the written approval of Shimadzu. The information contained herein is provided to you "as is" without warranty of any kind including without limitation warranties as to its accuracy or completeness. Shimadzu does not assume any responsibility or liability for any damage, whether direct or indirect, relating to be the use of this publication. This publication is based upon the information available to Shimadzu on or before the date of publication, and subject to change without notice.

SHIMADZU
Excellence in Science

5. Food Industry

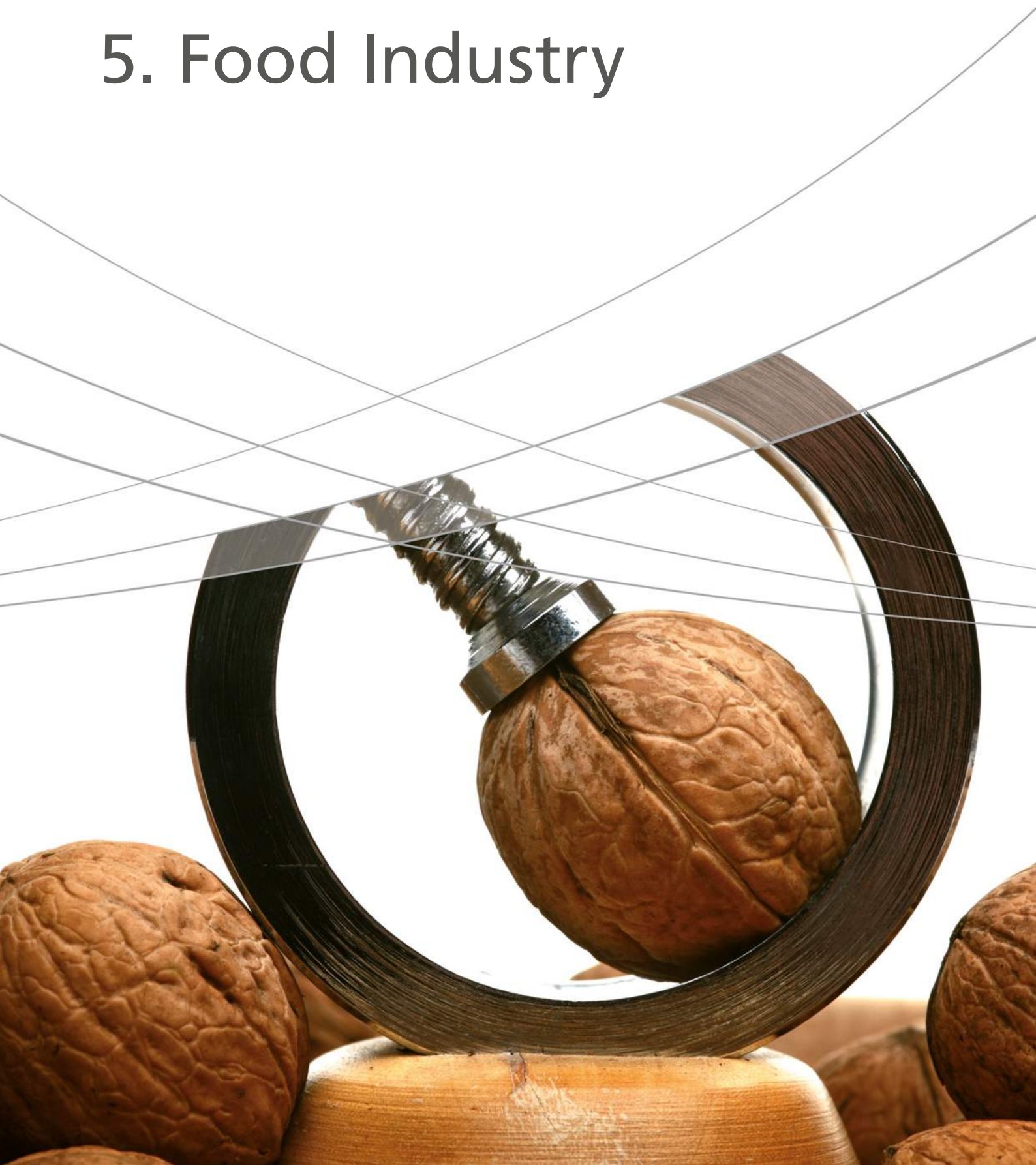

5. Food Industry

CONSISTENT QUALITY FOR THE RIGHT LOOK, FEEL, SHAPE AND TASTE

Food & beverages are very emotional products: although people either like or dislike certain products, food is in general associated with fun and enjoyment, with culture, style and way-of life. A further psychological aspect around food: we give food access into our bodies.

To stimulate consumption on a regular basis, food products also have to have a consistent quality regarding the right look, feel, shape and taste. Food designers, manufacturers and processors are aware of these challenges, particularly when handling natural products.

Today, food and beverages production is run and controlled by advanced technologies. They are used for natural, agricultural and meat products, but also for food and beverages which have been mixed in laboratories or production plants.

Food texture is the sense of touch when food is handled, the visual sense recorded by eye and oral touch sensation and palatability. Food products are tested for their mechanical characteristics, hardness, cohesive and elastic qualities as well as adhesiveness.

Whether butter, margarine, agar, pork, jelly bears or pickled plums – please see the multitude of applications on the following pages.

Szczesniak Texture Profile Analysis
Mechanical characteristics

1st characteristic	2nd characteristic	General Term	Characteristic content
Hardness		Soft / teeth resistance / hard	Required force for even deformation and internal binding power providing food product shape
Cohesive quality	Brittleness	Crumbly / Munchy / Brittle	Related to the force, hardness and cohesive quality when chewing a food product
	Masticable quality	Soft / tough	Relation between energy, hardness, cohesive quality and elastic quality required for mastication up to the point of swallowing a compressed food product
	Gum quality	Easy loss of shape / powder state / paste state / rubber state	Relation between energy, hardness and cohesive quality, required for mastication up to the point of swallowing a semi-compressed food product
Cohesiveness		Dry / cohesive	Degree of fluidity at force for displacement
Elastic quality		Plasticity / elasticity	Rate at which food that is deformed by an external force but returns to original shape after external force is released
Adhesiveness		Glutinous / adhesiveness / stickiness	The force required to overcome traction between the surface of a food product and items such as tongue teeth, and palate

5. Food Industry

No.i246	Texture evaluation of care food
No.11	Evaluation of foods for people with dysphagia
No.21	Compression tests of microcapsules containing aroma components
No.12	evaluation of food texture
SCA_300_003	An application of Shimadzu flowtester model CFT to food products
SCA_300_004	An evaluation of viscosity of non-vulcanized rubber by Shimadzu flow tester
SCA_300_005	Cereal compression shear test evaluation of food
SCA_300_006	Chewing properties of gummy bears test
SCA_300_015	Evaluation of texture using a multi-piercing jig evaluation of food
SCA_300_016	Evaluation test of butter and margarine evaluation of foods
SCA_300_027	Measurement of texture characteristics of rice using title line the EZ test Shimadzu texture analyzer
SCA_300_032	Texture evaluation of cheese and agar jelly
SCA_300_042	Evaluation test of foods for people with difficulty swallowing
SCA_300_046	Measurement of texture of pork by a penetrating strength test
SCA_300_048	Multifaceted measurement of plums pickled in plum wine
SCA_300_051	Texture analysis of "soumen" japanese vermicelli
SCA_300_052	Texture analysis of ikura salted
SCA_300_053	Texture evaluation of cheese and agar jelly

SHIMADZU

Application News

No.i246

Material Testing System

Texture Evaluation of Care Food

Introduction

The development of care food, which is processed to be soft and easy to eat, is steadily progressing to the point that the shape, color and taste are nearly indistinguishable from ordinary food, except that the texture is softened to enable crushing using just the gums and tongue. These commercially available products are a great boon to the elderly and individuals with internal mouth injuries who may have inadequate strength for chewing and drinking, and are helping these disadvantaged groups to better enjoy the pleasures of tasting and eating. Meanwhile, according to the Health Promotion Law in Japan, the Japan Consumer Affairs Agency is authorized to conduct reviews of the suitability of "foods for people with dysphagia" as regulated special purpose foods, and based on these reviews, permit the display of such foods.

Here, we conducted measurements of commercially available care food based on the test methods specified for reviewing the suitability of foods for people with dysphagia. We then classified the food according to the specific standard based on the obtained hardness, adhesiveness, and cohesiveness data.

Testing Equipment and Specimens

The instrument used for this evaluation was the Shimadzu EZ Test Texture Analyzer, with a 5N test force measurement load cell. The samples used consisted of 3 commercially available care food products (sample names: A – C).

Test Conditions

An overview of the measurement setup is shown in Fig. 1. The sample diameter was 40 mm, and the sample was loaded to a height of 15 mm in the 20 mm high sample container. Using a plastic plunger 20 mm in diameter and 8 mm in height, compression testing was conducted twice at a speed of 10 mm/sec with a clearance of 5 mm. The test was conducted using a sample temperature of 20 °C.

Test Results

The results obtained from testing of 3 types of food products are shown in the force – time graphs of Fig. 2 – Fig. 4.

Fig. 1 Overview of Texture Test

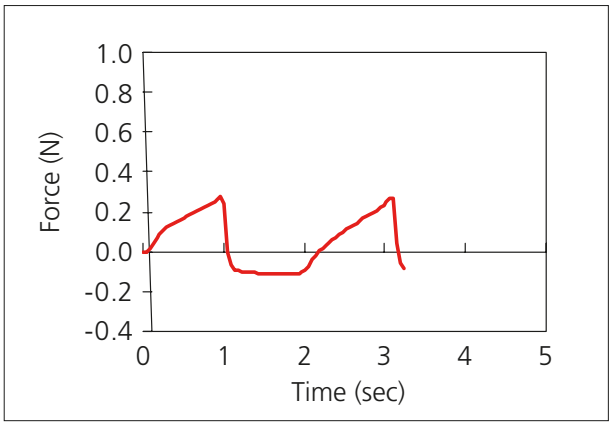

Fig. 2 Food A (vegetable soup)

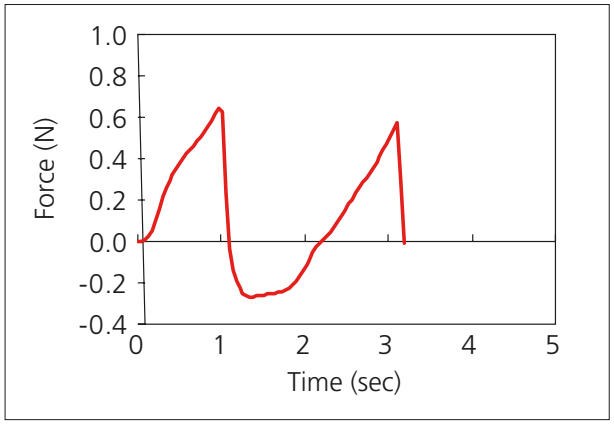

Fig. 3 Food B (rice gruel)

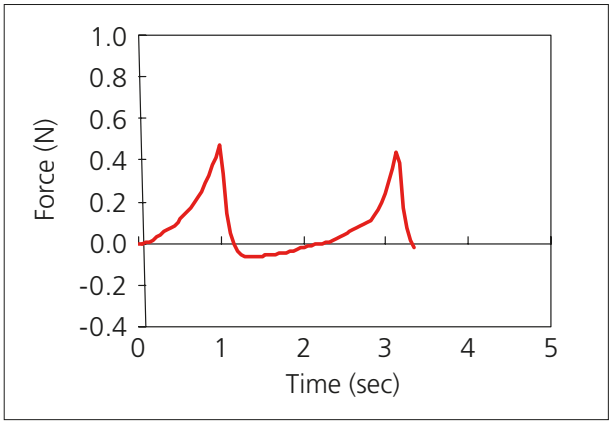

Fig. 4 F ood C (sukiyaki)

The results obtained from the series of measurements are shown in Table 1.

Table 1

Sample	Hardness		Adhesiveness		Cohesiveness		Permissible Standard (Overall Judgment)
	Measured Value (N/m^2)	Judgment	Measured Value (J/m^3)	Judgment	Measured Value	Judgment	
Food A	0.84×10^3	Ⅰ, Ⅱ, Ⅲ	0.19×10^3	Ⅰ, Ⅱ, Ⅲ	0.82	Ⅰ, Ⅱ	Ⅲ
Food B	1.97×10^3	Ⅰ, Ⅱ, Ⅲ	0.41×10^3	Ⅰ, Ⅱ, Ⅲ	0.76	Ⅰ, Ⅱ	Ⅲ
Food C	1.88×10^3	Ⅰ, Ⅱ, Ⅲ	0.08×10^3	Ⅰ, Ⅱ, Ⅲ	0.52	Ⅰ, Ⅱ	Ⅲ

The measured values for hardness, adhesiveness and cohesiveness that are within the range of the permissible standard are indicated with a □ that surrounds the standards in the Judgment field. Food A does not satisfy the hardness standards Ⅰ and Ⅱ, so the permissible standard was designated as Ⅲ. In the case of foods B and C, item Ⅰ is not satisfied, so the permissible standard would be presumed to be Ⅱ. However, the permissible standard becomes Ⅲ in the final evaluation, because food B and food C contain non-homogeneous ingredients. Thus, by defining the numerical value and comparing it with the judgment standards, the judgment can be made as to which permissible standard it corresponds.

[Reference]
(Permissible Standards of Foods for People with Dysphagia Note 1))
Note 1) Regarding permission to display special usage foods (Excerpted from Ministry of Health, Labour and Welfare Food Safety Notification No. 0212001)

Standard*1	Permissible Standard Ⅰ *2	Permissible Standard Ⅱ *3	Permissible Standard Ⅲ *4
Hardness (Resistance during compression at constant rate) (N/m^2)	2.5×10^3 - 1×10^4	1×10^3 - 1.5×10^4	3×10^2 - 2×10^4
Adhesiveness (J/m^3)	4×10^2 or less	1×10^3 or less	1.5×10^3 or less
Cohesiveness	0.2 - 0.6	0.2 - 0.9	-

*1 Within the permissible range of the standard under conditions of either of ambient temperature or the normal temperature at which eating takes place.
*2 Homogeneous items (for example, jellied foods)
*3 Homogeneous items (for example, jellied or smooth foods). However, this excludes foods that satisfy permissible standard Ⅰ.
*4 Includes non-homogeneous foods (for example, rice gruel which is easily clumped or collected, soft paste-like or jellied foods). However, this excludes foods that satisfy permissible standard Ⅰ or permissible standard Ⅱ.

First Edition: January, 2012

SHIMADZU

SHIMADZU Corporation
www.shimadzu.com/an/

For Research Use Only. Not for use in diagnostic procedures.
The contents of this publication are provided to you "as is" without warranty of any kind, and are subject to change without notice.
Shimadzu does not assume any responsibility or liability for any damage, whether direct or indirect, relating to the use of this publication.

© Shimadzu Corporation, 2012

SHIMADZU
Excellence in Science

Application Data Sheet

No.11

EZTest Compact Table-Top Universal Tester

Material Testing & Inspection

Evaluation of Foods for People with Dysphagia

Consumer Affairs Agency, Government of Japan, Food Labeling Notification No. 277
(Permission of Labeling for Foods for Special Dietary Uses)

Introduction

Foods for people with dysphagia are easy to swallow, and intended to prevent pulmonary aspiration and suffocation. In recent years, there has been an increase in people with dysphagia due to an aging population, so the demand for these commodities has increased. In the home medical care context, selecting appropriate meals is important, and using foods for people with dysphagia is one aspect of this. This article introduces a system for measuring hardness, adhesion, and agglomeration, evaluation items based on the Consumer Affairs Agency of Japan's Food Labeling Notification No. 277 (Permission of Labeling for Foods for Special Dietary Uses).

F. Yano

Measurements and Jigs

Fig. 1 shows a schematic diagram of the tools used in evaluating foods for people with dysphagia. The sample is used to fill a container with a diameter of 40 mm to a height of 15 mm. Compression measurement is then done twice using a resin plunger with a diameter of 20 mm and a height of 8 mm, at a compression speed of 10 mm/sec and a clearance of 5 mm. For foods that are chilled or eaten at room temperature, the test is conducted at 10 °C ± 2 °C and 20 °C ± 2 °C. For foods that are eaten warmed, the test is conducted at 20 °C ±2 °C and 45 °C ± 2 °C.

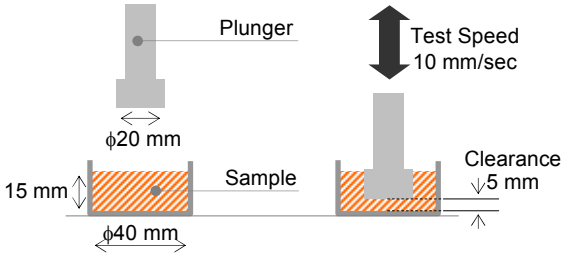

Fig. 1: Schematic Diagram of the Evaluation Test for Foods for People with Dysphagia

Measurement Results

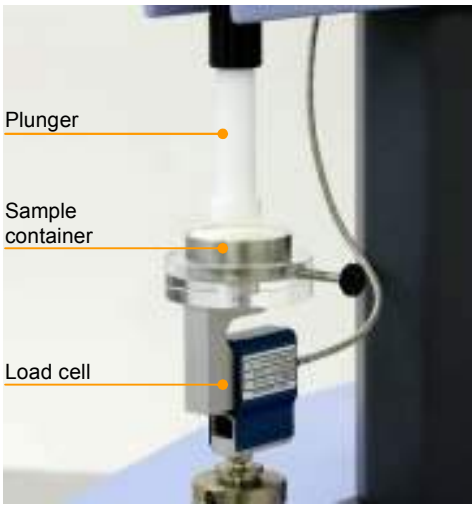

Fig. 2: Food Test Evaluation Jigs

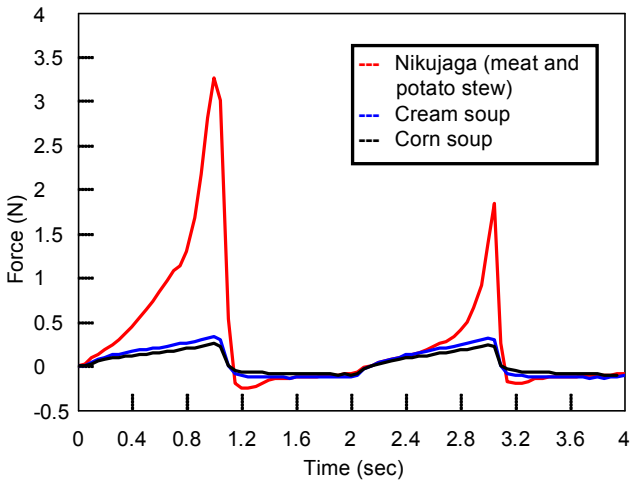

Fig. 3: Food Test Evaluation Results

Table 1: Test Conditions

Item	Set Value
Test Speed	10 mm/s
Clearance	5 mm
No. of Repetitions	2
Test Temperature	20 °C

Table 2: Test Results

Sample	Hardness (N/m²)	Adhesion (J/m³)	Agglomeration	Standard (judgment)
Nikujaga (meat and potato stew)	1.04×10^4	0.246×10^3	0.21	III
Cream soup	1.07×10^3	0.206×10^3	0.78	II
Corn soup	0.81×10^3	0.129×10^3	0.78	III

Evaluation System for Foods for People with Dysphagia

Tester:	EZ-SX
Load Cell:	50 N
Test Jig:	Universal Design Food Test Set
Software:	TRAPEZIUM X Texture
Thermostat:	Thermo-constant cooler/heater (separately installed)

EZTest Compact Table-Top Universal Tester

Features

- Light and compact
  The compact size fits easily on tables. Testing can be performed in a corner of the office.
- A high-precision load cell is adopted. (The high-precision type is class 1; the standard-precision type is class 0.5.)
  Accuracy is guaranteed over a wide range, from 1/500 to 1/1 of the load cell capacity. This supports highly reliable test evaluations.
- Jog controller (optional)
  This allows hand-held control of the crosshead position. Fine position adjustment is possible using the jog dial.
- TRAPEZIUM X Texture operational software
  This is the optimal software for a variety of pharmaceutical and cosmetic quality evaluations and physical characteristics measurements, as well as food texture measurements. It can create flexible control patterns and data processing items specific to foods, including hardness, brittleness, and energy.
- A wealth of specialized jigs
  Supporting the many needs of our customers with special jigs and applications for a number of fields, including foods, pharmaceuticals, electrical machinery & electronics, and plastics.

First Edition: February 2013

SHIMADZU

Shimadzu Corporation

www.shimadzu.com/an/

For Research Use Only. Not for use in diagnostic procedures.
The content of this publication shall not be reproduced, altered or sold for any commercial purpose without the written approval of Shimadzu.
The information contained herein is provided to you "as is" without warranty of any kind including without limitation warranties as to its accuracy or completeness. Shimadzu does not assume any responsibility or liability for any damage, whether direct or indirect, relating to the use of this publication. This publication is based upon the information available to Shimadzu on or before the date of publication, and subject to change without notice.

© Shimadzu Corporation, 2013

SHIMADZU
Excellence in Science

Application Data Sheet

No. 21

Micro Compression Testing Machine

Material Testing & Inspection

Compression Tests of Microcapsules Containing Aroma Components

Introduction

Recently, some washing agents include microcapsules containing aroma components, in order to sustain the smell of clothes after washing. The diameter of these microcapsules is in the order of several tens of μm, and when the appropriate pressure or friction is applied, the beads burst open and the fragrance is released. This Application Data Sheet describes compression tests carried out on microcapsules containing aroma components using an MCT Series Micro Compression Testing Machine.

F Yano

Measurement and Jigs

The diameters of the microcapsule particles measured with an optical microscope were about 10 to 20 μm, and a flat indenter with a tip diameter of 120 μm was used as the upper pressure indenter. Table 1 shows the test conditions.

Table 1 Test Conditions

Item	Set Value
Test speed	3.87 mN/s
Indenter	Flat indententer 120 μm dia.

Fig.1 Photograph Taken Using a Microscope

Measurement Results

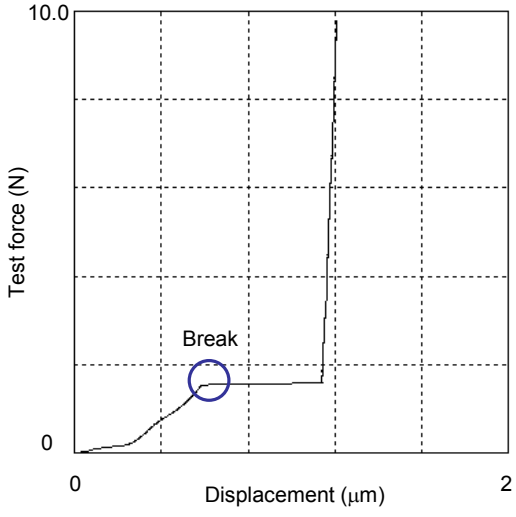

Fig. 2 Test Results

Table 2 Bead Compression Testing Results

Test Force at Break	Displacement at Break	Particle Diameter
1.57 mN	0.96 μm	9.01 μm

Microcapsule Compression Test System

Tester:	MCT
Indenter:	Truncated cone flat indenter (dia.: 120 μm)
Length measurement	Length measurement kit
Side observation:	Side observation kit

MCT Micro Compression Testing Machine

Features

■ Measurement of Minute Compression Displacements
In order to evaluate the compression properties of minute test specimens, two types of testers with different measurement ranges are provided, for measurements up to 100 μm with a resolution of 0.001 μm, and for measurements up to 10 μm and resolution of 0.0001 μm.

■ Wide Loading Range
In order to compress minute test specimens, two types are provided with maximum forces of 4903 mN and 1961 mN respectively.

■ High Accuracy Measurements
The accuracy of measurement is within ±1 % of the set or displayed test force, whichever is greater.

■ Sample Size Measurement Function Provided as Standard
The sample size measurement function using an overhead image is provided as standard. It allows determination of the geometric mean diameter, length, etc.

■ Length Measurement on PC Screen and Saving of Images (optional)
Use the length measurement kit (color or monochrome) to display the overhead image on the PC screen to measure the length of the sample. The image can be saved as digital data.

■ Display of Sample Images During Compression (optional)
Images captured in side observation during compression can be displayed (the optional side observation kit is required).

■ Testing Possible under High-Temperature Conditions (optional)
Testing can be performed in temperature conditions ranging from 50 to 250 °C.

First Edition: February 2013

SHIMADZU

Shimadzu Corporation
www.shimadzu.com/an/

For Research Use Only. Not for use in diagnostic procedures.
The content of this publication shall not be reproduced, altered or sold for any commercial purpose without the written approval of Shimadzu.
The information contained herein is provided to you "as is" without warranty of any kind including without limitation warranties as to its accuracy or completeness. Shimadzu does not assume any responsibility or liability for any damage, whether direct or indirect, relating to the use of this publication. This publication is based upon the information available to Shimadzu on or before the date of publication, and subject to change without notice.
© Shimadzu Corporation, 2013

SHIMADZU
Excellence in Science

Application Data Sheet

No.12

EZTest Compact Table-Top Universal Tester

Material Testing & Inspection

Evaluation of Food Texture

Introduction

Universal Design Foods is a term for foods that have been designed with consideration to texture or being easy to eat, and which can be used for everything from everyday meals to nursing-care foods. In Japan, with its rapidly aging society, a variety of nursing-care foods are currently available, and such meals must be suitable for patients.
The Japan Care Food Conference has established the Universal Design Foods concept, which is classified into 4 categories by hardness and viscosity. In this article, we introduce a system for measuring hardness.

F. Yano

Measurements and Jigs

Fig. 1 shows a schematic diagram of the test jigs used to evaluate the texture of foods. A cycle of compression and unloading is used to measure the hardness. Table 1 shows the relationship between the categories and the hardness upper limit values.

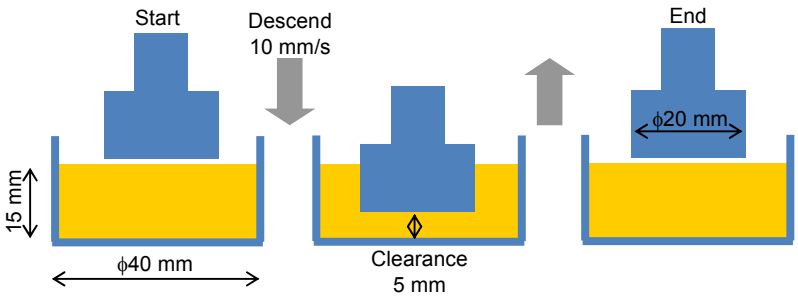

Fig. 1: Schematic Diagram of Universal Design Food Hardness Test

Table 1: Universal Design Food Categories and Upper Limit Values

Category	Hardness Upper Limit (N/m2)
1 (Easy to chew)	5×10^5
2 (Can be broken up using the gums)	5×10^4
3 (Can be broken up by the tongue)	Sol: 1×10^4 Gel: 2×10^4
4 (Does not need chewing)	Sol: 3×10^3 Gel: 3×10^3

Measurement Results

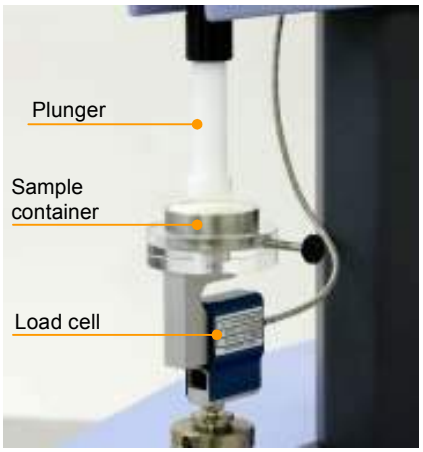

Fig. 2: Food Test Evaluation Jigs

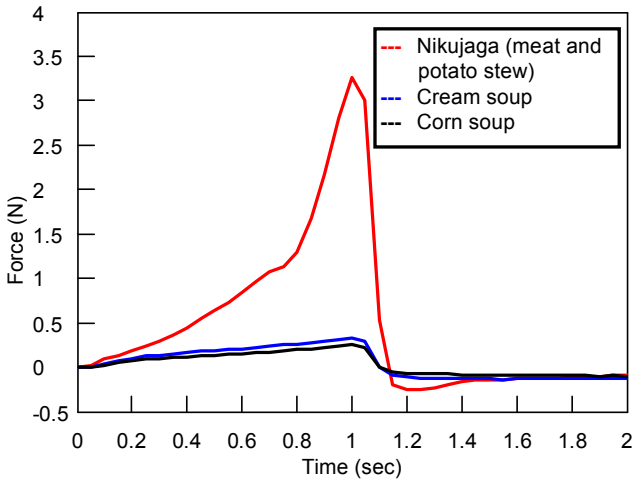

Fig. 3: Food Test Evaluation Results

Table 2: Test Conditions

Item	Set Value
Test Speed	10 mm/s
Clearance	5 mm
Test Temperature	20 °C

Table 3: Results for Food Hardness and Categories

Sample	Hardness (N/m²)	Classification
Nikujaga (meat and potato stew)	1.04×10^4	2
Cream soup	1.07×10^3	4
Corn soup	0.81×10^3	4

Food Hardness Evaluation System

Tester: EZ-SX

Load Cell: 50 N

Test jig: Universal Design Food Test Set

Software: TRAPEZIUM X Texture

Thermostat: Thermo-constant cooler/heater (separately installed)

EZTest Compact Table-Top Universal Tester

Features

■ Light and compact
The compact size fits easily on tables. Testing can be performed in a corner of the office.

■ A high-precision load cell is adopted. (The high-precision type is class 1; the standard-precision type is class 0.5.)
Accuracy is guaranteed over a wide range, from 1/500 to 1/1 of the load cell capacity. This supports highly reliable test evaluations.

■ Jog controller (optional)
This allows hand-held control of the crosshead position. Fine position adjustment is possible using the jog dial.

■ TRAPEZIUM X Texture operational software
This is the optimal software for a variety of pharmaceutical and cosmetic quality evaluations and physical characteristics measurements, as well as food texture measurements. It can create flexible control patterns and data processing items specific to foods, including hardness, brittleness, and energy.

■ A wealth of specialized jigs
Supporting the many needs of our customers with special jigs and applications for a number of fields, including foods, pharmaceuticals, electrical machinery & electronics, and plastics.

First Edition: February 2013

SHIMADZU

Shimadzu Corporation

www.shimadzu.com/an/

For Research Use Only. Not for use in diagnostic procedures.
The content of this publication shall not be reproduced, altered or sold for any commercial purpose without the written approval of Shimadzu.
The information contained herein is provided to you "as is" without warranty of any kind including without limitation warranties as to its accuracy or completeness. Shimadzu does not assume any responsibility or liability for any damage, whether direct or indirect, relating to the use of this publication. This publication is based upon the information available to Shimadzu on or before the date of publication, and subject to change without notice.

© Shimadzu Corporation, 2013

SHIMADZU
Excellence in Science

Application News

No. SCA_300_003

Material Testing System CFT

An Application of Shimadzu Flowtester Model CFT to Food Products
Measurement of stickiness and flowability of rice cake paste Model CFT to Food Products

Shimadzu Flowtester Model CFT, usually used for testing the flow of high polymer materials for data of their flowability properties - viscosity and softening - or for determination of their forming process conditions, is expanding its application to the field of food testing as well. The following is an introduction of the result of flow tests on three different types of rice cakes available on the market.

■ Flowability properties of viscosity and softening were measured with a constant rate heating method on three types of rice cake paste; two of them pounded manually with a cooking pestle, and the other by a mixing machine

■ Test conditions:

Specimens:	(1) Rice cake A by cooking pestle, much moisture
	(2) Rice cake B by cooking pestle, little moisture
	(3) Rice cake C by mixing machine
Test temperature:	initial temperature 40 °C (preheated for 180 sec.)
	heated thereafter at constant rate of 2 °C/min.
Extruding conditions :	extruding pressure: 10 kgf/cm^2,
	Die: D1 x 1 mm (diam. x length)
Testing machine :	Shimadzu Flowtester Model CFT

■ Softening - flowability characteristic curves

As shown in Fig.1, the softening - fluidifying process is presented in relation to temperature. The three cakes were softened at the ascending temperature in the order of cake A, cake C and cake B.

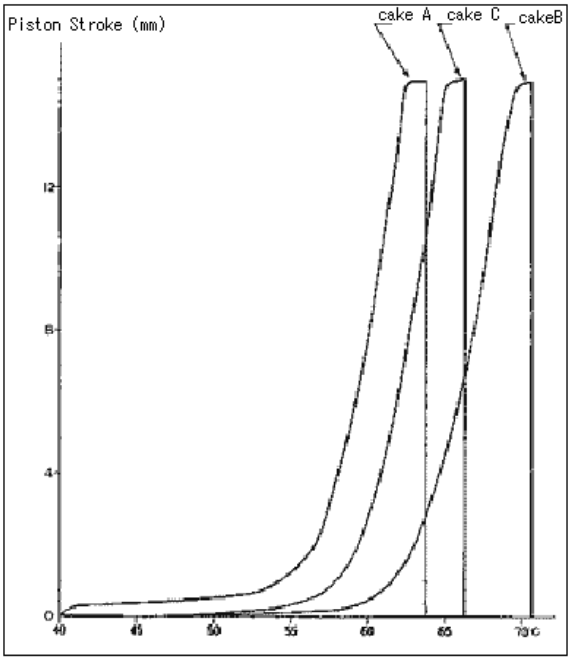

Fig. 1 Softening- Flowability Characteristic Curves

Note: The piston stroke in Fig.1 is equivalent to the quantity of specimen extruded (stroke of 1 mm = 0.1 ml).

* Please be advised that data obtained before the implementation of the current Weights and Measures Law may be presented in terms of gravimetric unit.

For Research Use Only. Not for use in diagnostic procedures.
The content of this publication shall not be reproduced, altered or sold for any commercial purpose without the written approval of Shimadzu. The information contained herein is provided to you "as is" without warranty of any kind including without limitation warranties as to its accuracy or completeness. Shimadzu does not assume any responsibility or liability for any damage, whether direct or indirect, relating to be the use of this publication. This publication is based upon the information available to Shimadzu on or before the date of publication, and subject to change without notice.

SHIMADZU
Excellence in Science

Application News

No. SCA_300_004

Material Testing System CFT

An evaluation of viscosity of non-vulcanized rubber by Shimadzu flow Tester

■ Introduction

In general, rubber for industrial use are processed through vulcanization in order to meet various requirements in hardness or elasticity (viscosity). Rubber is usually evaluated by Mooney Viscometers at the vulcanization process, but it can also be tested by Flow Testers to obtain useful information of its viscosity as well.

The following sections are dedicated to reporting comparison and evaluation of the test result on three kinds of non-vulcanized rubber, using a Mooney viscometer and a Shimadzu Flow Tester.

Table 1 shows the test result by the Mooney Viscometer.

Test parameters are: test temperature 100 °C, pre-heating time 1 min., test time 4 min. and rotor type L.

Sample Code	ML $_{1+4}$(100 °C)
Sample 1	83
Sample 2	78
Sample 3	73

Table 1: Measured Mooney viscosity value

The same samples were measured by the Shimadzu Flow Tester of constant load (pressure) extrusion capillary rheometer type, with the following result.

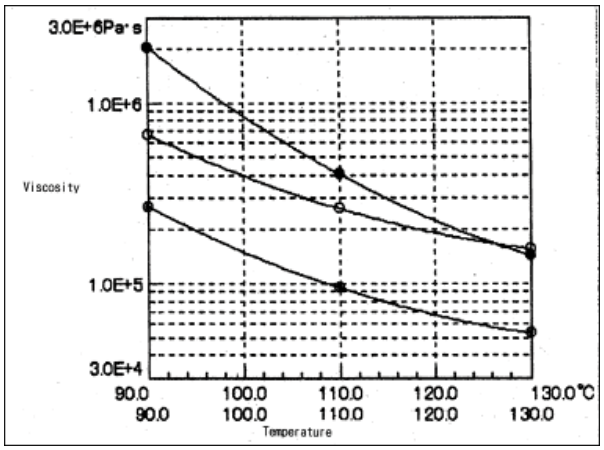

Fig. 1: Viscosity – Temperature Curve

Fig.1 shows the result of tests with the extruding pressure (load) of 3.432 MPa (35 kgf) and at the temperature of three different steps of 90.0 °C, 110 °C, and 130 °C. In the lower temperature range, difference between the three samples is clearly observed. Sample 1 has the highest viscosity followed by Sample 2 and sample 3 in Mooney viscosity. This order in terms of Mooney viscosity, however, is upset between sample 1 and sample 2 in the test result by the Shimadzu Flow Tester. At 130 °C however, the three samples are in the same order between the Mooney viscosity tester and the Shimadzu Flow tester. This fact indicates that the sample 2 has a nature of being vulnerable to thermal influence on its viscosity fluctuation.

Another test was exercised with different extruding pressures (loads) in an effort of searching further difference among the three samples.
The result is shown in Fig.2.

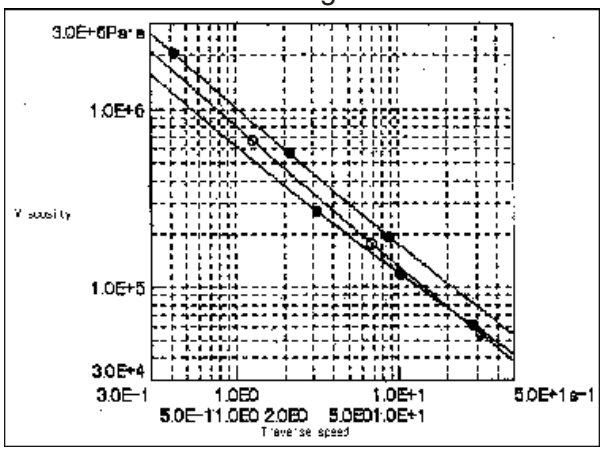

Fig. 2 Viscosity – shearing speed curve

Tests were performed with the test temperature of 90 °C and three different extruding pressures of 3.432 MPa (35 kgf), 4.903 MPa (50 kgf), and 6.865 MPa (70 kgf). The test result rearranged in terms of shearing speed are shown in Fig. 2. Traverse speed accounts for the flowing out speed of sample, which is one of the important factors for the engineering process including extruder forming. It is observed from Fig. 2 that the difference in shearing speed does not cause such an obvious difference as observed in the difference of temperature. The curves show a trend similar to that of Fig. 1 in the low extruding pressure (low shearing speed) range, while the order of the curves for sample 1 and 3 is upset each other in the high extruding pressure (high shearing speed) range. This is another trend different from that of Mooney viscosity. The curves of Fig. 2 also indicates that viscosity of sample 3 is less influenced by extruding pressure than the other two samples.
As seen above, tests with different apparatus having different evaluation tolls will provide an opportunity for reviewing from a different angle.
Shimadzu flow tester, which is a viscosity evaluation equipment for plastics in general, is also useful in viscosity evaluation of other various materials as it permits a wide range of test parameter choice. Materials, like rubber, for instance, which is hard and has high viscosity, can well be evaluated with a larger die (nozzle). The above data were obtained by use of a die with hole dia. of 3 mm and die length of 3 mm.

* Please be advised that data obtained before the implementation of the current Weights and Measures Law may be presented in terms of gravimetric unit.

SHIMADZU
Shimadzu Europa GmbH
www.shimadzu.eu

For Research Use Only. Not for use in diagnostic procedures.
The content of this publication shall not be reproduced, altered or sold for any commercial purpose without the written approval of Shimadzu. The information contained herein is provided to you "as is" without warranty of any kind including without limitation warranties as to its accuracy or completeness. Shimadzu does not assume any responsibility or liability for any damage, whether direct or indirect, relating to be the use of this publication. This publication is based upon the information available to Shimadzu on or before the date of publication, and subject to change without notice.

SHIMADZU
Excellence in Science

Application News

Material Testing System EZ-Test

No. SCA_300_005

Cereal Compression Shear Test Evaluation of Foods

■ Introduction

The following describes using a specialized Kramer shear cell jig to measure the hardness of breakfast cereal. The overall hardness and crunchiness of the cereal can be evaluated based on the initial slope of the test force curve and the jaggedness of the curve that results from individual cereal pieces breaking.

When evaluating samples that have nonuniform shapes, non-uniform internal characteristics, or include a mixture of various kinds of substances, it can be difficult to interpret meaning from the resulting graph and to obtain reproducible data. This is caused by the influence the testing location and characteristics of individual samples have on the data. To minimize such effects, multiple blades are used to perform compression shear tests. By using multiple blades, the resulting test force curve indicates the total test force for multiple blades, allows obtaining reproducible data.

Compression Shear Test of Cereal
Using Kramer Shear Cell Jig

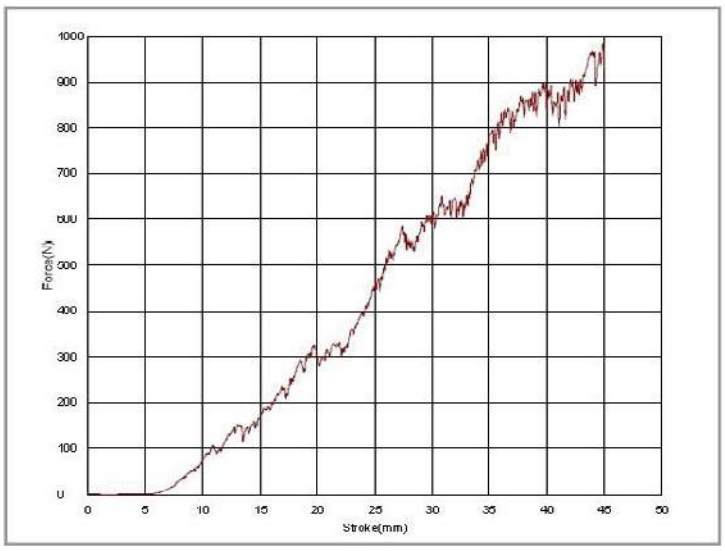

Results from Compression Shear Test of Cereal

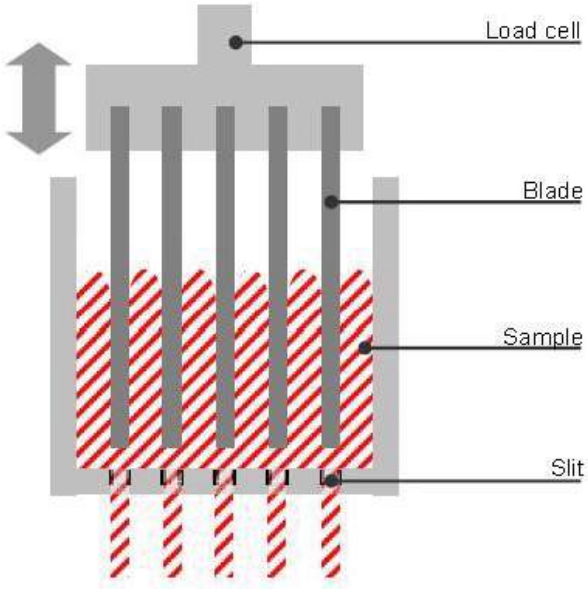

The Kramer shear cell is a specialized jig with five or ten blades used for compression, shear and extrusion tests. The 3 extrude the samples through slits located below the blades. Grooves on either side of the container guide the blades to ensure that the sample is sheared in a vertical direction. The blades can be disassembled from the container to allow easy cleaning after tests.

Examples of Sample Evaluation Tests

- Extent to which beans are cooked
- Breakfast cereal hardness
- Cheese curing level
- Hardness of boiled pasta
- Heating process of chunky sauces
- Hardness and brittleness of putty
- Hardness and processing level of vegetables and fruits
- Extent to which retort cooked rise is heated

Examples of Evaluation Parameters

- Stickiness/adhesion
- Cooking quality
- Fibrousness
- Fluidity
- Shear hardness
- Hardness/toughness
- Softness
- Flexibility
- Viscosity

SHIMADZU

Shimadzu Europa GmbH
www.shimadzu.eu

For Research Use Only. Not for use in diagnostic procedures.
The content of this publication shall not be reproduced, altered or sold for any commercial purpose without the written approval of Shimadzu. The information contained herein is provided to you "as is" without warranty of any kind including without limitation warranties as to its accuracy or completeness. Shimadzu does not assume any responsibility or liability for any damage, whether direct or indirect, relating to be the use of this publication. This publication is based upon the information available to Shimadzu on or before the date of publication, and subject to change without notice.

SHIMADZU
Excellence in Science

Application News

Material Testing System EZ-X

No. SCA_300_006

Chewing properties of gummy bears test

■ Purpose and Definition

Food texture is a very important characteristic when we eat. We want our meal or snack to be crispy, soft, creamy, crunchy, sticky, hard and so on. Another important reason to test texture is production efficiency. The testing of chewing properties of, for example gummy bears, is important to make production time as short as possible. By testing chewing properties the producer can optimize the time the gummy sweets need to stay in a stove oven during production, hereby optimizing production time, and produce a product with consistent quality and properties.

■ Equipment used:

Testing machine:
EZ-LX or SX/ AGS-XTable top

Load cell:
200N,1/500 Class1

Jig:
Compression plate

Software:
TrapeziumX, Texture / Compression

Environment: Room temp. 21 °C, +/-2 °C, humidity appr. 50 +/-5% RH.

Fig.1 EZ-SX

■ Test Jig

The jigs used were the standard lower Ø 100 mm compression plate, 343-08095, (346-51687-12 can also be used) and the Tooth pushrod A. (346-52258-02).

Fig.2 Test Jig

■ Test execution:

Five samples were tested where we are looking for elastic properties as well as adhesive and hardness properties. These are all factors which affects the chewing properties of a gummy sweet.

A method is prepared as described under “Creating a chewing test method” in the help section of the TrapeziumX software.

Test type is Texture and compression.
Test speed is set to 50 mm/min and the test is performed by doing two compressions to 6 mm in this case with a return to 0 mm between each compression. It is necessary to completely off-load the sample to get the negative force from the stickiness, which gives the adhesive properties of the sample.
TrapeziumX is already prepared for this test so the method description can be found in the help section including how to prepare the calculations needed in the calculator of TrapeziumX.

Fig.3 Test Setup

	Area1	Area2	Area3	Area4
Act.	Down	Up	Down	Up
	Stroke	Stroke	Stroke	Stroke
	50.000	50.000	50.000	50.000
	mm/min	mm/min	mm/min	mm/min
	Details	Details	Details	Details
Change point	Channel	Channel	Channel	Channel
	Stroke	Stroke	Stroke	Stroke
	6	1	6	0
	mm	mm	mm	mm
	Set	Set	Set	Set
GetData	None	None	None	None
Samplings	10msec	Same as prev. area	Same as prev. area	Same as prev. area
Loop	None	None	None	None

Fig.4 Test Method

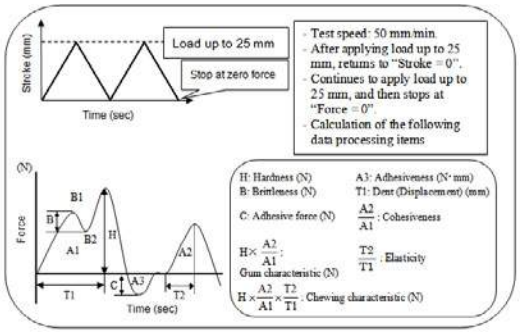

Fig. 5 Test Definition

■ Test Results:

By testing chewing properties the producer can optimize the time the gummy sweets need to stay in a stove oven during production, hereby optimizing production time, and produce a product with consistent quality and properties. The Texture module of the Trapezium software provides pre-defined data points for this type of tests and for the chewing properties test we used the guideline in the Trapezium help section. Some of the results presented are hardness, elastic properties, cohesiveness and adhesiveness.
HARDNESS is the force required to compress the sample to a pre-defined point.

ELASTICITY is the rate with which a deformed sample returns to its original length/size after deformation.

COHESIVENESS is the strength of the internal bonds making up the body of the product. (Greater the value the greater the cohesiveness).

ADHESIVENESS is the work necessary to overcome the adhesive forces between the surface of the sample and the surface of other materials with which the sample comes into contact with.

Force required to pull food away from surface. All together important properties of a gummy candy and the base for the texture experience we all expect when putting that wine gum or gummy bear in to our mouths.

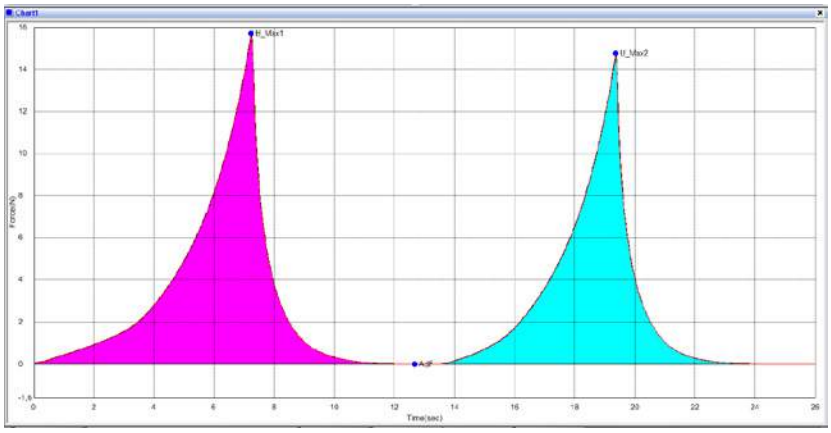

Fig. 6 Test Results

Results(Batch)

Name	Adhesive_Force_Force	Hardness_Force	Springness	Gumminess	Chewiness	Cohesiveness	Adhesiveness	Elastic
Parameter	2th Time	1th Time					2th Node- Next Node	Force 2 - 4 N
Pass/Fail								
Unit	N	N		N	N		J	N/mm2
Print	☑	☑	☑	☑	☑	☑	☑	☑
Gummibear _ 1	-0,0024	15,7016	0,68744	12,9853	8,92656	0,82700	0,02514	0,27281
Gummibear _ 2	0,0257	16,2005	0,57070	13,2673	7,57157	0,81894	0,02532	0,24825
Gummibear _ 3	-0,0062	16,5263	0,70705	13,5662	9,59195	0,82089	0,02593	0,26748
Gummibear _ 4	-0,0381	17,8539	0,56816	14,5252	8,25256	0,81356	0,02726	0,25762
Gummibear _ 5	0,0232	20,5296	0,60158	16,7512	10,0773	0,81596	0,03131	0,26603
Average	-0,0191	17,3624	0,62699	14,2190	8,88399	0,81927	0,02699	0,26244
Standard Deviation	0,01472	1,94165	0,06584	1,52968	1,00600	0,00515	0,00255	0,00962
Range	0,03570	4,82800	0,13889	3,76590	2,50573	0,01344	0,00617	0,02456

Fig. 7 Test Results

For Research Use Only. Not for use in diagnostic procedures.
The content of this publication shall not be reproduced, altered or sold for any commercial purpose without the written approval of Shimadzu. The information contained herein is provided to you "as is" without warranty of any kind including without limitation warranties as to its accuracy or completeness. Shimadzu does not assume any responsibility or liability for any damage, whether direct or indirect, relating to be the use of this publication. This publication is based upon the information available to Shimadzu on or before the date of publication, and subject to change without notice.

SHIMADZU
Excellence in Science

Application News

Material Testing System EZ-Test

Evaluation of Texture Using a Multi Piercing Test of Jam Evaluation of Foods

No. SCA_300_015

■ Introduction

Piercing tests are often used to evaluate food texture. Due to air bubbles, hard particles, or other variations in the internal structure of samples, however, test results can vary depending on where the sample is pierced, making evaluation difficult. To minimize such effects, tests can be performed by piercing samples with multiple probes. This process measures the total test force applied collectively to all probes, rather than the force applied to individual probes. Therefore, it results in data with higher reproducibility.

Piercing Test of Jam

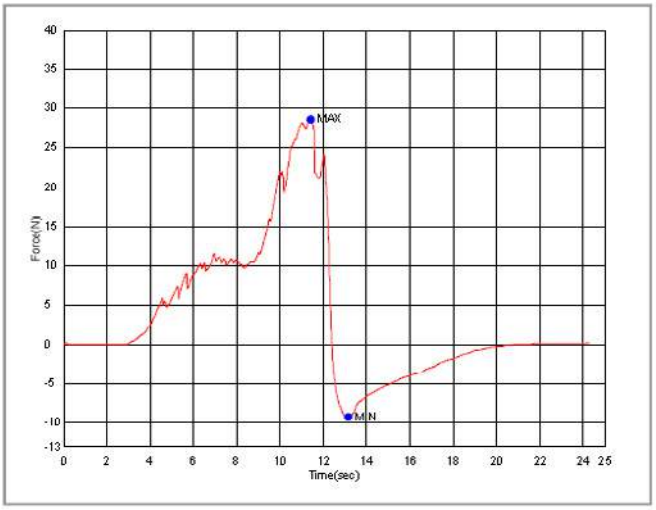

Jam Piercing Test Results

Piercing Hardness Test of Lettuce

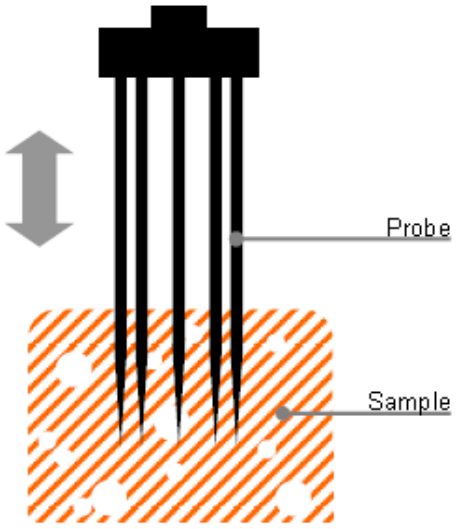

■ Multi-Piercing Jig

The multi-piercing jig consists of nine 3-mm diameter stainless steel rods used to test samples by piercing/penetration. It is used to test jams with pieces of fruit, ice cream with cookie pieces, or other foods that vary in level of hardness or consistency, or to test the hardness of vegetables with multiple overlapping leaves. This jig minimizes measurement error and achieves a average evaluation of samples.

For Research Use Only. Not for use in diagnostic procedures.
The content of this publication shall not be reproduced, altered or sold for any commercial purpose without the written approval of Shimadzu. The information contained herein is provided to you "as is" without warranty of any kind including without limitation warranties as to its accuracy or completeness. Shimadzu does not assume any responsibility or liability for any damage, whether direct or indirect, relating to be the use of this publication. This publication is based upon the information available to Shimadzu on or before the date of publication, and subject to change without notice.

SHIMADZU
Excellence in Science

Application News

Material Testing System EZ-Test

No. SCA_300_016

Evaluation Test of Butter and Margarine Evaluation of Foods

■ Introduction

There are many commercial butter and margarine products available, each characterized by certain features, such as smoothness, softness, low fat, and low calories. When developing such products or controlling their quality, it is necessary to measure, compare and quantify various characteristics, such as hardness, smoothness, and ease of spreading butter (spreadability).

Previously, this type of evaluation required spreading the product by hand and visually evaluating the spreadability. However, we recommend evaluating butter, for which it is easy to obtain samples with relatively uniform characteristics, using jigs specialized for each evaluation parameter.

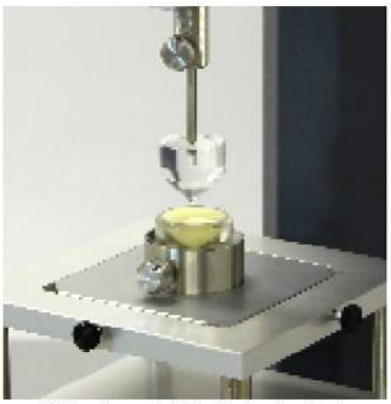

Butter Spreadability Evaluation Test

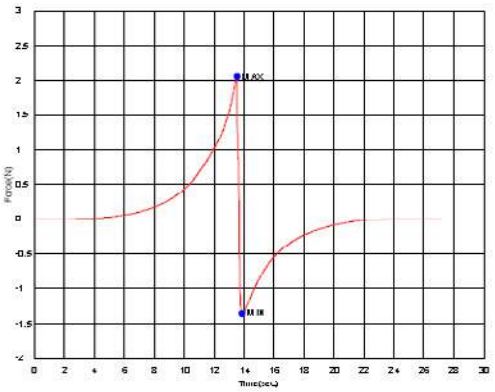

Butter Spreadability Evaluation Test Results

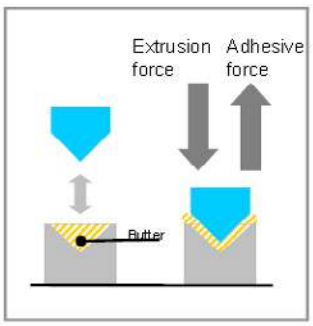

Evaluate spreadability by measuring the extrusion force, and evaluate viscosity by measuring the adhesive strength.

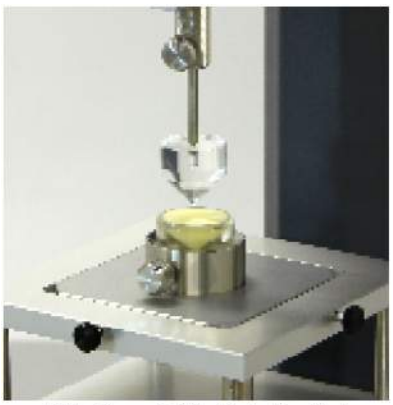

Butter Spreadability Evaluation Test

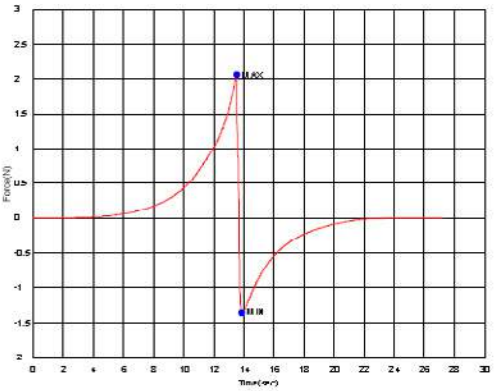

Butter Spreadability Evaluation Test Results

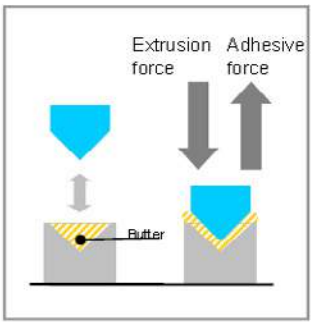

Evaluate spreadability by measuring the extrusion force, and evaluate viscosity by measuring the adhesive strength.

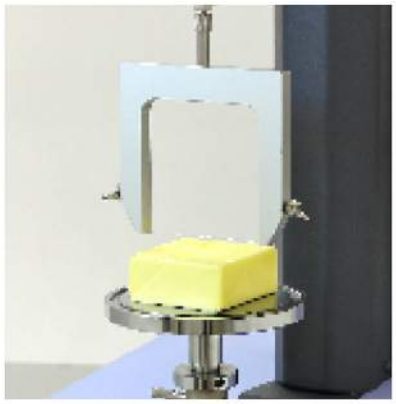

Butter Wire-Cutting Evaluation Test

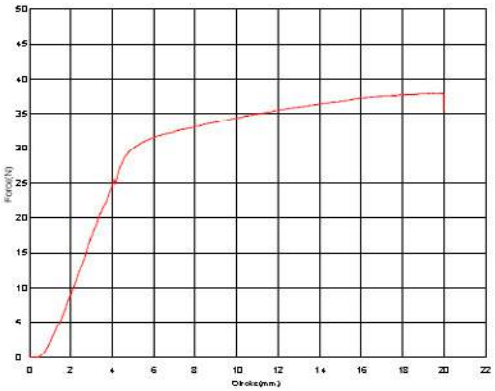

Butter Cutting Evaluation Test Result

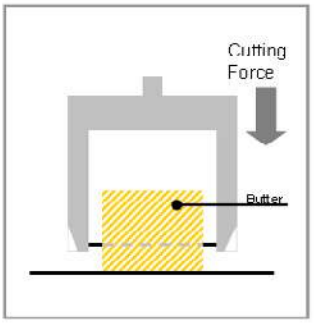

Wire cutting force measurements can be used as an index for evaluating the hardness of butter.

SHIMADZU

Shimadzu Europa GmbH
www.shimadzu.eu

For Research Use Only. Not for use in diagnostic procedures.
The content of this publication shall not be reproduced, altered or sold for any commercial purpose without the written approval of Shimadzu. The information contained herein is provided to you "as is" without warranty of any kind including without limitation warranties as to its accuracy or completeness. Shimadzu does not assume any responsibility or liability for any damage, whether direct or indirect, relating to be the use of this publication. This publication is based upon the information available to Shimadzu on or before the date of publication, and subject to change without notice.

SHIMADZU
Excellence in Science

Application News

Material Testing System EZ-Test

Measurement of Texture Characteristics of Rice Using Title Line the EZ Test Shimadzu Texture Analyzer

No. SCA_300_027

■ Introduction

Recently, numerical conversion of texture of materials and products is becoming more important. Especially in the food industry, various types of evaluation are performed on a wide range of materials, from raw ingredients to product packaging for quality assurance and development of new products. The EZ Test Shimadzu Texture Analyzer is used for various purposes such as numerical conversion of texture characteristics of foods such as chewiness, firmness, and palatability; quality evaluation based on the change of hardness; and strength evaluation of food packaging. The Analyzer is usable for such a wide range of purposes because a wide variety of jigs can be selectively used according to the type of test being performed. We conducted texture characterization of rice using the Texture Analyzer.

■ Samples and Testing Machines

Three types of rice; blended rice, Koshihikari (one of the most popular brands of rice), and rice with barley were used as samples in the measurement. Fig. 1 shows the appearance of the EZ Test Shimadzu Texture Analyzer used in the measurement.

(1)	Rice was cooked and left as is for one hour.
(2)	Rice was made into 10 g units.
(3)	Each unit of rice was then formed with a mold into a 20 mm high cylindrical form with a diameter of 25 mm

Table 1 Test Piece Making Process

Main Unit	EZ Test
Load Cell	Capacity 100 N
Jig	50 mm dia. compression plate
Software	TRAPEZIUMX Texture

Table 2 System Configuration

The analyzer has an exceptionally operable, compact frame and is perfect for texture characterization of foods. Table 1 shows the process to make test pieces and table 2 shows the configuration of the system used for the measurement.

Fig. 1 Appearance of Texture Analyzer

■ Test Conditions

Table 3 shows test conditions.
Fig. 2 shows how a test piece is placed.

Test Speed	50 mm/min
Pressing Amount	15 mm
Temperature	28 °C
Humidity	60 %

Table 3 Test Conditions

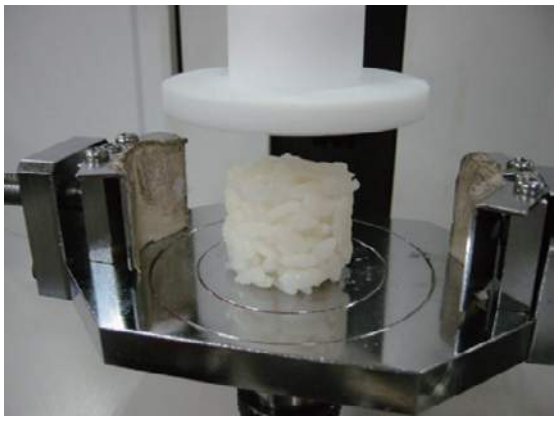

Fig. 2 Test Piece Placed

■ Test Results

Table 4 shows "Summary of Test Results (Average Values)" and Fig. 3 shows a "Force-Time" measurement example.

Sample	Hardness [N]	Cohesion Strength [N]]	Cohesiveness [Nmm]
Blended Rice	7.86	0.54	0.967
Koshihikari	16.3	1.09	2.78
Rice with Barley	7.67	0.33	0.603

Table 4 Summary of Test Results (Average Values)

Hardness: The maximum force loaded when compressed
Cohesion Strength: The maximum force required to pull off the jig after compression
Cohesiveness: A value calculated by multiplying the force required to pull off the jig after compression by the distance

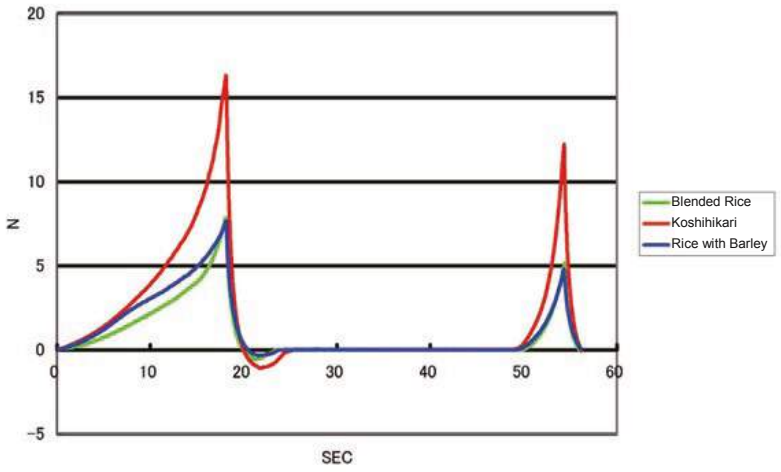

Fig. 3 Force-Time Graph

■ Summary

Koshihikari showed over twice as high values as compared to the other two types of rice for all items; hardness, cohesiveness, and cohesion strength. Cohesiveness is believed to closely indicate the sensation people fell when they actually eat rice. The test result for cohesiveness clearly indicates Koshihikari's characteristics. The use of the EZ Test Texture Analyzer is recommended for evaluating food texture because it provides easier texture characterization as compared to sensory evaluations and is highly operable

SHIMADZU

Shimadzu Europa GmbH
www.shimadzu.eu

For Research Use Only. Not for use in diagnostic procedures.
The content of this publication shall not be reproduced, altered or sold for any commercial purpose without the written approval of Shimadzu. The information contained herein is provided to you "as is" without warranty of any kind including without limitation warranties as to its accuracy or completeness. Shimadzu does not assume any responsibility or liability for any damage, whether direct or indirect, relating to be the use of this publication. This publication is based upon the information available to Shimadzu on or before the date of publication, and subject to change without notice.

SHIMADZU
Excellence in Science

Application News

Material Testing System EZ-Test

No. SCA_300_032

Texture Evaluation of Cheese and Agar Jelly

There are various factors to determine the tastiness of foods including the five senses; sight, taste, smell, touch, and hearing as well as physiological factors such as the state of hunger and full stomach, psychological factors, and dietary habits. It has been generally clarified that physical matters heavily influence sensory factors. Texture evaluation is a way to convert physical senses (texture) into numerical values.

■ Mastication Test on Cheese and Agar Jelly

A mastication test was conducted using load cell 20N and compression test jig (3 mm dia. plunger type) on the EZ Test Shimadzu Compact Table-Top Testing Machine in two cycles from 0 to 6 mm compression at a test speed of 50 mm/min. (Fig.1) Figs. 2 and 3 show the test force-displacement curve of each sample. Table 1 shows representative physical properties calculated based on the data. The test results clearly show that the texture evaluation showcased the difference between cheese and agar jelly in their physical properties. It is evident that the differences in their properties described below were accurately converted into numerical values. Agar jelly is chewier, more brittle and lighter in texture, and harder to stick to the teeth as compared to cheese.

Properties can be calculated as hardness, brittleness, cohesion strength, cohesiveness, elastic quality, cohesive quality, and adhesion as representative values. The section below introduces the results of a mastication test and shearing test conducted on cheese and agar jelly using the EZ Test Shimadzu Compact Table-Top Testing Machine as a texture evaluation example.

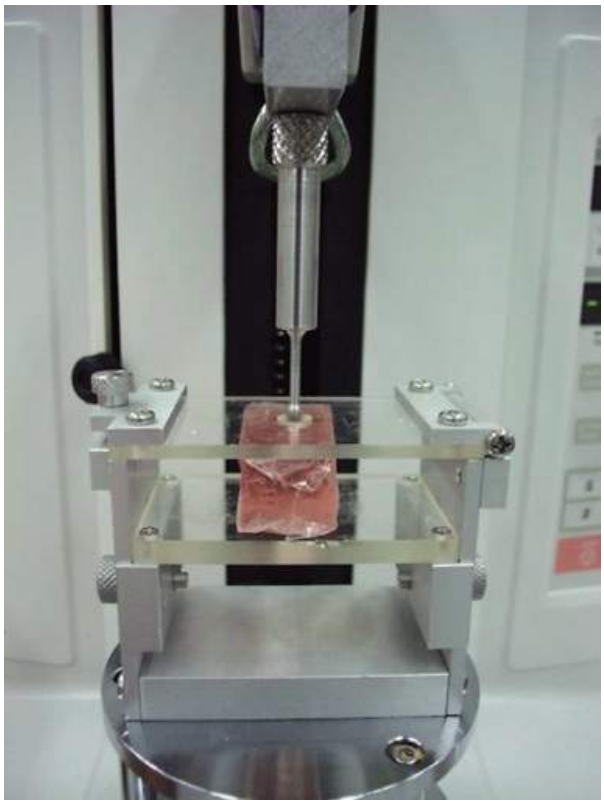

Fig. 1 Mastication Test

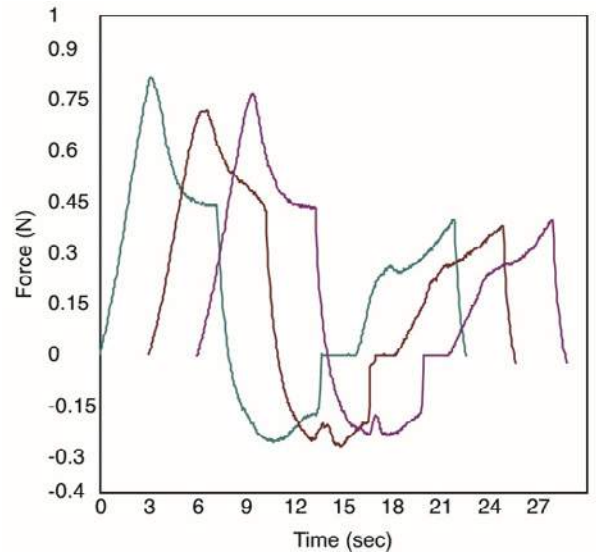

Fig. 2 Force-Displacement Curve for Cheese

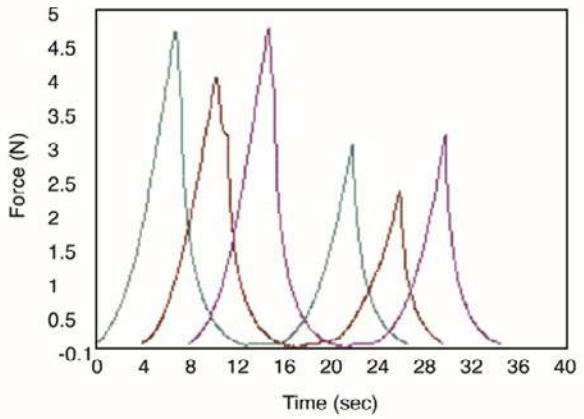

Fig. 3 Force-Displacement Curve for Agar Jelly

Parameter	Hardness	Cohesion Strength	Cohesiveness	Indentation	Cohesive Quality	Elastic Quality	Gum Quality	Masticable Quality
Unit	N	N	J	mm				
Agar Jelly	4.48	-0.04	-0.0001	5.58	203.358	1.08529	916.504	988.558
Cheese	0.77	-0.25	-0.00095	2.84	132.789	2.14723	102.315	220.447

Table 1 Texture Evaluation Values of Cheese and Agar Jelly (Mastication Test)

■ Shearing Test on Cheese and Agar Jelly

A shearing test was conducted using a shearing jig to evaluate hardness and chewiness as evaluation examples just like the mastication test described above. (Fig. 4) Figs.5 and 6 show the force-displacement curve of each sample as the test results. The data also clearly indicate the difference between the properties of cheese and agar jelly.

Fig. 4 Shearing Test

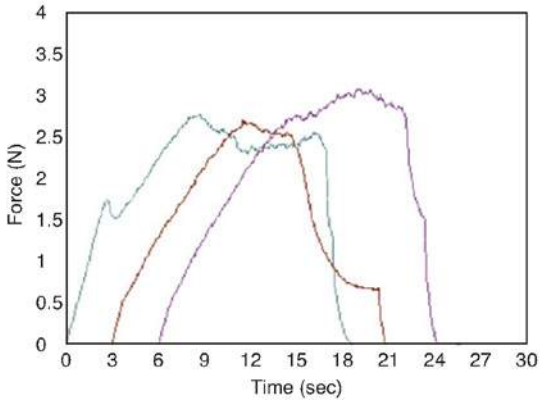

Fig. 5 Force-Displacement Curve for Cheese

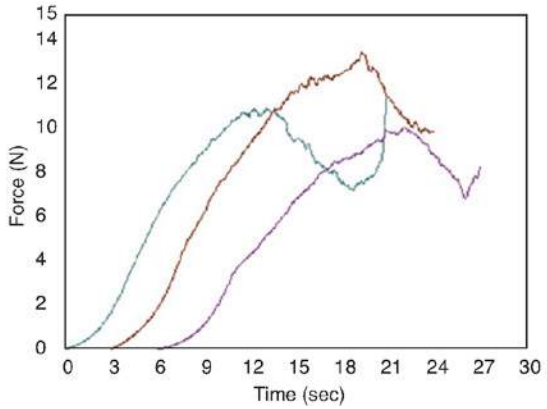

Fig. 6 Test Force-Displacement Curve for Agar Jelly

As shown in the examples above, using the EZ Test Shimadzu Compact Table-Top Testing Machine, a wide range of texture measurement can be easily conducted by adding various test jigs (there is a wide range of variation) for compression, shearing, and other purposes as well as the functions of a texture software.

[Reference]
Major texture evaluation terms
H : Hardness
B : Brittleness
C : Cohesion Strength
A3 : Cohesiveness
T1 : Indentation A2/A1 : Cohesive Quality
T2/T1 : Elastic Quality
H × A2/A1 : Gum Quality
H × A2/A1 × T2/T1 : Masticable Quality

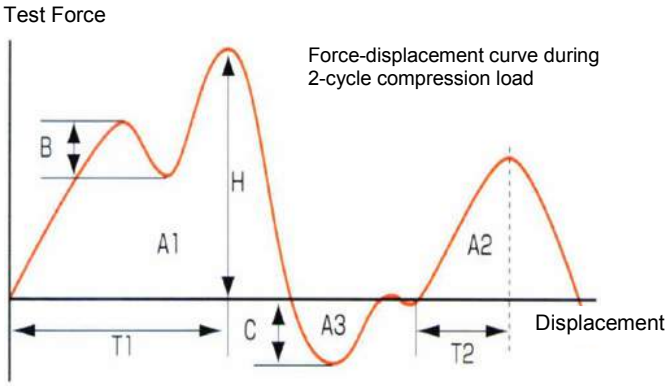

For Research Use Only. Not for use in diagnostic procedures.
The content of this publication shall not be reproduced, altered or sold for any commercial purpose without the written approval of Shimadzu. The information contained herein is provided to you "as is" without warranty of any kind including without limitation warranties as to its accuracy or completeness. Shimadzu does not assume any responsibility or liability for any damage, whether direct or indirect, relating to be the use of this publication. This publication is based upon the information available to Shimadzu on or before the date of publication, and subject to change without notice.

SHIMADZU
Excellence in Science

Application News

Material Testing System EZ-Test

No. SCA_300_042

Evaluation Test of Foods for People with Difficulties Swallowing

■ Introduction

The Japanese Consumer Affairs Agency, Food Labeling Div. Notification No. 277 (Labeling requirements for special-application foods) specifies standards for labeling foods intended for people who have difficulties swallowing. The following describes a system able to easily measure the parameters to determine conformance to the evaluation standards – hardness, adhesiveness, and cohesiveness. It was possible to determine which standard range was applicable by measuring food intended for nursing care applications and comparing characteristic values to the specified standards.

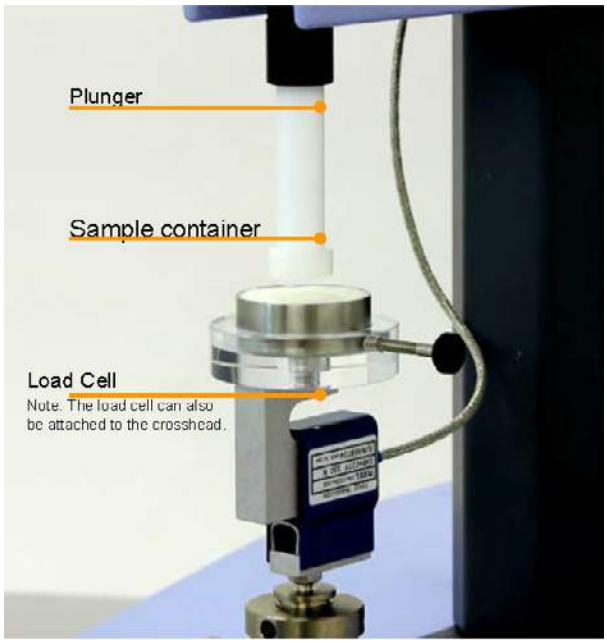

Jig for Evaluation Test of Foods for People with Difficulty Swallowing

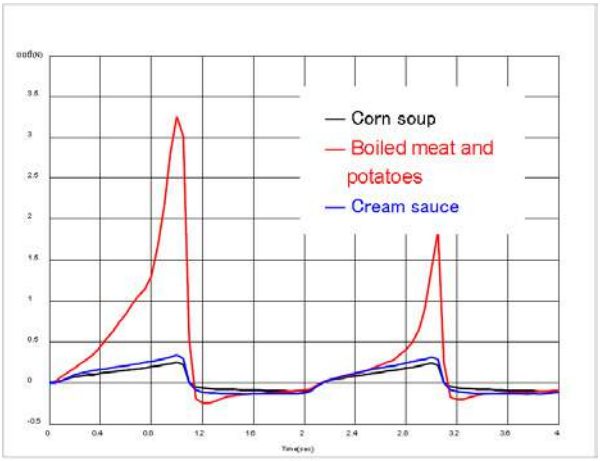

Evaluation Test Results of Foods for People with Difficulties Swallowing

- Test speed: 10 mm/sec
- Stroke Displacement: 10 mm
- Repetitions: 2
- Test Temperature: 20 °C

Sample	Hardness (N/m^2)	Adhesiveness (J/m^3)	Cohesiveness	Standard (judgment)
Corn soup	0,805 $X10^3$	0,129 $X10^3$	0,78	III
Boiled meet and potato	1,04 $X10^4$	0,246 $X10^3$	0,21	III
Cream sauce	1,07 $X10^3$	0,206 $X10^3$	0,78	II

Table 1: Test Results

Test Method for Foods for People with Difficulty Swallowing (CAA, Food Labeling Div., Notification No. 277). Fill samples to a height of 15 mm in a container 20 mm tall and 40 mm in diameter (a 15 mm tall container is acceptable if there is no possibility of sample overflowing). Use an instrument capable of measuring compressive stress by means of a liner motion to measure compressive stress two times using a plastic plunger 8 mm tall and 20 mm in diameter to compress samples at a rate of 20 mm/sec, with a bottom clearance of 5 mm.

The measurement temperature ranges are within 10 °C ±2 °C and within 20 °C ±2 °C for foods served cooled or at room temperature, and within 20 °C ±2 °C and within 45 °C±2 °C for foods served heated.

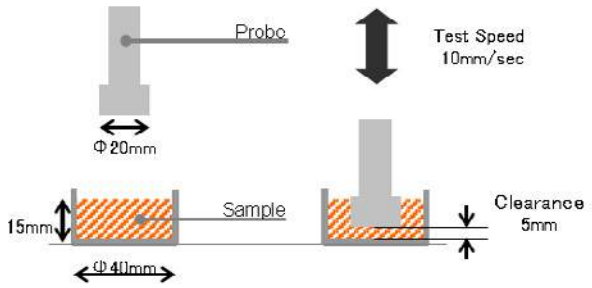

Testing Jig

Standard	Allowable Range I	Allowable Range II	Allowable Range III
Hardness［N/m2］ (resistance to compression applied at constant speed)	2,5 $X10^3$ - 1$X10^4$	1 $X10^3$ - 1,5$X10^4$	3 $X10^2$ - 2$X10^4$
Adhesiveness (J/m^3)	Max. 4 $X10^2$	Max. 1 $X10^3$	Max. 1,5 $X10^3$
Cohesiveness	0,2 – 0,6	0,2 – 0,9	-----

For Research Use Only. Not for use in diagnostic procedures.
The content of this publication shall not be reproduced, altered or sold for any commercial purpose without the written approval of Shimadzu. The information contained herein is provided to you "as is" without warranty of any kind including without limitation warranties as to its accuracy or completeness. Shimadzu does not assume any responsibility or liability for any damage, whether direct or indirect, relating to be the use of this publication. This publication is based upon the information available to Shimadzu on or before the date of publication, and subject to change without notice.

SHIMADZU
Excellence in Science

Application News

Material Testing System EZ-Test

No. SCA_300_046

Measurement of Texture of Pork by a Penetrating Strength Test

Today, Japanese people eat more pork than any other type of meat, 10 kg per person per year. Let's look at the history of eating pork in Japan. Generally, it is believed that Japanese people started to eat pork in the Meiji Era (1868-1912). In ancient times, they ate wild boar meat. It has been discovered that people kept wild boar during the Yayoi Era (1000 BC to 300 AD). It is imagined that people kept them free-range instead of penned in cages, fed them leftover food scraps, and ate them during festivals or special occasions.
People nowadays like tender meat more than chewy meat.

Therefore, various measures are taken to make pork tender, for example by soaking it in water or in protein degrading enzyme solution to quickly achieve an adequate level of tenderness.
Two cuts of store-bought Boston pork butt were soaked for 20 hours, one in water and the other in a protein degrading enzyme solution. A penetrating strength test was then performed on them and their textures were converted into numerical values for comparison. Fig. 1 is the penetrating test force- penetrating depth curve of store-bought Boston pork butt. Fig. 2 shows how the penetrating strength test was performed

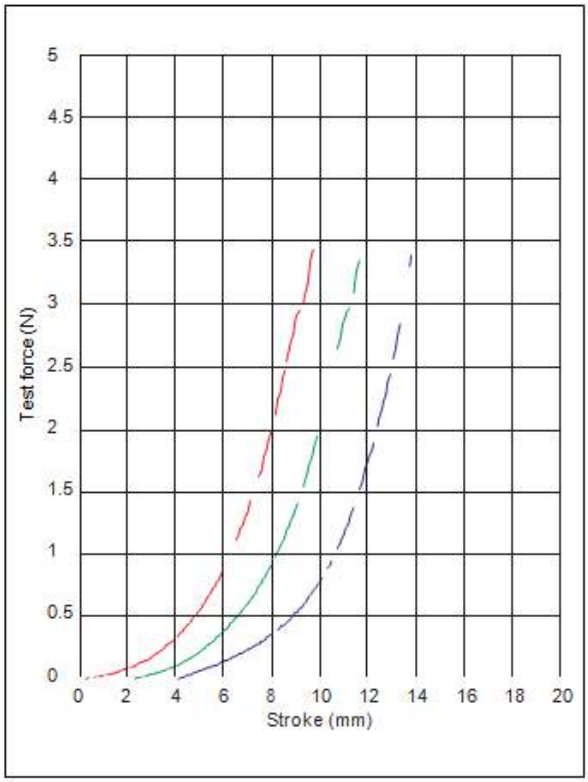

Fig. 1 Penetrating Test Force- Penetrating Depth Curve on Store-Bought Boston Pork Butt

Fig. 2 Penetrating Strength Test being performed on Pork

The EZ Test Shimadzu Table-Top Universal Tester was used in the test.
Fig. 3 is the penetrating test force-penetrating depth curve of pork soaked in water for 20 hours. Fig. 4 shows the results of soaking meat in a protein degrading enzyme solution for 20 hours.

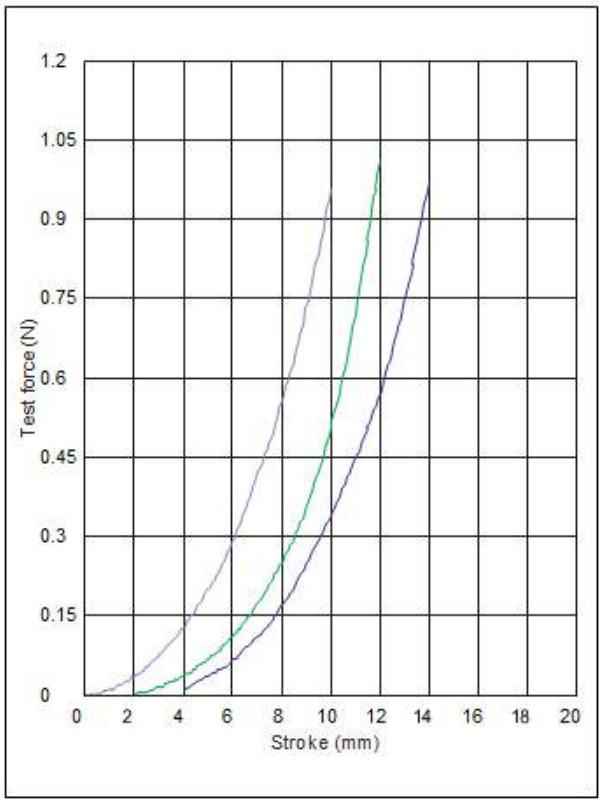

Fig. 3 Curve of Pork soaked in Water for 20 Hours

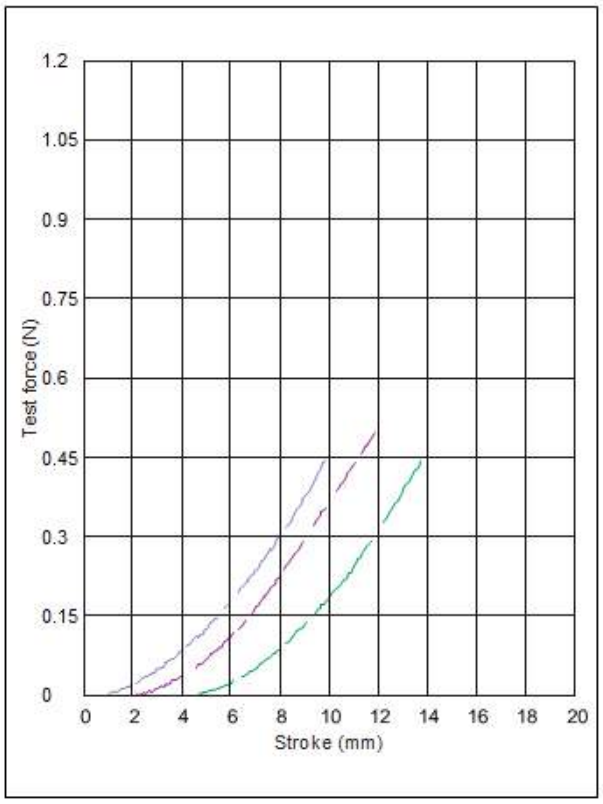

Fig. 4 Curve of Pork soaked in Enzyme Solution for 20 Hours

In these tests, the strength was measured at the point where a 5 mm diameter penetration elasticity jig penetrated a 20 mm thick cut of Boston Pork Butt to a depth of 10 mm at a speed of 100 mm/min. When the results shown in Fig. 3 and Fig. 4 are compared, the jig went deeper into the pork soaked in enzyme solution for 20 hours as compared to the pork soaked in water for 20 hours when the same test force was used, indicating the former is more tender.

When Fig. 1 and Fig. 3 are compared, approximately four times the strength is necessary to penetrate store-bought pork to the same depth as pork soaked in water for 20 hours, clearly indicating the difference in hardness. As shown in these figures, the texture of pork was converted into numerical values from the pork penetrating test strength- penetrating depth curve. Table 1 below shows the maximum penetrating test strength of these three tests.

Table 1

Sample	Average Value of Maximum Test Force N
Store-Bought Boston Pork Butt	3.90
Boston Pork Butt Soaked in Water for 20 hours	0.98
Boston Pork Butt Soaked in Enzyme Solution for 20 hours	0.49

The EZ Test Shimadzu Table-Top Universal Tester can be used to convert texture-related properties such as crispness of croquettes, resilience of bread, and firmness of boiled fish paste (kamoboko) as well as tenderness of pork reported in this document.

SHIMADZU

Shimadzu Europa GmbH
www.shimadzu.eu

For Research Use Only. Not for use in diagnostic procedures.
The content of this publication shall not be reproduced, altered or sold for any commercial purpose without the written approval of Shimadzu. The information contained herein is provided to you "as is" without warranty of any kind including without limitation warranties as to its accuracy or completeness. Shimadzu does not assume any responsibility or liability for any damage, whether direct or indirect, relating to be the use of this publication. This publication is based upon the information available to Shimadzu on or before the date of publication, and subject to change without notice.

SHIMADZU
Excellence in Science

Application News

Material Testing System EZ-Test

No. SCA_300_048

Multifaceted Measurement of Plums Pickled in Plum Wine

■ Introduction

Plum is not only a food but also used as a medicinal foodstuff to recover from fatigue and treat food poisoning. There are many types of plums such as the well-known Gojiro, Shirakaga, Sugita, Akebono, and Nankoh varieties. Yellowish unripened plums are used to make pickled plums and plum wine.
Texture and smell of four types of store-bought plums pickled in plum wines were converted into numerical values for comparison. The analysis and measurement items are listed below.

(1) Measurement of hardness and elastic quality which corresponds to chewiness using the EZ Test Shimadzu Compact Table-Top Testing Machine X-Ray Inspection System to see how pickled it is.

(2) Fluoroscopy of the inside of fruit flesh using the SMX-1000 Shimadzu Microfocus X-Ray Inspection System to see how pickled it is.

■ Measurement of Elastic Quality of Pickled Plums

Fig. 1 is a photo of elasticity measurement where fruit flesh was penetrated to a depth of 6 mm twice by a 0.5R penetration elasticity test jig.

Fig. 1 Penetrating Test Performed on Pickled Plum

Figs. 2-1 to 2-4 show the force (penetrating resistance [N]-vertical axis)-displacement (penetrating depth [mm]-horizontal axis) curves obtained using TRAPEZIUMX Texture software. In the curves, the higher the highest peak is, the harder the plum. The deeper the lower peak of the curve below the horizontal axis is, the higher the cohesiveness. And, the greater the height ratio between the height of the moderate curve slightly above the horizontal axis and the highest peak is, the higher the elasticity. In the test performed, the result was A≈B>D>C for all hardness, elastic quality, and cohesiveness.

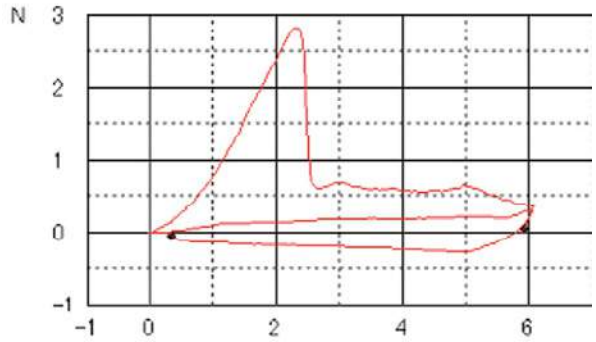

Fig. 2-1 Pickled Plum A

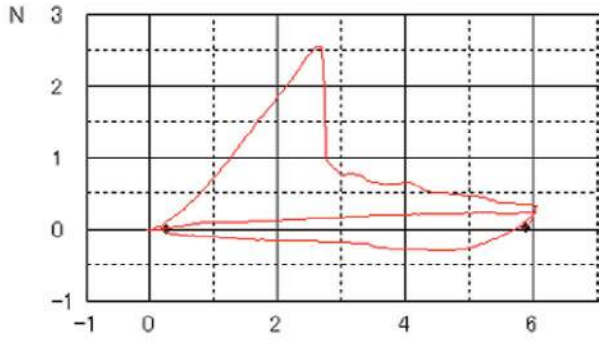

Fig. 2-2 Pickled Plum B

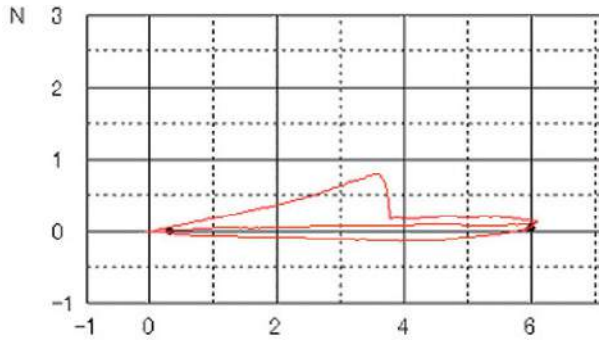

Fig. 2-3 Pickled Plum C

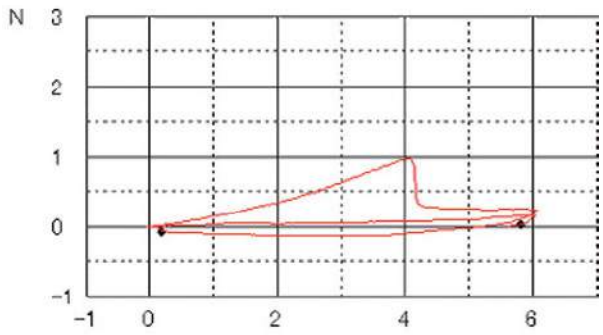

Fig. 2-4 Pickled Plum D

■ Fluoroscopic Observation of the Inside of Pickled Plums Using the X-Ray Inspection System

X-ray fluoroscopy was performed on pickled plums A through D at a certain fluoroscopic magnification and resolution (X-ray tube voltage 90 kV, X-ray tube current 110 μA, magnification 5×). The results are shown in Figs. 3-1 to 3-4. In general, areas with a higher density are displayed darker (blacker) and areas with a lower density are displayed lighter (whiter) in fluoroscopic images.

In Figs. 3-1 to 3-4, darkness of pickled plums A and B are similar, which indicates that the density of fruit flesh is relatively high. The entire fruit flesh of pickled plum C looks whitish, which indicates that liquid (distilled spirit in this case) has penetrated. In pickled plum D, a portion of fruit flesh close to the skin looks swollen because of liquid.

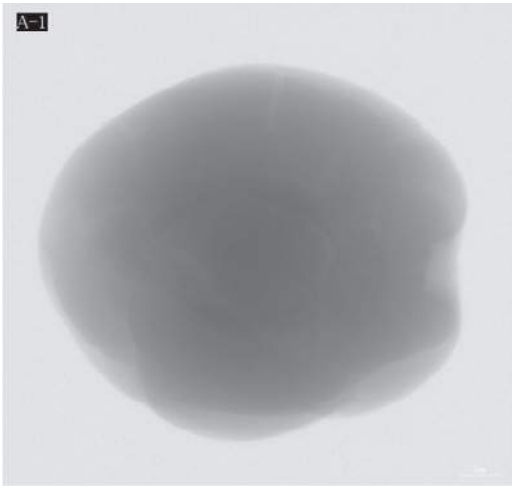

Fig. 3-1 Pickled Plum A

Fig. 3-2 Pickled Plum B

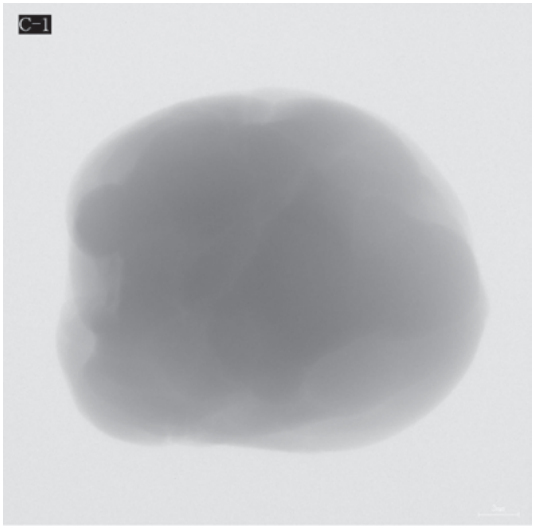

Fig. 3-3 Pickled Plum C

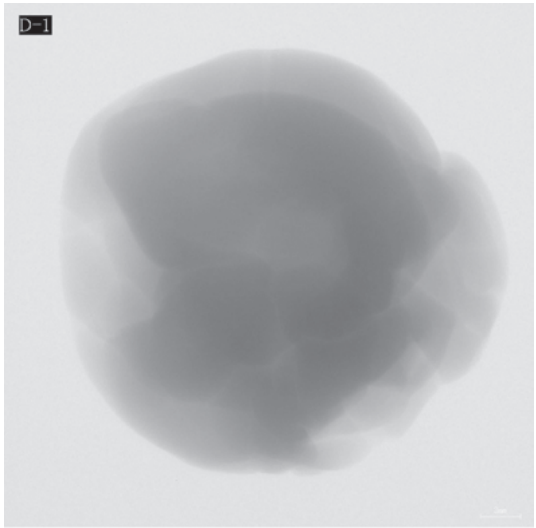

Fig. 3-4 Pickled Plum D

According to the above, the degree of penetration of distilled spirit (degree of swelling) was evaluated to be A≈B>C>D. The result was the same as how people felt (how pickled the plums were) when they put the plums in their mouth. However, the order of plums for hardness, elasticity, and cohesiveness was different from the data.

Fig. 4 SMX-1000 Shimadzu Microfocus X-Ray Inspection System

■ Summary

In the test, pickled plums were evaluated by a mechanical test, image observation. Although the results were sufficiently convincing, multifaceted analysis and measurement are believed to help convert the texture of food into numerical values.

For Research Use Only. Not for use in diagnostic procedures.
The content of this publication shall not be reproduced, altered or sold for any commercial purpose without the written approval of Shimadzu. The information contained herein is provided to you "as is" without warranty of any kind including without limitation warranties as to its accuracy or completeness. Shimadzu does not assume any responsibility or liability for any damage, whether direct or indirect, relating to be the use of this publication. This publication is based upon the information available to Shimadzu on or before the date of publication, and subject to change without notice.

SHIMADZU
Excellence in Science

Application News

Material Testing System EZ-Test

No. SCA_300_051

Texture Analysis of “Soumen” Japanese Vermicelli

■ Introduction

The evaluation of the mechanical properties of foods, such as strength and hardness, is becoming widely used for the numerical comparison and control of food texture. This Application News introduces the tensile test and cutting test of Japanese soumen vermicelli to evaluate the texture. Soumen vermicelli is originated in Nara Prefecture in Japan. It was made by hand by kneading wheat, salt and water; applying food oil and starch; and then stretching, drying, and maturing. Nowadays, it is generally machine-made.

According to JAS (Japan Agricultural Standards) standards, noodles less than 1.3 mm diameter are "soumen"; those from 1.3 mm to 1.7 mm diameter are "hiyamugi"; and larger noodles are classified as "udon”.

■ Testing Equipment and Specimens

Two types of commercially available soumen (Sample A, Sample B) were used as specimens for these tests. However, the diameters varied between 0.8 mm and 1.3 mm due to the degree of drying (the state in which it was sold). Therefore, the noodle diameters were measured with Vernier calipers to select specimens of approximately the same diameter.

The specimens were added to boiling water and boiled for three minutes and then washed in cold water for ten seconds. Ten specimens each of Sample A and Sample B were tested within five minutes.

Testing was performed using a Shimadzu EZTest tabletop tester (Fig. 1).

Fig. 1 EZTest Tabletop Tester

■ Tensile Test

The specimens were grasped in grips (sponge was attached to the grip faces to prevent destruction of the specimens), and the grips were mounted in the tester through universal joints. Tensile test was performed under the following conditions:

1) Force measurement - Load cell (1 N)
2) Extension measurement - Internal extensometer in tester
3) Test speed - 50 mm/min.

Fig. 2 and Fig. 3 show an overview of the grips and a specimen mounted in the tester.

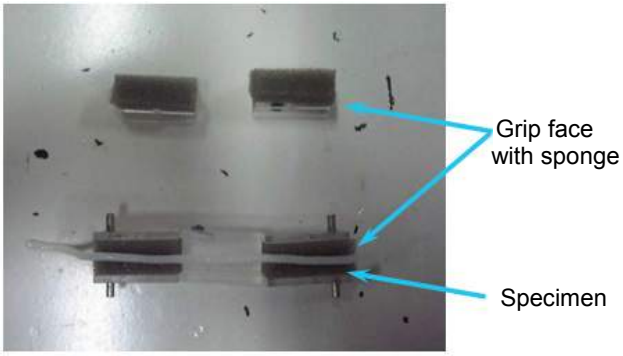

Fig. 2 Grips for Tensile Test

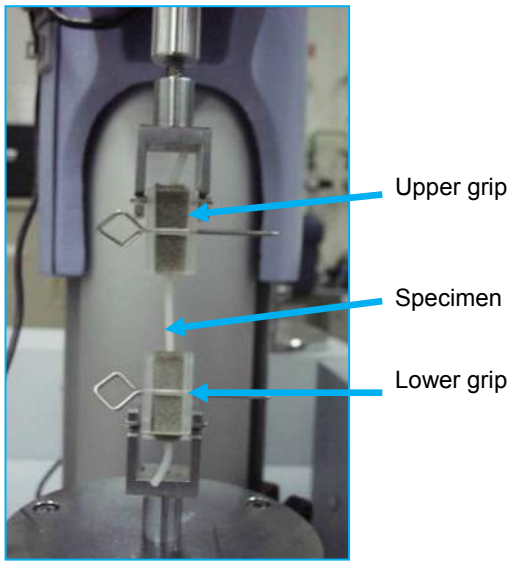

Fig. 3 Overview of Tensile Test

Fig. 4 shows the tensile test results as force-displacement (extension) curves. (Curves are superimposed for all ten specimens). The results indicate a maximum force of 164 mN and break displacement of 56 mm for Sample A and 120 mN. maximum test force and break displacement of 37.8 mm for Sample B. Sample A exhibits greater extension and strength than Sample B. (All values are averages of ten samples.)

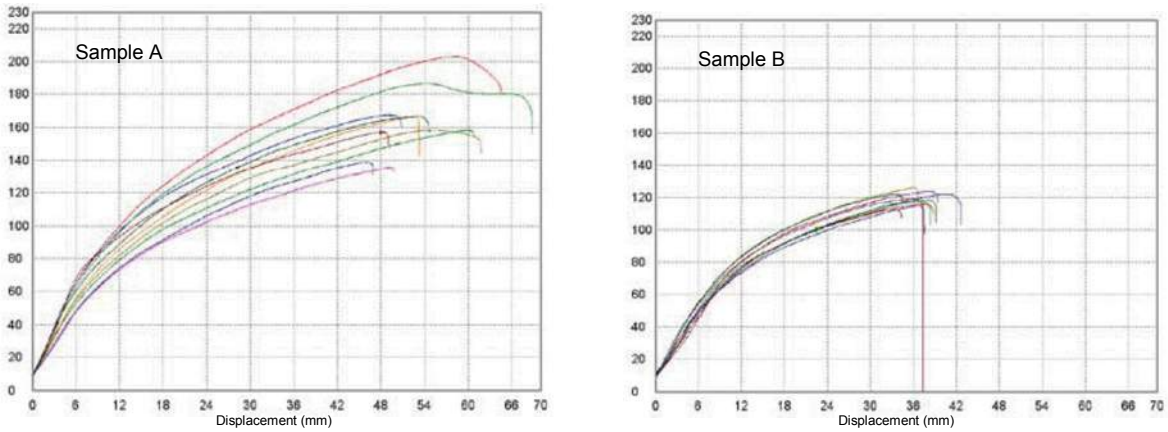

Fig. 4 Tensile Test Results

■ Cutting Test

Cutting test can be performed as an evaluation method that approximates biting through foods. For cutting test, the specimen is placed on the compression plate and the cutting test jig (tooth-shape press: R 0.2 mm knife-edge tip) is pressed down on the sample from above. The test conditions are as follows:

1) Force measurement - Load cell (1 N).
2) Indentation measurement - Internal extensometer in tester.
3) Test speed - 5 mm/minute.

Fig. 5 shows a specimen mounted in the tester.

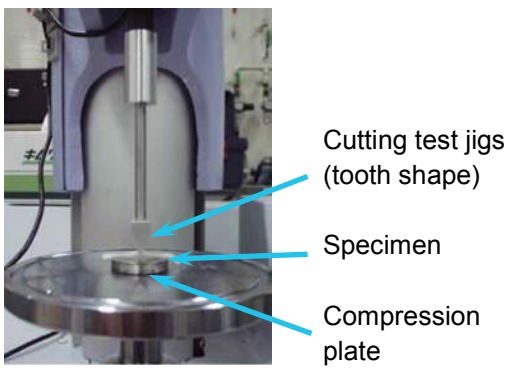

Fig. 5 Overview of Cutting Test

Fig. 6 shows the cutting test results as force-displacement (indentation) curves. (Curves are superimposed for all ten specimens.)

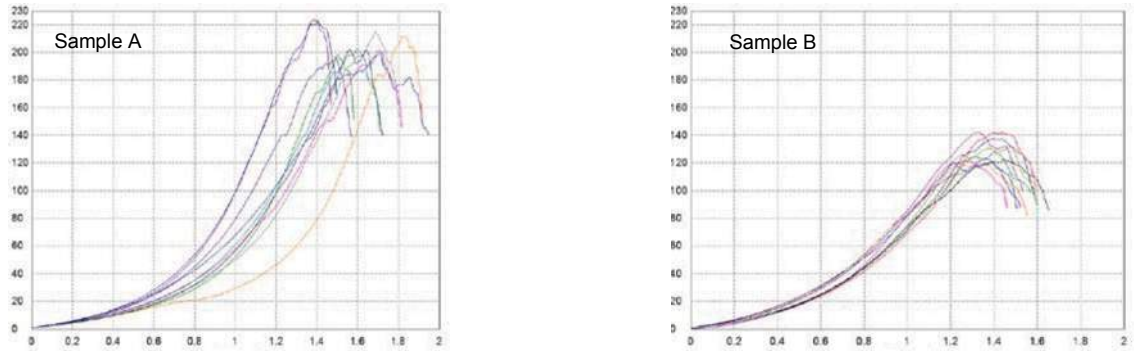

The results indicate a maximum force of 207 mN for Sample A and 129 mN maximum test force for Sample B. (All values are averages of ten samples.)

Fig. 6 Cutting Test Results

The tensile and cutting test results above provide a numerical evaluation that Sample A has a firmer texture than Sample B. The results confirm that the materials tester is effective for quantification for functional testing.

For Research Use Only. Not for use in diagnostic procedures.
The content of this publication shall not be reproduced, altered or sold for any commercial purpose without the written approval of Shimadzu. The information contained herein is provided to you "as is" without warranty of any kind including without limitation warranties as to its accuracy or completeness. Shimadzu does not assume any responsibility or liability for any damage, whether direct or indirect, relating to be the use of this publication. This publication is based upon the information available to Shimadzu on or before the date of publication, and subject to change without notice.

SHIMADZU
Excellence in Science

Application News

Material Testing System EZ-Test

No. SCA_300_052

Texture Analysis of "Ikura" Salted Salmon Roe by EZTest

■ Introduction

The numeric quantification of sensations has become increasingly important in recent years to provide the basic information for the accurate determination, improvement, and differentiation of the goods that surround us in our everyday lives. Sensations were conventionally evaluated mainly by the human five senses. However, numeric quantification of sensations is an effective method for the improvement and differentiation of goods. In the food industry, in particular, the quantitative evaluation of food texture is now commonly used for various purposes including the quality control and development of new food products.

The Shimadzu EZTest texture analyzer offers dedicated texture-analysis software and a comprehensive range of specialized test jigs for the quantitative evaluation of food texture, including crunchiness, crispiness, and palatability. It is a general-purpose tester that can be used for the strength testing of packaging materials in addition to the development, improvement, and quality control of foods.
This Application News introduces the use of EZTest for the texture analysis of salted salmon roe from different regions.

■ Testing Equipment and Test Conditions

Two samples of salted salmon roe (Sample A, Sample B) produced in different areas were tested. Testing was performed using a Shimadzu EZTest texture analyzer (Fig. 1).

Fig. 1 Overview of EZTest Texture Analyzer

EZTest features a compact frame that is extremely easy to operate. In addition to texture analysis, it can be used for the strength testing of other small samples.

Table 1 shows the configuration of the tester used, including the accessories.

Table 1 Tester Configuration

Main unit	EZTest EZ-S-5N
Load cell	Capacity 5 N
Jig	15 mm dia. compression plate (upper)
Software	TRAPEZIUM Rheometer texture analysis software

The texture was evaluated under compressive loads. Table 2 lists the test conditions and Fig. 2 shows an overview of the progress of a test.

Table 2 Test conditions

Test mode	Compression test (One egg from the salmon roe is placed on the compression plate and subjected to compressive oads.)
Test speed	10 mm/minute (constant speed)
Stroke	3 mm (Stroke to crush roe after compression.)
Ambient temperature	20 ˚C
Ambient humidity	60 %

Fig. 2 Overview of Texture Testing of Salted Salmon Roe

Table 3 Test Results

Sample Name	Hardness (N)	Breaking Strength
A	0.54	0.02
B	1.38	0.08

* Hardness: Maximum test force under compression
Breaking strength: Maximum stress calculated from maximum test force and size of the egg

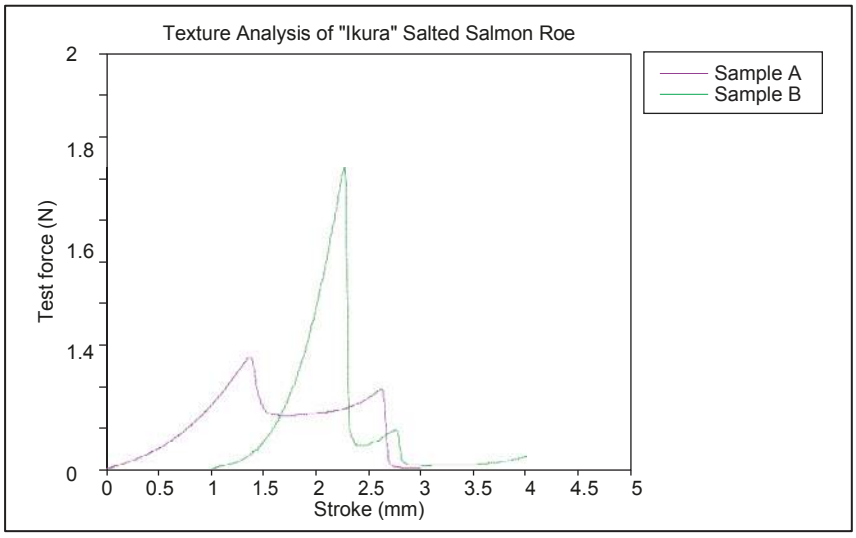

Fig. 3 Test Force-Stroke Curves for Typical Samples

These curves indicate that Sample A achieves over twice the hardness and breaking strength values of Sample B. Differences in the failure process of roe are also apparent. These differences are sensed as differences in texture, which can be difficult to express. Therefore, numeric quantification offers the advantage of providing an indicator for the quantitative comparison of food textures.

For Research Use Only. Not for use in diagnostic procedures.
The content of this publication shall not be reproduced, altered or sold for any commercial purpose without the written approval of Shimadzu. The information contained herein is provided to you "as is" without warranty of any kind including without limitation warranties as to its accuracy or completeness. Shimadzu does not assume any responsibility or liability for any damage, whether direct or indirect, relating to be the use of this publication. This publication is based upon the information available to Shimadzu on or before the date of publication, and subject to change without notice.

SHIMADZU
Excellence in Science

Application News

Material Testing System EZ- Test

No. SCA_300_053

Texture Evaluation of Cheese and Agar Jelly

■ Introduction

There are various factors to determine the tastiness of foods including the five senses; sight, taste, smell, touch, and hearing as well as physiological factors such as the state of hunger and full stomach, psychological factors, and dietary habits. It has been generally clarified that physical matters heavily influence sensory factors. Texture evaluation is a way to convert physical senses (texture) into numerical values. Properties can be calculated as hardness, brittleness, cohesion strength, cohesiveness, elastic quality, cohesive quality, and adhesion as representative values. The section below introduces the results of a mastication test and shearing test conducted on cheese and agar jelly using the EZ Test Shimadzu Compact Table-Top Testing Machine as a texture evaluation example.

■ Mastication Test on Cheese and Agar Jelly

A mastication test was conducted using load cell 20N and compression test jig (3 mm dia. plunger type) on the EZ Test Shimadzu Compact Table-Top Testing Machine in two cycles from 0 to 6 mm compression at a test speed of 50 mm/min (Fig.1). Figures 2 and 3 show the test force-displacement curve of each sample. Table 1 shows representative physical properties calculated based on the data. The test results clearly show that the texture evaluation showcased the difference between cheese and agar jelly in their physical properties. It is evident that the differences in their properties described below were accurately converted into numerical values. Agar jelly is chewier, more brittle and lighter in texture, and harder to stick to the teeth as compared to cheese.

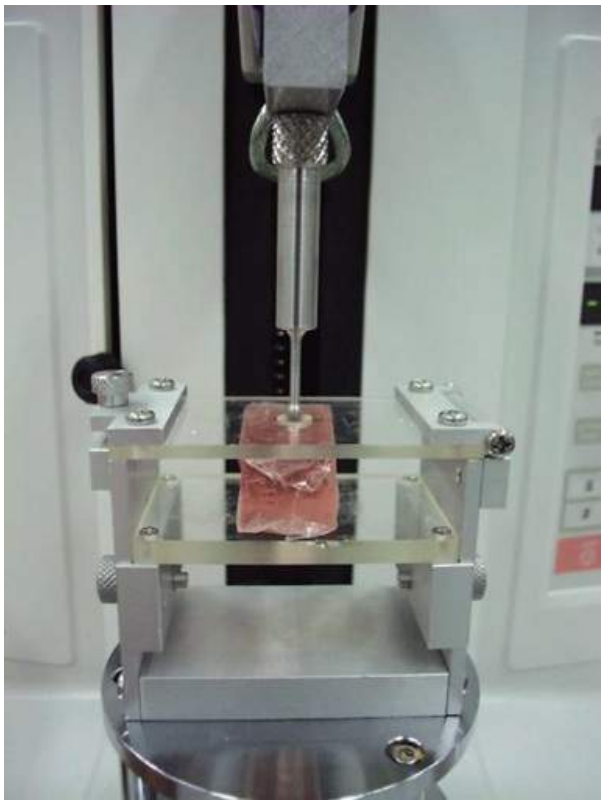

Fig. 1 Mastication Test

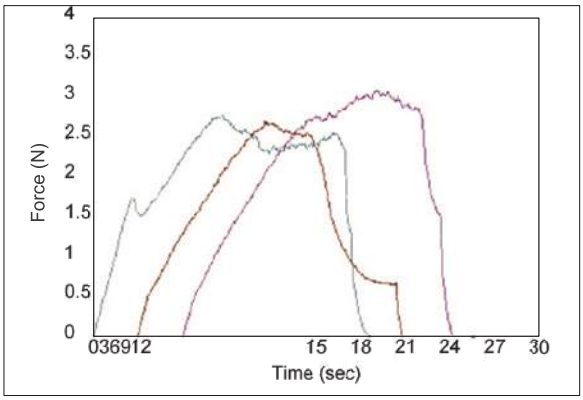

Fig. 2 Force-Displacement Curve for Cheese

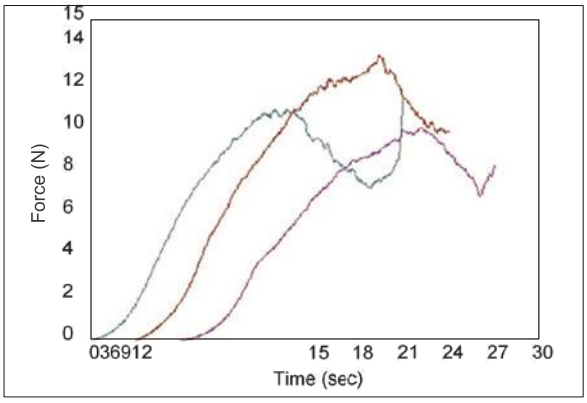

Fig. 3 Test Force-Displacement Curve for Agar Jelly

Parameter	Hardness	Cohesion Strength	Cohesiveness	Indentation	Cohesive Quality	Elastic Quality	Gum Quality	Masticable Quality
Unit	N	N	J	mm				
Agar Jelly	4.48	-0.04	-0.0001	5.58	203.358	1.08529	916.504	988.558
Cheese	0.77	-0.25	-0.00095	2.84	132.789	2.14723	102.315	220.447

Table 1 Texture Evaluation Values of Cheese and Agar Jelly (Mastication Test)

■ Shearing Test on Cheese and Agar Jelly

A shearing test was conducted using a shearing jig to evaluate hardness and chewiness as evaluation examples just like the mastication test described above. (Fig.4) Figs.5 and 6 show the force-displacement curve of each sample as the test results. The data also clearly indicate the difference between the properties of cheese and agar jelly.

Fig. 4 Shearing Test

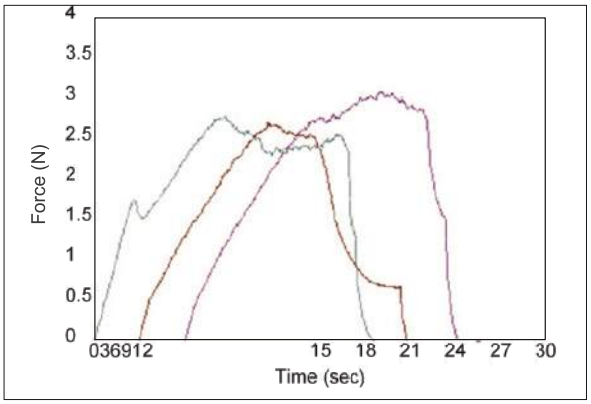

Fig. 5 Force-Displacement Curve for Cheese

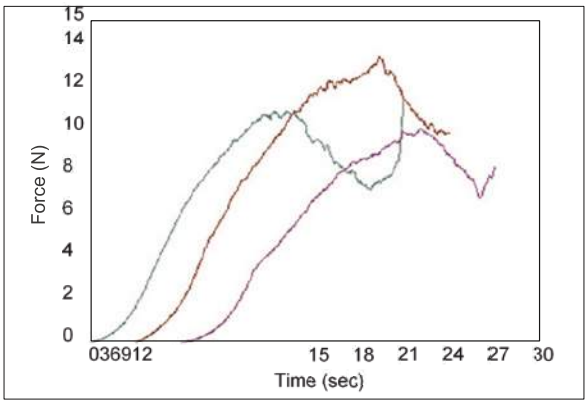

Fig. 6 Test Force-Displacement Curve for Agar Jelly

As shown in the examples above, using the EZ Test Shimadzu Compact Table-Top Testing Machine, a wide range of texture measurement can be easily conducted by adding various test jigs (there is a wide range of variation) for compression, shearing, and other purposes as well as the functions of a texture software.

[Reference]
Major texture evaluation terms

H : Hardness	A2/A1	: Cohesive Quality
B : Brittleness	T2/T1	: Elastic Quality
C : Cohesion Strength	H × A2/A1	: Gum Quality
A3 : Cohesiveness	H × A2/A1 × T2/T1	: Masticable Quality
T1 : Indentation		

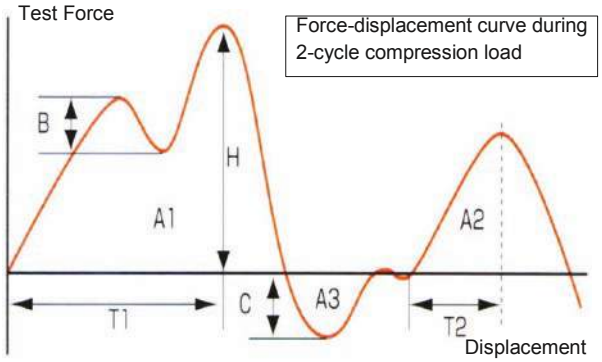

SHIMADZU

Shimadzu Europa GmbH
www.shimadzu.eu

For Research Use Only. Not for use in diagnostic procedures.
The content of this publication shall not be reproduced, altered or sold for any commercial purpose without the written approval of Shimadzu. The information contained herein is provided to you "as is" without warranty of any kind including without limitation warranties as to its accuracy or completeness. Shimadzu does not assume any responsibility or liability for any damage, whether direct or indirect, relating to be the use of this publication. This publication is based upon the information available to Shimadzu on or before the date of publication, and subject to change without notice.

SHIMADZU
Excellence in Science

6. Metal Industry

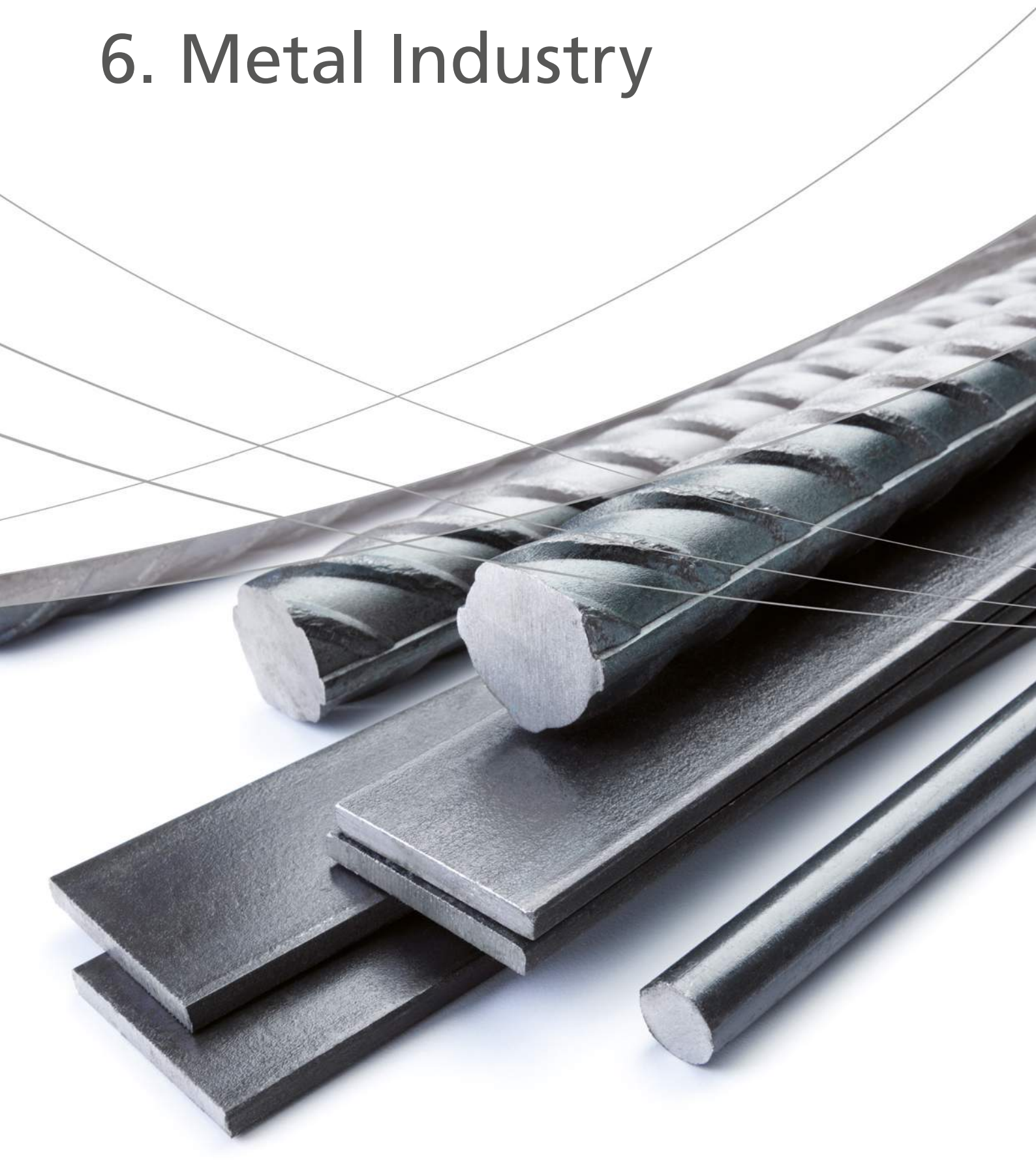

6. Metal Industry

DESTRUCTIVE AND NON-DESTRUCTIVE TESTING

The metal industries cover non-ferrous metals (e.g. aluminium, copper and zinc) and ferrous materials such as iron and steel. From an economic perspective, iron is the most important metal and is used in steel, cast iron and many alloys.

In ancient times, metals have been drivers of human culture and civilization. Today, they are the backbone of many industries and are used in uncountable products and applications. Main buyers are the automotive, construction and manufacturing, and mechanical engineering industries. Although processing of iron is an approx. 3000 years old technology, the steel industry is innovative, and many steel qualities have been developed in recent years.

Metals are tested mostly with two methods: non-destructive testing (NDT) and destructive testing (Destructive Physical Analysis DPA). Non-destructive testing evaluates properties of materials and components without damaging them. Using different methods, destructive testing examines specimens in order to understand their performance, failure and material behavior.

Stress, crash and hardness tests are typical destructive testing methods. They are easier to carry out than non-destructive testing, and deliver more information which is easier to interpret. Where significant hazard or economic loss can occur, non-destructive testing is the method of choice for prevention of component failure.

6. Metal Industry

C225-E032	Ultrasonic fatigue testing system with an average stress loading mechanism
No_i244	Tensile test for metallic materials using strain rate control and stress rate control
No.14	Tensile testing metallic materials stress rate contro lKM
No.15	Tensile testing metallic materials strain rate contro lKM
SCA_300_023	Measurement of carburized case depth of steel with Shimadzu micro hardness tester model HMV i45
SCA_300_024	Measurement of hardness of the machining deterioration layer of stainless steel with Shimadzu dynamic ultra micro hardness tester DUH
SCA_300_034	A hardness measurement of steel surface treatment layer with Shimadzu dynamic ultra micro hardness tester, model DUH
SCA_300_035	A hardness measurement of surface treatment layer on a steel sample using Shimadzu dynamic ultra micro hardness tester, model DUH
SCA_300_036	A thickness measurement of a Ni-plating layer on a stainless-steel sample with Shimadzu dynamic ultra micro hardness tester, mode DUH
SCA_300_045	Jigs for measuring Bauschinger effect
SCA_300_047	Measurement of the surface treatment depth of steel with Shimadzu micro hardness tester model HMV
SCA_300_050	Strength evaluation on metallic fine particles with Shimadzu micro compression testing machine model MCT
SCA_300_061	Compressive strength of metallic micro-spheres and dependence on heat treatment temperature MCT
eV021	Observation of bending fatigue testing of metal plate at ultrasonic frequency

SHIMADZU
Excellence in Science

Ultrasonic Fatigue Testing System with an Average Stress Loading Mechanism

For Gigacycle Fatigue Tests with Average Stress Loaded

Actual components are rarely used under conditions in which the average stress is zero. Despite this, the USF-2000A, a standard ultrasonic fatigue testing system, can only perform testing under zero average stress conditions.
Using an ultrasonic fatigue testing system equipped with an average stress loading mechanism, gigacycle fatigue tests can be performed with average tensile stress loaded.

System Appearance

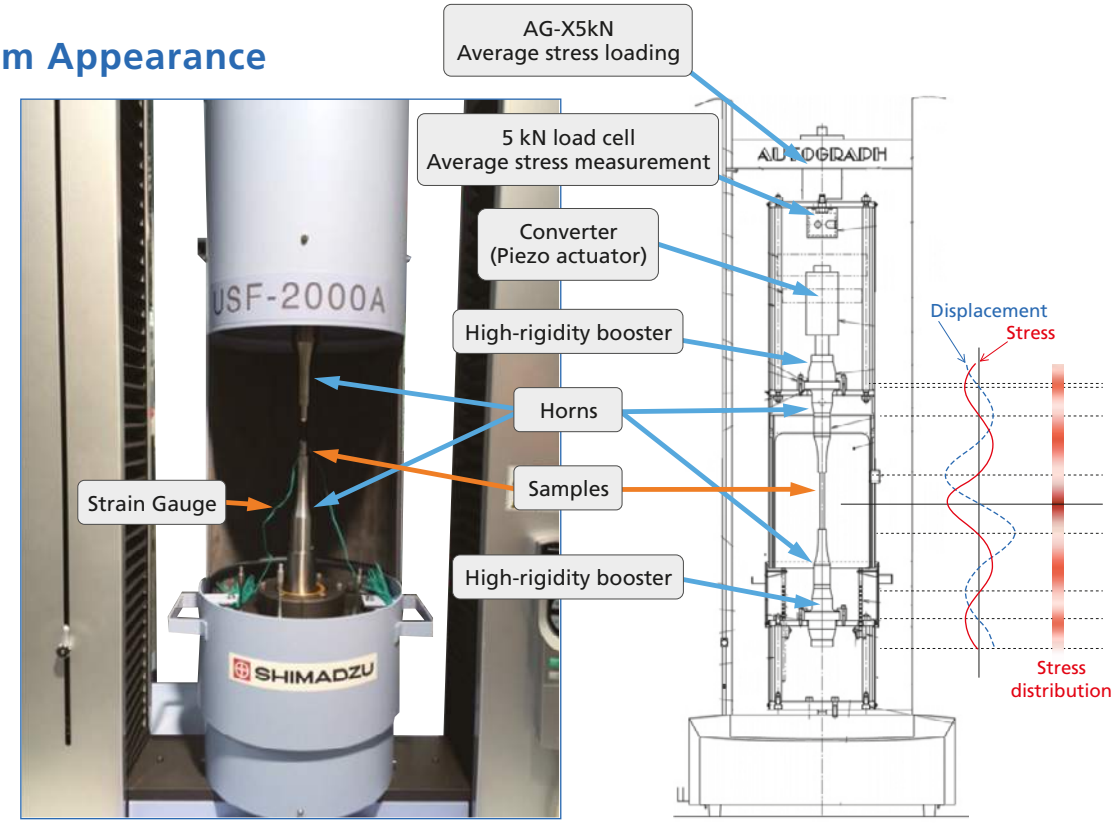

Ultrasonic Fatigue Testing System Effective for Gigacycle Fatigue Tests

With fatigue tests of high-strength steels, it is evident that internal fracture (fish-eye fracture), which is caused by inclusions and other micro defects, occurs at 107 cycles or more, a value considered the conventional fatigue limit.
An ultrasonic fatigue testing system is extremely effective when performing this sort of gigacycle fatigue test. (With a 100 Hz fatigue testing system, this would take 3 years, but if a 20 kHz ultrasonic fatigue testing system is used, testing can be completed in one week.)

Main Specifications

1) Test Frequency: 20 kHz ± 500 Hz

- The recommended test range is 20 kHz ± 30 Hz.
- The test frequency is determined by the resonance frequency of the sample.

2) Horn End Face Amplitude

Min. approx. ±10 µm
Max. approx. ±50 µm

- The minimum and maximum amplitudes are the end face amplitude values at amplitude outputs of 20 % and 100 % respectively. Accordingly, the minimum and maximum amplitude values will change somewhat depending on the shape of the sample.

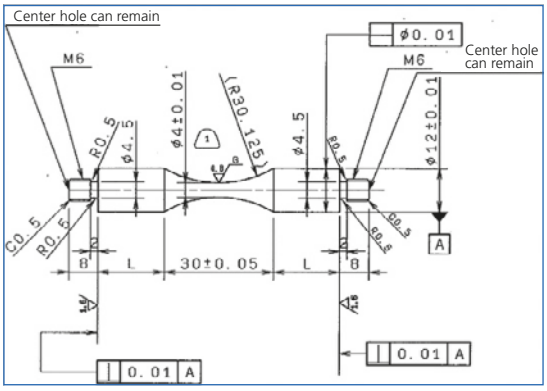

Standard Circular Tapered Sample

3) Test Stress

Standard circular tapered sample
Stress Min. 237 MPa
Max. 1186 MPa

- The test stress range can be changed by changing the sample shape.
- The minimum and maximum values are calculated with the end face amplitude values of 10 µm and 50 µm respectively.
- These are the values when the stress is within the elasticity range.

4) Average Stress

Max. 1.5 kN (tensile only)

- Average stress loads exceeding 1.5 kN are possible, but will have an impact on the service life of the horn.

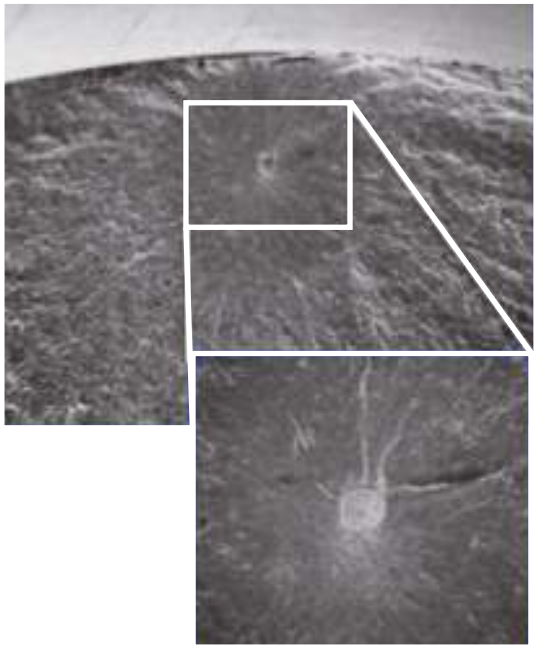
Surface of the Fatigued Fracture Originating from the Inclusion

■ Components

1	Ultrasonic resonance system Power supply, converter, booster (1 pair), horn (1 pair)
2	Personal computer (OS Windows 7) ADA/PIO interface board
3	Software Ultrasonic test control measurement software
4	Cooling system Air dryer, air piping • A separate 140 L/min air source is required.
5	Strain meter unit (option)
6	AG-X plus Autograph 5 kN + 250 extension
7	Average stress loading mechanism

Shimadzu Corporation
www.shimadzu.com/an/

For Research Use Only. Not for use in diagnostic procedure.
This publication may contain references to products that are not available in your country. Please contact us to check the availability of these products in your country.
Company names, product/service names and logos used in this publication are trademarks and trade names of Shimadzu Corporation or its affiliates, whether or not they are used with trademark symbol "TM" or "®". Third-party trademarks and trade names may be used in this publication to refer to either the entities or their products/services. Shimadzu disclaims any proprietary interest in trademarks and trade names other than its own.

The contents of this publication are provided to you "as is" without warranty of any kind, and are subject to change without notice. Shimadzu does not assume any responsibility or liability for any damage, whether direct or indirect, relating to the use of this publication.

© Shimadzu Corporation, 2016

First Edition: August 2016

SHIMADZU

Application News

No.i244

Material Testing System

Tensile Test for Metallic Materials Using Strain Rate Control and Stress Rate Control

Introduction

International standards for tensile testing of metallic materials have been revised as specified in ISO 6892 and JIS Z2241, such that strain rate control, where strain is measured with an extensometer, has recently been added as a test item to the current stress rate control method, in which a load is applied to a material until its yield point is reached. As a result, it can be assumed that there will be situations where both stress rate control and strain rate control tensile testing of metallic materials will be required.
Here, we introduce examples of strain rate control and stress rate control tensile testing of metallic samples, including cold-rolled steel, austenitic stainless steel, aluminium alloy and brass, according to ISO 6892, using the Shimadzu Autograph AG-50kNX Precision Universal Tester, and the SSG50-10H strain gauge type one-touch extensometer (Fig. 1, Fig. 2).

Fig. 1 Overview of Universal Testing System

Fig. 2 Specimen and Jigs for Tensile Testing

Specimens and Test Conditions

Information on the sample specimens are shown in Table 1, and the test conditions are shown in Table 2.

Table 1 Test Specimens

Sample Name	A	B	C	D
Material	Cold-rolled steel	Stainless steel (austenitic)	Aluminium alloy	Brass
Sample size	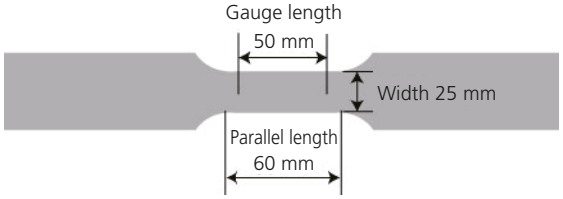 Width 25 mm, thickness 1 mm, gauge length 50 mm, parallel length 60 mm (JIS Z 2241 No. 5 test specimen)			

Table 2 Test Conditions

1) Load cell capacity	50 kN
2) Jig	50 kN Non-shift wedge type grips (file teeth for flat specimen)
3) Test speed	See Table 3
4) Test temperature	Ambient temperature
5) Software	TRAPEZIUMX (single)

Fig. 3 shows an image diagram of the test speed, and Table 3 and Table 4 show the applicable test speeds for the strain control and stress control tests, respectively.

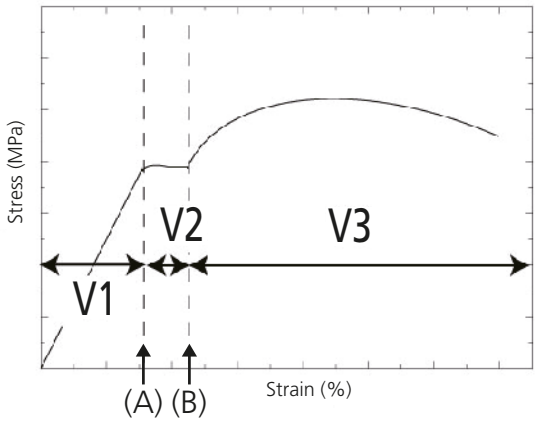

(A): Upper yield point (or its corresponding point)
(B): Upper limit of strain measurement (point after proof strength point)

Fig. 3 Image of Test Strain Rate

Table 3 Test Strain Rate (based on strain rate control)

V1: Strain rate	0.00025/s (1.5 %/min)
V2: Strain rate	0.00025/s (1.5 %/min)
V3: Predicted strain rate	0.0067/s (40 %/min)

Table 4 Test Stress Rate (based on stress rate control)

V1: Stress rate	10 MPa/s
V2: Strain rate	0.00083/s (5 %/min)
V3: Predicted strain rate	0.0067/s (40 %/min)

Test Results

Fig. 4 shows a diagram of the stress – stroke displacement for each sample using strain-rate control, and Table 5 shows their characteristic values. In Fig. 4, the point at which the stress becomes discontinuous, as indicated by the jump in the stress-stroke displacement curve, corresponds to the point at which the strain rate is switched.

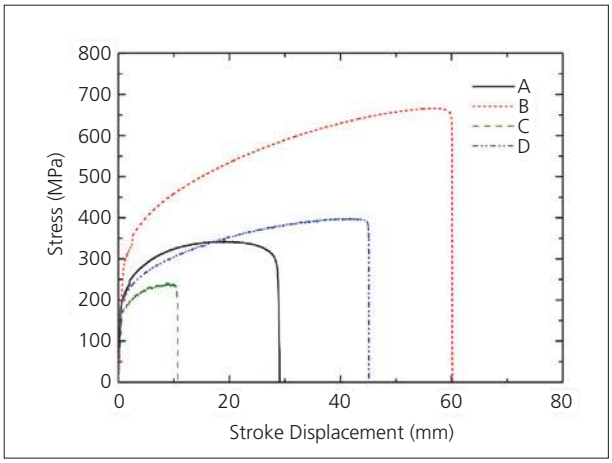

Fig. 4 Test Results for Each Metallic Material (stress-stroke curve based on strain rate control)

Table 5 Test results (Average n = 3)

Sample Name	Elastic Modulus (GPa)	0.2 % Proof Strength (MPa)	Tensile Strength (MPa)	Elongation at Break (%)
A (cold-rolled steel)	194	185.5	341.5	43.3
B (stainless steel)	200	278.5	660.8	55.0
C (aluminum)	71	170.1	236.3	13.0
D (brass)	109	193.1	398.1	49.1

Note 1) Strain rate refers to the amount of increase in strain, obtained using an extensometer to measure the gauge length of a test specimen, per unit time.
Note 2) Predicted strain rate was obtained using the displacement of the testing machine crosshead at each point in time and the test specimen's parallel length. Thus, it is defined as the increase in strain of the specimen's parallel length per unit time.

Fig. 5 (a) – (d) shows the strain rate and predicted strain rate obtained from tensile testing of the respective metallic materials using strain rate control. The red solid lines show the strain rate, the blue solid lines the predicted strain rate, and the black broken lines show the stress. In addition, the green dotted lines represent the permissible value ±20 % relative tolerance in the strain rate control (as specified in ISO 6892). As for the actual load rate, it is clear that the values are well within the permissible strain rate control range, indicating excellent strain rate control. Regarding samples A and B, displacement is measured up to 2 % of the gauge length using an extensometer. In the case of samples C and D, the strain measured using an extensometer was only up to 0.8 %, because of the appearance of serration when strain corresponding to about 1 % was applied.

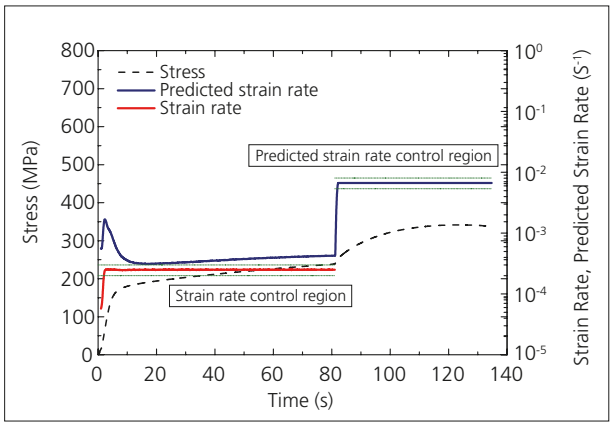

Fig. 5 (a) Test Results (Sample A)

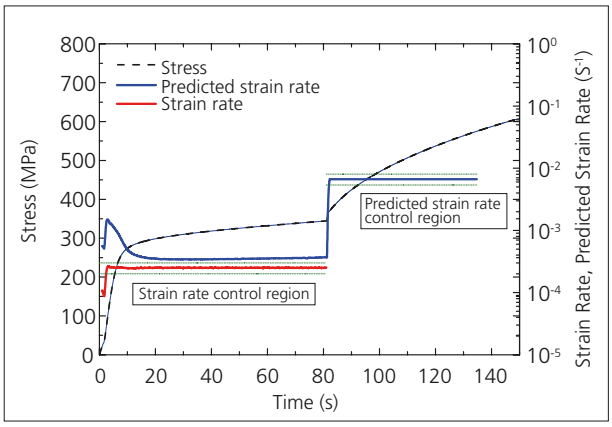

Fig. 5 (b) Test Results (Sample B)

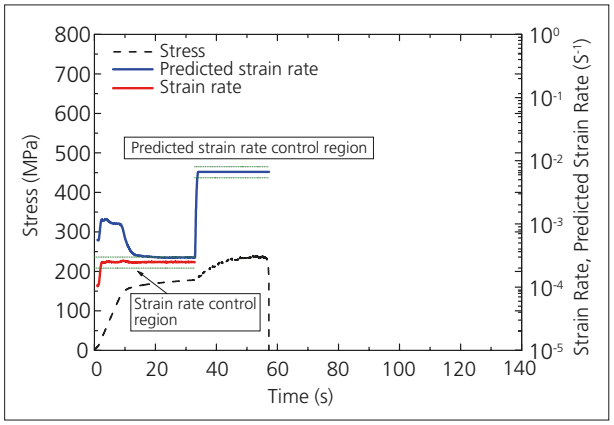

Fig. 5 (c) Test Results (Sample C)

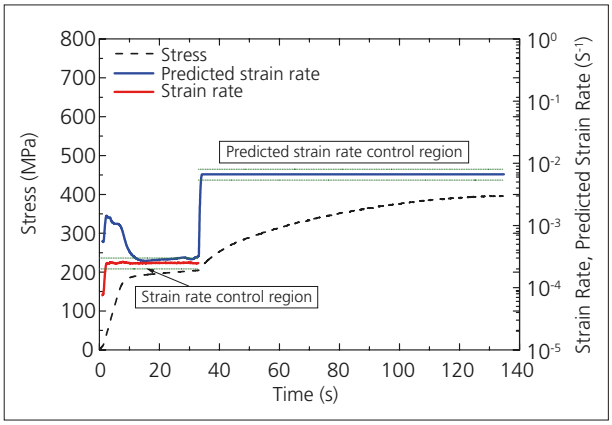

Fig. 5 (d) Test Results (Sample D)

Fig. 6 shows the stress-stroke displacement curve diagram obtained from tensile testing of each of the metallic materials using stress rate control, and the characteristic values are shown in Table 6.

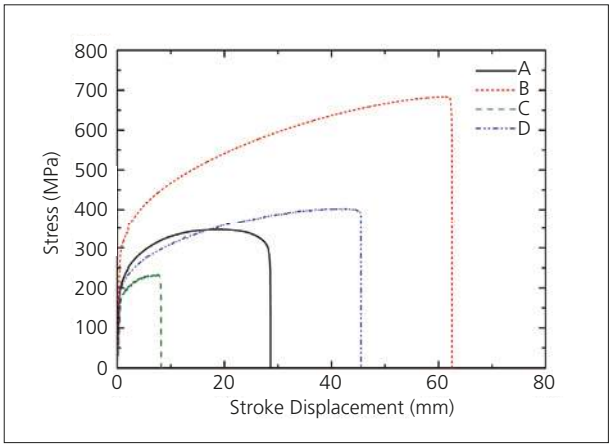

Fig. 6 Test Results (stress-stroke curve based on stress rate control)

Table 6 Test Results (Average n = 3)

Sample Name	Elastic Modulus (GPa)	0.2 % Proof Strength (MPa)	Tensile Strength (MPa)	Elongation at Break (%)
A (cold-rolled steel)	194	193.3	349.3	42.0
B (stainless steel)	205	290.7	687.0	54.8
C (aluminum)	69	177.0	233.5	12.6
D (brass)	112	196.7	405.5	48.8

Fig. 7 (a) – (d) shows the strain rate and predicted strain rate obtained from tensile testing of the respective metallic materials using stress rate control. The pink solid lines show the stress rate, the blue solid lines the predicted strain rate, and the black broken lines show the stress.

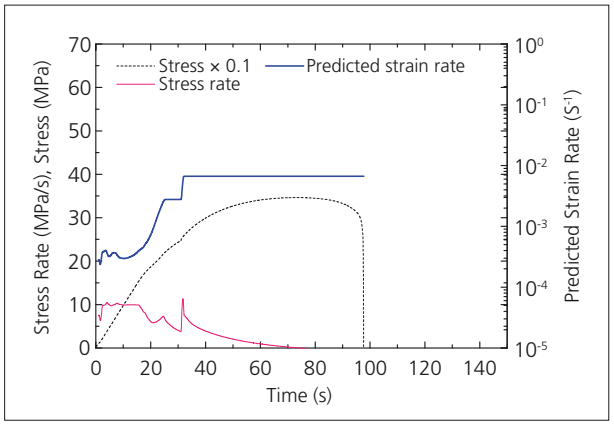

Fig. 7 (a) Test Results (Sample A)

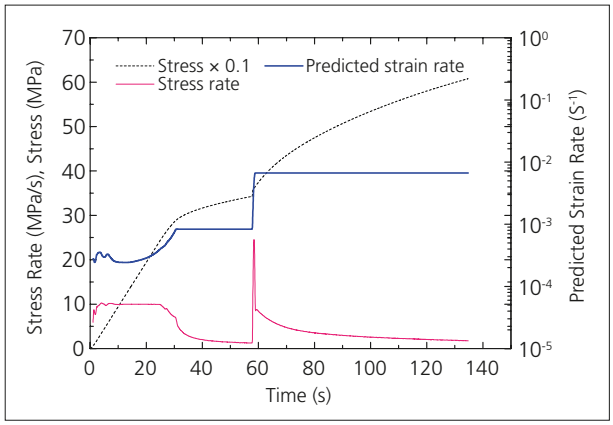

Fig. 7 (b) Test Results (Sample B)

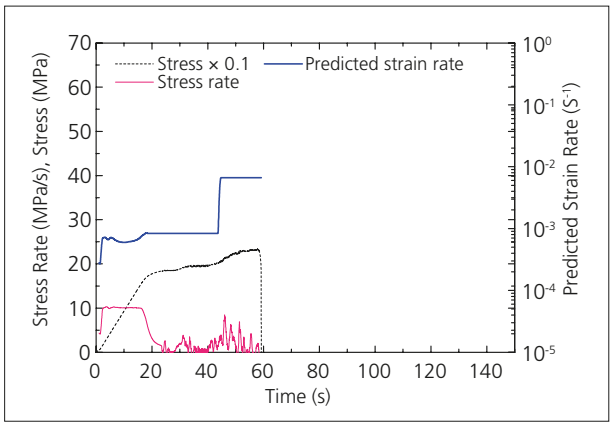

Fig. 7 (c) Test Results (Sample C)

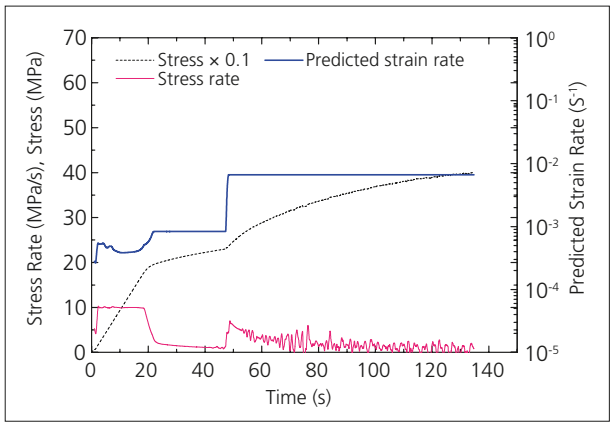

Fig. 7 (d) Test Results (Sample D)

It is clear that at the set rates, suitably stable data could be acquired for both stress rate and predicted strain rate.

The above results demonstrate that in the tensile testing of the various types of metallic materials using the Shimadzu Autograph AG-50kNX Precision Universal Tester, the strain rate control values were well within the range of the permissible values (± 20 %) specified in ISO 6892. Similarly, stable testing using stress rate control was also achieved. When using typical universal testing machines, testing control methods other than the crosshead rate control, e.g. strain rate control and stress rate control, normally require burdensome adjustment of the control gain depending on the material being tested. However, with this instrument, strain rate control and stress rate control in tensile testing of any metallic material are easily conducted because the gain is adjusted automatically (auto-tuning feature).

First Edition: January, 2012

SHIMADZU

SHIMADZU Corporation
www.shimadzu.com/an/

For Research Use Only. Not for use in diagnostic procedures.
The contents of this publication are provided to you "as is" without warranty of any kind, and are subject to change without notice.
Shimadzu does not assume any responsibility or liability for any damage, whether direct or indirect, relating to the use of this publication.

© Shimadzu Corporation, 2012

SHIMADZU
Excellence in Science

Application Data Sheet

No. 14

Autograph Precision Universal Tester

Material Testing & Inspection

Tensile Testing of Metallic Materials with Stress Rate Control

Standard No. ISO6892:2009 (JIS Z 2241: 2011)

Introduction

Metallic materials have excellent extensibility and ductility and are comparatively easy to mechanically process. Consequently, they are widely used in industrial components, building materials, and everyday goods. Tensile tests using stress rate control have long been used for quality control and new material development as a means of evaluating the mechanical properties of metallic materials. This Application Data Sheet introduces examples of static tensile testing using stress rate control performed on dumbbell-shaped test specimens of 4 types of metallic materials (cold-rolled steel, austenitic stainless steel, aluminium alloy, brass), in which basic mechanical properties such as tensile strength and elongation are evaluated.

T. Murakami

Measurement and Jigs

Most metallic materials have tensile strengths higher than those of resin and rubber materials, so it is necessary to select grips that are capable of reliably and stably holding the material during testing up to fracture. For tensile testing of metallic materials, non-shift wedge-type or hydraulic grips are used for samples with a large test force. For samples with a small maximum test force, pneumatic flat and screw-type flat grips are also used.

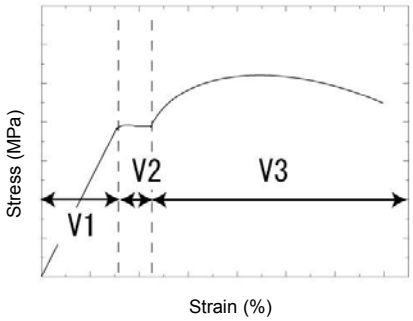

Fig. 1: Image of Controlling Rates

Table 1: Sample Information

Sample	A	B	C	D
Material	Cold-rolled steel	Stainless steel	Aluminum alloy	Brass

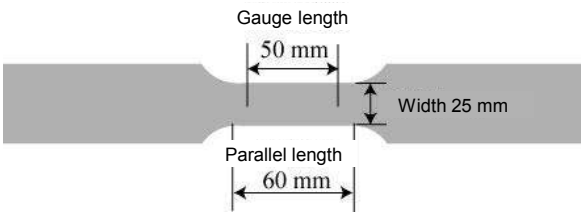

Width: 25 mm, thickness: 1 mm, gauge length: 50 mm, parallel length: 60 mm

Fig. 2: Sample Shape

V1: Rate of increase of stress: 10 MPa/s
V2: Estimated strain rate: 0.00084/s (5 %/min)
V3: Estimated strain rate: 0.0067/s (40 %/min)
Point of switching rate from V1 to V2: Point at which V1 exceeds V2 value
Point of switching rate from V2 to V3: Point at which measurement of displacement by extensometer is terminated

Note: The estimated strain rate is obtained based on the displacement per unit time of the crosshead of the testing machine and the parallel length of the test specimen. It is the increment of strain in the parallel length of the test specimen per unit time.

Measurement Results

Table 2: Test Results

Sample	Elastic modulus (GPa)	Proof strength (offset method) (MPa)	Tensile strength (MPa)	Percentage elongation after fracture (%)
A (Cold-rolled steel)	194	193.3	349.3	42.0
B (Stainless steel)	205	290.7	687.0	54.8
C (Aluminum alloy)	69	177.0	233.5	12.6
D (Brass)	112	196.7	405.5	48.8

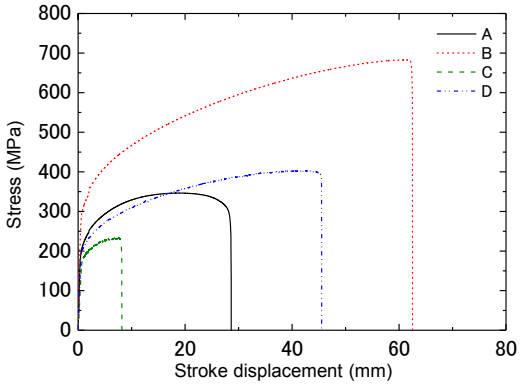

Fig. 3: Stress–Stroke Displacement Curves for Each Metal Material

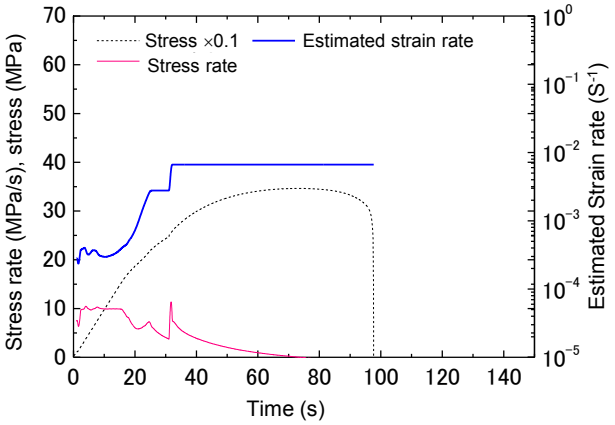

Fig. 4: Example of Stress Rate Results (Sample A: Cold-rolled steel plate)

Fig. 4 shows the stress rate and the estimated strain rate obtained from tensile testing the cold-rolled steel plate using stress rate control. It can be seen that stable data has been acquired in accordance with the set speed, for both the stress rate and estimated strain rate.

Metal Stress Rate Control Tensile Testing System

Tester:	AG-Xplus
Load Cell:	50 kN
Test Jig:	50 kN non-shift wedge type grips
Extensometer:	Strain gauge type one-touch extensometer: SSG50-10H
Software:	TRAPEZIUM X (Single)

AG-Xplus Floor-Type Precision Universal Tester

Features

- A high-precision load cell is adopted. (The high-precision type is class 0.5; the standard-precision type is class 1.) Accuracy is guaranteed over a wide range, from 1/1000 to 1/1 of the load cell capacity. This supports highly reliable test evaluations.
- Crosshead speed range
  Tests can be performed over a wide range from 0.0005 mm/min to 1,000 mm/min.
- High-speed sampling
  Ultrafast sampling, as fast as 0.2 msec, allows assessment of sudden changes in test force, such as when brittle materials fracture.
- TRAPEZIUMX X operational software
  Designed for intuitive operation, it offers a variety of convenient and user-friendly features.
- Smart controller
  Real-time test force and position data are readily confirmed, and the manual dial enables fine adjustments to jig positioning.
- Optional Test Devices
  A variety of tests can be performed by switching between an abundance of jigs in the lineup.

First Edition: February 2013

Shimadzu Corporation
www.shimadzu.com/an/

For Research Use Only. Not for use in diagnostic procedures.
The content of this publication shall not be reproduced, altered or sold for any commercial purpose without the written approval of Shimadzu.
The information contained herein is provided to you "as is" without warranty of any kind including without limitation warranties as to its accuracy or completeness. Shimadzu does not assume any responsibility or liability for any damage, whether direct or indirect, relating to the use of this publication. This publication is based upon the information available to Shimadzu on or before the date of publication, and subject to change without notice.
© Shimadzu Corporation, 2013

SHIMADZU
Excellence in Science

Application Data Sheet

No. 15

Autograph Precision Universal Tester

Material Testing & Inspection

Tensile Testing of Metallic Materials with Strain Rate Control

Standard No. ISO6892:2009 (JIS Z 2241: 2011)

Introduction

The international standard for tensile testing of metallic materials, ISO 6892, includes a strain rate control test method (strain measurement with an extensometer). This is in addition to the conventional stress rate control method as the loading method up to the yield point of the material. It is expected that tensile testing of metallic materials using both stress rate control and strain rate control will increase in the future. As a result, many existing testing machine users are interested in whether or not it is possible to obtain stable data from both test methods using existing and/or new testing machines. This Application Data Sheet introduces examples of static tensile tests using strain rate control carried out on dumbbell-shaped test specimens of 4 types of metallic material (cold-rolled steel, austenitic stainless steel, aluminium alloy, brass), in which basic mechanical properties such as tensile strength and elongation are evaluated.

T. Murakami

Measurement and Jigs

Most metallic materials have tensile strengths higher than those of resin and rubber materials, so it is necessary to select grips that are capable of reliably and stably holding the material during testing up to fracture. For tensile tests of metallic materials, non-shift wedge-type or hydraulic grips are used for samples with a large test force. For samples with a small maximum test force, pneumatic flat and screw-type flat grips are also used.

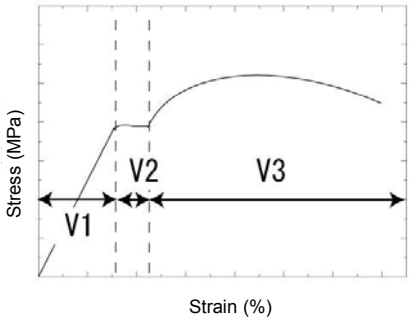

Fig. 1: Image of Controlling Rates

Table 1: Sample Information

Sample	A	B	C	D
Material	Cold-rolled steel	Stainless steel	Aluminum alloy	Brass

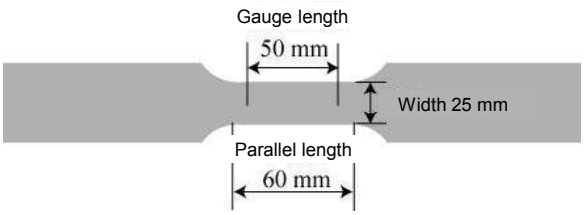

Width: 25 mm, thickness: 1 mm, gauge length: 50 mm, parallel length: 60 mm

Fig. 2: Sample Shape

V1, V2: Strain rate: 0.00025/s ±20 % (feedback of strain from extensometer to testing machine)
V3: Estimated strain rate: 0.0067/s (40 %/min) ±20 %
Point of switching rate from V2 to V3: Point at which measurement of displacement by extensometer is terminated (For samples A and B, displacement was measured using an extensometer up to 2 % of the gauge length. For samples C and D, serrations occurred when a strain equivalent to 1 % was applied, so measurement with the extensometer was used up to 0.8 %.)

Note: The estimated strain rate is obtained based on the displacement per unit time of the crosshead of the testing machine and the parallel length of the test specimen. It is the increment of strain in the parallel length of the test specimen per unit time.

Measurement Results

Table 2: Test Results

Sample	Elastic modulus (GPa)	Proof strength (offset method) (MPa)	Tensile strength (MPa)	Percentage elongation after fracture (%)
A (Cold-rolled steel)	194	185.5	341.5	43.3
B (Stainless steel)	200	278.5	660.8	55.0
C (Aluminum alloy)	71	170.1	236.3	13.0
D (Brass)	109	193.1	398.1	49.1

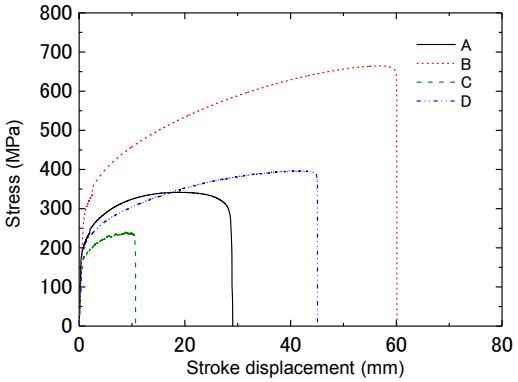

Fig. 3: Stress-Stroke Curves

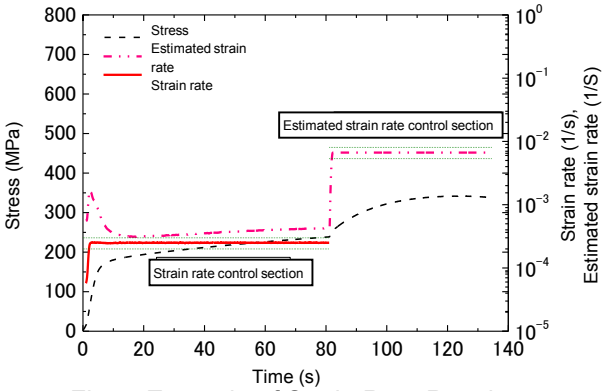

Fig. 4: Example of Strain Rate Results (Sample A: Cold-rolled steel plate)

Fig. 3 shows an example of the strain rate and estimated strain rate obtained from tensile testing the cold-rolled steel plate using strain rate control. The red solid line indicates strain rate, the pink double dotted broken line indicates the estimated strain rate, and the blue broken line indicates the stress. The green dotted line indicates the tolerance of the strain increase rate (±20 % specified by ISO 6892). The actual load rate is sufficiently within the tolerance of the strain rate control range, which indicates that good strain rate control has been performed.

Metal Strain Rate Control Tensile Testing System

Tester:	AG-Xplus
Load Cell:	50 kN
Test Jig:	50 kN non-shift wedge type grips
Extensometer:	Strain gauge type one-touch extensometer SSG50-10H
Software:	TRAPEZIUM X (Single)

TRAPEZIUM X

AG-Xplus Floor-Type Precision Universal Tester

Features

- A high-precision load cell is adopted. (The high-precision type is class 0.5; the standard-precision type is class 1.) Accuracy is guaranteed over a wide range, from 1/1000 to 1/1 of the load cell capacity. This supports highly reliable test evaluations.
- Crosshead speed range
  Test can be performed over a wide range from 0.0005 mm/min to 1,000 mm/min.
- High-speed sampling
  Ultrafast sampling, as fast as 0.2 msec, allows the assessment of sudden changes in test force, such as when brittle materials fracture.
- TRAPEZIUMX X operational software
  Designed for intuitive operation, it offers a variety of convenient and user-friendly features.
- Smart controller
  Real-time test force and position data are readily confirmed, and the manual dial enables fine adjustments to jig positioning.
- Optional Test Devices
  A variety of tests can be performed by switching between an abundance of jigs in the lineup.

First Edition: February 2013

SHIMADZU

Shimadzu Corporation

www.shimadzu.com/an/

For Research Use Only. Not for use in diagnostic procedures.
The content of this publication shall not be reproduced, altered or sold for any commercial purpose without the written approval of Shimadzu.
The information contained herein is provided to you "as is" without warranty of any kind including without limitation warranties as to its accuracy or completeness. Shimadzu does not assume any responsibility or liability for any damage, whether direct or indirect, relating to the use of this publication. This publication is based upon the information available to Shimadzu on or before the date of publication, and subject to change without notice.

© Shimadzu Corporation, 2013

SHIMADZU
Excellence in Science

Application News

No. SCA_300_023

Material Testing System HMV-G

Measurement of Carburized Case Depth of Steel with Shimadzu Micro Hardness Tester Model HMV

■ Introduction

Micro hardness testers are indispensable instruments for hardness evaluation, including surface composition, surface quenching layers, and machining transformation layers in research and development as well as quality control of parts of precision instruments, wires, metal foils, and electronic elements. The method for measuring the depth of layers hardened by carburizing or carburizing and quenching is specified in JIS-G-0557 "Method of measuring case depth hardened by carburizing treatment for steel." According to it, the effective depth or whole depth of hardened layer should be determined from the hardness distribution curve obtained on the cross section perpendicular to the hardened layer by use of a micro hardness tester.

The Shimadzu Micro Hardness Tester, which features very high reliability and excellent operability due to its built-in data processing functions, is best suitable for efficient measurement of the depth of carburized layers. The following is an example of such a measurement.

■ Measurement of hardness distribution in a carburized layer of Ni-Cr-Mo steel

A specimen was prepared by molding a cross section of steel into resin and finished by buffing. Hardness was measured at every 0.1mm on the test surface. The printer output is shown in **Fig.1**. The hardness distribution plotted from the measured data is shown in **Fig.2** JIS-G-0557 defines the effective depth of hardened layer as the distance between the surface and the point at which Vickers hardness matches 550. In this test, the effective depth is 0.6 mm. Shimadzu Micro Hardness Tester, featuring completely automatic load change, loading, and unloading, is used for quality control of low to high hardness's of small parts such as the gears and cams of watches, sewing machines, cameras and optical devices, and electronic elements like ICs and LSIs.

Date of test	Date 1987 2 14
Testing parameter file No	File No.
Specimen Number	Sample No.
Number of tests	Test 13
Number of lots	Lot 1
Testing mode	Vickers
Type of specimen surface	Flat
Repetitive number to read data	Read 2
Testing load	Load 200 GF
Load duration time	Loading Time 15 Sec
Correction coefficient	Correct 0,1273 µm
Number of lots and number of tests for a specimen	Lot = 1, Test = 1
Diagonal length of the indentation	D1 = 22,8
	D2 = 22,6
Vickers hardness	HV = 718
	Lot = 1, Test = 2
	D1 = 22,2
	D2 = 22,6
	HV = 735
	Lot = 1, Test = 3
	D1 = 22,3
	D2 = 22,6
	HV = 734
	Lot = 1, Test = 4
	D1 = 30,9
	D2 = 31,5
	HV = 380
Result of statistical calculation	--Statistics--
Measuring mode	HV
Number of lots	Lot = 1
Mean hardness	X = 572
Standard deviation	S = 143,7
Coefficient of variation	CV = 25,08 %
Minimum value in the lot	Min. = 380
Maximum value in the lot	Max. = 739

Fig. 1 Printer output of measured values

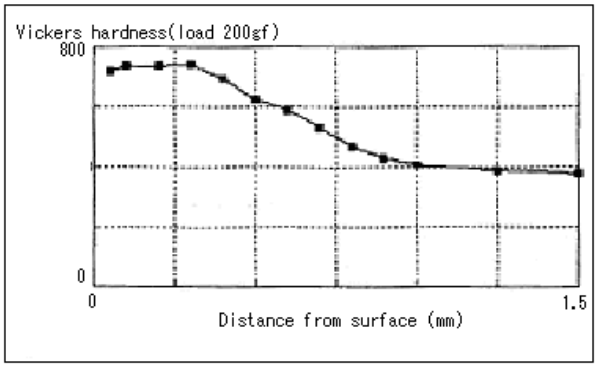

Fig. 2 Hardness Distribution in Carburized layer

* Please be advised that data obtained before the implementation of the current Weights and Measures Law may be presented in terms of gravimetric unit.

For Research Use Only. Not for use in diagnostic procedures.
The content of this publication shall not be reproduced, altered or sold for any commercial purpose without the written approval of Shimadzu. The information contained herein is provided to you "as is" without warranty of any kind including without limitation warranties as to its accuracy or completeness. Shimadzu does not assume any responsibility or liability for any damage, whether direct or indirect, relating to be the use of this publication. This publication is based upon the information available to Shimadzu on or before the date of publication, and subject to change without notice.

SHIMADZU
Excellence in Science

Application News

Material Testing System DUH

Measurement of Hardness of the Machining Deterioration Layer of Stainless Steel with Shimadzu Dynamic Ultra Micro Hardness Tester DUH

No. SCA_300_024

■ Introduction

When a metallic material is processed with lathes, milling machines, or grinders, the upper portion of the material*s surface is transformed into a so-called machining deterioration layer. This layer, which results from plastic transformation and increased temperature during the machining process, comprises an amorphous layer, a plastic deterioration layer, a fine particle layer, and micro structure deterioration layers. These have greater displacement than the inner part of the material, producing residual stress.

The following presents the results of dynamic indentation hardness testing on a thin surface layer (1-3 µm) of machine processed stainless steel (SUS304) performed with the Shimadzu Dynamic Ultra Micro Hardness Tester Model DUH.

This machine is widely applicable to a range of hard to soft materials as it measures hardness of thin films and thin layers in terms of the indentation depth of an indenter (dynamic indentation hardness) or the diagonal length of indentation (Vickers hardness).

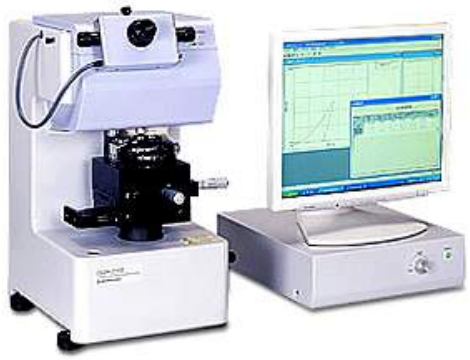

■ Test conditions

1) Specimen : Stainless steel SUS304
Processing:

A) Solution heat treatment only
B) Polishing finish after solution heat treatment
C) Turning and polishing by polishing paper after solution heat

■ Testing procedure

Dynamic indentation hardness (hereafter called hardness) was calculated from the relation of load versus depth at 0.2 µm intervals from the surface with load being applied via indenter to each of three specimens finished in different ways. Load was continuously applied up to 100 gf.

■ Test results

Table 1 displays the values measured under the processing condition A (others under processing conditions B and C are omitted), Table 2 the variation of hardness (averaged) along the depth direction for each of the processing conditions, and Fig.1 the depth versus hardness curves. The tendency of curve B to approach A at a depth of around 2 µm and to overlap A thereafter suggests that the machining deterioration layer remains influential until an indentation depth of around 2 µm, but the hardness of the matrix material is predominant thereafter. Curve C suggests that the respective machining deterioration layer keeps its influence down to a significantly greater depth than curve B, as sample C has undergone a turning process just prior to the polishing paper finish.

No.	Load (gf)	Depth	Hardness
1	0.640	0.20	603.41
2	1.300	0.40	170.66
3	2.720	0.60	170.46
4	4.260	0.80	162.71
5	6.260	1.00	181.49
6	8.480	1.20	159.05
7	10.960	1.40	150.25
8	13.680	1.60	142.45
9	16.720	1.80	144.15
10	20.100	2.00	147.06
11	23.720	2.20	132.13
12	27.300	2.40	132.12
13	31.680	2.60	131.67
14	36.100	2.80	125.24
15	40.720	3.00	131.53
16	45.440	3.20	122.39
17	50.500	3.40	126.31
18	55.900	3.60	129.71
19	61.600	3.80	130.86
20	67.200	4.00	115.21
21	73.220	4.20	122.12
22	79.520	4.40	122.96
23	85.840	4.60	144.29
24	92.360	4.80	112.87
25	99.020	5.00	109.63

No.	Load (gf)	Depth	Hardness
1	0.640	0.20	603.41
2	1.360	0.40	126.85
3	2.380	0.60	134.12
4	3.560	0.80	111.99
5	5.100	1.00	130.57
6	7.000	1.20	141.99
7	9.300	1.40	154.27
8	11.940	1.60	155.80
9	14.920	1.80	156.86
10	18.220	2.00	155.81
11	21.820	2.20	153.40
12	23.720	2.40	151.38
13	25.720	2.60	146.06
14	34.200	2.80	139.23
15	38.640	3.00	128.13
16	43.420	3.20	131.80
17	48.640	3.40	140.11
18	54.080	3.60	136.36
19	59.720	3.80	132.29
20	65.420	4.00	122.86
21	71.940	4.20	146.46
22	78.320	4.40	128.18
23	84.660	4.60	116.69
24	91.720	4.80	133.71
25	98.860	5.00	120.38

No.	Load (gf)	Depth	Hardness
1	0.700	0.20	662.16
2	1.620	0.40	179.93
3	2.940	0.60	184.68
4	4.600	0.80	175.00
5	6.460	1.00	149.01
6	8.760	1.20	165.34
7	11.220	1.40	143.00
8	14.020	1.60	147.37
9	17.040	1.80	139.21
10	20.440	2.00	146.18
11	23.900	2.40	127.990
12	27.640	2.40	128.53
13	31.500	2.60	124.12
14	35.880	2.80	129.77
15	48.580	3.00	136.78
16	45.360	3.20	123.04
17	50.420	3.40	126.32
18	55.340	3.60	108.31
19	61.00	3.80	130.32
20	66.960	4.00	131.37
21	73.060	4.20	125.75
22	79.440	4.40	126.30
23	86.280	4.60	133.59
24	93.260	4.80	128.40
25	100.100	5.00	114.48

Table 1: Measured Values under Processing Condition A (measured in three trials

No.	Depth (µm)	Dynamic Indentation Hardness (DH)		
		A	B	C
1	0.20	-	-	-
2	0.40	159.15	403.21	477.13
3	0.60	139.09	372.56	155.11
4	0.80	149.90	297.51	432.84
5	1.00	153.69	223.65	376.67
6	1.20	155.46	190.37	348.49
7	1.40	149.44	168.84	328.97
8	1.60	148.54	164.00	312.09
9	1.80	146.74	157.75	296.65
10	2.00	169.68	149.26	273.96
11	2.20	141.00	138.73	270.36
12	2.40	137.41	146.23	272.86
13	2.60	140.62	135.57	261.47
14	2.80	131.41	138.12	264.10
15	3.00	132.15	128.96	254.45
16	3.20	126.68	124.28	247.20

Table 2: Variation of Dynamic Indentation Hardness along Depth Direction for Each of Three Different Processing Conditions

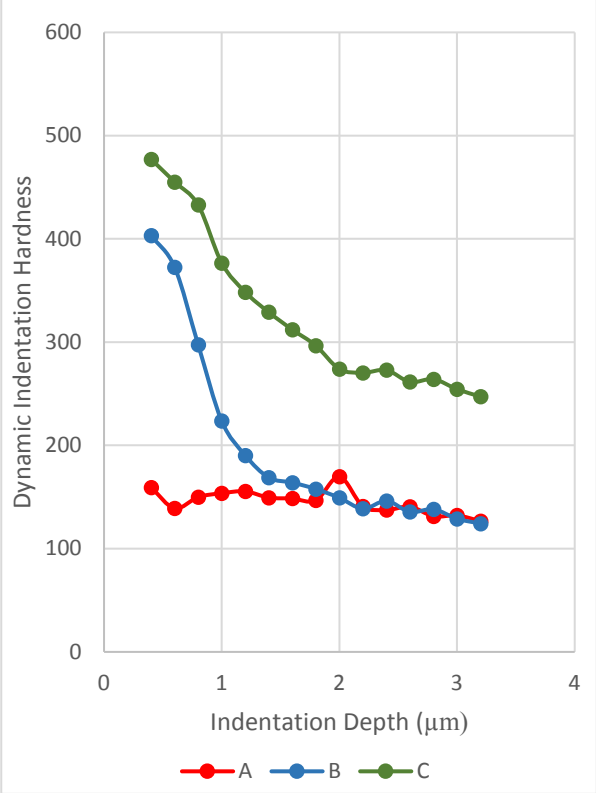

$$DH_n = 37{,}838 \cdot \frac{P_n}{(D_n - D_{n-1})^2} \cdot \left(1 - \sqrt{\frac{P_{n-1}}{P_n}}\right)^2$$

DH_n: Dynamic Hardness in the sequence of n-th

P_n: Load in sequence of n-th (gf)

P_{n-1}: Load in sequence of n-1-th (gf)

D_n: Indentation depth in the sequence of n-th (µm)

D_{n-1}: Indentation depth in the sequence of n-1-th (µm)

* Please be advised that data obtained before the implementation of the current Weights and Measures Law may be presented in terms of gravimetric unit.

For Research Use Only. Not for use in diagnostic procedures.
The content of this publication shall not be reproduced, altered or sold for any commercial purpose without the written approval of Shimadzu. The information contained herein is provided to you "as is" without warranty of any kind including without limitation warranties as to its accuracy or completeness. Shimadzu does not assume any responsibility or liability for any damage, whether direct or indirect, relating to be the use of this publication. This publication is based upon the information available to Shimadzu on or before the date of publication, and subject to change without notice.

SHIMADZU
Excellence in Science

Application News

Material Testing System DUH

No. SCA_300_034

A hardness measurement of steel surface treatment layer with Shimadzu Dynamic Ultra Micro Hardness Tester, Model DUH

A variety of surface treatment is exercised to every part of industrial products, so that their functionality, corrosive resistively, or decorating nature of the surficial layer should be made best fitted to their respective role. The following example is dedicated to represent an effective method for a dynamic hardness measurement by indenting onto the thin hardening layer (4 - 5μm deep) on the cut section, the surface of which is perpendicular to the longitudinal direction of a steel bar.

■ Testing parameters

1) Sample: steel (surficial hardening treatment), see Fig.1

2) Indenter: tip angle 136°, square pyramid indenter (Vickers indenter)

3) Measuring mode: load-load hold test (mode 1)

4) Test load: 1.0 gf

5) Loading speed: 0.0725 gf/sec.

6) Load hold-time: 10 sec.

■ Testing parameters

As the measuring area is limited to a very narrow range(4 - 5 μm) of hardening treatment thin layer, the diagonal length of an indentation must be as small as about a fifth (0.8 - 1mμ or less) of the width of the hardening layer so that the measurement would not undergo dimensional restriction. Accordingly, an optional X100 objective lens of was selected instead of standard X50, thus obtaining an overall magnifying power of X1000 with combined use of X10 eyepiece lens. This permits the measurement observing the indentation always near at the center of the surficial hardening layer through the optical monitor.

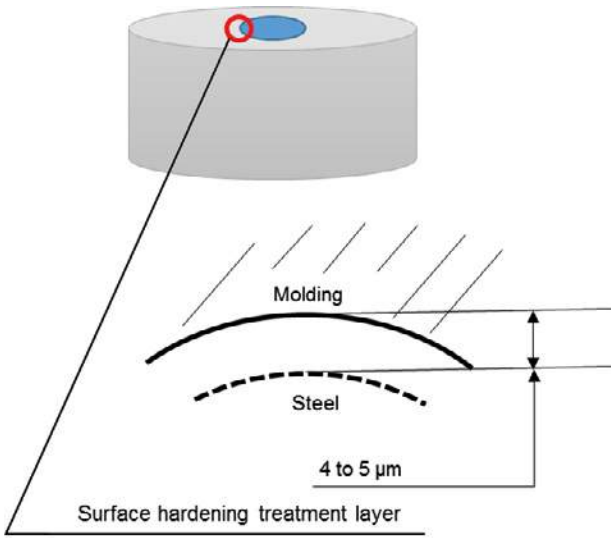

Fig. 1 Sample

■ Test Result

1) The average of three measurements are shown in Table 1, and the load - indentation depth curves are in Fig.2.

Load (gf)	Depth (μm)	Dynamic Hardness DHV
1,0015	0,126	2387

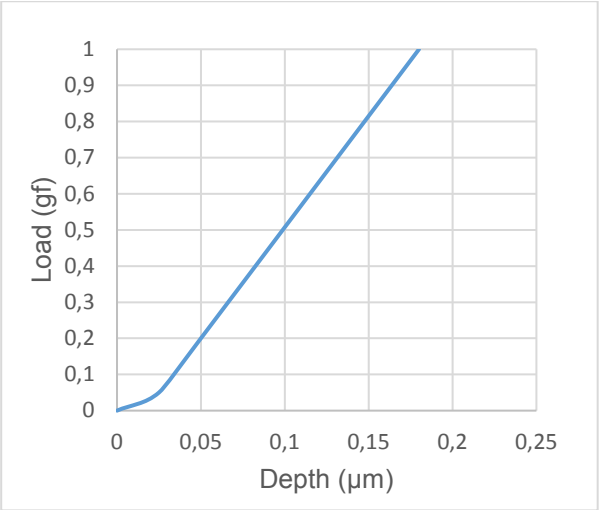

Fig. 2 Load- Indentation depth curve (in mode 1)

Dynamic Hardness was determined by the following formula:

$$DHV = \frac{37{,}838 \cdot P}{h^2}$$

Where:

DHV: Dynamic hardness by Vickers Indenter

P: Test Load (gf)

H: Indentation depth (μm)

2) Diagonal length of an indentation is known to be seven times of the indentation depth (using a Vickers indenter). Accordingly, the diagonal length is supposed to be about 0.9 μm in this case, which permits the measurement being not affected from the thickness of surficial hardening layer.

3) Fig.3 shows a photograph of the tested indentation (approx. X1000).

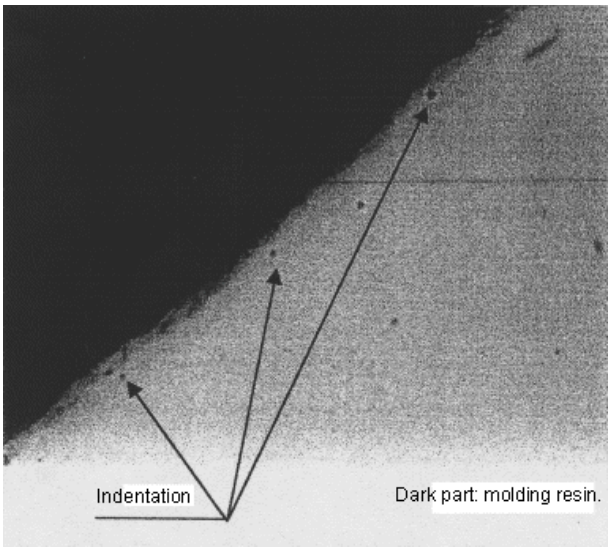

Fig. 3 Tested Indentation

For Research Use Only. Not for use in diagnostic procedures.
The content of this publication shall not be reproduced, altered or sold for any commercial purpose without the written approval of Shimadzu. The information contained herein is provided to you "as is" without warranty of any kind including without limitation warranties as to its accuracy or completeness. Shimadzu does not assume any responsibility or liability for any damage, whether direct or indirect, relating to be the use of this publication. This publication is based upon the information available to Shimadzu on or before the date of publication, and subject to change without notice.

SHIMADZU
Excellence in Science

Application News

Material Testing System DUH

No. SCA_300_035

A hardness measurement of surface treatment layer on a steel sample using Shimadzu Dynamic Ultra Micro Hardness Tester, Model DUH

Recent years have seen intensive requests for engineering materials with higher function ability and longer life, and as a result, surface treatment for such materials has become popular. Under this circumstance, hardness testers with micro load are enjoying an increasing demand. In this regards, a test report is herein introduced on the hardness distribution measured from the sample surface toward depth direction with an interval of 2 µm, using Shimadzu Dynamic Ultra Micro Hardness Tester Model DUH.

■ Test Parameters

1) Sample: plating layer on a metal plate (See Fig. 1)

2) Indenter: tip angle 136°, square pyramid indenter (Vickers indenter)

3) Measuring mode: load-load-hold test (mode 1)

4) Test load: 2.0 gf

5) Loading speed: 0.029 gf/sec.

6) Load hold-time: 10 sec.

■ Test Method

1) Vickers Hardness
Testing procedures, the distance between the indentation center and the sample edge shall be 2.5 time the diagonal length or more (the diagonal length is 2.6 µm or less). The test load was determined in accordance with this specification, and the tests were performed near the mid depth of the plating layer.

2) Hardness distribution measurements were performed at the location and with the depth intervals of 2 µm starting from the sample surface as shown in Fig. 2

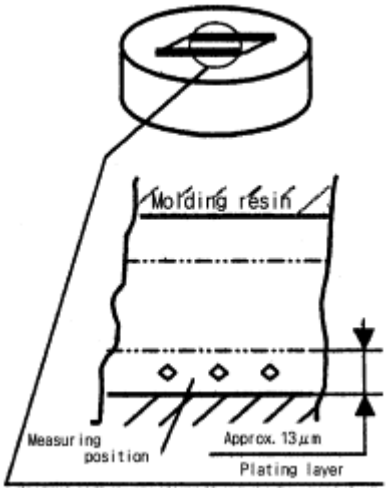

Fig. 1

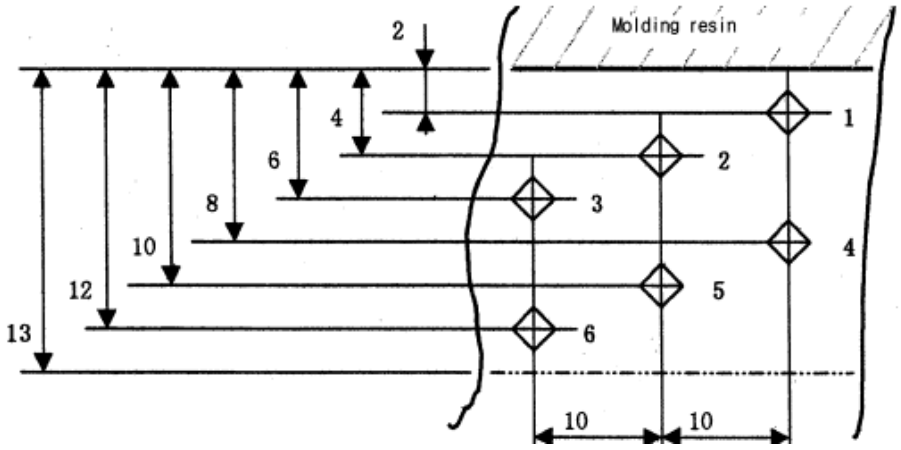

Fig. 2

■ Test Results

The average of five measurements is shown in Table 1, and the load-indentation depth curve is in Fig. 3

Test Load (gf)	Depth (μm)	Dynamic Hardness DHV
2,001	0,206	1065

Table 1 Hardness Test Result

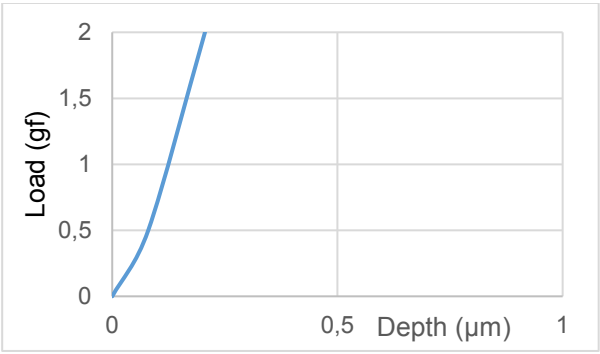

Fig. 3 Load-Indentation depth curve

Dynamic Hardness was determined by the following formula:

$$DHV = \frac{37{,}838 \cdot P}{h^2}$$

Where:

DHV: Dynamic hardness by Vickers Indenter

P: Test Load (gf)

H: Indentation depth (μm)

■ Test Results

Result of five tests with a depth interval of 2 μm is listed in Table 2.

Test Load (gf)	DHV					
	1	2	3	4	5	6
2,0	847	1001	1070	1103	966	925

Table 2 Hardness Distribution

..

■ **Dynamic hardness was determined by the same formula as item 1) above.**

The Relation of depth and hardness is shown in Fig. 4.

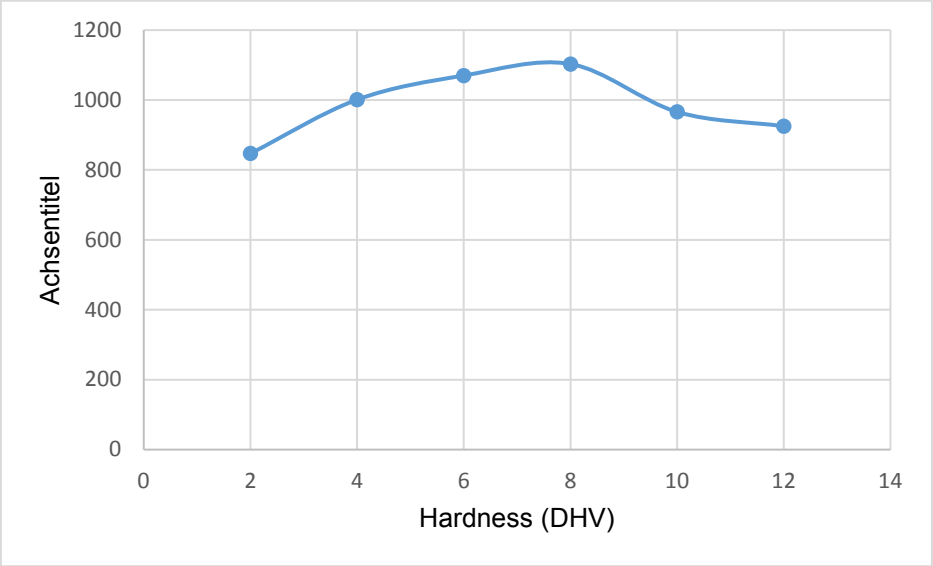

Fig. 4

Fig. 4 indicates a tendency that hardness increases as depth increases, reaches the max. at mid depth of the plating layer, and decreases thereafter.

For Research Use Only. Not for use in diagnostic procedures.
The content of this publication shall not be reproduced, altered or sold for any commercial purpose without the written approval of Shimadzu. The information contained herein is provided to you "as is" without warranty of any kind including without limitation warranties as to its accuracy or completeness. Shimadzu does not assume any responsibility or liability for any damage, whether direct or indirect, relating to be the use of this publication. This publication is based upon the information available to Shimadzu on or before the date of publication, and subject to change without notice.

SHIMADZU
Excellence in Science

Application News

Material Testing System DUH

No. SCA_300_036

A thickness measurement of a Ni-plating layer on a stainless-steel sample with Shimadzu Dynamic Ultra Micro Hardness

■ Introduction

In general, Shimadzu Dynamic Ultra Micro Hardness Tester Model-DUH series (measuring depth 0 – 10 µm) are widely used for measuring hardness of thin films and surface treatment layer, and it can also be applied to the thickness measurement of thin layers (thickness below 10 µm). The followings is a test example in which thickness of Ni-plating on a stainless-steel sample was measured with Shimadzu Dynamic Ultra Micro Hardness Tester Model DUH-201S.

■ Test parameters

1) Sample: Ni-plating layer on stainless steel (See Fig.1)
2) Indenter: Triangle pyramid indenter,tip angle 115° (Berkovich Indenter)
3) Measuring mode: load-load hold test (mode 1)
4) Test load: 100 gf
5) Loading speed: 3.6 gf/sec.
6) Load hold-time: 10 sec.

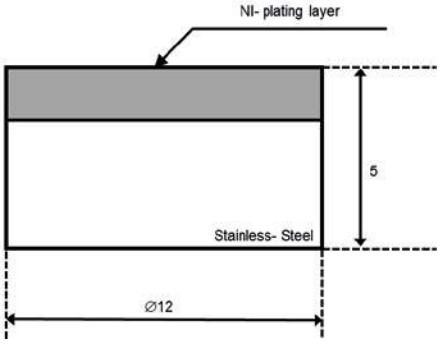

Fig. 1 Test Sample

■ Testing parameters

1) Measure each hardness while changing the test loads. Select 'Hardness-Indentation depth Curve between Two Points' in the data analysis menu and study how the state of curve changes, referring item 2) below.

2) At the earlier step when the test load is small and it makes an indentation of very shallow depth compared with the whole thickness of the plating layer, the indentation represents the hardness of the plating layer only, and its variation is moderately slow as the test load increases.

As the test load further increases, however, the indentation gradually undergoes the influence of the base-material, stainless-steel, and the indication of hardness changes steeply downward (or upward if the base-material is harder than the plating layer). The critical point (h1) will be observed, if the test load is further increased. There appears another critical point (h2), where the indentation is under significant influence from the hardness of base-material. The thickness of the plating layer can be estimated from these critical points.

3) In case of DUH series, the test load of the above item 2) need not be repeated many times but a few times only, just like 100 gf and 200 gf, the max. test load, for example.

■ Test Result

Fig. 2 shows the Load-Indentation depth Curve by the test using parameters in the above item 1. Fig. 3 is a 'Hardness-Depth Curve between Two Points' corresponding to the Fig.2.

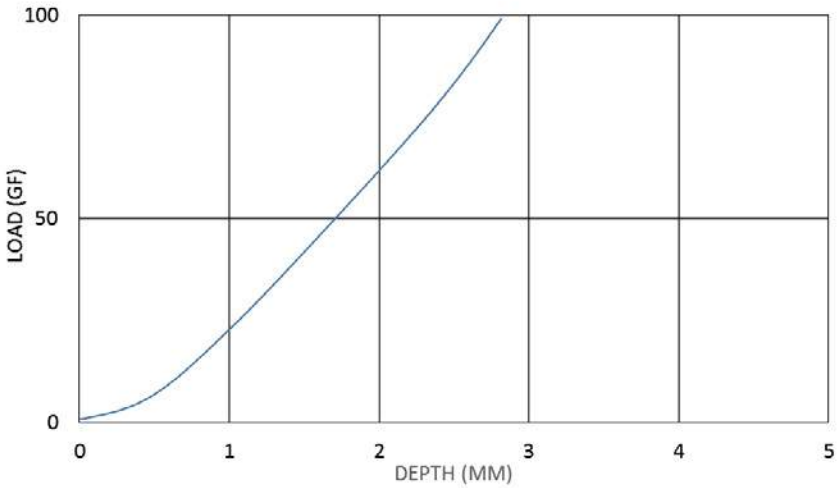

Fig. 2 Load- Indentation depth Curve (test mode 1)

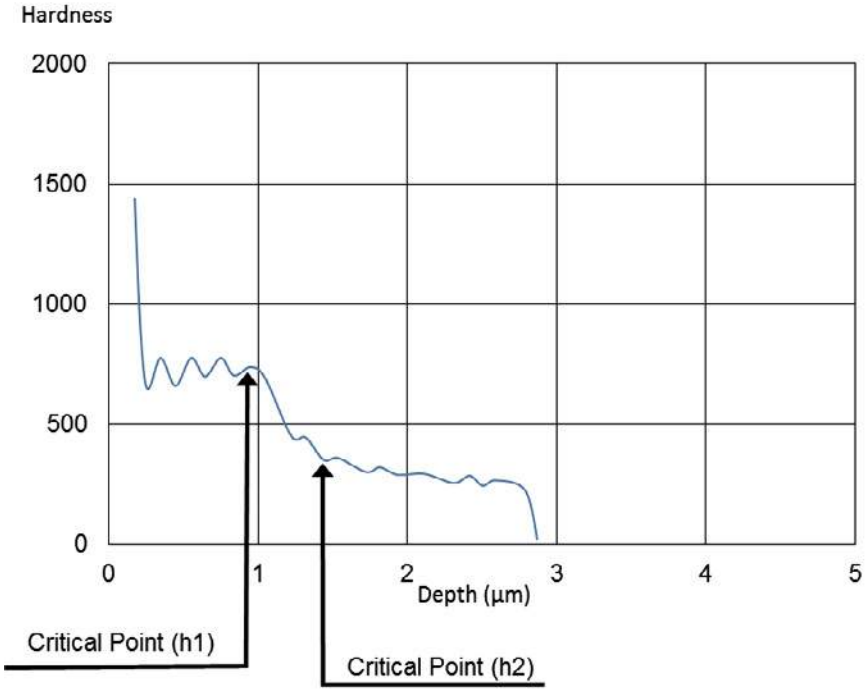

Fig. 3 Hardness- Depth Curve (test mode 1)

The thickness of the plating layer is estimated approx.1 µm from the critical point (h1) of Fig.3.

For Research Use Only. Not for use in diagnostic procedures.
The content of this publication shall not be reproduced, altered or sold for any commercial purpose without the written approval of Shimadzu. The information contained herein is provided to you "as is" without warranty of any kind including without limitation warranties as to its accuracy or completeness. Shimadzu does not assume any responsibility or liability for any damage, whether direct or indirect, relating to be the use of this publication. This publication is based upon the information available to Shimadzu on or before the date of publication, and subject to change without notice.

SHIMADZU
Excellence in Science

Application News

Material Testing System AG-X

No. SCA_300_045

Jigs for Measuring Bauschinger Effect

Use Autograph to simply perform in-plane reverse loading tests on sheet metal.

■ In-Plane Reverse Loading Test

It is a testing method, where a sheet metal is subjected to tensile ➡ compression ➡ tensile reverse loading and continuously measuring the stress-strain curve. It can be used to make highly accurate measurements of the Bauschinger effect or the strain dependence of the elastic modulus required for forming simulation. In-plane reverse loading is possible by gripping the specimen with a die (comb grips) movable in the testing axis direction to prevent a specimen from buckling.

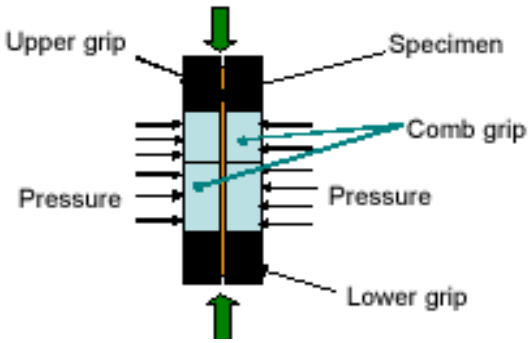

■ Features

Space-saving:

Perform tests by attaching the jigs to Autograph. No specialized equipment required.

Good operability:

The jigs can be used sideways, making specimen setting easy. All operations from attachment of the jigs to testing can be performed by one person.

Simple displacement measurement:

Extension of the specimen can be measured using the strain gauge type extensometer. No need to attach a strain gauge to the specimen, making it possible to perform tests more efficiently.

Simple operation:

Any straightening pressure can be set easily using the hydraulic jack and hydraulic hand pump.

■ External View of Jigs

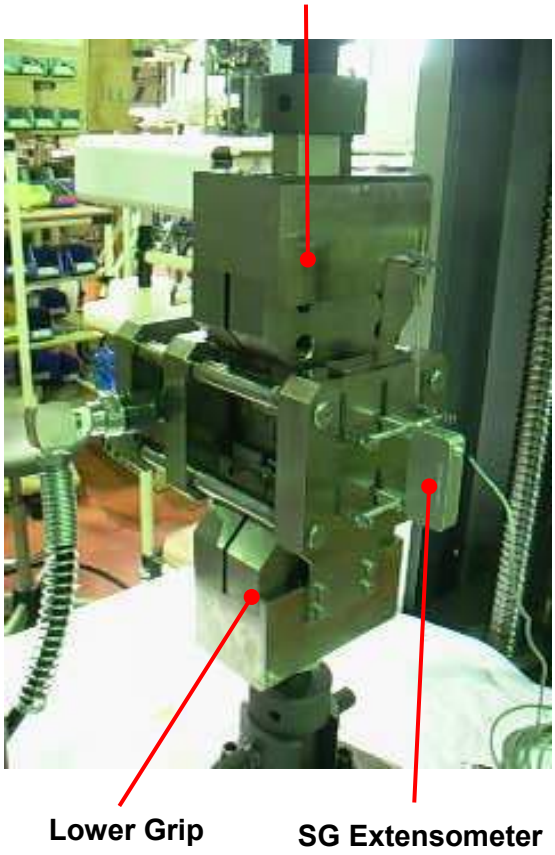

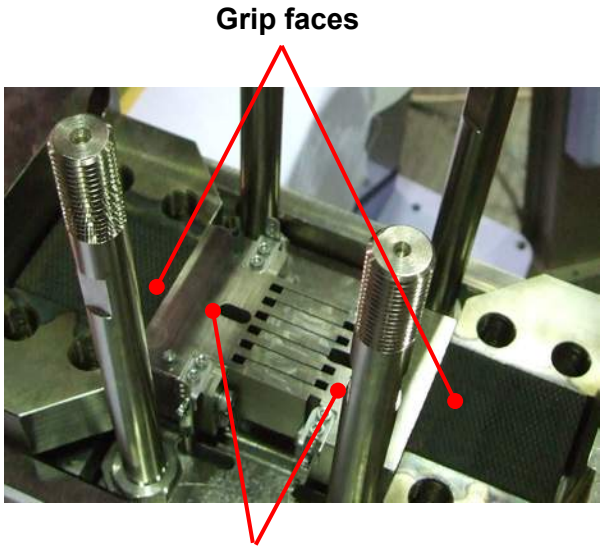

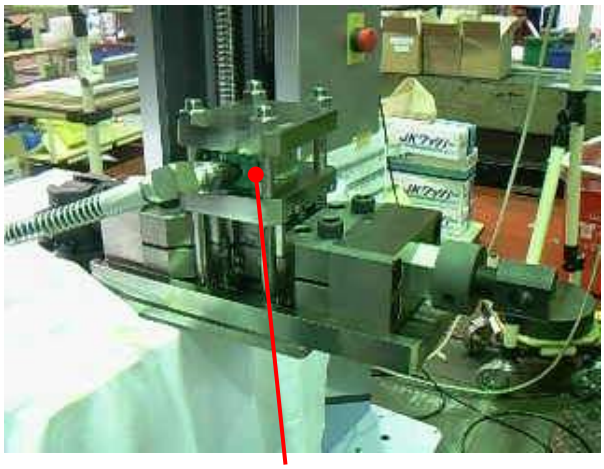

■ Example of Test Results True Stress-True Strain Curve

Specimen: DP780 high strength steel, sheet thickness 1.4 mm

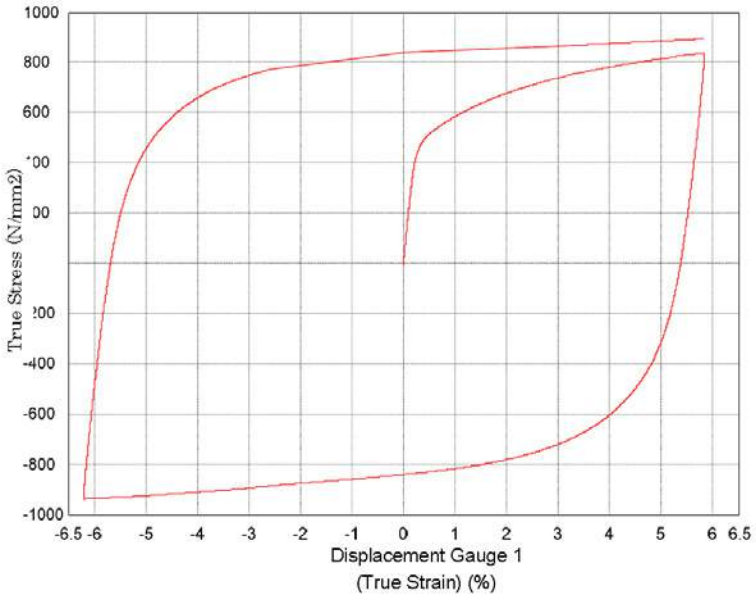

Specifications		
Applicable Testing Machine		AG-100kN
Loading Capacity		Tensile: 100 kN / Compression: 100 kN
Buckling Prevention Unit	Hydraulic Unit	Hydraulic hand pump
	Straightening Pressure	Max. 40 kN
Extensometer	Type	Strain gauge type
	Gauge Length	50 mm
	Measurement Range	+50 %/-10 %
	Measurement Precision	JIS B 7741 Class 1
Applicable Specimen	JIS 5	L200 mm x W40 mm
		Parallel section L60 mm x W40 mm
		1–3 mm thick
	JIS 5 Special Size (Wide specimen)	L200 mm x W45 mm
		Parallel section L60 mm x W35 mm
		1–3 mm thick
Operational Temp. Range		Room temperature

The test data is used with kind permission from G-TEKT Corporation

For Research Use Only. Not for use in diagnostic procedures.
The content of this publication shall not be reproduced, altered or sold for any commercial purpose without the written approval of Shimadzu. The information contained herein is provided to you "as is" without warranty of any kind including without limitation warranties as to its accuracy or completeness. Shimadzu does not assume any responsibility or liability for any damage, whether direct or indirect, relating to be the use of this publication. This publication is based upon the information available to Shimadzu on or before the date of publication, and subject to change without notice.

SHIMADZU
Excellence in Science

Application News

Material Testing System HMV

No. SCA_300_047

Measurement of the surface treatment depth of steel with Shimadzu Micro Hardness Tester Model HMV

The following is an example of output data obtained through a measurement of surface treatment depth of a steel sample with the Shimadzu Micro Vickers Hardness Tester, Model HMV. (Fig. 1)

Fig. 1 Shimadzu Micro Vickers Hardness Tester, Model HMV

■ Testing parameters

1) Sample: steel (surface hardening)

2) Measuring indenter: Square pyramid diamond indenter tip angle of 136° (Vickers indenter)

3) Test load: 1000 gf

4) Load hold-time: 10 sec

■ Testing method

1) A steel block is cut perpendicularly to the hardening surface. The surface of the cut section, after being polished, is applied to hardness measurement. Surface hardness shall be measured in the direction perpendicular to the cut section surface.

2) Hardness measurement shall be repeated starting from position 1 (surface) as shown in Fig. 2 until no substantial difference of hardness can be observed.

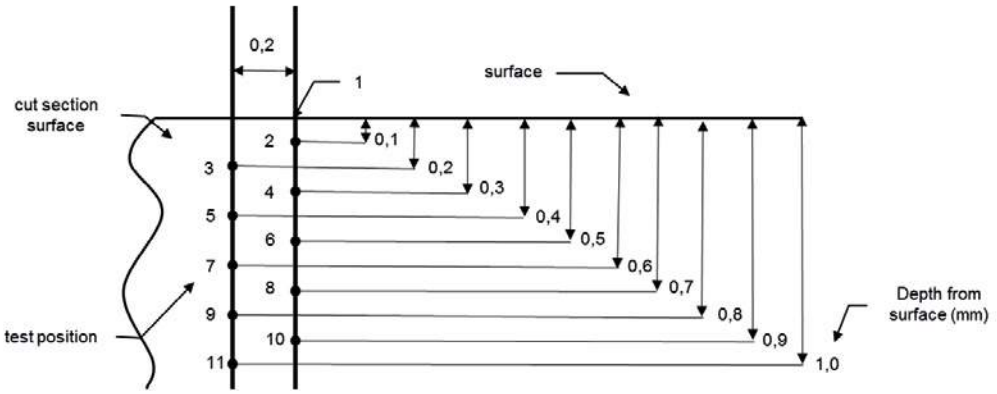

Fig. 2

■ Test results

1) Hardness at respective test positions is listed in Table 1, while the printer outputs of the test result and the plotted test result are shown in Table 1 and Fig. 3 respectively.

2) It is known from Table 1 and Fig. 3 that the depth of the hardening layer is 0.6 mm.

Depth (‡o)	Test position No.	Hardness (HV)
Surface	1	1070
0.1	2	905
0.2	3	847
0.3	4	687
0.4	5	591
0.5	6	397
0.6	7	251
0.7	8	229
0.8	9	225
0.9	10	217
1.0	11	215

Table 1 Test Results of hardness

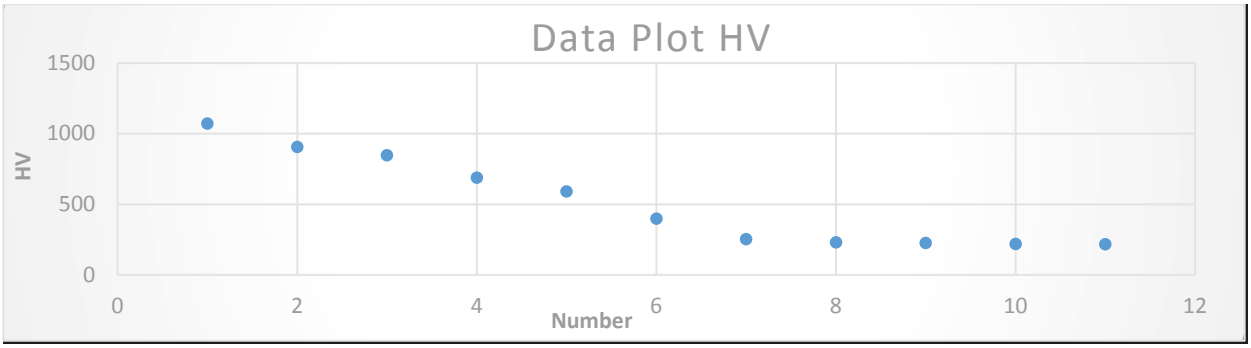

Fig. 3 Plot of Hardness

For Research Use Only. Not for use in diagnostic procedures.
The content of this publication shall not be reproduced, altered or sold for any commercial purpose without the written approval of Shimadzu. The information contained herein is provided to you "as is" without warranty of any kind including without limitation warranties as to its accuracy or completeness. Shimadzu does not assume any responsibility or liability for any damage, whether direct or indirect, relating to be the use of this publication. This publication is based upon the information available to Shimadzu on or before the date of publication, and subject to change without notice.

SHIMADZU
Excellence in Science

Application News

Material Testing System MCT

Strength Evaluation on Metallic Fine Particles with Shimadzu Micro Compression Testing Machine Model MCT

No. SCA_300_050

■ Introduction

The role of fine particles and related technologies is becoming more and more important as one of the basic factors supporting the current high technology boom.

Powders and fine particles display characteristic behaviors which distinguish them from normal liquids and solids. They can be easily mixed, moved, split, scattered in liquid and gas, and they also have comparatively large surface area for their volume. As a particle body is an aggregation of fine solid particles, it has properties of an individual particle and of a mass of particles. For this reason, diametric compressive fracture load applied to individual particles is a critical factor in particle processing technology.

The following is an example of an examination of the physical behaviors of metallic fine particles of different hardness's under pressing loads performed with the Shimadzu Micro Compression Testing Machine Model MCTM.

The MCTM applies a pressing load of electromagnetic force at a constantly increasing rate onto a specimen placed between an upper pressing indenter and a lower anvil. It automatically measures the deforming behavior of a specimen and processes data for its relation to load. The MCTM is optimized for the evaluation of the physical strength of various micro parts, powders and fine particle bodies, micro fibers, etc.

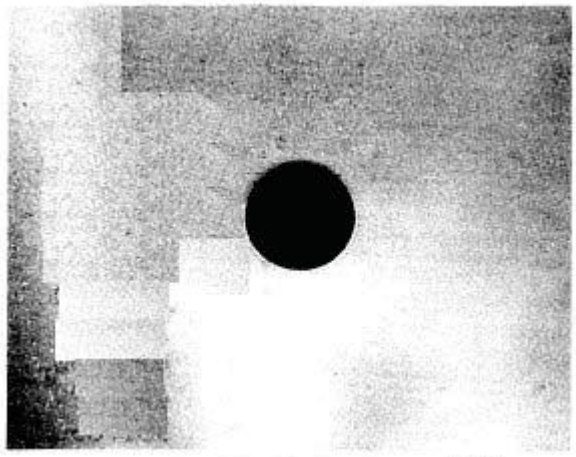

Fig. 1 Spherical particle ├ 100 µm ┤

■ Specimens

1) Name: metallic fine particles

2) Kinds: three different hardness's, A, B, and C

3) Shape: spherical (See Fig. 1)

■ Testing Method

1) Test mode : Compression

2) Load: 500 gf

3) Loading rate constant: 1 (4,230 gf/sec)

4) Numbers of tests : 10 tests

5) Calculation of strength: Strength was calculated by the following equation from the load and particle diameter when displacement reached 10% of diameter, since the three specimens did not reach compressive fracture. The calculated values in this method is shown as tentative strength with "-" before the figure, being distinguished from compressive fracture strength.

$$St = \frac{2{,}8 \cdot P}{\pi \cdot d^2}$$

St: Tensile Strength /kg/mm^2)

P: Load (kgf)

d: Particle diameter (mm)

Specimen No.	Applied Loads (gf)	Strain (μm)	Diameter (μm)	Diameter (μm)	Mean Diameter (μm)	Tentative Strength
1	230,650	8,15	81,50	81,50	81,50	-30,965
2	225,800	8,27	83,00	82,50	82,75	-29,405
3	262,150	8,32	83,00	83,50	83,25	-33,729
4	223,100	8,50	85,00	85,00	85,00	-27,535
5	277,150	8,42	84,50	84,50	84,25	-34,843
6	221,750	8,10	81,00	81,00	81,00	-30,139
7	277,150	8,15	81,50	81,50	81,50	-37,207
8	228,600	8,15	81,50	81,50	81,50	-30,689
9	232,600	8,25	83,00	82,50	82,50	-30,474
10	215,450	8,21	82,00	82,50	82,00	-28,572
Mean Value	239,456	8,25	82,60	82,53	82,53	-31,356

Table 1 Test Result of Particle A

Specimen No.	Applied Loads (gf)	Strain (μm)	Diameter (μm)	Diameter (μm)	Mean Diameter (μm)	Tentative Strength
1	364,250	8,25	82,50	82,50	82,50	-47,722
2	405,450	8,30	83,00	83,00	83,00	-52,482
3	342,450	8,32	83,50	83,80	83,25	-44,061
4	393,650	8,30	83,00	83,00	83,00	-50,955
5	357,830	8,10	81,00	81,00	81,00	-48,629
6	412,350	8,45	84,50	84,50	84,50	-51,497
7	403,900	8,45	84,50	84,50	84,50	-50,442
8	381,850	8,10	81,00	81,00	81,00	-51,898
9	389,950	8,31	83,00	83,00	83,00	-50,359
10	365,300	8,30	83,00	83,00	83,00	-47,285
Mean Value	381,605	8,29	82,90	82,85	82,87	-49,533

Table 2 Test Result of Particle B

Specimen No.	Applied Loads (gf)	Strain (μm)	Diameter (μm)	Diameter (μm)	Mean Diameter (μm)	Tentative Strength
1	426,000	8,20	82,00	82,00	82,00	-56,495
2	402,300	8,28	82,00	82,00	82,00	-53,352
3	410,850	8,50	85,00	85,00	85,00	-50,708
4	444,450	8,40	84,00	84,00	84,00	-56,169
5	494,150	8,50	85,00	85,00	85,00	-60,989
6	413,900	8,12	81,50	81,50	81,25	-55,908
7	443,250	8,32	83,00	83,50	83,25	-57,031
8	431,900	8,15	81,50	81,50	81,50	-57,982
9	457,050	8,30	83,00	83,00	83,00	-59,161
10	455,100	8,22	82,50	82,00	82,25	-59,988
Mean Value	437,895	8,29	82,90	82,95	82,93	56,778

Table 3 Test Result of Particle C

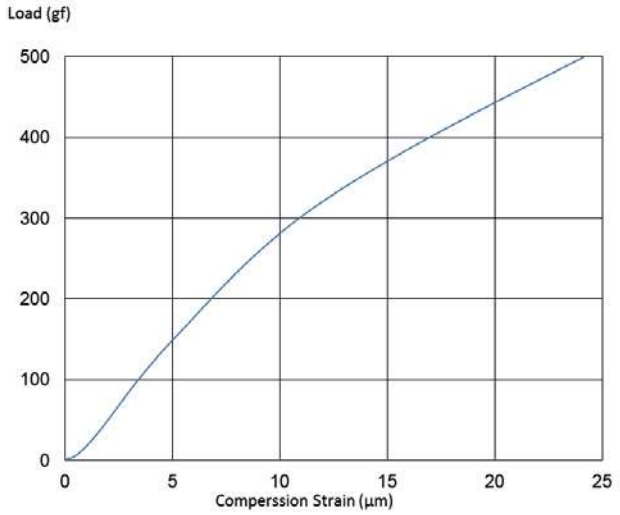

Fig. 2 Load- Strain Curve for Particle A

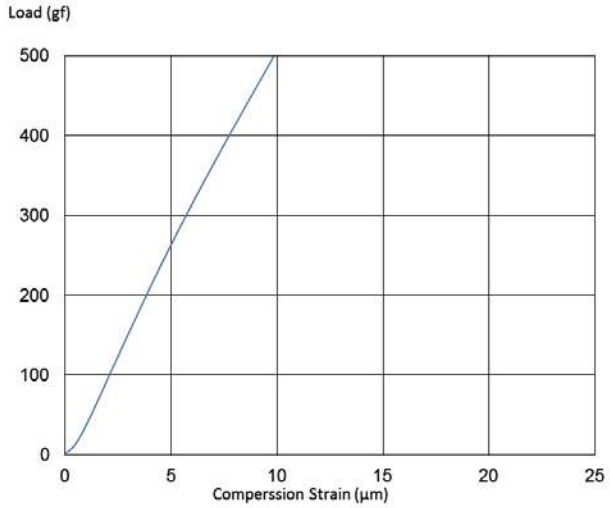

Fig. 3 Load- Strain Curve for Particle B

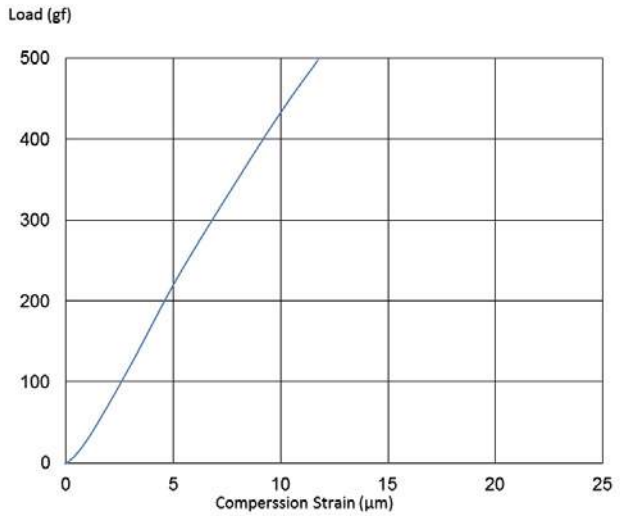

Fig. 4 Load- Strain Curve for Particle C

Kinds of Specimen	Compression Test		Hardness Test
	Tensile Strength (kgf/mm^2)	Standard Deviation (kgf/mm^2)	HRC [2)]
A	31.36	3.00	34
B	49.53	2.60	52
C	56.78	3.07	57

Table 4 summary of the test results

■ Test Conditions

Sample No	1
Test	5
Indenter	Vickers Flat
Read Time	2
Load	100 g
Loading Time	15 sec

	Kinds of Specimen		
	A	B	C
Test	1	1	1
D1	23,3	18,4	17,0
D2	23,4	18,1	16,8
HV	339	555	648
Test	2	2	2
D1	23,6	18,7	16,8
D2	23,3	18,3	17,2
HV	336	541	640
Test	3	3	3
D1	23,0	18,5	17,2
D2	23,2	18,2	17,0
HV	347	535	633
Test	4	4	4
D1	23,7	18,8	17,1
D2	23,6	18,4	16,7
HV	331	535	648
Test	5	5	5
D1	23,5	18,5	17,0
D2	23,8	18,7	17,2
HV	331	535	633
Average HV	337	543	640
Min HV	331	535	633
Max HV	347	555	648

Table 5 Result of Vickers Hardness

■ Comment on test results

Table 4 shows a summary of the test results, while Tables 1 through 3 and Figs. 2 through 4 present measured data. Figs. 2 through 4 show examples of load-strain curves for each kind of specimen having the same diameter. Vickers Hardness Indexes are shown in Table 5 for each respective particle specimen.

Table 4 indicates the correlation between tensile strength and Rockwell Hardness. Figs. 2 through 4 indicate that the order of strain size at a given load shows the same trend as that of hardness. According to these results, hardness decreases as strain increases, and increases as strain decreases.

For Research Use Only. Not for use in diagnostic procedures.
The content of this publication shall not be reproduced, altered or sold for any commercial purpose without the written approval of Shimadzu. The information contained herein is provided to you "as is" without warranty of any kind including without limitation warranties as to its accuracy or completeness. Shimadzu does not assume any responsibility or liability for any damage, whether direct or indirect, relating to be the use of this publication. This publication is based upon the information available to Shimadzu on or before the date of publication, and subject to change without notice.

SHIMADZU
Excellence in Science

Application News

No. SCA_300_061

Material Testing System MCT

Compressive Strength of Metallic Microspheres and Dependence on Heat Treatment Temperature. Shimadzu MCTM-500 Micro Compression Testing Machine

■ Introduction

One advance in metallurgy is the recent development in forming technology for the production of metal powders composed of microspherical particles ranging in size from several μm to 100μm. Evaluation of the mechanical properties of these particles as individual microspheres and as aggregates is required. The MCTM was applied to compression strength testing of Al-Ni alloy microspheres subjected to various heat treatments, and dependence of compression strength on the treatment temperature was observed.

The Model MCTM applies a pressing load of electromagnetic force at a constantly increasing rate onto a specimen placed between an upper pressing indenter and a lower anvil for automatic measurement of deforming behavior of the specimen and data processing for its relation to load. This testing machine is optimized for evaluating the physical strength of various micro-scale parts, powders and fine particle bodies, micro fibers, etc.

■ Specimens

1) Material name	Al-Ni type alloy
2) Kinds	Three different heat treatments • no heat treatment, • 200 °C heat treatment, • 400 °C heat treatment
3) Shape	micro sphere

■ Testing conditions

1) Testing mode	compression test
2) Upper pressing indenter	flat, diameter 50μmD(diamond)
3) Lower platen	SKS flat plate
4) Strength calculation	A 10% strength was calculated from the load value and particle diameter when strain reached 10% of particle diameter with the following equation, as the three specimens did not reach the state of breakage or fracture. The values hereby obtained are shown on the data sheet as tentative strength with a minus sign (-) to discriminate from fracture strength.

(Quoted from the equation by Hiramatsu, et al.)

$$St = \frac{2{,}8 \cdot P}{\pi \cdot d^2}$$

St: tensile strength (kgf/mm^2)

P: Load (kgf)

d: Diameter of particle (mm)

Note: Mr. Hiramatsu, Mr. Oka, Mr. Kiyama, Mining Association Journals

If particle diameter is 6,7 μm, strength is calculated with a load of 1,085 gf (P1) at a compression displacement of 0,67 mm (D1)

S10=21,553 kgf/mm^2)

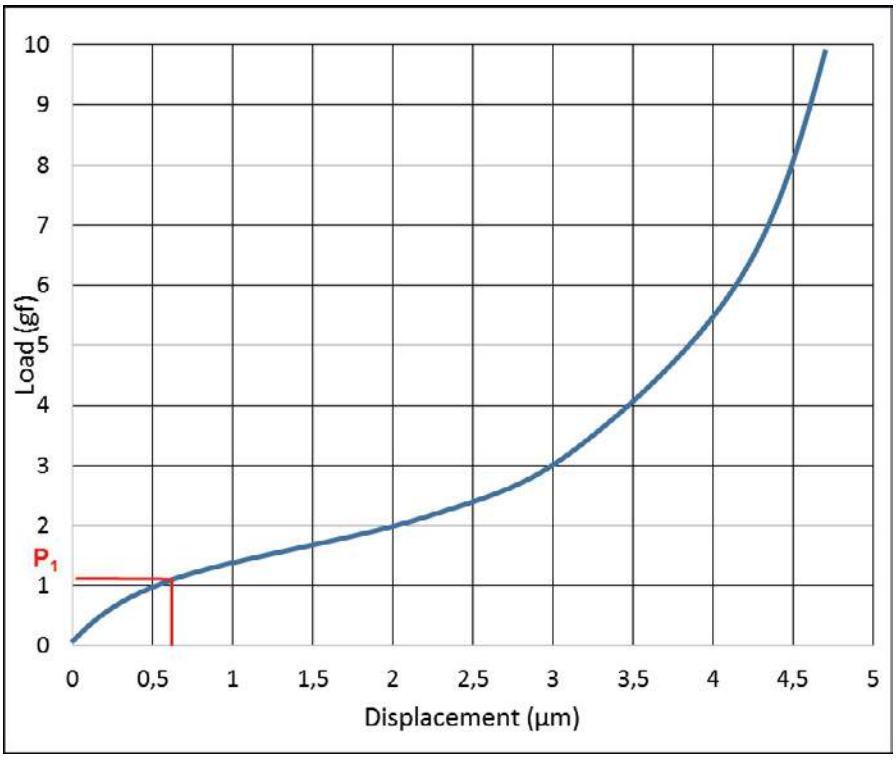

Fig. 1 Load-Displacement Curve

Table 1 Test results for untreated sample

	Testing Conditions						
		File No.		AN408.D1			
Test mode	1	Indenter:		Flate plate 50			
Sample name	Aluminium-Nickel alloy						
Sample No.	4						
Testing load	100.00 (gf)		Loading rate constant: 1				
Displacement scale	10 (μm)						
No.	Load (gf)	Displacement (μm)	Diameter (μm)	Diameter (μm)	Average (μm)	Strength (kgf/mm^2)	Tentative strength
1	1.085	0.67	6.70	6.70	6.70		-21.553
2	1.335	0.75	7.40	7.30	7.35		-22.036
3	6.480	1.49	15.00	14.90	14.95		-25.854
4	6.765	1.53	15.20	15.40	15.30		-25770
5	11.860	1.88	18.90	18.70	18.80		-29.922
6	14.320	1.90	19.00	19.00	19.00		-35.372
7	13.430	1.92	19.20	19.20	19.20		-32.486
8	19.125	2.14	21.50	21.40	21.45		-37.066
9	20.860	2.18	21.90	21.80	21.85		-38.962
10	29.785	2.59	25.90	25.90	25.90		-39.594
11	27.975	2.71	27.10	27.10	27.10		-33.967
12	31.035	3.05	30.60	30.50	30.55		-29.652
13	36.040	3.35	33.50	33.50	33.50		-28.637
14	49.100	3.94	39.20	39.20	39.20		-28.493
15	61.400	4.46	44.60	44.70	44.65		-27.463
Average	-----	-----	23.05	23.02	23.03		
Average	22.040	2.30				-----	-30.455

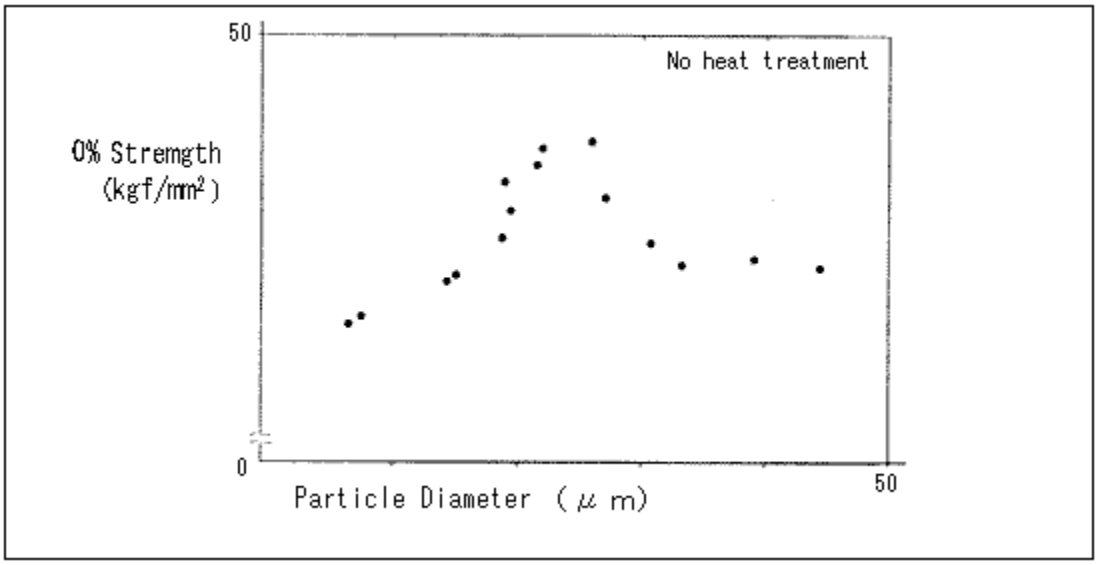

Fig. 2 10%Strentgh - Particle Diameter plot for untreated sample

Table 2 Test results for treated sample at 200 °C

	Testing Conditions						
		File No.		4-200.D2			
Test mode	1	Indenter:		Flate plate 50			
Sample name	Aluminium-Nickel alloy						
Sample No.	4-200						
Testing load	100.00 (gf)		Loading rate constant: 1				
Displacement scale	10 (μm)						
No.	Load (gf)	Displacement (μm)	Diameter (μm)	Diameter (μm)	Average (μm)	Strength (kgf/mm^2)	Tentative strength
1	1.580	0.65	6.30	6.30	6.45		-33.866
2	2.390	0.78	7.90	7.90	7.85		-34.585
3	4.705	1.12	11.20	11.20	11.20		-33.447
4	6.400	1.25	12.50	12.40	12.45		-36.819
5	12.515	1.67	16.70	16.70	16.70		-40.015
6	13.885	1.80	18.00	18.00	18.00		-38.215
7	15.235	1.83	18.20	18.40	18.30		-40.567
8	20.010	2.07	20.80	20.70	20.75		-41.442
9	23.460	2.26	22.60	22.70	22.65		-40.777
10	29.380	2.54	25.40	25.40	25.40		-40.608
11	34.765	2.85	28.80	28.30	28.55		-38.033
12	43.475	3.42	34.20	34.30	34.25		-33.048
13	43.970	3.81	38.20	38.00	38.10		-27.011
14	49.555	4.13	41.30	41.30	41.30		-25.907
15	46.455	4.16	41.60	41.70	41.65		-23.875
Average	-----	-----	22.91	22.90	22.91		
Average	23.185	2.29				-----	-35.214

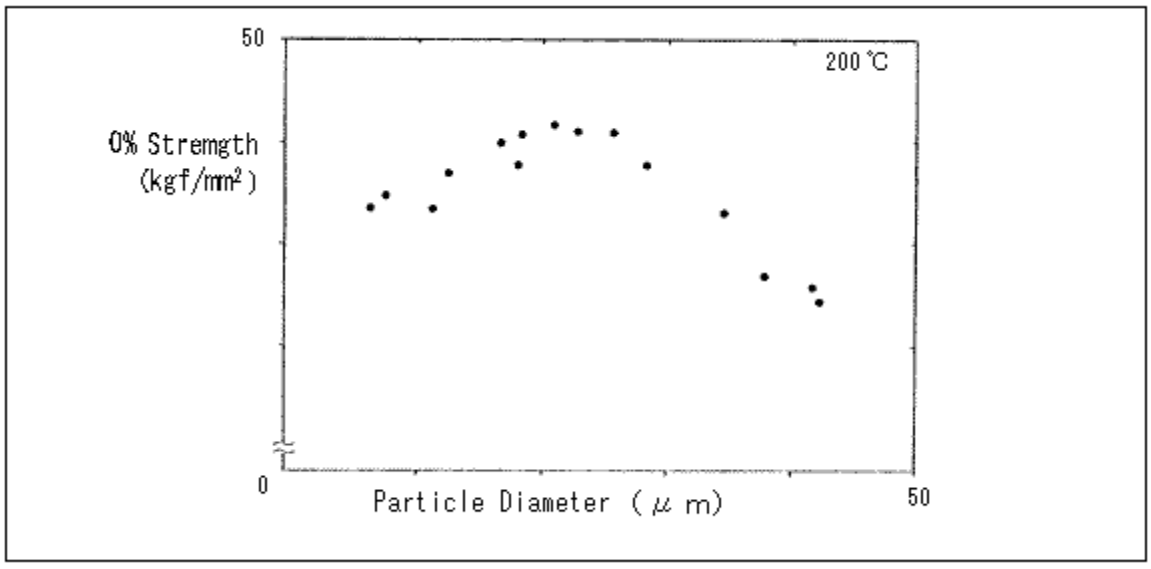

Fig. 3 10%Strentgh - Particle Diameter plot for sample treated at 200 °C

Table 3 Test results for treated sample at 400 °C

	Testing Conditions						
		File No.		4-200.D3			
Test mode	1	Indenter:		Flate plate 50			
Sample name	Aluminium-Nickel alloy						
Sample No.	4-400						
Testing load	100.00 (gf)		Loading rate constant: 1				
Displacement scale	10 (μm)						
No.	Load (gf)	Displacement (μm)	Diameter (μm)	Diameter (μm)	Average (μm)	Strength (kgf/mm^2)	Tentative strength
1	1.170	0.68	6.80	6.90	6.85		-22.235
2	1.655	0.83	8.20	8.20	8.20		-21.948
3	3.205	1.11	11.00	11.00	11.00		-23.620
4	5.145	1.35	13.60	13.40	13.50		-25.174
5	7.000	1.54	15.40	15.40	15.40		-26.320
6	9.880	1.91	19.20	19.00	19.10		-24.150
7	10.945	1.99	19.90	20.00	19.95		-24.522
8	12.190	2.10	21.00	21.00	21.00		-24.649
9	14.170	2.26	22.60	22.70	22.65		-24.630
10	18.190	2.73	27.40	27.20	27.30		-21.764
11	22.520	3.00	30.10	29.90	30.00		-22.313
12	24.550	3.11	31.10	31.20	31.15		-22.561
13	34.590	3.73	37.30	37.40	37.75		-22.110
14	44.200	4.06	40.60	40.60	40.60		-23.911
15	41.850	4.30	43.80	42.20	43.00		-20.183
42.20	-----	-----	23.20	23.07	23.14		
23.07	16.751	2.31				-----	-23.339

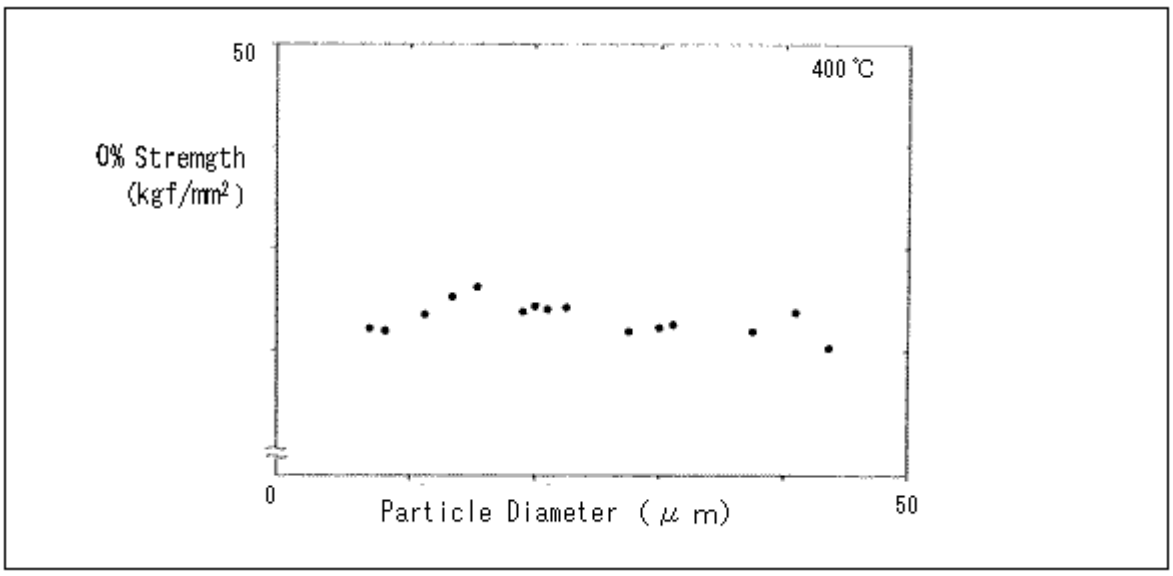

Fig. 4 10%Strentgh - Particle Diameter plot for sample treated at 400 °C

■ **Test results** Measured data are given in Tables 1 - 3 and Figs. 2 - 4.

Figs. 2 through 4 display 10% strength - particle diameter plots. The strength of the sample without heat treatment abruptly rises to approx. 40 kgf/mm^2 at a particle diameter of around 25 µm, as shown in Fig. 2. Compared with the specimen without heat treatment, the specimen with heat treatment at 200 °C has a high level of strength at 35 to 40 kgf/mm^2 in the lower particle diameter range (below 20 µm). The strength of the sample with heat treatment at 400 °C remains at a low level of around 25 kgf/mm^2 without any significant variation across diameters. As shown above, this data provides much information about the difference of strength depending on diameter size or method of heat treatment.

* Please be advised that data obtained before the implementation of the current Weights and Measures Law may be presented in terms of gravimetric unit.

For Research Use Only. Not for use in diagnostic procedures.
The content of this publication shall not be reproduced, altered or sold for any commercial purpose without the written approval of Shimadzu. The information contained herein is provided to you "as is" without warranty of any kind including without limitation warranties as to its accuracy or completeness. Shimadzu does not assume any responsibility or liability for any damage, whether direct or indirect, relating to be the use of this publication. This publication is based upon the information available to Shimadzu on or before the date of publication, and subject to change without notice.

SHIMADZU
Excellence in Science

Application News

No.V21

High-Speed Video Camera

Observation of Bending Fatigue Testing of Metal Plate at Ultrasonic Frequency

Introduction

Fatigue failure refers to the fracture of a component due to repeated load cycles, which can occur using a force much smaller than the static fracture strength. Also, because fatigue-related failure occurs suddenly, there are cases where this has led to serious accidents involving ships and aircraft. Therefore, knowledge of the fatigue properties of materials used in products is very important. However, determination of fatigue characteristics typically requires time-consuming testing using 10^7 repetitions (as per JIS Z2273, General Rules for Fatigue Testing of Metals), which at 10 Hz, takes about 12 days to complete. Also, due to enhancements in equipment efficiency and speed, there are now requests for fatigue evaluation with more than 10^7 repetitions. In response to this, an ultrasonic testing machine capable of 20 kHz ultrasonic fatigue testing is now in use. However, due to the very rapid vibration that is generated during measurement with this instrument, visual confirmation of the movement and deformation of the specimen is not possible. Therefore, a high-speed video camera was used to observe the movement of a metal plate vibrating while conducting a 20 kHz bending fatigue test. Previously, gaining an understanding of the overall movement of the test specimen required incremental repositioning of a displacement gauge, but with the high-speed video camera, it is possible to evaluate the movement of the specimen in a single observation process. Further, the possibility of determining the amount of movement of the specimen from captured images was also demonstrated.

Measurement System

The USF-2000 Ultrasonic Fatigue Testing System and the HPV-X2 high-speed video camera were used for this experiment. Table 1 lists all the instrumentation that was used. Shooting during the test can be conducted at any desired timing. Fig. 1 shows a photograph of the test specimen. For the bending vibration, the vibration modes shown in Fig. 2 are available, with a test specimen dimensioned to resonate for each vibration mode. Here, a test specimen was prepared to provide a second-order bending mode.

Table 1 Imaging Equipment

High-speed video camera	: HPV-X2
Microscope	: Z16 APO
Lighting	: Strobe
Testing apparatus	: USF-2000

Table 2 Measurement Conditions

Measurement speed	: 2 million frames/sec
Test frequency	: 20 kHz
Test specimen size	: 10.0 × 3.020 × 0.406 mm

Fig. 1 Specimen

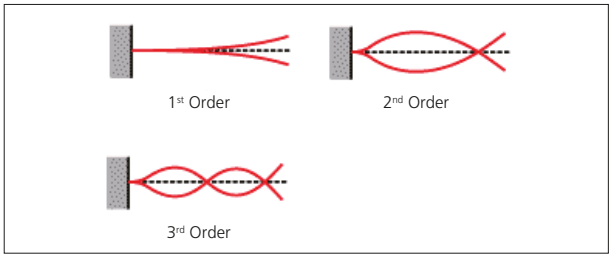

Fig. 2 Bending Mode Examples

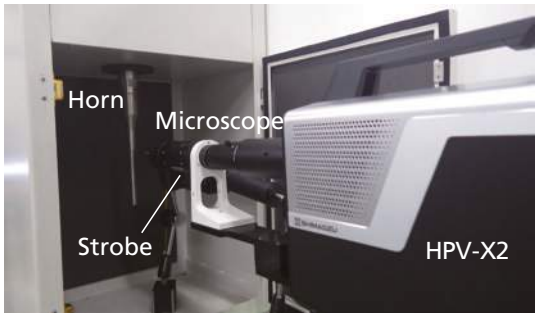

Fig. 3 Overview of Test

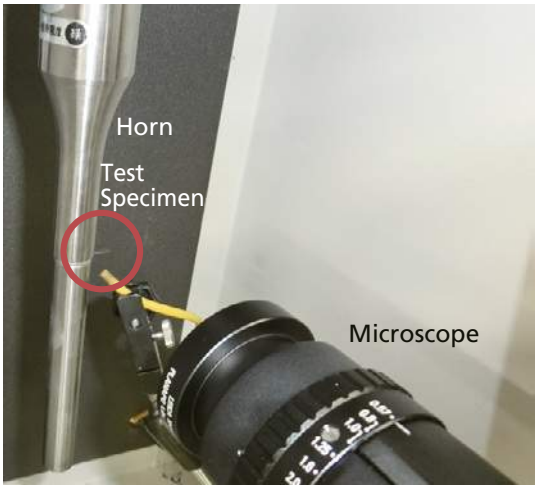

Fig. 4 Periphery of Specimen

Measurement Results

Fig. 3 shows an overview of the test setup, and Fig. 4 shows a close-up view of the vicinity of the specimen. The vibration generated by the actuator is amplified by the horn, causing the specimen to vibrate. Table 2 shows the measurement conditions. To obtain image data at more than 100 frames per cycle, the shooting speed must be set to two million frames/sec. Fig. 5 shows a series of captured images. The blue line traversing the images in Fig. 5 is situated at the center of the specimen in image (1). The central portion of the specimen is shifted in the downward direction as the images proceed from (1) to (3). Then, the center portion of the specimen shifts in the upward direction, reaching a maximum at image (9). From image (9), the specimen center descends once again, returning at image (11) to the same position as in image (1). From the above, the vibration cycle of the specimen was determined to be 20 kHz. Also, from Fig. 5, the specimen tip does not move very much, although it can be seen that the specimen is in a second-order bending mode due to movement of the test specimen center. Applying image processing software to the captured images permits determination of the range of movement of the test specimen. Here, we determined the amount of movement of the central part of the specimen. Fig. 6 shows the relationship between time and the amount of movement of the specimen center. Also, from Fig. 6, the amplitude in the bending test is determined to be about 80 µm, and the vibration frequency is determined to be 20 kHz.

Conclusion

Fatigue testing of a target component conducted using the ultrasonic frequency was documented using the HPV-X2, and the movement characteristics of the test specimens were confirmed. The HPV-X2 proved to be effective in capturing the high-speed movement generated during the test, and installation of a microscope permitted visual documentation of these minute movements. Aside from this confirmation of movement in the specimen during the test, the actual degree of movement in the test specimen can be determined from the captured images. The USF-2000 calculates the stress amplitude from the amplitude of vibration, thereby permitting the determination of the stress load on the test specimen from the images. Thus, the HPV-X2 can effectively serve in the very important fatigue testing process during product development.

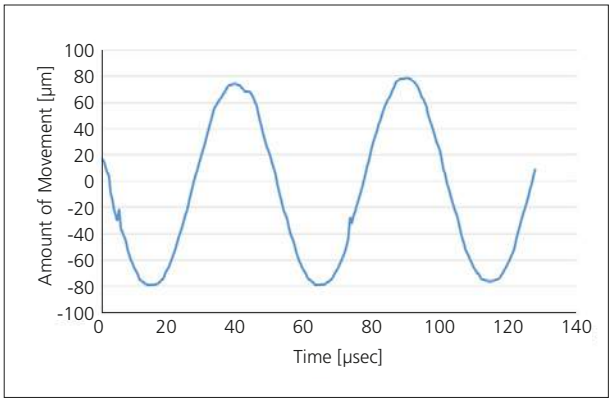

Fig. 6 Amount of Movement of Specimen

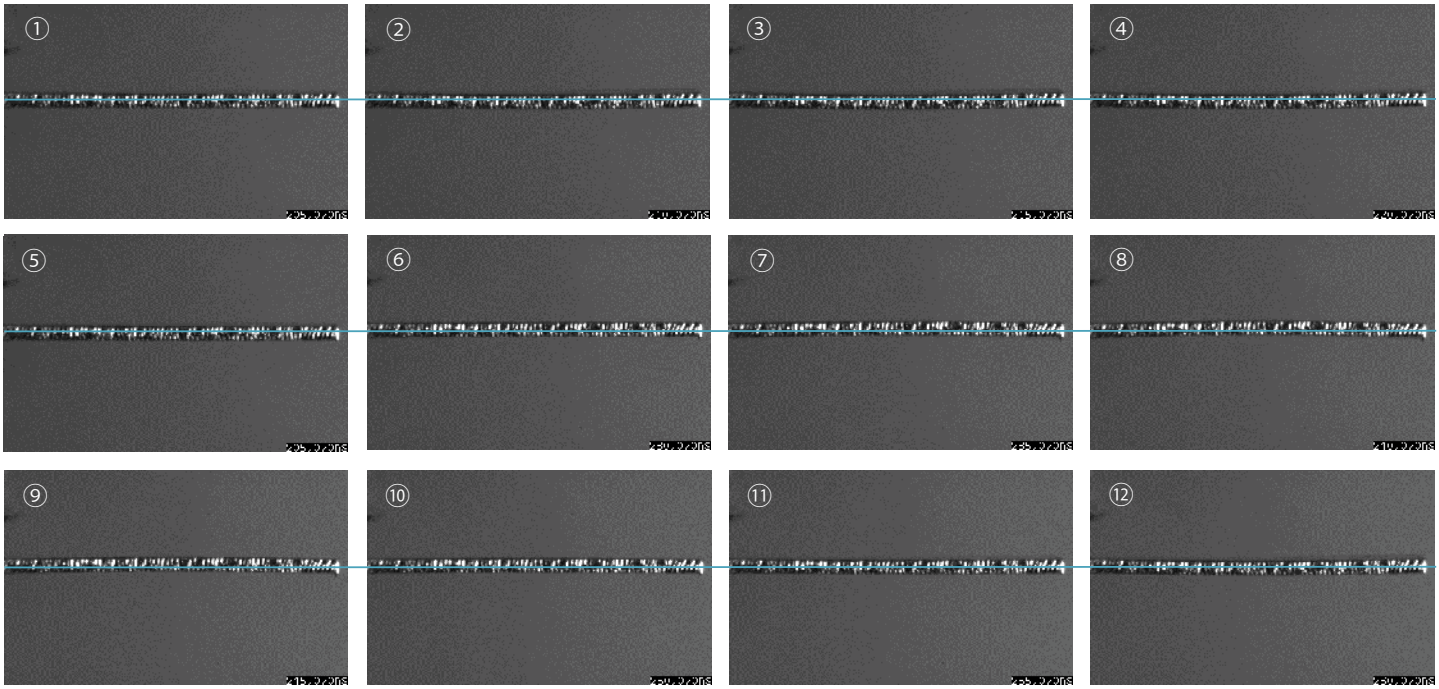

Fig. 5 High-Speed Images (Imaging interval: 5 µsec)

First Edition: Sep. 2015

Shimadzu Corporation
www.shimadzu.com/an/

For Research Use Only. Not for use in diagnostic procedures.
The content of this publication shall not be reproduced, altered or sold for any commercial purpose without the written approval of Shimadzu.
The information contained herein is provided to you "as is" without warranty of any kind including without limitation warranties as to its accuracy or completeness. Shimadzu does not assume any responsibility or liability for any damage, whether direct or indirect, relating to the use of this publication. This publication is based upon the information available to Shimadzu on or before the date of publication, and subject to change without notice.

© Shimadzu Corporation, 2015

SHIMADZU
Excellence in Science

7. Railroad Industry

7. Railroad Industry

DEVELOPMENT OF THE RAILROAD INDUSTRY

Railroads have a long history as both a day-to-day means of transport for people, and a means of transporting freight over land. Railroad technology has made huge strides, changing its power source and component members in response to the desire to travel farther, faster and in more comfort, for lower cost and in a way that is better for the passengers.

Railroad technology has achieved superior levels of safety, comfort, speed, accuracy and energy savings. Gaining of these levels has required a wide range of evaluation testing. Such technical innovation is never-ending, and continues to increase in scale.

Evaluation instruments have also made similar strides. They are routinely used in the evaluation of physical characteristics in materials development as well as for quality control of components. Furthermore, they are applied in performance evaluation of actual cars as well as reliability evaluation for infrastructure used in the operation of the railroads, and they continue to play a part in the assessment of a range of aspects of railroad development and operation.

Shimadzu has acquired a wealth of technical ability in regard to strength and endurance testing in the development of a range of materials and simulation testing on the actual sample, and is actively engaged in applying this knowledge in the railroad industry.

Shimadzu provides solutions for evaluation of safety and comfort during travel, e.g. through chassis tests as well as wheels and axles endurance evaluation. In addition, the company evaluates endurance and reliability of the track through ultrasonic flaw detection or rail fatigue lifespan test.

7. Railroad Industry

C225-E032	Ultrasonic fatigue testing system with an average stress loading mechanism
C225-E033	Three-axis endurance evaluations of automobile steering mechanisms

SHIMADZU
Excellence in Science

Ultrasonic Fatigue Testing System with an Average Stress Loading Mechanism

For Gigacycle Fatigue Tests with Average Stress Loaded

Actual components are rarely used under conditions in which the average stress is zero. Despite this, the USF-2000A, a standard ultrasonic fatigue testing system, can only perform testing under zero average stress conditions.
Using an ultrasonic fatigue testing system equipped with an average stress loading mechanism, gigacycle fatigue tests can be performed with average tensile stress loaded.

System Appearance

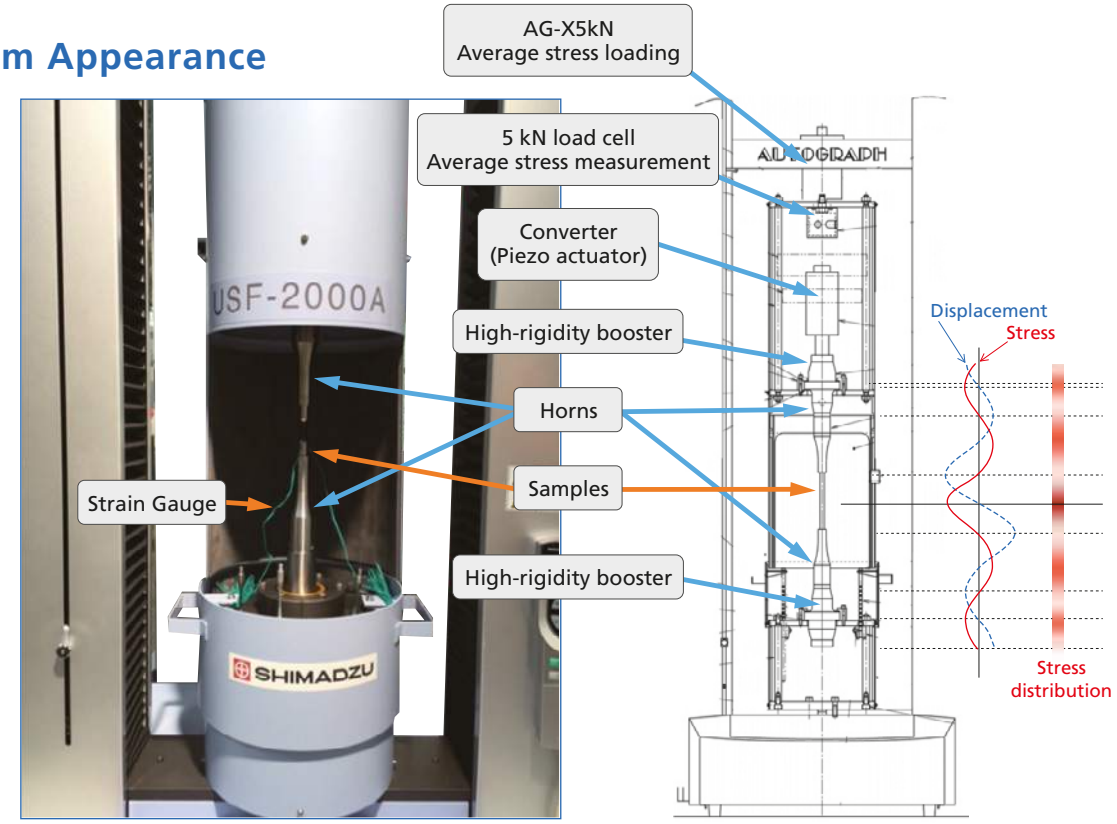

Ultrasonic Fatigue Testing System Effective for Gigacycle Fatigue Tests

With fatigue tests of high-strength steels, it is evident that internal fracture (fish-eye fracture), which is caused by inclusions and other micro defects, occurs at 107 cycles or more, a value considered the conventional fatigue limit.
An ultrasonic fatigue testing system is extremely effective when performing this sort of gigacycle fatigue test. (With a 100 Hz fatigue testing system, this would take 3 years, but if a 20 kHz ultrasonic fatigue testing system is used, testing can be completed in one week.)

Main Specifications

1) Test Frequency: 20 kHz ± 500 Hz

- The recommended test range is 20 kHz ± 30 Hz.
- The test frequency is determined by the resonance frequency of the sample.

2) Horn End Face Amplitude

Min. approx. ±10 µm
Max. approx. ±50 µm

- The minimum and maximum amplitudes are the end face amplitude values at amplitude outputs of 20 % and 100 % respectively. Accordingly, the minimum and maximum amplitude values will change somewhat depending on the shape of the sample.

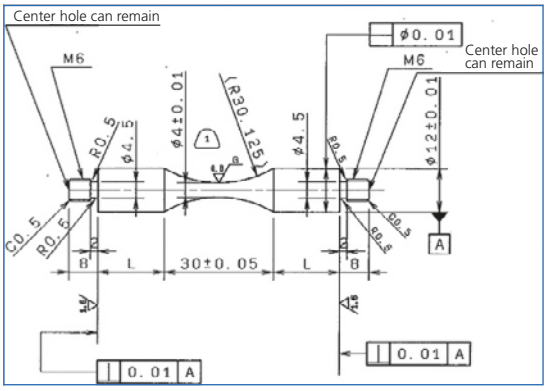

Standard Circular Tapered Sample

3) Test Stress

Standard circular tapered sample
Stress Min. 237 MPa
Max. 1186 MPa

- The test stress range can be changed by changing the sample shape.
- The minimum and maximum values are calculated with the end face amplitude values of 10 µm and 50 µm respectively.
- These are the values when the stress is within the elasticity range.

4) Average Stress

Max. 1.5 kN (tensile only)

- Average stress loads exceeding 1.5 kN are possible, but will have an impact on the service life of the horn.

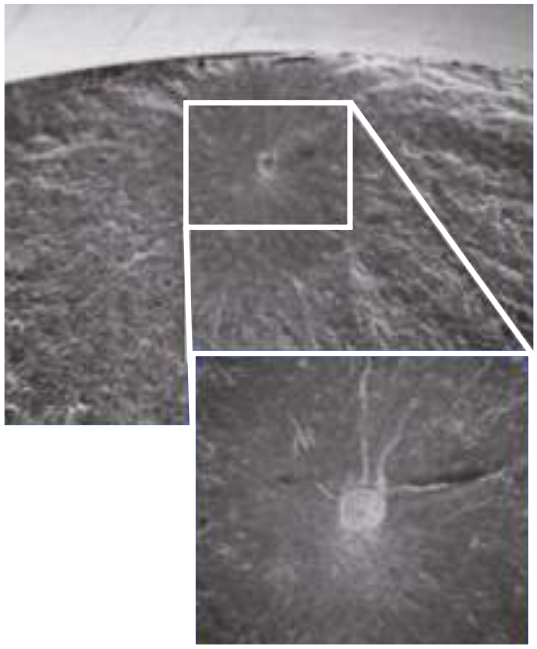
Surface of the Fatigued Fracture Originating from the Inclusion

■ Components

1	Ultrasonic resonance system Power supply, converter, booster (1 pair), horn (1 pair)
2	Personal computer (OS Windows 7) ADA/PIO interface board
3	Software Ultrasonic test control measurement software
4	Cooling system Air dryer, air piping • A separate 140 L/min air source is required.
5	Strain meter unit (option)
6	AG-X plus Autograph 5 kN + 250 extension
7	Average stress loading mechanism

Shimadzu Corporation
www.shimadzu.com/an/

For Research Use Only. Not for use in diagnostic procedure.
This publication may contain references to products that are not available in your country. Please contact us to check the availability of these products in your country.
Company names, product/service names and logos used in this publication are trademarks and trade names of Shimadzu Corporation or its affiliates, whether or not they are used with trademark symbol "TM" or "®". Third-party trademarks and trade names may be used in this publication to refer to either the entities or their products/services. Shimadzu disclaims any proprietary interest in trademarks and trade names other than its own.

The contents of this publication are provided to you "as is" without warranty of any kind, and are subject to change without notice. Shimadzu does not assume any responsibility or liability for any damage, whether direct or indirect, relating to the use of this publication.

© Shimadzu Corporation, 2016

First Edition: August 2016

SHIMADZU
Excellence in Science

Three-Axis Endurance Evaluations of Automobile Steering Mechanisms

With Control via Actual Data, Endurance Evaluations Approximating Real Motion Can Easily Be Performed

Automobile steering units are important components that must be highly durable. There are also significant differences in driver arm strengths, so many cars are equipped with a power steering mechanism, which complicates the structure. In contrast, with luxury cars and sports cars, specifications are required that can achieve an operable feeling that heightens the sense of enhanced value. In regards to these new and diversified requirements, quantitation, not only evaluations by people, is increasingly needed. By combining three actuators with the 4830 controller, which is capable of high-accuracy control, this system can easily perform endurance tests under close to real conditions.

System Appearance

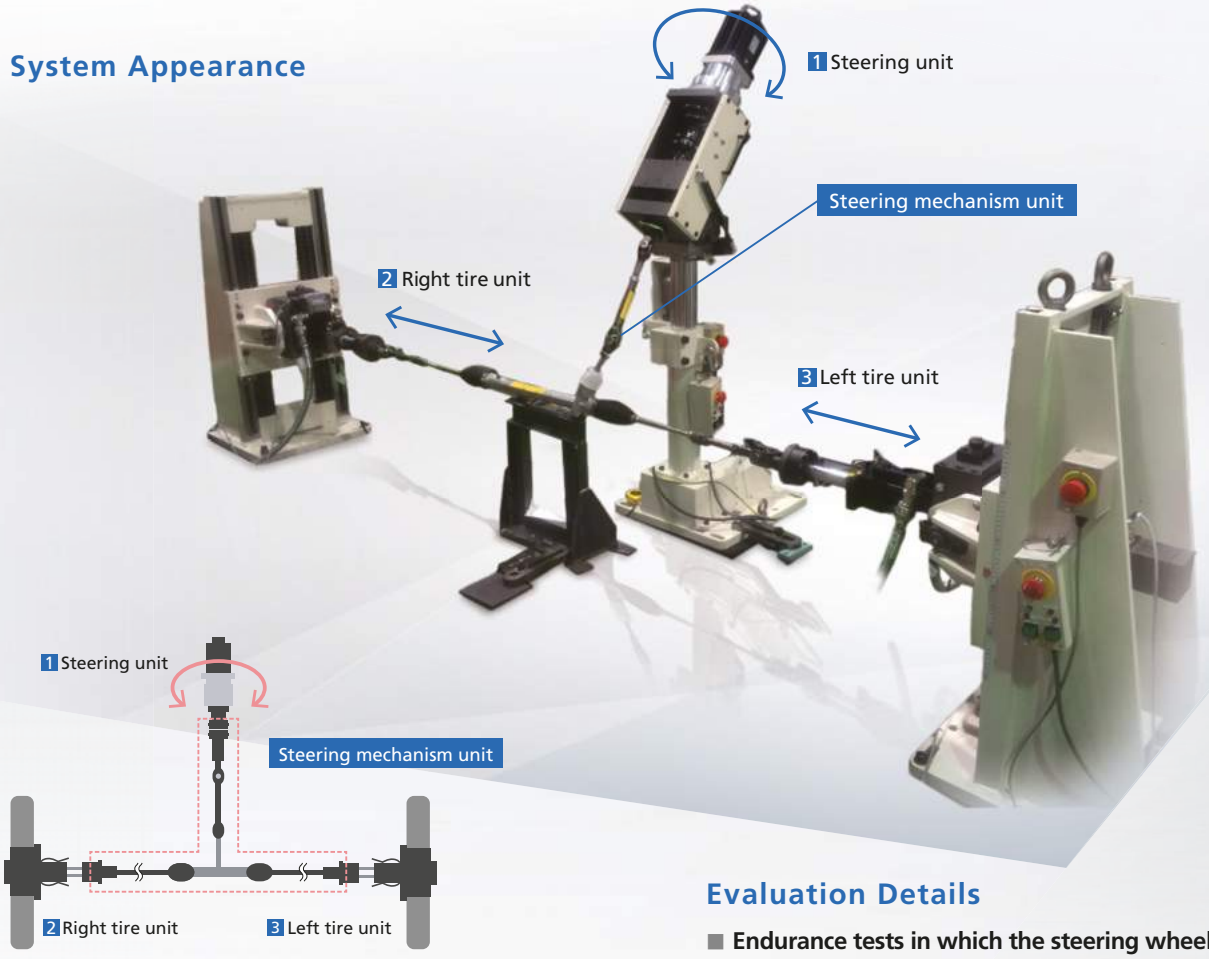

Endurance tests of the steering mechanism unit are performed by adding a rotational force via the steering wheel 1, and producing a reaction force originating from the tires in 2 and 3.

The reaction force from 2 and 3 corresponding to the rotational angle in 1 is obtained for use from an actual car.

Evaluation Details

- **Endurance tests in which the steering wheel is moved left and right more than one million times**
- **Endurance tests in which excessive force is applied to turn the steering wheel to the left or the right**
- **Quantitation of the sense of enhanced value (Rotational torque and angle of 1 and test force at 2 and 3 at each rotation point)**

Main Specifications

Left/Right Tire Units

1) Rated capacity: ±10 kN stroke ±100 mm
   (static maximum load capacity ±13 kN)
2) With trunnion pin
3) Maximum speed: 500 mm/sec
   (20 L/min hydraulic source, when unloaded)

Lifting Stand
(For the left/right tire units)

1) Height: 300 mm to 800 mm
   (electric lift, manual bolt fastening)
2) Angle: top/bottom ±10°
   (can change fastened or mobile) and horizontal ±10°

Steering Unit

1) Rated capacity: ±200 Nm, Angle: ±1080 deg
2) Maximum speed: 360 deg/sec
3) Excitation frequency: 0.01 Hz to 2 Hz (±5 deg or more)

4830 Controller

Lifting Stand
(For the steering unit)

1) Height: 800 mm to 1200 mm (electric lift, manual bolt fastening)
2) Angle: top/bottom 0° to 60° (can change fastened or mobile)

Data Processing Example (PC Screen)

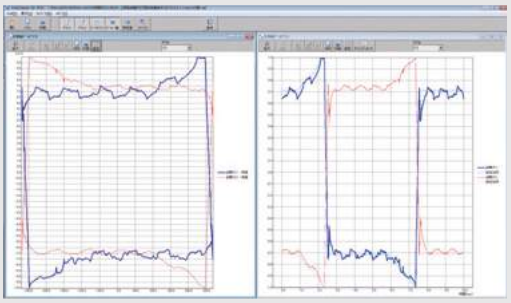

The left window shows the data chart results when the steering unit is turned to the left and right from the center position, and then returns to the center.

The window on the left shows a chart of angle versus test force.

The window on the right shows a chart of time versus test force.

The blue line is the test force for the right tire unit.

The red line is the test force for the left tire unit.

SHIMADZU

Shimadzu Corporation

www.shimadzu.com/an/

For Research Use Only. Not for use in diagnostic procedure.
This publication may contain references to products that are not available in your country. Please contact us to check the availability of these products in your country.
Company names, product/service names and logos used in this publication are trademarks and trade names of Shimadzu Corporation or its affiliates, whether or not they are used with trademark symbol "TM" or "®". Third-party trademarks and trade names may be used in this publication to refer to either the entities or their products/services. Shimadzu disclaims any proprietary interest in trademarks and trade names other than its own.

The contents of this publication are provided to you "as is" without warranty of any kind, and are subject to change without notice. Shimadzu does not assume any responsibility or liability for any damage, whether direct or indirect, relating to the use of this publication.

© Shimadzu Corporation, 2016

First Edition: August 2016

SHIMADZU
Excellence in Science

8. Plastics and Rubber Industry

8. Plastics and Rubber Industry

EVALUATION OF RUBBER AND PLASTICS

Rubber and plastic products are used in a wide variety of industrial areas such as packaging, construction, automotive, electronics, furniture, household goods, agriculture and medical. Plastomers, thermosetting plastic and elastomer materials are commonly used in various applications. Physical properties determine their important features, e.g. lightweight, hardness, density, resistance to heat, flexibility, moldability and chemical resistance.

Plastics and rubber are growing industries, and they are produced worldwide. They are also part of the supply chain in many industries. Evaluation of their basic performance and determined components is indispensable to product development and quality control. Applications include evaluation of rheological, thermal, statical and dynamic strength properties of additives and harmful materials as well as observation and measurement.

Shimadzu not only offers a wide array of evaluation instruments, but also provides comprehensive support from application to after-sales service. On the following pages are over 30 applications covering most versatile cases of material testing and inspection.

Testing, Weighing and Analytical Instruments For Rubber and Plastics

8. Plastics and Rubber Industry

C225-E034	System to test fatigue and endurance of rubber in clean environment
No.1	Tensile test of various plastic materials
No.2	Flexural test of plastic ISO178
No.3	Tensile tests of plastic materials at low ISO527 1
No.4	Tensile test of rubber dumb bell specimens ISO37
No.5	Tear test of crescent shaped ISO34 1
No.6	Tear tests of angle shaped rubber specimens ISO34 1
No.7	Tensile tests of films ISO527 3
No.9	Measurements of modulus of elasticity and poisson's ratio for films ISO527
No.17	Measurement of friction coefficient of film
No.18	90 degree peel resistance test of adhesive tape
No.19	180 degree peel resistance test of adhesive tape
No.20	Measurement of friction coefficient of film
No_05	Fluidity evaluation of unvulcanized rubber
No_06	Evaluation of the temperature characteristics of general plastics
No_07	CFT EX useful to evaluation of LED package
No_08	Why is CFT used to evaluate thermosetting resins
No_09	Fluidity evaluation of epoxy resin
No_10	Fluidity evaluation of ic sealant
SCA_300_010	Endurance testing and dynamic visco-elasticity measurement of EVA Film by MMT-100N
SCA_300_013	Evaluation of mooney viscosity by Shimadzu mooney viscometer, model SMV
SCA_300_014	Evaluation of surface hardness of audio-tapes with Shimadzu dynamic ultra micro hardness tester model DUH
SCA_300_017	Flow tests of various kinds of plastics with Shimadzu flowtester model CFT
SCA_300_021	Hardness measurement of plastic tubes using the Shimadzu dynamic ultra micro hardness tester DUH
SCA_300_026	Measurement of surface hardness of erasers with Shimadzu dynamic ultra micro hardness tester
SCA_300_028	Measuring and controlling performance of Shimadzu mooney viscometer model SMV in viscosity tests on rubber materials
SCA_300_031	Test on thermosetting resin with Shimadzu flow tester model CFT
No.ei253	Tensile test of plastic materials
No.ei249	Three-point bending flexural test of plastics (ISO178, JIS K 7171)
SCA_300_038	Deformation of rubber vibration isolators
SCA_300_039	Evaluation of elastic recovery in hardness measurement of plastic materials with Shimadzu dynamic ultra micro hardness tester
SCA_300_043	Fluidity evaluation of unvulcanized rubber
SCA_300_054	Viscosity evaluation of thermoplastic resins (epoxies)
SCA_300_057	Breaking strain measurement of ABS resin

SHIMADZU
Excellence in Science

System to Test Fatigue and Endurance of Rubber in a Clean Environment

Oil-Less, Electrically-Driven, Long Stroke, High Speed, and High Precision

Rubber vibration isolators are important parts for quiet operation of cars and industrial systems. To design rubber, factors including spring constant, damping coefficient, and loss factor need to be measured in conditions from static to high cycle rates. Using the EMT testing system, these tests can be performed easily. Fatigue and endurance testing can be performed simply by connecting the system to a 200 V outlet. Highly-reliable data can be acquired by using the system with an extremely rigid four-frame structure that is resistant to resonance, electrically-driven actuator that reproduces input waveforms accurately, and 4830 controller that has been well-received for high-precision control.

Product Lineup (EMT Series)

Model	EMT-1kNV-30	EMT-1kNV-50	EMT-5kNV-30	EMT-5kNV-50
Max. Test Force	±1 kN (static/dynamic)		±5 kN for dynamic, ±3.5 kN for static	
Stroke	±30mm	±50mm	±30mm	±50mm
Max. Speed	1m/s	2m/s	1m/s	1m/s
Max. Frequency	200Hz	200Hz	200Hz	100Hz
Accuracy	Test force: ±0.5 % of the indicated value, Stroke: ±1 % of the indicated value			

4830 Controller

*The auto-tuning function helps to input load waveforms accurately.
*The waveform strain correction function allows accurate control for the target waveform.

Standard Circular Tapered Sample

EMT Series

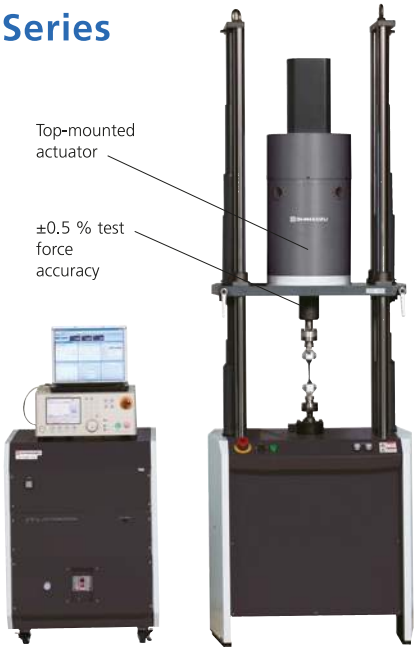

Standard Circular Tapered Sample

Standard Circular Tapered Sample

Application Example—Multi-Sample Measurement and Measurement in Various Testing Environments

Rubber is a raw material that requires a lot of testing, including evaluation of each production lot.
Since performance of rubber significantly varies according to the temperature, tests are performed under various temperature conditions.
In order to satisfy the demand for these tests, a multi-sample system (2-sample, 4-sample, 8-sample types) is available to provide high testing efficiency and save space for installing testing systems. By using the optional thermostatic chamber, tests can be performed at various temperatures from a low temperature of -35 ° C to a high temperature of +150 ℃ which rubber is used at in products. A light resistance test and endurance test can be performed simultaneously using the latest system in combination with a light resistance testing machine.

System Type of a 4-Sample EMT
+ Thermostatic Chamber (-30 to 150 °C)

Bottom-mounted actuator

System Type of a 2-Sample EMT
+ Light Resistance Testing Machine

Xenon irradiation equipment

SHIMADZU

SHIMADZU Corporation
www.shimadzu.com/an/

Company names, product/service names and logos used in this publication are trademarks and trade names of Shimadzu Corporation and its affiliates, whether or not they are used with trademark symbol "TM" or "®".
Third-party trademarks and trade names may be used in this publication to refer to either the entities or their products/services. Shimadzu disclaims any proprietary interest in trademarks and trade names other than its own.

For Research Use Only. Not for use in diagnostic procedures.
The contents of this publication are provided to you "as is" without warranty of any kind, and are subject to change without notice. Shimadzu does not assume any responsibility or liability for any damage, whether direct or indirect, relating to the use of this publication.

© Shimadzu Corporation, August,2016

SHIMADZU
Excellence in Science

Application Data Sheet

No. 1

Autograph Precision Universal Tester

Material Testing & Inspection

Tensile Test of Various Plastic Materials

Standard No. ISO527-1:2012 (JIS K 7161: 1994)

Introduction

Tensile tests are widely used to evaluate plastic materials, and the results are used as indices for new materials development and for implementing quality control. Items evaluated as tensile characteristics of plastic materials include the tensile modulus, strength, and break strain. In this Data Sheet, the tensile modulus of polypropylene (PP), polyvinyl chloride (PVC), and polycarbonate (PC) specimens (dumbbell shaped and cut types) was calculated based on displacement data acquired using an extensometer. The strength and break strain for the respective plastic materials are then determined from the test force values and crosshead travel distances detected with the tester.

T. Murakami

Measurements and Jigs

To find a sample's tensile modulus, it is necessary to use an extensometer capable of measuring tiny deformations of the sample with high accuracy. Measurements of crosshead travel distances include errors not only from sample deformation, but also from load cell and test jig deformation. When the deformation region is very small, the ratio of the error becomes significant, so this data is not suitable for tensile modulus calculations. In such cases, an extensometer that can measure changes in the gauge length with an accuracy of at least ±1 % must be used. When measuring the modulus of elasticity with a 50 mm gauge length, this corresponds to an accuracy of ±1 μm. In this test, a strain gauge type one-touch extensometer that meets the above-mentioned conditions was used to measure elongation.

Measurement Results

Fig. 1: Test Status

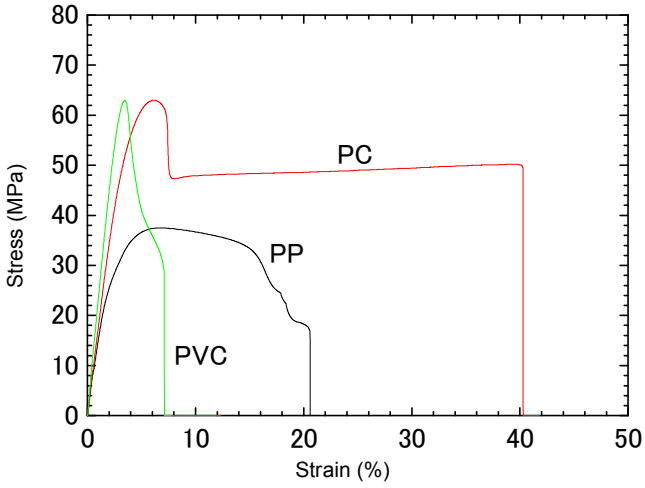

Fig. 2: Relationship Between Stress and Strain

Elongation was measured using the extensometer at a test speed of 1 mm/min within the elasticity region. After removing the extensometer, the test continued at a test speed of 50 mm/min until fracture of the specimen.

Table 1: Test Results

Sample	Tensile Modulus (MPa)	Strength (MPa)	Break Strain (%)
PP	1950	37.5	21.0
PVC	2390	62.4	7.2
PC	3060	63.0	42.2

Plastic Material Tensile Test System

Tester:	AGS-X
Load Cell:	5 kN
Test Jig:	5 kN pneumatic flat grips (single-side file teeth grip faces)
Extensometer:	Strain gauge type one-touch extensometer SSG50-10SH
External Amplifier:	ESA-CU200
Software:	TRAPEZIUM LITE X

AGS-X Table-Top Precision Universal Tester

Features

- A high-precision load cell is adopted. (The high-precision type is class 0.5; the standard-precision type is class 1.) Accuracy is guaranteed over a wide range, from 1/500 to 1/1 of the load cell capacity. This supports highly reliable test evaluations.
- Crosshead speed range
  Tests can be performed over a wide range from 0.001 mm/min to 1,000 mm/min.
- High-speed sampling
  High-speed sampling, as fast as 1 msec.
- TRAPEZIUMX LITE X operational software
  This is simple, highly effective software.
- Jog controller (optional)
  This allows hand-held control of the crosshead position. Fine position adjustment is possible using the jog dial.
- Optional Test Devices
  A variety of tests can be conducted by switching between an abundance of jigs in the lineup.

First Edition: February 2013

Shimadzu Corporation
www.shimadzu.com/an/

For Research Use Only. Not for use in diagnostic procedures.
The content of this publication shall not be reproduced, altered or sold for any commercial purpose without the written approval of Shimadzu.
The information contained herein is provided to you "as is" without warranty of any kind including without limitation warranties as to its accuracy or completeness. Shimadzu does not assume any responsibility or liability for any damage, whether direct or indirect, relating to the use of this publication. This publication is based upon the information available to Shimadzu on or before the date of publication, and subject to change without notice.
© Shimadzu Corporation, 2013

SHIMADZU
Excellence in Science

Application Data Sheet

No. 2

Autograph Precision Universal Tester

Material Testing & Inspection

Flexural Testing of Plastics

Standard No. ISO178: 2010 (JIS K 7171: 1994)

Introduction

In recent years, a large variety of synthetic resin (plastic) materials has become available for use in a diversity of products. They are used in applications that take advantage of their respective characteristics. For example, polyethylene (PE) is cheap and easy to mold, and thus used for containers, packaging film, and other everyday applications. In contrast, polycarbonate (PC) is transparent, has a high mechanical strength, and is heat-resistant; consequently, it is used for CDs and DVDs in the electrical and electronics fields, as well as in transportation equipment, optics, and medical fields.

In this Data Sheet, flexural testings are performed on four materials, including polyvinyl chloride (PVC) and polypropylene (PP).

T. Murakami

Measurements and Jigs

In plastic flexural testings, the width of the two supports and central loading edge must be larger than the width of the specimen, and parallelism within ± 0.2 mm is required. The loading edge radius is 5 mm ±0.1 mm, and the supports radius is specified as 2 mm ± 0.2 mm for specimens with a thickness of 3 mm or less, and 5 mm ± 0.2 mm for specimens with a thickness exceeding 3 mm. The span must be adjusted to a value of 16 (± 1) times the specimen thickness. In this test, since a 4 mm-thick specimen is used, the span is set to 64 mm (specimen thickness of 4 mm × 16 = 64 mm).

Measurement Results

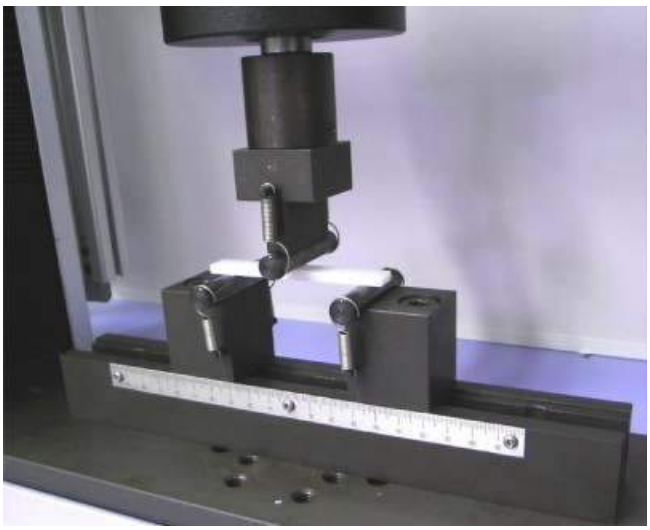

Fig. 1: Test Status

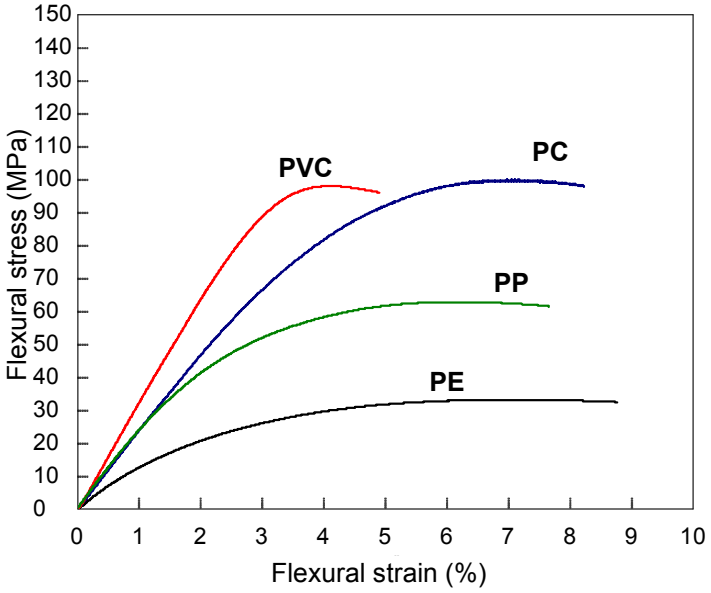

Fig. 2: Relationship Between Flexural Stress and Flexural Strain

Table 1: Test Conditions

Item	Set Value
Test Speed	2 mm/min
Span	64 mm

Table 2: Test Results

Sample	Flexural Modulus (MPa)	Flexural Strength (MPa)
PE (polyethylene)	1527	33.0
PC (polycarbonate)	2378	99.7
PVC (polyvinyl chloride)	3257	97.8
PP (polypropylene)	2559	62.6

Plastic Flexural Testing System

Tester:	AGS-X
Load Cell:	1 kN
Test Jig:	Three-point bending test jig for plastics (loading edge radius.: 5 mm, supports radius.: 3 mm)
Software:	TRAPEZIUM LITE X

AGS-X Table-Top Precision Universal Tester

Features

- A high-precision load cell is adopted. (The high-precision type is class 0.5; the standard-precision type is class 1.) Accuracy is guaranteed over a wide range, from 1/500 to 1/1 of the load cell capacity. This supports highly reliable test evaluations.
- Crosshead speed range
  Tests can be performed over a wide range from 0.001 mm/min to 1,000 mm/min.
- High-speed sampling
  High-speed sampling, as fast as 1 msec.
- TRAPEZIUMX LITE X operational software
  This is simple, highly effective software.
- Jog controller (optional)
  This allows hand-held control of the crosshead position. Fine position adjustment is possible using the jog dial.
- Optional Test Devices
  A variety of tests can be conducted by switching between an abundance of jigs in the lineup.

First Edition: February 2013

Shimadzu Corporation
www.shimadzu.com/an/

For Research Use Only. Not for use in diagnostic procedures.
The content of this publication shall not be reproduced, altered or sold for any commercial purpose without the written approval of Shimadzu.
The information contained herein is provided to you "as is" without warranty of any kind including without limitation warranties as to its accuracy or completeness. Shimadzu does not assume any responsibility or liability for any damage, whether direct or indirect, relating to the use of this publication. This publication is based upon the information available to Shimadzu on or before the date of publication, and subject to change without notice.
© Shimadzu Corporation, 2013

SHIMADZU
Excellence in Science

Application Data Sheet

No. 3

Autograph Precision Universal Tester

Material Testing & Inspection

Tensile Tests of Plastic Materials at Low Temperatures (-40 °C)

Standard No. ISO527-1: 2012 (JIS K 7161: 1994)

Introduction

Tensile tests are widely used to evaluate plastic materials, and the results are used as indices for new materials development and for implementing quality control. Items evaluated as tensile characteristics of plastic materials include the tensile modulus, strength, and break strain. In this Data Sheet, the tensile modulus of polypropylene (PP) and polyvinyl chloride (PVC) specimens (dumbbell shaped and cut types) was calculated based on displacement data acquired using an extensometer at a low temperature of -40 °C. In addition, the strength and break strain for the respective plastic materials were also evaluated.

T. Murakami

Measurements and Jigs

In finding a sample's tensile modulus, it is necessary to use an extensometer capable of measuring tiny deformations of the sample with high accuracy. Measurements of crosshead travel distances include errors not only from sample deformation, but also from load cell and test jig deformation. When the deformation region is very small, the ratio of the error becomes significant, so this data is not suitable for tensile modulus calculations. In such cases, an extensometer that can measure changes in the gauge length with an accuracy of at least ±1 % must be used. When measuring the modulus of elasticity with a 50 mm gauge length, this corresponds to an accuracy of ±1μm. In this test, a one-touch contact type extensometer, capable of operating even in a -40 °C environment, was used.

Measurement Results

Fig. 1: Test Status

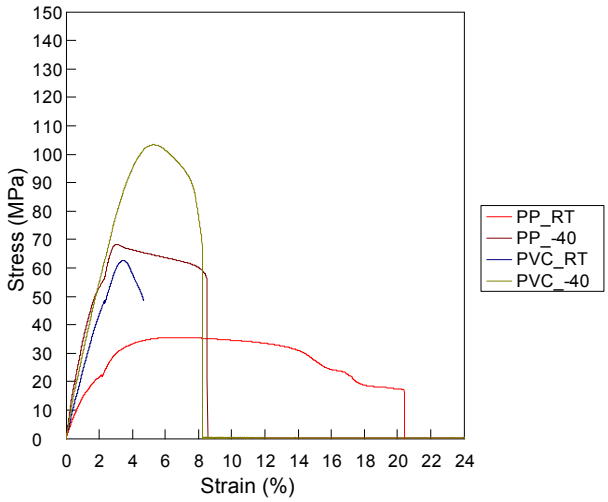

Fig. 2: Relationship Between Stress and Strain

In the results, samples with an "RT" suffix were measured in a room temperature environment, and those with a "-40" suffix were measured at -40 °C. In all cases, measurement was performed at a test speed of 1 mm/min up to 2 %, and then at a test speed of 50 mm/min. In the room temperature measurements, the extensometer measurement range was exceeded, so the extensometer was removed at the 2 % position.

Table 1: Test Results

Sample	Tensile Modulus (MPa)	Strength (MPa)	Break Strain (%)
PP_RT	1955	36	20.2
PP_-40	5333	68	7.8
PVC_RT	3150	63	4.3
PVC_-40	3942	103	7.1

Plastic Material Thermostatic Tensile Test System

Tester:	AGS-X
Load Cell:	5 kN
Test Jig:	5 kN pneumatic flat grips (Single-side file teeth grip faces)
Extensometer:	Strain gauge type one-touch extensometer EPC-50-10
External Amplifier:	ESA-CU200
Thermostatic Chamber:	TCR2W
Software:	TRAPEZIUM LITE X

AGS-X Table-Top Precision Universal Tester

Features

- A high-precision load cell is adopted. (The high-precision type is class 0.5; the standard-precision type is class 1.) Accuracy is guaranteed over a wide range, from 1/500 to 1/1 of the load cell capacity. This supports highly reliable test evaluations.
- Crosshead speed range
  Tests can be performed over a wide range from 0.001 mm/min to 1,000 mm/min.
- High-speed sampling
  High-speed sampling, as fast as 1 msec.
- TRAPEZIUMX LITE X operational software
  This is simple, highly effective software.
- Jog controller (optional)
  This allows hand-held control of the crosshead position. Fine position adjustment is possible using the jog dial.
- Optional Test Devices
  A variety of tests can be conducted by switching between an abundance of jigs in the lineup.

First Edition: February 2013

Shimadzu Corporation
www.shimadzu.com/an/

For Research Use Only. Not for use in diagnostic procedures.
The content of this publication shall not be reproduced, altered or sold for any commercial purpose without the written approval of Shimadzu.
The information contained herein is provided to you "as is" without warranty of any kind including without limitation warranties as to its accuracy or completeness. Shimadzu does not assume any responsibility or liability for any damage, whether direct or indirect, relating to the use of this publication. This publication is based upon the information available to Shimadzu on or before the date of publication, and subject to change without notice.
© Shimadzu Corporation, 2013

SHIMADZU
Excellence in Science

Application Data Sheet

No. 4

Autograph Precision Universal Tester

Material Testing & Inspection

Tensile Tests of Rubber Dumb-bell Specimens

Standard No. ISO37: 2005 (JIS K6251: 2010)

Introduction

Rubber materials have characteristic mechanical properties including elasticity and flexibility, and are widely used for industrial parts, construction materials, and housewares. In particular, a diverse range of synthetic rubber materials with differing properties suited to match their application have been developed. Measuring these mechanical properties is extremely important to ensure quality control and for new materials development. This Data Sheet introduces an example of the evaluation of three synthetic rubber (main components: chloroprene [1]; urethane [2]) specimens (dumb-bell test pieces). Static tensile tests were performed, and the specimens were evaluated with respect to tensile strength, stress at given elongation, and elongation at break, which are aspects of their basic mechanical properties.

T. Murakami

Measurements and Jigs

In tensile tests of rubber dumb-bell specimens, the grips must tighten automatically. When tensile loads are applied to rubber materials, they elongate and their thickness decreases. For this reason, if there is no automatic tightening mechanism, the specimen will inadvertently break free of the grip before the maximum load is applied, making favorable measurements impossible. Accordingly, in rubber tensile tests, it is necessary to use pneumatic parallel grippers, pantograph grips, eccentric roller type grips, Henry Scott type grips, or other grips equipped with this feature.

Measurement Results

Fig. 1: Test Status

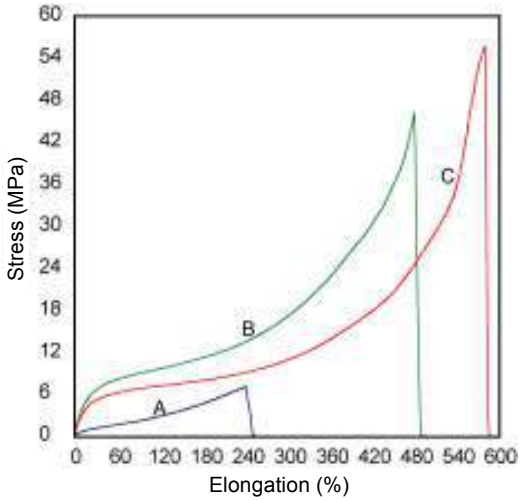

Fig. 2: Relationship Between Stress and Elongation

Table 1: Test Conditions

Item	Set Value
Test Speed	500 mm/min
Initial Distance between Grips	60 mm
Gauge Length	20 mm

Table 2: Test Results

Sample	Main Component	Tensile Strength (MPa)	Stress at 100 % Elongation (MPa)	Stress at 200 % Elongation (MPa)	Elongation at Break (%)
A	Chloroprene	7.1	2.4	5.4	242.3
B	Urethane	47.1	9.3	11.9	478.1
C	Urethane	55.5	7.0	8.4	572.6

The tensile test results for the three samples are shown in Table 2. A graph showing the stress-elongation relationship for the samples is shown in Fig. 2. Clear differences in mechanical properties such as tensile strength and elongation at break are apparent between the samples.

Rubber (Dumb-bells test pieces) Tensile Test System

Tester:	AGS-X
Load Cell:	1 kN
Test Jig:	1 kN pneumatic flat grips (Single-side file teeth grip faces)
Extensometer:	SES-1000 type extensometer for soft specimens
Software:	TRAPEZIUM LITE X

AGS-X Table-Top Precision Universal Tester

Features

- A high-precision load cell is adopted. (The high-precision type is class 0.5; the standard-precision type is class 1.) Accuracy is guaranteed over a wide range, from 1/500 to 1/1 of the load cell capacity. This supports highly reliable test evaluations.
- Crosshead speed range
  Tests can be performed over a wide range from 0.001 mm/min to 1,000 mm/min.
- High-speed sampling
  High-speed sampling, as fast as 1 msec.
- TRAPEZIUMX LITE X operational software
  This is simple, highly effective software.
- Jog controller (optional)
  This allows hand-held control of the crosshead position. Fine position adjustment is possible using the jog dial.
- Optional Test Devices
  A variety of tests can be conducted by switching between an abundance of jigs in the lineup.

First Edition: February 2013

Shimadzu Corporation
www.shimadzu.com/an/

For Research Use Only. Not for use in diagnostic procedures.
The content of this publication shall not be reproduced, altered or sold for any commercial purpose without the written approval of Shimadzu.
The information contained herein is provided to you "as is" without warranty of any kind including without limitation warranties as to its accuracy or completeness. Shimadzu does not assume any responsibility or liability for any damage, whether direct or indirect, relating to the use of this publication. This publication is based upon the information available to Shimadzu on or before the date of publication, and subject to change without notice.
© Shimadzu Corporation, 2013

SHIMADZU
Excellence in Science

Application Data Sheet

No. 5

Autograph Precision Universal Tester

Material Testing & Inspection

Tear Tests of Crescent-shaped Rubber Specimens

Standard No. ISO34-1: 2004 (JIS K6252: 2007)

Introduction

Rubber materials have characteristic mechanical properties including elasticity and flexibility, and are widely used for industrial parts, construction materials, and housewares. In particular, a diverse range of synthetic rubber materials with differing properties suited to match their application have been developed. Measuring these mechanical properties is extremely important to ensure quality control and for new materials development. This Data Sheet introduces an example of the evaluation of two synthetic rubber specimens (crescent-shaped specimens). Tear tests were performed, and the specimens were evaluated with respect to tear strength, one of their basic mechanical properties.

T. Murakami, J. Sakai

Measurements and Jigs

Tear tests of crescent-shaped rubber specimens require grips that tighten automatically as the tear force increases. When tensile loads are applied to rubber materials, they elongate and their thickness decreases. For this reason, if there is no automatic tightening mechanism, the specimen will inadvertently break free of the grips before the maximum tear force is applied, making favorable measurements impossible. Accordingly, in rubber tear tests, it is necessary to use pneumatic parallel grippers, pantograph grips, eccentric roller type grips, Henry Scott type grips, or other grips equipped with this feature.

Measurement Results

Fig. 1: Test Status

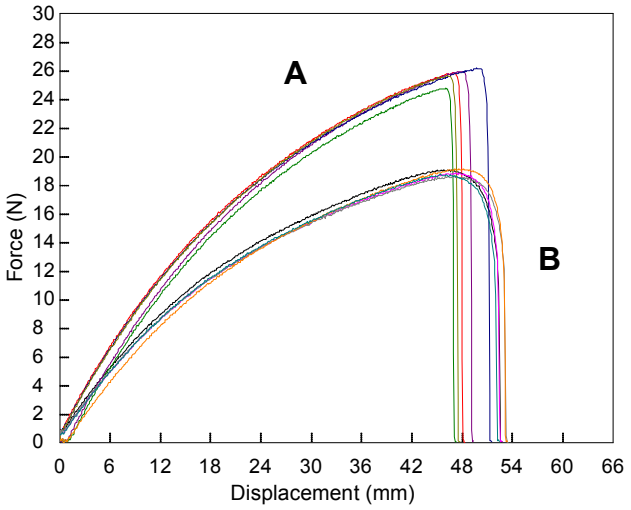

Fig. 2: Relationship Between Force and Displacement

Table 1: Test Conditions

Item	Set Value
Test Speed	500 mm/min
Initial Distance between Grips	60 mm

Table 2: Test Results (Average)

Sample	Main Component	Max. Force (N)	Tear Strength (kN/m)
A	CR rubber (black)	25.9	13.0
B	CR rubber (white)	18.9	9.5

The tear test results for the two samples are shown in Table 2. A graph showing the force-displacement relationship for each sample is shown in Fig. 2. Differences in tear strength between the samples are clearly apparent.

Rubber Tear Test System

Tester:	AGS-X
Load Cell:	1 kN
Test Jig:	1 kN pneumatic flat grips (Single-side file teeth grip faces)
Software:	TRAPEZIUM LITE X

AGS-X Table-Top Precision Universal Tester

Features

- A high-precision load cell is adopted. (The high-precision type is class 0.5; the standard-precision type is class 1.) Accuracy is guaranteed over a wide range, from 1/500 to 1/1 of the load cell capacity. This supports highly reliable test evaluations.
- Crosshead speed range
  Tests can be performed over a wide range from 0.001 mm/min to 1,000 mm/min.
- High-speed sampling
  High-speed sampling, as fast as 1 msec.
- TRAPEZIUMX LITE X operational software
  This is simple, highly effective software.
- Jog controller (optional)
  This allows hand-held control of the crosshead position. Fine position adjustment is possible using the jog dial.
- Optional Test Devices
  A variety of tests can be conducted by switching between an abundance of jigs in the lineup.

First Edition: February 2013

Shimadzu Corporation
www.shimadzu.com/an/

For Research Use Only. Not for use in diagnostic procedures.
The content of this publication shall not be reproduced, altered or sold for any commercial purpose without the written approval of Shimadzu.
The information contained herein is provided to you "as is" without warranty of any kind including without limitation warranties as to its accuracy or completeness. Shimadzu does not assume any responsibility or liability for any damage, whether direct or indirect, relating to the use of this publication. This publication is based upon the information available to Shimadzu on or before the date of publication, and subject to change without notice.
© Shimadzu Corporation, 2013

SHIMADZU
Excellence in Science

Application Data Sheet

No. 6

Autograph Precision Universal Tester

Material Testing & Inspection

Tear Tests of Angle-Shaped Rubber Specimens

Standard No. ISO34-1: 2004 (JIS K6252: 2007)

Introduction

Rubber materials have characteristic mechanical properties including elasticity and flexibility, and are widely used for industrial parts, construction materials, and housewares. In particular, a diverse range of synthetic rubber materials with differing properties suited to match their application have been developed. Measuring these mechanical properties is extremely important to ensure quality control and for new materials development. This Data Sheet introduces an example of the evaluation of two synthetic rubber specimens (angle-shaped specimens). Tear tests were performed, and the specimens were evaluated with respect to tear strength, one of their basic mechanical properties.

T. Murakami, J. Sakai

Measurements and Jigs

Tear tests of angle-shaped rubber specimens require grips that tighten automatically as the tear force increases. When tensile loads are applied to rubber materials, they elongate and their thickness decreases. For this reason, if there is no automatic tightening mechanism, the specimen will inadvertently break free of the grips before the maximum tear force is applied, making favorable measurements impossible. Accordingly, in rubber tear tests, it is necessary to use pneumatic parallel grippers, pantograph grips, eccentric roller type grips, Henry Scott type grips, or other grips equipped with this feature.

Measurement Results

Fig. 1: Test Status

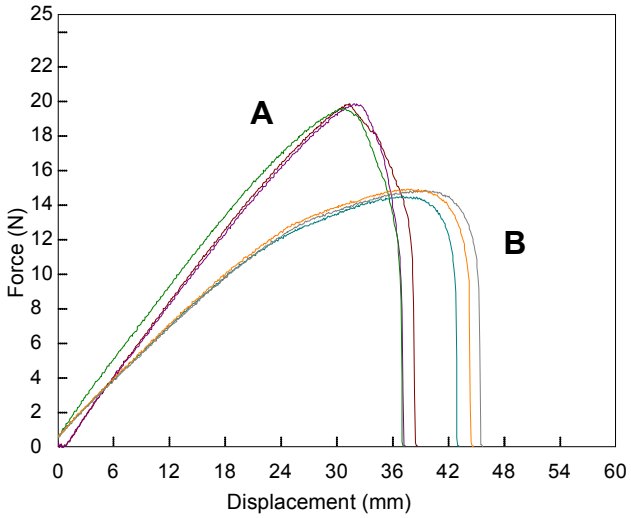

Fig. 2: Relationship Between Force and Displacement

Table 1: Test Conditions

Item	Set Value
Test Speed	500 mm/min
Initial Distance between Grips	60 mm

Table 2: Test Results (Average)

Sample	Main Component	Max. Force (N)	Tear Strength (kN/m)
A	CR rubber (black)	19.7	9.85
B	CR rubber (white)	14.7	7.35

The tear test results for the two samples are shown in Table 2. A graph showing the force-displacement relationship for each sample is shown in Fig. 2. Differences in tear strength between the samples are clearly apparent.

Rubber Tear Test System

Tester:	AGS-X
Load Cell:	1 kN
Test Jig:	1 kN pneumatic flat grips (Single-side file teeth grip faces)
Software:	TRAPEZIUM LITE X

AGS-X Table-Top Precision Universal Tester

Features

- A high-precision load cell is adopted. (The high-precision type is class 0.5; the standard-precision type is class 1.) Accuracy is guaranteed over a wide range, from 1/500 to 1/1 of the load cell capacity. This supports highly reliable test evaluations.
- Crosshead speed range
  Tests can be performed over a wide range from 0.001 mm/min to 1,000 mm/min.
- High-speed sampling
  High-speed sampling, as fast as 1 msec.
- TRAPEZIUMX LITE X operational software
  This is simple, highly effective software.
- Jog controller (optional)
  This allows hand-held control of the crosshead position. Fine position adjustment is possible using the jog dial.
- Optional Test Devices
  A variety of tests can be conducted by switching between an abundance of jigs in the lineup.

First Edition: February 2013

Shimadzu Corporation
www.shimadzu.com/an/

For Research Use Only. Not for use in diagnostic procedures.
The content of this publication shall not be reproduced, altered or sold for any commercial purpose without the written approval of Shimadzu.
The information contained herein is provided to you "as is" without warranty of any kind including without limitation warranties as to its accuracy or completeness. Shimadzu does not assume any responsibility or liability for any damage, whether direct or indirect, relating to the use of this publication. This publication is based upon the information available to Shimadzu on or before the date of publication, and subject to change without notice.
© Shimadzu Corporation, 2013

SHIMADZU
Excellence in Science

Application Data Sheet

No. 7

Autograph Precision Universal Tester

Material Testing & Inspection

Tensile Tests of Films

Standard No. ISO527-3: 2012 (JIS K 7127: 1999)

Introduction

Tensile tests are widely used to evaluate plastic materials, and the results are used as indices for new materials development and for implementing quality control. Items widely evaluated as tensile characteristics of plastic materials include the tensile modulus, strength, and break strain. In this Data Sheet, break strain was measured based on displacement data acquired using an extensometer. The strength was also evaluated.

T. Murakami

Measurements and Jigs

Non-contact type extensometers capable of displacement measurements without affecting the sample properties are effective for accurately measuring the break strain of a film. In measuring such physical properties, the sample must be gripped evenly, suppressing the occurrence of wrinkles, so it is important to choose the grips carefully. As in this test, the use of a non-contact type extensometer/width sensor and foil grips is recommended for film tensile tests.

Measurement Results

Fig. 1: Test Status

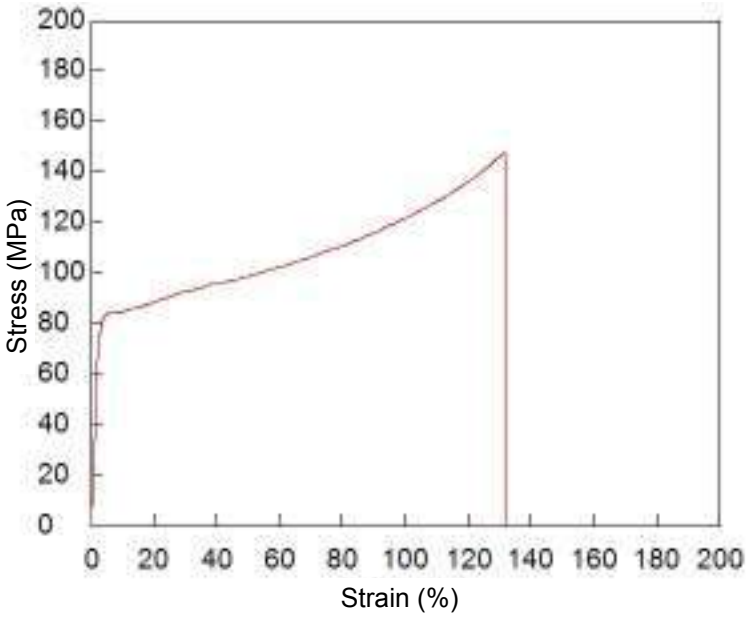

Fig. 2: Relationship Between Stress and Strain

Table 1: Test Conditions

Item	Set Value
Test Speed	50 mm/min
Initial Distance between Grips	100 mm

Table 2: Test Results

Sample	Thickness (μm)	Strength (MPa)	Break Strain (%)
PET Film	150	148	132

Film Tensile Test System

Tester:	AGS-X
Load Cell:	1 kN
Test Jig:	1 kN grips for foils
Extensometer:	TRViewX 240S non-contact extensometer/width sensor
Software:	TRAPEZIUM X

AGS-X Table-Top Precision Universal Tester

Features

- A high-precision load cell is adopted. (The high-precision type is class 0.5; the standard-precision type is class 1.) Accuracy is guaranteed over a wide range, from 1/500 to 1/1 of the load cell capacity. This supports highly reliable test evaluations.
- Crosshead speed range
  Tests can be performed over a wide range from 0.001 mm/min to 1,000 mm/min.
- High-speed sampling
  High-speed sampling, as fast as 1 msec.
- TRAPEZIUMX operational software
  Designed for intuitive operation, this software offers excellent convenience and user friendliness.
- Jog controller (optional)
  This allows hand-held control of the crosshead position. Fine position adjustment is possible using the jog dial.
- Optional Test Devices
  A variety of tests can be conducted by switching between an abundance of jigs in the lineup.

First Edition: February 2013

SHIMADZU

Shimadzu Corporation

www.shimadzu.com/an/

For Research Use Only. Not for use in diagnostic procedures.
The content of this publication shall not be reproduced, altered or sold for any commercial purpose without the written approval of Shimadzu.
The information contained herein is provided to you "as is" without warranty of any kind including without limitation warranties as to its accuracy or completeness. Shimadzu does not assume any responsibility or liability for any damage, whether direct or indirect, relating to the use of this publication. This publication is based upon the information available to Shimadzu on or before the date of publication, and subject to change without notice.

© Shimadzu Corporation, 2013

SHIMADZU
Excellence in Science

Application Data Sheet

No. 9

Autograph Precision Universal Tester

Material Testing & Inspection

Measurements of Modulus of Elasticity and Poisson's Ratio for Films

Standard Nos. ISO527-3: 2012 (JIS K 7127: 1999)
ISO527-1: 2012 (JIS K 7161: 1994)

Introduction

Tensile tests are widely used to evaluate plastic materials, and the results are used as indices for new materials development and for implementing quality control. Items evaluated as tensile characteristics of plastic materials include the tensile modulus, Poisson's ratio, strength, and break strain. With films, there are no standards specified with respect to test methods for the tensile elastic modulus and Poisson's ratio, yet there are demands for measurements of these values. In this Data Sheet, measurements of the tensile modulus and Poisson's ratio were performed for a PET film based on elongation and width data acquired using a non-contact type extensometer/width sensor.

T. Murakami

Measurements and Jigs

Non-contact type extensometers/width sensors capable of fine displacement measurements without affecting the sample properties are required to accurately obtain the tensile modulus and Poisson's ratio for a film. In measuring such physical properties, the sample must be gripped evenly, suppressing the occurrence of wrinkles, so it is important to choose the grips carefully. The use of a non-contact type extensometer/width sensor and foil grips is recommended for film tensile tests.

Measurement Results

Fig. 1: Test Status

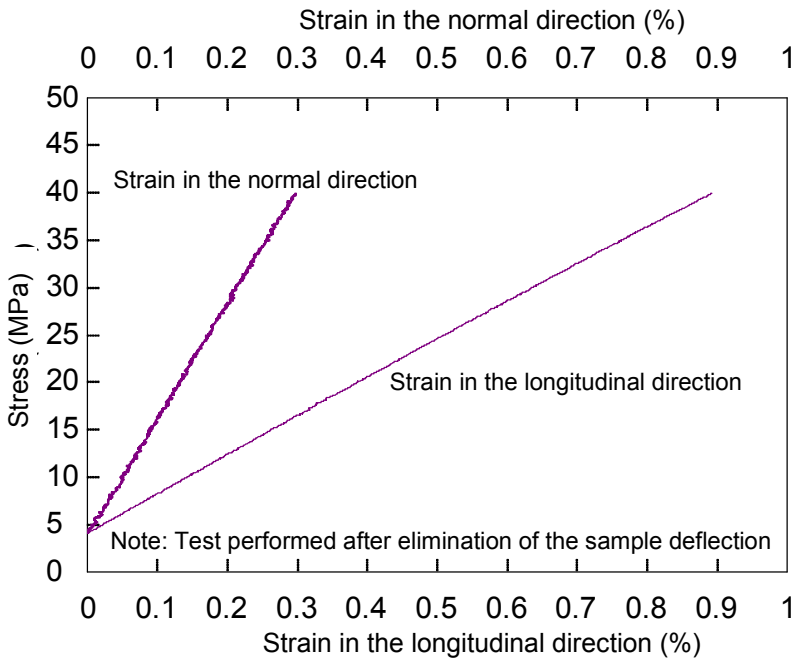

Fig. 2: Relationship Between Stress and Strain

Table 1: Test Conditions

Item	Set Value
Test Speed	1 mm/min
Initial distance Between Grip	100 mm
Gauge Length	40 mm

Table 2: Test Results

Sample	Thickness (μm)	Tensile Modulus (MPa)	Poisson's Ratio
PET Film	25	4139	0.37

Young's Modulus Measurement System for Film

Tester:	AG-Xplus
Load Cell:	1 kN
Test Jig:	1 kN grips for foils
Extensometer:	TRViewX 55S non-contact extensometer/width sensor
Software:	TRAPEZIUM X (Single)

AG-Xplus Table-Top Precision Universal Tester

Features

- A high-precision load cell is adopted. (The high-precision type is class 0.5; the standard-precision type is class 1.) Accuracy is guaranteed over a wide range, from 1/1000 to 1/1 of the load cell capacity. This supports highly reliable test evaluations.
- Crosshead speed range
  Tests can be performed over a wide range from 0.0005 mm/min to 1,500 mm/min.
- High-speed sampling
  Ultrafast sampling, as fast as 0.2 msec. Sudden changes in test force, such as when brittle materials fracture, can be assessed.
- TRAPEZIUMX X operational software
  Designed for intuitive operation, this software offers excellent convenience and user friendliness.
- Smart controller
  Real-time test force and position data is readily confirmed, and the manual dial can be used for fine adjustments to jig positioning.
- Optional Test Devices
  A variety of tests can be conducted by switching between an abundance of jigs in the lineup.

First Edition: February 2013

Shimadzu Corporation
www.shimadzu.com/an/

For Research Use Only. Not for use in diagnostic procedures.
The content of this publication shall not be reproduced, altered or sold for any commercial purpose without the written approval of Shimadzu.
The information contained herein is provided to you "as is" without warranty of any kind including without limitation warranties as to its accuracy or completeness. Shimadzu does not assume any responsibility or liability for any damage, whether direct or indirect, relating to the use of this publication. This publication is based upon the information available to Shimadzu on or before the date of publication, and subject to change without notice.
© Shimadzu Corporation, 2013

SHIMADZU
Excellence in Science

Application Data Sheet

No. 17

Autograph Precision Universal Tester

Material Testing & Inspection

Measurement of Friction Coefficient of Film

Standard No. ISO 8295: 1995 (JIS K 7125: 1999)

Introduction

Plastic films are used for coating or wrapping of various materials. It is often necessary to measure sliding friction between two films or between a film and a different material. For example, the coefficient of friction of film for foods and that of protection film for smartphones are measured. In this Application Data Sheet, measurement examples of the static and dynamic coefficients of friction for polyethylene film in accordance with the ISO standard are introduced.

F. Yano

Measurement and Jigs

The standard specifies the method of measuring the coefficients of starting and sliding friction of plastic films and sheets. This method measures the coefficient of friction of plastic films and sheets that are not sticky up to 0.5 mm thickness. The test requires 2 test specimens of size about 80 mm × 200 mm, and the test apparatus generally includes a horizontal testing table, a sliding member, and a drive mechanism that produces relative motion between the test table and the sliding member. In these tests, the AGS-X Table-Top Precision Universal Tester and friction coefficient measuring apparatus were used to evaluate polyethylene film.

Measurement Results

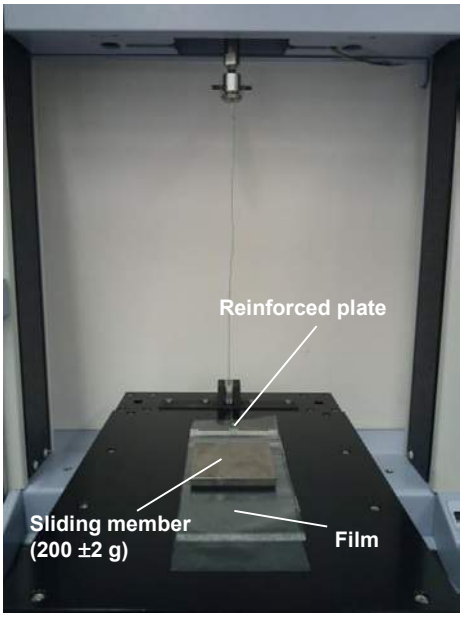

Fig. 1 Test Status

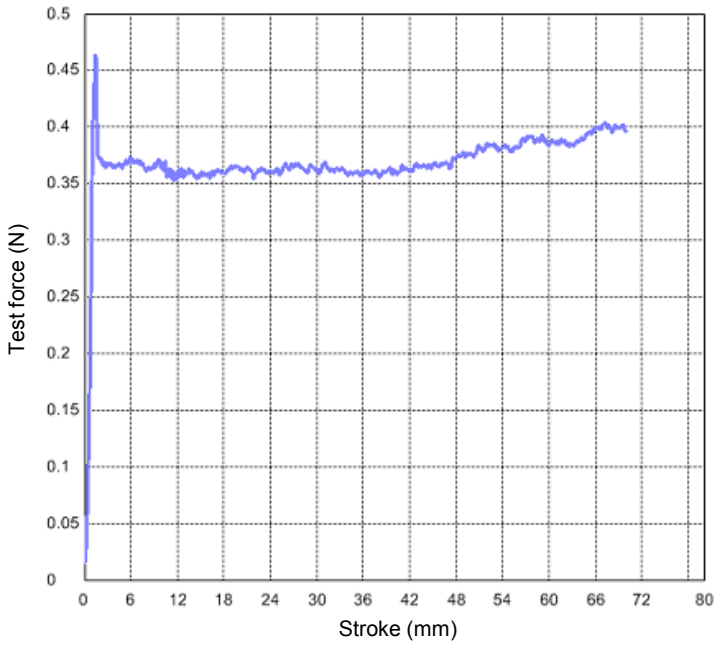

Fig.2 Test Results

Table 1 Test Conditions

Item	Set Value
Test speed	100 mm/min
Load cell capacity	5 N

Table 2 Test Results

Static Coefficient of Friction	Dynamic Coefficient of Friction
0.23	0.19

Friction Coefficient Measurement System

Tester: AGS-X
Load Cell: 5 N
Test Jig: Friction coefficient measuring apparatus
Software: TRAPEZIUM LITE X

AGS-X Table-Top Precision Universal Tester

Features

- A high-precision load cell is adopted. (The high-precision type is class 0.5; the standard-precision type is class 1.) Accuracy is guaranteed over a wide range, from 1/500 to 1/1 of the load cell capacity. This supports highly reliable test evaluations.
- Cross head speed range
  Test can be performed over a wide range from 0.001 mm/min to 1,000 mm/min.
- High speed sampling
  High speed sampling, as fast as 1 msec.
- TRAPEZIUMX LITE X operational software
  This is simple, highly effective software.
- Jog controller (optional)
  This allows hand-held control of the crosshead position. Fine position adjustment is possible using the jog dial.
- Optional Test Devices
  A variety of tests can be accommodated by switching between an abundance of jigs in the lineup.

First Edition: February 2013

SHIMADZU
Shimadzu Corporation
www.shimadzu.com/an/

For Research Use Only. Not for use in diagnostic procedures.
The content of this publication shall not be reproduced, altered or sold for any commercial purpose without the written approval of Shimadzu.
The information contained herein is provided to you "as is" without warranty of any kind including without limitation warranties as to its accuracy or completeness. Shimadzu does not assume any responsibility or liability for any damage, whether direct or indirect, relating to the use of this publication. This publication is based upon the information available to Shimadzu on or before the date of publication, and subject to change without notice.
© Shimadzu Corporation, 2013

SHIMADZU
Excellence in Science

Application Data Sheet

No. 18

Autograph Precision Universal Tester

Material Testing & Inspection

90-Degree Peel Resistance Test of Adhesive Tape

Sandard No. ISO29862: 2007 (JIS Z 0237 :2009)

Introduction

Adhesives are widely used in many industrial fields such as electronics and electrical machinery. Starting from the use of materials such as glue to join solids together, adhesives that use synthetic polymers as the raw material have been commercialized with the progress of the chemical industry. In this Application Data Sheet, examples of the 90-degree peeling test for adhesive material used for adhesive tape are introduced.

T. Murakami

Measurement and Jigs

General adhesive tape cut to a width of 24 mm and length of 300 mm was used as the test sample, and a SUS304 stainless steel plate was used as the test plate for setting the sample. An adhesive tape peel resistance test apparatus that was capable of peeling the sample at a constant 90 degree to the test plate was used.

Measurement Results

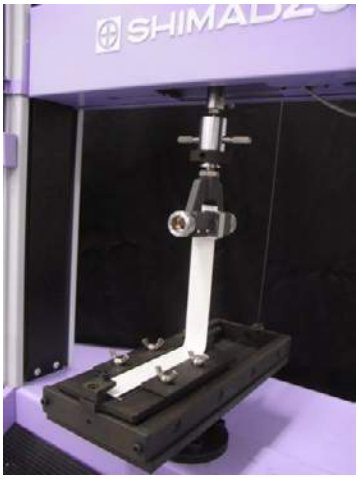

Fig. 1 Test Status

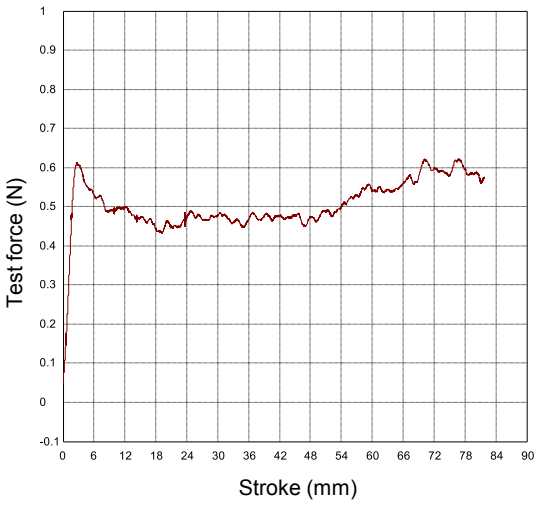

Fig. 2 Relationship Between Test Force and Stroke

The tests were carried out at a load rate of 300 mm/min. The measured values for the initial 25 mm length after start of testing were ignored, and the subsequent adhesion force measurement values for subsequent 50 mm length peeled from the test plate were averaged to obtain the peel adhesion force.

Table 1 Test Results

Peel Adhesion Force
0.238 N/10 mm

Plastic Material Tensile Test System

Tester: AGS-X
Load Cell: 50 N
Test Jig: Adhesive tape peel resistance test apparatus
Software: TRAPEZIUM LITE X

AGS-X Table-Top Precision Universal Tester

Features

- A high-precision load cell is adopted. (The high-precision type is class 0.5; the standard-precision type is class 1.) Accuracy is guaranteed over a wide range, from 1/500 to 1/1 of the load cell capacity. This supports highly reliable test evaluations.
- Cross head speed range
  Test can be performed over a wide range from 0.001 mm/min to 1,000 mm/min.
- High speed sampling
  High speed sampling, as fast as 1 msec.
- TRAPEZIUMX LITE X operational software
  This is simple, highly effective software.
- Jog controller (optional)
  This allows hand-held control of the crosshead position. Fine position adjustment is possible using the jog dial.
- Optional Test Devices
  A variety of tests can be accommodated by switching between an abundance of jigs in the lineup.

First Edition: February 2013

SHIMADZU

Shimadzu Corporation
www.shimadzu.com/an/

For Research Use Only. Not for use in diagnostic procedures.
The content of this publication shall not be reproduced, altered or sold for any commercial purpose without the written approval of Shimadzu.
The information contained herein is provided to you "as is" without warranty of any kind including without limitation warranties as to its accuracy or completeness. Shimadzu does not assume any responsibility or liability for any damage, whether direct or indirect, relating to the use of this publication. This publication is based upon the information available to Shimadzu on or before the date of publication, and subject to change without notice.

© Shimadzu Corporation, 2013

SHIMADZU
Excellence in Science

Application Data Sheet

No. 19

Autograph Precision Universal Tester

Material Testing & Inspection

180-Degree Peel Resistance Test of Adhesive Tape

Sandard No. ISO29862: 2007 (JIS Z 0237 :2009)

Introduction

Adhesives are widely used in many industrial fields such as electronics and electrical machinery. Starting from the use of materials such as glue to join solids together, adhesives that use synthetic polymers as the raw material have been commercialized with the progress of the chemical industry. In this Application Data Sheet, examples of the 180-degree peeling test for adhesive material used for adhesive tape are introduced.

T.Murakami

Measurement and Jigs

General adhesive tape cut to a width of 24 mm and length of 300 mm was used as the test sample, and a SUS304 stainless steel plate was used as the test plate for setting the sample. When the sample was peeled, the ends of the tape were held and folded through 180 degree so that the back of the tape was overlapped. After the sample was peeled 25 mm from the test plate, one end of the test plate from which the tape had been peeled was fixed in the lower jig set in the testing machine, and the adhesive tape was fixed in the upper jig.

Measurement Results

Fig. 1 Test Status

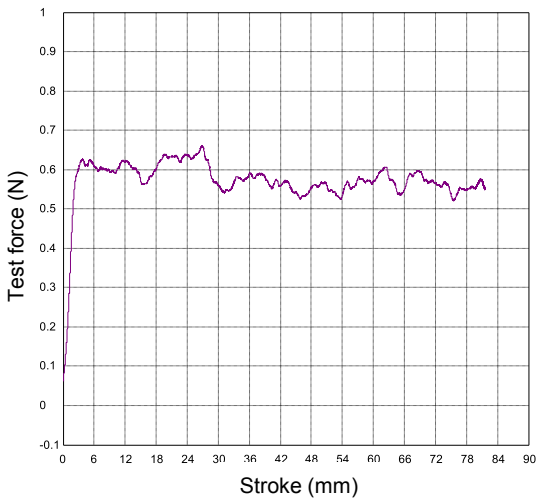

Fig. 2 Relationship Between Test Force and Stroke

The tests were carried out at a load rate of 300 mm/min. The measured values for the initial 25 mm length after start of testing were ignored, and the subsequent adhesion force measurement values for subsequent 50 mm length peeled from the test plate were averaged to obtain the peel adhesion force.

Table 1 Test Results

Peel Adhesion Force
0.217 N/10 mm

Plastic Material Tensile Test System

Tester:	AGS-X
Load Cell:	50 N
Test Jig:	50 N pneumatic flat grips (plane teeth)
Software:	TRAPEZIUM LITE X

AGS-X Table-Top Precision Universal Tester

Features

- A high-precision load cell is adopted. (The high-precision type is class 0.5; the standard-precision type is class 1.) Accuracy is guaranteed over a wide range, from 1/500 to 1/1 of the load cell capacity. This supports highly reliable test evaluations.
- Cross head speed range
  Test can be performed over a wide range from 0.001 mm/min to 1,000 mm/min.
- High speed sampling
  High speed sampling, as fast as 1 msec.
- TRAPEZIUMX LITE X operational software
  This is simple, highly effective software.
- Jog controller (optional)
  This allows hand-held control of the crosshead position. Fine position adjustment is possible using the jog dial.
- Optional Test Devices
  A variety of tests can be accommodated by switching between an abundance of jigs in the lineup.

First Edition: February 2013

SHIMADZU

Shimadzu Corporation

www.shimadzu.com/an/

For Research Use Only. Not for use in diagnostic procedures.
The content of this publication shall not be reproduced, altered or sold for any commercial purpose without the written approval of Shimadzu.
The information contained herein is provided to you "as is" without warranty of any kind including without limitation warranties as to its accuracy or completeness. Shimadzu does not assume any responsibility or liability for any damage, whether direct or indirect, relating to the use of this publication. This publication is based upon the information available to Shimadzu on or before the date of publication, and subject to change without notice.

© Shimadzu Corporation, 2013

SHIMADZU
Excellence in Science

Application Data Sheet

No. 20

Autograph Precision Universal Tester

Material Testing & Inspection

Measurement of Friction Coefficient of Film

Standard No. ASTM D 1894 - 95 (JIS K 7312 - 1996)

Introduction

Plastic films are used for coating or wrapping of various materials. It is often necessary to measure sliding friction between two films or between a film and a different material. For example, the coefficient of friction of film for foods and that of protection film for smartphones are measured. In this Application Data Sheet, measurement examples of the static and dynamic coefficients of friction for polyethylene film in accordance with the ASTM standard are introduced.

F. Yano

Measurement and Jigs

The standard specifies the method of measuring the coefficients of starting and sliding friction of plastic films and sheets. These tests were carried out on polyethylene film using the AGS-X Table-Top Precision Universal Tester and friction coefficient measuring apparatus. Two test samples were prepared: a movable sample and a fixed sample. The measurements were carried out with the movable sample (a square test specimen of side 63.5 mm) fastened to a metal sled using double-sided tape, and the fixed sample (rectangular test specimen of width 130 mm and length 250 mm minimum) fastened to a platform using double-sided tape.

Measurement Results

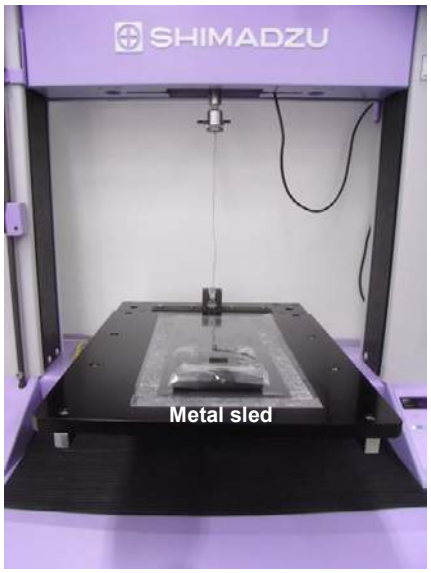

Fig. 1 Test Status

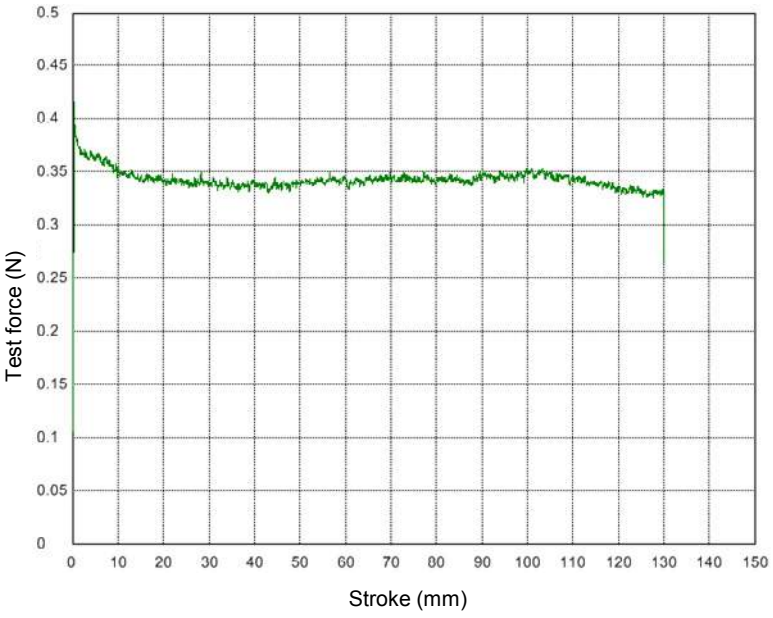

Fig.2 Test Results

Table 1 Test Conditions

Item	Set Value
Test speed	150 mm/min
Moving distance	130 mm
Load cell capacity	5 N

Table 2 Test Results

Static Coefficient of Friction	Dynamic Coefficient of Friction
0.21	0.17

Friction Coefficient Measurement System

Tester: AGS-X
Load Cell: 5 N
Test Jig: Friction coefficient measuring apparatus
Software: TRAPEZIUM LITE X

AGS-X Table-Top Precision Universal Tester

Features

- A high-precision load cell is adopted. (The high-precision type is class 0.5; the standard-precision type is class 1.) Accuracy is guaranteed over a wide range, from 1/500 to 1/1 of the load cell capacity. This supports highly reliable test evaluations.
- Cross head speed range
  Test can be performed over a wide range from 0.001 mm/min to 1,000 mm/min.
- High speed sampling
  High speed sampling, as fast as 1 msec.
- TRAPEZIUMX LITE X operational software
  This is simple, highly effective software.
- Jog controller (optional)
  This allows hand-held control of the crosshead position. Fine position adjustment is possible using the jog dial.
- Optional Test Devices
  A variety of tests can be accommodated by switching between an abundance of jigs in the lineup.

First Edition: February 2013

Shimadzu Corporation
www.shimadzu.com/an/

For Research Use Only. Not for use in diagnostic procedures.
The content of this publication shall not be reproduced, altered or sold for any commercial purpose without the written approval of Shimadzu.
The information contained herein is provided to you "as is" without warranty of any kind including without limitation warranties as to its accuracy or completeness. Shimadzu does not assume any responsibility or liability for any damage, whether direct or indirect, relating to the use of this publication. This publication is based upon the information available to Shimadzu on or before the date of publication, and subject to change without notice.
© Shimadzu Corporation, 2013

Shimadzu Flowtester

CFT-EX Series

Application Topic ＃05

Fluidity Evaluation of Unvulcanized Rubber

Rubber products are produced by forming rubber compounds (mixtures of rubber and additives that provide specific functional characteristics) in a mold and then applying heat to provide an elastic body. Therefore, the fluidity of rubber compounds can have a major effect on molding quality. Unformed rubber compounds change their characteristics after long storage periods, which can cause fluidity to deteriorate or the molding process to fail, depending on how they are stored.

Here, the example which evaluated the fluidity change by the storage method of the unvulcanized rubber is introduced.

Fluidity Change by the Storage Method of Unvulcanized Rubber

In this case, a rubber compound was stored at ambient temperature and low temperature for 14 days and 28 days immediately after kneading and then the fluidity was evaluated.

The results showed that the given sample could be stored at low temperatures without a significant change in fluidity, even after one month.
Using the CFT-EX series allows evaluating the rubber compounds storage temperatures and storage periods without actually having to mold any parts.

Test condition

Test Method	Constant temperature test
Die Diameter	0.5 mm
Die Length	1 mm
Test Temperature	280 ℃
Test Pressure	20.1 MPa
Preheating Time	0 sec
Sample Size	1.6 g

Test result

Storage Temperature	Storage Period	Viscosity (Pa.s)
Ambient Temperature	0	395.7
	14	568.1
	28	600.0
Low Temperature	0	395.7
	14	447.5
	28	419.3

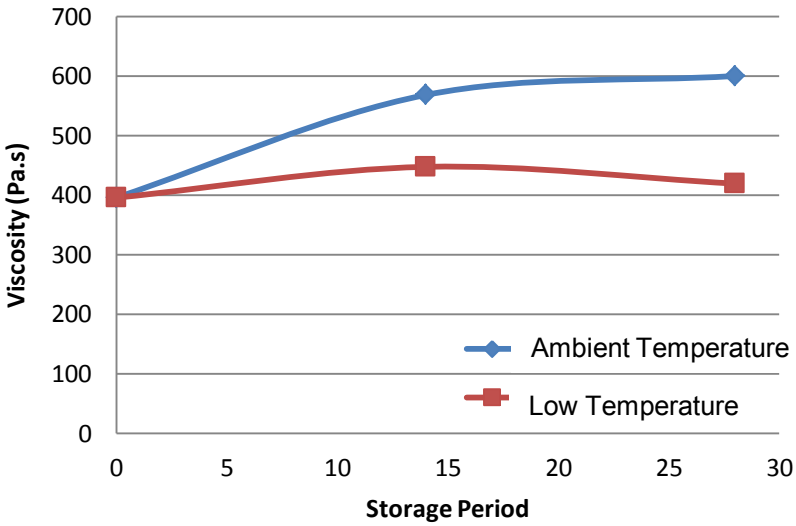

Changes in Viscosity Due to Storage Methods

CFT-EX can use evaluation of unvulcanized rubber

CFT-EX which can evaluate thermosetting and thermoplastic resin in evaluation of unvulcanized rubber is recommended.

The feature of CFT-EX

- Higher Level Evaluation Using a Variety of Analysis Methods
  ・・・The evaluation of thermosetting resin and constant heating rate test is possible.
- Smooth, Easy Test Flow
  ・・・New software compatible with Win7, 8.1
- Supported by More Than 50 Years of Technology and Know-How
  ・・・Abundant applications cultivated for years

Shimadzu Flowtester

CFT-EX Series

Thermosetting resins

Thermoplastic resins

Rubbers

The fluidity of various materials & Evaluation of the heat characteristic

Ceramics

Toners

Composites

SHIMADZU

Shimadzu Corporation

www.shimadzu.com/an/

For Research Use Only. Not for use in diagnostic procedures.
The content of this publication shall not be reproduced, altered or sold for any commercial purpose without the written approval of Shimadzu.
The information contained herein is provided to you "as is" without warranty of any kind including without limitation warranties as to its accuracy or completeness. Shimadzu does not assume any responsibility or liability for any damage, whether direct or indirect, relating to the use of this publication. This publication is based upon the information available to Shimadzu on or before the date of publication, and subject to change without notice.

Shimadzu Flowtester

CFT-EX Series

Application Topic ＃06

Evaluation of the Temperature Characteristics of General Plastics

The optimal measuring method is the constant heating rate method test that measuring the temperature where resins start softening and flowing, and their fluidity properties. Here, the example which tested with the constant heating rate method of typical general-purpose resin is shown.

The stroke-temperature graph shows that the sample starts flowing after it exceeds the flow beginning temperature and decreases in viscosity as the temperature increases (graph slope increases). The viscosity can be calculated for each temperature after initial flow.

To accurately determine the viscosity at each temperature, we recommend using the constant temperature method.

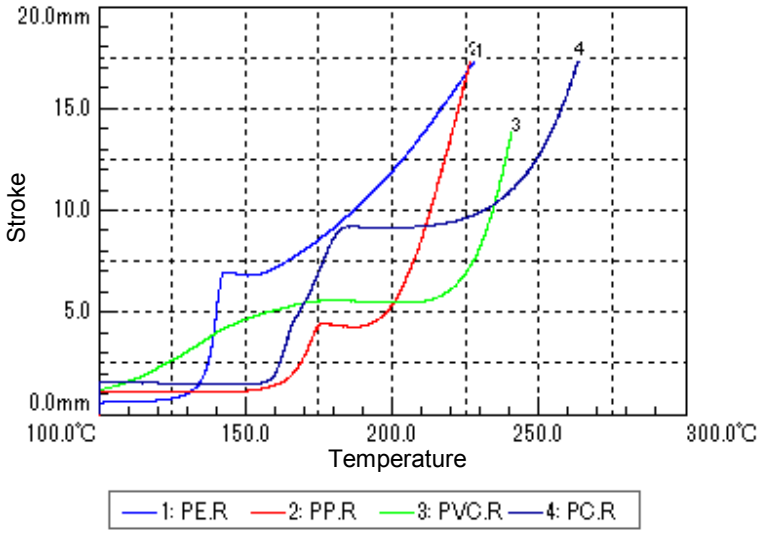

Stroke-Temperature Graph

Test condition

Test Method	Constant heating rate test
Die Diameter	1 mm
Die Length	1 mm
Beginning Temperature	100 ℃
Ending Temperature	300 ℃
Heating Rate	5 ℃/min
Test Pressure	0.98 MPa
Preheating Time	300 sec
Sample Size	1.2 g

Test result

Sample Name	Softening Temperature (°C)	Flow Beginning Temperature (°C)	1/2 Method Temperature (°C)	1/2 Method Viscosity(Pa・s)
Polyethylene	142.4	153.6	203.6	16,370
Polypropylene	175.6	187.2	215.6	5,716
Polyvinyl chloride	175.3	208.2	234.4	6,138
Polycarbonate	183.1	205.1	253.9	10,590

Cylinder Cooling Fan Improves Cycle Time for Constant Heating Rate Tests

Constant heating rate test measurements start at a low and finish at a high temperature. The cylinder cooling fan can be quickly attached to the bottom of the furnace to force-cool the cylinder, which can significantly shorten the cooling time.

A piston for force-cooling the cylinder with compressed air is also available.

CFT-EX can use evaluation of general plastic.

CFT-EX is recommended for evaluation of a general-purpose plastic because it can simply evaluated about the flow characteristic for the temperature of resin by the constant heating rate method.

The feature of CFT-EX

- Higher Level Evaluation Using a Variety of Analysis Methods
  ・・・The evaluation of thermosetting resin and constant heating rate test is possible.
- Smooth, Easy Test Flow
  ・・・New software compatible with Win7, 8.1
- Supported by More Than 50 Years of Technology and Know-How
  ・・・Abundant applications cultivated for years

Shimadzu Flowtester

CFT-EX Series

Thermosetting resins

Thermoplastic resins

Rubbers

The fluidity of various materials & Evaluation of the heat characteristic

Ceramics

Toners

Composites

SHIMADZU

Shimadzu Corporation

www.shimadzu.com/an/

For Research Use Only. Not for use in diagnostic procedures.
The content of this publication shall not be reproduced, altered or sold for any commercial purpose without the written approval of Shimadzu.
The information contained herein is provided to you "as is" without warranty of any kind including without limitation warranties as to its accuracy or completeness. Shimadzu does not assume any responsibility or liability for any damage, whether direct or indirect, relating to the use of this publication. This publication is based upon the information available to Shimadzu on or before the date of publication, and subject to change without notice.

Shimadzu Flowtester

CFT-EX Series

Application Topic ＃07

CFT-EX Useful to Evaluation of LED Package

LEDs are used in various fields for their beneficial features such as long lifetime, low energy consumption, and small size. We often see LEDs in our everyday life since they are used in illuminations, traffic signals, lighting, backlights for LCD televisions, cellular phones, and car lights. To manufacture LEDs, electrode or other parts are attached on elements, wires are connected, and then the parts are sealed with resin for protection. This process is called packaging. In addition to more efficient elements, optimized packaging technology helps to draw light from LED elements efficiently and enhance light directionality.

Round LED Package

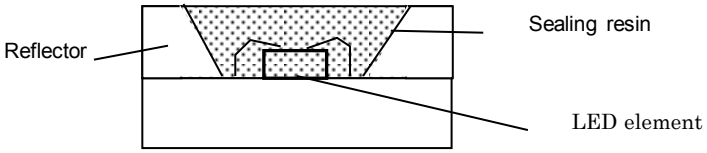

Mounted LED Package

Resins used in LED packages have a lens-like function to focus light or a reflector-like function and also disperse phosphors for white LEDs. For the lens, thermoplastic resins such as transparent acrylic resin and polycarbonate resins are used. For resin material to mold LED elements, thermosetting resins such as epoxy resin and silicon resin are used. The optimum resin selection, higher functions, and more consistent quality are demanded for easier molding and higher adhesiveness with elements and other parts.

Recently, there has been a growing awareness about white LEDs which are expected to be applied to a wide range of products, from backlights for televisions to general lighting fixtures. (The global market of sealing materials for LEDs is estimated to grow to 22.7 billion yen in year 2013 which is approximately three times larger than the market size in 2008.) Mainstream white LEDs are currently created by combining blue diode and phosphor. White LEDs have a problem of shorter lifetime due to deterioration of packaging resins caused by heat along with higher luminance and deterioration caused by UV ray generated by luminance of phosphor. In order to solve these problems, there is a growing demand for higher heat resistance and UV-proof functions on packaging resins.

Shimadzu flowtester is an optimum system to evaluate these resins for packaging LEDs because fluidity properties and hardening properties (by heating test) can be measured easily and accurately.

For LED lighting

The replacement from a filament lamp to white LED lighting is progressing because of the energy-saving, and the new product has come out one after another. One of the big features of LED lighting is a longer operating life (20,000 hours: filament lamp is 1,500 hours), and the major factor which influences the life is "heat." For this reason, the heat-resistant design and the heat dissipation design are important.

Therefore, the filler of a carbon system or a ceramic system is used for resin, or the material which made insulation and heat dissipation compatible by unification with a printed circuit board is developed, and the manufacturing cost reduction which includes a moldability as a metaled substitute article is proposed.

The moldability (fluidity) is an important item for evaluation of plastic new materials. CFT-EX is the optimal equipment at this evaluation.

CFT-EX can use evaluation of LED

CFT-EX which can evaluate thermosetting and thermoplastic resin in evaluation of the LED package for which various resin is used is recommended.

The feature of CFT-EX

- Higher Level Evaluation Using a Variety of Analysis Methods
  ・・・The evaluation of thermosetting resin and constant heating rate test is possible.
- Smooth, Easy Test Flow
  ・・・New software compatible with Win7, 8.1
- Supported by More Than 50 Years of Technology and Know-How
  ・・・Abundant applications cultivated for years

Shimadzu Flowtester

CFT-EX Series

Thermosetting resins

Thermoplastic resins

Rubbers

The fluidity of various materials & Evaluation of the heat characteristic

Ceramics

Toners

Composites

SHIMADZU

Shimadzu Corporation

www.shimadzu.com/an/

For Research Use Only. Not for use in diagnostic procedures.
The content of this publication shall not be reproduced, altered or sold for any commercial purpose without the written approval of Shimadzu.
The information contained herein is provided to you "as is" without warranty of any kind including without limitation warranties as to its accuracy or completeness. Shimadzu does not assume any responsibility or liability for any damage, whether direct or indirect, relating to the use of this publication. This publication is based upon the information available to Shimadzu on or before the date of publication, and subject to change without notice.

Shimadzu Flowtester

CFT-EX Series

Application Topic ＃08

Why Is CFT Used to Evaluate Thermosetting Resins?

What is thermosetting resins?

Resins are generally classified into thermoplastic resins and thermosetting resins.

Similar to chocolate, thermoplastic resins soften and become deformed when heated. They can be processed when they are soft and harden when cooled. They soften if heated again and can be used repeatedly. Major examples are polyethylene terephthalate (PET) used in PET bottles and polypropylene (PP) used in kitchen goods.

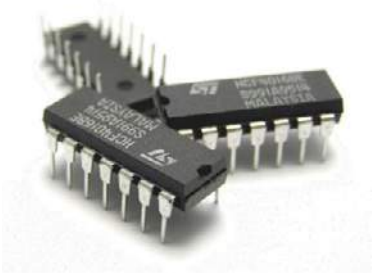

By contrast, though thermosetting resins also soften and become fluidized at the early stage of heating, they gradually harden due to chemical reaction and do not soften again, no matter how long they are heated. (They are often compared to biscuits.) Major examples are phenol resin (PF) used in engine parts; epoxy resin (EP) used in packaging of electronic parts such as ICs, semiconductors; and unsaturated polyester resin (UP) used in bathtubs .

Why Is CFT Suitable to Evaluate Thermosetting Resins?

Although thermosetting resins get fluidized at the early stage of heating, they gradually harden when heated more. The relationship between the temperature and viscosity is an important parameter for molding.

In CFT-EX, viscosity is calculated by measuring the piston's travel distance (travel rate) in the constant test force extrusion method. In this method, even if a thermosetting resin hardens due to heating, only the displacement of the piston stops. Therefore, measurement is very easy and data with a high rate of reproducibility can be obtained.

Applications of Thermosetting Resins

- Phenol resin (PF)
  - Automobile field: Engine-related parts, electric parts, disk pads, clutch facing, or other bonding materials
  - Electric fields: Parts such as switches and breakers, power supply transformer bobbins
  - Bonding material for grind stones
- Epoxy resin (EP)
  - Cast products: Circuit units of AC transformers and open/close equipments
  - Laminated products: Printed circuit boards, insulating boards
  - Molded products: Packaging and connectors of electronic parts such as ICs, semiconductors, and LEDs
- Urea resin (UF)
  - Molding materials: Wiring instrument parts, lighting apparatus parts, lacquerware
- Melamine resin (MF)
  - Adhesives and paints
  - Molding: Dishes, kitchen utensils, electric parts
- Unsaturated polyester resin (UP)
  - Unsaturated polyester resin (UP) is mostly used for fiber reinforced plastics (FRP).
  - Building material field: Water tanks, bathtubs, bathroom vanities, kitchen counters, septic tanks
  - Industrial equipment field: Chemical tanks, pipes, ducts, helmets
  - Transportation field: Fishing vessels, boats, yachts, car bodies, aero parts
  - Other than FRP: Cast molding (cultured marble, resin concrete, floor materials), paints, decorative boards
- Diallyl phthalate resin (PDAP or DAP)
  - Often used in the electric and electronic fields.: Sealing of connectors, switches, relay parts, coils/elements
- Other: Binder for decorative boards or grind stones

CFT-EX can use evaluation of epoxy resin (thermosetting resin).

Thermosetting resin can also be evaluated very easily with CFT-EX which has adopted the constant test force extrusion type.

The feature of CFT-EX

- Higher Level Evaluation Using a Variety of Analysis Methods
  ・・・The evaluation of thermosetting resin and constant heating rate test is possible.
- Smooth, Easy Test Flow
  ・・・New software compatible with Win7, 8.1
- Supported by More Than 50 Years of Technology and Know-How
  ・・・Abundant applications cultivated for years

Shimadzu Flowtester

CFT-EX Series

Thermosetting resins

Thermoplastic resins

Rubbers

The fluidity of various materials & Evaluation of the heat characteristic

Ceramics

Toners

Composites

SHIMADZU

Shimadzu Corporation

www.shimadzu.com/an/

For Research Use Only. Not for use in diagnostic procedures.
The content of this publication shall not be reproduced, altered or sold for any commercial purpose without the written approval of Shimadzu.
The information contained herein is provided to you "as is" without warranty of any kind including without limitation warranties as to its accuracy or completeness. Shimadzu does not assume any responsibility or liability for any damage, whether direct or indirect, relating to the use of this publication. This publication is based upon the information available to Shimadzu on or before the date of publication, and subject to change without notice.

Shimadzu Flowtester

CFT-EX Series

Application Topic ＃09

Fluidity Evaluation of Epoxy Resin

Epoxy resin or epoxy resin with filler are used for Printed Circuit Board. To make the throughput high and keep the quality constant you need more fast extrusion and fast hardening conditions and materials. To obtain such conditions or materials the viscosity, hardening time and hardening temperature of material are very important.

Epoxy resins are also used for the package of LSI. The main focus of LSI manufacturer is also how to make the throughput high. It means how to make the extrusion speed higher and how to make the hardening time shorter. Many researchers try to find more excellent combination of compounds. And to find such conditions CFT is the most suitable equipment.

With using CFT you can obtain the viscosity vs. time properties and the time up to hardening. Because these results are changed with the compounds, temperature and pressure, it is also very important to check the properties of compound to control the product line.

The right graph shows the Viscosity vs. Time curve of Epoxy resin under constant temperature test. Samples are same for both data but the temperature under extrusion test is deferent. Extrusion pressure is 0.98Mpa.

You can see the difference on Viscosity and the time of lowest viscosity. CFT-EX is the most suitable equipment in order to find such conditions.

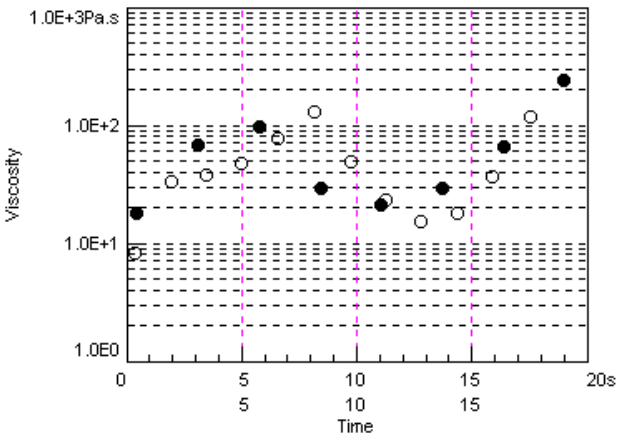

Filename	Viscosity1	Viscosity2	Viscosity3
SMTC1.c1	4.624E+1	4.316E+1	2.298E+1
SMTC2.c1	8.514E+1	2.357E+1	4.184E+1

The Example Measured by Three Kinds of Epoxy Resins

The right graph shows the differences of 3 kinds of Epoxy. Temperature condition of these results was at 150 degree C. And the below table shows the calculated viscosity number at 10, 20, 30, 40 and 50 sec from the beginning of extrusion. You can see the big difference between samples.

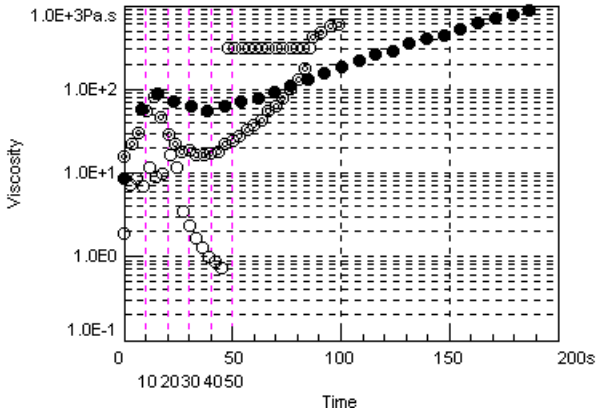

Filename	Viscosity1	Viscosity2	Viscosity3	Viscosity4	Viscosity5
SMTC11.c1	7.498E+0	1.241E+1	2.417E+0	9.470E-1	3.016E+2
SMTC12.c1	6.284E+1	7.762E+1	6.313E+1	5.534E+1	6.499E+1
SMTC13.c1	4.727E+1	3.133E+1	1.789E+1	1.684E+1	2.337E+1

CFT-EX can use evaluation of epoxy resin (thermosetting resin).

Thermosetting resin can also be evaluated very easily with CFT-EX which has adopted the constant test force extrusion type.

The feature of CFT-EX

- Higher Level Evaluation Using a Variety of Analysis Methods
  ・・・The evaluation of thermosetting resin and constant heating rate test is possible.
- Smooth, Easy Test Flow
  ・・・New software compatible with Win7, 8.1
- Supported by More Than 50 Years of Technology and Know-How
  ・・・Abundant applications cultivated for years

Shimadzu Flowtester

CFT-EX Series

Thermosetting resins

Thermoplastic resins

Rubbers

The fluidity of various materials & Evaluation of the heat characteristic

Ceramics

Toners

Composites

SHIMADZU

Shimadzu Corporation

www.shimadzu.com/an/

For Research Use Only. Not for use in diagnostic procedures.
The content of this publication shall not be reproduced, altered or sold for any commercial purpose without the written approval of Shimadzu.
The information contained herein is provided to you "as is" without warranty of any kind including without limitation warranties as to its accuracy or completeness. Shimadzu does not assume any responsibility or liability for any damage, whether direct or indirect, relating to the use of this publication. This publication is based upon the information available to Shimadzu on or before the date of publication, and subject to change without notice.

Shimadzu Flowtester

CFT-EX Series

Application Topic ＃10

Fluidity Evaluation of IC Sealant

Epoxy resin or epoxy resin with filler are used for Printed Circuit Board. To make the throughput high and keep the quality constant you need more fast extrusion and fast hardening conditions and materials. To obtain such conditions or materials the viscosity, hardening time and hardening temperature of material are very important.

Epoxy resins are also used for the package of LSI. The main focus of LSI manufacturer is also how to make the throughput high. It means how to make the extrusion speed higher and how to make the hardening time shorter. Many researchers try to find more excellent combination of compounds. And to find such conditions CFT is the most suitable equipment.

With using CFT you can obtain the viscosity vs. time properties and the time up to hardening. Because these results are changed with the compounds, temperature and pressure, it is also very important to check the properties of compound to control the product line.

The right graph shows the stroke-time curve of IC sealant (epoxy resin + filler) measured by the constant temperature test. The sample is comparing by an unsettled and an dried resin.

The result that the sample 1 is an unsettled resin, its hardening time is long, and viscosity is low. On the other hand, the sample 2 which dries the sample 1, its hardening time is short, and viscosity is high.

Thus, the check of the viscosity difference of two kinds of samples, i.e., the ease of fabrication and a storage state(moisture absorption etc.) can be evaluated easily.

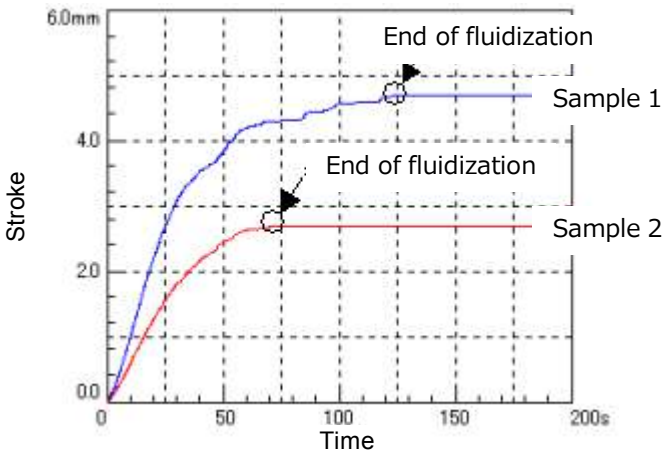

Evaluation by Constant Heating Rate Method

In addition to the constant temperature method which maintaining test temperature at constant temperature, the constant heating rate methods which measure the dependence of the viscosity to temperature as heating sample temperature at a fixed rate can be used.

Especially, the constant heating rate method is a original method of flowtester and its feature is that rheology character of a wide temperature span to reach a flow region through a rubber domain from the solid region of a sample can be measured at one time. And there is not in other capillary rheometers.

A right graph is a viscosity-time graph at the time of testing IC sealant by the constant heating rate method as minimum viscosity (viscosity change) evaluation.
It has the minimum viscosity near 117 degree C as the graph shown.

Thus, the change of physical properties to temperature or temperature can be evaluated easily, namely, the moldability at molding temperature can be evaluated.

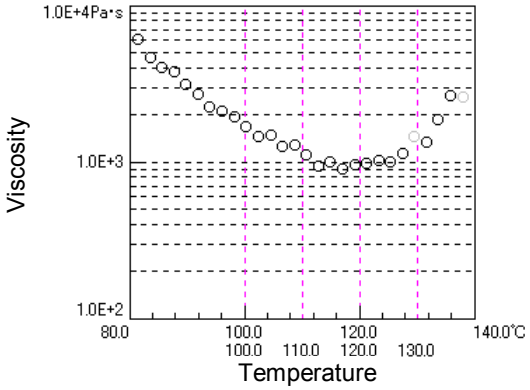

CFT-EX can use evaluation of IC sealant (thermosetting resin)

Thermosetting resin can also be evaluated very easily with CFT-EX which has adopted the constant test force extrusion type.
Furthermore, since the constant heating rate method is also possible in addition to the constant temperature method, efficient evaluation is possible.

The feature of CFT-EX

- Higher Level Evaluation Using a Variety of Analysis Methods
  ・・・The evaluation of thermosetting resin and constant heating rate test is possible.
- Smooth, Easy Test Flow
  ・・・New software compatible with Win7, 8.1
- Supported by More Than 50 Years of Technology and Know-How
  ・・・Abundant applications cultivated for years

Shimadzu Flowtester

CFT-EX Series

Thermosetting resins

Thermoplastic resins

Rubbers

The fluidity of various materials & Evaluation of the heat characteristic

Ceramics

Toners

Composites

SHIMADZU

Shimadzu Corporation
www.shimadzu.com/an/

For Research Use Only. Not for use in diagnostic procedures.
The content of this publication shall not be reproduced, altered or sold for any commercial purpose without the written approval of Shimadzu.
The information contained herein is provided to you "as is" without warranty of any kind including without limitation warranties as to its accuracy or completeness. Shimadzu does not assume any responsibility or liability for any damage, whether direct or indirect, relating to the use of this publication. This publication is based upon the information available to Shimadzu on or before the date of publication, and subject to change without notice.

SHIMADZU
Excellence in Science

Application News

Material Testing Systems MMT

Endurance Testing and Dynamic Viscoelasticity Measurement of EVA Film by MMT-100N

No. SCA_300_010

■ Introduction

EVA (ethylene vinyl acetate) film, highly elastic, yet stress crack resistant, is widely used as a film for bonding of solar cells. Solar cells reach high temperatures in the daytime when exposed to sunlight, but cool down at night. This requires that the EVA film has sufficient durability to withstand the daily range of thermal expansion and thermal contraction.

EVA film is also gradually deteriorated with prolonged usage due to the constant exposure to ultraviolet rays during the daytime. Here, we introduce examples of tensile fatigue (endurance) testing and dynamic visco-elasticity measurement of EVA film before and after ultraviolet irradiation.

■ Endurance Testing of EVA Film

Two types of EVA film samples were used for the endurance testing. One type consisted of original film samples ((1), (2), (3)) that had never been exposed to UV radiation, and the other consisted of samples ((4), (5), (6)) that had been exposed to UV radiation for 100 hours. The samples consisted of EVA film strips measuring 40 (L) × 20 (W) × 0.5 (T) mm. The testing machine and load jigs (grips) are shown in Fig. 1 and Fig. 3, respectively. The load stress in the endurance testing was set based on the static tensile strength (TS = 9 MPa) of the samples unexposed to UV radiation. These unirradiated samples showed an endurance of 100,000 cycles at a stress equal to 20 % (1.8 MPa) of static tensile strength. On the other hand, the samples that had been irradiated for 100 hours exhibited an endurance of 100,000 cycles at a stress equal to 10 % (0.9 MPa) of static tensile strength, but broke prior to reaching 100,000 cycles at a stress equal to 15 %(1.4 MPa) of static tensile strength. The results are summarized in Table 1.

Fig. 1 Microservo MMT-100N

UV Irradiation Conditions	Not Irradiated			Irradiated for 100 Hours		
Sample No.	(1)	(2)	(3)	(4)	(5)	(6)
Maximum load stress (MPa)	1.8	1.4	0.9	1.8	1.4	0.9
Minimum load stress (MPa)	0,9	0,7	0,45	0,9	0,7	0,45
Repetitions before break	100,000*	100,000*	100,000*	139	4,883	100,000

Table 1 Results of Endurance Testing of EVA Film

The * indicates that the sample did not break.

Using the endurance test data obtained for samples (1)-(6), an SN curve was plotted with stress amplitude on the Y-axis, and the number of cycle repetitions before breaking on the X-axis, as shown in Fig. 2. Based on the data, it can be concluded that ultraviolet irradiation of EVA film is a large factor that significantly contributes to diminished longevity with respect to loading frequency. Therefore, when evaluating the long-term reliability of solar cell products that will be used for long periods, this type of endurance testing is extremely important for assessing the parameters that include both stress due to the temperature effect (daily range of thermal expansion and contraction) and the amount of ultraviolet radiation received.

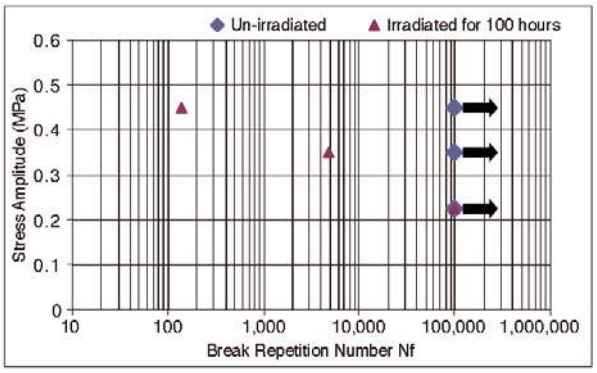

Fig.2 SN Curve for EVA Film

■ Dynamic Viscoelasticity Measurement of EVA Film

The dynamic viscoelasticity (as indicated by absolute spring constant, storage spring constant, loss spring constant, damping factor, and loss factor) of a sample can be measured using the Microservo endurance testing software. Here, focusing on the torage Young's modulus and loss Young's modulus obtained from the test force and testing machine's piston displacement measured using the number of cycles in the endurance test,we compared the changes in these constants while increasing the number of load cyclerepetitions. Fig. 3 shows the history of the storage spring constant and loss spring constant for samples (2) and (5) from the 100th load cycle onward. At the 100th cycle, the storage spring constant of the sample (5), irradiated for 100 hours, is 25 % smaller than that of the unirradiated sample (2), and as the number of cycles is increased, they both show a gradual decreasing trend. In addition, the loss spring constant at the early load stage is slightly less in sample (5) than in sample (2), and the degree of the gradual decrease in the loss spring constant is greater in sample (5). Furthermore, the storage spring constant and loss spring constant of sample (2) level off and exhibit a plateau region between 60,000 cycles and 100,000 cycles.

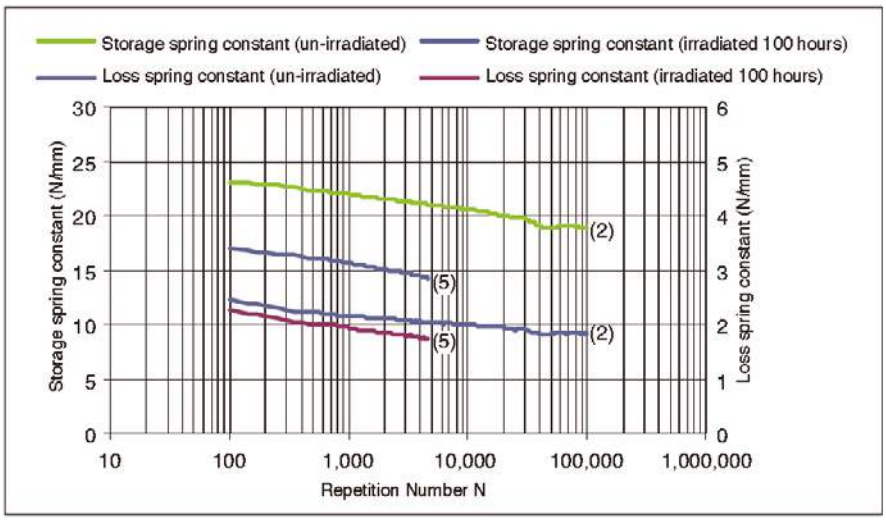

Fig. 3 Storage and Loss Spring Constants of EVA Film

Fig. 4 Grips and EVA Film

Thus, the Microservo is a material testing system that offers simultaneous endurance testing and dynamic viscoelasticity measurement of samples. Since this system adopts an electromagnetic actuator, not only is testing conducted in a green environment, but a variety of evaluations become possible using a temperature atmospheric chamber and other optional attachments.

■ Reference Information

Absolute spring constant: $|K^*| = \frac{F_0}{x_0}$

Storage spring constant: $K' = |K^*| \cdot \cos(\delta)$

Loss spring constant: $K'' = |K^*| \cdot sin(\delta)$

Damping factor: $c = \frac{K''}{2 \cdot \pi \bullet Frequency}$

Loss factor: $Lt = \frac{K''}{K'}$

The loss angle δ is calculated below using FFT based on the test force and displacement waveform relative to time.

Loss angle $\delta = 2\pi \bullet \Delta t \cdot$ Frequency

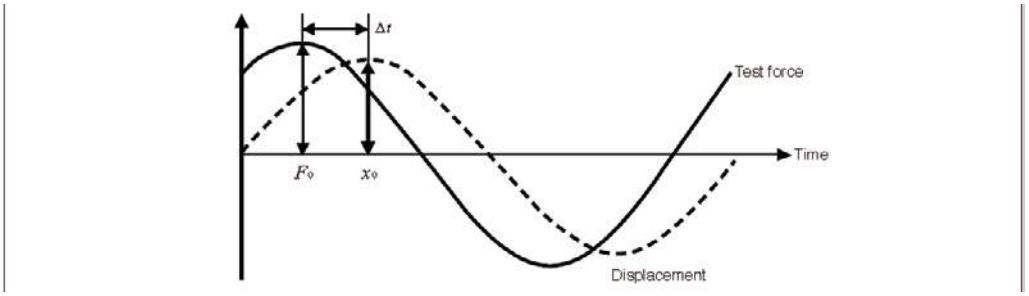

Fig. 5 Test Force and Displacement Waveform

SHIMADZU
Shimadzu Europa GmbH
www.shimadzu.eu

For Research Use Only. Not for use in diagnostic procedures.
The content of this publication shall not be reproduced, altered or sold for any commercial purpose without the written approval of Shimadzu. The information contained herein is provided to you "as is" without warranty of any kind including without limitation warranties as to its accuracy or completeness. Shimadzu does not assume any responsibility or liability for any damage, whether direct or indirect, relating to be the use of this publication. This publication is based upon the information available to Shimadzu on or before the date of publication, and subject to change without notice.

SHIMADZU
Excellence in Science

Application News

Material Testing System SMV

No. SCA_300_012

Evaluation of Mooney Viscosity by Shimadzu Mooney Viscometer, Model SMV Title Line 1 (Arial 14)

The Shimadzu Mooney Viscometer features excellent performance of the Mooney viscosity test and the Mooney scorch test on unvulcanized rubber, with high efficiency ensured by controlling system.

The following is an introduction of Mooney viscosity tests on the standard samples of the NBS (National Bureau of Standards) which demonstrate this viscometer with enhanced precision, labor saving efficiency, and operational safety.

■ Standard procedure for Mooney viscosity test: JIS K6300, ASTM D 1646

1. Test temperature is set at 100 °C.
2. Preheating time, working time, and pressure releasing time are set.
3. Test starts.

• Press the START button after inserting the rotor bearing specimens into the rotation shaft, and test starts in accordance with the preset conditions.
• The rotors are ejected automatically following release of pressure (upper heating plate lifts).

4. Mooney values.

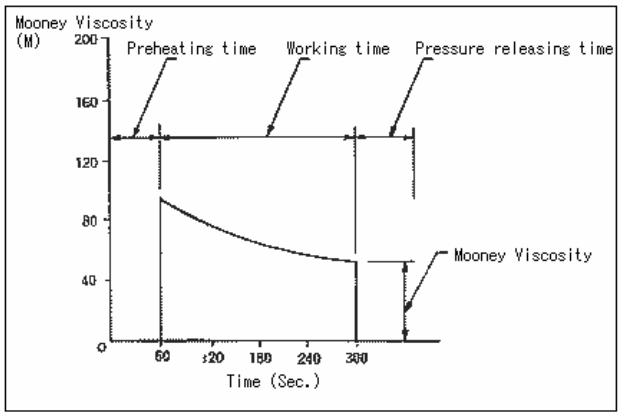

Fig.1 Results of Mooney Viscosity Test

■ Examples of Mooney viscosity measurement on NBS standard samples

1. NBS standard sample No.388L
   • Standard Mooney value ML1+8 (100 °C) 71.5 +/- 0.2
2. Values measured by Shimadzu Mooney Viscometer
   • Number of tested samples: 4
   • Measured values

(1)	71.6
(2)	71.7
(3)	71.6
(4)	71.4
Mean	71.58

The time base recording of Mooney viscosity is shown in Fig. 2

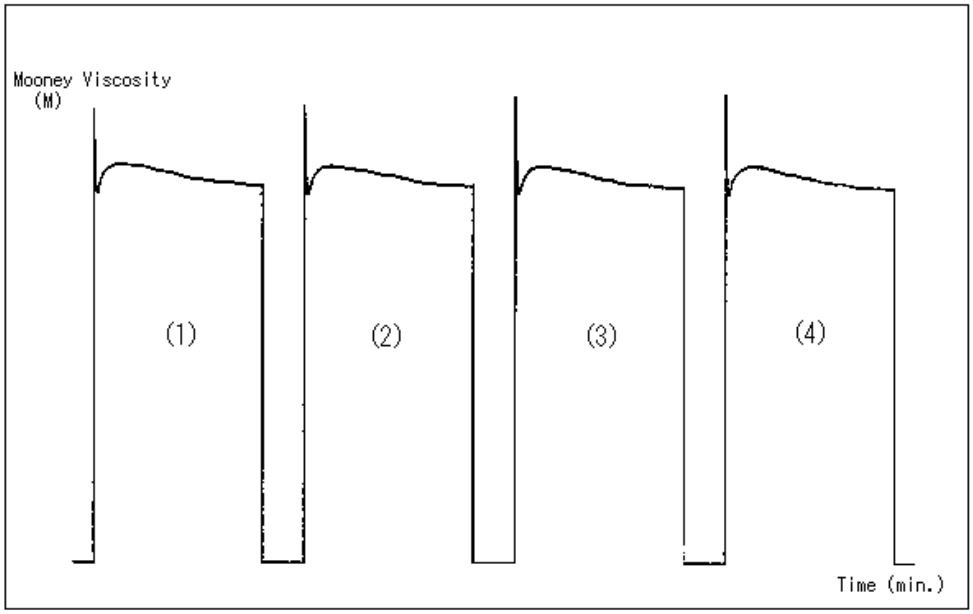

Fig. 2 Time Base Recording of Mooney Value

* Please be advised that data obtained before the implementation of the current Weights and Measures Law may be presented in terms of gravimetric unit.

For Research Use Only. Not for use in diagnostic procedures.
The content of this publication shall not be reproduced, altered or sold for any commercial purpose without the written approval of Shimadzu. The information contained herein is provided to you "as is" without warranty of any kind including without limitation warranties as to its accuracy or completeness. Shimadzu does not assume any responsibility or liability for any damage, whether direct or indirect, relating to be the use of this publication. This publication is based upon the information available to Shimadzu on or before the date of publication, and subject to change without notice.

SHIMADZU
Excellence in Science

Application News

Material Testing System DUH

No. SCA_300_014

Evaluation of Surface Hardness of Audiotapes with Shimadzu Dynamic Ultra Micro Hardness Tester Model DUH

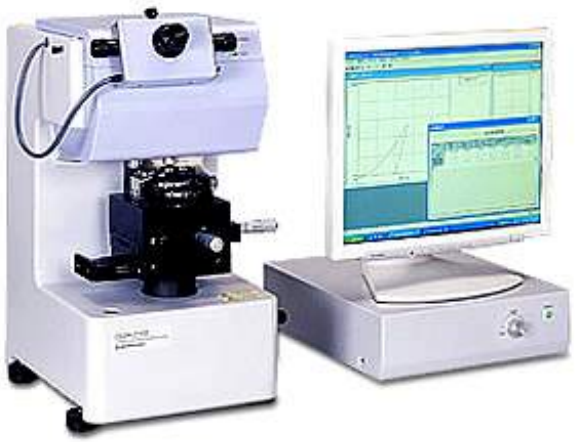

■ Introduction

Music cassette tapes are used by an enormous number of music lovers to enjoy beautiful sounds whenever and wherever they wish. High quality audiotapes with low noise levels are required to reproduce the full dynamic range of any music with a stable and balanced sound volume.

Ultra micro magnetic particles are scattered on the surface of the high polymer substrates of audiotapes. Audiotapes are classified into several types depending on the kinds of magnetic materials, each of which have respective frequency characteristics.

The following presents the result of surface hardness evaluation performed on audiotapes from several manufacturers using the Shimadzu Dynamic Ultra Micro Hardness Tester Model DUH. This unit works on the principle of a micro area measuring technique for providing information about the surface hardness of tape materials.

Measurement of hardness of audiotapes

(1) Samples:

Brand A TYPE1 (NORMAL)
Brand B TYPE1 (NORMAL)
Brand C TYPE2 (CrO_2)
Brand D TYPE2 (CrO_2)
Brand E TYPE4 (METAL)
Brand F TYPE4 (METAL)

(2) Testing machine

1) Shimadzu Dynamic Ultra Micro Hardness Tester Model DUH
2) Thin film attachment (type 2)

Test Mode	2
Cal. Mode	1 (115° triangular pyramid indenter)
Auto or Manual	Auto
F.S. Depth	2μm
Max. Load	0,5gf
Loading Speed	5 or 10
After Time	5sec
Pre Time	5sec
LOT	3

Table 1 Test Conditions

Fig.1 shows dynamic hardness determined by the difference of displacement at two different loads.

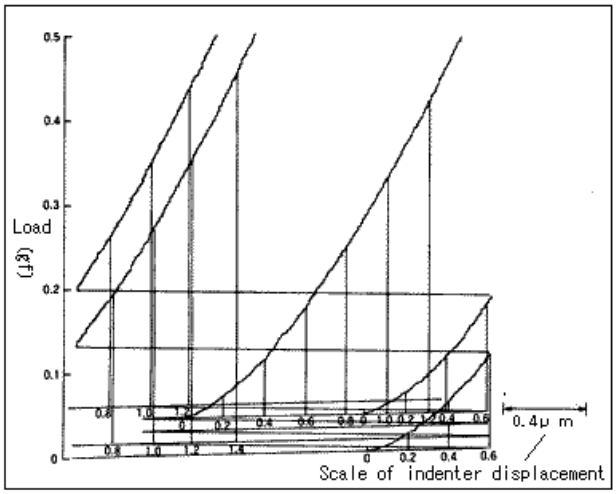

Fig. 1 Load – Indentation Depth Curves for Audiotape (Type 1)

Dynamic hardness was calculated by the following equation:

$$DH(115°) = 37{,}838 \cdot \frac{P_2}{(D_2 - D_1)^2} \cdot \left(1 - \sqrt{\frac{P_1}{P_2}}\right)^2$$

DH(115°): Dynamic Hardness
P1: Small testing load (gf)
P2: Large testing Load (gf)
D1: Indentation depth at P1 (μm)
D2: Indentation depth at P2 (μm)

Figs.2, 3 and 4 show hardness variations of respective tapes of types 1, 2, and 4 at various depths. The tape type 2 of brand C showed the highest surface hardness. The tape type 2 from brand D showed a hardness peak at 0.4 to 0.6 μm, suggesting a hard layer at that depth. The metallic tapes of type 4 from brands E and F show similar hardness properties. As seen above, useful information is attainable for evaluating micro hardness differences due to different processing or treatments of tape surfaces.

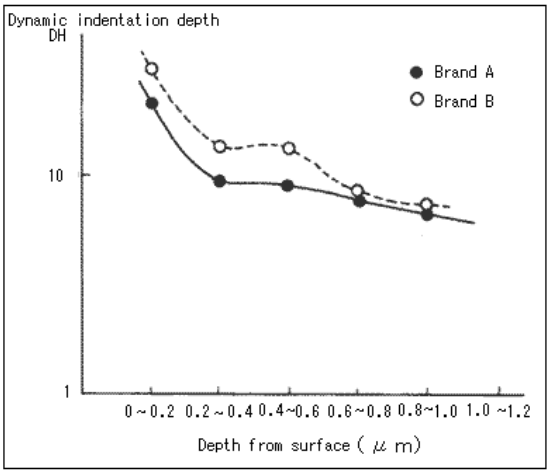

Fig. 2. Hardness from Surface towards Depth Direction on Audiotape Type 1

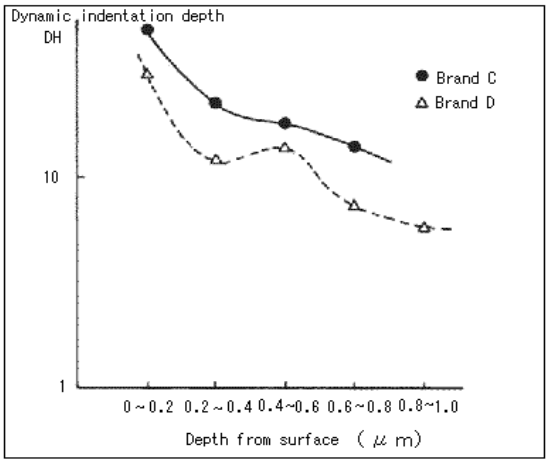

Fig. 3 Hardness from Surface towards Depth Direction on Audiotape Type 2

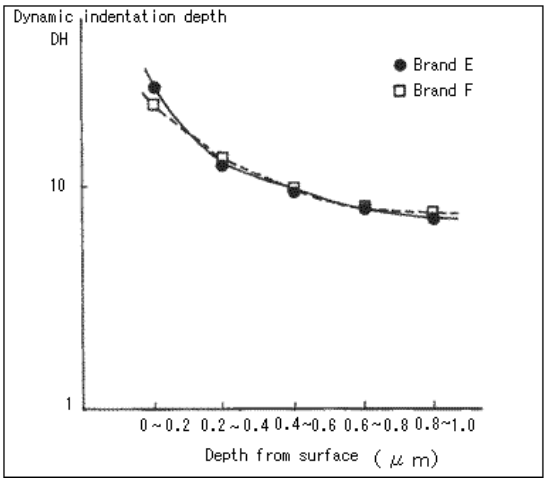

Fig. 4 Hardness from Surface towards Depth Direction on Audiotape Type 4

SHIMADZU
Shimadzu Europa GmbH
www.shimadzu.eu

For Research Use Only. Not for use in diagnostic procedures.
The content of this publication shall not be reproduced, altered or sold for any commercial purpose without the written approval of Shimadzu. The information contained herein is provided to you "as is" without warranty of any kind including without limitation warranties as to its accuracy or completeness. Shimadzu does not assume any responsibility or liability for any damage, whether direct or indirect, relating to be the use of this publication. This publication is based upon the information available to Shimadzu on or before the date of publication, and subject to change without notice.

SHIMADZU
Excellence in Science

Application News

Material Testing System CFT

No. SCA_300_017

Flowtester Flow Tests of Various Kinds of Plastics with Shimadzu Flowtester Model CFT

The Shimadzu Flowtester Model CFT is used for measurement of melting viscosity and rheological properties of raw materials such as thermo plastics, thermosetting resins, and ceramics, or for determination of temperature and pressure of pressing or injection molding.

Two testing modes are available, the constant temperature mode and constant heating rate mode. The former is a method of pressing specimens in a condition of constant temperature, and is suitable for general quality control. The latter is a method pressing specimens in a constant rate heating mode and is often used in measurements of softening and hardening temperatures for flowability evaluation.

The following presents the results of flow tests performed in the constant heating rate mode on four kinds of plastics.

■ Softening - flowability curve of polycarbonate resin in constant heating rate mode (Fig.1)

■ Test conditions:

Test temperature:	preset temperature 250 °C to max. 300 °C
Constant heating rate:	6 °C / min
Pressing condition:	Pressure: 10 kgf/cm^2 Die: 1 mm D x 10mm (diam. x length)

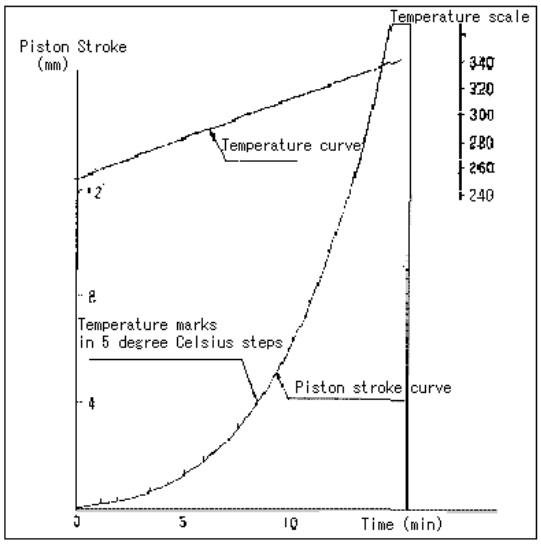

Fig. 1
Softening – Flowability Curve of Polycarbonate Resin in Constant Heating Rate Mode

■ Softening - flowability curve of polyurethane resin in constant heating rate mode (Fig. 2)

Test temperature:	Preset temperature 100 °C to max. 200 °C
Constant heating rate:	5 °C/min
Pressing conditions:	Pressure: 10 kgf/cm^2 Die: D1 x 1 mm（diam. x length)

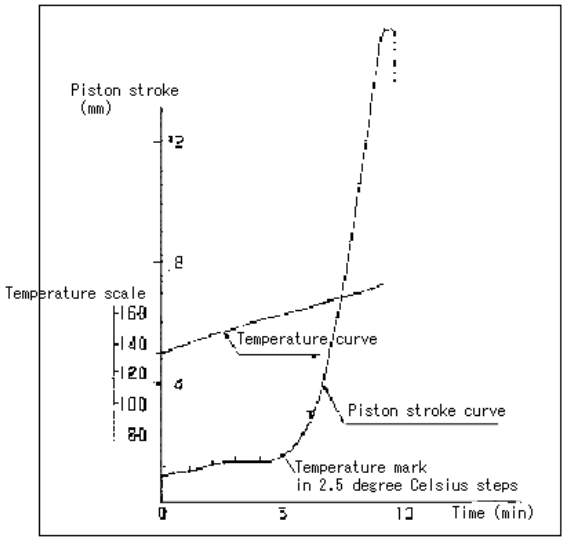

Fig. 2
Softening- Flowability of Polyurethane Resin in Constant Heating Rate Mode

■ Softening - flowability curve of polyester resin in constant heating rate mode (Fig. 3)

Test temperature:	preset temperature 220 °C to max. 350 °C
Constant heating rate:	3 °C/min
Pressing conditions:	Pressure: 50 kgf/cm^2 Die: D 0.5 x 1 mm (diam. x length)

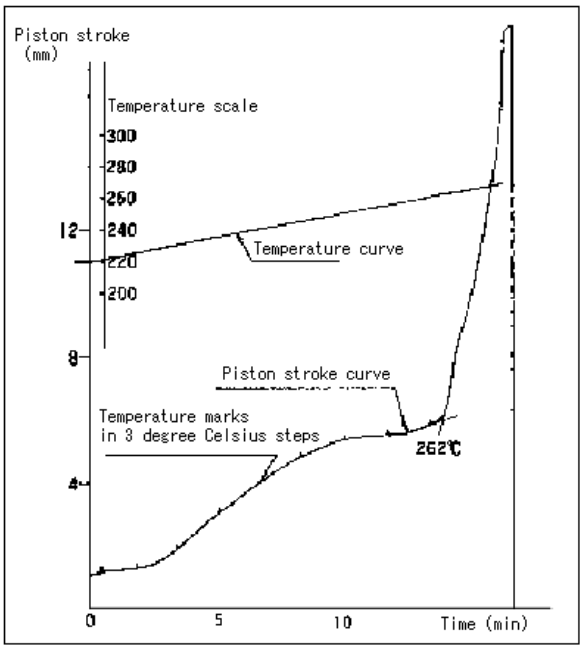

Fig. 3
Softening- Flowability of Polyester Resin in Constant Heating Rate Mode

■ Softening - flowability curve of polychlorinated resin in constant heating rate mode (Fig.4)

Test temperature:	Preset temperature 150 °C to max. 300 °C
Constant heating rate:	6 °C/min
Pressing conditions:	200 kgf/cm^2 Die: D1 x 10 mm (diam. x length)

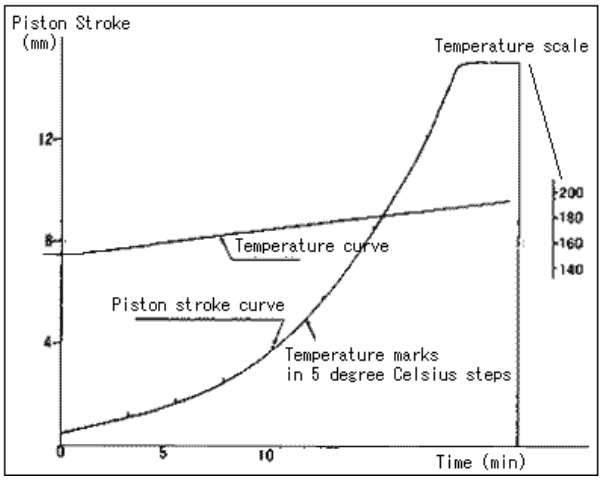

Fig. 4
Softening- Flowability of Polychlorinated Vinyl in Constant Heating Rate Mode

* Please be advised that data obtained before the implementation of the current Weights and Measures Law may be presented in terms of gravimetric unit.

■ Softening - flowability characteristic curves

As temperature is elevated at a given constant rate, the flow rate, apparent viscosity, shear rate, or shearing stress of respective resin specimens can be recorded at any test temperature.

For Research Use Only. Not for use in diagnostic procedures.
The content of this publication shall not be reproduced, altered or sold for any commercial purpose without the written approval of Shimadzu. The information contained herein is provided to you "as is" without warranty of any kind including without limitation warranties as to its accuracy or completeness. Shimadzu does not assume any responsibility or liability for any damage, whether direct or indirect, relating to be the use of this publication. This publication is based upon the information available to Shimadzu on or before the date of publication, and subject to change without notice.

SHIMADZU
Excellence in Science

Application News

Material Testing System DUH

No. SCA_300_021

Hardness Measurement of Plastic Tubes using the Shimadzu Dynamic Ultra Micro Hardness Tester DUH-W211S

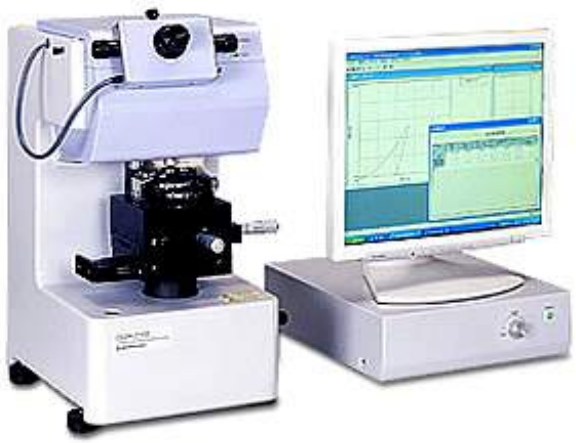

■ Introduction

Light, strong and rust-free plastic tubes (pipes) are widely used for transporting liquids and gases, and for insulating and protecting electrical wiring. In these fields, the hardness of the tube material is an important factor that affects the usage conditions. If the tube is cut lengthways and held flat before measuring its hardness, the elasticity of the plastic causes minute bending (see Fig. 1) that impedes accurate measurement. Here, we present results from a test method that is ideal for such situations.

1. Sample

(Plastic Tube)

1) Sample name: Plastic tube
2) Sample No.: No.1 to No.3
3) Sample size: ⌀2.2 (Outer diameter) x ⌀1.2 (Internal diameter) x 10 (Length) mm

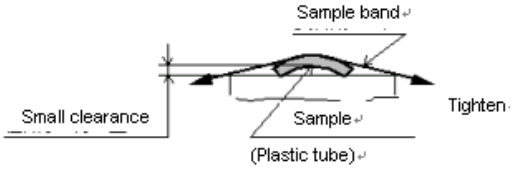

Fig.1

2. Test conditions

1) Testing machine: Shimadzu Dynamic Ultra Micro Hardness Tester DUH-W201S
2) Indenter: Triangular pyramid indenter with tip angle 115° (Berkovitch type)
3) Test mode: Load - Load hold test
4) Test force: 9.8 mN
5) Loading rate: 0.284 mN/sec
6) Sample holding time: 1 sec
7) Temperature: 25 ℃

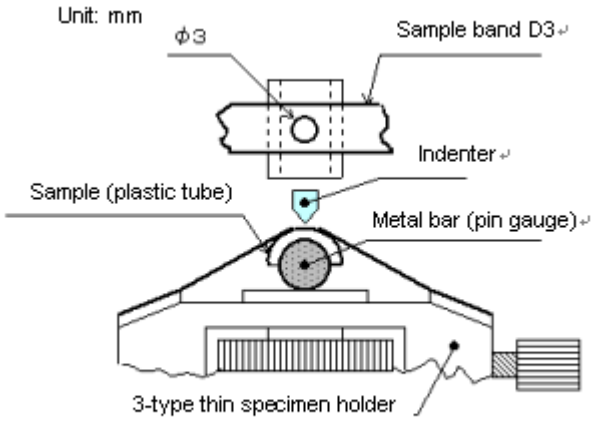

Fig.2

1. Test Method

The sample (plastic tube) was cut lengthways into two and set on a metal bar (pin gauge ⌀ 1.2) as shown in Fig.2 to measure its hardness by indentation.

2. Test Results

1) Results of the hardness measurements are shown in Table 1, Fig.3 and Fig.4.
2) The DHT_{115} values in Table 1 shows that the Sample No.1 is the hardest, followed by No.2 and No.3 in that order, when tested with the test force of 9.8 mN. Fig.4 (graph that presents the relation of test force and indentation depth) shows that the elasticity of the tube is correctly detected, validating the effectiveness of the data.

Table 1 Hardness measurement results (mean values)

Sample name	Sample No.	Dynamic hardness (DHT_{115})	Test force (mN)	Indentation depth (μm)
Tube A	No. 1	15.6	9.8	1.55
Tube B	No. 2	13.7	9.8	1.66
Tube C	No. 3	11.7	9.8	1.8

Ref.) Dynamic hardness was calculated as follows:

DHT_{11S}=3,8584 P/ D^2
DHT_{115}:Dynamic hardness (115° triangular indenter)
P: Test force (mN)
D: Indentation Depth (μm)

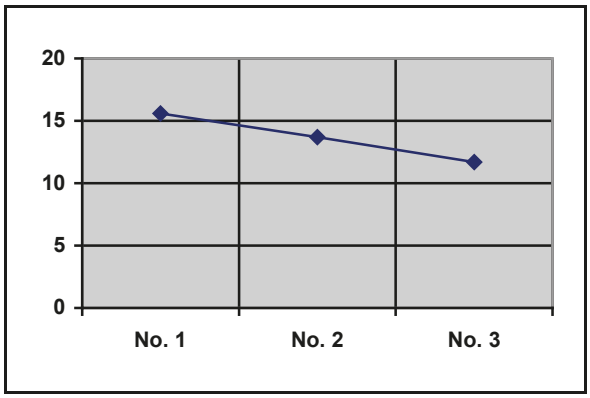

Fig. 3
Sample number and dynamic hardness (DHV)

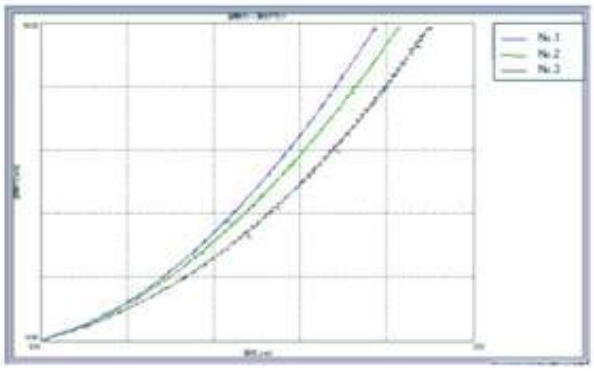

Fig. 4 Test force – indentation depth curve

* Please be advised that data obtained before the implementation of the current Weights and Measures Law may be presented in terms of gravimetric unit.

For Research Use Only. Not for use in diagnostic procedures.
The content of this publication shall not be reproduced, altered or sold for any commercial purpose without the written approval of Shimadzu. The information contained herein is provided to you "as is" without warranty of any kind including without limitation warranties as to its accuracy or completeness. Shimadzu does not assume any responsibility or liability for any damage, whether direct or indirect, relating to be the use of this publication. This publication is based upon the information available to Shimadzu on or before the date of publication, and subject to change without notice.

SHIMADZU
Excellence in Science

Application News

No. SCA_300_026

Material Testing System DUH

Measurement of Surface Hardness of Erasers with Shimadzu Dynamic Ultra Micro Hardness Tester

-Surface hardness evaluation of soft materials-

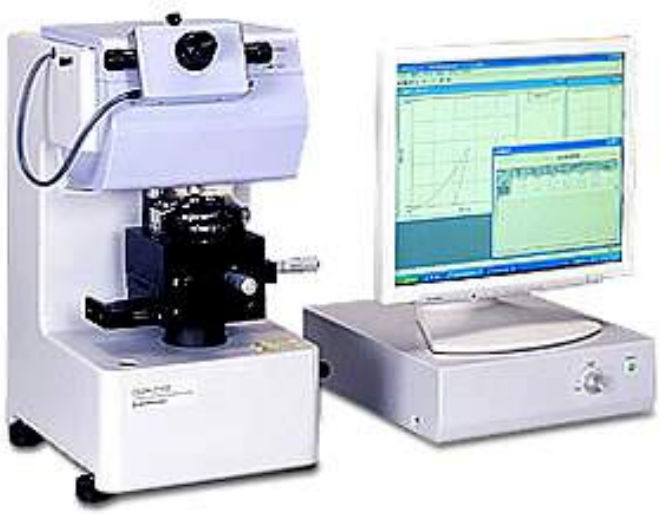

■ Introduction

JIS S6004 stipulates a fixed set of conditions for product tests on erasers, while hardness tests should be conducted according to JIS K6301 (Physical testing methods for vulcanized rubber). Since the erasing ability (erasing rate) is affected by the mechanical properties of the eraser surface which comes in contact with paper, the hardness near its surface is a particularly important factor for evaluation.

The Shimadzu Dynamic Ultra Micro Hardness Tester allows you to measure the hardness of thin films and thin layers, using the indentation depth of the indenter (dynamic indentation hardness) or the diagonal length of indentation (micro Vickers hardness). This instrument can thus measure the hardness of various specimens from hard to soft materials, and has an extremely broad range of applications. Here, we will introduce an example of a test in which this Hardness Tester was used to measure the hardness of three types of pencil erasers and two types of soft rubbers in terms of the relationship between the load and the indentation depth.

Test results

Eraser (A)							
No.	Load (gf)	Depth (μm)	Hardness	No.	Load (gf)	Depth (μm)	Hardness
1	0.114	21.85	0.0090	2	0.114	21.53	0.0093
3	0.098	19.94	0.0094				
Average	0.109	21.11	0.0092				

Eraser (B)							
No.	Load (gf)	Depth (μm)	Hardness	No.	Load (gf)	Depth (μm)	Hardness
1	0.127	15.17	0.0209	2	0.115	14.50	0.0207
3	0.114	13.44	0.0238				
Average	0.118	14.37	0.0218				

Eraser (C)							
No.	Load (gf)	Depth (μm)	Hardness	No.	Load (gf)	Depth (μm)	Hardness
1	0.179	13.28	0.0384	2	0.147	12.33	0.0366
3	0.159	13.71	0.0320				
Average	0.162	13.11	0.0357				

Soft rubber (A)							
No.	Load (gf)	Depth (μm)	Hardness	No.	Load (gf)	Depth (μm)	Hardness
1	0.029	17.71	0.0035	2	0.033	19.21	0.0034
3	0.028	17.27	0.0036				
Average	0.030	18.06	0.0035				

Soft rubber (B)							
No.	Load (gf)	Depth (μm)	Hardness	No.	Load (gf)	Depth (μm)	Hardness
1	0.312	17.82	0.0372	2	0.342	18.86	0.0364
3	0.370	19.47	0.0369				
Average	0.342	18.72	0.0369				

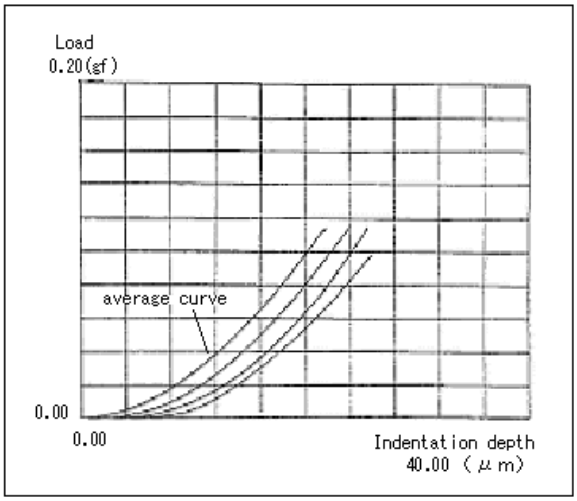

Fig. 1 Eraser (A)

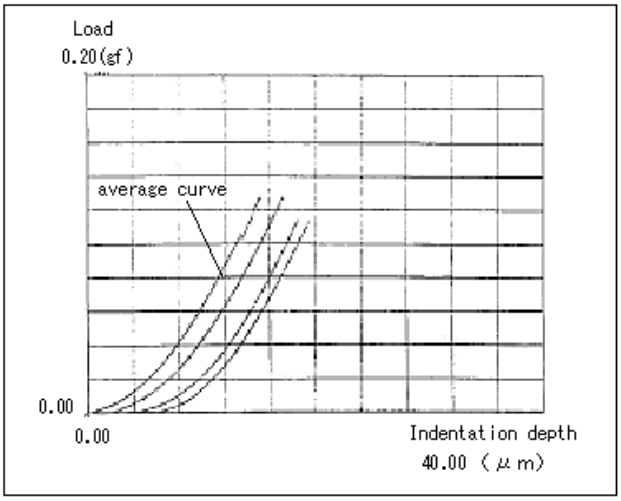

Fig. 2 Eraser (B)

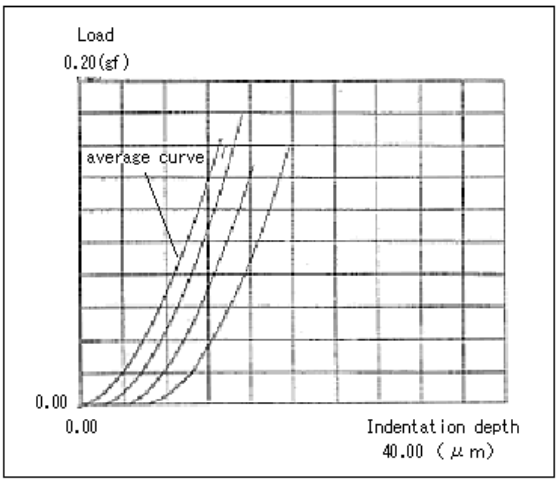

Fig. 3 Eraser (C)

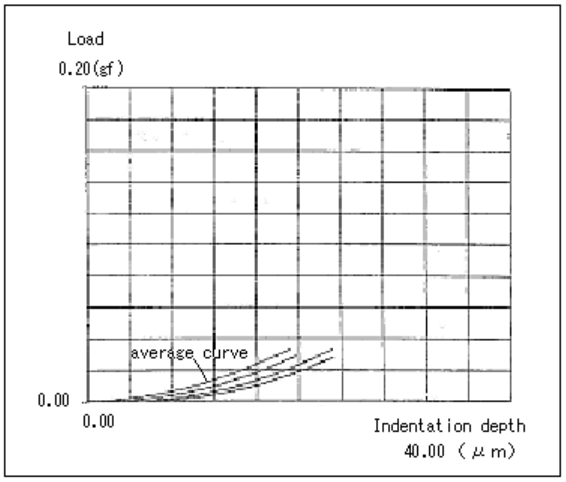

Fig. 4 Soft Rubber (A)

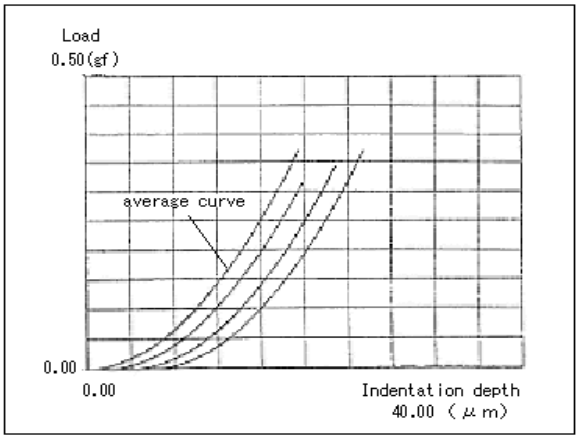

Fig. 5 Soft Rubber (B)

Figs. 1, 2 and 3 are diagrams of the test results that indicate the load-indentation depth relationships for pencil erasers (A), (B), and (C) respectively. **Figs. 4 and 5** display those for soft rubbers (A) and (B).
In each respective diagram, the data obtained from three tests and their average values are indicated as four curves. The average value is shown in the first curve in each diagram. For the hardness (DH) measurement, a triangular pyramid indenter with a tip angle of 115 degrees was used, and the calculation was performed using the following equation:

DH= 37,838 P/h2
P: Test Load (gf)
h: Indentation depth (μm)

For Research Use Only. Not for use in diagnostic procedures.
The content of this publication shall not be reproduced, altered or sold for any commercial purpose without the written approval of Shimadzu. The information contained herein is provided to you "as is" without warranty of any kind including without limitation warranties as to its accuracy or completeness. Shimadzu does not assume any responsibility or liability for any damage, whether direct or indirect, relating to be the use of this publication. This publication is based upon the information available to Shimadzu on or before the date of publication, and subject to change without notice.

SHIMADZU
Excellence in Science

Application News

Material Testing System SMV

No. SCA_300_028

Measuring and Controlling Performance of Shimadzu Mooney Viscometer Model SMV in Viscosity Tests on Rubber Materials

■ Introduction

Some of today's synthetic rubbers feature unique properties such as minimal elasticity or a thermoplastic nature that needs no vulcanization, which make them particularly appropriate for some applications. Such new features and functions of synthetic rubbers are blurring the line between rubbers and plastics. Many kinds of rubbers are appearing on the market due to the development of new rubber materials, fillers, vulcanizing agents, plasticizers etc.

The viscosity test of rubber materials is one important method for evaluating various functions for rubber. The Shimadzu Automatic Mooney Viscometer is an excellent machine for the efficient performance of Mooney viscosity and Mooney scorch tests.

■Test results of Mooney viscosity and scorch

(1) Butyl type rubber (Fig.1)

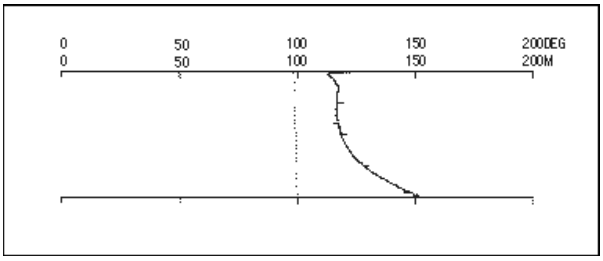

Fig. 1 Butyl Type Rubber

(2) Natural rubber (Fig. 2)

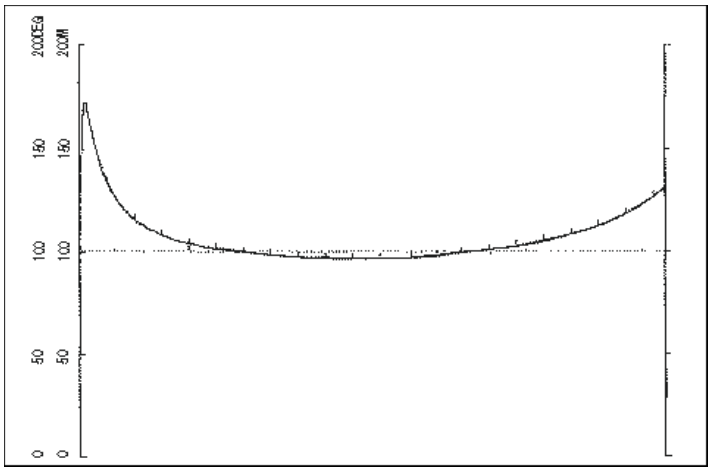

Fig. 2 Natural Rubber

(3) Nitrile rubber (Fig. 3)

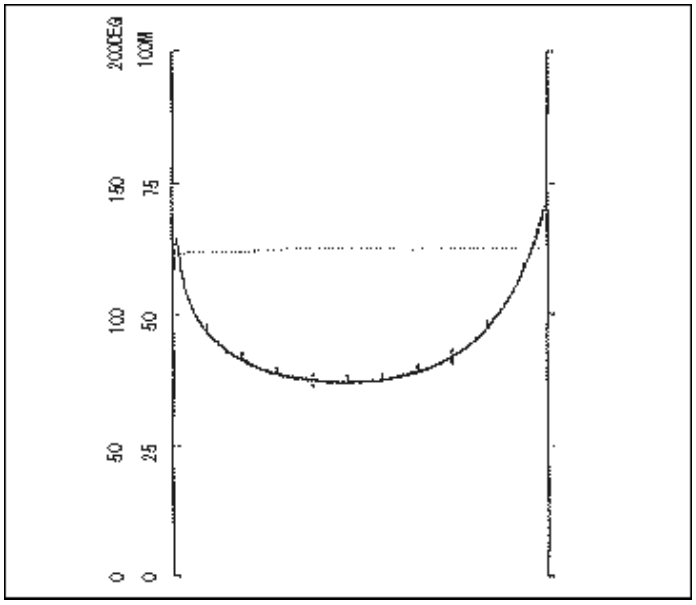

Fig. 3 Nitrile Rubber

---

* Please be advised that data obtained before the implementation of the current Weights and Measures Law may be presented in terms of gravimetric unit.

For Research Use Only. Not for use in diagnostic procedures.
The content of this publication shall not be reproduced, altered or sold for any commercial purpose without the written approval of Shimadzu. The information contained herein is provided to you "as is" without warranty of any kind including without limitation warranties as to its accuracy or completeness. Shimadzu does not assume any responsibility or liability for any damage, whether direct or indirect, relating to be the use of this publication. This publication is based upon the information available to Shimadzu on or before the date of publication, and subject to change without notice.

SHIMADZU
Excellence in Science

Application News

Material Testing System CFT

No. SCA_300_031

Test on Thermosetting Resin with Shimadzu Flow Tester Model CFT

Epoxy resin, characterized by its excellent electrical, mechanical and adhesive properties as well as its chemical proof properties, is utilized in a wide range of materials including electric insulators, paints, structural assemblies, adhesive agents, etc.
The thermosetting nature of epoxy resin materials, processed in combination with curing agent, has to be evaluated in terms of curing speed by the extruding type flow test method, and not by usual physical strength methods. The Shimadzu Flow Tester Model CFT, with the ability to test flow rates under pressures and shear rates similar to those of the usual forming process, can be used not only for testing thermoplastic resin, but also thermosetting resin, adhesive agents, copying toner, rubber materials, ceramic materials, foods, cosmetics, medicines, etc. The following presents the results of measurement in curing time of epoxy resin performed with the Shimadzu Flow tester Model CFT.

■ Outline of Shimadzu flow tester CFT

1) Method of pressure application: Constant load extruding
2) Extruding pressure: Max. 500 kgf/cm^2
3) Testing mode: Constant temperature or constant heating rate
4) Test temperature: Max. 400 °C
5) Cylinder diameter: 11.329 mm (1 cm^2 cross sectional area)

■ Testing conditions

Specimen: Epoxy resins
Couring agent: Anhydrous phtalic acid + acid absorption amine
Temperature conditions: Constant temperature mode, 150 °C.
Extruding condition: Pressure kgf/cm^2
Die irifice: Diam 1.0 x Length 1.0 mm

■ Test results

Figs.1, 2 and 3 show flow curves of three different epoxy resins with different concentrations of curing agent. Flow starting times, curing times etc. for respective specimens can be discerned immediately from these curves. Test conditions and data such as shear stress, flow rate, shear rate, viscosity, etc. are simultaneously printed automatically at the portion above the graph, presenting all necessary information on a sheet.
The three curves of Figs.1, 2 and 3 are shown in Fig. 4 in overlap mode for at-a-glance comparison with each other. Overlap mode helps present mean values and deviation of test data for a single specimen as well.

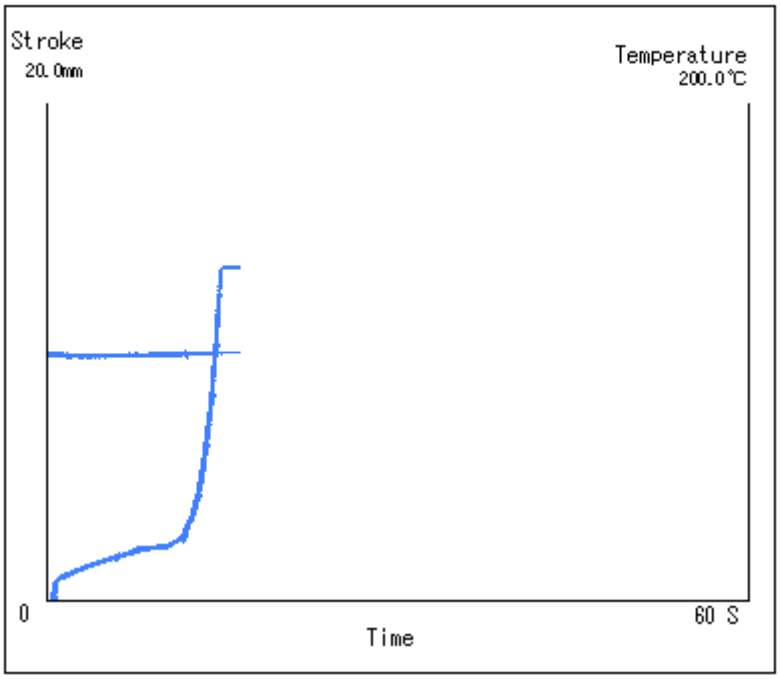

Figure 1: Flow curve of epoxy resin (A)

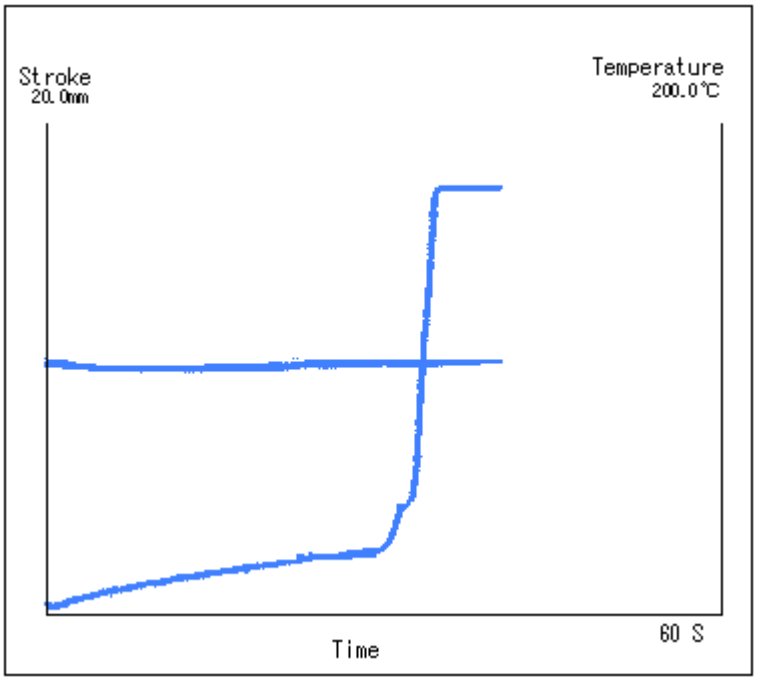

Figure 2: Flow curve of epoxy resin (B)

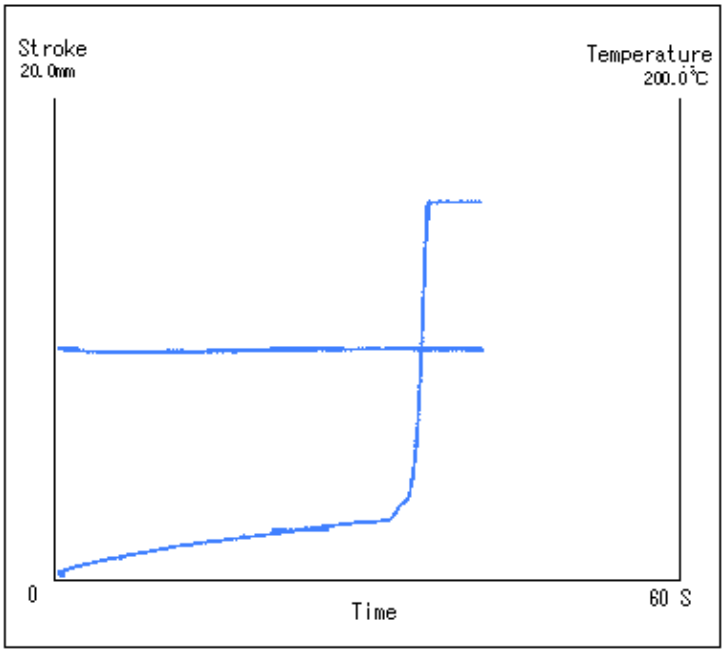

Figure 3: Flow curve of epoxy resin (C)

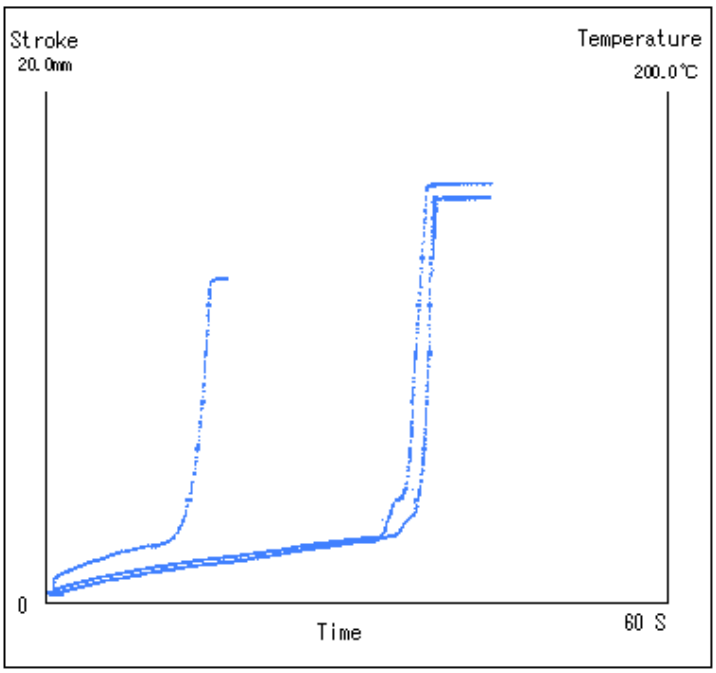

Figure 4: Overlapping flow curves of epoxy resins (A, B and C)

* Please be advised that data obtained before the implementation of the current Weights and Measures Law may be presented in terms of gravimetric unit.

For Research Use Only. Not for use in diagnostic procedures.
The content of this publication shall not be reproduced, altered or sold for any commercial purpose without the written approval of Shimadzu. The information contained herein is provided to you "as is" without warranty of any kind including without limitation warranties as to its accuracy or completeness. Shimadzu does not assume any responsibility or liability for any damage, whether direct or indirect, relating to be the use of this publication. This publication is based upon the information available to Shimadzu on or before the date of publication, and subject to change without notice.

SHIMADZU
Excellence in Science

Application News

No.i253

Material Testing System

Tensile Test of Plastic Materials

Introduction

The physical characteristics of plastic materials are an essential part of product design and quality control. Various materials tests are performed because of this, of which the most basic test is tensile testing that is cited in many product specifications. The tensile properties of plastic materials assessed by tensile testing include strength, elastic modulus, and breaking strain. Tensile testing of plastics was once performed according to the standard test methods described in ISO 527-1 (JIS K 7161), but ISO 527-1 was revised substantially in 2012 (and JIS K 7161 in 2014). This revision resulted in a number of important changes, of which the main changes are summarized below.

First, the preferred gauge length for type 1A geometry specimens was changed to 75 mm. The previous gauge length of 50 mm is still allowed, but since it became possible to set a longer gauge length, a gauge length of 75 mm is preferred since using this length makes it easier to produce a break within the gauge length. Also, a gauge length of 75 mm is recommended due to the relationship between gauge length and extensometer accuracy that is mentioned below. ISO 527-1 (JIS K 7161) noted that tests must be performed within a standard error of 1 % to calculate elastic modulus accurately. Fig. 1 shows absolute values for the extensometer accuracy required when using a 75 mm and 50 mm gauge length. It shows the absolute accuracy of a 75 mm gauge length is ±1.5 µm, while the absolute accuracy of a 50 mm gauge length is ±1.0 µm. In other words, performing the same test with a 75 mm gauge length increases the permissible range of absolute accuracy. This widens the choice of extensometers and allows the TRViewX non-contact digital video extensometer (absolute accuracy of ±1.5 µm) to be used for standard testing.

The revision also added a method for calculating strain at yield point. The previous Method A calculated strain with equation (1). The newly added Method B calculates strain with equation (2).

$$\varepsilon_t = \frac{L_t}{L} \quad (1)$$

$$\varepsilon_t = \varepsilon_y + \frac{\Delta L_t}{L} \quad (2)$$

ε_t : Nominal strain
L : Initial distance between grips [mm]
L_t : Increase in distance between grips [mm]
ε_y : Yield strain
ΔL_t : Increase in distance between grips beyond the yield point [mm]

Method B is preferred for materials that exhibit yielding and necking. Fig. 2 shows an illustrated image of a strain calculation performed using Method B. Shimadzu's TRAPEZIUM X software supports both Method A and Method B.

In this article, PP (polypropylene), PVC (polyvinyl chloride) and PC (polycarbonate) specimens are tested in accordance with current standards.

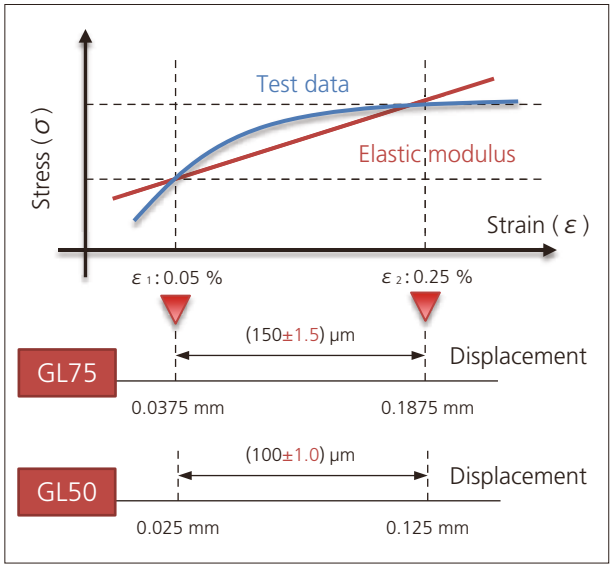

Fig. 1 Comparison of Absolute Accuracy between 75 mm and 50 mm Gauge Lengths

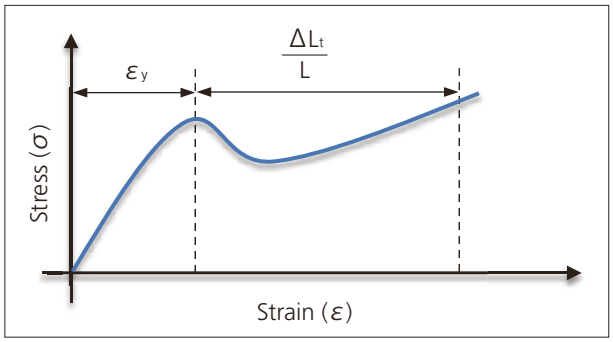

Fig. 2 Strain Calculated by Method B

Measurement System

Measurements were made using an AGS-X table-top precision universal testing instrument, a contact extensometer, and a non-contact digital video extensometer. A gauge length of 75 mm was used with both extensometers. Table 1 shows a list of the equipment used.

Table 1 Experimental Equipment

Testing Machine	: AGS-X
Load Cell	: 5 kN
Gripping Device	: Pneumatic parallel gripping device
Gripping Teeth	: Single-cut file teeth
Software	: TRAPEZIUM X (Single)
Displacement Gauge	: SG75-10, TRViewX 240S

Measured Results

An initial test speed of 1 mm/min was switched to 50 mm/min at 1 mm displacement. The contact extensometer was removed at 1 mm displacement. Fig. 3 shows testing with the SG75-10 and Fig. 4 shows testing with the TRViewX. The respective test results are shown in Table 2 and Table 3, and the stress-strain curve obtained using the SG75-10 is shown in Fig. 5. The results shown in Table 2 and Table 3 confirm that tests were performed successfully since there is almost no difference between them.

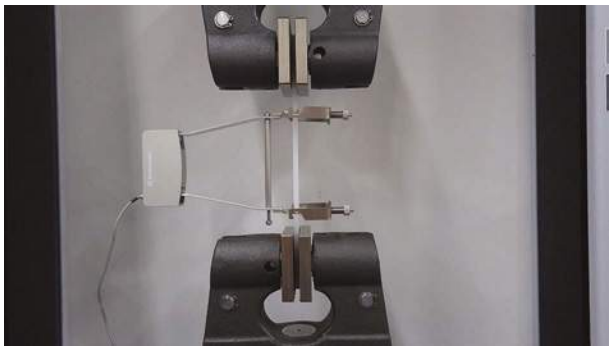

Fig. 3 Testing with SG75-10

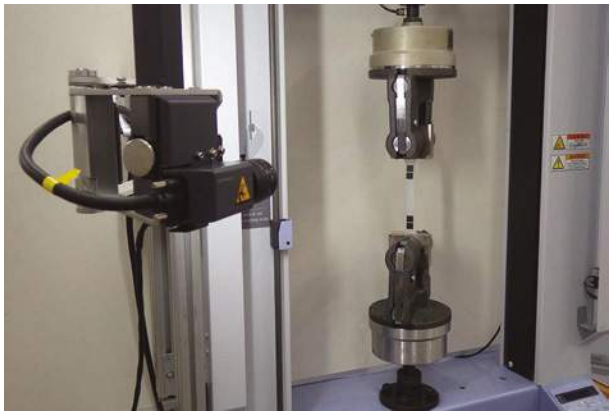

Fig. 4 Testing with TRViewX

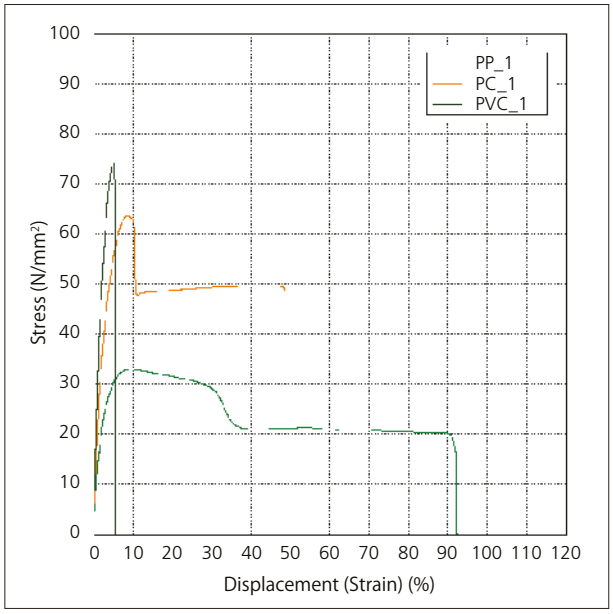

Fig. 5 Test Results Using SG75-10

Table 2 Test Results Using SG75-10

Specimen	Strength [MPa]	Elastic Modulus [GPa]
PP	32.5	1.66
PC	63.3	2.30
PVC	73.4	3.23

Table 3 Test Results Using TRViewX

Specimen	Strength [MPa]	Elastic Modulus [GPa]
PP	32.5	1.63
PC	63.7	2.26
PVC	73.4	3.12

Conclusion

The testing standard for tensile testing of plastic materials has undergone an important revision. Introduction of a 75 mm gauge length brings benefits that include an increased choice of extensometers for elastic modulus measurement and an easier break within the gauge length. Introducing Method B for calculating strain allows a more accurate determination of strain, in materials that exhibit yielding and necking in particular. Testing according to the current ISO 527-1: 2012 (JIS K 7161-1: 2014) standard can be performed successfully using the equipment described in this article.

First Edition: Aug. 2016

Shimadzu Corporation
www.shimadzu.com/an/

For Research Use Only. Not for use in diagnostic procedure.
This publication may contain references to products that are not available in your country. Please contact us to check the availability of these products in your country.

The content of this publication shall not be reproduced, altered or sold for any commercial purpose without the written approval of Shimadzu. Company names, product/service names and logos used in this publication are trademarks and trade names of Shimadzu Corporation or its affiliates, whether or not they are used with trademark symbol "TM" or "®". Third-party trademarks and trade names may be used in this publication to refer to either the entities or their products/services. Shimadzu disclaims any proprietary interest in trademarks and trade names other than its own.

The information contained herein is provided to you "as is" without warranty of any kind including without limitation warranties as to its accuracy or completeness. Shimadzu does not assume any responsibility or liability for any damage, whether direct or indirect, relating to the use of this publication. This publication is based upon the information available to Shimadzu on or before the date of publication, and subject to change without notice.

© Shimadzu Corporation, 2016

SHIMADZU
Excellence in Science

Application News

No.i249

Material Testing System

Three-Point Bending Flexural Test of Plastics (ISO 178, JIS K 7171)

Introduction

Based on their thermal properties and light weight, plastics have recently come to be used in a variety of applications and sectors, from small gears to airplane fuselages. A variety of tests must be performed to evaluate these materials, from tensile tests to flexural tests and compression tests. Of these, a flexural test is performed to examine material characteristics when flexed by an external force. Because components subject to an external force will flex in reaction to a bending moment, the flexural test is one of the most basic tests used to evaluate materials.

Previous testing standards described a three-point bending flexural test for plastics did not require the deflection-measuring system. As a result, tests detected specimen, instrument deflection and indenter depression together as a total, which is a method not suited to accurate measurements of flexural modulus of elasticity. New standards (ISO178:2010, Amd.1:2013 and JIS K 7171:2016) have been revised and include either use of a deflection-measuring system with "ISO 9513 Class 1" absolute accuracy of within 1 %, or use of compliance correction to remove testing machine deflection. A three-point bending flexural test was performed on PC, PVC, and GFRP specimens in compliance with the new standards, where the flexural modulus of elasticity of each plastic was calculated using compliance correction and the deflection-measuring instrument.

Measurement System

Measurements were performed using an AGS-X Table-Top Type Universal Testing Instrument and the deflection-measuring system with a measurement accuracy of within 3.4 µm. The requirements of the new standards when mean specimen thickness is 4 mm are shown in Fig. 1. The value relevant to flexural modulus calculation is 341 µm, where a deflection measuring instrument with absolute accuracy of 1 % of this value (3.4 µm) is required (Fig. 1 shows the flexural modulus of elasticity calculated based on the slope at two points, though the flexural modulus of elasticity could also be calculated based on the linear regression of the curve).

Table 1, 2 and 3 show details of the instruments, specimens, and test conditions used. Fig. 2 shows the test apparatus layout. The new standards describe a method A that uses a constant test speed, and a method B that increases the test speed after flexural modulus measurement. Test method A was used with GFRP that has a small maximum flexural strain, and test method B was used with PC and PVC that have a large maximum flexural strain, and the test speed changeover point was set at 0.3 % flexural strain. Furthermore, since the proportion of external force accounted for by shearing force increases when the span between supports is small[1], standards recommend the span between specimen supports is 16±1 times the mean specimen thickness.

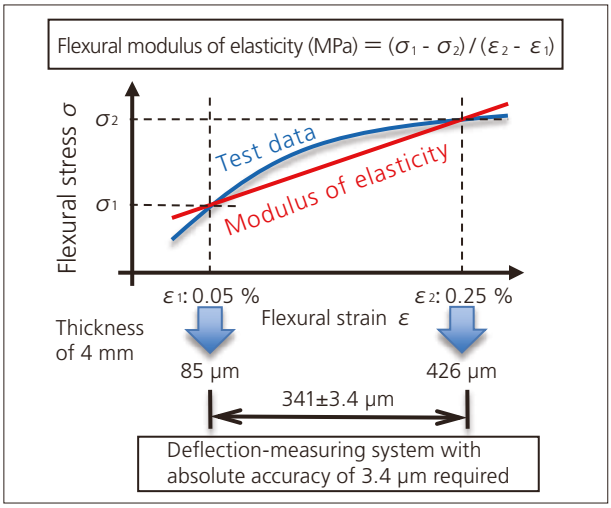

Fig. 1 New Standard Requirements

Table 1 Equipment Details

Testing Machine	: AGS-X
Load cell	: 1 kN
Deflection-measuring system	: Deflection measuring device
Bending jigs	: Loading edge R5, supports R5

Table 2 Specimen Information

Dimensions	: 80 mm × 10 mm × 4 mm
Type	: PC, PVC, GFRP (short fiber)

Table 3 Test Conditions

Test speed	: 2 mm/min
Test speed after measurement of flexural modulus of elasticity	: 100 mm/min (method B)
Span between specimen supports	: 64 mm

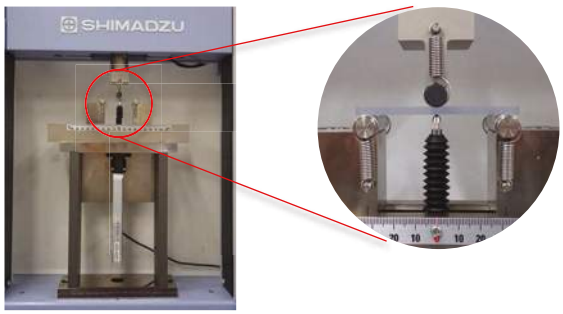

Fig. 2 Attachment of deflection-measuring system to Testing Machine

Test Results

Fig. 3 shows a flexural stress/flexural strain curves. Flexural strain on the horizontal axis was calculated based on results measured using the deflection-measuring system. The curve shows a sudden decrease in flexural stress with GFRP, but no sudden decrease in flexural stress with PC and PVC as these specimens did not break suddenly. Table 4 shows the results obtained for flexural strength and flexural modulus of elasticity for each material.
Table 5 shows the difference in flexural modulus when calculated based on the deflection-measuring system and compliance correction. The results show a difference of around 1 to 2 % for plastics like PC and PVC with a flexural modulus of elasticity of 2 to 3 GPa, and a difference of around 3 % for specimens like GFRP with a high flexural modulus of elasticity.

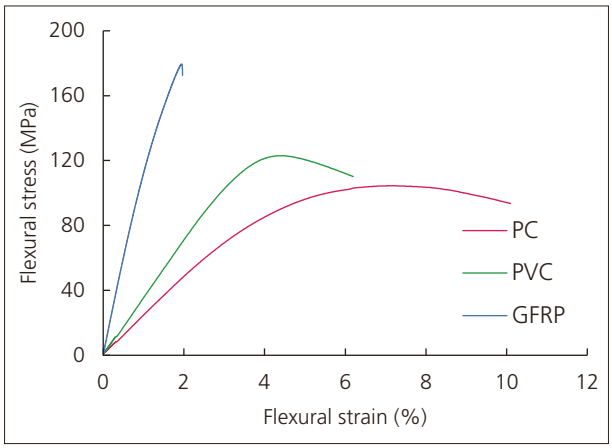

Fig. 3 Test Results

Table 4 Test Results

	Flexural strength [MPa]	Flexural modulus of elasticity [GPa]
PC	104.4	2.44
PVC	123.0	3.48
GFRP	179.4	12.1

Table 5 Difference in Flexural Modulus of Elasticity Results Using Compliance Correction and Deflection-Measuring System

	Flexural Modulus of Elasticity [GPa] Deflection-Measuring System	Flexural Modulus of Elasticity [GPa] Compliance Correction	Difference (%)
PC	2.44	2.42	1.1
PVC	3.48	3.41	2.1
GFRP	12.1	11.7	3.3

Deflection according to compliance correction and the deflection-measuring system is compared in Fig. 4, which shows deflection obtained by each method during the initial period of the test of GFRP. Results obtained from the deflection-measuring system are represented by the solid line, and results obtained by compliance correction are represented by the dotted line. The graph shows the difference between the lines.

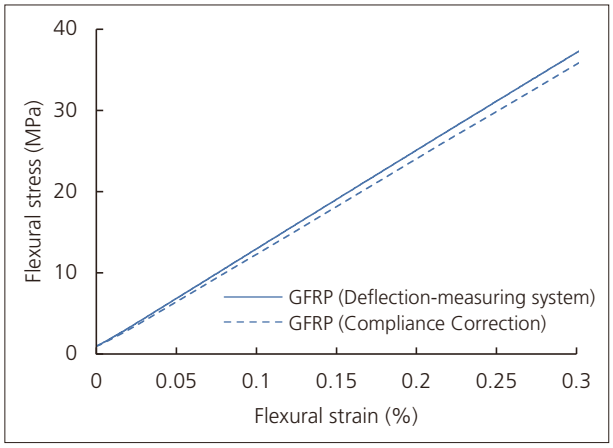

Fig. 4 Flexural Stress/Flexural Strain Curve of GFRP (Flexural strain 0 % to 0.3 %)

Conclusion

Plastics were subjected to a three-point bending flexural test with a method compliant with new standards (ISO178:2010, Amd.1:2013 and JIS K 7171:2016). Results showed the higher the flexural modulus of elasticity of a material, the larger the difference between the flexural modulus of elasticity calculated using a deflection-measuring system and compliance correction. Exact measurement of displacement with a deflection-measuring system is required for a proper evaluation of materials in compliance with the new standards.
The equipment setup employed in this article can be used to perform three-point bending flexural tests of plastics in compliance with the new standards.

Reference
1) Takeshi Murakami, Shimadzu Review Vol. 71, Issue 3/4 (2014)

First Edition: Dec. 2016

Shimadzu Corporation
www.shimadzu.com/an/

For Research Use Only. Not for use in diagnostic procedure.
This publication may contain references to products that are not available in your country. Please contact us to check the availability of these products in your country.

The content of this publication shall not be reproduced, altered or sold for any commercial purpose without the written approval of Shimadzu. Company names, product/service names and logos used in this publication are trademarks and trade names of Shimadzu Corporation or its affiliates, whether or not they are used with trademark symbol "TM" or "®". Third-party trademarks and trade names may be used in this publication to refer to either the entities or their products/services. Shimadzu disclaims any proprietary interest in trademarks and trade names other than its own.

The information contained herein is provided to you "as is" without warranty of any kind including without limitation warranties as to its accuracy or completeness. Shimadzu does not assume any responsibility or liability for any damage, whether direct or indirect, relating to the use of this publication. This publication is based upon the information available to Shimadzu on or before the date of publication, and subject to change without notice.

© Shimadzu Corporation, 2016

SHIMADZU
Excellence in Science

Application News

Material Testing System AGS-X

No. SCA_300_038

Tension - Compression Major Deformation Test of Rubber Vibration Isolator by Shimadzu Autograph Series

The Autograph Series features the ability to freely change test conditions while testing in addition to the reciprocating function (tension - compression).

Shown below is an example of a tension - compression major deformation test. This test is popular for evaluating the dynamic characteristics of rubber vibration isolators, executed by the Autograph.

Measurement was taken to record changes in energy loss (absorbed energy) on a hysteresis loop. Load and deformation were applied to an anti-vibration rubber developed for use in the architecture and civil engineering fields, load and deformation were then increased at return point per cycle...

■ Test conditions

1) Cycle test by means of load control

Test Mode	Cycle Tens/Comp. (Tens.)
Minimum Load	-50 kgf
Maximum Load	50 kgf
Test Speed	2 mm/min
Load Cell	10000 kgf
F/S Load	500 kgf

The above were load conditions at first cycle (+/- 50 kgf).+/- 100 kgf, +/- 200 kgf, +/- 300 kgf and +/-400 kgf were applied successively thereafter

Test Mode	Cycle Tens/Comp. (Tens.)
Minimum Stroke	-1 mm
Maximum Stroke	1 mm
Test Speed	2 mm/min
Load Cell	10000 kgf
F/S Load	500 kgf

The above were displacement conditions at first cycle (+/- 1 mm).
+/- 2 mm, +/- 3 mm, +/- 4 mm and +/- 5 mm were applied successively thereafter.

■ Test results

1) Cycle test by means of load control

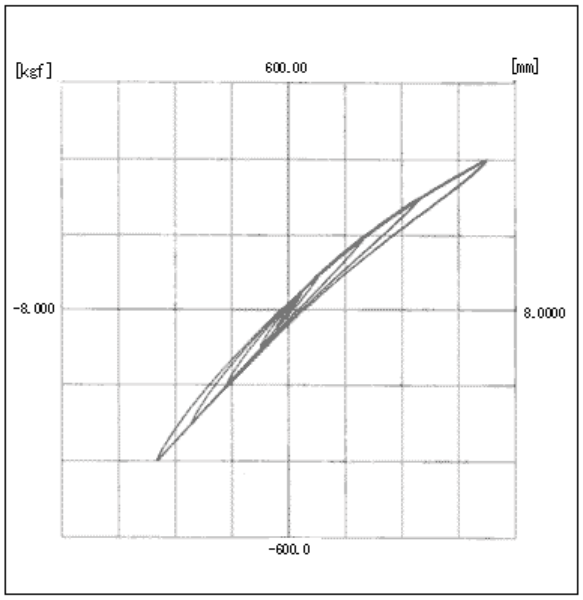

Fig. 1 Load versus Displacement Curve of Rubber Vibration Isolator (cycle test by load control)

2) Cycle test by means of displacement control

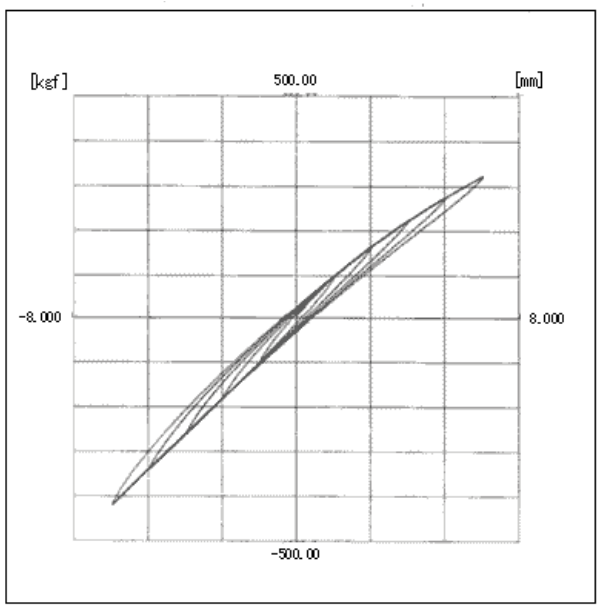

Fig. 2 Load versus Displacement Curve of Rubber Vibration Isolator (cycle test by stroke control)

* Please be advised that data obtained before the implementation of the current Weights and Measures Law may be presented in terms of gravimetric unit.

For Research Use Only. Not for use in diagnostic procedures.
The content of this publication shall not be reproduced, altered or sold for any commercial purpose without the written approval of Shimadzu. The information contained herein is provided to you "as is" without warranty of any kind including without limitation warranties as to its accuracy or completeness. Shimadzu does not assume any responsibility or liability for any damage, whether direct or indirect, relating to be the use of this publication. This publication is based upon the information available to Shimadzu on or before the date of publication, and subject to change without notice.

SHIMADZU
Excellence in Science

Application News

Material Testing System DUH

No. SCA_300_039

Evaluation of Elastic Recovery in Hardness Measurement of Plastic Materials with Shimadzu Dynamic Ultra Micro Hardness Tester

Plastics often show viscoelasticity. They can be deformed by a relatively small external force, but return to their original state if the external force is removed. In addition, many plastics have a hardness dependent on their mechanical properties. Elastic recovery and temperature are the essential factors for the evaluation of the mechanical hardness of plastics.

The Shimadzu Dynamic Ultra Micro Hardness Tester allows you to measure the hardness of thin films and thin layers using the indentation depth of the indenter (dynamic indentation hardness) or the diagonal length of indentation (micro Vickers hardness). This instrument can thus measure the hardness of various specimens from hard to soft materials, and has an extremely broad range of applications. Here, we will introduce an example of a hardness test in which this Ultra Micro Hardness Tester, installed in a room of constant temperature, was used to measure and compare the elastic recovery of two types of plastics, which have similar dynamic indentation hardness: nylon 66 and polyethylene.

Test conditions

Indenter:	Vickers
Maximum load:	50 gf
Retention time:	1 sec
Deformation scale:	10 μm

Test method

Load is applied up to 50 gf using the cyclic loading function of the Ultra Micro Hardness Tester. After the load is retained for one second, the load begins to decrease until it reaches zero. The depth of the indenter is measured at two points, when the load reaches 50 gf and when it returns to zero. The discrepancy in load between these two points is regarded as the amount of elastic recovery. The dynamic indentation hardness when the Vickers indenter is used is calculated by the following equation:

$DH = 37{,}838\ P/h^2$
P : Test load (gf)
H : Indentation depth (μm)

Table 1 Test Results

	Nylon 66	Polyethylene
Load (gf)	50,00	50,00
Indentation depth when load reaches 50gf (μm)	18,20	19,13
Indentation depth when load returns to 0 (μm)	7,65	13,06
Amount of elastic recovery (μm)	10,55	6,07
Dynamic indentation hardness	5,71	5,17

Test results

The test results are shown in Table 1, Figure 1 and 2.

As indicated by the table and figures, there is a major difference in the amount of elastic recovery between these two types of plastics despite their similar dynamic indentation hardness (that of nylon 66 is slightly greater than that of the other). It is therefore presumed that in the method to measure the diagonal length of indentation, nylon 66 will exhibit a considerably higher hardness than that of polyethylene.

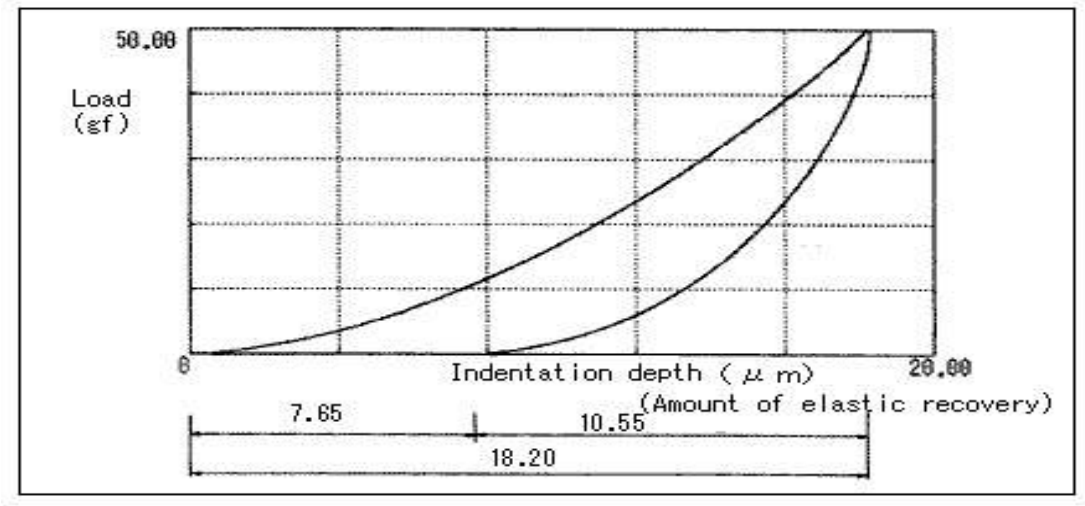

Fig. 1 Diagram of load Indentation Depth Relationship for Nylon 66

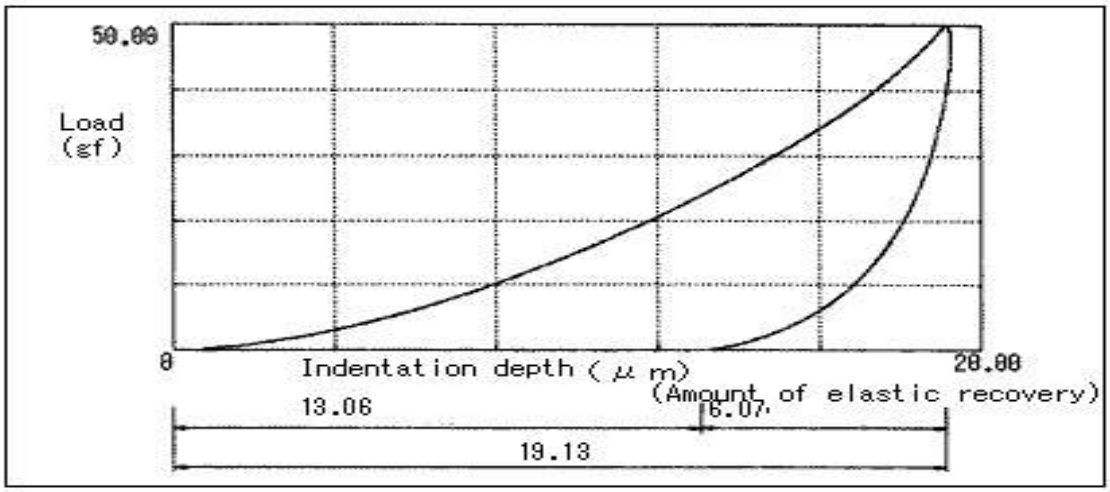

Fig. 2 Diagram of load Indentation depth for Polyethylene

* Please be advised that data obtained before the implementation of the current Weights and Measures Law may be presented in terms of gravimetric unit.

For Research Use Only. Not for use in diagnostic procedures.
The content of this publication shall not be reproduced, altered or sold for any commercial purpose without the written approval of Shimadzu. The information contained herein is provided to you "as is" without warranty of any kind including without limitation warranties as to its accuracy or completeness. Shimadzu does not assume any responsibility or liability for any damage, whether direct or indirect, relating to be the use of this publication. This publication is based upon the information available to Shimadzu on or before the date of publication, and subject to change without notice.

SHIMADZU
Excellence in Science

Application News

Material Testing System CFT

No. SCA_300_043

Fluidity Evaluation of Unvulcanized Rubber

■ Introduction

Rubber products are produced by forming rubber compounds (mixtures of rubber and additives that provide specific functional characteristics) in a mold and then applying heat to provide an elastic body. Therefore, the fluidity of rubber compounds can have a major effect on molding quality. Unformed rubber compounds change their characteristics after long storage periods, which can cause fluidity to deteriorate or the molding process to fail, depending on how they are stored. Here, the example, which evaluated the fluidity change by the storage method of the unvulcanized rubber, is introduced.

■ Fluidity Change by the Storage Method of Unvulcanized Rubber

In this case, a rubber compound was stored at ambient temperature and low temperature for 14 days and 28 days immediately after kneading and then the fluidity was evaluated. The results showed that the given sample could be stored at low temperatures without a significant change in fluidity, even after one month. Using the CFT-EX series allows evaluating the rubber compounds storage temperatures and storage periods without actually having to mold any parts.

Test Method	Constant temperature test
Die Diameter	0,5 mm
Die Length	1 mm
Test Temperature	280 ℃
Test Pressure	20,1 MPa
Preheating Time	0 sec
Sample Size	1.6 g

Test Conditions

Storage Temperature	Storage Temperature	Viscosity(Pa•s)
Ambient Temperature	0	395,7
	14	568,1
	28	600,0
Low Temperature	0	395,7
	14	447,5
	28	419,3

Test Result

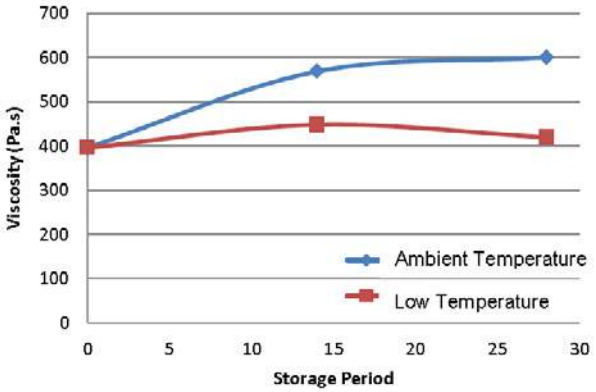

Changes in Viscosity Due to Storage Methods

■ CFT-EX can use evaluation of unvulcanized rubber

CFT-EX, which can evaluate thermosetting and thermoplastic resin in evaluation of unvulcanized rubber, is recommended.

The feature of CFT-EX

- Higher Level Evaluation Using a Variety of Analysis Methods
  The evaluation of thermosetting resin and constant heating rate test is possible.
- Smooth, Easy Test Flow
  New software compatible with Win7, 8.1
- Supported by More Than 50 Years of Technology and Know-How
  Abundant applications cultivated for years

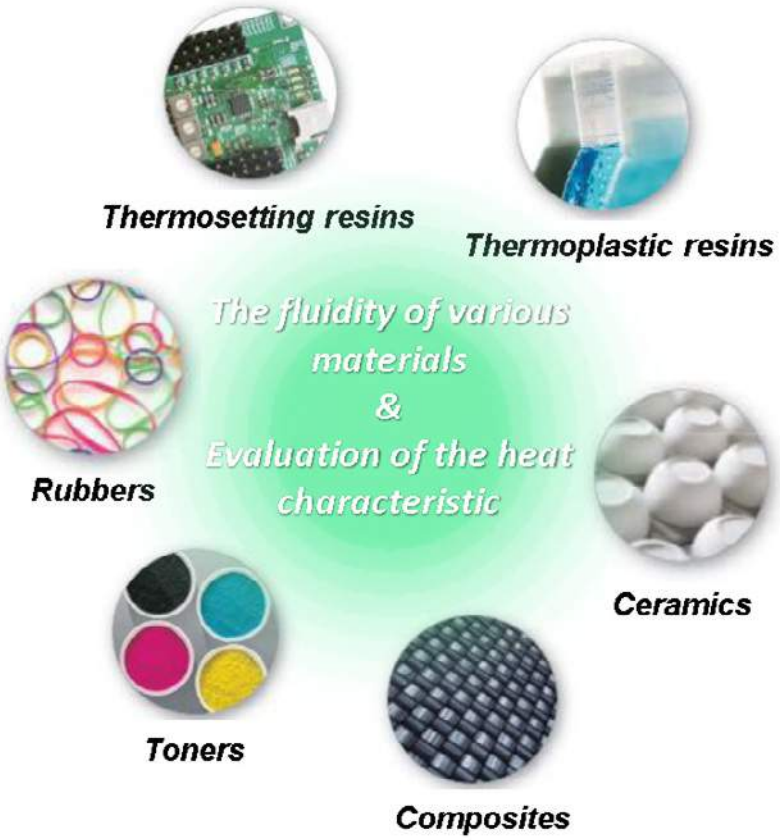

SHIMADZU

Shimadzu Europa GmbH
www.shimadzu.eu

For Research Use Only. Not for use in diagnostic procedures.
The content of this publication shall not be reproduced, altered or sold for any commercial purpose without the written approval of Shimadzu. The information contained herein is provided to you "as is" without warranty of any kind including without limitation warranties as to its accuracy or completeness. Shimadzu does not assume any responsibility or liability for any damage, whether direct or indirect, relating to be the use of this publication. This publication is based upon the information available to Shimadzu on or before the date of publication, and subject to change without notice.

SHIMADZU
Excellence in Science

Application News

Material Testing System CFT

No. SCA_300_054

Viscosity Evaluation of Thermoplastic Resins (Epoxies)

When thermosetting resins are heated, they melt and are able to flow, but further increases causes curing. The minimum viscosity value, the time it takes to reach that minimum, curing depend on the temperature used to melt the resin. Unless these viscosity and time molding process, they can result in molding defects. For resins, characteristic values due to other factors. Therefore, controlling the resin viscosity is very important to ensure vary and good products are produced.

■ Measurement of the Minimum Melt Viscosity Value

The fluidity properties of thermosetting resins are often measured using constant temperature testing. Unlike thermoplastic resins, the thermoset viscosity is constantly changing. Therefore, the minimum melt viscosity value can be determined automatically by using automatic constant temperature testing. In this case, three types of thermosetting resins were tested using the constant temperature method. The testing pressure was selected so that the sample would melt and flow and then stop flowing due to curing. Test condition Viscosity-Temperature Graph The viscosity-time graph, which shows the change in viscosity over time, indicates that the sample melts and starts to flow after about 3 seconds, reaches its minimum viscosity after about 10 seconds, and then stops flowing after about 18 seconds. The CFT calculates viscosity by measuring the amount of piston movement (movement speed) during constant test force extrusion.

Therefore, even when the sample cures due to heating, the piston displacement merely stops, which has no effect on controlling test force. Consequently, it provides extremely stable and highly reproducible test.

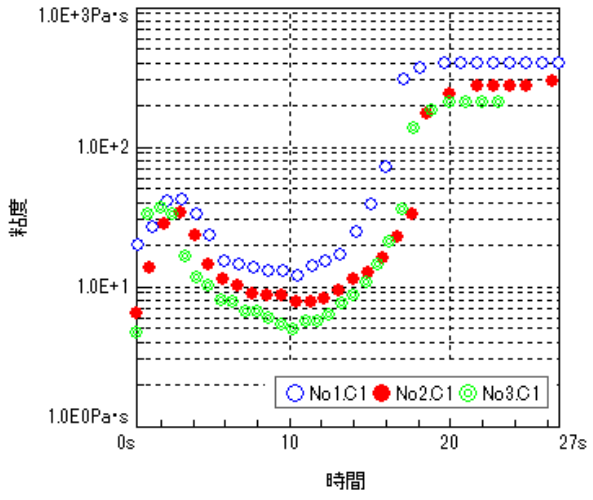

Viscosity-Temperature Graph

Test Method	Constant Temperature Test
DIE Diameter	0,5 mm
DIE Length	10 mm
Test Temperature	185 °C
Test Pressure	245 Mpa
Preheating Time	15 sec
Sample Size	2,5 g (Pellets)

Test Conditions

Sample Number	Shear Rate (S^{-1})	Viscosity (Pa•s)
1	2,471	12,4
2	4,073	7,5
3	5,810	5,3

Test Result

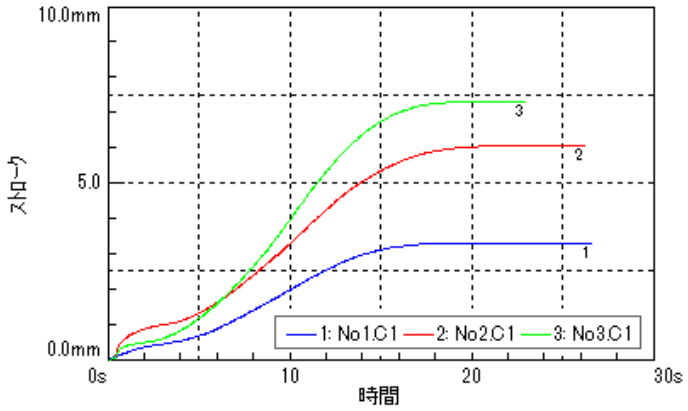

Stroke-Temperature Graph

■ A Split Nozzle Makes Cleaning Easy

Due to the relatively low minimum melt viscosity and high fluidity of thermosetting resins, long nozzles with small hole diameters are often used. Therefore, it can be difficult to remove the residual resin inside the nozzle once the resin has cured after measurements. However, using a split nozzle, which splits into two halves down its center, allows the resin to be removed easily, thereby cleaning and measuring more efficiently.

■ CFT-EX Series

SHIMADZU

Shimadzu Europa GmbH
www.shimadzu.eu

For Research Use Only. Not for use in diagnostic procedures.
The content of this publication shall not be reproduced, altered or sold for any commercial purpose without the written approval of Shimadzu. The information contained herein is provided to you "as is" without warranty of any kind including without limitation warranties as to its accuracy or completeness. Shimadzu does not assume any responsibility or liability for any damage, whether direct or indirect, relating to be the use of this publication. This publication is based upon the information available to Shimadzu on or before the date of publication, and subject to change without notice.

SHIMADZU
Excellence in Science

Application News

Material Testing System HITS

No. SCA_300_057

Breaking strain measurement of ABS resin

Increasingly high performance engineering resins are being developed for use in a wide range of fields, such as the automotive industry, consumer electronics, office automation equipment, for their various functional characteristics. Some of the criteria that have become especially important for evaluating the performance of such materials is impact resistance and its associated material properties, such as strength and rigidity. In addition to evaluating materials in terms of conventional static tensile strength, high-rate tensile strength, longitudinal elasticity, and strain measurements up to the breakpoint are expected to become important new parameters for materials development. This example describes testing the high- rate tensile strength of a flat plate specimen of ABS resin and measuring strain up to the breakpoint.
Images of the high-rate tensile test were captured with a high-speed video camera and image analysis software was used to measure the strain between gauge length on the specimen.

■ Tensile test specimen

Fig. 1 shows the dumbbell-shaped flat ABS resin tensile test specimen mounted in the grips of the high- rate tensile testing machine. A chuck extensometer, capable of measuring the relative displacement of the fixed end and the upper grip, is attached to the top right of the specimen. A matrix of black dots is printed on the surface of the specimen. The strain between gauge length can be measured by using a high-speed video camera to record a moving image of the tensile test and automatically tracking the movement of the specified dots.

(1) Specimen Material: ABS resin
(2) Specimen Dimensions: 110 (L) × 10 (W) × 3 (T) mm and 19 mm wide grip tab
(3) Dot Specifications: 0.5 mm diameter, spaced 2 mm apart

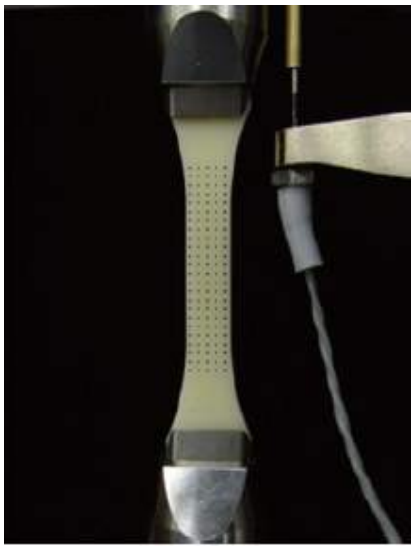

Figure 1: Tensile test specimen mounted in grips

■ Measuring High-Rate Tensile Strength and Recording Video Image

Tensile test was performed using the HITS-T10 hydroshoot hydraulic tensile machine. The HPV-2A high speed camera was mounted in front of the testing machine to capture 100 video frames of the specimen of the specimen behavior during tensile testing. Conditions for tensile testing and recording video in this example are indicated below:

(1) Tensile rate: 3 m/s
(2) Grip distance: 75 mm
(3) Gauge length measuring strain: 30 mm
(4) Test force measurement: 10 KN load cell
(5) Data collection: 250 KHz
(6) Recording speed: 32 kfps
(7) Light source metal halide light

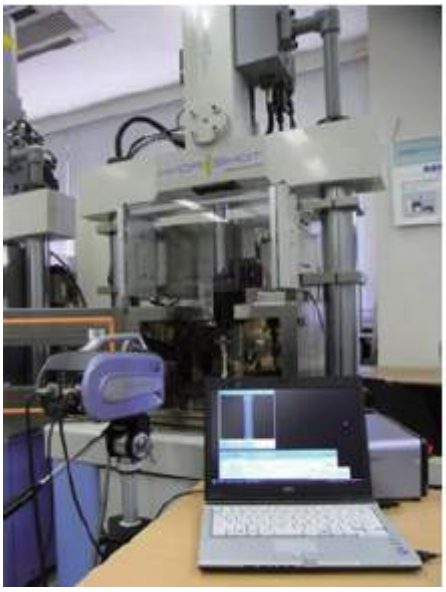

Figure 2: Setup of high rate test and video recording

■ Video high rate tensile test of ABS resin

Images of the ABS resin specimen (4 frames) before and after breakpoint during the high-rate tensile test are shown in Fig. 3. In this example, the recording speed was 32 kfps. The interval between frames was 32 microseconds.

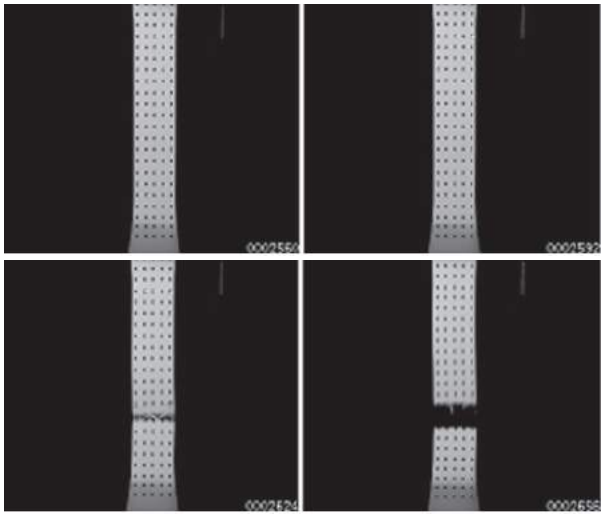

Figure 3: Four fames of specimen before and after breakpoint

■ Video high rate tensile test of ABS resin

A time history of strain between gauge length is determined by using image analysis software to analyze the images obtained. In this case, gauge length was specified longitudinally 30 mm apart on an image of the specimen not moving (16 consecutive dots apart at the center of the specimen), then that gauge length was automatically tracked as a function of time to measure the longitudinal strain. The resulting time history of strain obtained is shown in Fig. 4. In addition, a time history of stress measured by the high- rate tensile testing machine or external data logger can be displayed simultaneously as well. Furthermore, images are displayed synchronized with strain and stress in terms of time. This tensile test example resulted in a tensile strength and breaking strain of ABS resin that was 70 MPa and 30 %, respectively.

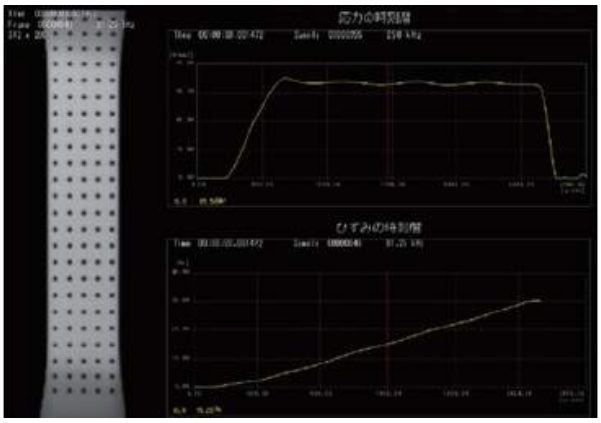

Figure 4: Video of tensile test and time history of strain and stress

■ Video high rate tensile test of ABS resin

Producing a stress-strain curve, which is easy for static tensile testing, is an extremely difficult technical challenge for high-rate tensile testing. Strain gauges can only measure a small range and contact type extensometers do not work for shock. In this example, a stress-strain curve was obtained for ABS resin by synchronizing the video image timing with the test force.

A stress-strain curve up to the specimen breakpoint is shown in Fig. 5.

In this way, combining a high-rate tensile testing machine, high-rate video camera, and image analysis software, enables simultaneously evaluating high-rate tensile properties, including breaking strain, and visualizing changes in the status of resins.

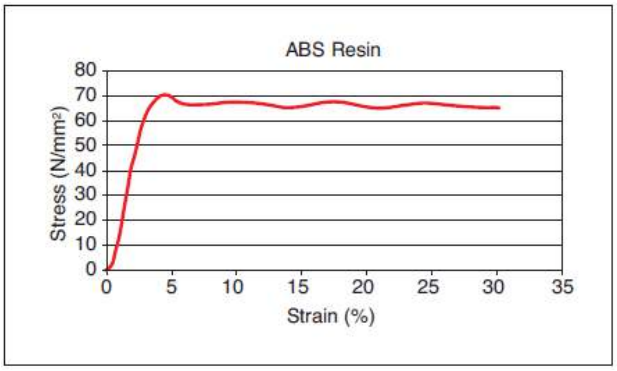

Figure 5: Stress-strain curve up to breakpoint

For Research Use Only. Not for use in diagnostic procedures.
The content of this publication shall not be reproduced, altered or sold for any commercial purpose without the written approval of Shimadzu. The information contained herein is provided to you "as is" without warranty of any kind including without limitation warranties as to its accuracy or completeness. Shimadzu does not assume any responsibility or liability for any damage, whether direct or indirect, relating to be the use of this publication. This publication is based upon the information available to Shimadzu on or before the date of publication, and subject to change without notice.

SHIMADZU
Excellence in Science

9. Others

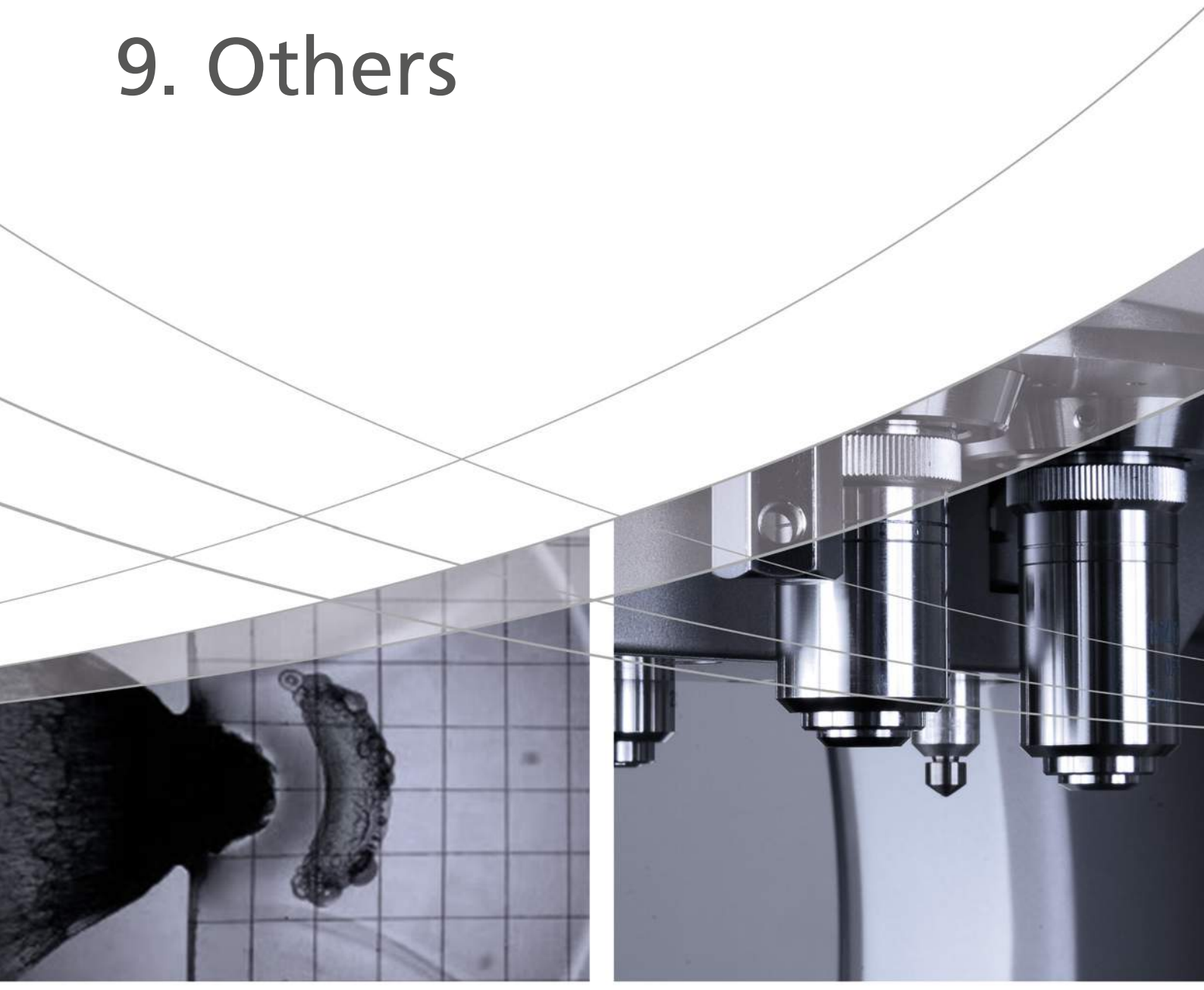

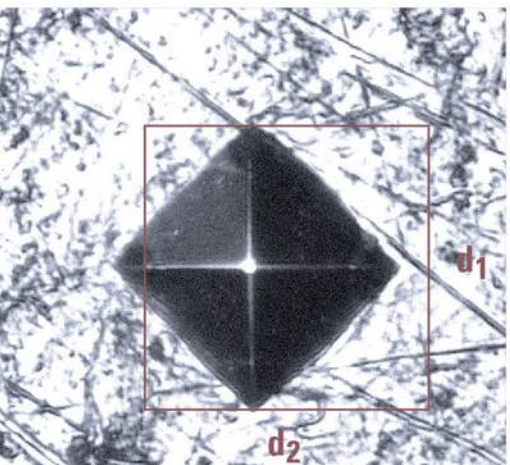

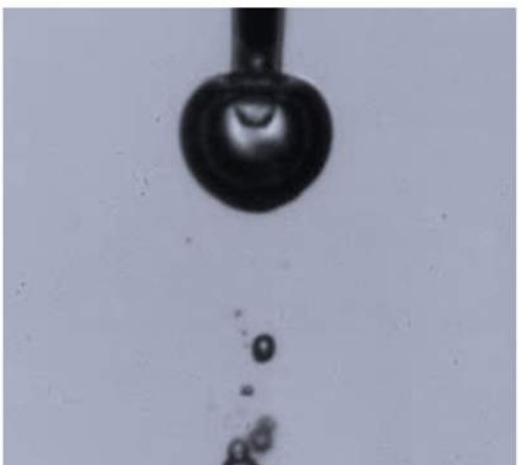

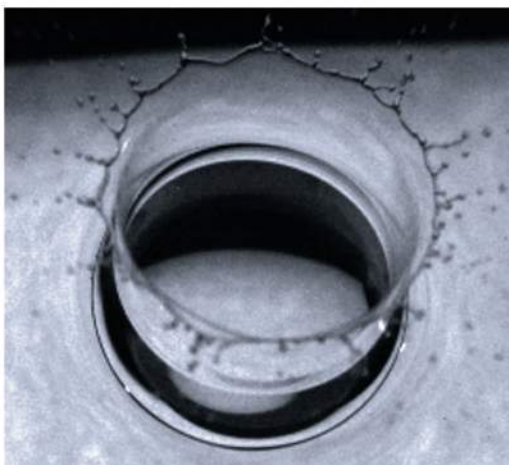

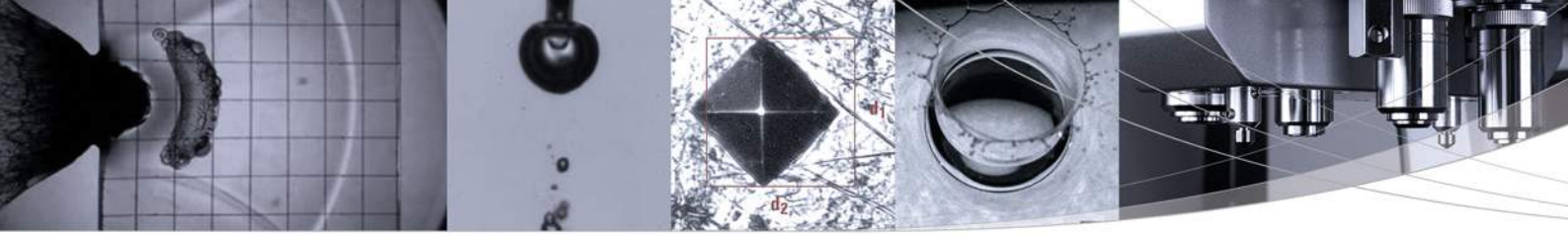

9. Others

UNIVERSAL, HARDNESS AND VISCOSITY AND FLOW TESTING

This chapter covers applications outside routine materials testing. They show that machine testing capabilities can also meet creativity of the laboratory staff.

To categorize the applications, they are allocated to the material testing machines. In total, 15 versatile and exciting applications are described on the following pages.

Micro Vickers Hardness Tester
Developed particularly for less experienced operators, the Micro Vickers Hardness testers feature automatic length measurement. The HMV-G series is capable of automatic recognition of total sample image and edges through easy-to-use software. Even complicated shapes can be recognized.

DUH Ultra Micro Hardness Tester
Shimadzu`s DUH tester is useful in a wide range of applications for evaluating the surface hardness of solid samples based on the relation between indenting load and indentation depth. The DUH series has been designed for testing of materials in the micro field that cannot be handled by regular testers. The DUH series focusses surface strength evaluations on every type of material, e.g. extra fine wire, pencil leads, pearl surface and hydrogen storage alloy as used in fuel cell batteries.

Autograph AGS-X universal material testing system
Providing high-level control and intuitive operation, the Autograph AGS-X series sets a new standard for strength evaluations. The series offers superior performance and practical testing solutions for a wide array of applications such as paper friction test, spring compression test and measurement of strength of glass.

EZ-X universal material testing system
The compact-sized EZ-X series provides accurate results due to a high-precision load cell. It supports a huge number of applications, e.g. medical, plastics, electronics, film/textile and food. In addition to the applications mentioned in this book, please see the Big Breakfast Test.

Material Testing System CFT
The CFT-EX series is ideal for research and development, production process and quality control. The system evaluates fluidity and thermal properties of various materials such as thermoplastic and thermosetting resins, toners, composites, rubbers and other flowable materials.

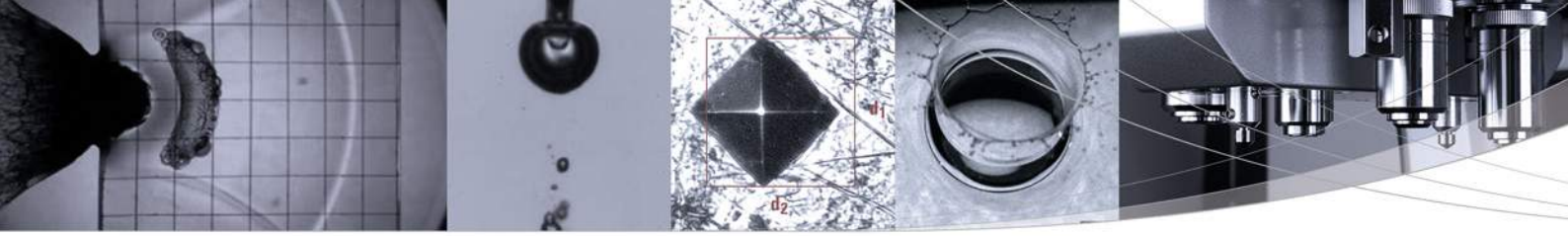

9. Others

No.i248	Mechanical strength evaluation of functional film used in smartphones
No.10	Measurment for monotonic equibiaxial flexural strength of glass ASTM C1499 01
SCA_300_007	Compression test of a liquid crystal spacer (columnar) under different temperatures
SCA_300_008	Compression tests of liquid crystal spacer using the Shimadzu dynamic ultra micro hardness tester DUH
SCA_300_009	DUH hardness test on extra fine wires
SCA_300_018	Hardness evaluation of pencil leads with Shimadzu dynamic ultra micro hardness tester-bmu
SCA_300_020	Hardness measurement of hydrogen storage alloy using the Shimadzu dynamic ultra micro hardness tester DUH
SCA_300_022	Hardness test of ion implanted specimens and valuable metals with Shimadzu dynamic ultra micro hardness tester model DUH
SCA_300_025	Measurement of pearl surface hardness using Shimadzu dynamic ultra micro hardness tester
SCA_300_029	Paper friction test friction test according to ASTM D1894
SCA_300_030	Paper tensile test tensile test according to ASTM-D 828, EN ISO 1924-2 or TAPPI T-494
SCA_300_033	Viscosity evaluation of toner for electronic photographs with Shimadzu flow tester model CFT
SCA_300_041	Evaluation of the temperature characteristics of toner
SCA_300_044	Hardness measurement of thin layer (resin layer) on Si wafer
SCA_300_060	Spring compression test
eV020	High-speed imaging of laser ablation process
eV023	Observation of microbubbles and cell behavior due to exposure to ultrasonic waves

SHIMADZU
Excellence in Science

Application News

No.i248

Material Testing System

Mechanical Strength Evaluation of Functional Film Used in Smartphones

Introduction

Plastic film is formed into thin film using techniques such as extrusion and stretch molding of the polymer film. A wide variety of products having special characteristics, such as water retentivity, light reflectivity, and selective permeability for specific substances, can be found all around us as industrial products, construction materials, as well as everyday necessities. Recently, a wide range of multi-functional films have been developed which possess a variety of special characteristics designed to provide such functionality as enhanced protection and visibility in display screens for smartphones and LCD televisions. These multi-functional plastic films can also be designed to provide enhanced security, insulation, and light shielding for automotive and architectural glass products.
This paper introduces an example of the strength evaluation of self-repair coating film used on the functional protective film that covers the LCD screens of such products as smartphones and tablets.

Test Conditions

Fig. 1 shows an overview of the test configuration, and Fig. 2 illustrates the structure of the sample. Table 1 shows the test conditions, and Table 2 presents detailed information about the sample.

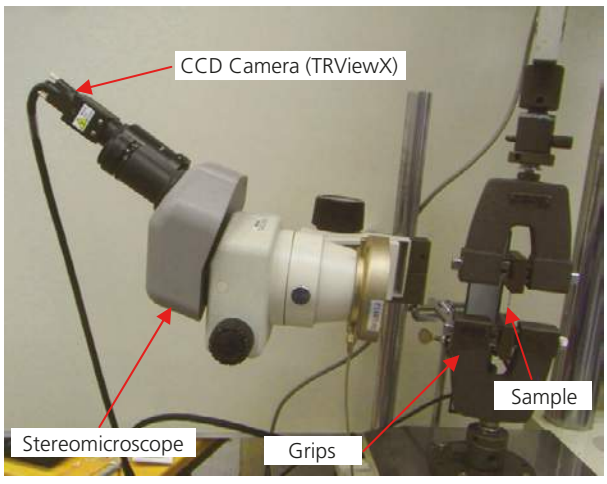

Fig. 1 Test Apparatus

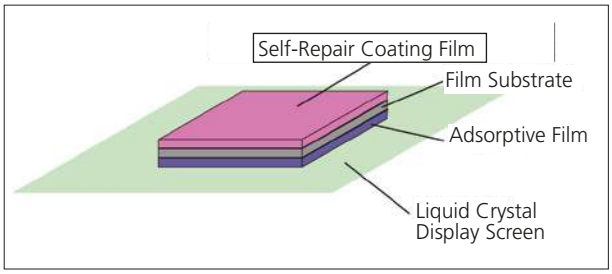

Fig. 2 Sample Structure

Table 1 Test Conditions

Instrument	Micro Autograph MST-1
Test Force Measurement	1 kN load cell
Test Speed	5 mm/min
Grips	1 kN screw type flat grips
Grip Teeth	File teeth
Video Observation	TRViewX Non-Contact Digital Video Extensometer
	Stereomicroscope
Software	TRAPEZIUM X (Single)

Table 2 Sample

Sample (dimensions)	Width 10 mm, length 40 mm (strip shape), thickness 150 µm
	PET self-repair film

To conduct this study, we used the Autograph MST-I micro strength tester with the CCD camera of a TRViewX video extensometer connected to a stereomicroscope to provide non-contact observation of state changes due to a tensile load. The samples evaluated in this study are used as protective film for liquid crystal displays in smartphones. In sequence from the top, the protective film structure includes a self-repair coating film, a film substrate, and an adhesive film for attaching the LCD screen to the protective film.
The non-contact TRViewX video extensometer can record changes in the sample state during tensile testing as an animation, making it possible to easily extract such information as the test force at the instant of deformation as well as the amount of deformation, using a built-in feature referred to as "Point Pick."
This Point Pick feature was used to quantitatively evaluate the whitening phenomenon (appearance of cloudiness in the self-repair film due to the occurrence of countless small cracks) that occurs in the self-repair film at the top of the three-layer functional film sample when a tensile load is applied.

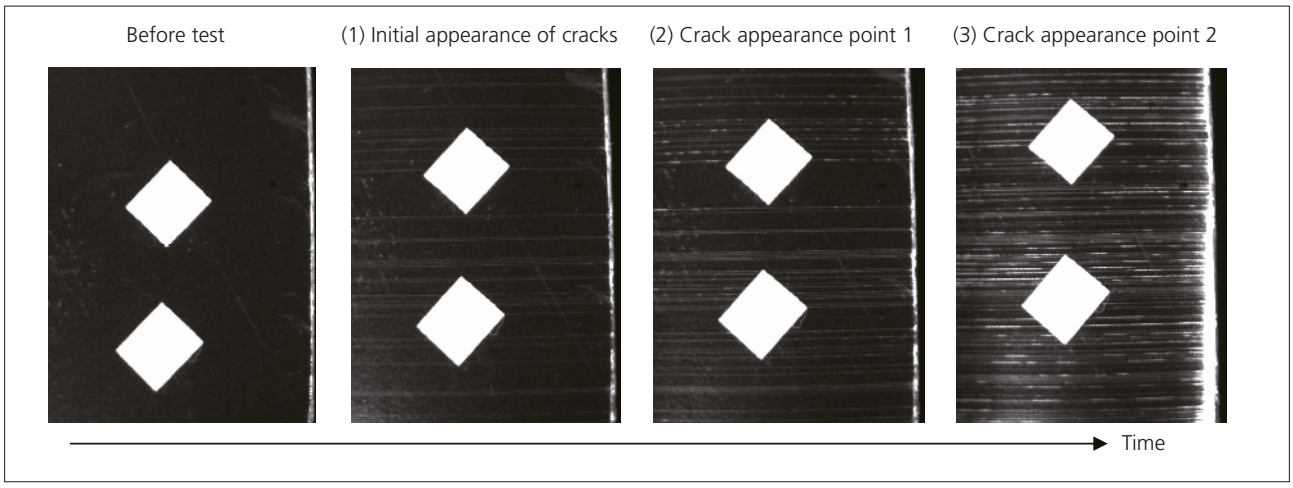

Fig. 3 State of Self-Repair Coating on Sample

Results

Fig. 3 shows the time-course changes in the self-repair coating film at the sample surface that were extracted from the TRViewX tensile test video. Here, the characteristic changes that occurred in the sample at various states during tensile loading are displayed in photographs. The captured states include: (1) Initial appearance of cracks: the point at which localized minute cracks first appear in self-repair coating film, (2) Crack appearance point 1: the point at which the cracks become clearly evident, and (3) Crack appearance point 2: the point at which the cracks become evident over the entire coating film, imparting a whitening effect.

Next, using the TRViewX Point Pick feature, we quantified the test force loaded onto the sample and the amount of deformation that occurred at states (1), (2), and (3) of the self-repair coating film. Fig. 4 shows the Test Force -Stroke curve.

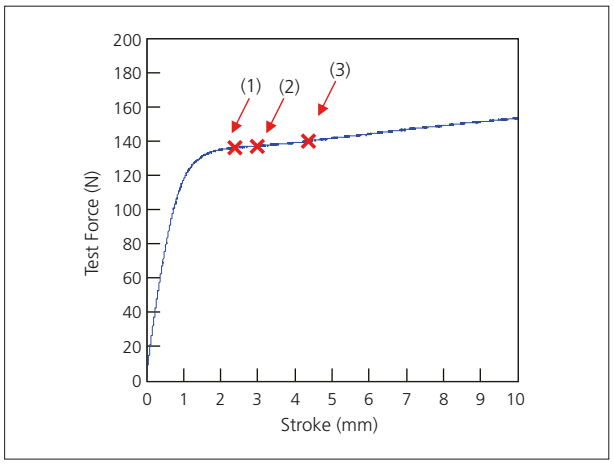

Fig. 4 Test Force - Stroke Curve

Table 3 Test Results

	Test Force (N)	Stroke (mm)
(1)	135.66	2.38
(2)	137.25	2.98
(3)	139.53	4.36

Fig. 4 reveals that the cracks occur in the self-repair coating film after the sample exhibits non-linear behavior - that is, when the plastic region has been reached. It is therefore presumed that the self-repair coating film possesses strength properties that prevent its damage in the elastic region. The cracks in the coating film appeared at about the 135 N load point, and after the cracks became clearly evident at a load point of about 137 N, the cracking suddenly became very pronounced over the range of 137 N-140 N.

From this study, we were able to quantitatively evaluate the strength characteristics of a self-repair coating film in functional film. Therefore, it is reasonable to expect that this test method for evaluating material strength in multilayer structures, previously difficult to evaluate, has the possibility of achieving widespread application, not only for functional films, but also for films coated on various surfaces.

First Edition: Mar. 2013

SHIMADZU
Shimadzu Corporation
www.shimadzu.com/an/

For Research Use Only. Not for use in diagnostic procedures.
The content of this publication shall not be reproduced, altered or sold for any commercial purpose without the written approval of Shimadzu.
The information contained herein is provided to you "as is" without warranty of any kind including without limitation warranties as to its accuracy or completeness. Shimadzu does not assume any responsibility or liability for any damage, whether direct or indirect, relating to the use of this publication. This publication is based upon the information available to Shimadzu on or before the date of publication, and subject to change without notice.
© Shimadzu Corporation, 2013

SHIMADZU
Excellence in Science

Application Data Sheet

No.10

AUTOGRAPH
Material Testing & Inspection

Measurement for Monotonic Equibiaxial Flexural Strength of Glass

Standard No. ASTM C1499-01

Introduction

In recent years, there has been an increase in smart phones, tablets and other mobile devices that use glass. Mobile products require the strength to resist bends, drops and other external forces, and any glass pieces must also be sufficiently strong. For glass, there are typically two types of strength, which are measured by different methods. One type is edge strength, which is obtained from 3-point (or 4-point) bending tests. When glass is cut, microscopic damage (microcracks) appears at the cut surface. With a 3-point (or 4-point) bending test, strength is determined by the fracture from these cracks. In other words, edge strength could be called an indicator of the degree of damage at a fracture surface. The other type is surface strength, which is determined from ring bending tests. In this method, fracture starts near the center of the glass, so there is no cut surface impact. In other words, surface strength could be called an indicator of the strength of the glass surface itself. In this article, we introduce an example of a ring bending test, as per the ASTM standard, to obtain the surface strength of glass.

F. Yano

Measurements and Jigs

Fig. 1 shows a schematic diagram of the jigs used with the ASTM standard (ASTM C1499-01). This standard includes precise specifications regarding the measurements and jigs, a portion of which are shown below.

- The radius of the ring tip is set to between 0.5 and 1.5 times the thickness of the test specimen
- The ratio of the diameters of the load ring and the support ring is between 0.2 and 0.5
- Setting the diameter ratio to 0.2 is recommended for high-strength objects (σ > 1 GPa) with a low elastic modulus (E < 100 GPa).
- Align the load ring and support ring axes using a 90° V block.
- To observe how the glass cracks develop, affix tape to the load ring prior to measurement.

The surface strength evaluated by the glass ring bending test is automatically calculated by a numerical formula preregistered with the software's configurable formula function.

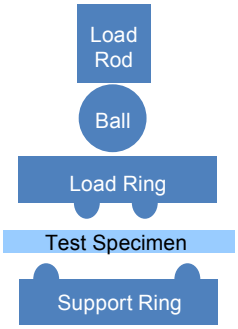

Fig. 1: Ring Bending Schematic

Measurement Results

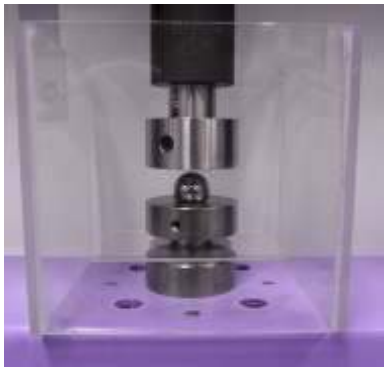

Fig. 2: Measurement Status

Note: A safety cover is required.

Fig. 3: The Glass After the Test

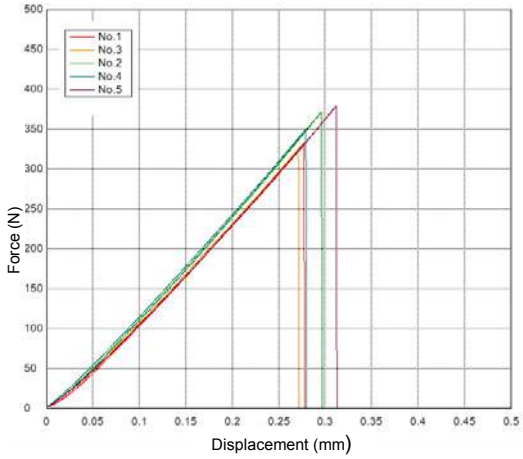

Fig. 4: Force - Displacement Curve

Table 1: Test Conditions

Item	Set Value
Load cell capacity	1 kN
Load speed	1 mm/min

Table 2: Test Results Average

Sample	Surface Strength (MPa)
Borosilicate glass	144

Glass Ring Bending Measurement System

Tester: AGS-X
Load Cell: 1 kN
Test Jig: Ring bending test jigs, safety cover
Software: TRAPEZIUM LITE X

AGS-X Table-Top Precision Universal Tester

Features

- A high-precision load cell is adopted. (The high-precision type is class 0.5; the standard-precision type is class 1.) Accuracy is guaranteed over a wide range, from 1/500 to 1/1 of the load cell capacity. This supports highly reliable test evaluations.
- Crosshead speed range
  Tests can be performed over a wide range from 0.001 mm/min to 1,000 mm/min.
- High-speed sampling
  High-speed sampling, as fast as 1 msec.
- TRAPEZIUMX LITE X operational software
  This is simple, highly effective software.
- Jog controller (optional)
  This allows hand-held control of the crosshead position. Fine position adjustment is possible using the jog dial.
- Optional Test Devices
  A variety of tests can be conducted by switching between an abundance of jigs in the lineup.

First Edition: February 2013

Shimadzu Corporation
www.shimadzu.com/an/

For Research Use Only. Not for use in diagnostic procedures.
The content of this publication shall not be reproduced, altered or sold for any commercial purpose without the written approval of Shimadzu.
The information contained herein is provided to you "as is" without warranty of any kind including without limitation warranties as to its accuracy or completeness. Shimadzu does not assume any responsibility or liability for any damage, whether direct or indirect, relating to the use of this publication. This publication is based upon the information available to Shimadzu on or before the date of publication, and subject to change without notice.
© Shimadzu Corporation, 2013

SHIMADZU
Excellence in Science

Application News

Material Testing System DUH

No. SCA_300_007

Compression Test of a Liquid Crystal Spacer (columnar) under Different Temperatures

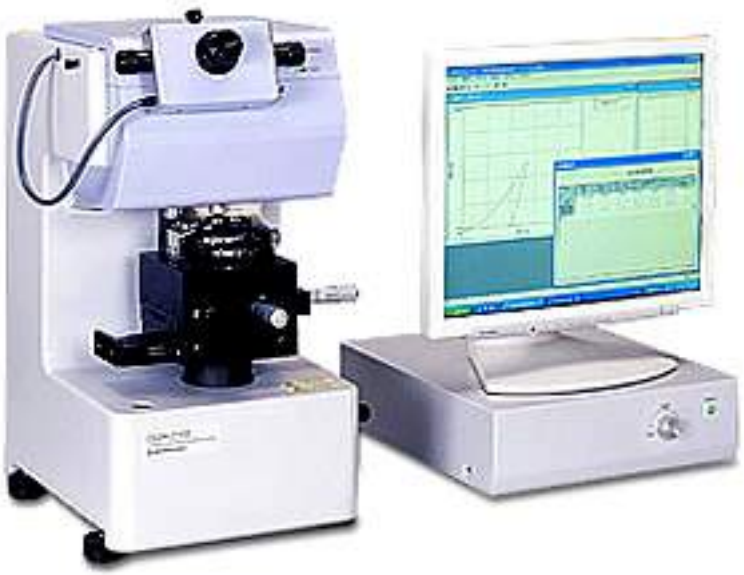

■ Introduction

Conventionally, beads (such as plastic, silica) were the item most commonly used as spacers in liquid crystal displays. However, dispersal of beads is difficult, and damage to the oriented film causes problems with the panel strength, display defects and light leaks. In recent times therefore, photolith (columnar) spacers featuring a variety of cross-sectional shapes (square, circular, elliptical etc.) have begun to be used. Introduced here is an example of a study into the compression temperature properties of a photolith spacer on a glass plate by heating it and using the DUH-W201S Shimadzu Dynamic Ultra Micro Hardness Tester equipped with a high temperature system and software for the MCT-W Micro Compression Testing Machine.

■ Specimen

1) Specimen name: Spacer on a glass plate (A,B,C) (**Fig.1)**
2) Specimen no.: No.1 to No.3
3) Size of Specimen: ⍉ 25 mm x 0.5 mm (glass plate)

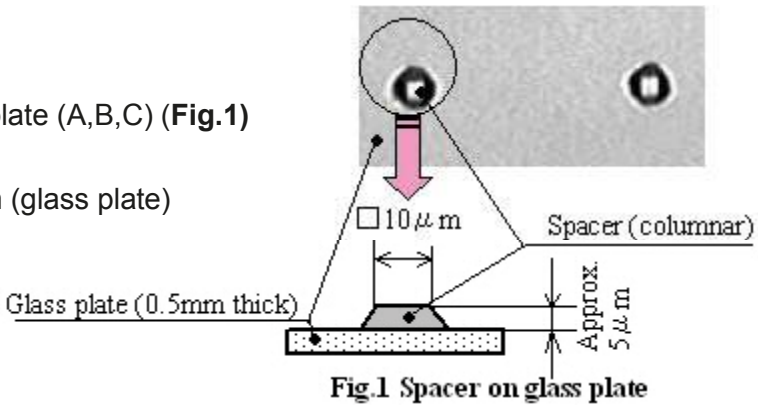

Fig.1 Spacer on glass plate

■ Test Conditions

Tester: DUH-W201S Shimadzu Dynamic Ultra Micro Hardness Tester equipped with high temperature system (Software: MCT-W) (Refer to **Fig. 2**)	
Measurement indenter:	f50 μm diamond surface indenter
Measurement mode:	Load-unload test
Test force:	10 (mN)
Loading rate:	0.284 (mN/sec)
Load retention time:	5 (sec)
Heating temps.	25 °C (room temp.), 180 °C

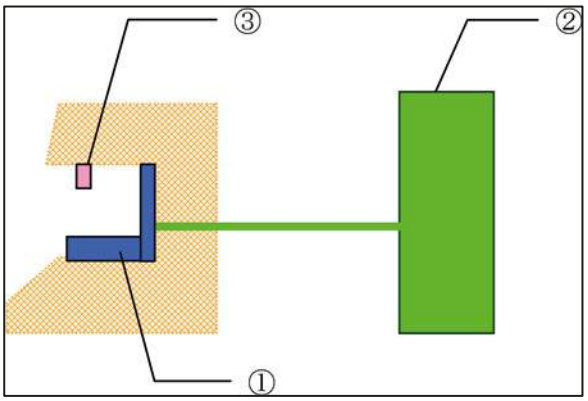

Fig. View of high temp DUH

①Heating unit 347-24675

②Temperature controller 347-23120-01

③Inver indenter 339-85898-21

■ Test Results

The Test force – Depth graphs for a test force of 10 mN are shown in **Figs.3** (specimen temp.: 25 °C) & **4** (specimen temp.: 180 °C), while a summary of the results (averages) are shown in **Table 1** & **Figs. 5 & 6**.

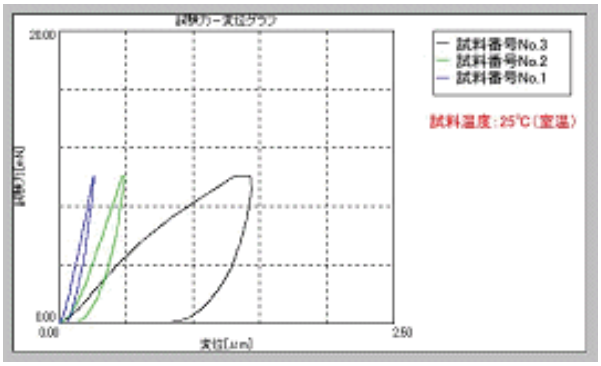

Fig. 3
Test force– Strain graph (Specimen temp.: 25 °C)

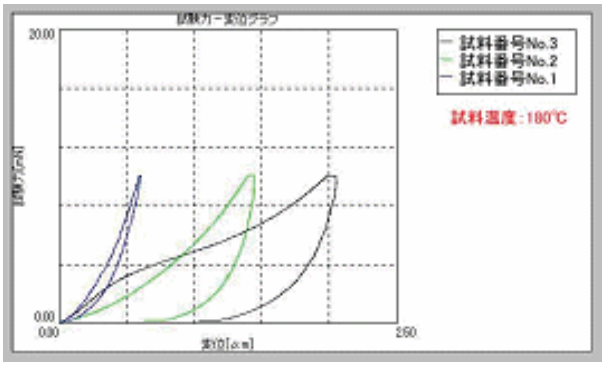

Fig. 4
Test force– Strain graph (Specimen temp.: 180 °C)

Specimen Temp	Results of Compression Test using the high temperature system equipped DUH (averages)							
25 °C	Specimen Name		Specimen No.	Strain 1 (μm)	Strain 2 (μm)	Particle size (μm)	Compress-ibility	Recovery (%)
	Spacer	A	No.1	0,248	0,046	10,0	2,484	2,020
		B	No.2	0,449	0,099	10,0	4,486	3,491
		C	No.3	1,384	0,795	10,0	13,837	5,884
180 °C	Specimen Name		Specimen No.	Strain 1 (μm)	Strain 1 (μm)	Particle size (μm)	Compress-ibility	Recovery (%)
	Spacer	A1	No.1	0,558	0,004	10,0		5,536
		B1	No.2	1,298	0,497	10,0		8,008
		C1	No.3	2,097	1,061	10,0		10,358

NOTES 1) One side of the square section of the spacer was taken to be particle size 'd'
2) Compressibility and recovery were calculated using the equation below

Compressibility Cr = (L1/d)x100
Recovery Rr = {(L1-L2)/d}x100
Cr: Compressibility (%)
Rr: Recovery (%)
D: Particle size (μm)
L1: Strain 1 (μm)
L2: Strain 2 (μm)

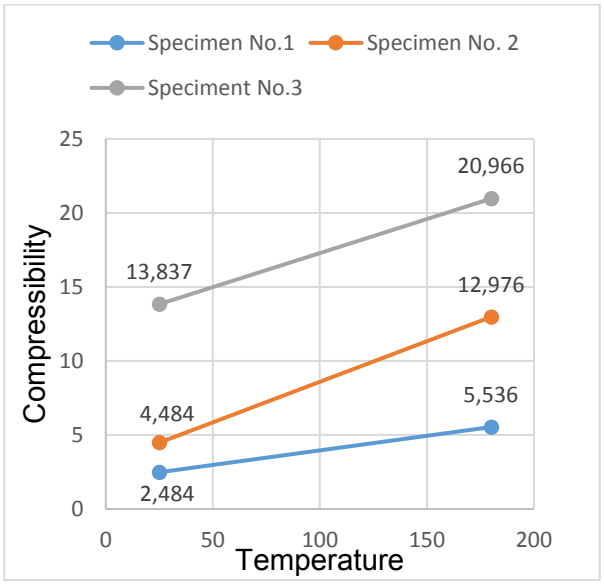

Fig.5 Temp. vs. compressibility each specimen

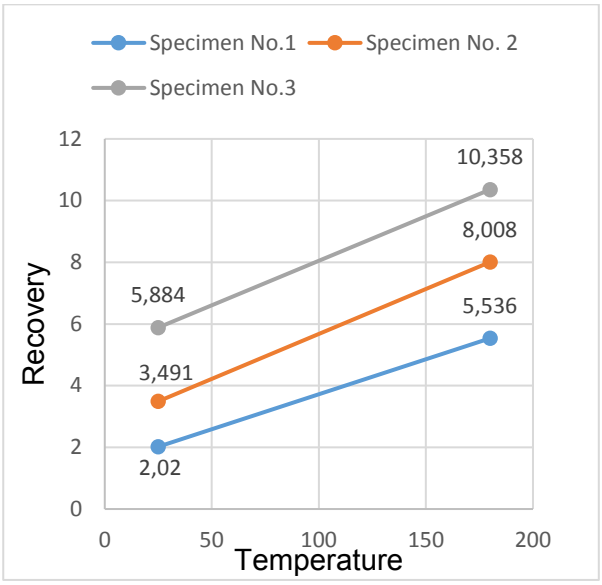

Fig.6 Temp. vs. recovery each specimen

2) From **Figs. 3 & 4** it can be seen that, even at the same test (compression) force, the strain is larger if the heating temperature is higher – in other words, these are thermoplastic materials. Furthermore, it can be seen from Figs. 5 & 6 that compressibility and recovery tend to become larger for each specimen as the temperatures rises. Therefore, if the same force as at room temperature is applied to a liquid crystal panel being used at a high temperature it needs to be taken into account that, although the material will recover, the degree of deformation will be larger.

■ Summary

Useful data on the strain properties of a variety of specimens with respect to temperatures ranging from room temperature to 250 °C can be obtained using the Shimadzu Dynamic Ultra Micro Hardness Tester equipped with a high temperature system (Software: MCT-W). Although in this example we have measured the strain against temperature for photolith spacers on glass plates used in liquid crystal, this instrument will also be useful in evaluating the dynamic temperature characteristics of materials used under heated conditions such as heat insulating and heat resistant materials.

* Please be advised that data obtained before the implementation of the current Weights and Measures Law may be presented in terms of gravimetric unit.

SHIMADZU

Shimadzu Europa GmbH

www.shimadzu.eu

For Research Use Only. Not for use in diagnostic procedures.
The content of this publication shall not be reproduced, altered or sold for any commercial purpose without the written approval of Shimadzu. The information contained herein is provided to you "as is" without warranty of any kind including without limitation warranties as to its accuracy or completeness. Shimadzu does not assume any responsibility or liability for any damage, whether direct or indirect, relating to be the use of this publication. This publication is based upon the information available to Shimadzu on or before the date of publication, and subject to change without notice.

SHIMADZU
Excellence in Science

Application News

Material Testing System DUH

Compression Tests of Liquid Crystal Spacer using the Shimadzu Dynamic Ultra Micro Hardness Tester DUH-211S

No. SCA_300_008

The following shows an example of compression tests carried out on liquid crystal spacers, an electronics component, to determine their breaking strength (See Fig.1).

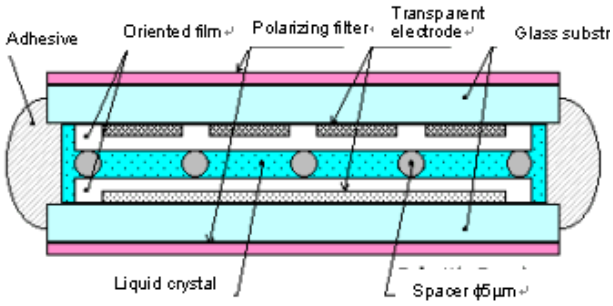

Figure 1: Liquid crystal spacers

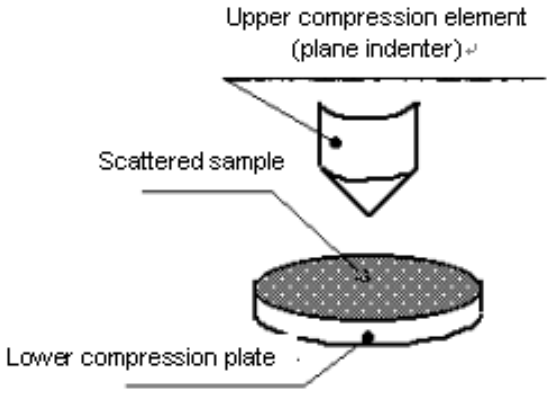

Figure 2: Compression test

■ Test conditions

1) Sample: Spacer (A), (B) (ϕ 5 μm)
2) Upper compression element: Plane ϕ 50 μm (Diamond)
3) Lower compression element: SKS plate
4) Test mode: Compression test (Mode 1: Indentation test)
5) Test force: 49 mN
6) Loading rate: 2.648 mN/sec

■ Test method (see Figure 2)

1) Replace the indenter (triangular or Vickers) with a plane one.
2) Scatter the sample (spacers) thinly on the lower compression plate.
3) Set the lower compression plate prepared in step 2) to the sample holder (3-type thin specimen holder).
4) Carry out compression tests on each particle.

■ Test results

1) Fig. 3 and Fig.4 show the graph setting screens for “Hardness calculations using the preset test force” of 5 data obtained from each sample.
2) Test forces at the rupture points can be determined by placing the cursor at the rupture points. They are as follows:
Test force at the rupture point for spacer A: 39.79 mN
Test force at the rupture point for spacer B: 23.01 mN
Table 1 shows the rupture strength calculated based on these values using EXCEL.
3) Table 1 shows that sample No.1 (spacer A) has higher rupture strength than No.2 (spacer B).
4) Fig.7 shows images of sample No.1 before and after measurement.

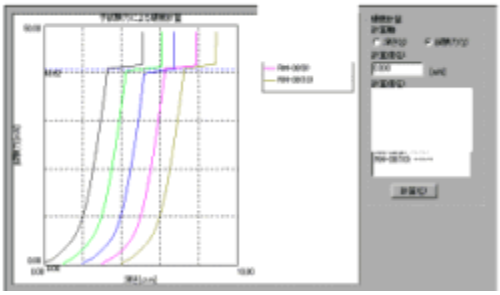

Figure 3: Spacer (A)

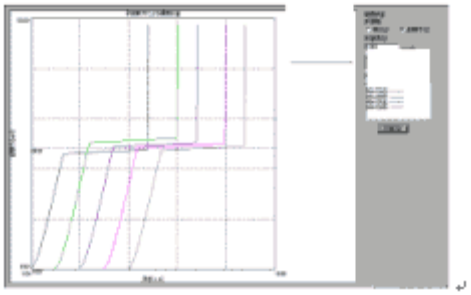

Figure 4: Spacer (B)

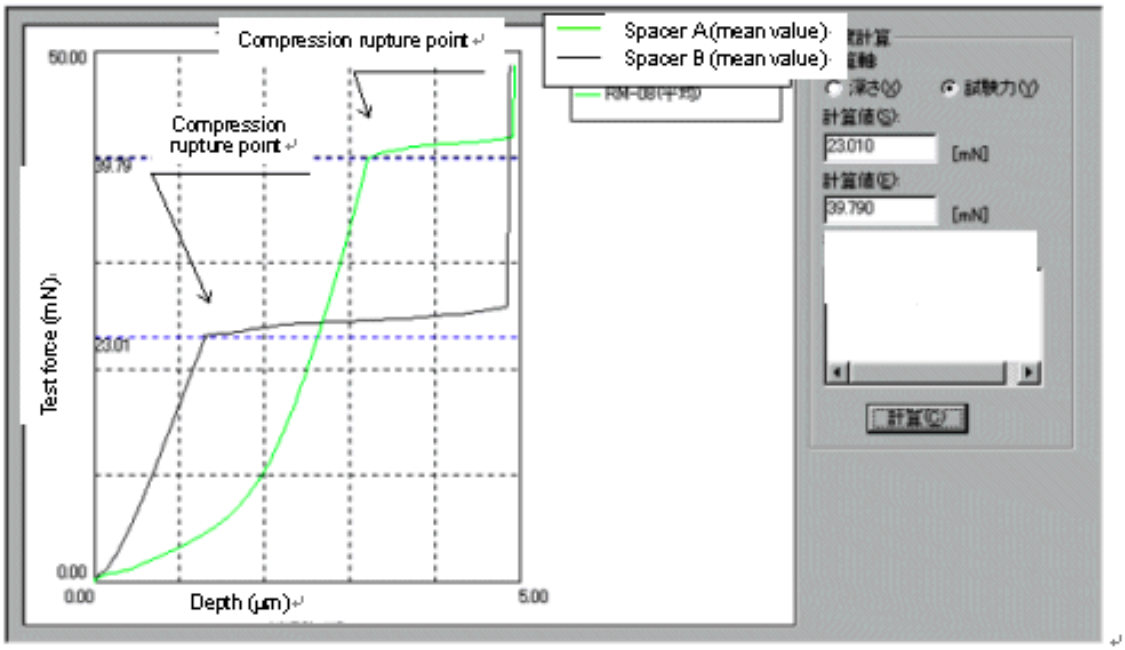

Figure 5: Setting screen for overlaid graph of mean values

■ Summary

Normally, the Shimadzu Micro Compression Testing Machine MCTM/MCTE is used for compression tests of micro particles. This example shows that hardness testers are also applicable for this purpose.

The Ultra Micro Hardness Tester DUH can be used for compression tests, as long as the sample displacement at the point of rupture is less than 10 µm and the testing force is less than 1980 mN. In addition, effective data can be obtained by calculating the rupture strength using EXCEL.

■ Bibliography

1) Fig.1: The Association of Powder Process Industry and Engineering, Japan, “7.6 Distribution of Spacers for Liquid Crystal Panels” in “Micro Particle Engineering” (AsakuraShoten).
2) Rupture strength formulae: Hiramatsu, Oka, Kiyama (Japan Mining Industry Association Journal 81.10.24 (1965))

Table 1 Compression test results using DUH				
Sample name	Sample No.	Force (N)	Particle Diameter (mm)	Rupture strength (MPa)
Spacer A	No. 1	3,979E-02	6,0E-03	985,60
Tube B	No. 2	2,301E-02	5,0E-03	820,74

Ref.) Rupture strength was calculated as follows:

$ST=2,8\ P/\pi d^2$
ST: Rupture strength (N/mm^2 or MPa)
P: Test force (N)
d: Particle diameter or fiber diameter (mm)

Source: Hiramatsu, Oka, Kiyama (Japan Minig Industry Association Journal)

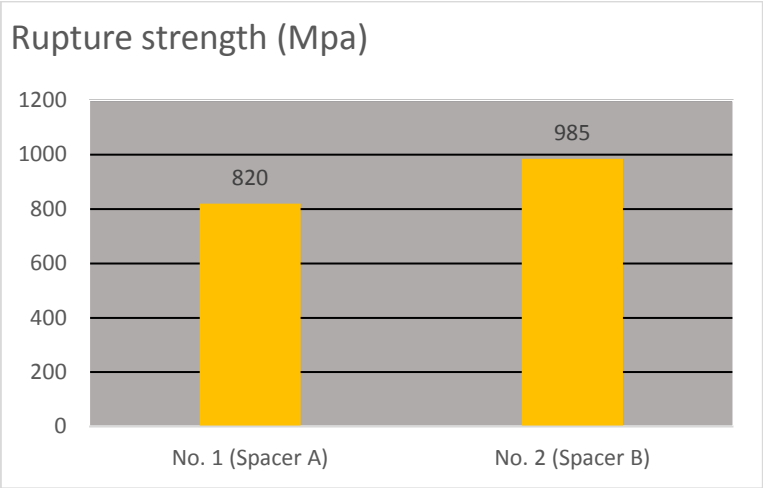

Figure 6: Rupture strength for each spacer

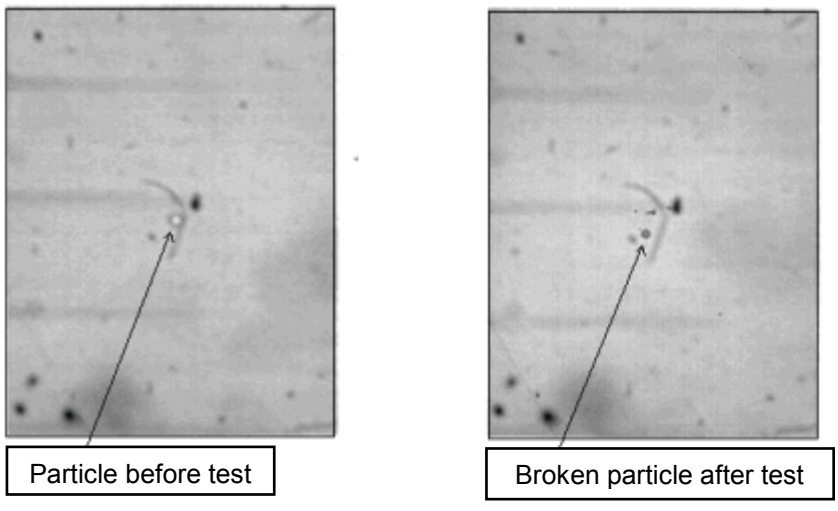

Figure 7: Sample No.1 before and after test

For Research Use Only. Not for use in diagnostic procedures.
The content of this publication shall not be reproduced, altered or sold for any commercial purpose without the written approval of Shimadzu. The information contained herein is provided to you "as is" without warranty of any kind including without limitation warranties as to its accuracy or completeness. Shimadzu does not assume any responsibility or liability for any damage, whether direct or indirect, relating to be the use of this publication. This publication is based upon the information available to Shimadzu on or before the date of publication, and subject to change without notice.

SHIMADZU
Excellence in Science

Application News

Material Testing System DUH

No. SCA_300_009

Hardness Test on Extra Fine Wire by Shimadzu DUH Dynamic Ultra Micro Hardness Tester

■ Introduction

A well-known method of testing the hardness of micro diameter wire is to grind the test surface of the wire specimen imbedded in resin and test the cross-section area of the wire. Though the hardness test by imbedding the specimen in resin is reliable, it is not a simple method since it involves imbedding the specimen in resin and grinding the specimen. The following introduces an example of a hardness test performed using the Shimadzu Dynamic Ultra Micro Hardness Tester without using the resin imbedded method.

■. Specimen

1) Specimen name	Extra Fine wire	
	W	SUS
2) Specimen No.	No. 1	No.2
3) Wire dia. (μm)	∅20	∅30
4) Material	Tungsten	Stainless steel

■ Test Conditions

1) Test Machine	Shimadzu DUH-Dynamic Ultra Micro Hardness Tester (See Fig. 1)
2) Indenter	Berkovich indenter (made of diamond)
3) Test type	Load-unload test
4) Test Force (mN)	9,8
5) Loading Rate (mN/sec)	0,711
6) Holding Time (sec)	5
7) Test Method	Both ends of the wire were fixed in place on an Si wafer with cellophane tape, and the hardness of the top of the cylindrical part of the wire was tested. (See Fig. 2)

Fig. 1 Overview of DUH

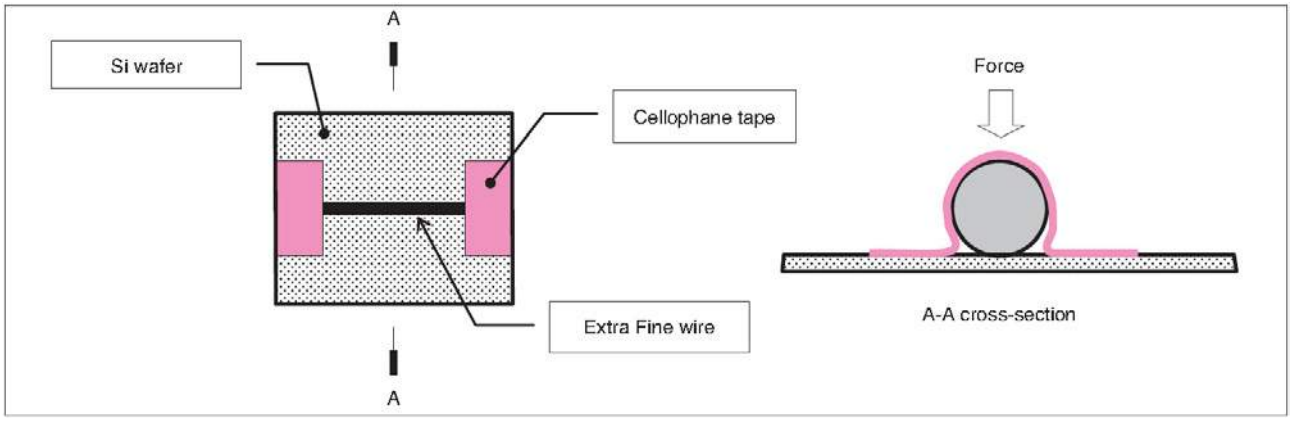

Fig. 2 Conceptual diagram

■ Test results

1) Table 1 summarizes the results (mean values) of testing by the test conditions in section 2.

Table 1 Hardness Measurement Results (Mean Values)

Specimen Name		Specimen No.	Maximum Force [mN]	Maximum Depth [μm]	Dynamic Hardness [DHT115-1]
Super-fine wire	W	No. 1	9,82	0,208	874,717
	SUS	No.2	9,85	0,243	644,253

Remarks: The calculation expression for dynamic indentation hardness is as follows:
DHT115-1 = 3.8584 P/h2 where,
DHT115-1 : Dynamic hardness of triangular pyramid indenter at load end
P : Maximum Force (mN)

2) Fig. 3 shows the force-depth graph after testing.

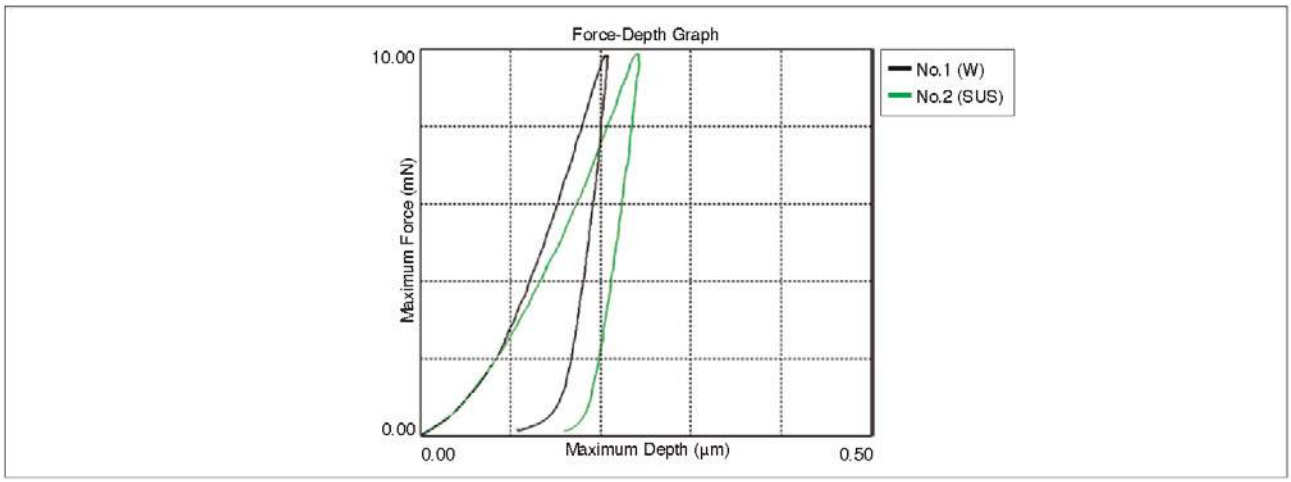

3) The order of specimen hardness in 1) is as follows: No. 1 (tungsten) > No. 2 (stainless steel)

4) Figs. 4 and 5 show images of the indentation.

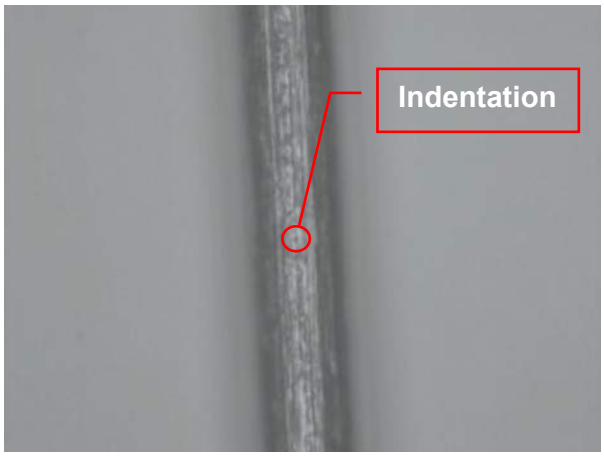

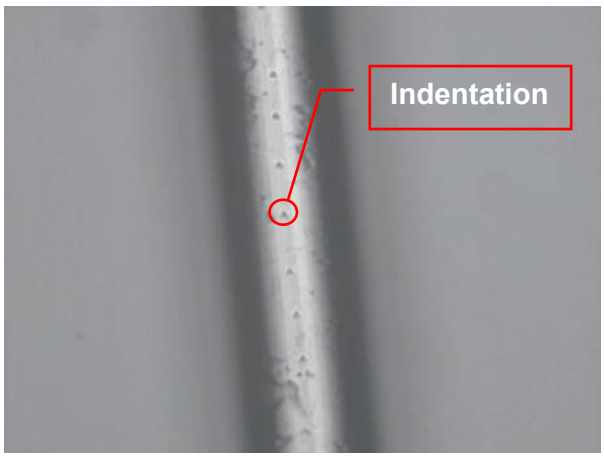

■ Summary

The Shimadzu DUH-W Dynamic Ultra Micro Hardness Tester allows specimen hardness to be simply evaluated without imbedding the

For Research Use Only. Not for use in diagnostic procedures.
The content of this publication shall not be reproduced, altered or sold for any commercial purpose without the written approval of Shimadzu. The information contained herein is provided to you "as is" without warranty of any kind including without limitation warranties as to its accuracy or completeness. Shimadzu does not assume any responsibility or liability for any damage, whether direct or indirect, relating to be the use of this publication. This publication is based upon the information available to Shimadzu on or before the date of publication, and subject to change without notice.

SHIMADZU
Excellence in Science

Application News

Material Testing System DUH

No. SCA_300_018

Hardness Evaluation of Pencil Leads with Shimadzu Dynamic Ultra Micro Hardness Tester

■ Introduction

Consumer commodities should measure up to a certain level of quality and function appropriate to their uses. Otherwise, their public reputation may suffer if consumers buy them and they are short of expectations. The Japan Industrial Standard (JIS) sets forth standards specifying quality requirements for products ranging from daily necessities to industrial products. The quality of leads for pencils and automatic pencils is also specified by JIS. It classifies leads in the order of their density and flexural strength, ranging from 9H down to 6B. This standard is used instead of the more reasonable standard of hardness and density because physical calculation of hardness is extremely difficult.

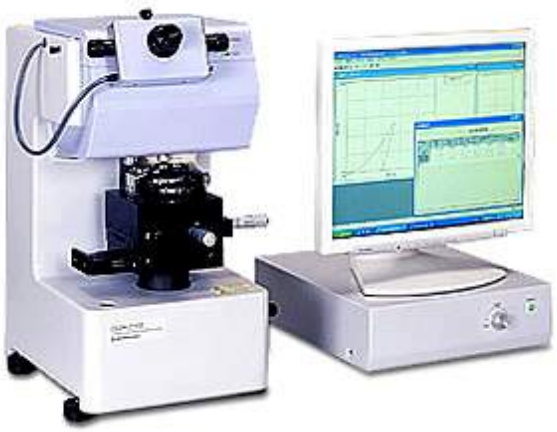

Fig. 1 External View of the DUH-211 Series

The following is an example of hardness measurements performed on pencil leads of different density, a property previously deemed very difficult to measure.

Hardness test on pencil leads

(1) Samples

Pencil leads of 5H, H, HB, B, 3B, 5B, and red pencil

(2) Testing machine

(a) Shimadzu Dynamic Ultra Micro Hardness Tester

(b) Standard vise

3) Test result

Load versus indenter displacement curves for pencil leads of 5H type and 5B type are shown as examples in Figs.1 and 2 respectively.

Table 1 Testing conditions

TEST MODE	2
CAL. MODE	115° TRIANG. PYRAMID INDENTER
MODE	AUTO
F.S. DEPTH	5 μm
MAX LOAD	20 gf
LOAD SPEED	0.65 gf/sec
AFTER TIME	5 sec
LOT	20
ROOM TEMP	23 – 24 °C

10 mgf (for automatic measurement of the indentation depth of an indenter), is applicable to the measurement of the hardness of a wide range of materials from soft materials such as rubbers and plastics to hard materials such as ceramics and diamonds.

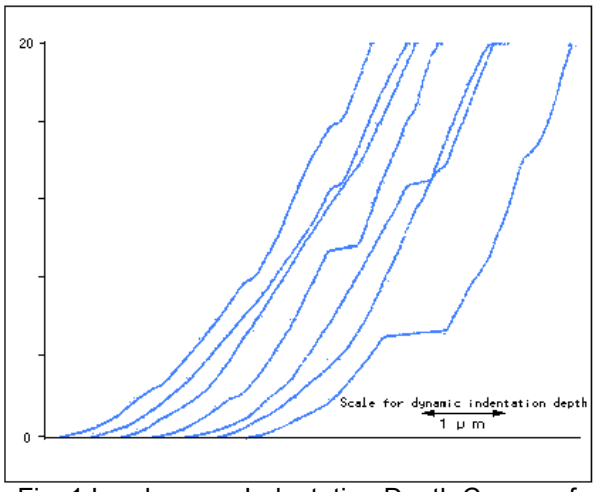

Fig. 1 Load versus Indentation Depth Curves of Pencil Leads of Type 5H

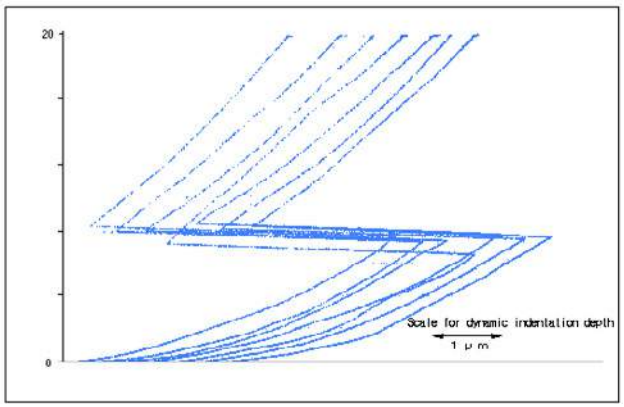

Fig. 2 Load versus Indentation Depth Curves of Pencil Leads of Type 5B

Note: One of the curves shows an abrupt increase of indentation depths due to internal slipping in the specimen.

Note: Curves exceeding the full scale of 5 μm for indentation depth are shown with the abscissa values deducted by 5 μm.

Table 2 DH Hardness and Flexural Strength of Pencil Leads

Specimen	Symbols for density or color	DH Hardness			Flexural strength
		Average	Standard deviation	Coefficient of variation	kg/m m^2
Pencil leads	5H	46.2	4.1	8.8%	7
	H	23.9	2.4	9.9%	6
	HB	18	2.8	15.5%	5
	B	14.9	1.2	8.2%	4
	3B	11.9	0.7	5.7%	3
	5B	9.5	0.5	5.4%	2
Lead of color pencil	Vermilion	6.3	0.4	6.0%	2

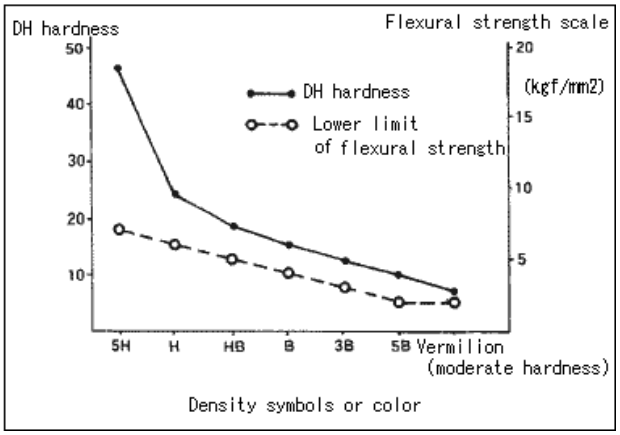

Fig. 3 DH Hardness and Flexural Strength of Pencil Leads

Table 2 and Fig.3 show a comparison between flexural strengths as specified in JIS S6005-1985 (Leads for pencils, coloured pencils and mechanical pencils) and dynamic hardness calculated from the dynamic indentation depth measured with the Shimadzu Dynamic Ultra Micro Hardness Tester. An appreciably good correlation is observed between flexural strength and dynamic indentation depth.
Admitting that there is deviation of data or variation due to different ingredients, this hardness tester is suitable for the quality control of products as long as data is statistically managed.

(Note: For details about hardness of automatic pencil leads, refer to Application News i30)

* Please be advised that data obtained before the implementation of the current Weights and Measures Law may be presented in terms of gravimetric unit.

SHIMADZU
Shimadzu Europa GmbH
www.shimadzu.eu

For Research Use Only. Not for use in diagnostic procedures.
The content of this publication shall not be reproduced, altered or sold for any commercial purpose without the written approval of Shimadzu. The information contained herein is provided to you "as is" without warranty of any kind including without limitation warranties as to its accuracy or completeness. Shimadzu does not assume any responsibility or liability for any damage, whether direct or indirect, relating to be the use of this publication. This publication is based upon the information available to Shimadzu on or before the date of publication, and subject to change without notice.

SHIMADZU
Excellence in Science

Application News

Material Testing System MCT

Hardness Measurement of Hydrogen Storage Alloy using the Shimadzu Dynamic Ultra Micro Hardness Tester DUH

No. SCA_300_020

The hydrogen storage alloy used in fuel cell batteries is generally extremely fragile when compared to the simple metals themselves. Furthermore, as a result of repeated expansion and contraction that occur during hydrogen storage and release, large distortions may be created, finally leading to cracks and pulverization of metal particles. Pulverization causes reduction in the hydrogen storage capacity, deteriorating the original function of the alloy.
The following shows an example of hardness measurements that compare the difference of hardness before and after hydrogen storage.

External appearance of DUH

■ Sample

1) Sample name: Hydrogen storage alloy
2) Sample number: No1 (before hydrogen storage) and No.2 (after hydrogen storage)
3) Sample size: See Fig.1

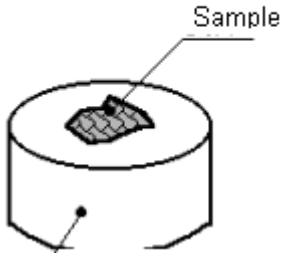

Fig.1 Sample Size

■ Test Conditions

1) Testing machine: Shimadzu Dynamic Ultra Micro Hardness Tester DUH-W201S
2) Indenter: Diamond shaped triangular indenter with tip angle 115
3) Test mode: Load-unload test
4) Test force: 49 mN
5) Loading rate: 2.684 mN/sec
6) Test force holding time: 10 sec
7) Sample fixing method: Standard vice

■ Test Results

1) Table 1 shows the measurement results (mean values) of load-unload tests with the test force of 49 mN. Fig.4 shows the Test force - indentation depth curve.

2) The dynamic hardness DHT115 in Table 1 shows that sample No.1 presents a large hardness than sample No.2 to the separator.

3) As the alloy becomes fragile after hydrogen storage, it was expected that the hardness increases by storing hydrogen. However, the measurements demonstrate the opposite results (see Fig.2 and Fig.3). It is assumed that the cracks caused by hydrogen storage act as springs, making the material appear to be less hard. This assumption requires further examination

Table 1 Hardness measurement results using DUH

Sample Name		Sample No.	Force	Depth (μm)	Dynamic Hardness (DHT115)	Elastic Modulus (Pa)	File Name	Figure
Hydrogen storage alloy	Before hydrogen storage	No. 1	49,217	0,537	555,27	1,39E+11	H-01	Fig. 4
	After hydrogen storage	No. 2	49,095	0,555	440,84	8,43E+10	H-02	

Note: Dynamic Hardness was calculated as follow

$$DHT115 = \frac{3{,}8584 \cdot P}{h^2}$$

DHT115: Dynamic hardness by triangular indenter with tip angle 115°
P: Test force (mN)
H: Indentation depth (μm)

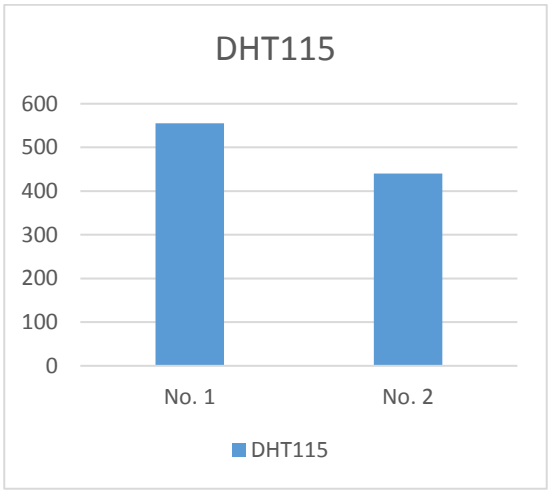

Fig. 2 Sample No. and Dynamic Hardness

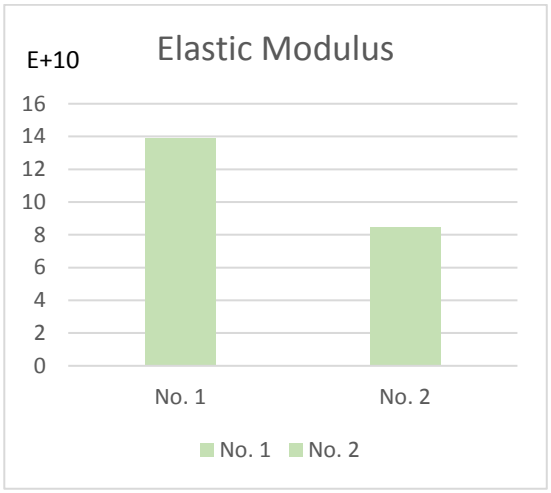

Fig. 3 Sample No. and elastic modulus

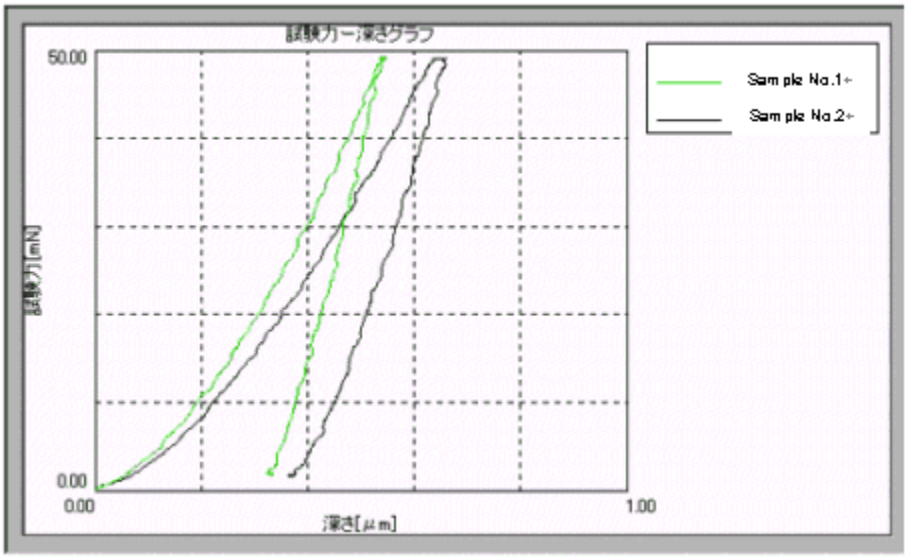

Fig.4 Test Force – Indentation depth curve

■ Summary

Hydrogen storage alloys are often used in ways that require repeated storage and release of hydrogen. Lanthanum/nickel alloy, for example, is said to be gradually pulverized while it repeats hydrogen storage and release. In this hardness measurement using the DUH, it has been confirmed that these alloys lose hardness by hydrogen storage.

For Research Use Only. Not for use in diagnostic procedures.
The content of this publication shall not be reproduced, altered or sold for any commercial purpose without the written approval of Shimadzu. The information contained herein is provided to you "as is" without warranty of any kind including without limitation warranties as to its accuracy or completeness. Shimadzu does not assume any responsibility or liability for any damage, whether direct or indirect, relating to be the use of this publication. This publication is based upon the information available to Shimadzu on or before the date of publication, and subject to change without notice.

SHIMADZU
Excellence in Science

Application News

No. SCA_300_022

Material Testing System DUH

Hardness Test of Ion Implanted Specimens and Valuable Metals with Shimadzu Dynamic Ultra Micro Hardness Tester Model DUH

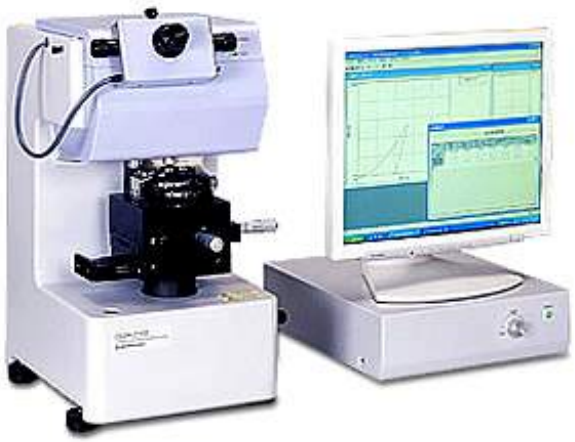

■ Introduction

The Shimadzu Dynamic Ultra Micro Hardness Tester Model DUH is a machine useful for a very wide range of applications for evaluating the surface hardness of solid samples based on the relation between indenting load and indentation depth.
The following presents the results of tests performed on nitrogen ion implanted sintered compact and fly cut platinum and gold specimens. (This data is courtesy of Prof. Kenichi Kanazawa of the Faculty of Machine Engineering, Chiba Institute of Technology, Japan.)

■ Ion implanted alumina ceramics

The test piece is a nitrogen ion implanted sintered compact of Al_2O_3 ceramic. Ion implantation conditions are 90 keV for the accelerating voltage and $2x10^{17}$ ions/cm^2 for the quantity of implanted ions. Within the load range below 1 gf, the difference in hardness was significant between the ion implanted specimen and the specimen without ion implantation, while the difference at the load range of over 1 gf is very small. This demonstrates the effectiveness of this ultra micro hardness tester at load ranges below 1 gf, unavailable to conventional Vickers hardness testers.

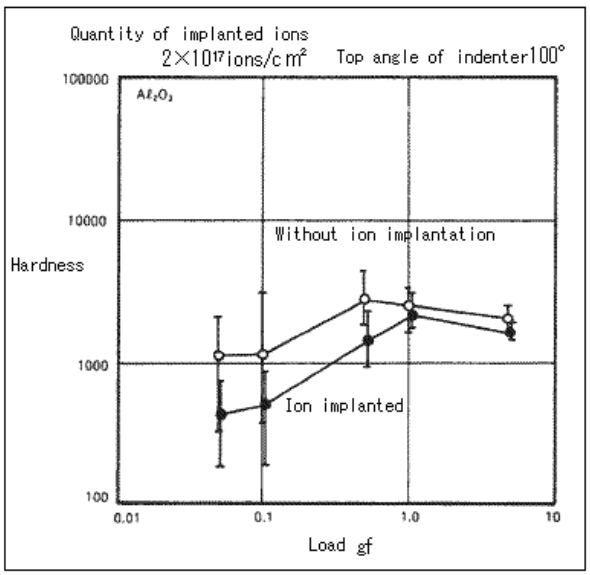

Fig.1 Relation between Hardness and Load in Nitrogen Ion Implanted Layer of Ceramic (AL_2O_3) (with $2x10^{17}$ ions/cm^2, triangular pyramid indenter of top angle 100°)

■ Ion implanted WC-Co sintered compact

The test piece is WC-Co type nitrogen ion implanted sintered hard alloy. Ion implantation conditions are 90 keV for the accelerating voltage and $5x10^{17}$ ions/cm^2 for the quantity of implanted ions. As the specimen was a sintered compact and hardness differed at each measured point, mean values for measured hardness were used for comparing data between the ion implanted specimen and the non-ion-implanted specimen. Just as on the results for the Al_2O_3 ceramic, differences of hardness that were not observed at loads over 1 gf were clearly shown at the load range below 1 gf. As evidenced above, the Model DUH, capable of performing tests with micro loads, is particularly fitted to the measurement of hardness differences in extreme surface layers.

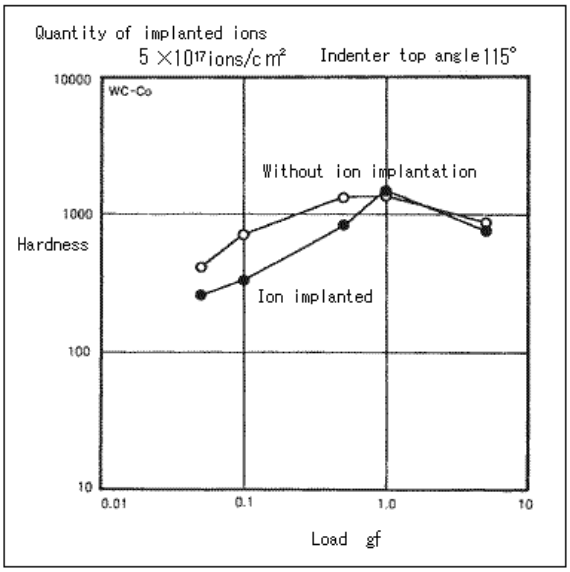

Fig.2 Relation between Hardness and Load in Nitrogen Ion Implanted Layer of Sintered Hard Alloy (WC-Co) (with $5x10^{17}$ ions/cm^2, triangular pyramid indenter of top angle 115°)

■ Fly cut pure platinum

Surface hardness was measured on a surface of high purity platinum cut with a high speed diamond cutting tool (fly cutting). Load versus indentation depth is plotted in **Fig.3**, from which hardness is calculated and plotted in relation to load in **Fig.4**.

DH100 with a triangular pyramid indenter of top angle 100 degrees is calculated by the following equation, where H represents indentation depth and P represents load: $DH_{100} = 147.28P/H^2$ the hardness varying in accordance with load is estimated to lie within the deviation of hardness.

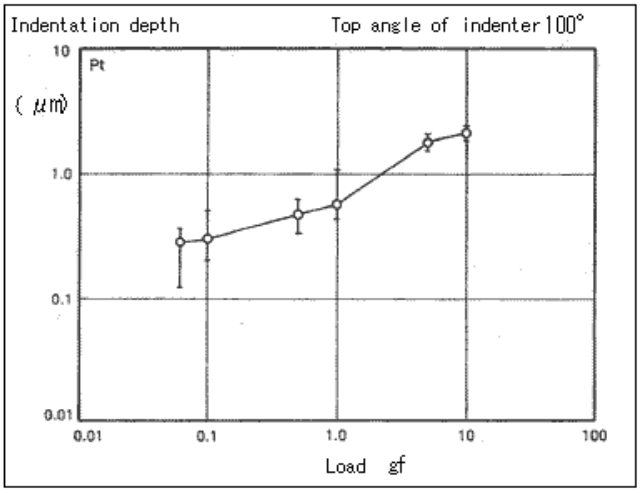

Fig. 3 Indentation Depth – Load Curve of Platinum (with triangular pyramid indenter of top angle 100°)

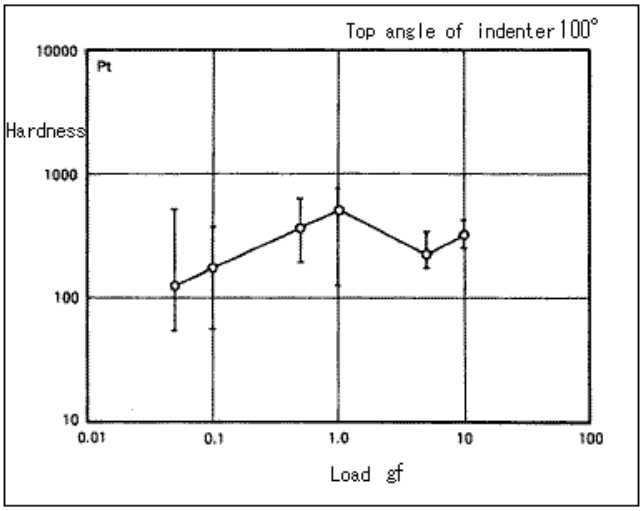

Fig. 4 Relation between Hardness and Load of Platinum (with triangular pyramid indenter of top angle 100°)

■ Fly cut pure gold

Just as in the case of platinum, this is a hardness test of fly cut pure gold. As a whole, the deviation of hardness is smaller than that of platinum, suggesting the possibility of hardness testing at a load of as small as 0.01 gf. The indicated hardness is significantly less than that of platinum.

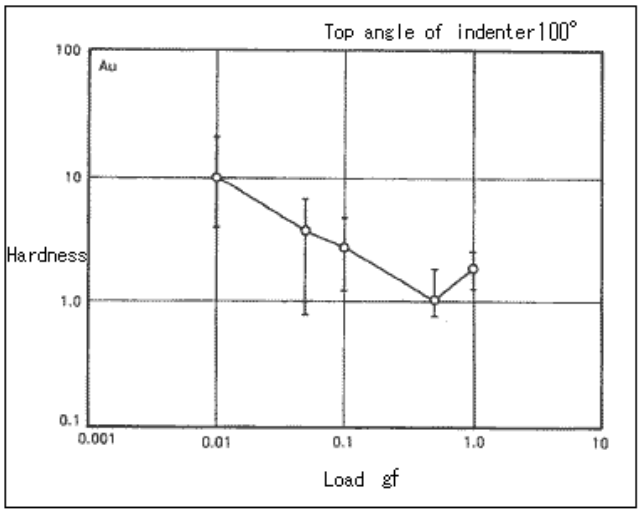

Fig. 5 Relation between Hardness and Load of Gold (with triangular pyramid indenter of top angle 115°)

* Please be advised that data obtained before the implementation of the current Weights and Measures Law may be presented in terms of gravimetric unit.

For Research Use Only. Not for use in diagnostic procedures.
The content of this publication shall not be reproduced, altered or sold for any commercial purpose without the written approval of Shimadzu. The information contained herein is provided to you "as is" without warranty of any kind including without limitation warranties as to its accuracy or completeness. Shimadzu does not assume any responsibility or liability for any damage, whether direct or indirect, relating to be the use of this publication. This publication is based upon the information available to Shimadzu on or before the date of publication, and subject to change without notice.

SHIMADZU
Excellence in Science

Application News

No. SCA_300_025

Material Testing System DUH

Measurement of Pearl Surface Hardness using Shimadzu Dynamic Ultra Micro Hardness Tester

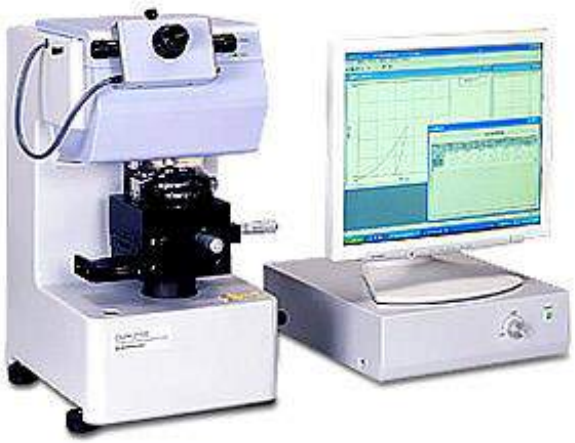

■ Introduction

Pearls are comprised of thin laminated layers of calcium carbonate of 0.3 to 0.5 mm secreted by Japanese pearl oysters or black-lip pearl oysters. The reflection and interference of light by these thin layers are considered to give the luster unique to pearls. In addition, a protein membrane of 0.02 mm is built atop these thin layers. Thus, the surface of a pearl assumes complex aspects.

Here, we will introduce an example of a hardness test in which the Shimadzu Dynamic Ultra Micro Hardness Tester was used to measure and compare the dynamic indentation hardness's of a pearl irradiated with ultraviolet rays (maltreated pearls) and an unimpaired pearl (one that has just been removed from pearl oysters).

The Shimadzu Dynamic Ultra Micro Hardness Tester allows you to measure the hardness of thin films and thin layers, using the indentation depth of the indenter (dynamic indentation hardness) or the diagonal length of indentation (micro Vickers hardness). This instrument can thus measure the hardness of various specimens from hard to soft materials, and has an extremely broad range of applications.

Test Conditions

Date	28.12.1989
Test Type	2
Speciment No.	Pearl
Maximum Load	A
Number of repetitions	200,00 gf
Retention Time	1
Pearl	10
File	SIN-A2, D1
Indenter	DH115
Minimum Load	0,00 gf
Load Speed	1
Deformation Scale	10 µm

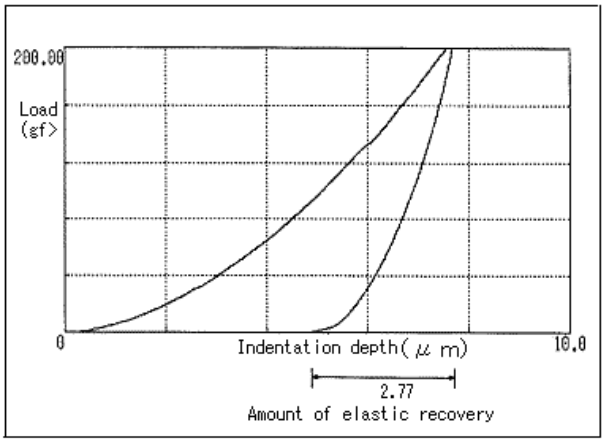

Fig. 1 Diagram of Load-Indentation Depth Relationship for Unipaired Pearl

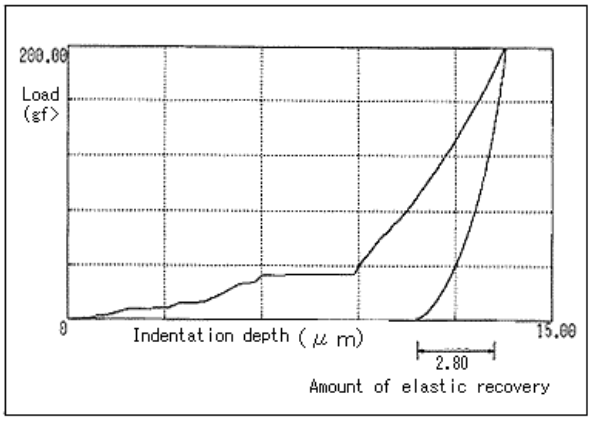

Fig. 2 Diagram of Load-Indentation Depth Relationship for Pearl Irradiated with Ultraviolet Rays

Test Conditions

Date	28.12.1989
Test Type	2
Speciment No.	Pearl
Maximum Load	E4
Number of repetitions	200,00 gf
Retention Time	1
Pearl	5
File	SINE21, D1
Indenter	DH115
Minimum Load	0,00 gf
Load Speed	1
Deformation Scale	10 µm

Table 1 Hardness of Unimpaired Pearl

No.	Load (gf)	Depth	Hardness
1	200,04	7,56	132,4
Average	200,04	7,56	132,4

Table 2 Hardness of Pearl Iradiated with Ultraviolet Rays

No.	Load (gf)	Depth	Hardness
1	199,92	13,51	41,45
Average	199,92	13,51	41,45

Table 3 Change in Hardness of Unimpaired Pearl

No.	Load (gf)	Depth	Hardness
1	1,720	0,50	260,33
2	5,980	1,00	226,27
3	12,540	1,50	205,84
4	19,780	2,00	187,11
5	29,260	2,50	177,14
6	39,180	3,00	164,70
7	51,980	3,50	160,56
8	64,820	4,00	153,29
9	80,340	4,50	150,12
10	96,760	5,00	146,45
11	115,420	5,50	144,37
12	113,140	6,00	139,94
13	152,280	6,50	136,38
14	173,660	7,00	134,10

Table 4 Change in Hardness of Pearl Irradiated with Ultraviolet Rays

No.	Load (gf)	Depth	Hardness
1	1,020	0,52	147,73
2	2,540	1,01	94,21
3	5,000	1,50	84,08
4	7,960	1,97	77,61
5	8,120	2,33	56,59
6	8,260	2,89	37,42
7	12,180	3,47	38,28
8	12,540	3,99	29,80
9	15,940	4,50	29,78
10	22,020	5,00	33,33
11	27,000	5,49	33,90
12	32,200	6,00	33,84
13	33,280	6,05	34,40
14	33,460	7,46	22,75
15	33,600	8,69	16,84
16	39,060	9,00	18,25
17	54,480	9,50	22,84
18	67,400	10,00	25,50
19	80,440	10,50	27,61
20	96,320	11,00	30,12
21	112,880	11,50	32,30
22	130,860	12,00	34,39
23	151,520	12,50	36,69
24	172,460	13,00	38,61
25	199,000	13,50	41,32

■ Test Results

The test results for the unimpaired pearl are shown in Tables 1 and 3, and in Fig. 1. Those for the pearl irradiated with ultraviolet rays are shown in Tables 2 and 4, and in Fig. 2.

As indicated by these results, a pearl irradiated with ultraviolet rays shows brittleness from its surface to a depth of approximately 9 mm. At a greater depth, the values for the average hardness in the depth direction (see Table 5) and the amount of elastic recovery (see Figs 1 and 2) of a pearl irradiated with ultraviolet rays are similar to those of an unimpaired pearl. Based on these data, the degree of the effect of ultraviolet irradiation can be estimated. At the same time, these data indicate that the substrate of a pearl irradiated with ultraviolet rays retains the hardness property of an unimpaired pearl.

Table 5 Average Hardness between Two Points in the Depth Direction

Specimen	Pearl irradiated with ultraviolet rays		Unimpaired pearls	
Depth (μm)	10,5	13.5	4,5	7,5
Load (gf)	80,44	199,00	80,34	196,94
Average hardness between 2 points (DH)	110,98		108,08	

The dynamic indentation depth is calculated by the following equation (in the case of the triangular pyramid indenter with a tip angle of 115 degrees)

$$DH = 37{,}838 \cdot \frac{P_2}{(D_2 - D_1)^2} \cdot \left(1 - \sqrt{\frac{P_1}{P_2}}\right)^2$$

For Research Use Only. Not for use in diagnostic procedures.
The content of this publication shall not be reproduced, altered or sold for any commercial purpose without the written approval of Shimadzu. The information contained herein is provided to you "as is" without warranty of any kind including without limitation warranties as to its accuracy or completeness. Shimadzu does not assume any responsibility or liability for any damage, whether direct or indirect, relating to be the use of this publication. This publication is based upon the information available to Shimadzu on or before the date of publication, and subject to change without notice.

SHIMADZU
Excellence in Science

Application News

Material Testing System AGS-X

No. SCA_300_029

Paper friction test
Friction test according to ASTM D1894

■ Purpose and Definition

Coefficient of friction testing measures the ease with which two surfaces in contact are able to slide over one another. There are two different values associated with the coefficient of friction –static and kinetic (also called dynamic).

Static friction applies to the force necessary to initialize motion between the two surfaces and kinetic (dynamic) friction is the resistance to moving once the surfaces are in motion over each other. ASTM D1894 is a general standard for Static and Kinetic Coefficients of Friction of Plastic Film and Sheeting which may also be applied on paper and other materials.

■ Equipment used

Load cell: 10N, 1/500 Class1
Jig: Friction Modulus Test Device, according to ASTM D1894
Software: Trapezium-X Single / Peel
Environment: Room temp 21°C +/-2 °C, humidity ca. 50 +/-5% RH

■ Test jig:

The friction jig consists of a fixed 240 x 360 mm, steel, sliding plane which is mounted on the testing machine table with two bolts.
The sled, which weighs 200 g and is 63,5 mm x 63,5 mm in size is connected to the load cell with a wire.

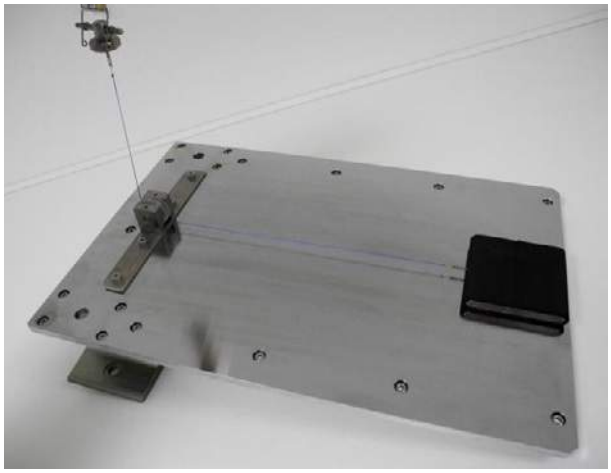

Fig. 1 Test Jig

Fig.2 Testing Machine

■ Test execution

Two samples are prepared, one for the plane and one for the sledge. The plane sample is 250 to 300 mm x 130 mm and is fixed using tape with the short end facing the machine. The sledge is wrapped with the paper sample approx. 63,5 mm wide and long enough to be wrapped around the sled and taped together on top.

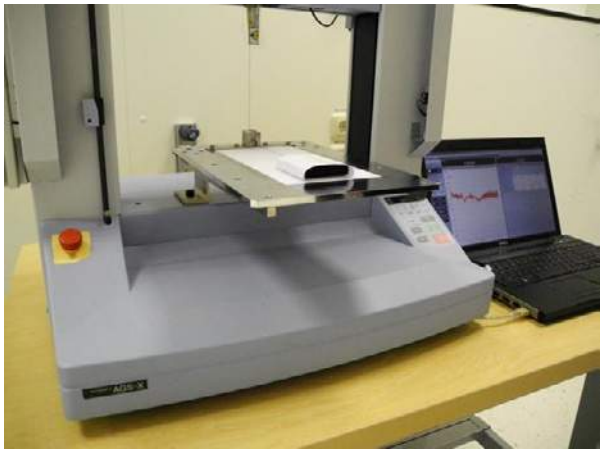

Fig.3 Setup 1

When testing card board or other rigid samples they are taped to the bottom side of the sled by using double sided tape.

Cleanliness is very important to avoid contaminating the samples with fat or other substances that might affect the friction properties of the sample, gloves may very well be used and the plane should be cleaned using some alcohol based cleaning fluid.

A method is prepared according to ASTM D1894.
Test type is single and peel.
Test speed is set to 130 mm/min (150 +/-30 mm/min is required.)
And stroke limit is set to 130 mm.
TrapeziumX is already prepared for this test so the necessary data points for friction, static COF and kinetic COF, are selectable points in the data processing menu.

A 50 N load cell was used and all results were below 1N. In this case it is important to set the sensitivity settings very low in the data processing window, default is 1%/FS, and this means that the smallest detectable change would be 0,1 N.

The differences between peaks and valleys are about 0,1 N and you might find that no results are presented after the test. This can of course always be adjusted after the test using the re-analyse function.

Fig. 4 Setup 2

For Research Use Only. Not for use in diagnostic procedures.
The content of this publication shall not be reproduced, altered or sold for any commercial purpose without the written approval of Shimadzu. The information contained herein is provided to you "as is" without warranty of any kind including without limitation warranties as to its accuracy or completeness. Shimadzu does not assume any responsibility or liability for any damage, whether direct or indirect, relating to be the use of this publication. This publication is based upon the information available to Shimadzu on or before the date of publication, and subject to change without notice.

SHIMADZU
Excellence in Science

Application News

Material Testing System EZ-X

No. SCA_300_030

Paper Tensile test
Tensile test according to ASTM-D 828, EN ISO 1924-2or TAPPI T-494.

■ Purpose and Definition

Tensile tests are a fundamental test within material science and is performed on more or less all materials including paper. Within the paper industry it is very important to know the tensile properties. Paper products are for example often printed in automated machines where the paper is run through big rolls over large distances and at very high speeds.
Also in the packaging industry the paper is delivered on big rolls which are then fed into machinery which produce different types of cartons for a great variation of applications and rely on high tensile quality during production.

■ Equipment used

Testing machine: EZ-LX Table top
Load cell: 1000 N, 1/500 Class1
Jig: PFG-1 kN Pneumatic grips.
Software: TrapeziumX Single / tensile.
Environment: Room temp 21 °C +/-2 °C, humidity ca. 50 +/-5% RH

■ Test execution

- 5 sets of samples were prepared.
- Sample length is 250 mm +/- 5 mm.
- Width is 25 mm +/-0,4 mm according to ASTM D828, (EN ISO1924 width shall be 15 +/-0,1 mm)
- The sample length has to be long enough to allow for 180 mm gauge length, grip separation, and still have enough sample for correct clamping.
- A method is prepared according to ASTM D828.
- Test type is single and tensile.
- Test speed is set to 20 mm/min (25 +/-5mm/min is required according to ASTM and 20 +/-5 mm/min according to EN ISO 1924).

Some data points which may be requested for in this test are:

- Tensile strength, kN/m,
- Elongation, %,
- Tensile energy absorption, J/m2,
- Tensile stiffness, kN/m,
- Breaking length, m,
- Tensile index, Nm/g.
- With the help of TrapeziumX and the calculator in the data processing menu it´s easy to create data points like the ones requested in the paper industry.

■ Test Results:

Tensile properties are always important in most materials and is the most common test made in universal testing machines. Generally a customer is looking for elastic, maximum and break properties.

Results in this case are presented according to the requirements in ASTM D828.
To obtain this result we have a great help from the calculator in TrapeziumX / data processing to present the results in a correct way.
Please refer to ASTM D828 for details

Results(Batch)

Name		Max_Force	Tensile strength	Tensile index	Break_Strain	A	TEA
Parameter		Calc. at Entire Areas			Sensitivity: 1	Calc. at Entire Areas	
Pass/Fail							
Unit		kN	kN/m	Nm/g	%	J	J/m²
Print		☑	☑	☑	☑	☑	☑
80g/m² _ 1	☑	0,20073	10,0365	100,365	1,87989	0,43186	94,7594
80g/m² _ 2	☑	0,18411	9,20550	92,0550	1,78297	0,36799	81,7715
80g/m² _ 3	☑	0,19289	9,64450	96,4450	1,94483	0,42123	93,3916
80g/m² _ 4	☑	0,18449	9,22450	92,2450	1,75497	0,36492	81,0084
80g/m² _ 5	☑	0,18095	9,04750	90,4750	1,77312	0,36157	80,3079
Average		0,18863	9,43170	94,3170	1,82716	0,38951	86,2478
Standard Deviation		0,00808	0,40397	4,03972	0,08172	0,03409	7,18074
Range		0,01978	0,98900	9,89000	0,18986	0,07029	14,4515

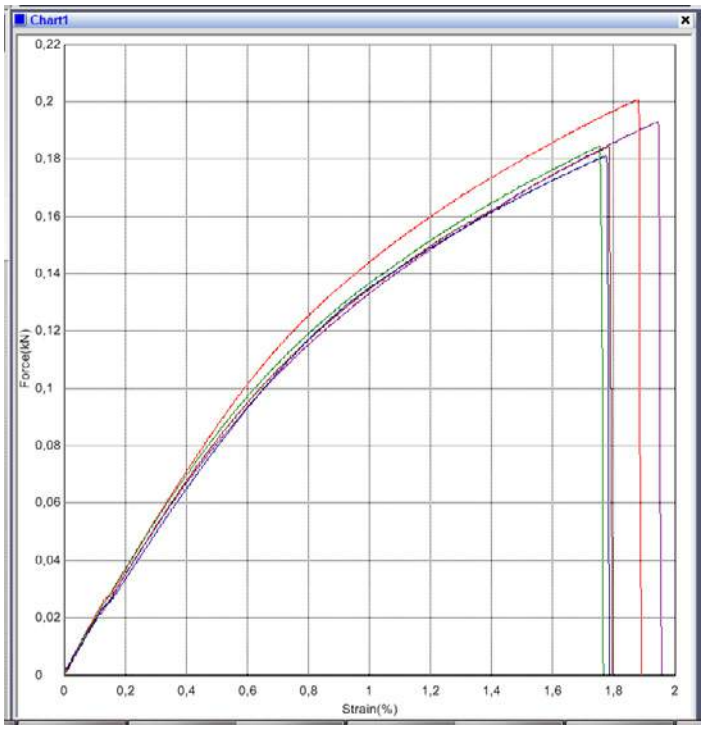

Examples of applicable standards:
Determination of tensile properties – ISO 1924-2
Tensile Properties of Paper and Paperboard Using ASTM D828
Tensile properties of paper and paperboard TAPPI T-494

SHIMADZU
Shimadzu Europa GmbH
www.shimadzu.eu

For Research Use Only. Not for use in diagnostic procedures.
The content of this publication shall not be reproduced, altered or sold for any commercial purpose without the written approval of Shimadzu. The information contained herein is provided to you "as is" without warranty of any kind including without limitation warranties as to its accuracy or completeness. Shimadzu does not assume any responsibility or liability for any damage, whether direct or indirect, relating to be the use of this publication. This publication is based upon the information available to Shimadzu on or before the date of publication, and subject to change without notice.

SHIMADZU
Excellence in Science

Application News

Material Testing System CFT

No. SCA_300_033

Viscosity Evaluation of Toner for Electronic Photographs with Shimadzu Flow Tester Model CFT

Heat fusing type toner for electronic photographs is used in copying machines and printers of electronic photographing or electrostatic printing type.
Toner images are fixed by any one of three methods: by heated roller for melting and fusing toner, by organic solvent for dissolving or softening the binder resin to fix toner, or by pressing toner for fixing. Toners are oriented for use with a particular one of these methods.

The most commonly used method at present is the heat roller fusing method, which requires application of heat and pressure simultaneously so that the toner image is in contact with the heated roller and fixed on an imaging sheet. Toners used in this method should be such that they can be fixed at as low a temperature as practicable, and particularly, it should permit quick fixing and a wide range of applicable temperatures. Toners should further agree with such requirements that the image density is good enough to ensure clear images of high resolution and that it allows stable and continuous use at any-time.
Toner for electronic photographs comprises binding resin, usually polyester resin, and colouring agents, the softening or melting points of which may be evaluated with the flow tester Model CFT. Thanks to its excellent reputation, the Shimadzu Flow Tester Model CFT is enjoying great demand in the toner industry.

The followings presents an example of viscosity evaluation of a toner for electronic photographs.
In general, a flow curve in constant heating rate mode with flow tester Model CFT takes a S-letter shape as shown in Fig. 1.
The lower and upper softening temperature limits and point of softening are usually determined from the intersecting points of straight line through the most linear portion of the obtained flow curve with the lines extended from flow starting point and terminating point.

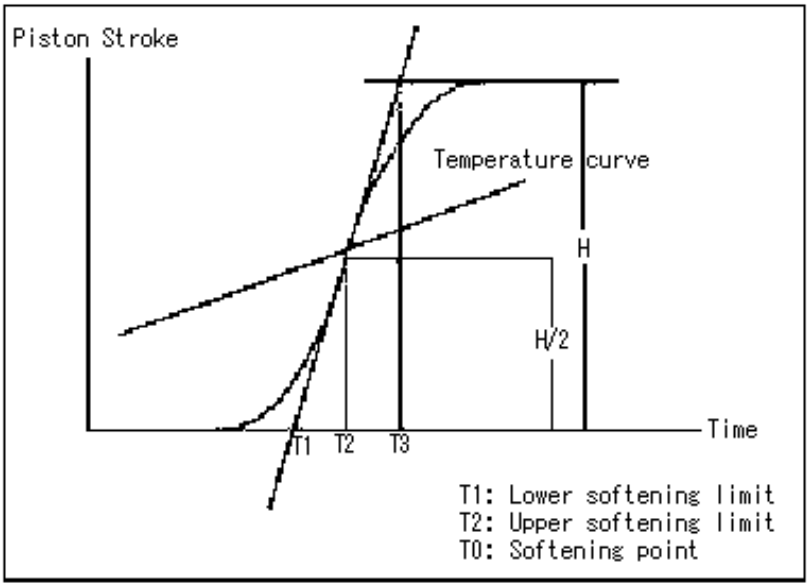

Figure 1: Flow curve of toner in constant heating rate mode

■ Flow curve of toner (A) in constant heating rate mode (Figure 2)

Test conditions

Test temperature:	80 °C to max 300 °C
Constant heating rate:	5 °C/min
Extruding conditions:	Pressure: 50 kgf/cm^2
	Die: D 0.5 x 1 mm (Diameter x Length)

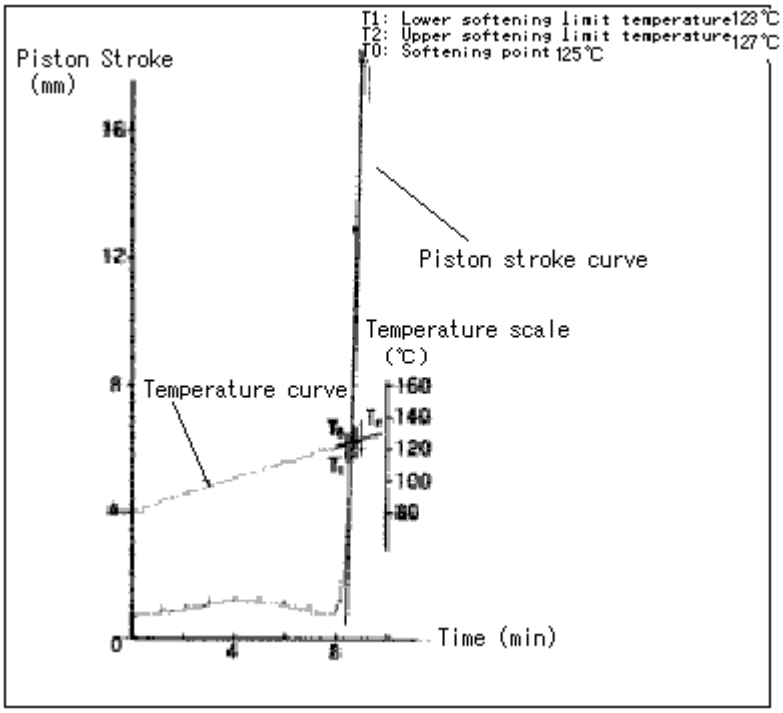

Figure 2: Flow curve of toner (A) in constant heating rate mode

■ Flow curve of toner (B) in constant heating rate mode (Figure 3)

Test conditions

Test temperature: 80 °C to max 300 °C
Constant heating rate: 5 °C/min
Extruding conditions: Pressure: 50 kgf/cm^2, Die: D 0.5 x 1 mm (Diameter x Length)

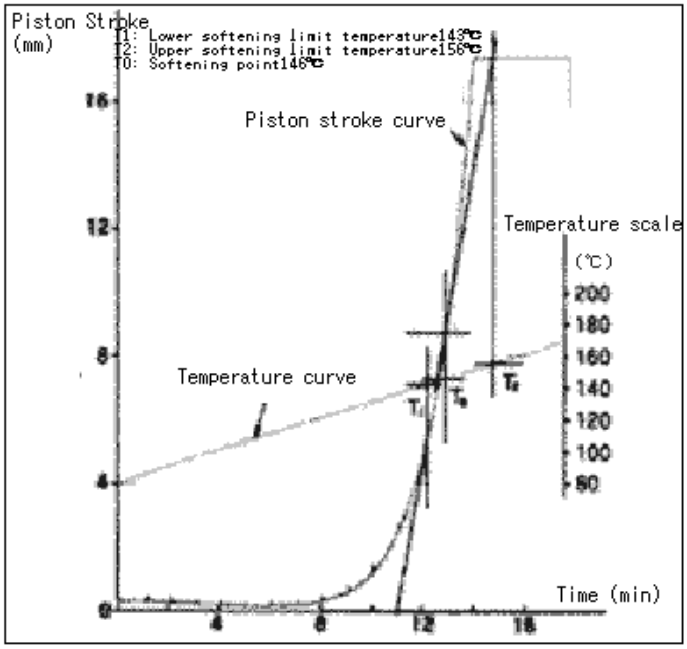

Figure 3: Flow curve of toner (B) in constant heating rate mode

■ Flow curve of toner (C) in constant heating rate mode

Test conditions

Test temperature: 80 °C to max 300° C
Constant heating rate: 5 °C/min
Extruding conditions: Pressure: 50 kgf/cm^2, Die: D 0.5 x 1 mm (Diameter x Length)

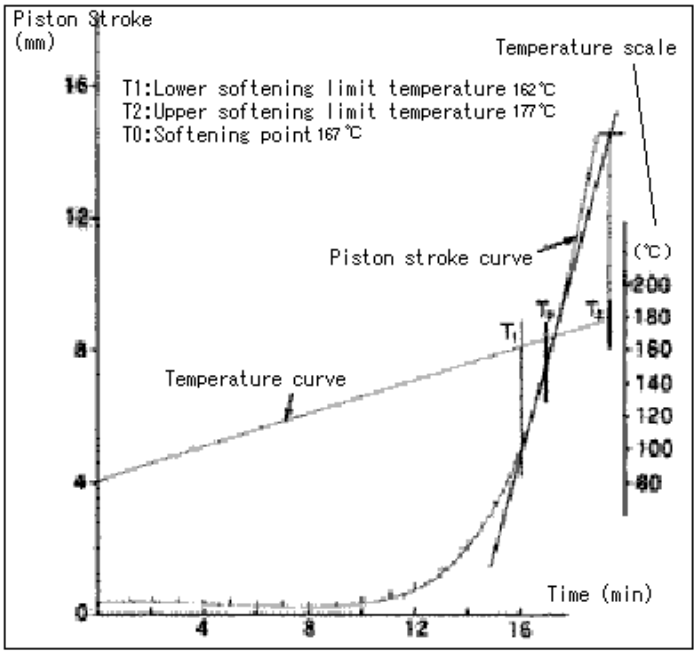

Figure 4: Flow curve of toner (C) in constant heating rate mode

High quality printing and copying free from defects like blots is required by the booming office automation movement from which the toner industry is enjoying an increasing demand for toner.
Softening temperature and flow properties are the fundamental factors for ensuring the commercial value of toner by quality control.

* Please be advised that data obtained before the implementation of the current Weights and Measures Law may be presented in terms of gravimetric unit.

Shimadzu Europa GmbH
www.shimadzu.eu

For Research Use Only. Not for use in diagnostic procedures.
The content of this publication shall not be reproduced, altered or sold for any commercial purpose without the written approval of Shimadzu. The information contained herein is provided to you "as is" without warranty of any kind including without limitation warranties as to its accuracy or completeness. Shimadzu does not assume any responsibility or liability for any damage, whether direct or indirect, relating to be the use of this publication. This publication is based upon the information available to Shimadzu on or before the date of publication, and subject to change without notice.

SHIMADZU
Excellence in Science

Application News

Material Testing System CFT

No. SCA_300_041

Evaluation of the Temperature Characteristics of Toner

During laser printing, toner powder, which has a particle diameter of about 5 µm, is transferred onto copy paper and heated so that it adheres to the paper. In the case of color laser printing, this process is repeated for four different colors. If the melting temperature and melt viscosity differ for the four colors, then it could cause bleeding or poor adhesion in areas printed first and reduce print quality. To prevent that, the temperature characteristics associated with toner flow must be the same for all four colors.

Fig. 1

■ Flow Beginning Temperature for Four Toner Colors by Constant Heating Rate Testing

The constant heating rate test was performed for all four color toners used in the same color printer (cyan, magenta, yellow, and black). The constant heating rate method was used to calculate characteristic values such the softening temperature, flow beginning temperature, ½ method temperature, and offset temperature.

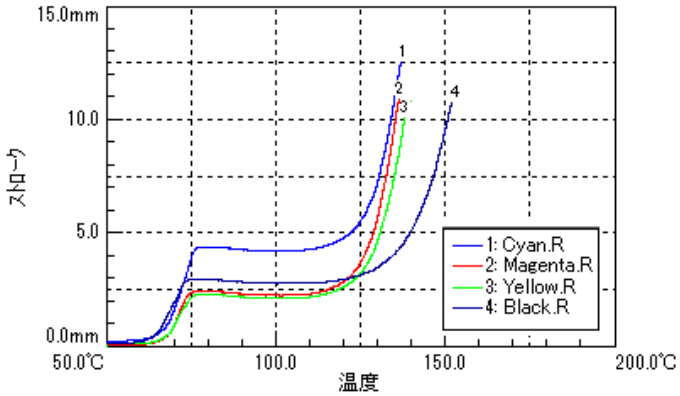

Fig. 2 Stroke- Temperature Graph

½ method temperature: Midpoint between flow beginning and flow ending temperatures
Offset temperature: Temperature at flow beginning stroke plus any arbitrary offset stroke. All four toner colors have very similar characteristic values. In particular, the values for the three non-black colors were almost identical. Ensuring that the respective temperature and fluidity characteristics are approximately the same is important for maintaining the print quality of color laser printers. Therefore CFT-EX series flowtesters serve an important role in toner research and development, and quality control applications.

Test Method	Constant Temperature Test
DIE Diameter	0,5 mm
DIE Length	1 mm
Beginning Temperature	50 °C
Ending Temperature	200 °C
Heating Rate	5 °C/min
Test Pressure	0,98 MPa
Preheating Time	240 sec
Sample Size	1 g (pallets)

Table 1: Test Conditions

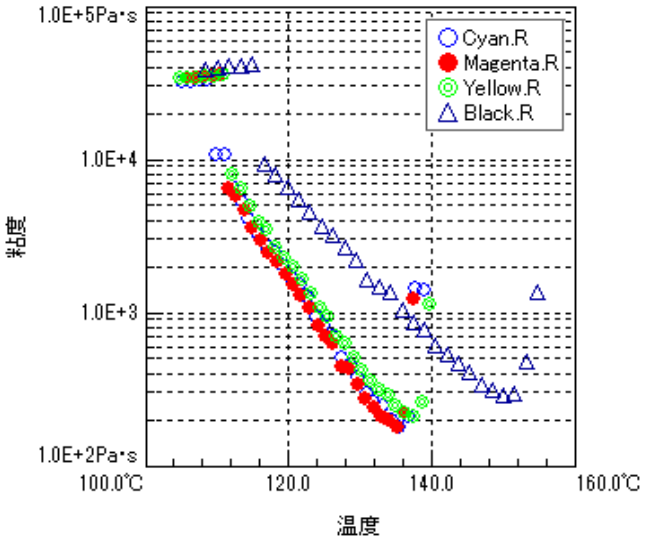

Fig. 3 Viscosity-Temperature Graph

Sample Name.	Softening Temperature (°C)	Flow Beginning Temperature (°C)	½ Methode Temperature (°C)	½ Methode Temperature (Pa•s)
Cyan	76,8	105,1	132,5	248,2
Magenta	75,4F	105,8	131,8	240,7
Yellow	76,3	104,8	133,5	285,8
Black	73,8	108,5	145,9	402,4

Table 2: Test Result

■ Press-Forming Powdered Samples for Efficient Measurement

Due to the small size of toner particles, samples could easily scatter if placed directly in the sample chamber or spill out from die orifices. Therefore, for samples such as these, a hand press and preforming die unit can be used to press them into a form that can be more easily placed in the sample chamber. Accurate values can be measured efficiently by placing only one pellet in the chamber. For thermosetting resin samples, measurements can fail due to ongoing curing during the time it takes to place samples in the sample chamber. Therefore, it is extremely important to pelletize samples before measurement.

For Research Use Only. Not for use in diagnostic procedures.
The content of this publication shall not be reproduced, altered or sold for any commercial purpose without the written approval of Shimadzu. The information contained herein is provided to you "as is" without warranty of any kind including without limitation warranties as to its accuracy or completeness. Shimadzu does not assume any responsibility or liability for any damage, whether direct or indirect, relating to be the use of this publication. This publication is based upon the information available to Shimadzu on or before the date of publication, and subject to change without notice.

SHIMADZU
Excellence in Science

Application News

No. SCA_300_044

Material Testing System DUH

Hardness Measurement of Thin Layer (Resin Layer) on Si Wafer using the Shimadzu Dynamic Ultra Micro Hardness Tester DUH-211S

The Shimadzu Dynamic Ultra Micro Hardness Tester DUH-211S allows hardness measurement with extremely small test force (from 0.1 mN). Therefore, by using this testing machine, characteristics of thin layers can be determined accurately not affected by the base material. The DUH-211S is being widely used for strength evaluation of various protective layers. The following presents an example where a thin layer (resin layer) on a 6-inch Si wafer was tested for hardness without being broken.

1. Sample

Sample Name	Sample No.	Thickness	Sample size and measurement position
Si Wafer			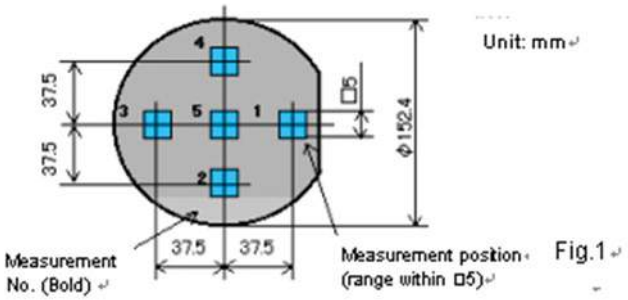
	No.1		
	No.2		
	No.3		

Fig.1

1. Test conditions

1. Testing machine: Shimadzu Dynamic Ultra Micro Hardness Tester DUH-211S
2. Indenter: Quadrangular pyramid indenter with 136° tip angle (Vickers indenter)
3. Test mode: Load-unload test
4. Test force: 4.9 mN
5. Loading rate: 0.284 mN/sec
6. Load holding time :10 sec

■ Sample fixing method

Sample was fixed by rubber plates and clamps as shown in Fig. 2.

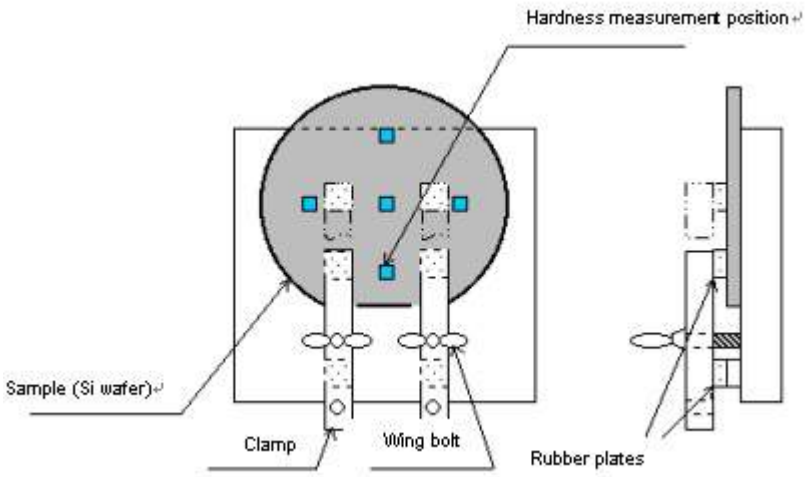

Fig. 2 Sample fixing method diagram

■ Test results

1) Fig.3 shows the “Test force? Indentation depth graph” of the mean values for each sample obtained from hardness measurements.
2) Table 1 shows the results (mean values) of hardness measurements.
   Dynamic hardness was calculated using the following formula:

   DHT115-1 = 3.8584P/D2
   DHT115-1: Dynamic hardness measured by triangular indenter with 115° tip angle
   P: Test force (mN)
   D: Indentation depth (mm)

3) Measurement results: According to the DHT115-1 values in Table 1, the hardness of the samples is ordered as follows:

   No.3 > No.2 > No.1

4) Measurement results: According to the elastic modulus in Table 1, elastic modulus of the samples is ordered as follows:

   No.3 > No.2 > No.1

5) For all samples, the elastic modulus decreases with the reduction in hardness.

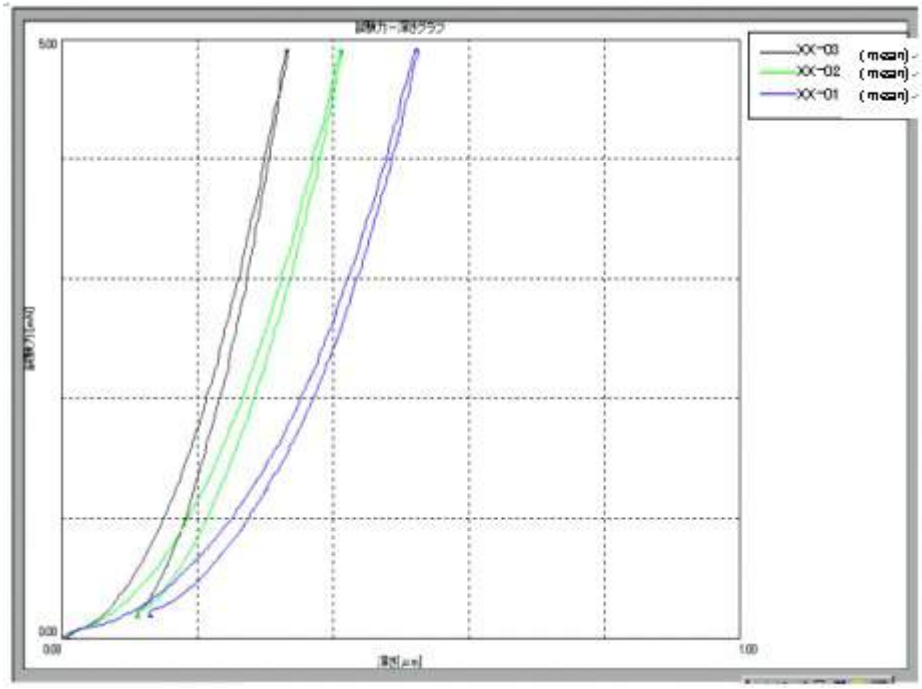

Fig. 3 Test Force Indentation Depth Diagram

Table 1 Hardness measurement results (mean values)				
Sample name	Sample No.	Dynamic hardness (DHT115-1)	Elastic modulus (PA)	Data file name
Si wafer resin layer				
	No.1	68	1.12E+10	XX-01
	No.2	111	1.74E+10	XX-02
	No.3	176	2.79E+10	XX-03
Ref.) "E+10" in the Elastic modulus columns means 1010				

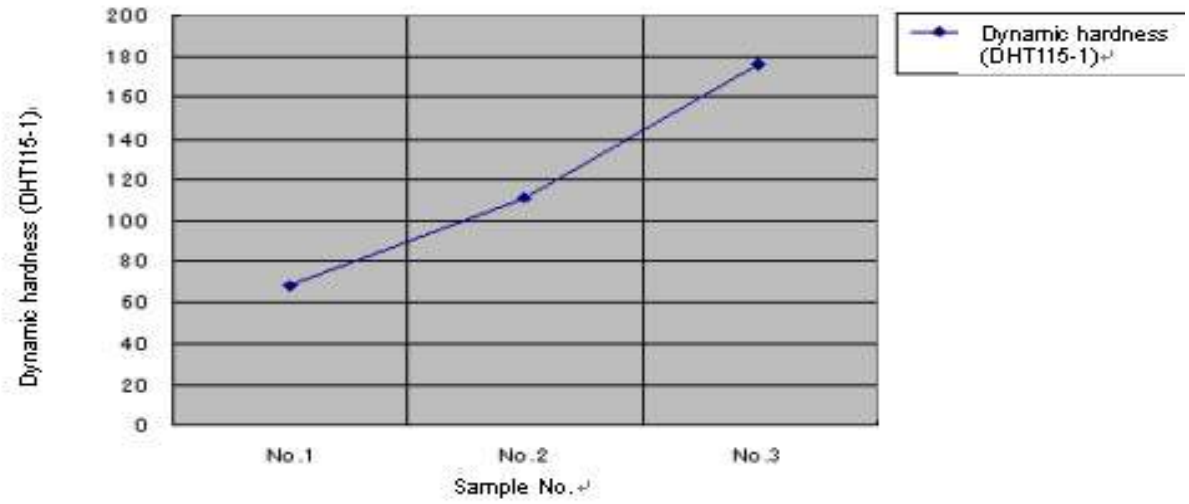

Fig.4 Sample No. and Dynamic Hardness (DHT-115-1)

■ Summary

The resin layer on wafer is increasingly resistant to abrasion as the hardness increases, and increasingly strong against damage such as thermal deformation as the elastic modulus increases. Therefore, layers with high hardness and elastic modulus are desirable, making sample No. 3 the best among the samples tested in this example.

For Research Use Only. Not for use in diagnostic procedures.
The content of this publication shall not be reproduced, altered or sold for any commercial purpose without the written approval of Shimadzu. The information contained herein is provided to you "as is" without warranty of any kind including without limitation warranties as to its accuracy or completeness. Shimadzu does not assume any responsibility or liability for any damage, whether direct or indirect, relating to be the use of this publication. This publication is based upon the information available to Shimadzu on or before the date of publication, and subject to change without notice.

SHIMADZU
Excellence in Science

Application News

Material Testing System AGS-X

No. SEG_300_060

Spring compression test

■ Purpose and Definition

All spring manufacturers has to test their type products in quality control and R&D. Tests are performed in tensile or compression direction depending on spring.
They have to make tensile tests according to ISO6892 on the spring wire and also tensile or compression tests on the final products. We will have a look at compression tests on helical springs. The results the customers normally are looking for are load at specified height, height at specified load, free height and spring constant.

■ Equipment used

Testing machine:	AGS-X 5kN
Load cell:	1kN, 1/500 Class 1
Jig:	Compression plates, Ø100 mm.
Software:	Trapezium-X, Spring
Environment:	Room temp 21°+/- 2 °C, humidity ca. 50 +/- 5% r.F.
Test jig:	Standard compression plates, Ø100 mm 343-08095.

For production control purposes the AGS-X series will be the suitable option. It´s performance and price together with TrapeziumX Spring software makes it a perfect tool for efficient spring testing with high throughput.

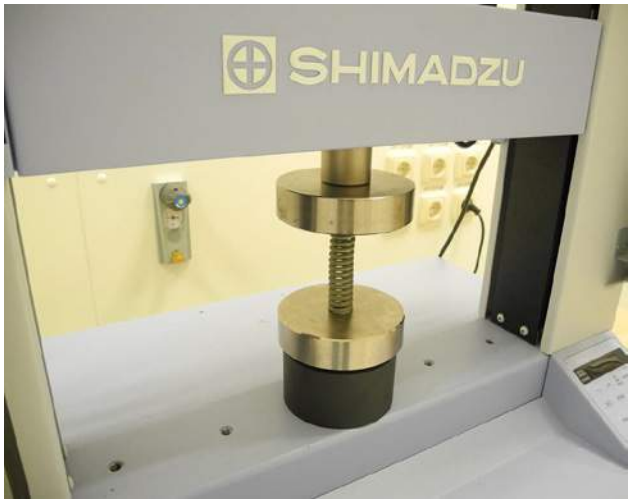

Fig. 1. Overview of AGS-X Spring Compression Test

■ Test execution

In TrapeziumX, spring we create a method with some typical data points for spring tests. You will find them for example in ASTM A125 where it´s exactly specified what should be selected. We select load at specified Height (LASE), height = spring length.
Height at specified load (EASL), free height with a sensitivity (detection point) of 0,01% of full scale (1kN) and spring constant. Free height is the height of the spring at the start of the test and is automatically measured by the instrument.

The main difference between a standard compression test and a spring test is that the instrument has to be able to detect the absolute position of the crosshead.
This is needed to be able to detect the spring height, which is an important parameter in a spring test.

A zero position reset has to be made whenever fixtures are changed or the machine is started. The software will ask for this procedure when started but it has to be done manually by the operator whenever he changes fixtures (= changes the zero position). The procedure itself is automated and easy to perform and you will be guided by the software.

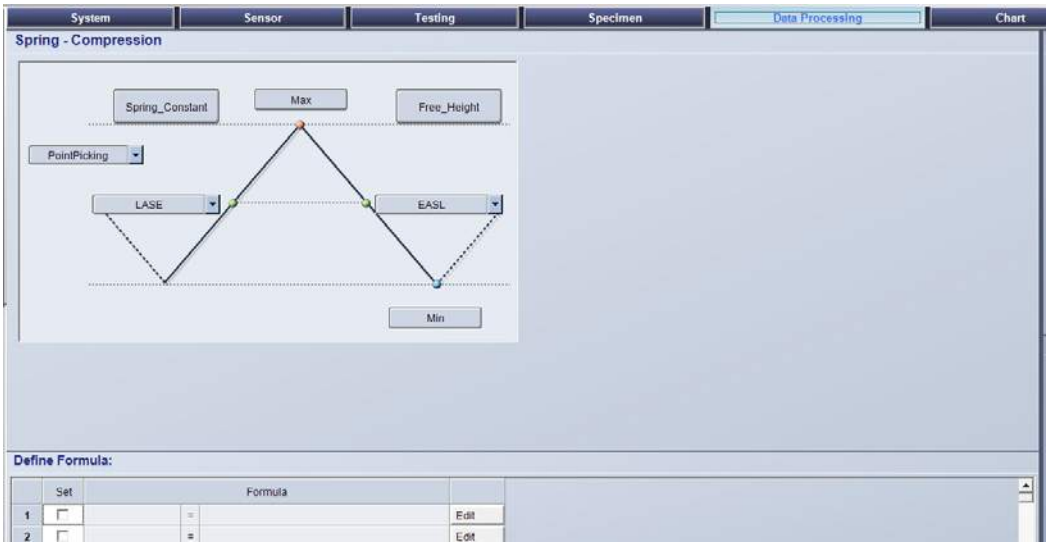

■ Test Results

Spring testing is important for the producer as well as the third party user.
Springs are used everywhere and many times in safety functions like spring loaded high pressure release valves.

Height changes at different loads and loads at different heights together with spring constant gives the user or producer important data regarding product quality.

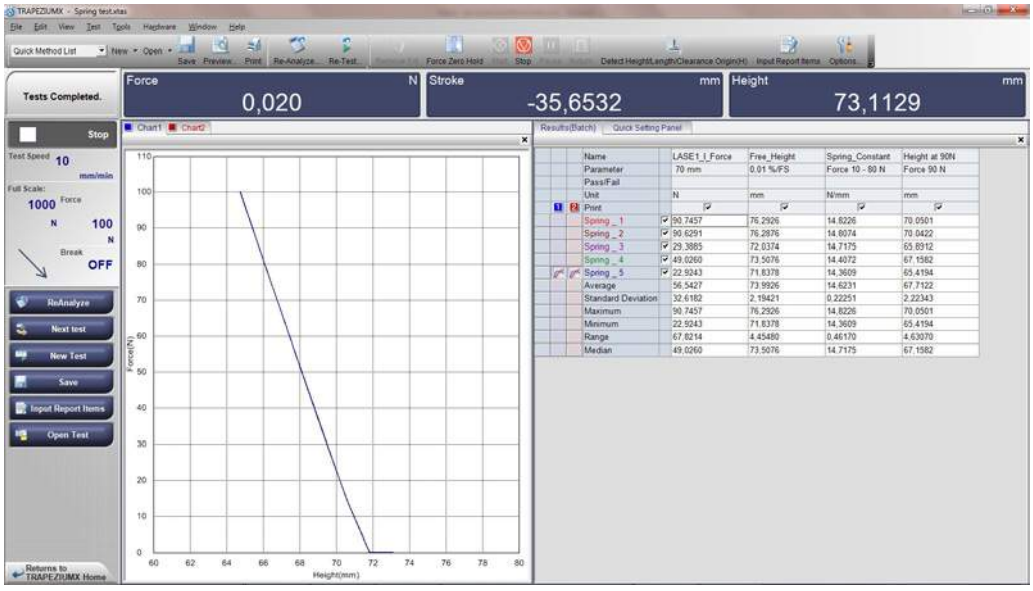

Examples of applicable standards: ASTM A125

SHIMADZU

Shimadzu Europa GmbH
www.shimadzu.eu

For Research Use Only. Not for use in diagnostic procedures.
The content of this publication shall not be reproduced, altered or sold for any commercial purpose without the written approval of Shimadzu. The information contained herein is provided to you "as is" without warranty of any kind including without limitation warranties as to its accuracy or completeness. Shimadzu does not assume any responsibility or liability for any damage, whether direct or indirect, relating to be the use of this publication. This publication is based upon the information available to Shimadzu on or before the date of publication, and subject to change without notice.

SHIMADZU
Excellence in Science

Application News

No.V20

High-Speed Video Camera

High-Speed Imaging of Laser Ablation Process

Introduction

Laser ablation is the process of removing material from a solid (or occasionally liquid) surface by irradiating it with a laser beam. At high irradiation intensities, material on the solid surface is vaporized and converted to plasma. Laser ablation is utilized in a wide range of fields, including product processing, medical, material manufacturing, and more.

Examples of product processing include electronic component processing by Q-switched Nd: YAG laser and microfabrication of plastics and ceramics by excimer laser. An example in the medical field is refractive surgery of the cornea using an ArF laser. In material production, it is notably used in thin film production apparatuses. Although this application of laser ablation is not suitable for mass production of thin films, the ability to easily create a thin film having the same composition ratio as a target (solid surface) and the ease with which the thickness can be changed, have led to its wide use in specialized applications. Observation of the substances discharged (plume) during ablation and elucidation of the behavior of the laser ablation plume make it possible to optimize the film-forming conditions and enhance development of thin films. It is believed that observation of the ablation plume using a high-speed video camera is important. Using the Shimadzu Hyper Vision HPV-X2 high-speed video camera, we were able to observe and document the laser ablation plume generated using AZO (transparent electrode material) as the target.

Experimental Method

The thin film production apparatus consisted of a laser device and a vacuum chamber for ablation. The laser was applied to the target, and film was formed on the substrate above. Fig. 1 shows the state of the experimental apparatus, the vacuum chamber, the Shimadzu HPV-X2, and the target. A target rotation accessory was installed to prevent repeated ablation at the same site on the target. Laser oscillation timing was used as the trigger for recording. Table 1 lists the imaging components.

Measurement Results

As indicated in Table 2, imaging was conducted at a speed of 10 million frames per second. Frame 2 of Fig. 2 shows that laser irradiation has occurred (indicated by white arrow). Ablation occurs in subsequent frames. The intensity of the ablation plume's emission gradually deteriorates as it spreads in a perpendicular direction to the target.

Table 1 Imaging Equipment

High-Speed Video Camera	: Shimadzu Hyper Vision HPV-X2
Lens	: 105 mm macro lens
Lighting	: Strobe

Table 2 Measurement

Recording speed	: 10 million frames per second

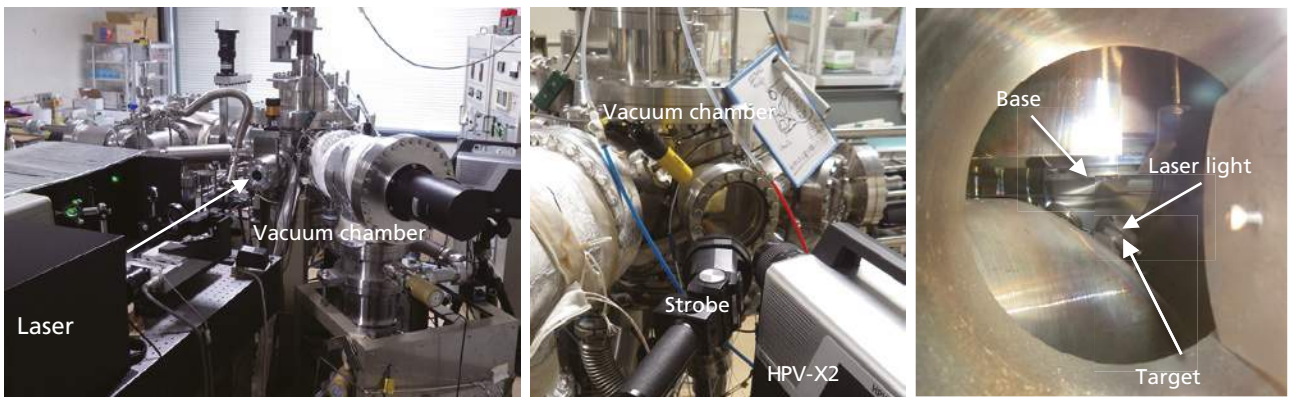

View of entire experimental apparatus (left), vacuum chamber, Shimadzu HPV-X2 (center), and target (right).

Fig. 1 Experiment Equipment

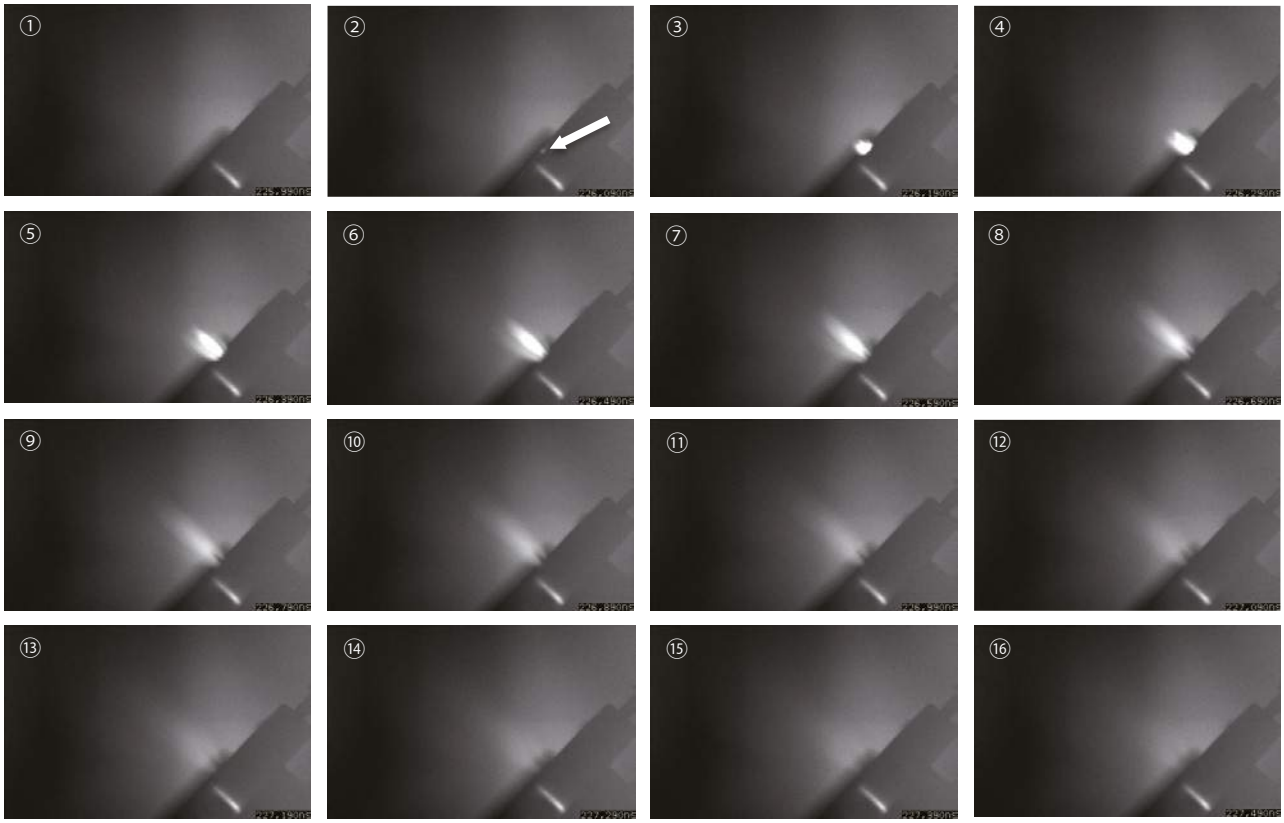

Data provided by Kyoto University, Tabe Laboratory

Fig. 2 High-Speed Images (framing interval: 100 nanoseconds)

Fig. 3 shows the relationship between distance from and brightness of the target vertically. Brightness corresponds to the brightness values obtained by subtracting the brightness of frame 1 (before laser irradiation) from each of the brightness values of frames 2 through 16, respectively. The spreading characteristics of the ablation plume can be comprehended from the graph. The speed of the laser ablation plume can be determined based on the 100-nanosecond frame interval.

Note: As the aperture was opened to record the entire ablation, some halation is evident in frames 3 through 7.

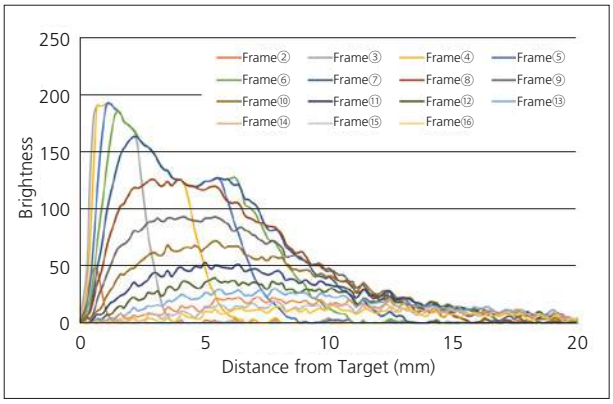

Fig. 3 Brightness of Laser Ablation Plume

Conclusion

Laser ablation is an ultra high-speed phenomenon and can be captured in exquisite detail with the newly developed Shimadzu Hyper Vision HPV-X2 high-speed video camera — featuring recording speeds up to 10 million frames per second and six times higher sensitivity compared to conventional video cameras. Video recording of this type has not been possible using conventional video cameras due to the difficulty of light reaching the target inside the vacuum chamber. The Shimadzu Hyper Vision HPV-X2 high-speed video camera is the best in its class, providing excellent video documentation of the laser ablation process.

First Edition: Sep. 2015

SHIMADZU

Shimadzu Corporation

www.shimadzu.com/an/

For Research Use Only. Not for use in diagnostic procedures.
The content of this publication shall not be reproduced, altered or sold for any commercial purpose without the written approval of Shimadzu.
The information contained herein is provided to you "as is" without warranty of any kind including without limitation warranties as to its accuracy or completeness. Shimadzu does not assume any responsibility or liability for any damage, whether direct or indirect, relating to the use of this publication. This publication is based upon the information available to Shimadzu on or before the date of publication, and subject to change without notice.

© Shimadzu Corporation, 2015

SHIMADZU
Excellence in Science

Application News

No.V23

High-Speed Video Camera

Observation of Microbubbles and Cell Behavior Due to Exposure to Ultrasonic Waves

Introduction

One type of drug delivery system (DDS) dosing method involves injecting pharmaceuticals into cells by filling microbubbles with pharmaceuticals, and then collapsing them after making them adhere to cells. In this method, it is important that the drug is injected by penetrating the cell wall, but without killing the cell, as a result of the jet when the microbubble collapses. Accordingly, it is important to observe the behavior of the cell when the bubble collapses. Bubbles are made to collapse by resonance with ultrasonic waves. Resonant frequencies are 1 MHz or higher, so high-speed imaging must be performed at 1 million frames/sec or faster. This article introduces observations of the behavior of cells and microbubbles due to exposure to ultrasonic waves, using the HPV-X2 high-speed video camera.

Measurement System

The HPV-X2 high-speed video camera was used for this experiment. Fig. 1 shows the imaging system, Fig. 2 shows the sample and ultrasonic horn, and Fig. 3 shows a schematic diagram of the imaging system. As in Fig. 2, cancer cells and PVC microcapsules (approximately 5 µm in diameter) are placed in a sample cell filled with physiological saline, which is then placed at the bottom of a water tank. The focus of the ultrasonic horn was aligned with the sample cell, the sample cell was exposed to 1 MHz ultrasonic waves for a total of 3 seconds, and the results were observed with the HPV-X2. The instruments used are indicated in Table 1.

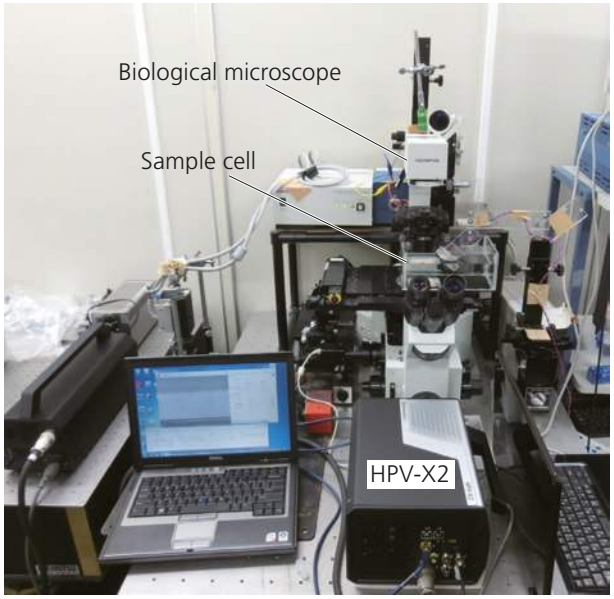

Fig. 1 Imaging System

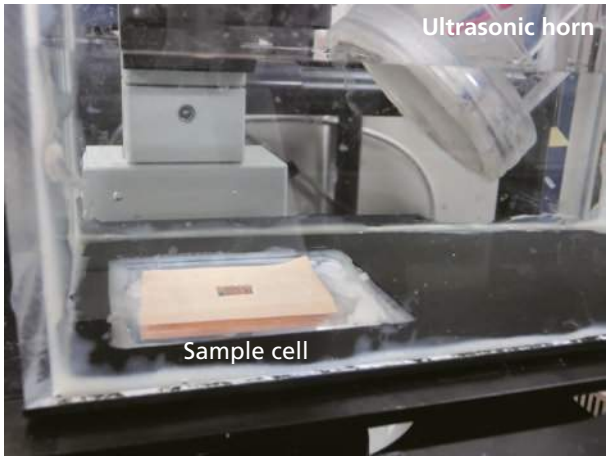

Fig. 2 Sample and Ultrasonic Horn

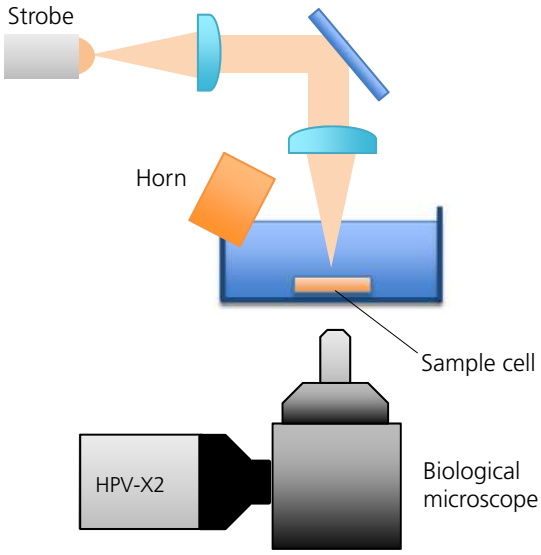

Fig. 3 Schematic Diagram of the Imaging System

Table 1 Imaging Equipment

High-speed video camera	: HPV-X2
Microscope	: IX70 Biological Microscope
Illumination	: Strobe

Measurement Results

Imaging was performed at a speed of 10 million frames/sec. Fig. 4 shows the imaging results. In Image 2 in Fig. 4, the sample is exposed to ultrasonic waves, and the microbubbles within the microcapsules are expanding. The two microbubbles shown by the arrows in Image 3 have made contact with the cell due to the expansion process and a load is being applied. The expansion of the microbubbles continues until Image 4, after which they contract until Image 11. The cell has become deformed at the two locations shown by the arrows in Image 11, and it can be confirmed that it is damaged.

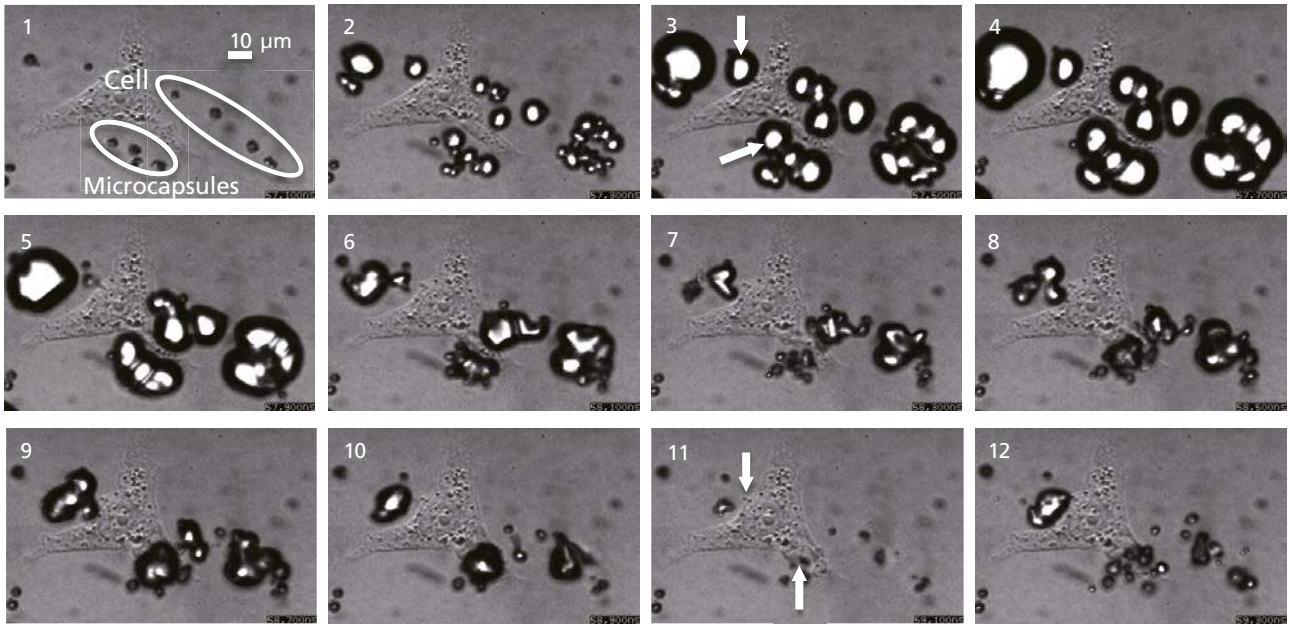

Fig. 4 High Speed Imaging Results (Interval Between Images is 200 ns)

Data provided by the Laboratory of Biomedical Engineering at Hokkaido University

Conclusion

The behavior of cells and microbubbles due to exposure to ultrasonic waves were observed using the HPV-X2 high-speed video camera. Samples were exposed to 1 MHz ultrasonic waves, so an imaging speed of at least 1 million frames/sec was required. Because a microscope was used for imaging, camera sensitivity was very important for these measurements. The newly developed HPV-X2 has at least six times the sensitivity of the conventional HPV-X, so favorable imaging was obtained, even using a microscope, at an imaging speed of 10 million frames/sec. Using the HPV-2 in this way will contribute to DDS development.

Note: Drug Delivery Systems

A drug delivery system (DDS) is a system for administering pharmaceuticals. It is a general term for a form of pharmaceutical administration designed to further enhance the effectiveness of medicinal agents, aiming to optimize the pharmaceutical administration route. In other words, the objective is to provide the required pharmaceuticals to the required location at the required time. When medicine is swallowed, only a tiny portion of the amount actually arrives at the affected area to have the intended effect. Some medicinal components are degraded within the body, while others cause side effects by acting at sites where they are not needed. Using a DDS enables more effective administration, which can be expected to reduce both the dosage of medicinal agents and their side effects, thereby improving the quality of life (QOL) for patients. In addition, expense reductions can be expected due to reductions in the number of times pharmaceuticals are administered.

First Edition: Mar. 2016

Shimadzu Corporation
www.shimadzu.com/an/

For Research Use Only. Not for use in diagnostic procedures.
The content of this publication shall not be reproduced, altered or sold for any commercial purpose without the written approval of Shimadzu.
The information contained herein is provided to you "as is" without warranty of any kind including without limitation warranties as to its accuracy or completeness. Shimadzu does not assume any responsibility or liability for any damage, whether direct or indirect, relating to the use of this publication. This publication is based upon the information available to Shimadzu on or before the date of publication, and subject to change without notice.
© Shimadzu Corporation, 2016

Founded in 1875, Shimadzu Corporation, a leader in the development of advanced technologies, has a distinguished history of innovation built on the foundation of contributing to society through science and technology. We maintain a global network of sales, service, technical support and application centers on six continents, and have established long-term relationships with a host of highly trained distributors located in over 100 countries.

For information about Shimadzu, and to contact your local office, please visit our website at www.shimadzu.eu

SHIMADZU

Shimadzu Europa GmbH
Albert-Hahn-Str. 6-10 · D-47269 Duisburg
Tel.: +49 - (0)203 - 76 87-0
Fax: +49 - (0)203 - 76 66 25
shimadzu@shimadzu.eu
www.shimadzu.eu